GEOLOGICAL SURVEY OF CANADA
BULLETIN 500

EXPLORING FOR MINERALS IN ALBERTA: GEOLOGICAL SURVEY OF CANADA GEOSCIENCE CONTRIBUTIONS, CANADA-ALBERTA AGREEMENT ON MINERAL DEVELOPMENT (1992-1995)

Edited by
R.W. Macqueen

1997

Natural Resources Canada   Ressources naturelles Canada

Canada

GEOLOGICAL SURVEY OF CANADA
BULLETIN 500

EXPLORING FOR MINERALS IN ALBERTA: GEOLOGICAL SURVEY OF CANADA GEOSCIENCE CONTRIBUTIONS, CANADA-ALBERTA AGREEMENT ON MINERAL DEVELOPMENT (1992-1995)

Edited by
R.W. Macqueen

1997

Catalogue No. M42-500E
ISBN 0-660-16725-5

Available in Canada from
Geological Survey of Canada offices:

601 Booth Street
Ottawa, Canada K1A 0E8

3303-33rd Street N.W.
Calgary, Alberta T2L 2A7

101-605 Robson Street
Vancouver, B.C. V6B 5J3

or from

Canadian Government Publishing
Public Works and Government Services Canada
Ottawa, Ontario K1A 0S9

A deposit copy of this publication is also available for reference
in selected public libraries across Canada

Price subject to change without notice

Cover illustration
An aerial view of Precambrian (Paleoproterozoic) granite and syenogranite terrain, northeastern Alberta, looking northeast towards Turtle Lake in the middle distance, centre of photograph. The typical rolling topography has been extensively scoured by glacial ice flowing from right to left across the trend in foliation. NTS 74M/7. Photograph by J.M. Bednarski.

Authors' addresses

H.J. Abercrombie
Birch Mountain Resources Ltd.
3100, 25 5th Avenue S.W.
Calgary, Alberta T2P 2V7

S.B. Ballantyne
Eldorado Gold Corporation
920, 1055 West Hastings Street
Vancouver, British Columbia V6E 2E9

D.C. Harris
23 Bentworth Crescent
Nepean, Ontario K2G 3X1

J. Mariano
Exxon Exploration Co. Ltd.
P.O. Box 42791
Houston Texas, U.S.A. 77210-42791

M.R. McDonough
Servicio Nacional De Geología y Minería
Oficina Técnica Puerto Varas
Avenida La Paz 406
Puerto Varas, Chile

V. Ruzicka
1053 Pinewood Crescent
Ottawa, Ontario K2B 5Y3

D.J. Teskey
6179 Voyageur Drive
Orleans, Ontario K1C 2X5

R. Feng, D.A. Leckie, R.W. Macqueen, G.M. Ross
Geological Survey of Canada (Calgary)
3303-33rd Street N.W.
Calgary, Alberta T2L 2A7

J.M. Bednarski
Terrain Sciences Division (Calgary)
3303-33rd Street N.W.
Calgary, Alberta T2L 2A7

B.W. Charbonneau, C-J. Chung, R.G. Garrett, R.J. Hetu, P.B. Holman, M.W. McCurdy, A.N. Rencz, A. Zhang
Mineral Resources Division
Geological Survey of Canada (Ottawa)
601 Booth Street
Ottawa, Ontario K1A 0E8

L. H. Thorleifson
Terrain Sciences Division
Geological Survey of Canada (Ottawa)
601 Booth Street
Ottawa, Ontario K1A 0E8

K.L. Currie, R. Dumont, B.A. Kjarsgaard, T.D. Peterson
Continental Geoscience Division
Geological Survey of Canada (Ottawa)
601 Booth Street
Ottawa, Ontario K1A 0E8

N.J. Bégin, R.E. Beiersdorfer, E.D. Ghent
University of Calgary
2500 University Dr. N.W.
Calgary, Alberta T2N 1N4

D. Craw
University of Otago
P.O. Box 56
Dunedin, New Zealand

Original manuscript submitted: 96.12.01
Final version approved for publication: 97.05.13

Contents

INTRODUCTION[1]

R.W. Macqueen
Geological Survey of Canada, Calgary

Abstract

In 1995, Alberta produced about 48.0% ($20.8 billion) of total Canadian mineral production - almost entirely oil, natural gas and coal. What of the non-fuel mineral potential? Canada-Alberta Agreement on Mineral Development (MDA) studies provide or enhance the geological framework, technology development, and economic aspects necessary to encourage exploration for base/precious metals, diamonds, industrial minerals and other non-fuel mineral commodities. Because they underlie an efficient and dynamic exploration community, geoscience studies expended about 65% of federal/provincial MDA funds available. This volume reports on federal MDA-supported Geoscience conducted mainly by Geological Survey of Canada (GSC) personnel. Regional studies of the exposed Canadian Shield of northeastern Alberta (~58% of MDA geoscience funding) include bedrock/Quaternary geological mapping at 1:50 000 scale, gamma ray spectrometry-magnetics-VLF geophysics, and geochemistry of lake sediments/waters. Many new data from these studies are available digitally. The potential of Athabasca Basin in Alberta for uranium-polymetallic mineralization is evaluated. A digitally based integration project contributes to assessment of the undiscovered mineral potential of northeastern Alberta. Diamond-related studies (~30% of MDA geoscience funds) include examination of minettes/kimberlites, regional indicator mineral/geochemical till/soil studies in southern Alberta, and a Cypress Hills aeromagnetic survey. Other studies reported on herein involve gold, including Fort McKay area microdisseminated Au-Ag-Cu minerals; gold/platinum group elements in Tertiary/Holocene gravels of central Alberta; and gold occurrences in lithified Cretaceous and Tertiary gravels/conglomerates of southwestern Alberta. Good potential exists for many commodities.

Résumé

En 1995, l'Alberta a été l'origine d'environ 48,0 % (20,8 milliards de dollars) de la production minérale totale au Canada, laquelle consistait presque entièrement en pétrole, en gaz naturel et en charbon. Qu'en est-il du potentiel en minéraux non combustibles? Les études réalisées dans le cadre de l'Entente Canada-Alberta sur l'exploitation minérale (EEM) ont permis d'établir ou d'améliorer les descriptions des contextes géologiques, le développement de technologies et la détermination des aspects économiques nécessaires pour encourager l'exploration des métaux communs et précieux, des diamants, des minéraux industriels et d'autres substances non-combustibles. Soixante-cinq pour cent (65%) des fonds fédéraux-provinciaux prévus pour l'EEM ont été injectés pour réaliser des études géoscientifiques, menées par une communauté scientifique efficace et dynamique se consacrant à l'exploration minière. Le présent volume contient un compte rendu des travaux géoscientifiques menés dans le cadre de l'EEM par le personnel de la Commission géologique du Canada (CGC). Les études régionales sur la partie affleurante du Bouclier canadien dans le nord-est d'Alberta (env. 58 % des fonds de l'EEM consacrés aux travaux géoscientifiques) ont notamment consisté à cartographier la géologie du substratum rocheux et des depôts quaternaires à une échelle de 1:50 000 et à réaliser des levés tant géophysiques (rayons gamma, magnétisme et VLF) que géochimiques (sédiments et eaux lacustres). De nombreuses nouvelles données recueillies dans le cadre de ces études sont disponibles sous forme numérique. On a entrepris l'évaluation du potentiel en minéralisation polymétallique riche en uranium du bassin d'Athabasca en Alberta. Un projet d'intégration des données numériques pour évaluer le potentiel minéral non-découvert du nord-est de l'Alberta a été mis sur pied. Parmi les études liées aux gites de diamants (env. 30 % des fonds de l'EEM consacrés aux travaux géoscientifiques), on compte un examen des minettes et des kimberlites, un échantillonnage régional des minéraux indicateurs ainsi que des tills et des sols (géochimie) dans le sud de l'Alberta et un levé aéromagnétique dans la région des collines Cypress. Les autres travaux portent, entre autres, sur les minéralisations Au-Ag-Cu de la région de Fort McKay, sur les teneurs en or et en elements du groupe du platine dans les graviers tertiaires et holocènes du centre de l'Alberta et sur les minéralisations en aurifères dans les graviers et conglomérats tertiaire et holocène du sud-ouest de l'Alberta. On a analysé les volcanites de Crowsnest (Crétacé) pour établir leur potentiel minéral. Il ressort de ces travaux qu'il existe un bon potentiel pour découvrir des concentrations de nombreuses substances.

[1]Canada-Alberta Agreement on Mineral Development, Project C1.61

INTRODUCTION

Ore deposits are rocks of unusual composition that can be mined at a profit, and result from the concentrated application of geological processes. Canada is a favoured nation in terms of geological processes responsible for ore deposits. For 1994-95, preliminary estimates indicate that Canada was the world's leading producer of zinc, uranium, potash, and possibly nickel (approximately equal in nickel production to that of Russia); second in asbestos (chrysotile) production (after the former Soviet Union); third in copper production (after Chile and U.S.A); fourth in gold production (after South Africa, U.S.A., and Australia); and one of the top six silver producers as well as a leading producer of salt, structural materials and other prized mineral commodities (Pilsworth and Kokkinos, 1996). Canada is also the world's largest exporter of minerals. Non-fuel mineral exports totalled approximately 16.3% of Canada's total domestic exports in 1995 (Godin, 1996, p. iii). Canada's proficiency in mineral exploration and services demonstrates that the country also is a leader in the export of technical expertise.

This is an enviable record, as is the fact that in terms of attracting non-petroleum mineral exploration investment capital between 1970 and 1995, Canada was first in the world for 14 years, second for eight years, and third for four years (Cranstone, 1996). Canadian reserves of some metals have, however, declined dramatically over the past two decades (e.g., base metals, which declined by one third to two thirds between 1980 and 1995, depending on the particular metal; Lemieux, 1996).

Many factors are involved in declines of reserves or production fluctuations in Canada and elsewhere, including low or variable commodity prices, saturated markets for certain mineral commodities, substitution of ceramics and plastics for certain metals, increasing levels of taxation or regulation, increasing competition in mineral production from less-developed countries, and other issues (see Keevil, 1988; Pilsworth and Kokkinos, 1996). Overlying all of these factors is perhaps the greatest challenge facing the Canadian mineral industry of the 1990s and beyond - an impending shift in the source of mineral supplies away from the traditional producers towards developing and newly industrialized countries, particularly those of Central and South America and Asia.

It is against this background that a series of Mineral Development Agreements (MDAs) were established between the Government of Canada and all provinces and territories with the exception of Prince Edward Island (see, e.g., Richardson, 1995; and others).

Alberta is a relative late-comer to the MDA process, partly because it has been so successful in the mineral fuels area. For example, in 1995 Alberta produced an estimated 48% ($20.8 billion) of the $43.4 billion of mineral wealth produced in Canada, including minerals and mineral fuels (Pilsworth and Kokkinos, 1996). More than 97% of Alberta's mineral production is, however, in the area of mineral fuels - oil, natural gas, natural gas liquids, and coal. For comparison, other provinces' total mineral production (minerals and mineral fuels) in 1995 were $5.8 billion for Ontario (13.4% of the Canadian total of $43.4 billion), $4.6 billion for Saskatchewan (10.7%), $4.5 billion for British Columbia (10.4%), $3.1 billion for Quebec (7.1%), $1.05 billion for Manitoba (2.4%), and $3.6 billion (7.9%) for the remaining six jurisdictions, four provinces and two territories (Pilsworth and Kokkinos, 1996, p. 1.6).

Given the degree of prominence of Alberta in mineral fuel wealth, perhaps it is not surprising that the province is not normally considered as a potential repository of non-fuel mineral resources. The preponderance of sedimentary rocks of the Western Canada Sedimentary Basin, deformed in the Eastern Cordillera of the Rocky Mountains and Foothills and relatively flat-lying in the Interior Platform of Alberta, also has discouraged those who believe that Precambrian and/or igneous and metamorphic rocks are the favoured hosts for metallic mineralization. Until the 1980s Alberta was under-explored (e.g., Alberta Chamber of Resources, 1987; Macqueen and Olson, 1988). Alberta's metallic and industrial mineral potential has not been adequately defined, and publicly available information on these mineral resources has been limited. Experience elsewhere verifies that without such information, little incentive exists for the mineral industry to increase its exploration effort.

Accordingly, one of the prime purposes of the Mineral Development Agreement, known as the Canada–Alberta Agreement on Mineral Development (1992-1995), was to conduct studies that will encourage non-fuel mineral exploration. What is the potential of Alberta for commodities such as base and precious metals, diamonds, structural materials and other non-fuel minerals? How can knowledge of the geological framework, which underlies successful exploration for such commodities, be improved? What is the scope for research in minerals-related technology development and economic development that could act as a stimulus to mineral exploration and production? These and other questions are central to the goals of the Canada-Alberta MDA. All Alberta MDA projects are summarized in "Canada-Alberta Partnership on Minerals" (1996). Appendix 1 lists all Alberta MDA projects.

GEOLOGY OF ALBERTA

Alberta contains portions of the three, main geological provinces of Western Canada: the Canadian Shield in the northeast, the Western Canada Sedimentary Basin (WCSB) over much of the province, and the Rocky Mountains and Foothills in the southwest (Fig. 1).

Canadian Shield and its subsurface extension in Alberta

The Canadian Shield of northeast Alberta consists of strongly deformed metamorphic and intrusive rocks of Archean and Proterozoic age, overlain by only slightly deformed Proterozoic sedimentary rocks of the Athabasca Basin, which contains the rich uranium deposits of northern Saskatchewan. Important earlier studies of the Precambrian rocks of Alberta include those of Godfrey (1986), Burwash et al. (1994) and others (see complete listing of mineral-related references to 1994 in Olson et al., 1994). Geological and geochronological, geochemical and geophysical studies of exposed Precambrian Shield rocks of North America over the past decade indicate that the Shield is made up of a tectonic collage of Archean crustal blocks separated by Proterozoic rocks of orogenic origin interpreted as zones of collision (Hoffman, 1989).

Deformed Archean and Proterozoic rocks form the basement beneath sediments of the WCSB. Over the past decade a new tectonic framework of basement domains has been established for the Precambrian crystalline rocks of Alberta, including the Precambrian crust underlying the WCSB. This new basement tectonic framework owes its origin to the synthesis of geological, geochronological and isotopic analyses of Precambrian basement drillcore intersected in petroleum exploration boreholes, combined with regional geophysical studies. Although there are nearly 200 000 drillholes in the WCSB, fewer than 4000 of these penetrated the basement.

The newly recognized Precambrian basement domains of Alberta are shown in Figure 2 (Ross et al., 1991; detailed documentation by Villeneuve et al., 1993). Major basement domains of Alberta include the Archean-aged Slave, Hearne and Rae provinces, further subdivided into a number of distinctive crustal blocks; Proterozoic-aged accreted terranes and magnetic lows; Proterozoic-aged magmatic arcs; and one domain of uncertain origin, the Lacombe domain (Fig. 2).

A better understanding of the basement beneath the sedimetary cover in Alberta and elsewhere in the

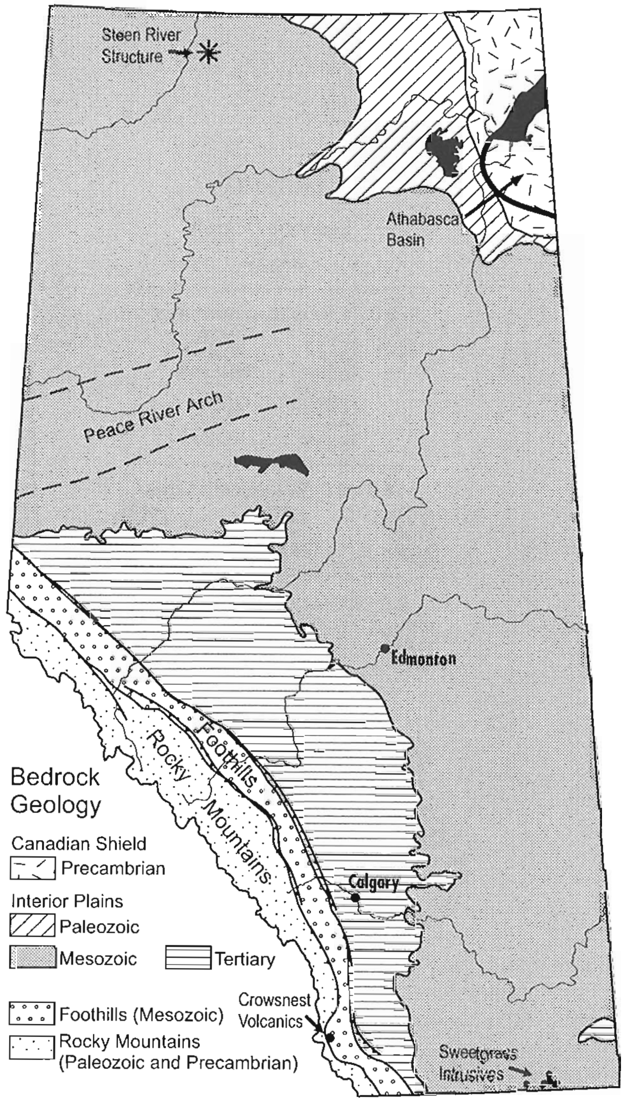

Figure 1. *Bedrock geology of Alberta. Modifed from Alberta Chamber of Resources (1987, Fig. 2) and Dufresne et al. (1996, Fig. 2).*

WCSB is important because of the possible role of basement structures in the evolution of the overlying sedimentary cover as well as its contained mineral resources. Indeed these Precambrian basement rocks, including their comparison with exposed shield rocks and their possible interactions with the overlying Phanerozoic rocks and underlying mantle rocks, are the subject of the Alberta Basement Transect LITHOPROBE project (see for example, Ross et al., 1994; and Clowes, 1996). Interactions between basement and cover rocks may be important in influencing structure and in governing fluid origin and migration, both important aspects of mineral and petroleum exploration. For specific commodities such as diamonds, the presence of Archean rocks at depth beneath Phanerozic cover rocks is judged to be important to the successful location of diamondiferous

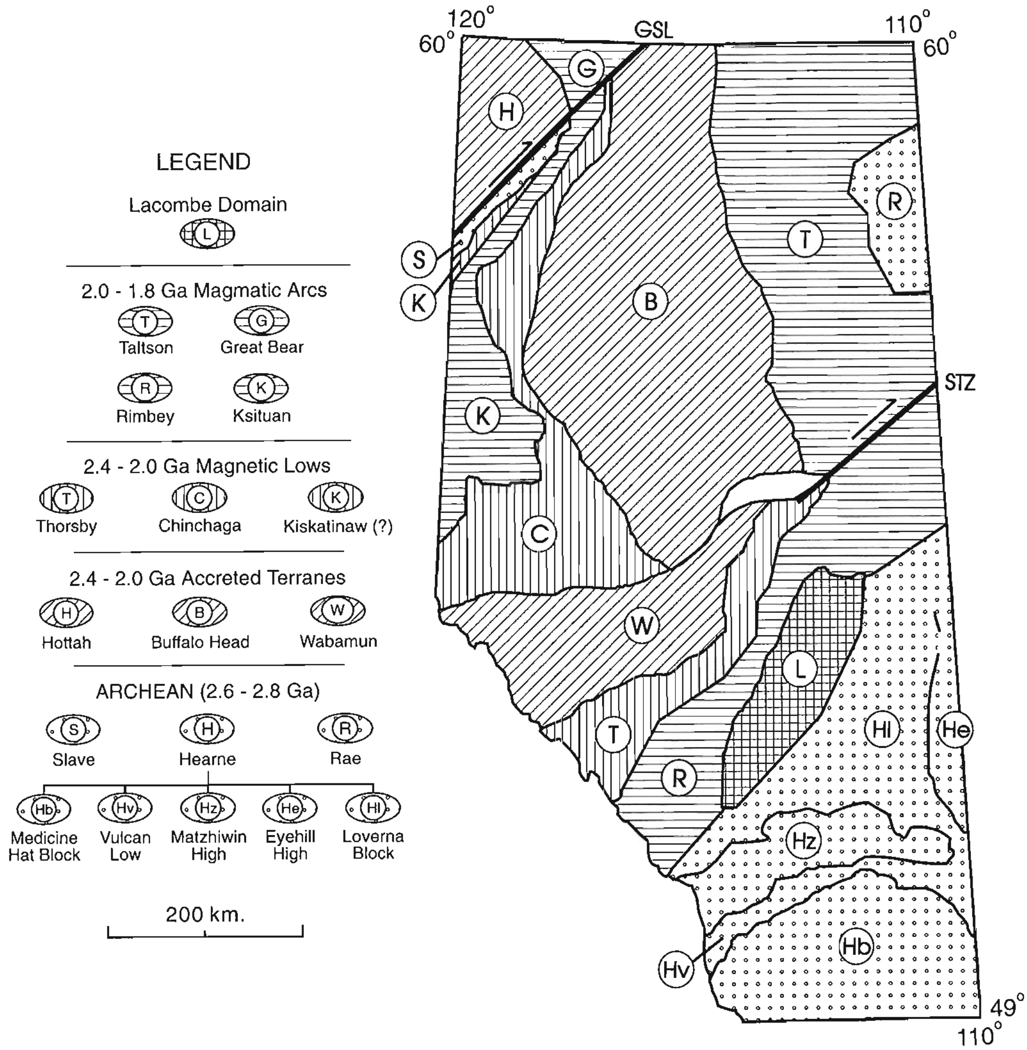

Figure 2. Exposed and subsurface basement terranes in Alberta based on geophysical properties and U-Pb zircon and monazite ages from Villeneuve et al. (1993). Arrows show relative sense of displacement along Great Slave Lake shear zone (GSL) and Snowbird Tectonic Zone (STZ). From Ross et al. (1991).

kimberlites and lamproites (e.g., Fipke et al., 1995). LITHOPROBE studies of the Alberta Basement Transect project supported the acquisition of nearly 2000 km of multichannel seismic reflection profiles, which are providing essential new perspectives on Precambrian continental assembly in western Canada as well as a regional perspective on the evolution of the overlying WCSB (e.g., Eaton et al., 1995; Ross et al., 1995).

Western Canada Sedimentary Basin

The undeformed portion of the WCSB consists of a northeasterly tapering wedge of Phanerozoic sedimentary rocks present from northeastern British Columbia eastward to Manitoba, and reaching a maximum thickness of more than 6 km in southwestern Alberta (Wright et al., 1994). These rocks represent two main successions. The underlying continental terrace wedge (Porter et al., 1982) is of Cambrian to mid-Jurassic age, and consists mostly of platformal carbonate, shale and evaporitic sediments, with clastics mainly derived from shield sources. The overlying foreland basin, of Late Jurassic to Early Tertiary age, is made up of westerly sourced clastics representing Cordilleran orogenesis. The foreland basin developed as a result of collisions between North America and two distinct tectonic collages that were accreted to the western margin of North America (Price, 1994). Both successions of the WCSB have been variably affected during or following deposition by a number of cratonic arches, including the Sweetgrass, Peace River and Western Alberta arches (Porter et al., 1982; Wright et al., 1994).

As noted above, the Alberta portion of the WCSB is host to Canada's major petroleum reserves to date. Important recent general sources of information on the WCSB include Mossop and Shetsen (1994), Ricketts (1989), and Stott and Aitken (1993). For the Foreland Basin specifically, a recent general reference is Macqueen and Leckie (1992).

Cordilleran Orogen in Alberta

WCSB rocks extend into the Canadian Cordillera, forming the foreland fold and thrust belt of westernmost Alberta (Fig. 1). This belt overlaps and deforms sediments of the foreland basin, and generally exhibits thin-skinned structural style. In the Alberta portion of the belt, thrust faulting with associated folding was the predominant mechanism of deformation. Dating from Late Jurassic to Paleocene time, the foreland basin clastic wedges that were shed into the WCSB in Alberta can be linked only generally to identified tectonic episodes of the Canadian Cordillera (e.g., Stockmal et al., 1992; Price, 1994). Because of the spectacular scenery and therefore strong recreational and tourist appeal, and the environmental fragility of the mountainous terrain, major parts of the Foohills and Rocky Mountains are designated as national or provincial parks or as protected areas, off-limits to mineral exploration.

MINERAL EXPLORATION IN ALBERTA

Major mineral deposits are known in jurisdictions adjacent to Alberta (Fig. 3), but there have been no major discoveries of economically promising mineral deposits in Alberta to 1997. This is despite the fact that Alberta has favourable and varied geology, a number of minor metallic mineral occurrences, a large (and growing) geological and geophysical database, a well-developed infrastructure in much of the province, and favourable regulatory and tax regimes (Alberta Chamber of Resources, 1987). These positive factors underlie the initiation of the Canada-Alberta Agreement on Mineral Development (1992-1995).

Regional metallogenic evaluation of Alberta

An important metallogenic evaluation of Alberta began before Canada-Alberta MDA studies were initiated (Olson et al., 1994). This study compiled a large volume of diverse geological and related data, identifying more than 630 mineral occurrences or

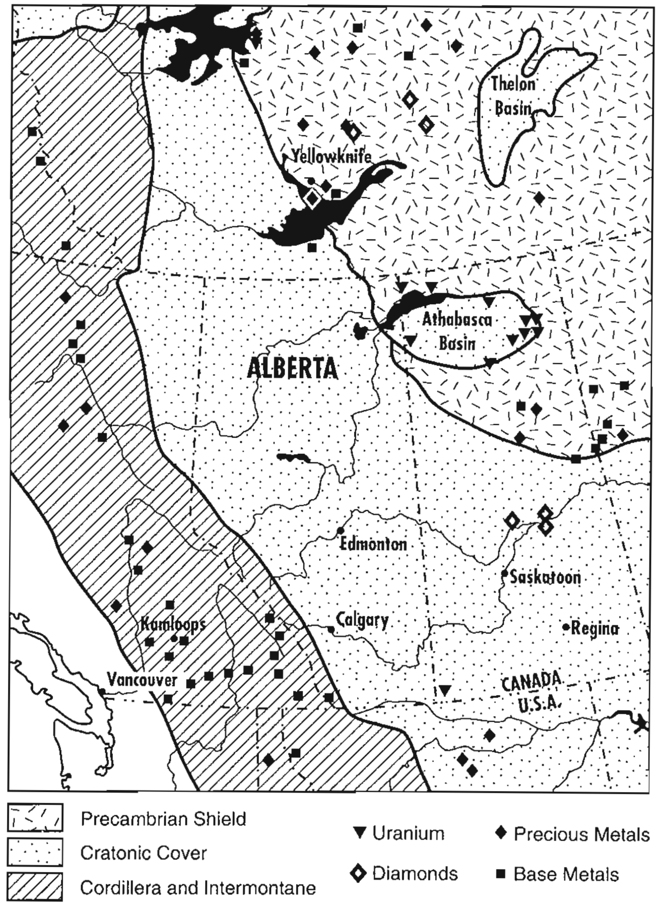

***Figure 3.** Known metallic and diamondiferous mineral deposits of Alberta and proximal regions. From Alberta Chamber of Resources (1987, Fig. 3) and R.A. Olson (pers. comm., 1996).*

geological, geochemical or geophysical anomalies in Alberta. The Olson et al. (1994) study suggested that potential exists in Alberta for a large number of metallic and precious mineral deposits, including bonanza lode and epithermal gold deposits, sediment-hosted base metal deposits including Mississippi Valley-type lead-zinc deposits, and a variety of typically Precambrian Shield deposits such as volcanogenic massive sulphides, granitoid-related precious metals, sandstone-hosted and vein type uranium deposits, diamondiferous diatremes, and various types of placer or paleoplacer precious metal deposits. The Olson et al. (1994) study is an important compilation of all available mineral exploration and assessment data to 1993-94, and thus should be required reading for those exploring for minerals in Alberta. For the WCSB as a whole, Hamilton and Olson (1994) provide maps, tables and a description of existing non-fuel mineral resources.

Recent mineral exploration in Alberta

Data compiled from provincial records (R.A. Olson, pers. comm., 1996) demonstrate the dramatic increase in mineral claim staking in Alberta, from fewer than several hundred thousand hectares and under $100,000 cumulatively to 1991, to 40 million hectares and 2 million dollars cumulatively by 1995. This increase in staking activity is accounted for mainly by a high level of interest in exploration for diamonds and gold, both influenced to some degree by Canada-Alberta MDA studies, and augmented by a change in the expenditures necessary to acquire and hold mineral properties (see Olson et al., 1994, p. 5-7).

OBJECTIVES AND DESCRIPTION OF THE CANADA-ALBERTA AGREEMENT ON MINERAL DEVELOPMENT (MDA)

The Canada-Alberta MDA sought to support both new and established metallic and industrial mineral industries by (a) providing a broader base of geological and resource inventory data; (b) supporting technological research into mining and processing opportunities; and, (c) evaluating market potential for current and new products. The initiative was jointly funded and administered by the two governments. The formal agreement was in effect for three years, 1992-1995, with a fourth year, 1995-96, devoted mainly to completion and publication of projects.

Each government was responsible for a different set of MDA projects. A noteworthy aspect of the Canada-Alberta MDA is the fact that a number of the projects were conducted by industry from funding provided by either level of government. A related unique aspect was direct industry participation in some of the management committees that oversaw funding requests and project approvals. This role by industry personnel in the MDA acted to ensure that MDA projects focussed on the needs of industry.

The Canada-Alberta MDA concentrated on three core elements: *geoscience*, the subject of this publication, *technology development*, and *economic development*. Geoscience studies were designed to provide baseline geoscience data. Mineral exploration is a sequential process, from exploration to discovery, delineation and development, and production. Geoscience is important at all stages of the process, but particularly at the exploration stage, where sound and reliable geoscience data have the greatest potential to have an impact on the mineral supply process, including attracting investment to mineral commodities and areas with promising economic potential.

CHOICE OF FEDERALLY FUNDED CANADA-ALBERTA MDA PROJECTS

Initial projects were chosen based on topics and approaches that are particularly suited to mineral exploration in Alberta, and on concepts and methods (e.g., geophysical and geochemical surveys) known to be successful elsewhere, commonly within other MDA programs. With the exception of two projects under the Diamond subprogram, both of which were approved in the final funded year of the program (1995-1996), all GSC projects are reported on herein. All federally supported projects were conducted as part of the Geological Survey of Canada's scientific program. All projects were also subject to review and approval by the Managment Committee of the Canada-Alberta Agreement on Mineral Development. Projects were evaluated and funded based on their potential to increase private sector investment in Alberta's developing and potential mineral industry.

Geoscience studies expended about 69% of the federal-provincial MDA funds available. Projects were conducted in the areas of regional mapping, geochemical and geophysical surveys, and mineral information system development. The objective of the *technology development* component was to enhance the competitive position of Alberta's mineral industry through the development of innovative technologies. This activity expended about 21% of the federal-provincial funds available. Projects were conducted in the areas of metallic minerals, industrial minerals, mineral processing and the environment. The aim of the *economic development* component was to develop and promote the mineral sector in Alberta by identifying the market potential for metallic and industrial minerals. This activity expended about 4% of the available funds, reflecting the fact that the Alberta non-fuels mineral industry is at an early stage of development. The remaining areas of funding included public information and program administration, together totalling about 6% of the funds available from 1992 to 1996.

FEDERALLY FUNDED GEOSCIENCE STUDIES: OVERVIEW

Regional Geological, Geophysical, Geochemical/Mineralogical Surveys

Sound geological mapping and field-related research are a prerequisite for successful mineral exploration. Most of the surveys discussed below have been published elsewhere as indicated. Overviews and interpretations are reported on in this volume.

Regional geological mapping projects carried out under the Northeastern Minerals subprogram include M.R. McDonough's 1:50 000 scale mapping of the Canadian Shield of northeastern Alberta, accompanied by J.M. Bednarski's studies of the surficial geololgy of the same area (Fig. 4). As noted by Hamilton (1989), accurate and up-to-date geological maps are a major stimulus in support of mineral exploration. Such studies are of continuing value to exploration programs for all sorts of commodities from precious and base metals to diamonds, sand and gravel, clays, etc.

Regional geophysical surveys are undertaken to identify magnetic, electrical, geochemical or other anomalies, and to outline geological structure and possible mineralization (see Shives et al., 1995). Canada-Alberta MDA federally supported studies of this kind include: (a) a regional airborne gamma ray spectrometer-magnetic-VLF survey of the Shield of northeastern Alberta (Northeastern Minerals subprogram), completed by B.W. Charbonneau and colleagues, including interpretation and follow-up studies (Charbonneau et al., 1994; and (b) a 1:100 000 scale aeromagnetic survey of the Cypress Hills area of southeastern Alberta, part of the Diamonds subprogram and flown to specifications typical of such surveys on the Canadian Shield, completed by contract under the leadership of P. Stone (Fig. 4) (Stone, 1993a, b).

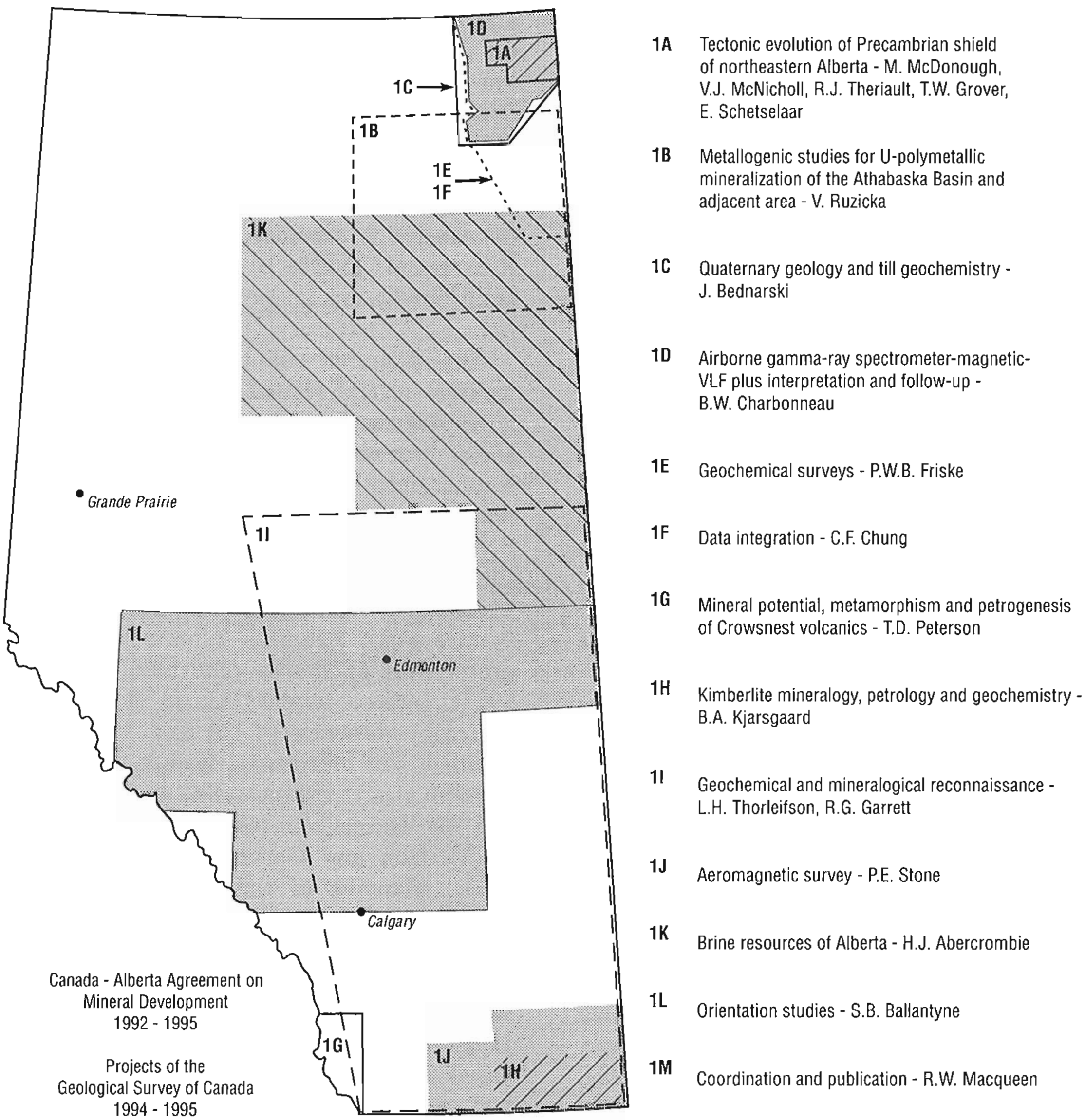

Figure 4. *Study areas of federally supported Canada-Alberta MDA projects 1A to 1M, 1992-1995. Modified from Macqueen (1995, Fig. 1) from data provided by D.G. Richardson (pers. comm., 1995).*

A *regional lake sediment and water geochemical survey* of northeastern Alberta was carried out under contract as part of the Northeastern Minerals subprogram. This survey, to standards of the National Geochemical Reconnaissance Program, was completed under the leadership of P W.B. Friske and colleagues (Friske et al., 1994).

A *geochemical and mineralogical reconaissance survey* was completed in the southern half of Alberta under the auspices of the Diamonds subprogram, and as one part of a series of similar surveys completed on the Canadian prairies (Garrett and Thorleifson, 1993; Thorleifson and Garrett, 1993; Thorleifson et al., 1994).

An important goal for the Northeastern Minerals subprogram was to *integrate geological, geophysical and geochemical data,* together with satellite-derived data (thematic mapper and synthetic aperture radar), to enable the construction of digitally produced mineral potential maps. C.-J. Chung and colleagues carried out this activity.

Commodity-related studies

According to Hamilton and Olson (1994) more than 50 industrial and metallic minerals either have been produced from the WCSB or offer potential for future production. To date the major production has been in the industrial minerals class, in which potash, sulphur, limestone and construction aggregates (mainly sand and gravel), account for the bulk of the production. Certain commodities are attracting particular interest in the Alberta context, however, including diamonds, uranium, and gold and platinum group elements. These commodities are reviewed briefly here to provide an introduction to the papers that follow.

Diamonds

Following the discovery of commercially viable diamond-bearing kimberlites in the Lac de Gras area of the N.W.T. in 1991 (Kjarsgaard, 1996a), and with commercial production of diamonds from this camp expected in 1998 (Boucher, 1996), "diamond fever" spread rapidly to most areas of Canada (e.g., LeCheminant et al., 1996), including Alberta. The high level of interest in diamonds in Canada is strongly related to the "size of the prize" - Fipke et al. (1995) noted that diamonds rank very high in value of world production. Interest in diamonds in Alberta was also strongly stimulated by discoveries in the Fort à la Corne region of the prairies of north-central Saskatchewan, where more than 70 kimberlite bodies, some diamondiferous, were discovered between 1988 and 1995, with initial discoveries resulting from Geological Survey of Canada regional aeromagnetic maps (Kjarsgaard, 1995c, 1996b).

Although the two most important diamond source rocks are peridotite and ecoglite, primary diamonds occur where kimberlite and lamproite magmas errupted, since these deep-seated magmas provide a medium for sampling diamond-bearing source rocks and for transporting diamonds and diamond indicator minerals to the surface (LeCheminant et al., 1996). Only about one in one hundred kimberlite or lamproite pipes are commercially productive of diamonds (Levinson et al., 1992). Diamond formation and preservation seems to be favoured by areas of thick and cool continental lithosphere, which extends into the diamond stability field at depths greater than ~150 km (see Fipke et al., 1995; Kjarsgaard, 1996a). Diamond exploration techniques including the use of indicator minerals are discussed by Fipke et al. (1995); exploration for diamonds in Canada is the subject of LeCheminant et al. (1996); and the diamond potential of Alberta is considered by Dufresne et al. (1996). Kjarsgaard (1995a,b) considers kimberlite- and lamproite-hosted diamond settings.

The Diamond subprogram of the Alberta MDA includes several related studies. Direct studies of the mineralogy and petrology of kimberlites and/or related rocks cropping out in the Sweet Grass Hills of southernmost Alberta and in the Mountain Lake area northeast of Grande Prairie have been conducted by B.A. Kjarsgaard and colleagues (Kjarsgaard, 1996b). Eleven kimberlite bodies have been discovered recently by Ashton Mining in the Buffalo Hills area of northwestern Alberta, in part by drilling isolated geophysical anomalies (Northern Miner, March 10, 1997). Indirect studies, aimed at detecting diamond indicator minerals in till and soil samples of the southern half of Alberta, include the geochemical and mineralogical reconnaissance studies of R.G. Garrett and H. Thorleifson (Garrett and Thorleifson, 1993; Thorleifson and Garrett, 1993; Thorleifson et al., 1994). Mapping of the Archean crust and tectonic domains of the sub-Phanerozoic Precambrian Shield in Alberta (Ross et al., 1991) provides important exploration information, as does detailed aeromagnetic surveying of the Cypress Hills and other areas (Stone, 1993a,b). Interest in Alberta continues to be high, based on known kimberlites in the Buffalo Hills area and the presence of ultrabasic rocks of deep-seated origin at Mountain Lake near Grande Prairie (Kjarsgaard, 1996b; Leckie, Kjarsgaard et al., 1997).

Precious metals: gold and platinum group elements (PGEs)

In recent years, gold has tended to become a commodity rather than a monetary metal (e.g., Green, 1993). As a commodity, its price tends to fluctuate with demand. In terms of dollar value, gold is commonly the leading metal produced in Canada (Couturier, 1996). One camp, Hemlo in Ontario, has three mines that produce close to half of Canada's annual production (Couturier, ibid.). Despite varied forecasts of supply and demand, the rapid growth in demand for jewellry in Asia has led to supply shortages that have been made up by forward selling by central banks (Couturier, ibid.). Thus the long-term future for gold seems to be good. Canada's situation with respect to present and future gold production is reviewed in a global context by Couturier (1996), who also notes that demand for gold is likley to continue to exceed gold production.

As noted above, geological, geochemical and geophysical studies of the Precambrian of northeastern Alberta were designed to provide or improve a framework for exploration for any mineral commodities, not only gold and PGEs. In regional geological mapping, however, emphasis was placed on identifying and mapping shear zones, known to be significant hosts for gold emplacement particularly following the discovery of the rich deposits at Hemlo, Ontario (Harris, 1989; Thompson, 1995). The Hemlo deposits are the outstanding Archean gold discovery of the 1980s (Green, 1993; Thompson, 1995). Although early interpretations of Hemlo favoured a syngenetic origin for these rich deposits, recent research supports ore deposition by hydrothermal fluids in the vicinty of ductile shear zones (Harris, 1989). In the Northeastern Minerals subprogram, geochemical surveys (Friske et al., 1994) and geophysical surveys (Charbonneau et al., 1994) were designed to identify anomalies of any kind, including anomalous values of gold, to encourage private sector exploration. The geochemical reconnaissance studies of Garrett and Thorleifson include gold and silver analyses for the southern prairies, also of interest in precious metal exploration. The mineral potential mapping of Chung and colleagues has the same purpose of detecting anomalies, and is well-suited to exploration for gold occurrences.

Meanwhile, within the Brines subprogram, work by Abercrombie and colleagues identified micro-disseminated gold in Phanerozoic sediments and underlying Precambrian rocks of the Fort McKay region. Following this discovery in 1993, the brines program quickly evolved to the study of micro-disseminated gold, driven by a high degree of interest in the mineral exploration community.

Known gold and PGE occurrences in Alberta consist of placer occurrences in river gravels of Tertiary and Holocene age in the Edmonton area, the subject of studies by Harris and Ballantyne (1994). These Canada-Alberta MDA studies were conducted to learn more about the nature and occurence, distribution, origin and importance of these placer occurences. A related paper on newly discovered paleoplacer gold occurrences in Cretaceous and Tertiary rocks of southwestern Alberta is included in this volume because of the interest in this topic, although this work was conducted independently of the Canada-Alberta MDA program.

One of the purposes of studies undertaken by Peterson and colleagues on the Crowsnest Volcanics of the Southwestern Minerals subprogram was to assess the potential of this unit for gold occurrences.

Uranium

Canada is the world's leading producer of uranium, most of it now being produced from the rich unconformity deposits of the Proterozoic-aged Athabasca Basin of northern Saskatchewan. Ruzicka (1995) showed the richness of the Athabasca Basin deposits, including Cigar Lake, Collins Bay, Key Lake, Midwest and others. Because the Athabasca Basin extends into Alberta (Fig. 1), Canada-Alberta MDA studies by Ruzicka were conducted to assess the possibility of economic deposits in Alberta's portion of the Athabasca Basin. Whillans (1996) recently reviewed uranium developments and prospects, concluding that the globally important deposits of Saskatchewan will form the basis of continued Canadian production well into the 21st century.

OUTLINE OF THIS VOLUME

Northeastern minerals

The first six papers deal with aspects of the Northeastern Minerals subprogram. Although M.R. McDonough's main efforts were directed at producing 1:50 000 scale bedrock geological maps of the Precambrian of northeastern Alberta, his paper outlines several kinds of sulphide mineralization encountered in this work; a full reference list is provided to new geological maps of the area. J.M. Bednarski discusses the surficial materials overlying the

Shield, including their nature, distribution and origin. A regional airborne gamma spectrometer-magnetic-VLF survey and its interpretation is outlined by B.W. Charbonneau and colleagues, and M.W. McCurdy discusses a regional geochemical lake sediment and water survey and its interpretation. C-J. Chung and colleagues have been concerned with integration of the crystalline Precambrian Shield data, with the goal of deriving digitally based mineral potential maps for this area; examples are given in their paper. Polymetallic and mono-metallic uranium occurrences in the Alberta portion of the uranium-rich Athabasca Basin are the subject of V. Ruzicka's paper.

Southwestern minerals

This subprogram was confined to study of the nature and origin of the Cretaceous-aged Crowsnest Volcanics and their mineral potential, topics dealt with in a paper by T.D. Peterson and colleagues.

Diamonds

This topic is treated in three papers. B.A. Kjarsgaard reviews known Alberta occurrences of igneous rocks of deep-seated origin and their possible relationship to diamonds, as well as the nature, origin and complex distribution patterns of associated indicator minerals. H. Thorleifson and R.G. Garrett review and interpret the results of regional kimberlite indicator and geochemical reconnaissance studies of the southern half of Alberta. G.M. Ross and colleagues, using the detailed Alberta MDA aeromagnetic survey data acquired for the Cypress Hills region of southeastern Alberta, note the presence of anomalies that support the concept that Eocene magmatism may have been more widespread in southernmost Alberta than previously known.

Precious metals and orientation studies

A new type of precious metal occurrence, micro-disseminated gold, silver and copper, has been found in the Fort McKay region of northern Alberta, and is outlined and interpreted by H.J. Abercrombie and R. Feng. Placer occurrences of gold, silver and platinum group elements, known to occur in the Edmonton region for more than 100 years, are the subject of a paper by S.B. Ballantyne and D.C. Harris. A related paper on previously unknown paleoplacer occurrences of gold in several Cretaceous units of southeastern Alberta by D.A. Leckie and D. Craw completes the scientific papers of the volume.

The volume ends with a summary and conclusions by R.W. Macqueen.

REFERENCES

Alberta Chamber of Resources
1987: Opportunites for Metallic Mineral Exploration. Alberta Chamber of Resources, Alberta Energy, Alberta Geological Survey, Edmonton, 40 p.

Boucher, M.A
1996: Diamonds. *In* 1995 Canadian Minerals Yearbook. Minerals and Metals Sector, Natural Resources Canada, E. Godin (ed.). Ottawa, p. 26.1-26.14.

Burwash, R.A., McGregor, C.R., and Wilson, J.A.
1994: Precambrian basement beneath the Western Canada Sedimentary Basin. *In* Atlas of Western Canada Sedimentary Basin, G.D. Mossop and I. Shetsen (compilers). Canadian Society of Petrolem Geologists and Alberta Research Council, p. 49-56.

Canada-Alberta Partnership on Minerals
1996: Program Summary. Alberta Geological Survey, Geological Survey of Canada, 104 p.

Charbonneau, B.W., Holman, P.B., and Hetu, R.J.
1994: Airborne geophyscal survey of northeastern Alberta NTS 74L/14,15, 74M/11-3, 6-11, 14,16. Geological Survey of Canada, Open File 2807.

Clowes, R.
1996: LITHOPROBE Phase IV: Multidisciplinary Studies of the Evolution of a Continent - A Progress Report. Geoscience Canada, v. 23, p. 109-123.

Couturier, G.
1996: Gold. *In* 1995 Canadian Minerals Yearbook. Minerals and Metals Sector, Natural Resources Canada, E. Godin (ed.). Ottawa, p. 28.1-28.19.

Cranstone, D.
1996: Canadian Mineral Exploration and Discovery Analysis. *In* 1995 Canadian Minerals Yearbook. Minerals and Metals Sector, Natural Resources Canada, E. Godin (ed.). Ottawa, p. 5.1-5.13.

Dufresne, M.B., Eccles, D.D., McKinstry, B., Schmitt, D.R., Fenton, M.M., Pawlowicz, J.G., and Edwards, W.A.D.
1996: The Diamond Potential of Alberta. Bulletin 63, Alberta Geological Survey, Edmonton, 158 p.

Eaton, D.W., Milkereit, B., Ross, G.M., Kanasewich, E.R., Geis, W., Edwards, D.J., Kelsh, L., and Varsek, J.
1995: Lithoprobe basin-scale seismic profiling in central Alberta: influence of basement on the sedimentary cover. Bulletin of Canadian Petroleum Geology, v. 43, p. 65-77.

Fipke, C.E., Gurney, J.J., and Moore, R.O.
1995: Diamond exploration techniques emphasising indicator mineral geochemistry and Canadian examples. Geological Survey of Canada, Bulletin 423, 86 p.

Friske, P.W.B., McCurdy, M.W., Day, S.J., Gross, H., Balma, R.G., Lynch, J.J., and Durham, C.C.
1994: National Geochemical Reconnaissance lake sediment and water data, northeastern Alberta (Parts of NTS 74E, 74L, and 74M). Geological Survey of Canada, Open File 2856.

Garrett, R.G. and Thorleifson, L.H.
1993: Prairie Kimberlite Study - Soil and till geochemistry and mineralogy, low density orientation survey traverses, Winnipeg-Calgary-Edmonton-Winnipeg, 1991. Geological Survey of Canada, Open File 2685, one diskette.

Godfrey, J.D.
1986: Geology of the Precambrian Shield in northeastern Alberta, NTS 74M and 74L N 1/2. Alberta Research Council Map EM 180, 1: 250 000 scale.

Godin, E. (ed.)
1996: 1995 Canadian Minerals Yearbook. Minerals and Metals Sector, Natural Resources Canada, Ottawa.

Green, T.
1993: The World of Gold. Rosendale Press, London, England, 388 p.

Hamilton, J.M.
1989: Earth Sciences in Canada from a User's Viewpoint. Geoscience Canada, v. 16, p. 213-220.

Hamilton, W.N. and Olson, R.A.
1994: Mineral Resources of the Western Canada Sedimentary Basin. *In* Atlas of Western Canada Sedimentary Basin, G.D. Mossop and I. Shetsen (compilers). Canadian Society of Petrolem Geologists and Alberta Research Council, p. 483-501.

Harris, D.C.
1989: The Mineralogy and Geochemistry of the Hemlo Gold Deposit, Ontario. Geological Survey of Canada, Economic Geology Report 38, 88 p.

Harris, D.C. and Ballantyne, S.B.
1994: Characterization of gold and PGE-bearing placer concentrates from the North Saskatchewan River, Edmonton, Alberta. *In* Current Research 1994-E. Geological Survey of Canada, p. 133-139.

Hoffman, P.F.
1989: Precambrian geology and tectonic history of North America. *In* The Geology of North America - an overview, A.W. Bally and A.R. Palmer. (eds.). Geological Society of America, The Geology of North America, v. A, p. 447-512.

Keevil, N. Jr.
1988: Future Challenges Facing the Canadian Minerals Industry: a Private Sector View. *In* Proceedings of the Eighteenth Centre for Resource Studies Policy Discussion Seminar, 1987, P.R. Richardson and R. Gesing (eds.). Centre for Resource Studies, Queen's University, Kingston, Ontario, p. 3-9.

Kjarsgaard, B.A.
1995a: Kimberlite-hosted diamond. *In* Geology of Canadian Mineral Deposit Types, O.R. Eckstrand, W.D. Sinclair and R.I. Thorpe (eds.). Geological Survey of Canada, Geology of Canada no. 8, p. 560-568.

1995b: Lamproite-hosted diamond. *In* Geology of Canadian Mineral Deposit Types, O.R. Eckstrand, W.D. Sinclair and R.I. Thorpe (eds.). Geological Survey of Canada, Geology of Canada no. 8, p. 568-572.

1995c: Research on kimberlites and applications of diamond exploration techniques in Saskatchewan. *In* Investigations completed by the Saskatchewan Geological Survey and the Geological Survey of Canada under the Geoscience Program of the Canada-Saskatchewan Partnership Agreement on Mineral Development (1990-1995), D.G. Richardson (ed.). Geological Survey of Canada, Open File 3119; Saskatchewan Geological Survey, Open File Report 95-3, p. 213-226.

1996a: Slave Province kimberlites, N.W.T. *In* Searching for Diamonds in Canada, A.N. LeCheminant, D.G. Richardson, R.N.W. DiLabio and K.A. Richardson (eds.). Geological Survey of Canada, Open File 3228, p. 55-60.

1996b: Prairie kimberlites. *In* Searching for Diamonds in Canada, A.N. LeCheminant, D.G. Richardson, R.N.W. DiLabio and K.A. Richardson (eds.). Geological Survey of Canada, Open File 3228, p. 67-72.

LeCheminant, A.N., Richardson, D.G., DiLabio, R.N.W., and Richardson, K.A.
1996: Foreword. *In* Searching for Diamonds in Canada, A.N. LeCheminant, D.G. Richardson, R.N.W. DiLabio and K.A. Richardson (eds.). Geological Survey of Canada Open File 3228, p. 1-3.

Leckie, D.A., Kjarsgaard. B.A. et al.
1997: Geology of a Late Cretaceous possible kimberlite at Mountain Lake, Alberta - chemistry, petrology, indicator minerals, aeromagnetic signature, age, stratigraphic position and setting. Geological Survey of Canada, Open File 3441, 200 p.

Lemieux, A.
1996: Canadian Reserves of Selected Major Metals, Recent Production Decisions, and Deposits Promising for Future Production. *In* 1995 Canadian Minerals Yearbook. Minerals and Metals Sector, Natural Resources Canada, E. Godin (ed.). Ottawa, p. 3.1-3.31.

Levinson, A.A. Gurney, J.J., and Kirkley, M.B.
1992: Diamond sources and production: Past, present and future. Gems and Gemology, Winter, 1992, p. 234-253.

Macqueen, R.W.
1995: Canada/Alberta Partnership on Minerals (Mineral Development Agreement) - projects and progress. *In* Proceedings of the Oil and Gas Forum '95 - Energy from Sediments, J.S. Bell, T. Bird, T.L. Hillier, and P. Greener (eds.). Geological Survey of Canada, Open File 3058, p. 73-77.

Macqueen, R.W. and Leckie, D.A. (eds.)
1992: Foreland Basins and Fold Belts. American Association of Petroleum Geologists, Memoir 55, 460 p.

Macqueen, R.W., and Olson, R.A.
1988: Introduction to Metallic Mineral Potential, Western Interior Platform and Underlying Precambrian. Geoscience Canada, v. 15, p. 83-84.

Mossop, G., and Shetsen, I. (compilers)
1994: Geological Atlas of the Western Canada Sedimentary Basin. Canadian Society of Petroleum Geologists and Alberta Research Council, 510 p.

Olson, R.A., Dufresne, M.B., Eccles, D.R., Richardson, R.J.H., and Freeman, M.E.
1994: Regional Metallogenic Evaluation of Alberta. Alberta Research Council, Open File Report 1994-8,150 p. + appendices.

Pilsworth, D. and Kokkinos, K.
1996: General Review. *In* 1995 Canadian Minerals Yearbook. Minerals and Metals Sector, Natural Resources Canada, E. Godin (ed.). Ottawa p. 1.1-1.17.

Price, R.A.
1994: Cordilleran Tectonics and the Evolution of the Western Canada Sedimentary Basin. *In* Atlas of Western Canada Sedimentary Basin, G.D. Mossop and I. Shetsen (compilers). Canadian Society of Petrolem Geologists and Alberta Research Council, p. 13-24.

Porter, J.W., Price, R.A., and McCrossan, R.G.
1982: The Western Canada Sedimentary Basin. *In* The Evolution of Sedimentary Basins, Proceedings of a Royal Society Discussion Meeting. Philosophical Transactions of the Royal Society of London, series A, v. 305, Royal Society, London. p. 169-192.

Richardson, D.G. (ed.)
1995: Investigations completed by the Saskatchewan Geological Survey and the Geological Survey of Canada under the Geoscience Program of the Canada-Saskatchewan Partnership Agreement on Mineral Development (1990-1995). Geological Survey of Canada, Open File 3119, 302 p.

Ricketts, B.D. (ed.)
1989: Western Canada Sedimentary Basin: a Case History. Canadian Society of Petroleum Geologists, Calgary, 320 p.

Ross, G.M., Broome, J., and Miles, W.
1994: Potential fields and basement structure, Western Canada Sedimentary Basin. *In* Atlas of Western Canada Sedimentary Basin, G.D. Mossop and I. Shetsen (compilers). Canadian Society of Petroleum Geologists and Alberta Research Council, p. 41-47.

Ross, G.M., Milkereit, B., Eaton, D., White, D., Kanasewich, E.R. and Burianyk, M.J.A.
1995: Paleoproterozoic collisional orogen beneath the western Canada sedimentary basin imaged by Lithoprobe crustal seismic reflection data. Geology, v. 23, p. 195-199.

Ross, G.M., Parrrish, R.R., Villeneuve, M.E., and Bowring, S.A.
1991: Geophysics and geochronology of the crystalline basement of the Alberta Basin, western Canada. Canadian Journal of Earth Sciences, v. 28, p. 512-522.

Ruzicka, V.
1995: Unconformity-type uranium deposits. *In* Mineral Deposit Modeling, Geological Association of Canada Special Paper 40, R.V. Kirkham, W.D. Sinclair, R.I. Thorpe and J.M. Duke (eds.). p. 125-149 (dated 1993).

Shives, R.B.K., Ford, K.L., and Charbonneau, B.W.
1995: Applications of Gamma ray spectrometric/magnetic/ VLF-EM Surveys. Geological Survey of Canada, Open File 3061, 82 p.

Stockmal, G.S., Cant, D.J., and Bell, J.S.
1992: Relationship of the stratigraphy of the western Canada foreland basin to Cordilleran tectonics: Insights from geodynamic models. *In* Foreland Basins and Fold Belts, R.W. Macqueen and D.A. Leckie (eds.). American Association of Petroleum Geologists, Memoir 55, p. 107-124.

Stone, P.E.
1993a: High resolution aeromagnetic total field survey of the Cypress Hills area, Alberta. 6 sheets (black and white). Scale 1:100 000. Geological Survey of Canada, Open File Report 2588, Map 1 - 82H/NE (south half); Map 2 - 72E/NW; Map 3 - 72E/NE; Map 4 - 82H/SE; Map 5 - 72E/SW; Map 6 - 72E/SE.

1993b: Coloured maps: aeromagnetic residual and total field colour interval maps with line contours, Cypress Hills area, southern Alberta. Scale 1:100 000. Map C9865G - 82H/NE (south half); Map C9866G - 72E/NW; Map C9867G - 72E/NE; Map C9868G - 82H/SE; Map C9869G - 72E/SW; Map C9870G - 72E/SE.

Stott, D.F. and Aitken, J.D. (eds.)
1993: Sedimentary cover of the craton in Canada. Geological Survey of Canada, Geology of Canada, no. 5, 826 p.

Thompson, J.F.H.
1995: Application of deposit models to exploration. *In* Mineral Deposit Modeling. Geological Association of Canada Special Paper 40, R.V. Kirkham, W.D. Sinclair, R.I. Thorpe, and J.M. Duke (eds.). p. 51-67. (dated 1993).

Thoreifson, L.H. and Garrett, R.G.
1993: Prairie kimberlite study - till matrix geochemistry and preliminary indicator mineral data. Geological Survey of Canada, Open File 2745, one diskette.

Thorleifson, L.H., Garrett, R.G., and Matile, G.
1994: Prairie kimberlite study indicator mineral geochemistry. Geological Survey of Canada, Open File 2875, one diskette.

Villeneuve, M.E., Ross, G.M., Theriault, R.J., Miles, W., Parrish, R.R., and Broome, J.
1993: Tectonic subdivision and U-Pb geochronology of the crystalline basement of the Alberta Basin, western Canada. Geological Survey of Canada, Bulletin 447, 86 p.

Willans, R.T.
1996: Uranium. *In* 1995 Canadian Minerals Yearbook. Mineral and Metals Sector, Natural Resources Canada, E. Godin (ed.). Ottawa, p. 64.1-64.17.

Wright, G.N., McMechan, M.E., and Potter, D.E.G.
1994: Structure and Architecture of the Western Canada Sedimentary Basin. *In* Atlas of Western Canada Sedimentary Basin, G.D. Mossop and I. Shetsen (compilers). Canadian Society of Petrolem Geologists and Alberta Research Council, p. 25-40.

STRUCTURAL CONTROLS AND AGE CONSTRAINTS ON SULPHIDE MINERALIZATION, SOUTHERN TALTSON MAGMATIC ZONE, NORTHEASTERN ALBERTA[1]

M.R. McDonough
Geological Survey of Canada, Calgary

Abstract

Northeastern Alberta is underlain by Precambrian rocks of the Taltson magmatic zone, a composite continental magmatic arc/collisional orogen developed between Rae craton (Archean) and the Buffalo Head terrane (Paleoproterozoic). Rutledge River basin (2.13–2.08 Ga) received pelitic/quartzitic sediments that probably covered the basement of the Taltson magmatic zone, and much of the western Rae Province, prior to Taltson magmatism (1.99–1.90 Ga). The basin was dismembered by the intrusion of Taltson plutons, and by development of a complex northward-trending regime of early granulite facies, mainly sinistral strike-slip shearing and subordinate thrusting (ca. 1.93 Ga), and later greenschist facies brittle-ductile dextral and sinistral shearing (ca. 1.86–1.80 Ga).

The Taltson magmatic zone contains three types of sulphide mineral occurrences. The first type is stratiform pyrite-arsenopyrite-gold mineralization, initially developed within pelitic gneisses of Rutledge River basin, commonly within 100 m of the contact with the underlying basement. The second type occurs in zones in which initial stratiform mineralization was subsequently remobilized within regions of greenschist grade deformation overprinting layer-parallel high-grade fabrics in pelitic gneisses. Gold values to 600 ppb and arsenic values to 3600 ppm were reported from these gneisses. The third type is pyrite-pyrrhotite, copper-gold mineralization found in greenschist grade shear zones associated with sheared amphibolite gneisses, with copper values ranging to 900 ppm. $^{40}Ar/^{39}Ar$ dating of micas indicates a 1.86 to 1.80 Ga age for regional greenschist grade deformation. This is inferred to be the time of recrystallization-reconcentration of mineralization in stratiform and shear zone-hosted occurrences.

Résumé

Dans le nord-est de l'Alberta, on observe des roches précambriennes de la zone magmatique de Taltson, laquelle témoigne d'un arc magmatique continental et d'un orogène de collision formé entre le craton de Rae (Archéen) et le terrane de Buffalo Head (Paléoprotérozoïque). Le bassin de Rutledge River (2,13–2,08 Ga) a reçu des sédiments pélitiques et quartzitiques qui ont probablement recouvert le substratum rocheux de la zone magmatique de Taltson et la presque totalité de la partie ouest de la Province de Rae et ce, avant l'épisode magmatique de Taltson (1,99–1,90 Ga). Le bassin a été démembré par l'intrusion des plutons de Taltson et la mise en place d'un régime complexe de déformation d'orientation nord. Ce dernier a d'abord été marqué par un cisaillement à décrochement principalement senestre et un chevauchement subordonné (vers 1,93 Ga) de roches métamorphisées au faciès des granulites et, par la suite, par un cisaillement cassant à ductile à décrochement dextre et senestre de roches métamorphisées au faciès des schistes verts (vers 1,86–1,80 Ga).

La zone magmatique de Taltson contient trois types d'indices minéralisés en sulfures. Le premier type est une minéralisation stratiforme de pyrite-arsénopyrite-or, initialement mise en place dans des gneiss pélitiques du bassin de Rutledge River et principalement observée à moins de 100 m du contact avec le substratum sous-jacent. Le deuxième type occupe des zones dans lesquelles la minéralisation stratiforme initiale a été ultérieurement remobilisée dans des régions où le

[1]Canada–Alberta Agreement on Mineral Development, Project C1.11

métamorophisme au faciès des schistes verts se surimpose aux fabriques de fort métamorphisme des gneiss pélitiques qui sont parallèles à la stratification. On a relevé dans ces gneiss des concentrations allant jusqu'à 600 ppb d'or et jusqu'à 3 600 ppm d'arsenic. Quant au troisième type, il est représenté par une minéralisation de pyrite-pyrrhotite riche en Cu-Au dans des zones de cisaillement métamorphisées au faciès des schistes verts associées à des gneiss amphibolitiques cisaillés; les concentrations de cuivre y atteignent 900 ppm. Des datations ^{40}Ar-^{39}Ar sur micas indiquent que le métamorphisme régional au faciès des schistes verts remonte à 1,86–1,80 Ga. Cet âge correspondrait à l'époque de recristallisation-reconcentration de la minéralisation dans des indices stratiformes et des indices encaissés dans les zones de cisaillement.

INTRODUCTION

The purpose of this paper is to outline the structural, stratigraphic, and temporal setting, and the metallogenic characteristics, of three types of sulphide mineral occurrences in the Precambrian Shield of northeastern Alberta: 1) stratiform Au occurrences associated with 2.13 to 2.08 Ga supracrustal gneisses of the Rutledge River basin (Bostock and van Breemen, 1994); 2) shear zone-hosted Cu-Au occurrences within 1.86 to 1.80 Ga greenschist grade mylonites (Plint and McDonough, 1995); and 3) pyrite–pyrrhotite Cu-Au occurrences in amphibolite within basement gneisses. New geochronological data support the premise that the host rocks to the mineral occurrences are Paleoproterozoic (2.5–1.6 Ga), and not Archean as once suspected. Therefore, the mineralization in these settings is likely Proterozoic. Other types of mineral occurrences in northeastern Alberta include tourmaline-vein-hosted pyrite–arsenopyrite, shear zone-hosted arsenopyrite, and potential volcanogenic massive sulphide occurrences (Langenberg et al., 1993, 1994) within the 2.008 to 1.971 Ga Waugh Lake basin (McNicoll and McDonough, 1995), and Prairie-type disseminated Au-Ag-Cu occurrences (Abercrombie and Feng, 1994, 1997 [*this volume*]; Feng and Abercrombie, 1994; McDonough and Abercrombie, 1995). These are also now known to be Proterozoic, except for the latter, which is likely Phanerozoic.

This paper provides a synthesis of new geological map data pertinent to the structural and metallogenic evolution of the Taltson magmatic zone, reported by McDonough et al. (1993, 1994a, b, c, d, e, 1995a; also see Godfrey, 1980a, b, 1984, 1986a; Godfrey and Langenberg, 1984a, b). It also incorporates new U-Pb isotopic data reported by McNicoll et al., (1994), Bostock and van Breemen (1994), McNicoll and McDonough (1995), and McDonough et al., (1995b, c), and $^{40}Ar/^{39}Ar$ geochronological data of Plint and McDonough (1995). Isotopic age data are summarized in Table 1. New evidence regarding the textural relationships of the various sulphide species to greenschist grade fabrics is utilized to argue that Au and Cu mineralization in stratiform and shear zone settings is syn- to epigenetic within zones of penetrative greenschist deformation.

GEOLOGICAL SETTING OF MINERAL OCCURRENCES

The Canadian Shield of northeastern Alberta is composed of the Taltson magmatic zone (TMZ), the exposed part of which is a 300 km long, northward trending belt of granitic basement gneiss, amphibolite, supracrustal gneisses, and Paleoproterozoic magmatic rocks, underlying northeastern Alberta and the District of Mackenzie. It is bounded to the north by the Great Slave Lake shear zone and to the south, in the subsurface, by the Snowbird tectonic zone (Hoffman, 1987; Hanmer et al., 1992, 1994; Fig. 1). The TMZ has been interpreted as a composite Andean-type continental magmatic arc and collisional orogen associated with the interaction of the subsurface 2.4 to 2.0 Ga Buffalo Head terrane to the west, and the largely Archean Rae Province to the east (Fig. 1; Hoffman, 1988, 1989; Ross et al., 1991, 1995; Thériault and Ross, 1991; Thériault, 1992; Villenueve et al., 1993; Plint and McDonough, 1995; McDonough et al., 1995c). The TMZ is considered to be the southern equivalent of the Thelon tectonic zone, a collisional and magmatic orogen between the Archean Slave and Rae provinces to the north of Great Slave Lake (e.g., Hoffman, 1987, 1988; Tirrul and Grotzinger, 1990; Henderson and van Breemen, 1991; Fig. 1).

The TMZ comprises voluminous 1.986 to 1.906 Ga magmatic rocks intruding an Archean to dominantly Paleoproterozoic basement and supracrustal gneiss sequence (Bostock et al., 1991; McDonough et al., 1993; Bostock and van Breemen, 1994; McNicoll et al., 1994; McDonough et al., 1995b, c). It is cut by ca.

Table 1

Geochronological data (all ages are reported in Ma) for the southern Taltson magmatic zone.

Unit	Lithology	Location	Age/Date	Mineral	Method	Comment
TBC[1]	granite	Leland Lakes	ca. 3200	zircon	U-Pb	age uncertain
TBC[1]	tonalite	Wylie Lake	3039 ± 14	zircon	U-Pb	crystallization age
TBC[1]	tonalite	Lake Athabasca	2559 ± 8	zircon	U-Pb	crystallization age
TBC[1]	granite	Mercredi Lake	ca. 2440	zircon	U-Pb	crystallization age
TBC[1]	peg granite	Andrew Lake	2430 ± 5	zircon	U-Pb	crystallization age, cuts older gn.
TBC[1]	granodiorite	Mercredi Lake	2287 ± 21	zircon	U-Pb	crystallization age, concordant
TBC[1]	syenogranite	Cornwall Lake	2138 ± 2	zircon	U-Pb	crystallization age, concordant
TBC[1]	syenogranite	Dore Lake	ca. 2300	zircon	U-Pb	age uncertain
TBC[1]	hbd granite	Cornwall Lake	ca. 2300	zircon	U-Pb	age uncertain
			Pre-tectonic Granitoid Units			
CoLP[2]	quartz diorite	Waugh Lake	1971 ± 4	zircon	U-Pb	crystallization age, cuts Waugh Gp
AnLP[2]	granodiorite	Andrew Lake	1962 + 16/-10	zircon	U-Pb	crystallization age, defmd in ALSZ
AnLP[3]	granodiorite	Andrew Lake	1959 ± 3	zircon	U-Pb	crystallization age, defmd in ALSZ
WyLP[2]	granodiorite	Florence Lake	1963 + 6/-4	zircon	U-Pb	crystallization age, defmd in ALSZ
ArLP[2]	syenogranite	Arch Lake	1938 + 1	zircon	U-Pb	cryst. age, defmd in CLSZ/LLSZ
			Post-tectonic Granitoid Units			
SLP[3]	granite	Leland Lakes	1933 ± 3	zircon	U-Pb	crystallization age, cuts LLSZ
ChLG[3]	granite	Charles Lake	1921–1932	monazite	U-Pb	crystallization age, intrudes CLSZ
CHIP[3]	granite	Flett Lake	1925 ± 8-6	zircon	U-Pb	crystallization age, cuts CLSZ
CoLG[3]	musc granite	Andrew Lake	1913–1933	monazite	U-Pb	crystallization age, cuts ALSZ
			Cooling Ages			
AnLP[3]	granodiorite	Andrew Lake	1932	monazite	U-Pb	metamorphic age?
RRBP[3]	pelitic gneiss	Myers Lake	1922–1928	monazite	U-Pb	cooling age (625°C)
AnLP[4]	granodiorite	Andrew Lake	1902 ± 11	hornblende	Ar-Ar	cooling age (525°C)
TBC[4]	amphibolite	Andrew Lake	1899 ± 12	hornblende	Ar-Ar	cooling age (525°C)
ChLG[4]	granite	Charles Lake	1799 ± 11	biotite	Ar-Ar	cooling age (325°C)
ChLG[4]	granite	Charles Lake	1856 ± 12	biotite	Ar-Ar	cooling age (325°C)
RRBP[4]	pelitic gneiss	Charles Lake	1803 ± 11	muscovite	Ar-Ar	cooling age (350°C)
ChLG[4]	granite	Charles Lake	ca. 1680	K-feldspar	Ar-Ar	cooling age (170°C)

Data sources: [1]McNicoll and McDonough, unpublished data, 1994; [2]McNicoll and McDonough (1995); [3]McDonough et al. (1995c); [4]Plint and McDonough (1995). Lithological Units: AnLP, Andrew Lake pluton; CHIP, Chipewyan granite; ChLG, Charles Lake granite; CoLG, Colin Lake muscovite granite; CoLP, Colin Lake pluton; RRBP, Rutledge River Basin pelitic gneiss; SLP, Slave pluton; TBC, Taltson basment complex; WyLP, Wylie Lake pluton. Shear zones: ALSZ, Andrew Lake shear zone; CLSZ, Charles Lake shear zone; LLSZ, Leland Lakes shear zone. Closure temperatures are from Parrish (1990) and Heaman and Parrish (1991).

1.93 Ga, granulite to upper amphibolite grade shear zones that form a sinistral transpression system (McDonough et al., 1995c). North of latitude 60°N, the main shear zone of this system, the Charles Lake shear zone, is thought to mark the eastern boundary of the TMZ (Bostock and van Breemen, 1994). However, south of latitude 60°N, a series of Taltson plutons lies to the east of the shear zone, such that the eastern border of the TMZ in Alberta lies near the Alberta–Saskatchewan border (McDonough et al., 1995c).

Lithologies and U-Pb age constraints

Northern Taltson magmatic zone

Taltson Basement Complex

Basement gneisses of the northern TMZ (between lat. 60°N and Great Slave Lake) comprise the mixed gneisses of Bostock et al. (1991), which include layered gneisses, amphibolite gneiss, and metaplutonic gneisses, lying for the most part to the east of the

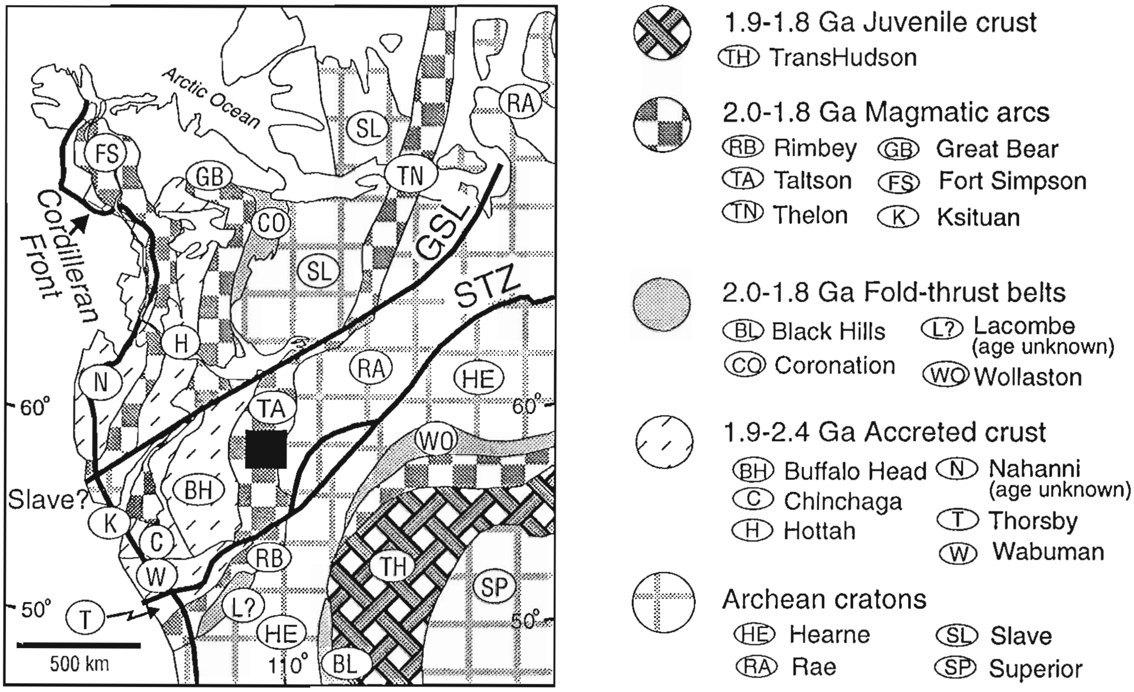

Figure 1. *Generalized lithotectonic map of western Laurentia (exposed units after Hoffman, 1988, and subsurface units after Ross et al., 1991). GSL, Great Slave Lake shear zone; STZ, Snowbird tectonic zone. The black box gives the location of Figure 2.*

Charles Lake shear zone. They considered these gneisses to form part of the Rae Province. Metaplutonic gneisses yielded U-Pb zircon ages ranging from 2.44 to 2.27 Ga. This age range is virtually the same as for Proterozoic basement gneisses of the southern TMZ (see below).

Rutledge River basin

Supracrustal gneisses in the northern Taltson magmatic zone comprise pelitic to quartzose paragneisses that form enclaves—elongate bodies that are enclosed by plutonic and basement gneisses. Quartzitic paragneiss enclaves in the northern TMZ have detrital zircon $^{207}Pb/^{206}Pb$ ages ranging from Archean to 2.13 Ga, and were interpreted to have formed part of a widespread precollisional basin deposited over the basement between 2.13 and 2.08 Ga, named the Rutledge River basin by Bostock and van Breemen (1994). Rutledge River basin gneisses have metamorphic zircon and monazite that record high-grade metamorphism at 2.08 to 2.05 Ga, and hydrothermal zircons that crystallized at 1.92 Ga (Bostock and van Breemen, 1994).

Taltson magmatism

The earliest magmatism in the TMZ comprises I-type magmatic rocks of the 1.986 Ga Deskenetlata gneiss (Bostock et al., 1991; Thériault, 1992). U-Pb zircon ages for the S-type Slave granites are 1.960 and 1.955 Ga (Bostock et al., 1987; Hanmer et al., 1992). These are older than the Slave granite of the southern TMZ. U-Pb monazite ages for S-type Konth syenogranite of the northern TMZ cluster around 1.935 Ga (Bostock et al., 1987, 1991).

Southern Taltson magmatic zone

Taltson Basement Complex

The oldest rocks of the TMZ comprise a package of ductilely deformed layered gneisses, amphibolites, and metaplutonic gneisses of the Taltson basement complex (TBC; McDonough et al., 1993), which underlies about 15 per cent of the southern TMZ, lying on either side of the Charles Lake shear zone. During Taltson magmatism, TBC gneisses formed either the western part of the Rae craton, or part of the Buffalo Head terrane, or both (McDonough et al., 1995b). TBC gneisses and Rutledge supracrustal gneisses were previously thought to be Archean, based on a poorly constrained 2.425 Ga Rb-Sr scatterchron from crosscutting pegmatites in the vicinity of the Charles Lake shear zone (Baadsgaard and Godfrey, 1972). However, new high-precision U-Pb zircon ages for TBC gneisses vary from Archean (three dates are ca. 3.20, 3.04, and 2.56 Ga) to Paleoproterozoic (five dates are 2.44 to 2.14 Ga; McNicoll et al., 1994; McDonough et al., 1995b; see Table 1). Archean material appears to be limited to tectonic slivers within a predominantly Paleoproterozoic basement complex. A second line of evidence that led to the original Archean basement interpretation was based on highly discordant bulk multigrain U-Pb zircon analyses (>200 mg) from the Charles Lake granite (Kuo, 1972; granite F of Godfrey, 1986a) having large amounts of inherited Archean Pb (see below). The new U-Pb isotopic information from TBC gneisses, Rutledge River supracrustal gneisses, and Taltson magmatic rocks, indicate that the basement of the Taltson zone is largely a Proterozoic, not an Archean, basement complex (McDonough et al., 1995b).

Rutledge River basin

Pelitic to quartzose enclaves of supracrustal gneiss in the southern Taltson magmatic zone in Alberta are interpreted to form part of the Rutledge River basin (Fig. 2). Detrital zircon dating is presently underway to confirm this correlation. Pelitic gneisses typically have the lower granulite facies mineral assemblage of K-feldspar–biotite–garnet–sillimanite–cordierite (Nielsen et al., 1981; Grover et al., 1993). Pelitic gneisses give metamorphic monazite ages of about 1.925 Ga, which are interpreted as cooling ages following lower granulite facies metamorphism (see Table 1; McDonough et al., 1995c; see Parrish, 1990). Supracrustal gneisses of the southern Taltson magmatic zone, and their mineral occurrences, were previously inferred to be Archean in age based on poorly constrained U-Pb and Rb-Sr isotopic data (see Baadsgaard and Godfrey, 1972; Kuo, 1972; Nielsen et al., 1981; Langenberg and Nielson, 1982; Godfrey, 1986a; Langenberg et al., 1993, 1994).

Taltson magmatism

U-Pb isotopic ages for southern TMZ magmatic rocks range from 1.97 to 1.92 Ga for surface exposures (Table 1; McNicoll et al., 1994; McDonough et al., 1995c), and 1.97 to 1.93 Ga for subsurface gneisses beneath the Western Canada Sedimentary Basin (Ross et al., 1991; Villenueve et al., 1993).

Magmatic rocks from the exposed southern Taltson magmatic zone were classified by McDonough et al. (1995c) as pre- to syntectonic or late- to post-tectonic with respect to granulite-grade shear zone deformation (see legend in Fig. 2). Pre-tectonic magmatic rocks of possible subduction-affinity? include hornblende-bearing granites and granodiorites of the Colin Lake (1.971 Ga), Wylie Lake (1.963 Ga), and Andrew Lake suites (1.962–1.959 Ga; McNicoll and McDonough, 1995; McDonough et al., 1995c). The Arch Lake pluton comprises K-feldspar megacrystic syenogranite gneiss that is strongly ductilely deformed in the Leland Lakes and Charles Lake shear zones, and is pre-tectonic. Preliminary zircon dating suggests that the Arch Lake is ca. 1.938 Ga (McDonough and McNicoll, unpublished data, 1995). It is magnetite-bearing, yet bears many of the characteristics of S-type crustal melts, such as hercynite and garnet, which suggests that it is collisional in origin. It is lithologically similar to, and spatially continous with, the ca. 1.935 Ga Konth syenogranite of the northern TMZ (U-Pb monazite ages; Bostock et al., 1991).

Post-tectonic units that intruded following high-grade shearing include the Slave granite, which is not ductilely deformed, and clearly intrudes and truncates granulite-grade mylonites in the Leland Lakes shear zone, leaving less than 500 m of the original width of the shear zone intact (McDonough et al., 1995c). These new field relations differ from the interpretation presented by Godfrey (1986a). Shear zone protoliths include the the Arch Lake granite, indicating that the Slave granite must be younger than 1.938 Ga. On the margin of the Slave pluton, a granite dyke that truncates high-grade fabrics in Leland Lakes shear zone has a U-Pb zircon age of 1.933 Ga, which is interpreted as the minimum age of the pluton (McDonough et al., 1995c). The new field relations and zircon dating strongly suggest that the Slave granite in Alberta is distinguished from the 1.955 and 1.960 Ga Slave plutons of the northern Taltson magmatic zone (see Bostock et al., 1991; Hanmer et al., 1992).

Other post-tectonic units include the ca. 1.92 Ga Charles Lake granite (see below), the 1.925 Ga Chipewyan granite, and the ca. 1.92 Ga muscovite-bearing granite of the Colin Lake suite. These were weakly to moderately deformed under amphibolite to greenschist conditions, and lack the extreme ductile fabrics typical of granulite-grade deformation conditions. They are anatectic, collisional granites that

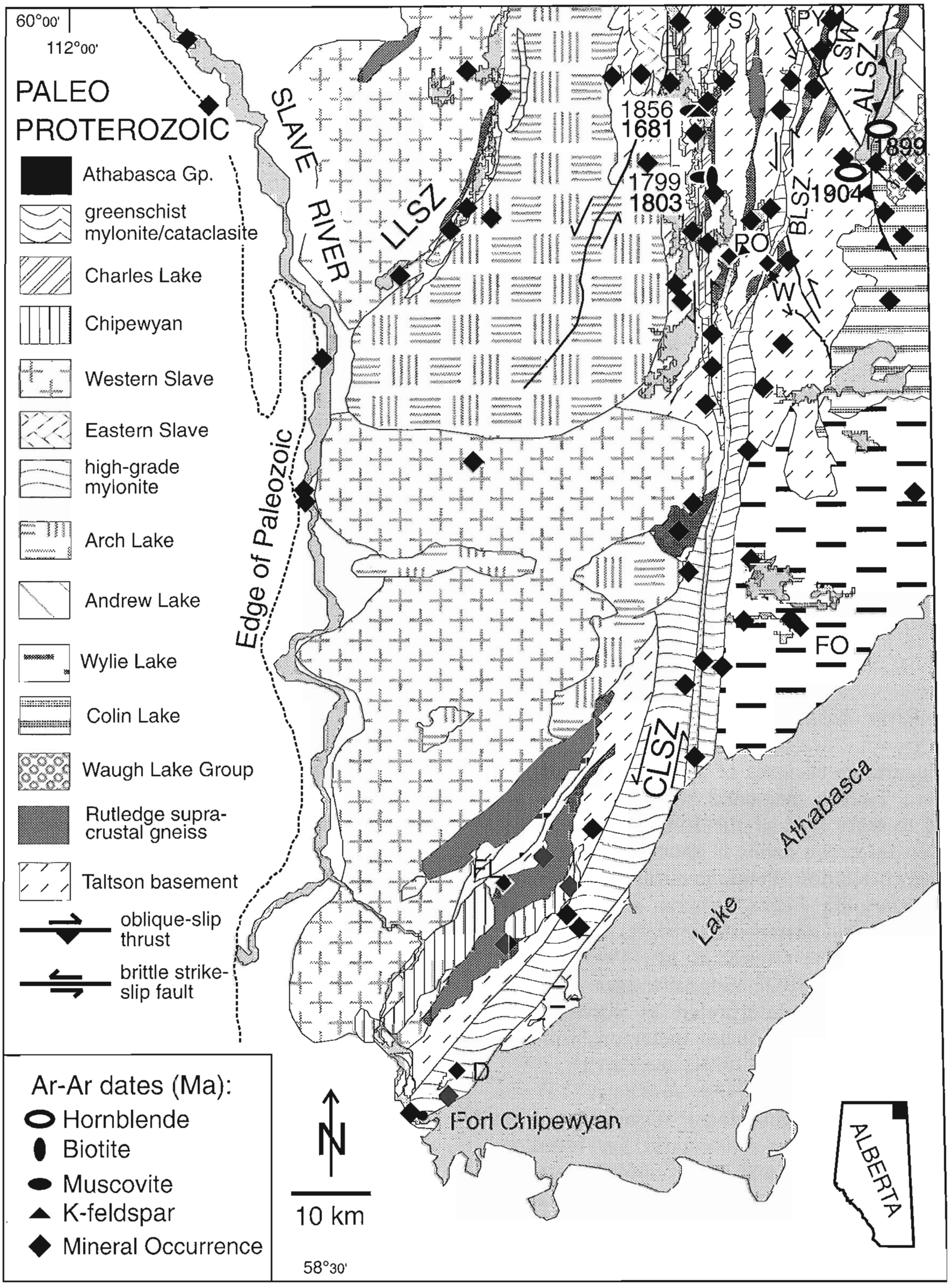

Figure 2. *Generalized geological map of the southern Taltson magmatic zone modified from Godfrey (1986a) and McDonough et al. (1993, 1994a, b, c, d, e, 1995a) showing locations of* $^{40}Ar/^{39}Ar$ *dates (Plint and McDonough, 1995) and mineral occurrences discussed in the text. D, Dore Lake; FL, Flett Lake; FO, Florence Lake; PO, Potts Lake; PY, Pythagoras Lake; W, Whaleback Lake; ALSZ, Andrew Lake shear zone; BLSZ, Bayonet Lake shear zone; CLSZ, Charles Lake shear zone; LLSZ, Leland Lakes shear zone; SW, Swinnerton window. Mineral occurrence data are from Godfrey (1986b) and McDonough (1995). Pre-tectonic units predate, and post-tectonic units postdate high-grade mylonite.*

are post-tectonic with respect to the highest grade of deformation (McDonough et al., 1995c).

The Charles Lake granite intrudes TBC gneisses, Rutledge River supracrustal gneisses, and high grade mylonites of the Charles Lake shear zone. The granite, and therefore the basement, supracrustal gneisses, and deformation, were all inferred to be Archean based on Kuo's (1972) U-Pb data (see Nielsen et al., 1981; Godfrey, 1986a). New zircon analyses from the Charles Lake granite are highly discordant, and yield variable upper intercept ages indicative of Pb inheritance. However, three new concordant single grain monazite U-Pb analyses give ages in the range from 1.932 to 1.919 Ga; the age of the Charles Lake granite is also interpreted in this range (McDonough et al., 1995c).

In total, U-Pb isotopic data for the northern and southern TMZ indicate a pulse of subduction-related? magmatic activity around 1.99 to 1.96 Ga, followed by a pulse of collision-related crustal anatexis and magmatism at 1.94 to 1.92 Ga (cf. Thériault, 1992). Anatectic magmatism is in part coincident with the culmination of granulite grade metamorphism and shear zone activity (McDonough et al., 1995c).

Shear zones

The southern TMZ is dissected by three regional, north-trending, ductile shear zones: the Leland Lakes, Charles Lake, and Andrew Lake shear zones (Fig. 2). The Leland Lakes (Warren fault of Godfrey, 1958) and Charles Lake (Allan fault of Godfrey, 1958) shear zones comprise mainly sinistral, vertical to subvertical, strike-lineated, granulite to upper amphibolite facies mylonites that exhibit extreme ductile deformation of K-feldspar, indicating mylonitization at temperatures greater than 700°C (McDonough et al., 1993, 1995c; cf. White and Mawer, 1992). Amphibolite to greenschist facies mylonites (both sinistral and dextral) occur as discrete narrow zones within the high-grade mylonites (Fig. 2). The Charles Lake shear zone (CLSZ) forms the master strike-slip fault of a crustal scale sinistral transpressional system having dip-lineated mylonites associated with thrusting on either side of the CLSZ (McDonough et al., 1995c). U-Pb constraints indicate that granulite grade sinistral shear in the Charles Lake shear zone was active prior to about 1.932 Ga, and was over by 1.933 Ga in the Leland Lakes shear zone (McDonough et al., 1995c).

The Andrew Lake shear zone (ALSZ), which separates layered basement gneisses to the west from Andrew Lake granodiorite to the east, is a southwest-dipping, high-grade thrust zone with dip-lineated mylonites, forming the eastern thrust of the transpressional system of the Taltson orogen (Fig. 2). It records dextral oblique, top-to-the-northeast displacement, and probably is linked temporally and kinematically to the Charles Lake shear zone. Basement and mineralized Rutledge River supracrustal gneisses of the hanging wall are in upper

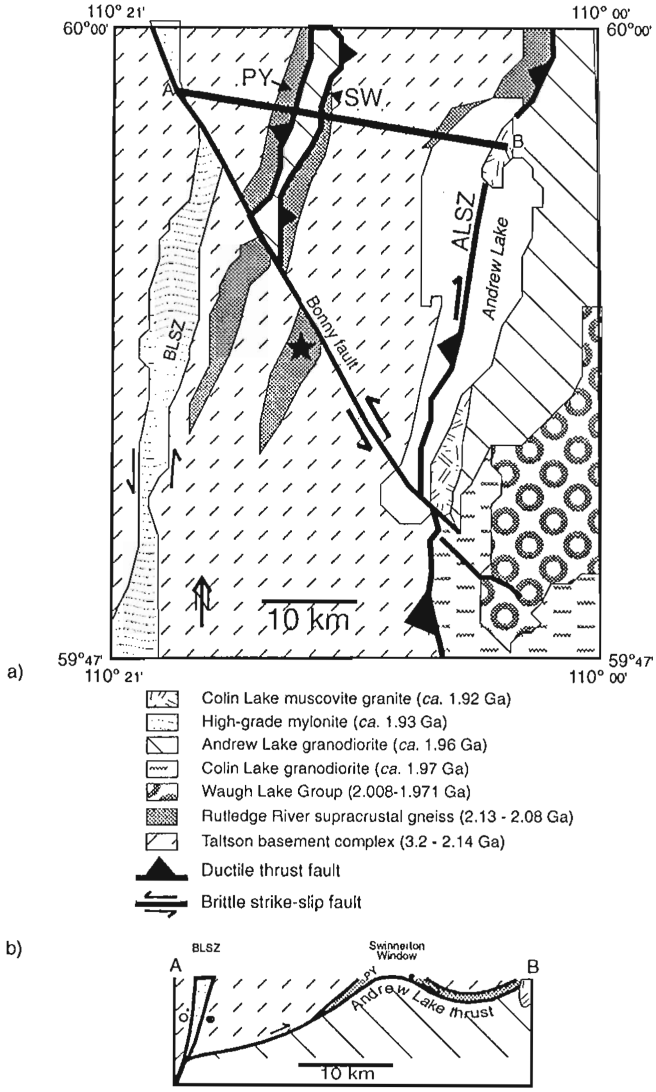

Figure 3. *Gelogical map* ***(a)*** *and schematic cross-section* ***(b)*** *of the Andrew Lake area showing the folded geometry of the Andrew Lake thrust at Swinnerton Window (SW). Rutledge River supracrustal gneisses of the Pythagoras Lake belt (PY) are in the hanging wall of the Andrew Lake thrust. Bayonet Lake shear zone (BLSZ) is a splay of the Charles Lake shear zone. The star gives the location of the Rutledge River supracrustal enclave at Holmes and Split lakes.*

amphibolite to granulite facies, whereas footwall rocks range from amphibolite facies at the thrust, to lower greenschist facies 2 km to the east (e.g., Waugh Lake Group; see Fig. 2). A tectonic window through the hanging wall exposes Andrew Lake granodiorite of the footwall near Swinnerton Lake, the Swinnerton window (Fig. 3). South of Andrew Lake, the character of the ALSZ changes from a narrow shear zone into a broad zone of dip-lineated L-S (linear-planar) fabrics within the Colin Lake granite (Fig. 2). U-Pb zircon data constrain the time of displacement to between 1.959 and 1.921 Ga. U-Pb monazite data suggest thrusting may have occurred around 1.932 Ga (McDonough et al., 1995c).

High-grade mylonites in the Leland Lakes and Charles Lake shear zones are overprinted by narrow zones of greenschist grade mylonites, which host pyrite-pyrrhotite shear zone occurrences.

MINERAL OCCURRENCES

Introduction

Mineral occurrences in the Canadian Shield of northeastern Alberta can be ascribed to the following general settings: 1) stratiform sulphide occurrences associated with Rutledge River basin pelitic gneisses, many of which occur within 100 m of the contact with the adjacent basement; 2) shear zone-hosted pyrrhotite-pyrite mineralization as typified by the Selwyn Lake occurrence; 3) ultramafic pyrite-pyrrhotite occurrences associated with lensoidal amphibolite bodies within TBC gneisses; and 4) arsenopyrite occurrences in tourmaline veins within the Waugh Lake basin (Langenberg et al., 1994). Au fire-assay values for all of these settings range to about 600 ppb (Langenberg et al., 1993, 1994; McDonough, 1995). The first three occurrence types are discussed here.

Stratiform sulphide occurrences, typified by the Pythagoras Lake, Potts Lake, and Whaleback Lake occurrences (Fig. 2), although classified as such due to their proximity to the basement contact, clearly have been influenced by younger deformation. They are related to penetrative greenschist grade deformation and therefore have been strongly influenced by epigenetic processes. A pyrrhotite occurrence at Selwyn Lake was interpreted within the context of a volcanogenic massive sulphide setting by Langenberg et al. (1994). However, based on fabric and textural evidence presented below, I argue that it is a shear zone-hosted occurrence. As such, it is unique in northeastern Alberta, but given the significant distribution of greenschist grade shear zones in the Taltson magmatic zone revealed by recent mapping, good potential exists for further shear zone-related discoveries.

Pythagoras Lake belt

The Pythagoras Lake belt (PY in Figs. 2, 3) forms a narrow, north-trending topographic trough that is underlain by pelitic to semi-pelitic supracrustal gneisses assigned to the Rutledge River basin, and is bounded by topographically high TBC gneisses to the west, and Andrew Lake granodiorite to the east. The Andrew Lake granodiorite occupies the Swinnerton Window in the footwall of the Andrew Lake shear zone (ALSZ), which is a thrust fault (McDonough et al., 1994a). Pelitic supracrustal gneisses at Pythagoras Lake, and westward-adjacent TBC gneisses, comprise the immediate hanging wall of the ALSZ (Fig. 3). The contact between TBC and supracrustal gneisses is a 50 to 100 m wide ultramylonite zone, which is interpreted to represent a sheared unconformity. Numerous gossans and sulphide mineral occurrences in supracrustal gneisses occurr within about 100 m of the basement-supracrustal gneiss contact on a regional basis (Fig. 2). The southern end of the Pythgoras Lake belt is terminated by the Bonny fault, a brittle oblique-slip fault. The preferred restoration of the Bonny fault that provides the best geological match across the fault indicates about 4 km of sinistral displacement, and probably less than 1 km of southwest-side-down dip-slip displacement. This restores the offset of the high-grade mylonites of the Bayonet Lake shear zone, and aligns the Pythagoras belt with the supracrustal gneiss body at Holmes and Split lakes (Fig. 3), where good potential for more stratiform sulphide mineralization exists. This restoration implies that the Andrew Lake granodiorite and the Andrew Lake thrust are in the shallow subsurface at Holmes and Split Lakes to the south of the Bonny fault.

Pelitic supracrustal gneisses of the Pythagoras Lake belt contain granulite to upper amphibolite grade mineral assemblages (Nielsen et al., 1981; Grover et al., 1993) associated with penetrative layer-parallel fabrics that completely obliterate any synsedimentary features normally associated with stratiform deposits (e.g., Morganti, 1981; McClay, 1983). Layer-parallel fabrics are overprinted by steeply dipping amphibolite to greenschist grade crenulation cleavage defined by chlorite and biotite (Fig. 4). Sulphides are concentrated within the crenulation cleavage, and therefore were

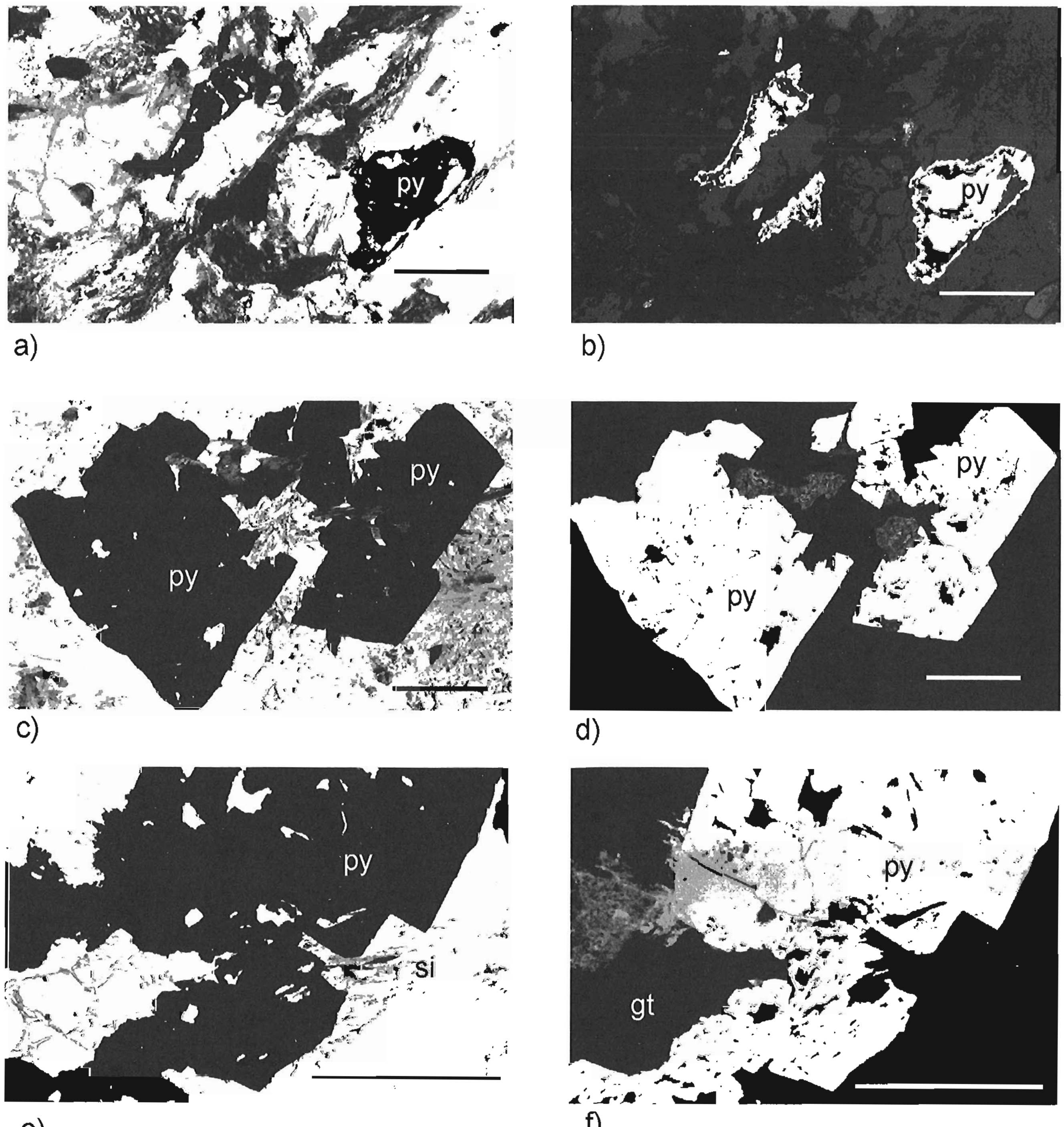

Figure 4. Photomicrographs of sulphides and their relationships to greenschist grade deformation fabrics in pelitic gneiss of the Pythagoras Lake area (sample WL2-08-29-04A; scale bars are 0.5 mm). ***a)*** *Pyrite (py) associated with greenschist grade crenulation cleavage with chlorite and biotite defining the foliation. Plane transmitted light, ISPG 4433-5.* ***b)*** *Reflected plane light image of (a) showing pyrite including matrix material. ISPG 4433-6.* ***c)*** *Plane transmitted light image of large pyrite crystals cutting and partly enclosing unoriented fine grained matrix of chlorite, biotite and muscovite. ISPG 4433-9.* ***d)*** *Plane reflected light image of (c). ISPG 4433-10.* ***e)*** *Large pyrite cyrstal cutting and including biotite-chlorite greenschist grade foliation that deforms an older high grade assemblage of garnet (gt) and sillimanite (si). ISPG 4433-19.* ***f)*** *Reflected plane light image of (e). ISPG 4433-20.*

either introduced or more likely remobilized during medium to low grade deformation. Also shown in Figure 4 are large porphyroblastic pyrite crystals cutting and/or enclosing greenschist grade mineral assemblages, indicating late- to post-deformational epigenetic sulphide crystallization. High Au (up to 603 ppb) and As (up to 3611 ppm) values are found at Pythagoras Lake in association with arsenopyrite occurrences (Langenberg et al., 1993, 1994).

Selwyn Lake pyrrhotite occurrence

The Selwyn Lake pyrrhotite occurrence is located on the west edge of a large splay of the Charles Lake shear zone (S in Fig. 2; McDonough et al., 1994a). It lacks the distinctive veining typical of brittle-ductile shear zone-hosted occurrences (e.g., Roberts, 1987), but clearly is hosted by greenschist mylonites. The key ingredients of this occurrence appear to be the interleaving of pelitic paragneiss and amphibolite gneiss within a narrow greenschist grade mylonite zone. Assay results indicate up to 895 ppm Cu, 65 ppm Ni, 57 ppm Co, and 17 ppb Au (see Langenberg et al., 1994 for the exploration history of this occurrence). A 15 m wide by 400 m long gossan occurs at a contact between sheared TBC gneisses and silicified mylonitic garnet-bearing paragneiss. Adjacent to the gossan, the mylonitic TBC gneisses contain strands of pulled apart amphibolite boudins with 2 to 3 m of strike separation, contained in a matrix of high-grade heteroclastic mylonite with sinistral σ-porphyroclasts. The gossan itself consists of highly silicified greenschist grade mylonite, with pyrrhotite, pyrite, and chalcopyrite forming the principal sulphide species (see Langenberg et al., 1994), occurring in association with the low grade mylonite.

Figures 5a and b illustrate a relatively unstrained pyrrhotite vein parallel to annealed greenschist grade mylonite fabric at the Selwyn Lake occurrence. The vein is interpreted to be syn- to epigenetic relative to the low grade fabric. The vein material encloses relic pull aparts of matrix material having the greenschist facies mineral assemblage of epidote, zoisite, chlorite, and deformed quartz. Pyrrhotite in the matrix has a preferred crystallographic orientation within the foliation, and probably is syngenetic relative to the low-grade foliation (Fig. 5a, b). A case can also be made for syngenetic origin for ductilely deformed pyrrhotite with a long tail oriented parallel to greenschist grade mylonite fabric with deformed chlorite, biotite, epidote, and quartz forming C-S fabric (Fig. 5c, d).

Whaleback Lake occurrences

Two sulphide occurrences near Whaleback Lake (W in Fig. 2) with Au assay values for grab samples ranging to 12 ppb (McDonough, 1995) are of note for their style of mineralization. The first is related to greenschist grade shearing along the margin of an amphibolite body within TBC gneisses. Greenschist grade mylonite fabric envelops a deformed feldspar porphyroclast that is pulled apart in a brittle fashion and infilled with pyrite and pyrrhotite (Fig. 5e, f). Therefore, the mineralization is interpreted to be syngenetic relative to greenschist grade shearing (or perhaps slightly younger).

The second Whaleback occurrence consists of stratiform sulphide mineralization found in a 3 to 5 m wide by 25 m long (minimum) gossan of altered chlorite-rich garnet-bearing pelitic gneiss within a small supracrustal enclave in TBC gneisses. Mineralization in the gossan occurs as veinlets of pyrite, chalcopyrite, and galena contained in irregularly shaped swaths of bright green argillic alteration. The alteration and mineralization are associated with vertical penetrative greenschist grade crenulation cleavage.

Other stratiform and shear zone-hosted occurrences

At Flett Lake (FL in Fig. 2), a large enclave of Rutledge River basin supracrustal gneiss has quartzose biotite garnet pelitic gneiss with numerous small stratiform gossanous zones and pyrite showings. In thin section, pyrite is replacing garnet, and is associated with chlorite alteration, and therefore is interpreted to be epigenetic (Fig. 6a, b). At Dore Lake (D in Fig. 2), a shear zone-hosted occurrence of altered, gossanous, biotite-rich TBC gneiss contains greenschist mylonite fabric in a 0.25 m wide by minimum 5 m long zone that extends downdip. The greenschist mylonite fabric in the gneiss is cut by a large porphyroblastic pyrite crystal, which encloses matrix epidote (Fig. 6c, d). An epigenetic origin is inferred. At Florence Lake (FO in Fig. 2), a 1.5 by 4 m stratiform? gossan occurs within a large xenolith of quartzose biotite-rich semi-pelitic gneiss in Wylie Lake granodiorite. Disseminated pyrite is concentrated along the foliation, which is parallel to the strike of the gossan. In thin section, pyrite is found in elongate forms parallel to strong biotite grade foliation, but in detail, it is void filling with oscillatory intergrowth of pyrite and minor chalcopyrite with magnetite (Fig. 6e, f). Void filling suggests that epigenetic mineralizing fluids invaded a greenschist grade foliation.

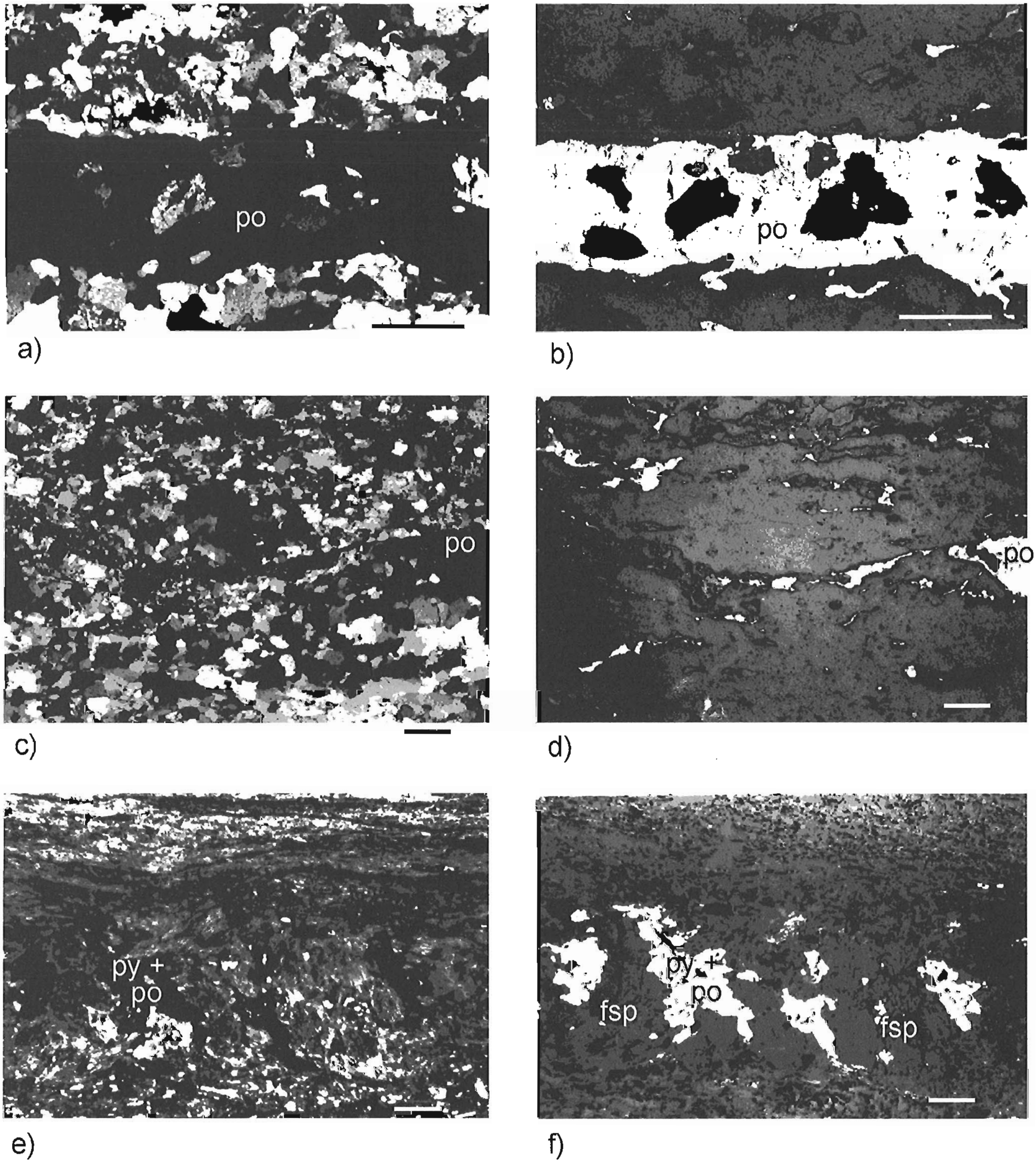

Figure 5. *Photomicrographs of sulphides and their relationships to greenschist grade deformation fabrics in sheared rocks (scale bars are 0.5 mm).* ***a)*** *Cross-polarized transmitted light image of a pyrrhotite (po) vein parallel to annealed greenshcist grade mylonite fabric, enclosing relic pull aparts of epidote, zoisite, and deformed quartz. Selwyn Lake pyrrhotite occurrence, sample MSB93-75A, ISPG 4419-3.* ***b)*** *Plane reflected light image of (a). ISPG 4419-4.* ***c)*** *Pyrrhotite (po) grown in greenschist grade mylonite fabric with deformed epidote and quartz forming C-S fabric. Selwyn Lake pyrrhotite occurrence, sample MSB93-75A, ISPG 4419-5.* ***d)*** *Plane reflected light image of (c). ISPG 4419-6.* ***e)*** *Greenschist grade mylonite in amphibolite protolith with brittle pulled-apart feldspar (fsp) infilled with pyrite (py) and pyrrhotite (po). Whaleback Lake, sample MSB93-45, ISPG 4419-40.* ***f)*** *Plane reflected light image of (e), ISPG 4419-42.*

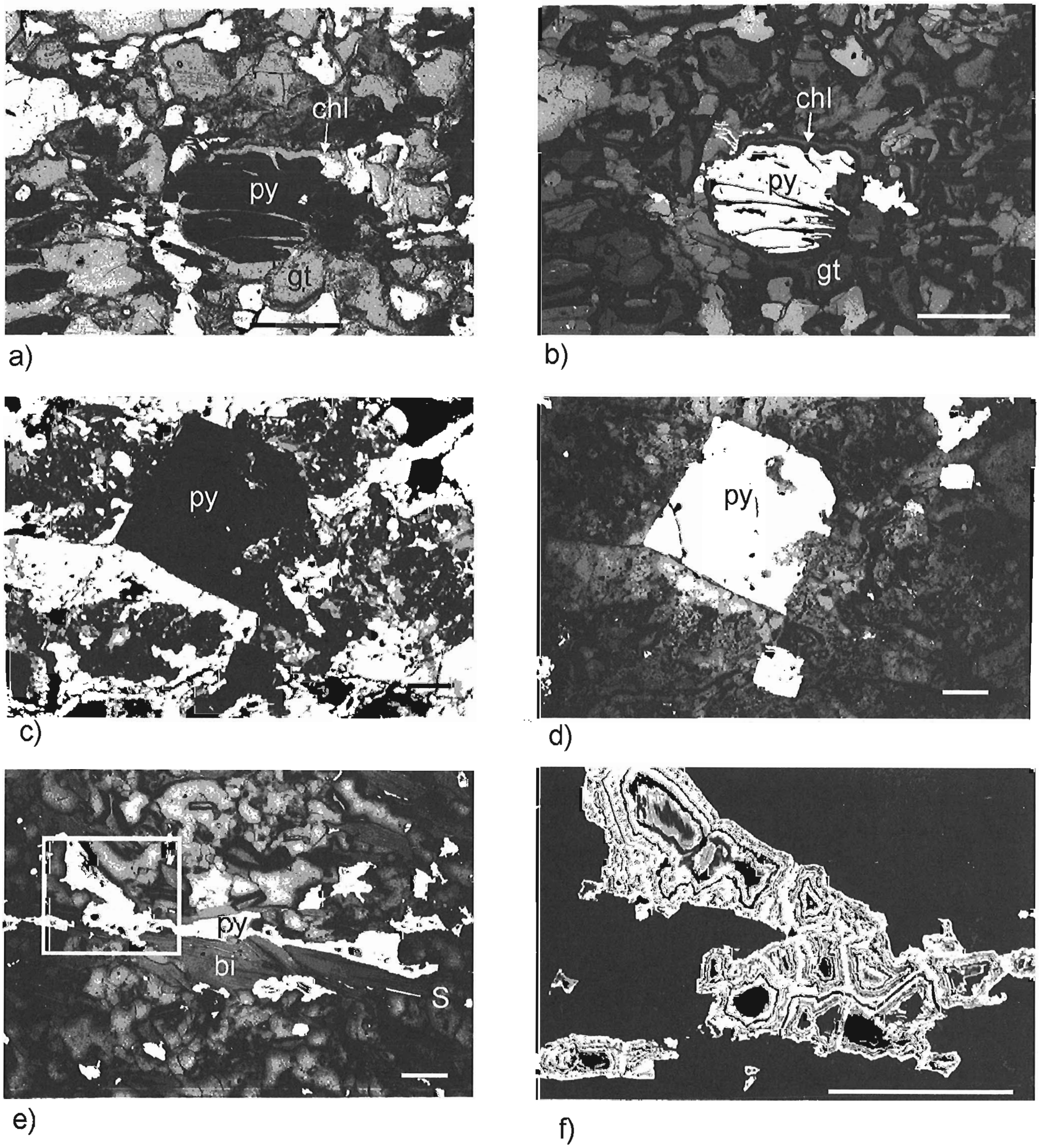

Figure 6. *Photomicrographs of sulphides and their relationships to deformation fabrics in pelitic and basement gneisses (scale bars are 0.5 mm).* ***a)*** *Plane transmitted light image of pyrite (py) replacing garnet (gt) that is rimmed by secondary chlorite (chl) in pelitic gneiss at Flett Lake. Sample MSB94-53, ISPG 4419-19.* ***b)*** *Plane reflected light image of (a). ISPG 4419-20.* ***c)*** *Plane transmitted light image of greenschist mylonite fabric in TBC basement gneiss cut by a large pyrite (py) crystal which encloses epidote. Dore Lake, sample MSB94-89, ISPG 4419-27.* ***d)*** *Plane reflected light image of (c). ISPG 4419-28.* ***e)*** *Plane reflected light image of biotite-rich semi-pelitic gneiss with pyrite (py) growing parallel to strong biotite (bi) grade foliation (S) from Florence Lake. White box outlines detail shown in (f). Sample MSB93-93, ISPG 4419-35.* ***f)*** *Plane reflected light image showing detail of (e) with void filling oscillatory growth of pyrite, oxide and minor chalcopyrite. ISPG 4419-37.*

Mafic-ultramafic-hosted occurrences

Pyrite–pyrrhotite occurrences are found in metre- to kilometre-scale lensoidal ultramafic–mafic bodies that form widely scattered tectonic slivers within TBC gneisses. Amphibolite gneiss from one of these bodies has been U-Pb zircon dated at ca. 2.29 Ga (McDonough et al., 1995b). Pyrite–pyrrhotite mineralization is disseminated in the matrix and also occurs as veins that are parallel to brittle fractures. The veins clearly cut the ca. 1.93 Ga ductile fabrics in the amphibolites and are therefore interpreted as epigenetic. Assay values range up to 18 ppb Au and 301 ppm Cu.

$^{40}Ar/^{39}Ar$ AND K/Ar CONSTRAINTS ON TIMING OF MINERALIZATION

Based on fabric evidence presented above, I contend that much of the sulphide mineralization in Rutledge River basin supracrustal gneisses and shear zones in northeastern Alberta was probably in part syngenetic, and later remobilized by epigenetic processes during or slightly after regional greenschist grade deformation and/or shear zone activity. Therefore, in order to assess the timing of much of the mineralization, the available $^{40}Ar/^{39}Ar$ and K/Ar data that constrain the timing of greenschist grade deformation are reviewed.

New $^{40}Ar/^{39}Ar$ dates for micas and K-feldspar are presented in Figure 7 (data are from Plint and McDonough, 1995). Muscovite (1803 ± 11 Ma) and biotite (1799 ± 11 and 1856 ± 12 Ma) $^{40}Ar/^{39}Ar$ dates agree within error with mean K-Ar dates for the area (muscovite, 1792 ± 40 Ma; and biotite, 1772 ± 40 Ma; Baadsgaard and Godfrey, 1972). An interpreted maximum $^{40}Ar/^{39}Ar$ cooling age for K-feldspar is 1681 ± 11 Ma, with a closure temperature of ca. 170°C calculated from diffusion experiments (Plint and McDonough, 1995). These data combined indicate regional slow cooling of about 2°C/Ma between ca. 1900 and 1700 Ma during amphibolite- to greenschist-grade deformation in the Taltson magmatic zone (Plint and McDonough, 1995), which is consistent with regional cooling ages for much of Alberta (Burwash et al., 1962).

$^{40}Ar/^{39}Ar$ dates for magmatic biotite from well preserved (nonmylonitic) lenses of the Charles Lake granite between greenschist grade splays of the Charles Lake shear zone indicate very slow cooling through 325°C between about 1860 Ma and 1800 Ma, and/or resetting of Ar systematics by fluids related to greenschist grade shearing (Plint and McDonough, 1995). Thus, greenschist grade mylonitization in the Charles Lake shear zone and the accompanying syngenetic to epigenetic mineralization of the Selwyn Lake pyrrhotite occurrence is probably no older than 1860 Ma.

A sample of Rutledge River supracrustal gneiss gave a muscovite $^{40}Ar/^{39}Ar$ plateau age of 1803 Ma, which is interpreted as a cooling age. Pelitic supracrustal gneisses locally contain late, texturally stable muscovite replacing high grade K-feldspar (Plint and McDonough, 1995). Greenschist grade dextral C-S fabrics that deformed muscovite in the Bayonet Lake shear zone, a splay of the Charles Lake shear zone, indicate deformation above 300°C, near or possibly above Ar closure in muscovite. Thus, an upper age limit on ductile greenschist grade shearing of 1.800 Ga can be established (Plint and McDonough, 1995). Therefore, syngenetic sulphide mineralization synchronous with low grade deformation in the Taltson zone probably occurred between 1.860 and 1.800 Ga. Truncation of greenschist grade fabrics by porphyroblastic sulphide growth indicates that at least some of the mineralization may be younger than 1.800 Ga.

DISCUSSION AND CONCLUSIONS

The single most important factor in the localization of sulphide mineralization in northeastern Alberta appears to be penetrative greenschist grade deformation within prospective host lithologies. Silicification and alteration of greenschist grade mylonites suggests that the low grade shear zones probably acted as conduits for mineralizing fluids.

Stratiform sulphide occurrences in enclaves of 2.13 to 2.08 Ga Rutledge River basin supracrustal gneisses are commonly found within 100 m of the contact with the adjacent basement, as exemplified by the Pythagoras Lake, Potts Lake, and Whaleback Lake occurrences. It is difficult to evaluate the significance of a synsedimentary component of mineralization due to the penetrative nature of granulite through greenschist metamorphism and deformation. However, the recurrent theme of "stratiform" occurrences in northeastern Alberta is that they occur close to the basement-supracrustal contact, and that the host rocks have experienced penetrative greenschist grade deformation. In many cases, structural control of mineralization is clearly evidenced by concentration of sulphides along greenschist grade crenulation surfaces. This mineralization is interpreted as syngenetic relative to the low grade deformation. In other cases, porphyroblastic sulphide species truncate and/or envelop greenschist grade mineral assemblages and therefore are interpreted to be epigenetic relative to the low grade fabrics.

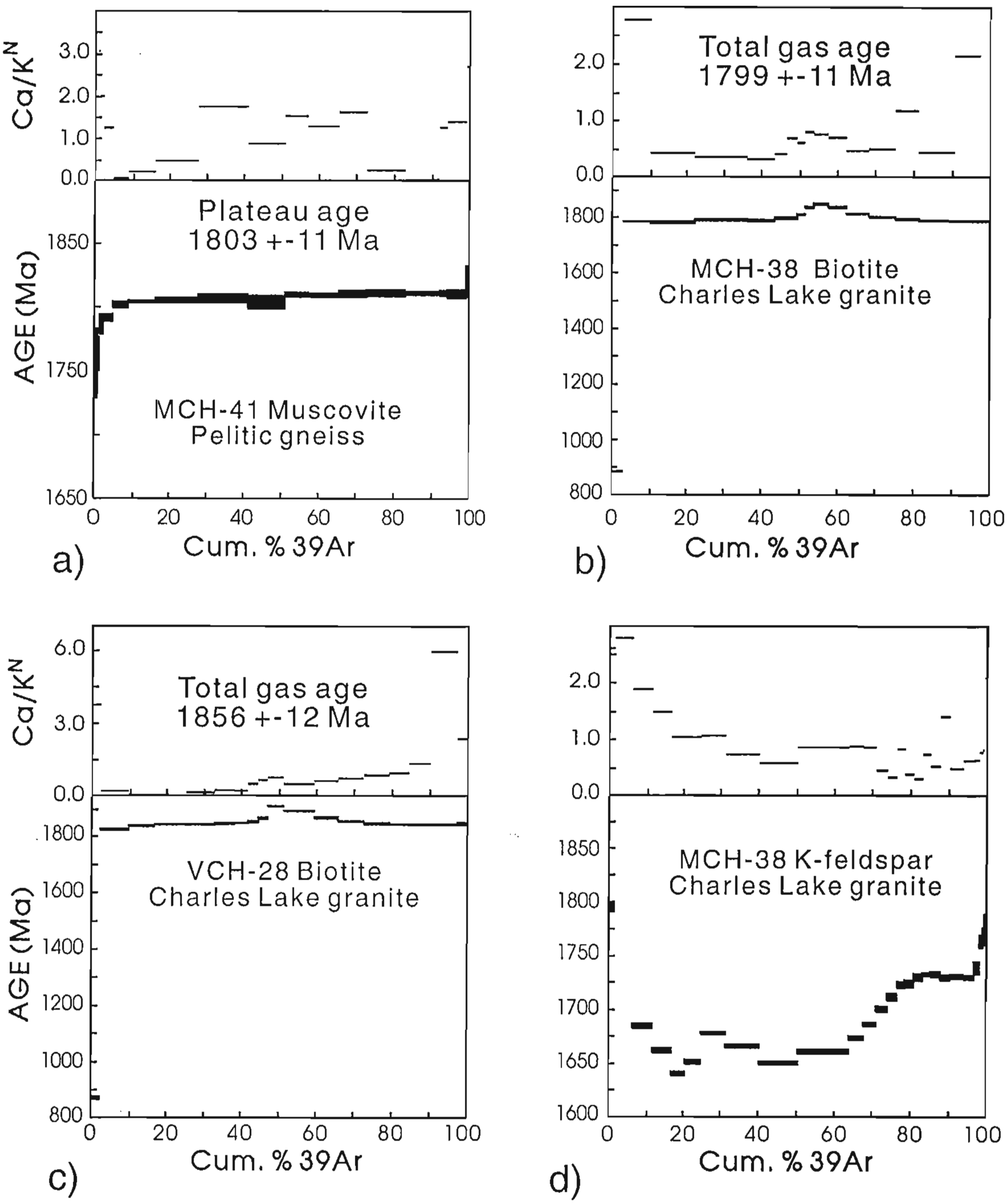

Figure 7. *$^{40}Ar/^{39}Ar$ age spectra and Ca/K ratios from the southern Taltson magmatic zone:* ***a)*** *muscovite from Rutledge River pelitic gneiss;* ***b)*** *and* ***c)*** *magmatic biotite from inclusions in K-feldspar megacrysts in Charles Lake granite; and* ***d)*** *K-feldspar from Charles Lake granite. Ca/K ratios are normalized to the integrated value of the ratio for all heating steps. Total gas ages for biotites exclude the first low-temperature, low-age step. The bar width represents 2σ analytical error (see Plint and McDonough, 1995 for details). All ages are considered as cooling ages with respect to the closure temperature of Ar retention in the mineral species (see Heaman and Parrish, 1991).*

Further structural control of sulphide mineralization by greenschist grade deformation is evident in the case of shear zone-hosted occurrences. At the Selwyn Lake pyrrhotite occurrence, a gossan is associated with greenschist grade mylonite that lies on the margin of high grade mylonites of the Charles Lake shear zone. Pyrite-pyrrhotite mineralization occurs as epigenetic veins that enclose fragments of the greenschist mylonite matrix, or as porphyroblastic sulphide that truncates and therefore postdates the low grade mylonite fabric.

Geological and geochronological data for the southern TMZ indicate a sinistral transpressive system of strike-slip and thrusting at granulite to upper amphibolite grade prior to ca. 1.932 Ga (McNicoll et al., 1994; McDonough et al., 1995c). Deformation continued through to mid-lower amphibolite and greenschist grades between 1.93 and 1.80 Ga (Plint and McDonough, 1995). Deformation affected gneisses that are largely Paleoproterozoic in age, with minor tectonic slices of Archean material. Such prolonged high temperature deformation probably destroyed or redistributed early stratiform sulphide mineralization such that the present distribution of sulphide mineralization is a function of greenschist grade syngenetic to epigenetic processes. Argon geochronometry indicates that deformation under greenschist grade conditions occurred between 1.86 and 1.80 Ga. Since both stratiform and shear zone sulphide mineralization is linked to greenschist grade deformation, it follows then that syngenetic to epigenetic sulphide mineralization probably occurred between 1.86 and 1.80 Ga, or perhaps slightly later.

Acknowledgments

Hewitt Bostock and Roger Macqueen are thanked for insightful reviews of earlier versions of the manuscript. Willem Langenberg is thanked for numerous discussions of the geology and mineral occurrences of northeastern Alberta, and for loan of polished thin sections. Heather Plint collected the $^{40}Ar/^{39}Ar$ data, and helped immensely in interpretation of those data. David Pattison and Glen DiPaoli are thanked for use of the reflected light microscope at the University of Calgary. J.A. van Ham and the Dog Head Blues Band provided field and inspirational assistance. Bill Sharman's photographic expertise is greatly appreciated.

REFERENCES

Abercrombie, H.J. and Feng, R.

1994: Prairie-type disseminated gold-silver-copper mineralization in the Western Canada Sedimentary Basin: Brine-associated native and alloyed metals, chlorides, oxides and carbonates. Geological Society of America, Abstracts with Programs, v. 26, no. 7.

1997: (*this volume*) Geological setting and origin of Microdisseminated Au-Ag-Cu minerals, Fort McKay region Northeastern Alberta. *In* Exploring for Minerals in Alberta: Geological Survey of Canada Geoscience Contributions, Canada–Alberta Agreement on Mineral Development (1992–1995), R.W. Macqueen (ed.). Geological Survey of Canada, Bulletin 500, p. 247-277.

Baadsgaard, H. and Godfrey, J.D.

1972: Geochronology of the Canadian Shield in northeastern Alberta I. Andrew Lake area. Canadian Journal of Earth Sciences, v. 4, p. 541–563.

Bostock, H.H. and van Breemen, O.

1994: Ages of detrital and metamorphic zircons and monazites from a pre-Taltson magmatic zone basin at the western margin of Rae Province. Canadian Journal of Earth Sciences, v. 31, p. 1353–1364.

Bostock, H.H., van Breemen, O., and Loveridge, W.D.

1987: Proterozoic geochronology in the Taltson magmatic zone, N.W.T. *In* Radiogenic Age and Isotopic Studies: Report 1. Geological Survey of Canada, Paper 87-2, p. 73–80.

1991: Further geochronology of plutonic rocks in northern Taltson magmatic zone, District of Mackenzie, N.W.T. *In* Radiogenic Age and Isotopic Studies: Report 4. Geological Survey of Canada, Paper 90-2, p. 67–78.

Burwash, R.A., Baadsgaard, H., and Peterman, Z.E.

1962: Precambrian K-Ar dates from the western Canada Sedimentary Basin. Journal of Geophysical Research, v. 67, p. 1617–1625.

Feng, R. and Abercrombie, H.J.

1994: Disseminated Au-Ag-Cu mineralization in the Western Canada Sedimentary Basin, Fort MacKay, northeastern Alberta: a new gold deposit type *In* Current Research, 1994-E. Geological Survey of Canada, p. 121–132.

Godfrey, J.D.

1958: Aerial photographic interpretation of Precambrian structures, north of Lake Athabasca. Alberta Research Council, Bulletin No. 1, 19 p.

1980a: Geology of the Alexander-Wylie Lakes District, Alberta. Alberta Research Council, Earth Sciences Report 78-1, scale 1:31 680.

1980b: Geology of the Fort Chipewyan District, Alberta. Alberta Research Council, Earth Sciences Report 78-3, scale 1:31 680.

1984: Geology of the Bocquene-Turtle Lakes District, Alberta. Alberta Research Council, Earth Science Report 84-5, scale 1:31 680.

1986a: Geology of the Precambrian Shield in northeastern Alberta. Alberta Research Council, Map EM 180, scale 1:250 000.

1986b: Mineral showings of the Precambrian Shield in northeastern Alberta. Alberta Research Council, Map EM 182, scale 1:250 000.

Godfrey, J.D. and Langenberg, C.W.
1984a: Geology of the Fitzgerald, Tulip-Mercredi-Charles Lakes District, Alberta. Alberta Research Council, Earth Science Report 84-7, scale 1:31 680.

1984b: Geology of the Myers-Daly Lakes District, Alberta. Alberta Research Council, Earth Science Report 84-6, scale 1:31 680.

Grover, T.W., McDonough, M.R., and McNicoll, V.J.
1993: Preliminary report of the metamorphic geology of the Taltson magmatic zone, Canadian Shield, northeastern Alberta. *In* Current Research, Part C. Geological Survey of Canada, Paper 93-1C, p. 233–238.

Hanmer, S., Bowring, S., van Breemen, O., and Parrish, R.
1992: Great Slave Lake shear zone, NW Canada: mylonitic record of Early Proterozoic continental convergence, collision and indentation. Journal of Structural Geology, v. 14, p. 757–773.

Hanmer, S., Parrish, R., Williams, M., and Kopf, C.
1994: Striding-Athabasca mylonite zone: Complex Archean deep-crustal deformation in the East Athabasca mylonite triangle, northern Saskatchewan. Canadian Journal of Earth Sciences, v. 31, p. 1287–1300.

Heaman, L..M. and Parrish, R.R.
1991: U-Pb geochronology of accessory minerals. *In* Application of Radiogenic Isotope Systems to Problems in Geology, L. Heaman and J.N. Ludden (eds.). Mineralogical Association of Canada, Short course handbook, v. 19, p. 59–102.

Henderson, J.B. and van Breemen, O.
1991: K-Ar (hornblende data) from the Healey Lake area, District of Mackenzie: A potential time constraint on the intracratonic indentation of the Slave Province into the Thelon Tectonic Zone. *In* Radiogenic Age and Isotopic Studies: Report 4, Geological Survey of Canada, Paper 90-2, p. 61–66.

Hoffman, P.F.
1987: Continental transform tectonics: Great Slave Lake shear zone (ca. 1.9 Ga), northwest Canada. Geology, v. 15, p. 785–788.

1988: United plates of America, the birth of a craton: Early Proterozoic Assembly and growth of Laurentia. Annual Reviews of Earth and Planetary Science Letters, v. 16, p. 543–603.

1989: Precambrian geology and tectonic history of North America. *In* The Geology of North America – An Overview, A.W. Bally and A.R. Palmer (eds.). Geological Society of America, The Geology of North America, v. A, p. 447–512.

Kuo, S.L.
1972: Uranium-lead geochronology in the Charles Lake area. M.Sc. thesis, University of Alberta, Edmonton, Alberta, 126 p.

Langenberg, C.W. and Nielsen, P.A.
1982: Polyphase metamorphism in the Canadian Shield of northeastern Alberta. Alberta Research Council, Bulletin 42, 80 p.

Langenberg, C.W., Salat, H.P., Skupinski, A., and Eccles, D.R.
1994: Mineral occurrences of the Selwyn Lake and Leland lakes areas, northeast Alberta. Alberta Research Council, Report 1994-5.

Langenberg, C.W., Salat, H.P., Turner, A., and Eccles, D.R.
1993: Evaluation of the economic mineral potential in the Andrew Lake–Charles Lake area of northeast Alberta. Alberta Research Council, Open File Report, 1993-08.

McClay, K.R.
1983: Deformation of stratiform Pb-Zn deposits. *In* Sediment-hosted stratiform lead-zinc deposits, D.F. Sangster (ed.). Mineralogical Association of Canada, Short Course Handbook, v. 8, Victoria.

McDonough, M.R.
1995: Whole rock major and trace element analyses of selected mineral occurrences, Taltson magmatic zone, Canadian Shield, northeastern Alberta (NTS 74M and 74L). Geological Survey of Canada, Open File 2893.

McDonough, M.R. and Abercrombie, H.J.
1995: Mineral occurrences in Middle Devonian carbonates, Salt River and Stony Islands (Slave River) areas, northeastern Alberta. *In* Current Research, 1995-B. Geological Survey of Canada, p. 125–130.

McDonough, M.R., Cooley, M.A., and Schetselaar, E.M.
1994: Geology, Hay Camp, Alberta (NTS 74M/11). Geological Survey of Canada, Open File 2832, scale 1:50 000.

McDonough, M.R., Grover, T.W., McNicoll, V.J., Cooley, M.A., Schetselaar, E.M., and Robinson, N.N.
1994: Geology, Cornwall Lake, Alberta (NTS 74M/10). Geological Survey of Canada, Open File 2896, scale 1:50 000.

McDonough, M.R., Grover, T.W., McNicoll, V.J., Cooley, M.A., Schetselaar, E.M., Robinson, N.N., and Bednarski, J.
1995: Geology, Colin Lake, Alberta–Saskatchewan (NTS 74M/9). Geological Survey of Canada, Open File 3047, scale 1:50 000.

McDonough, M.R., Grover, T.W., McNicoll, V.J., and Lindsay, D.D.
1993: Preliminary report of the geology of the southern Taltson magmatic zone, northeastern Alberta (74M/14, 74M/15 and 74M/16). *In* Current Research, Part C. Geological Survey of Canada, Paper 93-1C, p. 221–232.

McDonough, M.R., Grover, T.W., McNicoll, V.J., Lindsay, D.D., Kelly, K.L., and Guerstein, P.G.
1994a: Revised Geology, Andrew Lake, Alberta-Saskatchewan-NWT (NTS 74M/16). Geological Survey of Canada, Open File 2905, scale 1:50 000.

1994b: Revised Geology, Mercredi Lake, Alberta-NWT (NTS 74M/15). Geological Survey of Canada, Open File 2904, scale 1:50 000.

1994c: Geology, Tulip Lake East-Half, Alberta-NWT (NTS 74M/14). Geological Survey of Canada, Open File 2820, scale 1:50 000.

McDonough, M.R., McNicoll, V.J., and Schetselaar, E.M.
1995: Age and kinematics of crustal shortening and escape in a two-sided oblique-slip collisional and magmatic orogen, Paleoproterozoic Taltson magmatic zone, northeastern Alberta. *In* Report of LITHOPROBE Alberta Basement Transects Workshop, G.M. Ross (ed.). LITHOPROBE Report #47, p. 264-308.

McDonough, M.R., McNicoll, V.J., and Thériault, R.J.
1995: Taltson Basement Complex: Basement to a Paleoproterozoic continental collisional and magmatic orogen. Geological Association of Canada, Program with Abstracts, v. 20, p. A68.

McNicoll, V.J. and McDonough, M.R.
1995: The Waugh Lake Basin: a 2.01-1.971 Ga back arc basin, southern Taltson magmatic zone, northeastern Alberta. *In* Report of LITHOPROBE Alberta Basement Transects Workshop, G.M. Ross (ed.). LITHOPROBE Report #47, p. 309-328.

McNicoll, V.J., McDonough, M.R., and Grover, T.W.
1994: U-Pb geochronological studies in the southern Taltson magmatic zone, northeastern Alberta. *In* Report of LITHOPROBE Alberta Basement Transects Workshop, G.M. Ross (ed.). LITHOPROBE Report #37, p. 270-273.

Morganti, J.M.
1981: Sedimentary-type stratiform ore deposits: Some models and a new classification. Geoscience Canada, v. 8, no. 2, p. 65-75.

Nielsen, P.A., Langenberg, C.W., Baadsgaard, H., and Godfrey, J.D.
1981: Precambrian metamorphic conditions and crustal evolution, northeastern Alberta, Canada. Precambrian Research, v. 16, p. 171-193.

Parrish, R.R.
1990: U-Pb dating of monazite and its application to geological problems. Canadian Journal of Earth Sciences, v. 27, p. 1431-1450.

Plint, H.E. and McDonough, M.R.
1995: $^{40}Ar/^{39}Ar$ and K-Ar constraints on shear zone evolution, southern Taltson magmatic zone, northeast Alberta. Canadian Journal of Earth Sciences, v. 32, p. 281-291.

Roberts, R.G.
1987: Archean lode gold deposits. Geoscience Canada, v. 14, no. 1, p. 37-52.

Ross, G.M., Milkereit, B., Eaton, D., White, D., Kanasewich, E.R., and Burianyk, M.J.A.
1995: Paleoproterozoic collisional orogen beneath western Canada sedimentary basin imaged by Lithoprobe crustal seismic reflection data. Geology, v. 23, no. 3, p. 195-199.

Ross, G.M., Parrish, R.R., Villeneuve, M.E., and Bowring, S.A.
1991: Geophysics and geochronology of the crystalline basement of the Alberta Basin, western Canada. Canadian Journal Earth Sciences, v. 28, p. 512-522.

Thériault, R.J.
1992: Nd isotopic evolution of the Taltson magmatic zone, Northwest Territories, Canada: Insights into Early Proterozoic accretion along the western margin of the Rae Province. Journal of Geology, v. 100, p. 465-475.

Thériault, R.J. and Ross, G.M.
1991: Nd isotopic evidence for crustal recycling in the ca. 2.0 Ga subsurface of western Canada. Canadian Journal of Earth Sciences, v. 28, p. 1140-1147.

Tirrul, R. and Grotzinger, J.P.
1990: Early Proterozoic collisional orogeny along the northern Thelon tectonic zone, Northwest Territories, Canada: Evidence from the foreland. Tectonics, v. 9, p. 1015-1036.

Villeneuve, M.E., Ross, G.M., Thériault, R.J., Miles, W., Parrish, R.R., and Broome, J.
1993: Tectonic subdivision and U-Pb geochronology of the crystalline basement of the Alberta Basin, western Canada. Geological Survey of Canada, Bulletin 447, 86 p.

White, J.C. and Mawer, C.K.
1992: Deep crustal deformation textures along megathrusts from Newfoundland and Ontario: implications for microstructural preservation, strain rates, and strength of the lithosphere. Canadian Journal of Earth Sciences, v. 29, p. 328-337.

METALLOGENIC FEATURES OF THE URANIUM-POLYMETALLIC MINERALIZATION OF THE ATHABASCA BASIN, ALBERTA, AND A COMPARISION WITH OTHER PARTS OF THE BASIN[1]

V. Ruzicka
Mineral Resources Division, Geological Survey of Canada

Abstract

Metallogenic studies of the Athabasca Basin metallogenic province in Alberta indicate favourability of the basement and overlying Athabasca Group rocks for uranium-polymetallic mineral deposits. The basement rocks include Archean and Aphebian granitoid and Aphebian metasedimentary rocks with layers of pyritic graphitic metapelites. Regolith is typically present at the top of the basement rocks. Elevated values of uranium are associated with granitic rocks, particularly with alkali feldspar-rich granitoids, the Fishing Creek granitoids, and grey foliated granitoids; and with felsic mylonite, chloritized graphitic-pyritic metapelite and altered pegmatoids. Nickel mineralization is associated locally with chloritized biotite gneiss. The Athabasca Group rocks contain polymetallic mineralization, particularly at the sub-Athabasca unconformity, where it is intersected by faults. A typical polymetallic assemblage contains uranium, nickel, arsenic, cobalt, molybdenum and zinc. Elevated contents of chromium have been found in rocks of the study area.

Résumé

Dans la région du bassin d'Athabasca en Alberta, des études métallogéniques révèlent que le substratum et les roches sus-jacentes du Groupe d'Athabasca pourraient être les encaissants de gisements polymétalliques riches en uranium. Les roches du substratum consistent en des granitoïdes archéens et aphébiens ainsi qu'en des roches métasédimentaires aphébiennes contenant des couches de métapélites à graphite et à pyrite. Un manteau d'altération (régolite) recouvre généralement le substratum. Les concentrations élevées d'uranium sont associées à des roches granitiques, en particulier des granitoïdes riches en feldspath alcalin (ceux de Fishing Creek) et des granitoïdes gris feuilletés; elles sont également associées à des mylonites felsiques, des métapélites chloritisées à graphite et à pyrite et des pegmatoïdes altérés. Quant à la minéralisation en nickel, elle est liée par endroits à des gneiss à biotite qui ont été chloritisés. Les roches du Groupe d'Athabasca sont l'encaissant d'une minéralisation polymétallique, surtout au niveau de leur discordance inférieure, où elles sont entrecoupées de failles. Un assemblage polymétallique typique contient de l'uranium, du nickel, de l'arsenic, du cobalt, du molybdène et du zinc. Des teneurs élevées en chrome ont été enregistrées dans des roches de la région à l'étude.

INTRODUCTION

Important metallogenic provinces hosting unconformity uranium deposits

The most significant metallogenic province for uranium-polymetallic deposits in respect to their sizes, grades and production is the Athabasca Basin, Saskatchewan and Alberta, Canada. Other, to some degree analogous, metallogenic provinces are the Pine Creek Geosyncline, Northern Territory, Australia, and the Thelon Basin region, Northwest Territories, Canada. Some geologists also consider the Paterson block, Western Australia, Australia, as a metallogenic province of this type (Jackson and Andrew, 1990). In addition to uranium, mineral deposits in these provinces also contain nickel, cobalt, arsenic and gold. All of these deposits have a common denominator: they are associated with sub-Middle Proterozoic unconformities and are commonly known as "unconformity deposits".

[1]Canada-Alberta Agreement on Mineral Development, Project C1.12

Athabasca Basin

The unconformity deposits in the Athabasca Basin occur in Lower (Aphebian) and Middle (Helikian) Proterozoic basement rocks at or in proximity to the pre-Helikian (sub-Athabasca) unconformity (Figs. 1, 2). The basement rocks include granitoid and metasedimentary rocks, including graphitic/pyritic metapelites. The Aphebian basement rocks, which underwent extensive uplift, erosion and weathering, are separated by an angular unconformity from overlying unmetamorphosed siliciclastic sedimentary rocks of the Athabasca Group, which is in turn overlain locally by Paleozoic rocks and Quaternary glacial sediments. Uranium mineralization, which includes pitchblende and coffinite, occurs either at the sub-Athabasca unconformity, beneath it in the basement rocks, or at some distance above the unconformity within the Athabasca Group rocks. The uranium minerals are commonly accompanied by minerals bearing nickel, cobalt, arsenic, and locally of molybdenum and zinc.

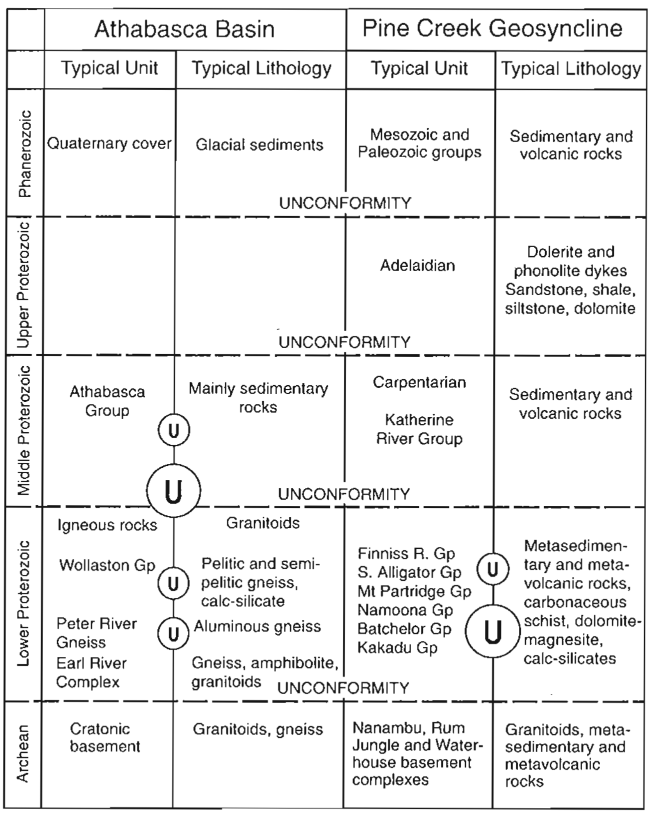

Figure 1. *Generalized geological columns of the Athabasca Basin, Canada, and Pine Creek Geosyncline, Australia. Circles and circle sizes denote geological position, importance, and relative sizes of uranium unconformity deposits within the sequence.*

Other metallogenic uranium provinces

In the Pine Creek Geosyncline of Australia, the Lower Proterozoic rocks, which consist of metasedimentary and metavolcanic rocks, carbonaceous schists, dolomite-magnesite and calc-silicates, rest unconformably on Archean granitoid basement complexes. The Lower Proterozoic rocks are unconformably overlain by Middle Proterozoic (Carpentarian) rocks, which include siliciclastic sedimentary and volcanic rocks, medium to coarse grained quartz sandstone, thin beds of siltstone, and pebbly sandstone and conglomerate of the Kombolgie Formation. The sequence is overlain by Upper Proterozoic, Paleozoic and Mesozoic rocks (Fig. 1). Unlike the Athabasca Basin, the unconformity deposits in the Pine Creek Geosyncline occur only in Lower Proterozoic rocks (i.e., below the pre-Middle Proterozoic unconformity; Figs. 1, 3; Battey et al., 1987; Needham, 1988). The mineralization, which consists of pitchblende, is locally accompanied by gold.

In the Thelon Basin region of the Northwest Territories, Canada, Archean rocks are overlain by belts of Aphebian metamorphosed rocks, which include quartzites, schists and banded iron formation, and have been intruded by granitoid rocks during late Hudsonian events. The basement rocks, which have been subjected to intensive uplift, erosion and weathering, are overlain by Helikian continental siliciclastic sedimentary rocks of the Thelon Basin. The Thelon Basin is comparable in the time of deposition, lithological and structural features, to the Athabasca Basin. The unconformity deposits typically occur within the basement rocks, but some occurrences have also been found in the Helikian cover rocks (Miller et al., 1989). The uranium mineralization, which consists mostly of pitchblende, occurs mainly in the basement rocks.

In the Paterson block of Western Australia, the Rudall Metamorphic Complex consists of granite gneiss of possible Archean age, surrounded by an older suite of metasedimentary rocks, which includes paragneiss, mica schist and iron formation, and by a younger suite, which includes quartzite, graphitic schist, and chlorite-quartz and chlorite-carbonate schist. The Rudall Metamorphic Complex is overlain, with angular unconformity, by the Proterozoic Coolbro Sandstone, which includes thick sequences of quartz sandstone and thin beds of mudstone and shale. The Precambrian rocks are, in turn, unconformably overlain by Permian rocks and Quaternary sediments. Uranium mineralization, which includes pitchblende and traces of a polymetallic assemblage, occurs within chlorite-quartz and chlorite-carbonate schists (Jackson and Andrew, 1990).

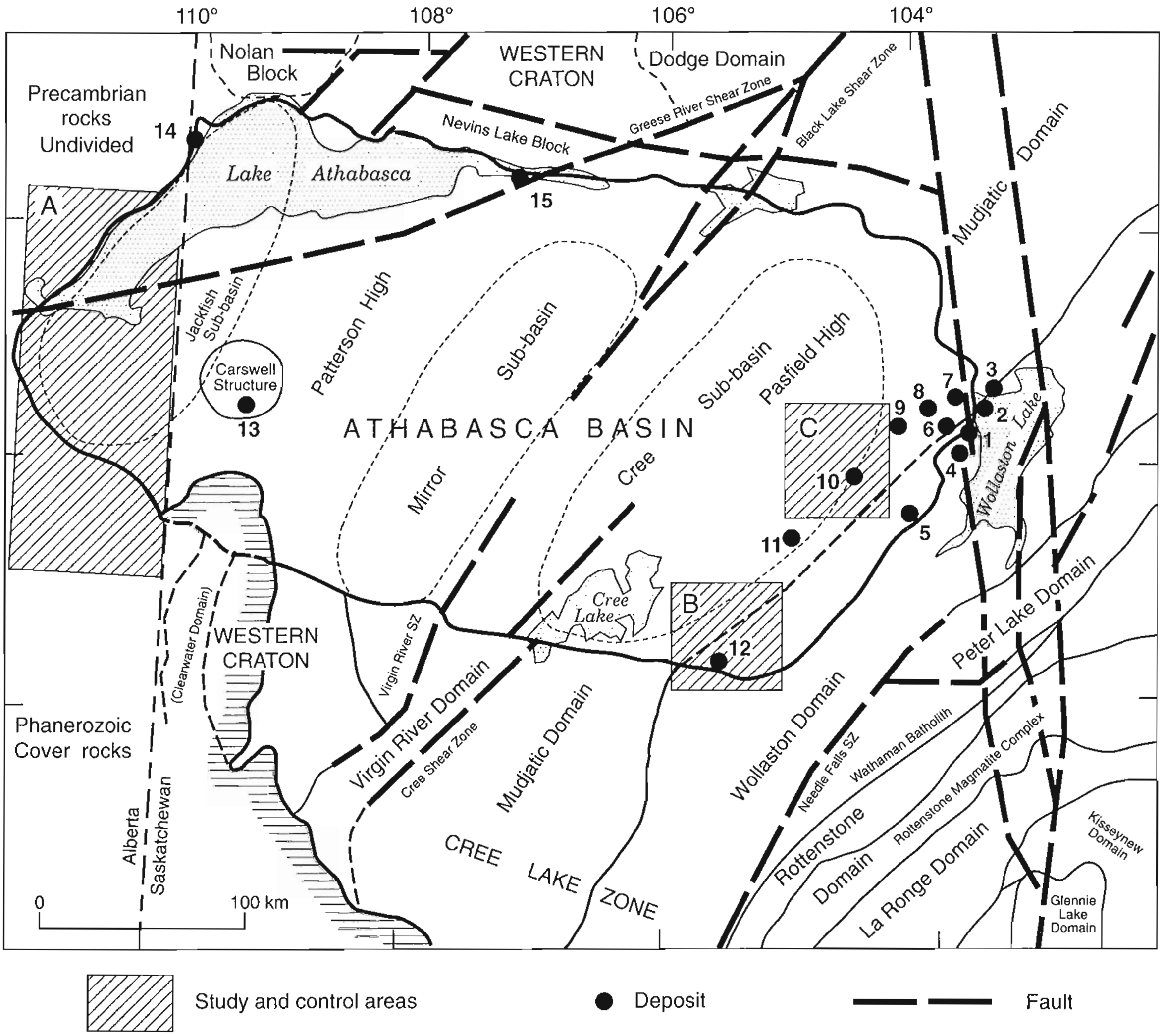

__Figure 2.__ Generalized geology and distribution of unconformity deposits in the Athabasca Basin Metallogenic Province, Canada. A, main study area, Alberta; B, control area at Key Lake; C, control area at Cigar Lake. Deposits (m, monometallic; p, polymetallic): 1, Rabbit Lake (m); 2, Collins Bay cluster (p); 3, Eagle Point (m); 4, Horseshoe and Raven (m); 5, West Bear (p); 6, McClean-Sue cluster (p); 7, JEB (m); 8, Dawn Lake (p); 9, Midwest (p); 10, Cigar Lake (p); 11, P2 North (McArthur River; p); 12, Key Lake (p); 13, Cluff Lake cluster (p, m); 14, Maurice Bay (p); 15, Fond-du-Lac (m). (Base map after Sibbald et al., 1990.)

Importance of the unconformity deposits

Unconformity deposits are the largest high-grade deposits of uranium known at present. Some of the unconformity-type deposits contain very large amounts of ore and have very high grades. The tonnage/grade graph for these deposits (Fig. 4) demonstrates these attributes for selected deposits from Canada and Australia. The graph shows sandstone-hosted, basement-hosted, monometallic and polymetallic deposits. As it is apparent from this graph, Canada has the world's largest high-grade deposit — the Cigar Lake deposit, which contains, in its core, 110 000 t U in ores grading 12.2 per cent U. A lower grade extension of this deposit (Cigar Lake tail) contains an additional 40 000 t U at a grade of 4.0 per cent U. For comparison, the recent mining grade of the uranium quartz-pebble conglomerate deposits at Elliot Lake, Ontario, is less than 0.1 per cent U.

World uranium production for 1993 is estimated to have amounted to about 33 kt of uranium metal (NEA/IAEA, 1994), from which about 26 per cent was produced from low-cost resources of the Athabasca Basin deposits. In 1993, the uranium production from Canadian unconformity deposits represented more than 92 per cent of the total Canadian uranium output. In the same year, Canadian sales of uranium amounted

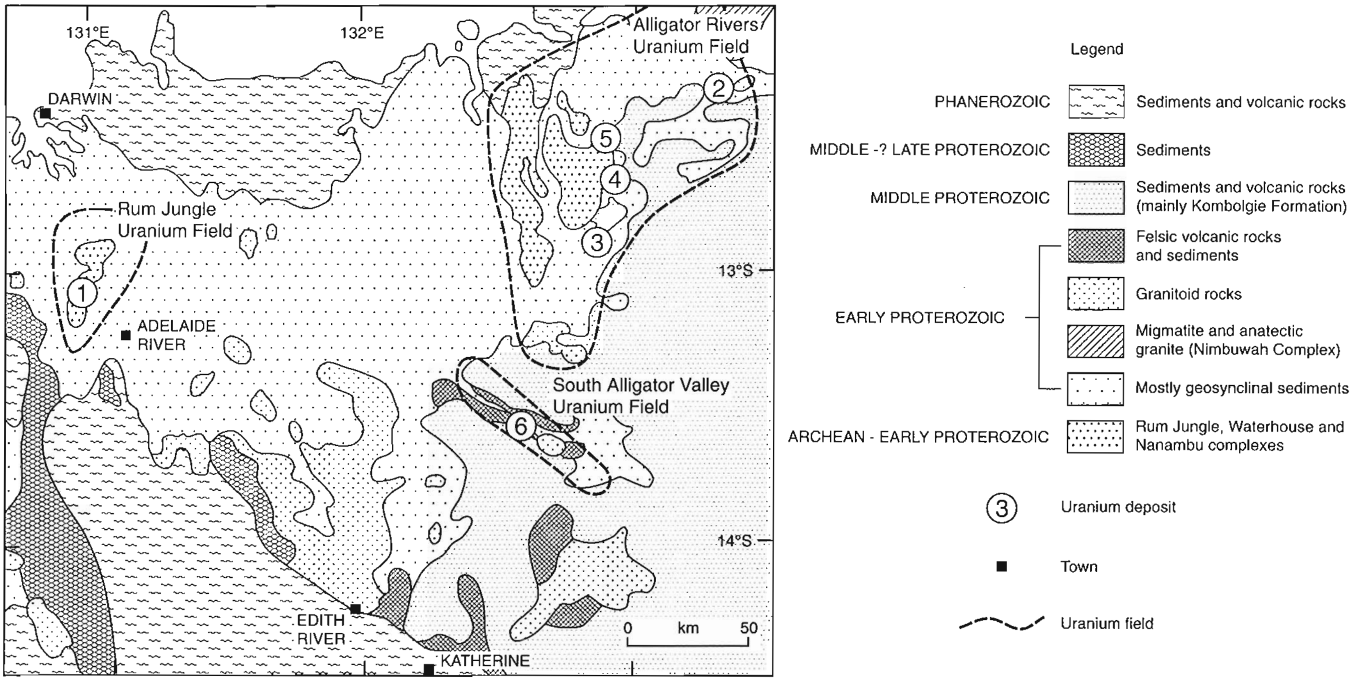

Figure 3. *Generalized geology and distribution of unconformity deposits in the Pine Creek Geosyncline, Australia (modified after Battey et al., 1987). Numbers in circles denote deposits: 1, Rum Jungle; 2, Nabarlek; 3, Koongarra; 4, Ranger 1; 5, Jabiluka 1, 2, 3; 6, Coronation Hill.*

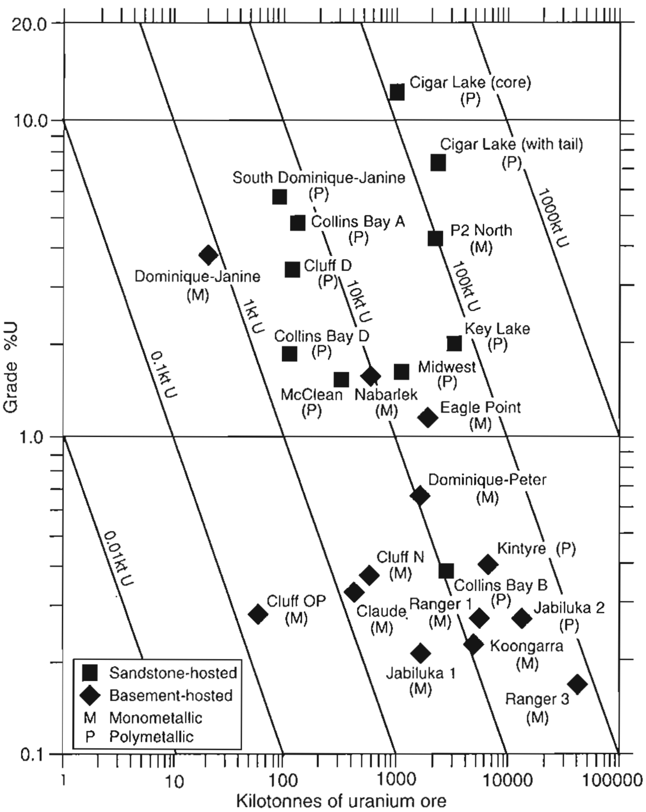

Figure 4. *Tonnage/grade graph for unconformity deposits, Canada and Australia. Data as of 1993 (after Ruzicka, 1993).*

to more than a half billion dollars and Canadian uranium mining operations employed in excess of 1300 persons (NRCan, 1994). It is expected that the world uranium supply will experience a deficit beyond the year 2000, and that the proportion of global uranium production from unconformity deposits will be even higher.

METALLOGENY OF THE ATHABASCA BASIN

Mineral deposits of the Athabasca Basin have been the subject of a number of papers, for example: Knipping (1974); Hoeve and Sibbald (1978); Tremblay (1982); Ruzicka (1984); Langford (1986); Wallis et al. (1986); Fouques et al. (1986); Andrade (1989); Kyser et al. (1989); Ramaekers (1990); Sibbald et al. (1990); Kotzer and Kyser (1990a, b); Kotzer (1992); Marlatt et al. (1992); Ey et al. (1992) and Ruzicka (1993a, b, 1996). The following summary is based mainly on these papers.

Regional metallogenic model

The regional metallogenic cycle of uranium and associated metals was initiated by the introduction of uranium with granitoid magmatism as much as 2.6 Ga

(Fig. 5). Uranium-rich zircons from an unfoliated, nonmagnetic, white granitic body at Colquhoun Lake, Saskatchewan (near Key Lake), yielded ages of 2.6 and 1.7 Ga respectively (Krogh and Clark, 1987). The time of crystallization of these uraniferous zircons apparently reflects the oldest age of the first uranium mineralization period in the Athabasca Basin region. Robinson (1955) reported a U-Pb age >2.2 Ga from pegmatites and mafic portions of metasedimentary rocks from the Beaverlodge area, which is located a short distance to the north of the Athabasca Basin.

Uranium was subsequently (at about 1.9 Ga) reconcentrated into pegmatitic mobilizates and into mafic portions of metasedimentary rocks of the Tazin Group (Koeppel, 1968). The age of the Viking Lake deposit, Saskatchewan, which is an example of a complex, radioactive, pegmatite dyke, and contains pyrochlore, magnetite, titanite, uranothorite, uraninite, cyrtolite, meta-allanite and pyrite, was determined by several methods to be about 1.9 Ga (Robinson, 1955; Baadsgaard, 1965; Koeppel, 1968).

Formation of vein deposits

Major mobilization of uranium in the west-central part of the Churchill Structural Province of the Canadian Shield was associated with the Hudsonian Orogeny (1.9–1.8 Ga) and led to the formation of epigenetic pitchblende-brannerite deposits in the Beaverlodge area. About 120 U-Pb isotope determinations for pitchblende specimens were statistically analyzed by Ward (1984), who suggested that the earliest ages are in the order of 1800 to 1700 Ma. An additional cluster of results falls in the range 1100 to 900 Ma. Episodic reworking occurred during the Phanerozoic.

Post-orogenic sedimentary processes

Paleoweathering of the metamorphic basement rocks prior to deposition of Athabasca Basin Middle Proterozoic clastic sedimentary rocks led to the formation of regolith (or saprolite). The regolith persists throughout the basin and shows many features compatible with present-day lateritic soil profiles formed in subtropical to tropical climates. Development of the regolith was characterized by chloritization and hematitic alteration of ferromagnesian minerals, sericitization, illitization or kaolinization of K-feldspars and saussuritization of plagioclase. However, some elements accompanying uranium, such as V, Mo, Pb, Ag, Ni, Co and As, survived weathering in chemically resistant oxide and

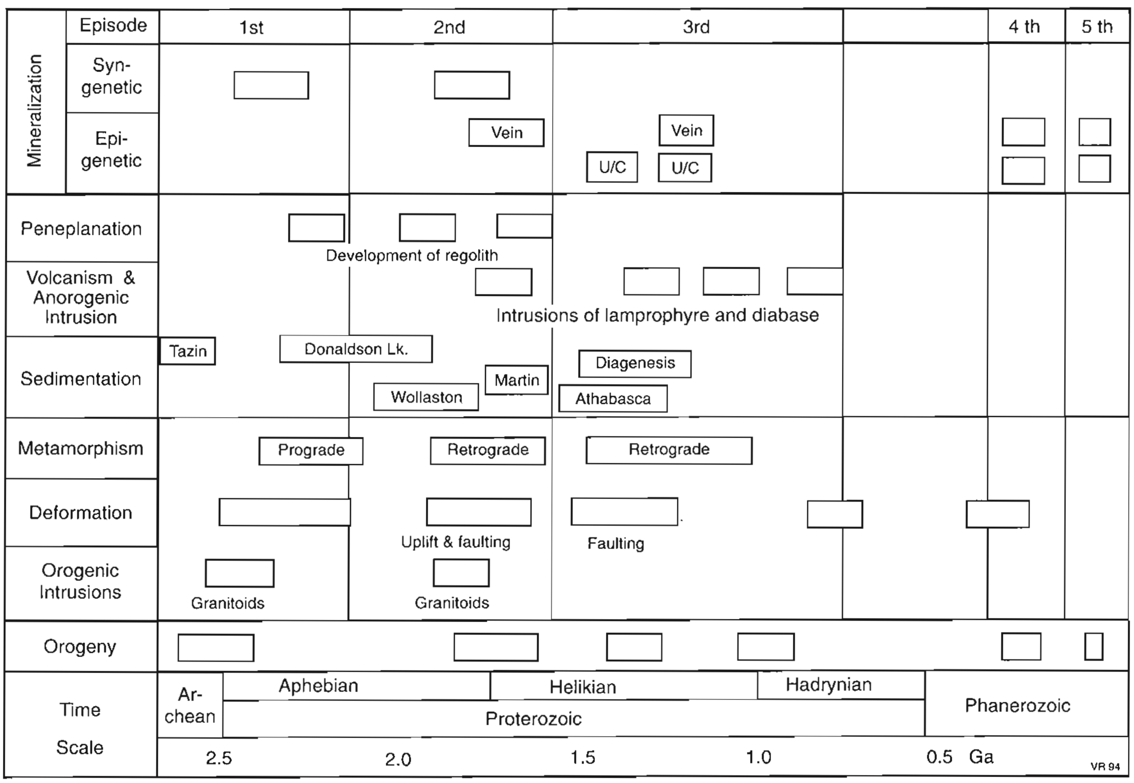

Figure 5. *Regional model for the Athabasca Basin region, Saskatchewan, Canada (modified after Ruzicka and LeCheminant, 1987). U/C, Unconformity deposits.*

heavy mineral phases and thus became available as detritus for subsequent sedimentary accumulation in the Athabasca Basin. The basin thus became a reservoir for specific metalliferous minerals that later were subjected to diagenetic leaching.

Uranium and accompanying metals were concentrated during a long period of weathering and diagenesis, including the development of extensive regolith. A later stage of epigenetic deposition, further concentrating uranium and associated metals, may be related to thermal events associated with either emplacement lamprophyre and diabase dykes, deformation, or retrograde metamorphism.

Conceptual genetic deposit model

The formation of the Athabasca Basin deposits was controlled by lithological, structural and geochemical factors, which are summarized in the following deposit model (Fig. 6).

Lithological controls

The lithological framework of the deposit model for the Athabasca Basin deposits consists of an Archean granitoid dome, reactivated during the Aphebian, and surrounded by metamorphosed Lower Proterozoic (Aphebian) shelf sediments, which include layers of euxinic rocks (graphitic and pyritic metapelites). The basement (Archean and Aphebian) rocks are unconformably overlain by unmetamorphosed Middle Proterozoic (Helikian) clastic sedimentary cover rocks filling the basin. Peneplanation and lateritic weathering of the Archean and Aphebian basement rocks resulted in the formation of regolith. Detritus, which was derived from the basement rocks by the weathering processes, was transported to and deposited in the intracratonic basin.

Spatial association of the deposits with Archean granitic domes is apparent, for example, from the location of the Cigar Lake deposit (Fig. 7), and particularly from the location of the Sue Zone, Rabbit Lake and Collins Bay deposits, which are spatially associated with the Collins Bay Dome (Fig. 8). The Cluff Lake deposits, Dominique-Peter, Dominique-Janine, and Cluff D are spatially associated with the Dominique-Peter Dome (Fig. 9). The relationship of the deposits to layers of graphitic and pyritic metapelitic rocks is apparent at most of the known deposits in the Athabasca Basin, particularly at Cigar Lake, Key Lake, Collins Bay, P2 North, Midwest, McClean Lake and Sue Zone.

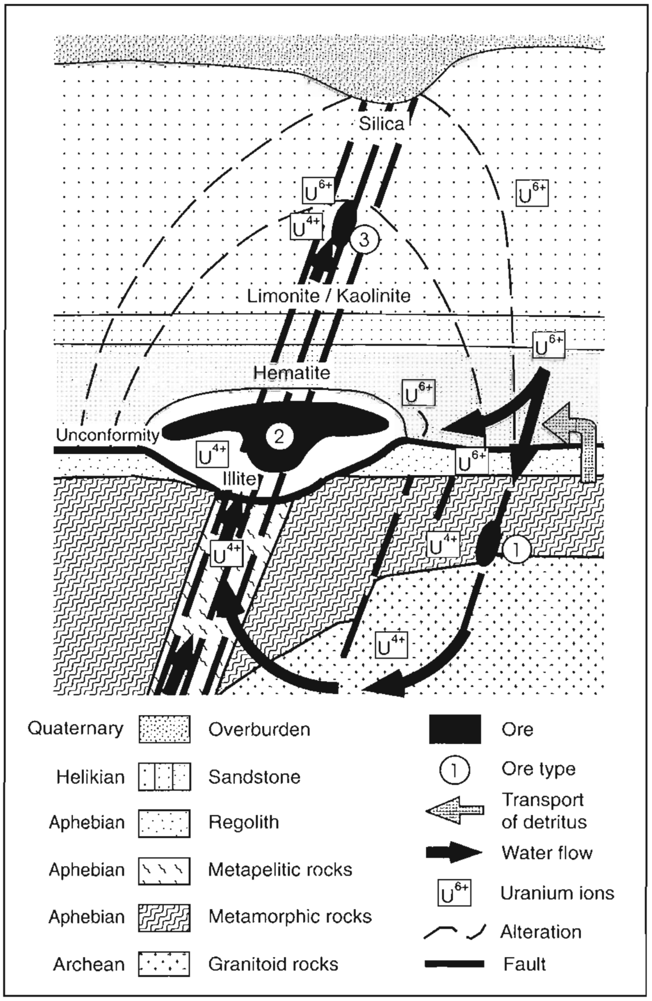

Figure 6. Deposit model for deposits associated with the sub-Athabasca unconformity (modified after Ruzicka, 1984). A generalized vertical cross-section. Arrows indicate flow paths of oxidized and reduced fluids. Circled numbers indicate locations of various styles of mineralization referred to in the text: 1, monometallic mineralization in the basement rocks; 2, typically polymetallic mineralization at the unconformity; 3, monometallic mineralization within the sedimentary cover rocks ("perched" above the unconformity).

Structural controls

The structural framework, which controls the distribution of uranium mineralization, consists of: (i) the sub-Athabasca unconformity, and (ii) faults or fracture zones, which may locally displace the unconformity (Fig. 6). The commonly subvertical fractures usually follow the graphitic pelitic layers in the basement rocks and extend to the sedimentary cover rocks.

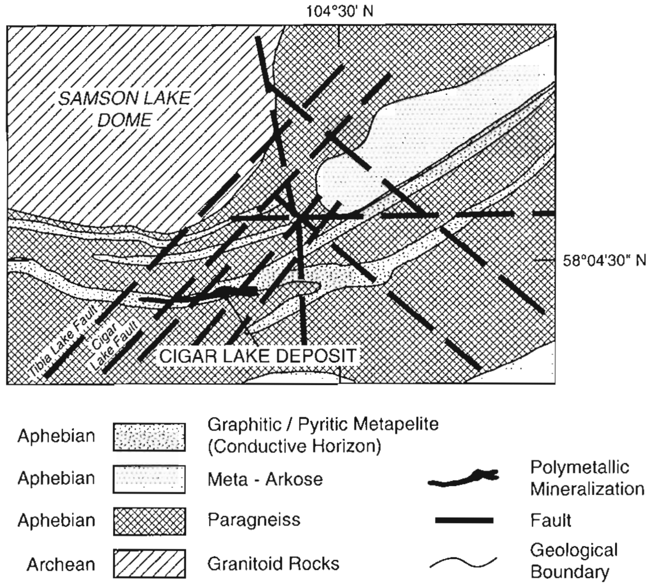

__Figure 7.__ Assumed outline of the paleosurface of the pre-Helikian rocks in the vicinity of the Samson Lake Dome, and location of the Cigar Lake deposit (modified after Fouques et al., 1986).

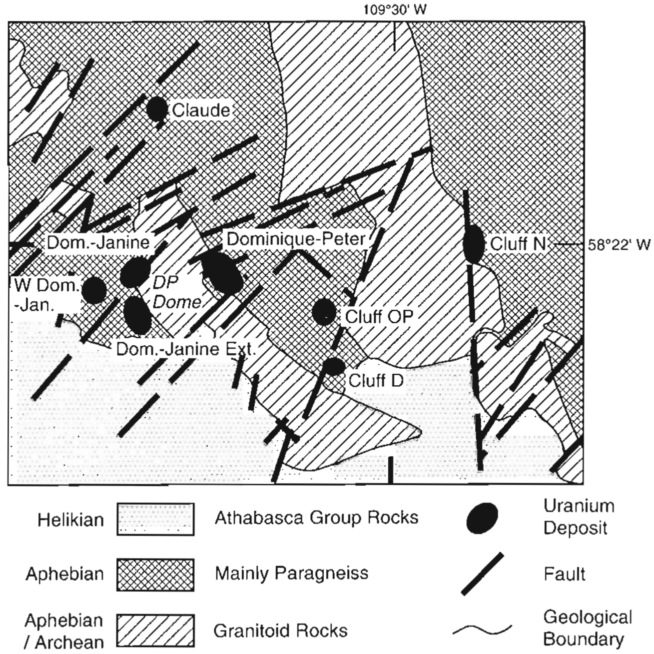

__Figure 9.__ Geology and location of uranium deposits in southwest part of Carswell Structure (after Cogema Resources Inc., unpub. report, 1993).

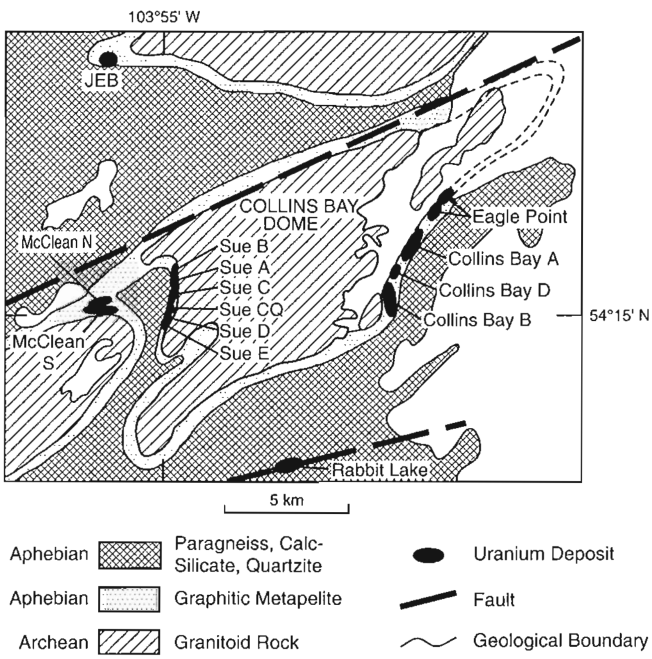

__Figure 8.__ Uranium deposits spatially associated with the Collins Bay Dome (after Ruzicka, 1992).

The unconformity (Fig. 6) represents a boundary between the commonly regolithic (clay-rich), less water-permeable, granitoid and metamorphic basement rocks, and the overlying porous, more-permeable, sedimentary rocks of the Athabasca Basin, and thus forms a barrier for water flow within the overlying aquifer. Conversely, the faults and fracture zones, which intersect the unconformity, represent channels for the fluids and thus are an important part of the "plumbing" system. In the Athabasca Basin, the pre-Middle Proterozoic (sub-Athabasca) unconformity is generally flat-lying. The intersecting faults and fracture zones typically have northeastern to eastern trends. For example, the Rabbit Lake deposit is localized at the intersection of the sub-Athabasca unconformity and the northeast-trending Rabbit Lake thrust fault. The Eagle Point deposit occurs in the hanging-wall of the eastward-trending Collins Bay Fault at its intersection with the sub-Athabasca unconformity. Localization of the Key Lake deposit apparently is controlled by the intersection of a regional northeast-trending steep fault with the sub-Athabasca unconformity. The unconformity is dislocated by the fault for about 30 m. The Cigar Lake deposit is located where the sub-Athabasca unconformity is intersected by an east-trending fracture zone that coincides with graphitic pelite layers in the Lower Proterozoic basement. The Dominique-Peter deposit in the Cluff Lake area is confined to a mylonite zone which occurs at the contact between two gneissic lithostratigraphic units, presumably not far below the unconformity.

The forms of the orebodies are also structurally controlled. The ores in basement rocks occur typically in lenses within veins and as thin, often anastomosing, veinlets in stockworks. Orebodies located in proximity to the unconformity commonly form pods and large lenses aligned along the controlling structures and, to a lesser extent, occurring as veinlets and impregnations in the host rocks. Typical shapes for such deposits are subhorizontal elongated orebodies, which formed from prevailing fluid flows along the unconformity, or plume-like lobes that formed from ascending fluids. The orebodies are, as a rule, surrounded by illite, chlorite, kaolinite or carbonate alteration haloes, overprinted by hematite and/or limonite staining. A silicification aureole commonly forms the outer zone of the alteration haloes. Later tectonic movements and alteration processes led to the formation of collapse structures above major orebodies.

Geochemical controls

Tectonic and thermal events, which could be related to subsidence of the basin or to intrusion of diabase dykes, activated hydrothermal systems causing convective cycling of fluids and mobilization of the metals from the reservoirs. Fluids from three sources took part in the hydrological system (Fig. 6): (i) oxidized basinal fluids, which also included metalliferous connate waters brought into the basins along with detritus; (ii) reduced basement fluids; and (iii) low temperature "retrograde" fluids derived from meteoric waters. These fluids became part of the hydrodynamic system; the oxidized basinal saline metalliferous fluids or brines having salinities up to 30 per cent of NaCl equivalent moved laterally and downward. Where these fluids encountered the hydrological barrier at the unconformity, they continued flowing laterally along the unconformity. However, part of the fluids also entered fault and fracture zones in the basement rocks, and consequently became reduced. These reduced artesian basement fluids, which became heated by deep circulation to as much as 200°C (from fluid inclusions), then re-entered the sedimentary rocks in ascending flows along faults and fracture zones, where they mingled with the laterally moving oxidized metalliferous basinal waters at the unconformity and at higher levels within the sedimentary sequence. Whether or not the ascending fluids also contained water from deep-seated sources is unknown. Under modern conditions, the hydrological barrier of the sub-Athabasca unconformity is, for instance, visible on the walls of the Deilmann open pit at Key Lake. Water flowing from the unconformity causes limonite staining on the underlying basement rocks in the open pit.

Deposition of the metals and associated gangue minerals took place at the interface between the oxidizing and reducing fluids (i.e., at the redox front) during the diagenesis of the sedimentary cover rocks (Fig. 6). Uranium was transported in hexavalent (U^{6+}) form as uranyl carbonate complexes and precipitated, due to reduction, to tetravalent (U^{4+}) form by reductants, such as CO_2, CH_4 and H_2S. Depending upon the location of the redox front, the mineralization took place in diverse parts of the basin and within various parts of the basement and cover rocks: (i) High grade mineralization typically formed at the interface of the oxidized basinal fluids with the reduced basement fluids in proximity to the unconformity (location 2 in Fig. 6). The high-grade polymetallic deposits, such as Key Lake and Cigar Lake, and the monometallic P2 North deposit are representative examples of this mineralization process. (ii) Medium-grade mineralization formed due to interaction of oxidized basinal fluids with the reducing basement rocks in fractures and faults below the sub-Athabasca unconformity (location 1 in Fig. 6). The medium-grade monometallic deposits, such as Rabbit Lake and Eagle Point, are characteristic examples of this mineralization process. (iii) Low-grade mineralization formed at interfaces between oxidized and reduced facies within the sedimentary sequence at some distance above the sub-Athabasca unconformity (location 3 in Fig. 6). The low grade Fond-du-Lac monometallic deposit is a typical example of this mineralization process.

The unconformity deposits (location 2 in Fig. 6) have associated zones of host rock alteration that appear to result from three distinct processes:

(i) Paleoweathering of the metamorphic basement rocks prior to deposition of the Middle Proterozoic (Helikian) clastic sedimentary rocks led to the formation of regolith (if the profile contains both autochthonous and allochthonous material) or saprolite (if the profile contains solely autochthonous material). The regolith or saprolite persist throughout the basin and shows many features compatible with present-day lateritic soil profiles formed in subtropical to tropical climates (Macdonald, 1985). For example, development of regolith at Key Lake was characterized by chloritization and hematitic alteration of ferromagnesian minerals, sericitization, illitization or kaolinization of K-feldspars and saussuritization of plagioclase (de Carle, 1986). The weathered material was an important source of metals for the Athabasca

Group rocks. Regolith is also host for mineralization of some deposits (Tremblay, 1982).

(ii) Diagenetic and epigenetic alteration processes, which were coeval with the mineralization, affected not only the rocks of the Athabasca Group but also the basement rocks, particularly in the vicinity of the deposits. Oxygen- and hydrogen-isotope analyses of illite, kaolinite and chlorite associated with uranium mineralization at the unconformity deposits in the Athabasca Basin (Table 1) indicate that: the basement fluids produced clinochlore and sudoite; the basinal fluids produced illite and kaolinite in the sedimentary cover rocks; and the retrograde fluids (i.e., meteoric waters that circulated along fault zones) produced a late-stage kaolinite (Kyser et al., 1989; Kotzer and Kyser, 1990a, b; Kotzer, 1992, 1993). The alteration processes had various forms and intensities depending on the character of the host rocks and the nature of the fluids. For example, at Key Lake, kaolinization of the Athabasca Group rocks was superimposed on illitization and extended laterally from the mineralization for several hundred metres. At Cigar Lake, the orebody was surrounded by an alteration halo, which contained hematite, illite, ferromagnesian illite, chlorite and its Al-Mg variety — sudoite, kaolinite, iron-rich kaolinite, locally unconsolidated sand (quicksand) and a quartz-cemented cap (Fouques et al., 1986; Percival, 1989; Percival and Kodama, 1989; Percival et al., 1993). At Rabbit Lake, where mineralization is entirely hosted by the basement rocks, chloritization, graphitic chloritic alteration and dolomitization are the main forms of alteration of host rocks. Uranium and boron at the Midwest deposit and boron and lead at Key Lake are enhanced in the host rocks around mineralization (Sopuck et al., 1983). The orebodies typically are enveloped by clay. Quartz grains in rocks at the unconformity are corroded or even totally replaced by clay. Silicification of the sandstone in the form of vein systems and pervasive cements has occurred in places in the overlying sandstone and is a manifestation of intense illitization and desilicification at depth. Partial destruction of graphite and carbon from metapelitic rocks, formation of limonite and hematite, and/or bleaching of the host rocks, are other characteristics of the alteration zones.

Table 1

Oxygen and hydrogen isotope equilibria with typical alteration minerals at selected unconformity deposits in the Athabasca Basin (after Kotzer, 1992, 1993)

Type of fluids	$\delta^{18}O$	δD	In equilibrium with
Saline basinal fluids	+4±2‰	-60±20‰	diagenetic illite and kaolinite
Basement fluids (a)	+2±4‰	-45 to -15‰	clinochlore
Basement fluids (b)	+7 to +9‰	-60 to -25‰	sudoite
Low temperature meteoric waters	-16±2‰	-130±10‰	kaolinite
Late (D-depleted) meteoric waters	+5±5‰	-110±30‰	illite
Retrograde fluids	-16±2‰	-130±10‰	late kaolinite

Brecciation, development of collapse structures in the immediate vicinity of the mineralization, and formation of "Zone à Boules" (Lainé et al., 1985) are associated with the alteration processes. The diagenetic and epigenetic alterations were apparently enhanced by ionization effects of the radionuclides, particularly by the radiolysis of water and by reactions of hydrogen and oxygen with the rocks. Effects of water radiolysis were observed at the Cigar Lake deposit (Cramer, 1986).

(iii) Post-ore alteration (about 1.2–0.8 Ga) succeeded the main episode of uranium mineralization. Tectonic uplift of the Athabasca Basin around 300 Ma (Hoeve and Quirt, 1984) triggered circulation of basinal fluids, which caused: corrosion of the ores; formation of new alteration minerals, particularly chlorite, smectite and mixed-layer clays; and kaolinization of illite and quartz (Ruhrmann and von Pechmann, 1989).

Kotzer and Kyser of the University of Saskatchewan and Irving of the Geological Survey of Canada (Kotzer et al., 1992) identified fluids associated with the development of several types of magnetism in hematites (Fig. 10): (a) fluids associated with development of 'A' magnetism with normal polarity in purple, coarse grained hematite in oxidized heavy mineral bands; (b) fluids associated with development of 'B' magnetism with reverse polarity in red, fine grained hematite, proximal to faults and uranium mineralization. This type of hematite with 'B'

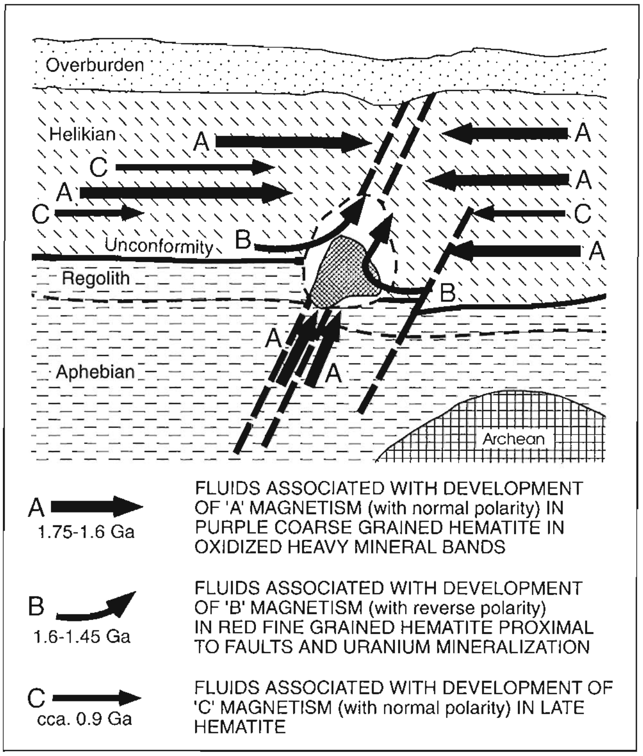

Figure 10. *Fluid flows forming hematite with various single-component magnetizations, Athabasca Basin (after Kotzer et al., 1992).*

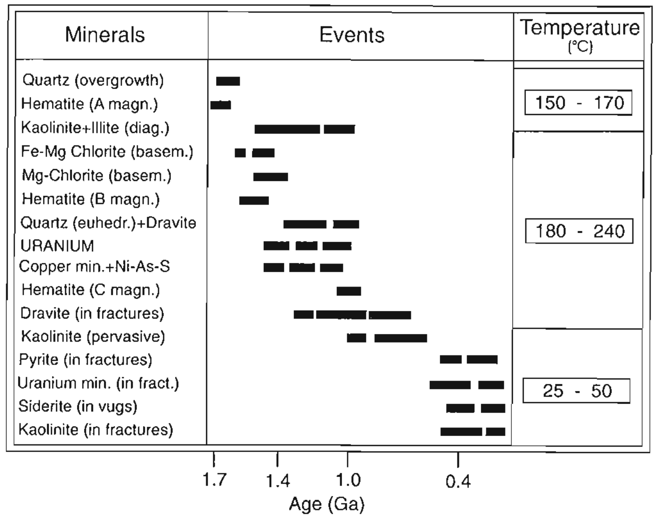

Figure 11. *Alteration changes and mineralization with time and temperature (after Kotzer, 1992, 1993). Magn., magnetization; diag., diagenetic; basem., basement rocks; fract., fractures; min., mineralization.*

magnetism has been identified only in association with large unconformity deposits in the basin; (c) fluids associated with development of 'C' magnetism with normal polarity in late hematite; (d) there also have been identified fluids associated with development of 'D' magnetism in hematite, but in very restricted amounts. Recognition of hematite with 'B' magnetism is an important exploration task, because of its association with uranium mineralization.

During various stages of the mineralization processes, which occupied a period of time from 1.7 Ga to Recent, the fluids had various temperatures and chemical compositions (Fig. 11): (a) Fluids preceding the mineralization stage had temperatures between 150° and 170°C (Kotzer, 1992), and caused the dissolution and recrystallization of quartz in vugs, hematitization with 'A' magnetism, and development of diagenetic kaolinite and illite. (b) Fluids associated with the ore-forming stage reached temperatures between 180° and 240°C (Kotzer, 1992), and caused magnesian metasomatism (development of Fe-Mg- and Mg-chlorites), tourmalinization (development of dravite) in basement rocks, hematitization with 'B' and 'C' magnetism and deposition of uranium, copper and nickel arsenides and sulpharsenide minerals. (c) During the post-ore stage, the fluids had reduced temperatures between 25° and 50°C (Kotzer, 1992), and caused pervasive kaolinization, and deposition of iron sulphides and carbonates, tourmaline (dravite) and redeposition of pitchblende in fractures.

The above-mentioned deposit model (Fig. 6) is supported by oxygen and hydrogen isotope analyses of illite, kaolinite and chlorite, associated with the mineralization (Kotzer, 1992; Fig. 12). These analyses, which are summarized in Table 1, indicate that: (i) The saline basinal fluids, which are in equilibrium with diagenetic illite + kaolinite and illite in sandstone, had $\delta^{18}O = +4 \pm 2‰$ and $\delta D = -60 \pm 20‰$. (ii) The basement fluids, which are in equilibrium with clinochlore, had $\delta^{18}O$ from +2 to +4‰ and δD from -45 to -15‰. (iii) The basement fluids, which are in equilibrium with late sudoite, had $\delta^{18}O$ from +7 to +9‰ and δD from -60 to -25‰. (iv) Low temperature meteoric waters, which are in equilibrium with recrystallized kaolinite, had $\delta^{18}O$ equal to -16 $\pm 2‰$ and δD $-130 \pm 10‰$ and temperatures from about 25° to about 50°C. (v) D-depleted meteoric waters, which are in equilibrium with illite, had $\delta^{18}O$ $+5 \pm 5‰$ and δD $-110 \pm 30‰$. (vi) Retrograde fluids, which are in equilibrium with late kaolinite in faults, had $\delta^{18}O$ $-16 \pm 2‰$ and δD $-130 \pm 10‰$, and temperatures below 50°C.

The alteration minerals (chlorite, illite, kaolinite) formed envelopes around the orebodies, which greatly reduced permeability of the host rocks and thus protected the orebodies from destruction by

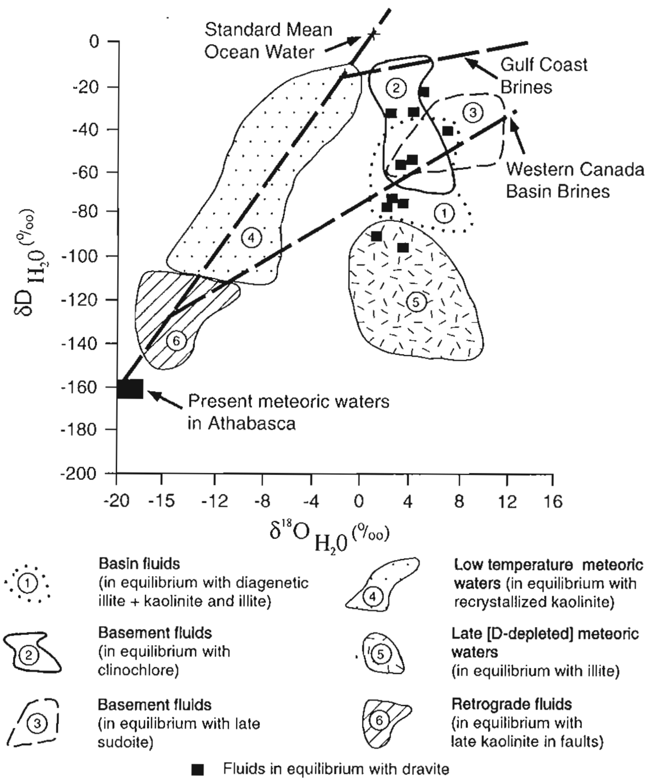

Figure 12. Hydrogen and oxygen isotope ratios in various environments (after Kotzer, 1992, 1993).

groundwater and transient basinal fluids (Ruzicka, 1993, 1996).

CANADIAN UNCONFORMITY URANIUM DEPOSITS

The majority of Canadian uranium deposits associated with pre-Middle Proterozoic (sub-Helikian) unconformities occur in the Saskatchewan part of the Athabasca Basin. Several deposits of this type have been discovered in the Thelon Basin region near Baker Lake, Northwest Territories. A few occurrences are also known from the Otish Basin, Quebec (Ruzicka, 1984).

Unconformity deposits in the Athabasca Basin

The Athabasca Basin is a part of the Churchill Structural Province. Its rocks fill an intracratonic Helikian depression on Archean and Lower Proterozoic (Aphebian) basement rocks. The basement rocks include granulites of the Western Craton (2.6–2.9 Ga, Sm-Nd model ages; Bickford et al., 1990) and metasedimentary and granitoid rocks of the Virgin River, Mudjatic and Wollaston domains. The granitoids, which were reactivated during the Hudsonian Orogeny, form elongated domes, which are flanked by shelf sedimentary rocks including graphitic, pyritic, and aluminous pelites and semipelites, calc-silicate rocks, banded iron formation, greywackes and volcanic rocks. These basement rocks experienced at least three main deformational events and various grades of metamorphism during early Proterozoic time (Lewry and Sibbald, 1980).

The crystalline Archean and Aphebian basement rocks were subjected to uplift, erosion, weathering and development of regolith prior to deposition of the Middle Proterozoic cover rocks of the Athabasca Group. The Athabasca Group rocks, which compose the Athabasca Basin, consist of fluviatile and marine redbed successions of unmetamorphosed, flat-lying and little disturbed sandstones, siltstones and conglomerates. The sediments were deposited on an intensely weathered surface or, where the regolith had been eroded, on the unaltered basement. Initially there were three northeastward-trending tectonic depressions, the western Jackfish, central Mirror and eastern Cree subbasins, which later coalesced into a single Athabasca basin (Fig. 2). Locally, sedimentation was accompanied by volcanism. The clastic sedimentary rocks underwent diagenetic changes, such as silicification, hematitization, clay alteration, and cementation by carbonates, and in some areas by phosphates. Layers of sulphides and organic substances, such as kerogen, occur locally. During late Proterozoic time, both the basement and cover rocks were intruded by diabase dykes.

The uranium deposits have been discovered in the southeastern, northern and west-central (Saskatchewan) parts of the Athabasca Basin; as demonstrated later in this paper, some uranium occurrences have also been identified in the western (Alberta) part of the basin. The deposits represent two main types of metal assemblages. Some deposits are monometallic (U) and generally occur either below or (rarely) at some distance above the sub-Athabasca unconformity. Others are polymetallic (U-Ni-Co-As) and occur in proximity to the unconformity.

Monometallic unconformity deposits

Deposits with mainly monometallic (solely uranium) mineralization generally occur either in basement rocks or in the upper parts of the Middle Proterozoic sedimentary succession of the Athabasca Basin. For instance, the Rabbit Lake, Eagle Point, Raven, Horseshoe and Dominique-Peter deposits are located within altered basement rocks beneath the unconformity; they are confined to various levels of the Lower Proterozoic succession, such as the Wollaston Group and Peter River Gneiss. The Fond-du-Lac deposit occurs within sandstone in the cover rocks of the Athabasca Basin, some distance above the unconformity. The more recently discovered McArthur River (P2 North) deposit, which consists of monometallic mineralization directly at the unconformity, represents the only known exception.

The principal host rocks of the **Rabbit Lake deposit** are albite-rich rocks, derived apparently from arkosic to semipelitic rocks, which were subjected to sodic metasomatism (producing rocks termed 'plagioclasites' by Sibbald, 1976, 1978; Appleyard, 1984), as well as meta-arkose, calc-silicate and graphitic granulites. The plagioclasites form part of the footwall complex of the deposit. The host rocks also include a unit of partly graphitic semipelite and a layer of dolomite. The metasedimentary sequence has been intruded by granitic rocks.

The **Eagle Point deposit** is hosted by the lower pelitic unit of the Wollaston Group, which consists of quartzofeldspathic gneiss that is locally graphitic, quartzite, and granite pegmatite. This suite unconformably overlies folded Archean granitoid rocks. In the Eagle Point deposit, Andrade (1989) identified: two generations of euhedral uraninite, which belong to the oldest phases of mineralization; three forms of pitchblende (veinlets, coatings and inclusions), which are younger than uraninite and represent the bulk of the mineralization; and minor amounts of boltwoodite and coffinite, which represent the youngest members of the uranium mineral assemblage.

The **Raven and Horseshoe deposits** occur within the quartz-amphibolite unit of the Wollaston Group, which consists of sillimanite meta-arkose, amphibolite, graphitic metapelite and quartzite, calc-silicate rocks, phosphates and sillimanitic quartzite. The metasedimentary succession has been folded into a syncline and intruded by dykes of granite pegmatite. The mineralization is confined mainly to the graphitic quartzite horizon, which is fractured and altered by sericitization, chloritization and argillization.

The **Dominique-Peter deposit**, which is located in the Carswell Structure, is confined to a mylonite zone. This zone is entirely within basement gneisses at a contact between the Peter River Gneiss and the Earl River Gneiss complexes. Most of the mineralization occurs in the mylonitized Peter River Gneiss.

The **Fond-du-Lac deposit** occurs in hematitized, carbonatized and silicified sandstone of the Athabasca Group, about 30 m above the unconformity. The mineralization is composed of a stockwork of steeply dipping fractures and the adjacent porous, coarse grained facies of the sandstone.

The **McArthur River (P2 North) deposit**, which is located about 70 km northeast of the Key Lake deposit (Fig. 2), contains prevailingly monometallic uranium (pitchblende) mineralization just above the sub-Athabasca unconformity and in the footwall of a thrust fault. The mineralized zone has been traced for 1850 m along strike by vertical drillholes. It averages 30 m wide and 7 m thick, but is locally more than 50 m wide and has a vertical thickness of as much as 46 m. The main orebody is located from about 500 to about 600 m below the surface. As of 1992 it was estimated that the deposit contained in excess of 76 000 t of uranium metal in ores grading 3.4 per cent U (Marlatt et al., 1992). The orebody consists of massive pitchblende and very minor amounts of galena, pyrite and chalcopyrite. The basement rocks in the footwall of the orebody consist of quartzite interbedded with garnetiferous and cordieritic gneisses, and are capped by a few metres of chloritic and hematitic regolith. The overthrust basement rocks consist of Aphebian graphitic and sericitic schists, quartzites and minor amounts of pegmatites and calc-silicate rocks. The basement rocks are unconformably overlain by conglomerate and sandstone of the Helikian Athabasca Group. The host rocks are strongly silicified, but otherwise only relatively weakly altered by illite, chlorite, kaolinite, hematite, limonite, siderite and dravite. Except for the silicification, the alteration of the deposit is restricted to a narrow aureole around the orebody. The mineralization has yielded two main U-Pb ages: an older and prevailing age of 1514 ± 18 Ma, and a younger age of 1327 ± 8 Ma (Cumming and Krstic, 1992). The older date represents the oldest known mineralization among the deposits associated with the sub-Athabasca unconformity.

As indicated later in this paper some monometallic occurrences have been identified in the Alberta part of the Athabasca Basin.

Polymetallic unconformity deposits

Deposits of polymetallic (U-Ni-Co-As) composition in the Athabasca Basin occur in proximity to the sub-Athabasca unconformity. Examples include the Key Lake, Cigar Lake, Collins Bay 'A', Collins Bay

'B', McClean, Midwest, Sue and Cluff Lake 'D' deposits (Fig. 2), which occur in the basal part of the Middle Proterozoic Athabasca Group clastic sedimentary sequence and/or the uppermost part of the Lower Proterozoic basement rocks.

The **Key Lake deposit** consists of two orebodies (Gärtner and Deilmann), which occur at the unconformity between the Athabasca Group rocks and the rocks of the underlying Wollaston Group. The deposition of the orebodies was controlled structurally by an intersection of the sub-Athabasca unconformity and a major reverse fault zone. The orebodies occur in proximity to graphitic metapelite layers of the Wollaston Group, which also contains biotite–plagioclase–quartz–cordierite gneiss, garnet–quartz–feldspar–cordierite gneiss, amphibolite, calc-silicate rocks, migmatite and granite pegmatite. The Wollaston Group rocks unconformably overlie Archean granitic rocks, which are exposed in northeastward elongated domal structures. The sedimentary rocks of the Athabasca Group have been subjected to alteration by diagenetic and epigenetic processes. The diagenetic alteration, which is preserved outside the mineralized zone, is characterized by clay alteration of feldspars, corrosion of quartz grains by kaolinite and chlorite, partial bleaching (removal of the original hematite), development of several generations of secondary hematite, and dravitization and carbonatization of the kaolinite matrix. In the immediate vicinity of ore, the Athabasca Group and the basement rocks have been altered to illite, chlorite and kaolinite.

The world's largest high grade uranium deposit, the **Cigar Lake deposit,** (with ores of the world's highest average grade), contains not only polymetallic, but also some monometallic mineralization. Most of the mineralization occurs in clay-altered rocks at the base of the Athabasca Group, immediately at the unconformity (Fig. 7; Fouques et al., 1986). Small amounts of mineralization are contained within altered basement rocks just beneath the unconformity and up to 200 m above the unconformity in fractured Athabasca sediments. The mineralization is present in three assemblages of elements: (i) uranium, nickel, cobalt and arsenic; (ii) uranium and copper; and (iii) uranium alone (Ruzicka and LeCheminant, 1986, 1987; Ruzicka, 1989).

The **Collins Bay 'A' and 'B' zones** occur at the unconformity, partly in clay-altered sedimentary rocks of the Athabasca Group and partly in altered metamorphic rocks of the Wollaston Group, along the Collins Bay Fault.

The **Sue deposits** occur within the Sue structural trend, which consists of a series of faults adjacent to the southwestern margin of the Collins Bay Granitic Dome (Fig. 8). The trend includes a layer of graphitic gneiss within the Aphebian sequence. The mineralization is predominantly polymetallic (U, Ni, Co, As, V, Cu and Pb) and hosted by sandstone, but in part monometallic (U) and hosted by basement rocks. The mineralization occurs in several zones, such as the Sue 'B', Sue 'A', Sue 'C', Sue 'CQ', Sue 'D' and Sue 'E'. The Sue deposits are excellent examples of the consanguinity of the sandstone- and basement-hosted mineralization (Ruzicka, 1992).

As indicated later in this paper, some polymetallic occurrences have been identified in the Alberta part of the Athabasca Basin.

Unconformity deposits in the Thelon and Otish basins

Monometallic deposits

Several monometallic uranium deposits associated with the sub-Thelon unconformity occur in the Kiggavik Trend, which approximately parallels the southeastern margin of the Thelon Basin, Northwest Territories.

The **Kiggavik deposit** represents a large uranium concentration associated with the sub-Thelon unconformity. The deposit occurs in Lower Proterozoic basement rocks, mica-rich nongraphitic quartzo-feldspathic metasedimentary rocks, and unmetamorphosed fluorite-bearing granite (Miller et al., 1984; Fuchs and Hilger, 1989; Ashton, 1988; Henderson et al., 1991; LeCheminant and Roddick, 1991; Dudas et al., 1991). The mineralization lies at an undefined distance below the assumed sub-Thelon unconformity (Fuchs and Hilger, 1989).

In the Otish Basin, Quebec, polymetallic uranium occurrences, such as the **Camie showing**, are associated with an unconformity between the Archean volcanic rocks and the overlying Lower Proterozoic unmetamorphosed Otish Group. Sedimentation in the Otish Group varied from fluvial in the basal Indicator Formation to marginal marine in the overlying Peribonca Formation. The basement and the sedimentary cover rocks have been intruded by gabbroic sills and dykes. Radiometric dating of the uranium mineralization and the associated rocks indicates Hudsonian events in the basin.

Polymetallic occurrences

In the Thelon Basin region, the only known polymetallic uranium occurrence is at **Boomerang Lake**, at the southwestern rim of the basin. The mineralization occurs at the unconformity in altered sandstone of the flat-lying Helikian Thelon Formation and in the underlying graphitic metapelites of the Elk River belt of inferred Early Proterozoic age (Davidson and Gandhi, 1989).

Geochronology of the unconformity deposits

Unconformity-associated uranium deposits in the Athabasca Basin region are hosted by Lower Proterozoic and Middle Proterozoic (Athabasca Group) rocks, the ages of which are bracketed by Archean granitoid units (about 2500 Ma) and by intrusion of diabase dykes of the Mackenzie diabase dyke swarm (U-Pb age of 1267 ± 2 Ma on baddeleyite; LeCheminant and Heaman, 1989). U-Pb analyses of fluorapatites from the Upper Wolverine Point and Fair Point formations of the Athabasca Group indicated at least two distinct ages in the range 1650 to 1700 Ma (Cumming et al., 1987). The mineralization is diagenetic and epigenetic, and formed during several stages.

Older granitic and metasedimentary rocks apparently were an important source of uranium. Archean granitic plutons containing above normal contents of uranium occur in the vicinity of most deposits. Uraninite-bearing pegmatites and metasedimentary rocks (U-Pb age >2.2 Ga; Robinson, 1955) are present in the Beaverlodge area, a short distance to the north of the Athabasca Basin. Hudsonian felsic intrusive rocks, and particularly their pegmatitic derivatives, are abundant, for instance, in the source area for the Manitou Falls Formation that surrounds the Key Lake deposits. Ray (1977, p. 22) speculated that "the initial Aphebian sedimentation under anaerobic conditions could have produced suitable conditions for syngenetic concentration of uranium within the basal pelites; these may have formed a source for some uranium deposits in northern Saskatchewan". Ramaekers (1981) considered the Athabasca Group sedimentary rocks as the immediate source for uranium found in the unconformity deposits at their base.

Numerous age determinations have indicated that the bulk of the ores in this region were formed and/or reworked during the period between 1.4 and 0.8 Ga (Cumming and Rimsaite, 1979; Worden et al., 1985). However, more recently, Cumming and Krstic (1992) presented results of geochronologic studies on a number of uranium deposits from the Athabasca Basin, including the major deposits at Collins Bay, Cigar Lake, Dawn Lake, Eagle Point, Midwest, Rabbit Lake and McArthur River, and concluded that "almost all the deposits formed in a restricted time interval between about 1330 and 1380 Ma. . . The one major exception is the recently discovered NiAs-free deposit at McArthur River, for which a well-determined age of 1514 ± 18 Ma (2σ) has been obtained" (Cumming and Krstic, 1992, p. 1623). Remobilization and redeposition of the mineralization took place at about 1070 Ma, 550 Ma and 225 Ma (op. cit.). The main 1330 to 1360 Ma stage of mineralization corresponds to the age of 1326 ± 10 Ma published earlier by Ruzicka and LeCheminant (1986) for ore from the main pod of the Cigar Lake deposit. Other age determinations also fall close to the main mineralization stage established by Cumming and Krstic (1992). For example, U-Pb isotope analyses for 26 anisotropic uraninites from the Key Lake deposit, done at the Institut für Geowissenschaften und Rohstoffe in Germany, yielded a slightly older age of crystallization for uraninite of 1386 ± 4 Ma (FIGNR, 1989).

A Rb-Sr isochron age of 1477 ± 57 Ma was obtained for illites from various deposits associated with the sub-Athabasca unconformity (Kotzer and Kyser, 1990b). This age apparently reflects the beginning of the diagenetic-hydrothermal ore-forming process that led to the accumulation of uranium and associated metals.

In the Thelon Basin, U-Pb isotope dating on ores in the Kiggavik deposit suggests three mineralization events: the oldest at 1400 Ma, a later one at about 1000 Ma, and a rejuvenation of mineralization at 10 Ma (Fuchs and Hilger, 1989). The mineralization thus postdates the deposition of the Thelon Formation, for which a minimum U-Pb age of 1720 ± 6 Ma was obtained by Miller et al. (1989) by dating uraniferous phosphate minerals that cement sedimentary units within the Thelon Basin, which is lithostratigraphically correlative with the Athabasca Basin. The mineralization associated with the sub-Thelon unconformity has been discussed by Miller (1983) and Miller et al. (1984).

Mineralogical features of the unconformity deposits

Ores of the monometallic deposits, such as Rabbit Lake and Eagle Point, consist of pitchblende (in massive, globular and sooty forms), coffinite and, locally, secondary uranium minerals such as boltwoodite, sklodowskite and kasolite. Carbonates (calcite, dolomite, siderite), sericite, chlorite, clay minerals (illite, kaolinite), celadonite and tourmaline (dravite) are common gangue minerals.

The polymetallic ores, such as those of the Key Lake, Cigar Lake, Collins Bay 'B' and Midwest deposits, consist of: several generations of pitchblende and coffinite; arsenides and sulpharsenides of nickel and cobalt; sulphides of nickel, copper, lead, molybdenum, iron and zinc; and oxides and hydroxides of iron. Silver, gold and platinum group minerals occur locally. Chlorite, illite, kaolinite and siderite are the most common gangue minerals.

Some deposits of the polymetallic subtype (e.g., Cigar Lake) have vertically zoned mineral assemblages. U-Ni-Co-Ag-As assemblages at the unconformity locally grade upward into a zone with the U-Cu assemblage, whereas monometallic uranium is found in upper and lower extremities of the orebodies. The zonal arrangement of these assemblages suggests that they are contemporaneous and are apparently related to the geochemical mobilities of individual elements and stabilities of the minerals.

The proportions of metals in ores of the polymetallic subtype differ from one deposit to another. In the Key Lake ores, the contents of the principal constituents, uranium and nickel, are 1:0.55 (A. de Carle, pers. comm., 1986); whereas in the ores of the main pod of the Cigar Lake deposit, the contents of these metals are 1:0.078 (Fouques et al., 1986).

Pitchblende is the principal uranium mineral in deposits of both the monometallic and polymetallic types. A crystalline variety of pitchblende (alpha-triuranium heptaoxide - U_3O_7 - tetrauraninite) has been identified in some deposits (e.g., Key Lake, Cigar Lake and Eagle Point). Coffinite is another common uranium mineral. Locally, thucholite and uranoan carbon are present as veinlets, globules and lenses. Thorium-bearing uraninite, brannerite and U-Ti mineral aggregates are much less common. Secondary uranium minerals are present in some deposits, even at depths exceeding 100 m (e.g., in the Eagle Point and Rabbit Lake deposits). They include uranophane, kasolite, boltwoodite, sklodowskite, becquerelite, vandendriesscheite, woelsendorfite, tyuyamunite, zippeite, masuyite, bayleyite and yttrialite (Ruzicka, 1989). Minerals of nonradioactive metals occur in relatively large quantities in the polymetallic subtype, but minor amounts are also present in the monometallic subtype. Nickeline and rammelsbergite are the most common arsenides. Skutterudite, pararammelsbergite, safflorite, maucherite and modderite occur locally. Gersdorffite is the most common representative of the sulpharsenides. Cobaltite, glaucodot and tennantite are relatively rare. Chalcopyrite, pyrite and galena are the most common sulphides; others include bornite, chalcocite, sphalerite, marcasite, bravoite, millerite, jordisite, covellite and digenite. Some deposits contain selenides, such as clausthalite, freboldite, trogtalite and guanajuatite. Tellurides, such as altaite and calaverite, occur in some deposits in the Carswell Structure. Locally, native metals such as gold, copper, and arsenic accompany the uranium mineralization. A detailed list of ore-forming minerals in individual deposits has been given by Ruzicka (1989).

The unconformity uranium deposits in the Athabasca Basin represent the world's richest and largest uranium orebodies. The deposits formed at redox fronts, similar to the deposits in Phanerozoic sandstones. However, whereas the Phanerozoic deposits formed at mobile redox fronts and their mineralization was subjected to local dispersion, the unconformity deposits formed at stationary redox fronts by accretion and their clay envelope protected them from destruction.

METALLOGENY OF THE ALBERTA PART OF THE ATHABASCA BASIN

Previous work

Geological investigations related to northeastern Alberta's potential for mineral deposits (e.g., Cameron, 1930; Godfrey, 1958, 1960, 1961; Godfrey and Peikert, 1963, 1964; Godfrey and Watanabe, 1964) initially were focused mainly on the exposed parts of the pre-Athabasca basement rocks. Discoveries of uranium deposits associated with the sub-Athabasca unconformity in Saskatchewan in the late 1960s triggered interest in exploration for mineral deposits and studies of mineral potential also in the Alberta part of the Athabasca Basin. Exploration for mineral deposits in the area was conducted by several companies, including Eldorado Nuclear Limited, Norcen Energy Resources Limited, Matagami Mines Limited, National Nickel Limited, and Uranerz Exploration and Mining Limited. Results of the exploration projects are contained in numerous assessment reports submitted to Alberta Energy and the Alberta Geological Survey, respectively. Studies of mineral potential for the Alberta part of the Athabasca Basin are contained in papers, such as those by Wilson

(1985, 1986, 1987), Edwards et al. (1991), Ruzicka (1993a) and Olson et al. (1994).

Methods of metallogenic investigations

Metallogenic investigations of the Alberta part of the Athabasca Basin for this study consisted of the writer's geological observations in the field, interpretation of previous geophysical and geochemical surveys conducted by the Geological Survey of Canada and by exploration companies, and examination of available mining company drillcores, deposited at the Alberta Geological Survey in Edmonton. In addition to geological data collected by the writer during the period from 1969 to 1991, the current studies included: 2687 gamma-ray spectrometric assays for total radioactivity, potassium, uranium and thorium; geological examination of 631 rock samples; and 16 984 geochemical analyses for 28 chemical constituents from the collected samples. The recent investigations funded by the Alberta Mineral Development Agreement were focused on the extension of previous studies, particularly those made by Wilson (1985, 1986, 1987) and by Edwards et al. (1991), and of results from exploration conducted by the mining industry in Alberta. The metallogenic research was oriented toward interpretation of processes leading to the evolution of mineral endowment and to the formulation of criteria applicable by the industry to exploration for uranium polymetallic and monometallic deposits.

Because the uranium mineral resources of the Saskatchewan part of the Athabasca Basin play an important role in the Canadian economy, special attention has been paid to investigations into whether or not the metallogenic observations on the Alberta part of the Athabasca Basin are compatible with the metallogenic features known from the Saskatchewan part of the basin.

In addition to the main study area 'A' in Alberta (Fig. 2), two control areas in the Saskatchewan part of the Athabasca Basin (Fig. 2) have been selected for the comparative study: area 'B', which is located in the proximity of the Key Lake deposit; and area 'C', which is located in the vicinity of the Cigar Lake deposit. The main principle of this comparative research was to proceed from known criteria scientifically established for the well-explored part of the Athabasca basin, to interpretation of metallogenic observations of the less explored, Alberta part of the basin. A preliminary comparison between the Alberta and Saskatchewan parts of the basin was reported during the earlier phase of the study (Ruzicka, 1993a).

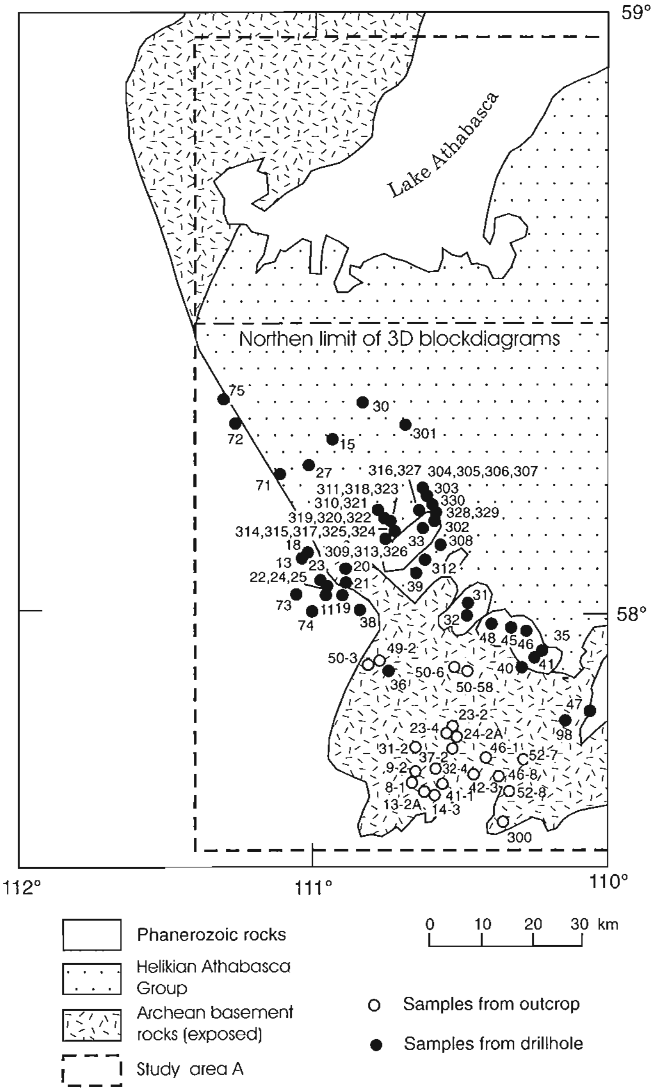

Figure 13. Index map of study area 'A', northeastern part of Alberta. See Table 4 for coordinates and other attributes of drillholes 301 to 330 (data from assessment files, Alberta Geological Survey, Edmonton, Alberta). For coordinates of the other drillholes and outcrops see Wilson (1985, p. 48-50).

General geology of the study area in Alberta

The area selected for the study (designated as area 'A' in Fig. 2) includes an approximately 500 m thick section of the westernmost part of the Athabasca Basin and its immediate vicinity (Fig. 13). This area is a part of the Churchill Structural Province and consists of Archean and Aphebian basement, Helikian Athabasca Group and Devonian sedimentary rocks.

On the basis of drillcore examination of basement rocks, Wilson (1986) distinguished four groups of granitoid rocks, two groups of mylonitic rocks, a group of metamorphic rocks, and pegmatites. The granitoid rocks include: (i) Wylie Lake granitoid, which consists of sericitized plagioclase, alkali feldspar, quartz and biotite with minor amounts of clinopyroxene, apatite, muscovite, zircon and carbonate veinlets; (ii) Fishing Creek granitoid, which could be classified as tonalite to granodiorite, and consists of quartz, plagioclase and biotite; (iii) alkali feldspar-rich granitoid, which consists of alkali feldspar, plagioclase and minor amounts of biotite, quartz and garnet; and (iv) grey foliated granitoid, which consists of quartz, alkali feldspar and plagioclase in a matrix of biotite and garnet. The mylonitic rocks are of two types: (i) felsic mylonites, which are apparently derived from granitoid rocks; and (ii) mafic mylonites, which are probably derived from granite gneiss or metasedimentary rocks. In addition, the basement rocks locally include garnet/cordierite gneiss, amphibole-plagioclase gneiss, amphibolite, graphitic metapelites, granite pegmatite and graphitic/pyritic pelitic gneiss.

Layers of graphitic and pyritic metamorphosed pelitic rocks are an important part of the conceptual genetic model for the unconformity deposits of the Athabasca Basin. Zones of graphitic and pyritic pelitic gneisses were identified in several samples of basement rocks from the study area (e.g., in samples from drillholes 302, 306, 311, 318, 323, 327, and 330; Fig. 13; Table 4). The distribution of graphite and pyrite in samples of pelitic gneiss from drillhole 302 is apparent on S.E.M. images (Plates 1a, b). The samples were collected from a drillcore about 5 m below a lens of massive pitchblende.

The basement rocks in Alberta are unconformably overlain by unmetamorphosed sedimentary rocks of the Athabasca Group (Wilson, 1985, 1986). The Athabasca Group has been divided by Wilson (1985) into the Fair Point, Manitou Falls, Wolverine Point, Locker Lake and Otherside formations from base to top. Ramaekers (1990), however, classified the basal part of the Wolverine Formation of Wilson (1985) as the Lazenby Lake Formation (Ramaekers, 1990, p. 13). Drill core observations made during the present studies confirm the presence of the Lazenby Lake Formation as far west as longitude 110°40′W. The basal Fair Point Formation consists mainly of hematitic, clay-rich, coarse fluviatile sandstone in a generally fining-upward sequence. The Manitou Falls Formation is made up of medium size, massive to crossbedded, weakly hematitic sandstone; the Lazenby Lake Formation consists of mainly coarse ferruginous sandstone.

The basement and the sedimentary cover rocks of the study area are locally altered. Typical regolith (or saprolite) at the top of the basement rocks was reported by Wilson (1985). During this study, chloritic, illitic and kaolinitic alterations were observed on core from several drillholes (e.g., from drillholes 301, 302, 306 and 308; Fig. 13; Table 4). Diagenetic and epigenetic alterations due to magnesian and ferroan metasomatism of authigenic carbonates are typically associated with unconformity deposits in the Athabasca Basin and Pine Creek Geosyncline, Australia. In the study area, variable magnesium and iron ratios were observed in zoned authigenic carbonates from sandstones of the Lazenby Lake Formation (Plates 1c, d). The samples were collected about 150 m above a lens of massive pitchblende.

General geology of the control areas in Saskatchewan

Control area 'B' (Key Lake) includes two orebodies (Gärtner and Deilmann), which formed at the unconformity between the Athabasca Group rocks and the rocks of the underlying Wollaston Group (Fig. 2). The deposition of the orebodies was controlled structurally by the intersection of the sub-Athabasca unconformity and a major reverse fault zone. The orebodies occur in both the Athabasca Group and the underlying basement rocks. The basement rocks are part of the Wollaston Group, which contains biotite–plagioclase–quartz–cordierite gneiss, garnet–quartz–feldspar–cordierite gneiss, amphibolite, calc-silicate rocks, migmatite, granite pegmatite and graphitic/pyritic metapelite layers. The Wollaston Group rocks, which are capped by regolith, overlie Archean granitic rocks, which are exposed in northeastward elongated domal structures. The sedimentary rocks of the Athabasca Group, which are represented by a thick section of Manitou Falls Formation at its base, have been subjected to alteration by diagenetic and mineralization processes. The diagenetic alteration, which is preserved outside the mineralized zone, is characterized by clay alteration of feldspars, corrosion of quartz grains by kaolinite and chlorite, partial bleaching (removal) of the original hematite, development of several generations of secondary hematite, and dravitization and carbonatization of the kaolinite matrix. In the immediate vicinity of ore, the Athabasca Group and the basement rocks are altered to illite, chlorite and kaolinite. As an average standard for area 'B', a core from the drillhole DP3A, which was located in the immediate vicinity of the Deilmann ore body and intersected both the Athabasca Group and basement rocks, was included in the study.

Control area 'C' (Cigar Lake) includes a part of the Athabasca Basin in the immediate vicinity of the Cigar Lake deposit (Fig. 2). It is made up of basement rocks, which consist of Archean granite gneiss and Aphebian metasedimentary rocks. The gneiss forms a large elongated structure, the Swanson Dome. The basement rocks, which are capped by regolith, are unconformably overlain by unmetamorphosed sedimentary rocks of the Athabasca Group, which are represented by a thick section of Manitou Falls Formation at its base. As an average standard for area 'C', a core from the drillhole Q27B-29, which was located at Natona Bay and intersected both the Athabasca Group and basement rocks, was included in the study.

In addition, some metallogenic features of area 'A' (Alberta) have been compared with those from the Cluff Lake and Maurice Bay deposits of Saskatchewan. The Cluff Lake deposits occur in the southern part of the Carswell Structure (Fig. 2) and the Maurice Bay deposit is located on the north shore of Lake Athabasca, near the Saskatchewan-Alberta border.

Lithogeochemical features of the study area, Alberta

In order to investigate the geochemical background of rocks in study area 'A', analyses for 28 elements from 548 samples from 30 drillholes (301-331; Fig. 13; Table 2) from the basement and sedimentary cover rocks were examined. The analytical values of these elemental constituents were compared with their corresponding clarke values (average crustal abundance; clarke values quoted in this paper are from Rickwood, 1983). The comparison was made for their mean and peak contents in the samples and compiled in Figures 14a to d.

The scattergram for the mean elemental contents of the basement rocks (Fig. 14a) indicates that they contain distinctly higher amounts of As (789 times!), Ni (16.8 times), Cd (8 times), B (7.7 times), Th (7 times), Mo (6.7 times), and U (5.9 times) than the crustal rocks (clarke values). The enrichment in some elements is even more apparent on the histogram for the peak values (Fig. 14b). Peak values for arsenic are more than 200 000 times(!), Ni more than 4000 times, U more than 600 times, Mo 298 times, B 170 times, Th 130 times, Y 78 times, Cd 47 times, and P 40 times the corresponding clarke values. High contents of phosphorus (in disseminated apatite and in monazite and yttrium phosphate) in pelitic basement rocks were found in the vicinity of uranium mineralization in drillholes 307 (Plate 1e), 308 (Plate 1f) and 303, where monazite is intimately intergrown with chalcopyrite (Plate 2a). The pelitic basement rocks commonly contain native (radiogenic) lead and its oxide (e.g., in drillhole 302; Plates 2b, c).

The histogram for the mean elemental contents of the sedimentary cover rocks (Fig. 14c) indicates that they contain distinctly higher amounts of As (14 times), Cd (more than 10 times), B (more than 10 times), Mo (more than 4 times), Th (3 times), Cr (2 times), and U (about 2 times) than the crustal rocks (clarke values). The peak enrichments of some elements (Fig. 14d), such as As (more than 1400 times), B and Cd (140 times), Pb (more than 90 times), Th (more than 80 times), U (more than 70 times), P (more than 40 times), Mo (more than 30 times), Ni (17 times) and Cr (more than 12 times), are apparent from the scattergram for the peak values. Abundant nickel arsenides (nickeline) associated with anhydrite have been identified in the Fair Point Formation in drillhole 306, about 3 m above a lens of massive pitchblende (Plate 2d).

In order to investigate relationships among the elemental constituents, the data for the same group of elemental constituents were analyzed by a statistical correlation method (Table 3). Within 15 512 analyses, strong correlations were found, particularly between Ni and As (1.000!), Ni and Co (0.982), Co and As (0.982), U and Ni (0.968), U and As (0.968), U and Co (0.953), Zn and Co (0.908), Ni and Zn (0.897), Zn and As (0.896), U and Zn (0.878), Mo and Co (0.860), Mo and As (0.846), Ni and Mo (0.846), U and Mo (0.824), and Mo and Zn (0.761).

For a visual demonstration of the statistical relationships within the lithogeochemical analytical data, selected elements (excluding oxides of Al, Fe, Ca, Mg, K, Na, P, Mn and Ti) have been treated using factor analysis. As the Unrotated Factor Plot (Fig. 15) indicates, a group of U, Ni, As, Co, Mo and Zn forms a distinct cluster, which is clearly separated from the remaining elemental constituents in the samples.

The very high correlation coefficients between Ni and As, Ni and Co, and Co and As, are also evident in the presence of discrete authigenic minerals in the rocks in which these elements occur, namely

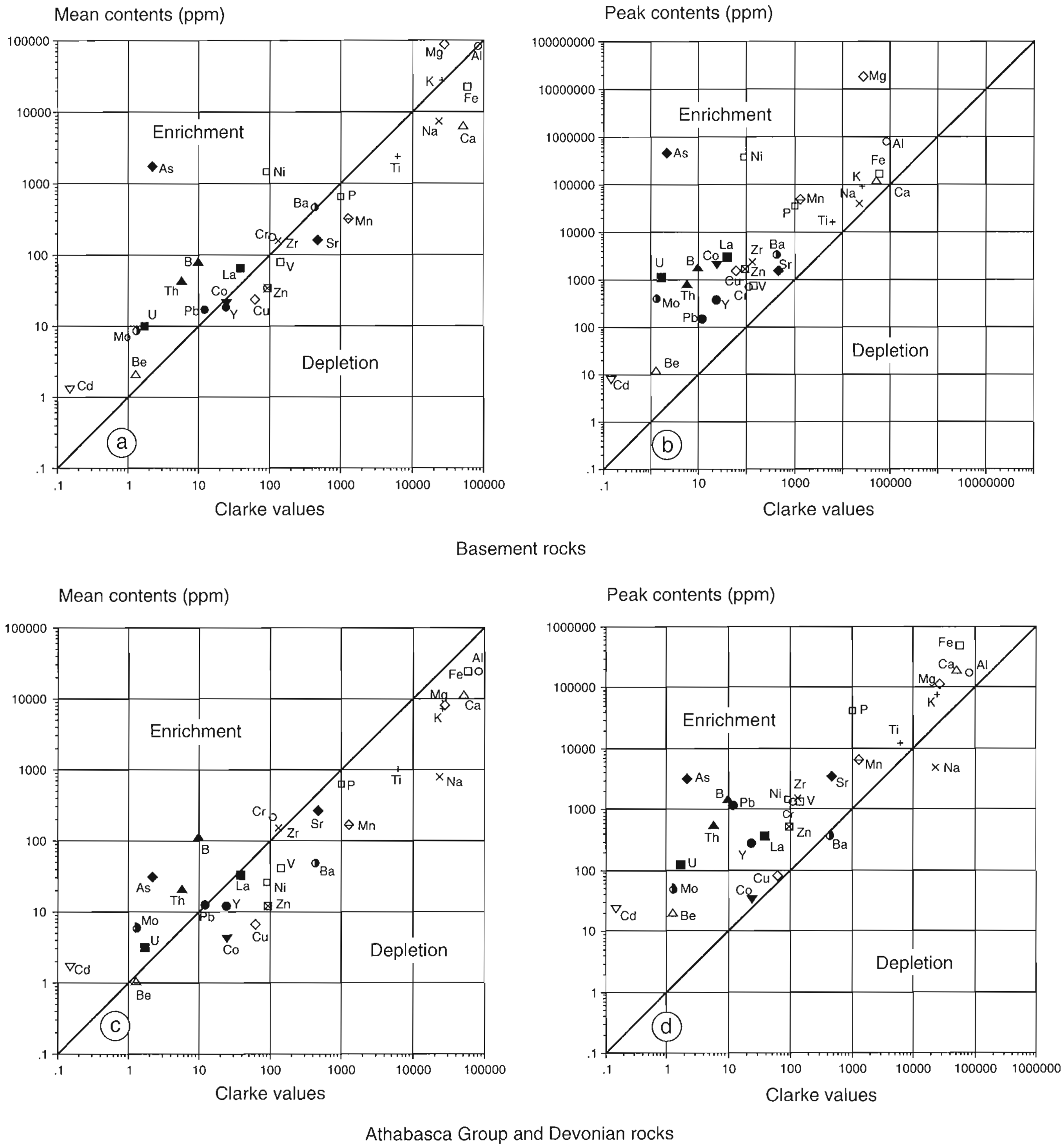

Figure 14. *Comparison between contents of elemental constituents in samples (n = 554) from the basement and sedimentary cover rocks in the Alberta part of the Athabasca Basin, with corresponding values of their crustal abundance. Vertical axes refer to the contents of elemental constituents. All data are in ppm. Scattergrams:* ***a.*** *mean contents in the basement rocks (n = 267);* ***b.*** *peak contents in the basement rocks (n = 267);* ***c.*** *mean contents in the sedimentary cover rocks (n = 287);* ***d.*** *peak contents in the sedimentary cover rocks (n = 287).*

Table 2

Summary table of geochemical analyses of samples from the study area (localities of drillhole 301-331; Fig. 13; Table 4), and the control areas (localities of drillholes S1 and S2; Fig. 13). Samples from localities 301 to 309, S1 and S2 were collected by the author; data for localities 310 to 331 are from Assessment Files, Alberta Geological Survey, Edmonton; and data for localities 13 to 75 are from Wilson (1986). Analyses of oxides in %; all other analyses in ppm

Locality	Analyses	Al2O3	Fe2O3	CaO	MgO	K2O	Na2O	Pb	U	B	As	Mo	P2O5	Zn	Cd	Co	MnO	Cr	V	Be	Cu	TiO2	Zr	Y	La	Th	Sr	Ba	Ni
313	n	10	10	10	10	10	10	10	10	10	10	10	10	10	10	10	10	10	10	10	10	10	10	10	10	10	10	10	10
	mean	12.73	2.72	0.81	0.57	1.62	0.243	9.6	6.1	79	3.6	5.5	0.93	9.5	1	11.3	0.012	154	38	2.2	13.2	0.36	151	48.1	46	26.1	359	184	13
	st. dev.	7.14	2.27	2.1	1.02	1.72	0.449	13.8	13	34	1.4	1.6	2.53	6.9	0	13.6	0.027	118	40	2.1	24.7	0.25	50	119.6	25.8	11.4	300	359	16
314	n	10	10	10	10	10	10	10	10	10	10	10	10	10	10	10	10	10	10	10	10	10	10	10	10	10	10	10	10
	mean	8.94	1.94	3.57	3.45	1.74	0.136	4.7	2.2	58	1.3	5	0.11	8.2	1	7.2	0.012	172	24	1.5	6.4	0.17	227	5	72.5	52.9	170	236	16
	st. dev.	6.74	2.01	3.82	2.44	2.06	0.162	3.7	1.5	44	1.6	0	0.14	7	0	5.7	0.011	49	23	1.3	2.3	0.14	430	3.6	151.1	110.8	301	585	14
315	n	8	8	8	8	8	8	8	8	8	8	8	8	8	8	8	8	8	8	8	8	8	8	8	8	8	8	8	8
	mean	13.97	2.44	0.09	2.05	1.59	0.194	5.5	2.2	96	4.6	5.9	0.08	8.8	1	12	0.005	218	34	1.8	6.4	0.47	189	9	64.5	36.8	203	187	30
	st. dev.	8.98	2.16	0.06	4.38	1.43	0.131	4.2	0.8	56	2.4	1.6	0.05	7.2	0	15	0.007	75	43	0.7	2.3	0.75	55	5	42.3	28	141	380	55
316	n	13	13	13	13	13	13	13	13	13	13	13	13	13	13	13	13	13	13	13	13	13	13	13	13	13	13	13	13
	mean	10.91	2.72	0.09	1.05	2.21	0.225	6.3	4.8	75	2.6	5.8	0.11	9.5	1.4	9.1	0.004	212	62	1.7	9.8	0.39	377	13.2	106.5	70.4	312	268	13
	st. dev.	6.83	3.34	0.09	1.54	1.84	0.133	4.5	5.1	41	2	1.3	0.08	8	1.4	7.9	0.005	87	88	1.4	5.5	0.47	624	17.8	157.7	133.5	227	402	10
317	n	9	9	9	9	9	9	9	9	9	9	9	9	9	9	9	9	9	9	9	9	9	9	9	9	9	9	9	9
	mean	7.75	1.36	4.92	4.96	1.86	0.21	4.2	4	94	2.1	5.2	0.09	13.6	1	7.1	0.011	237	30	1.4	9.1	0.17	114	8.9	63.7	19	53	154	19
	st. dev.	6.8	0.7	4.87	2.32	1.4	0.071	5.3	2.3	54	2.4	0.4	0.14	5.1	0	4.5	0.005	91	36	0.5	3	0.23	32	6.6	135.3	12.4	19	273	12
309	n	22	22	22	22	22	22	22	22	22	22	22	22	22	22	22	22	22	22	22	22	22	22	22	22	22	22	22	22
	mean	14.24	5.33	0.62	1.75	2.6	1.027	16.9	3.5	37	2	6.9	0.19	58	1	17	0.041	240	70	2.6	37.3	0.59	185	26.4	74.3	31.3	136	493	25
	st. dev.	4.42	2.41	0.69	1.65	1.78	0.868	13.5	5.3	26	2.7	3.2	0.52	47	0	10.8	0.032	97	46	2.1	57	0.37	71	27.1	132.2	62.5	121	435	18
318	n	10	10	10	10	10	10	10	10	10	10	10	10	10	10	10	10	10	10	10	10	10	10	10	10	10	10	10	10
	mean	8.26	2.54	2.6	3.52	0.66	0.186	6.4	2.5	117	3.7	6.6	0.09	10.2	1.1	9.6	0.007	264	83	1.8	9.2	0.35	138	17.5	32.1	14.5	102	42	21
	st. dev.	7.19	4.31	5.28	5.01	0.46	0.068	3.9	1.5	106	4.8	2.3	0.1	9.6	0.3	21.3	0.009	89	207	2.5	7	0.82	70	26.7	25.6	13.2	68	34	24
319	n	17	17	17	17	17	17	17	17	17	17	17	17	17	17	17	17	17	17	17	17	17	17	17	17	17	17	17	17
	mean	16.87	2.45	0.68	182.86	2.87	0.285	30.8	11	278	15.5	10.4	0.16	55.4	1.4	15.1	0.007	183	125	2.8	16.3	0.54	390	44.3	56.1	31.6	451	251	179
	st. dev.	10.25	2.58	1.52	734.73	3.27	0.13	36.9	11.3	381	17	18.8	0.2	81.5	0.9	16.2	0.01	104	181	2.7	32	0.53	404	37.7	59.6	28.2	676	666	218
320	n	23	23	23	23	23	23	23	23	23	23	23	23	23	23	23	23	23	23	23	23	23	23	23	23	23	23	23	23
	mean	9.91	3.21	1.09	1.07	3.65	1.278	18.5	2.7	47	3.7	5	0.08	11.2	1.7	6.3	0.27	299	13	1.1	11.6	0.14	147	7.8	45.2	45.1	138	390	11
	st. dev.	5.16	6.61	1.53	1.14	2.45	1.107	14.5	1.8	53	6	0.2	0.08	7.5	2.9	4.9	1.249	245	10	0.3	11.8	0.08	57	7.1	31	29.9	177	388	9
310	n	31	31	31	31	31	31	31	31	31	31	31	31	31	31	31	31	31	31	31	31	31	31	31	31	31	31	31	31
	mean	10.14	4.52	0.78	1.32	3.75	0.777	14.4	2.9	96	2.8	5.6	0.11	32.2	2.4	5.6	0.031	293	86	2.2	13.7	0.2	171	15.1	44	32.9	464	210	10
	st. dev.	5.22	9.96	1.78	1.49	2.45	1.012	9.3	2.4	90	4.2	1.5	0.15	91.5	4.4	5.8	0.063	147	251	3.2	10.9	0.3	191	18.5	72.5	51.4	781	207	6
321	n	24	24	24	24	24	24	24	24	24	24	24	24	24	24	24	24	24	24	24	24	24	24	24	24	24	24	24	24
	mean	9.4	1.54	0.3	0.59	3.82	1.174	24	3.6	37	1.2	6.3	0.06	12.4	1	4.6	0.007	272	10	1.2	26.9	0.14	171	8.7	42.2	39.7	136	438	6
	st. dev.	4.82	0.69	0.3	0.49	2.84	1.043	18	3.3	35	1.7	2.3	0.02	12	0	2.9	0.006	100	5	0.4	74.5	0.06	41	4.3	19.1	23.8	85	434	2
322	n	12	12	12	12	12	12	12	12	12	12	12	12	12	12	12	12	12	12	12	12	12	12	12	12	12	12	12	12
	mean	8.14	2.17	1.03	2.32	1.3	0.228	5.2	2.5	49	3	5.1	0.12	16.1	1	7.6	0.009	304	40	1.4	9.8	0.2	138	24.8	26.3	8.9	138	245	26
	st. dev.	6.97	1.04	2.98	2.23	1.69	0.108	3.5	1.9	29	2.9	0.3	0.11	19.7	0	5.4	0.01	173	30	0.7	9.8	0.16	55	49.4	18	7.1	137	660	15
323	n	12	12	12	12	12	12	12	12	12	12	12	12	12	12	12	12	12	12	12	12	12	12	12	12	12	12	12	12
	mean	9.75	2.01	2.53	3.04	0.74	0.255	14.9	5.3	65	6.3	5	0.19	10.8	1	19.7	0.01	251	76	1.9	9	0.22	205	14.2	45.2	145.4	325	76	70
	st. dev.	7.27	1.37	4.93	5.08	0.76	0.107	11.3	5.9	51	9.6	0	0.26	14.7	0	33	0.013	165	170	1.8	7.3	0.22	190	15.6	55.9	247.1	607	89	190
311	n	9	9	9	9	9	9	9	9	9	9	9	9	9	9	9	9	9	9	9	9	9	9	9	9	9	9	9	9
	mean	8.02	2.03	2.12	3.01	0.93	0.263	5.9	3.1	52	2.1	5.2	0.16	12.4	1.1	8.6	0.013	298	42	1.8	10.1	0.35	196	47.7	40.2	30.7	209	188	37
	st. dev.	6.67	1.8	5.73	3.92	1.12	0.138	5.3	2.5	47	1.2	0.7	0.26	16.6	0.3	6.6	0.022	114	37	1.1	14	0.24	117	87.1	26.9	30.5	151	370	38
324	n	12	12	12	12	12	12	12	12	12	12	12	12	12	12	12	12	12	12	12	12	12	12	12	12	12	12	12	12
	mean	9.22	6.04	1.16	2.46	1.08	0.395	10.6	2.3	46	4.7	5.4	0.37	21.7	1.8	16.8	0.024	286	118	1.2	14.6	0.37	138	15.9	48.8	39.8	220	168	30
	st. dev.	5.45	6.79	1.92	3.3	1.3	0.558	14.4	1.1	37	5.8	1.4	0.56	25.1	1.9	18.7	0.034	153	131	0.5	18.7	0.38	77	15.6	42	41.6	247	266	29
325	n	12	12	12	12	12	12	12	12	12	12	12	12	12	12	12	12	12	12	12	12	12	12	12	12	12	12	12	12
	mean	11.57	5.11	6.22	9.18	1.96	0.399	8.3	3.8	58	1.1	5.3	0.11	18.4	1.7	20.9	0.022	159	107	1.5	10.9	0.66	102	17.9	38.3	28.7	94	184	34
	st. dev.	7.23	6.29	8.92	5.12	1.32	0.364	6.9	3.7	53	2.3	1.2	0.11	13.7	1.4	26.8	0.017	105	99	0.8	12	0.74	56	15.2	58.1	56.2	58	183	22
312	n	13	13	13	13	13	13	13	13	13	13	13	13	13	13	13	13	13	13	13	13	13	13	13	13	13	13	13	13
	mean	9.47	2.2	6.04	5.05	1.98	0.405	9	3.3	86	1.2	5.4	0.09	16.5	1.1	6.5	0.015	237	35	1.2	9.8	0.18	93	12.6	25.4	33.9	90	152	18
	st. dev.	6.84	1.1	6.06	3.83	1.04	0.735	14.2	2.4	71	0.8	1.4	0.06	11.7	0.3	7.4	0.011	93	46	0.6	11.9	0.16	52	18.7	29.5	70.9	67	253	13
326	n	20	20	20	20	20	20	20	20	20	20	20	20	20	20	20	20	20	20	20	20	20	20	20	20	20	20	20	20
	mean	19.23	2.96	2.72	1.6	2.66	2.356	17.8	4	49	2	5.9	0.15	37.4	1.5	10.9	0.032	213	33	2.3	10.2	0.38	170	13.1	58.8	33.4	220	715	13
	st. dev.	30.66	1.78	3.99	2.77	1.28	1.876	10.4	2.6	68	3.6	2.1	0.1	30.9	1	6.2	0.025	43	35	1.5	6.3	0.26	62	8.6	39.2	43.1	159	650	9
327	n	13	13	13	13	13	13	13	13	13	13	13	13	13	13	13	13	13	13	13	13	13	13	13	13	13	13	13	13

Table 2 (cont.d')

	mean	9.72	2.13	0.57	1.44	1.34	0.38	16.4	3.2	88	2.1	5.5	0.09	18.6	1	7.8	0.01	330	38	1.6	11.8	0.27	131	13.7	43.1	21	190	181	24
	st. dev.	10.14	1.15	1.17	1.58	1.36	0.703	19.8	3.2	45	1.5	1.3	0.04	21.8	0	3.8	0.016	131	24	1	20.4	0.2	54	7.9	41.3	21.9	104	201	15
328	n	14	14	14	14	14	14	14	14	14	14	14	14	14	14	14	14	14	14	14	14	14	14	14	14	14	14	14	14
	mean	7.26	0.81	0.29	1.49	1.12	0.317	12.9	3.7	78	4.3	8.1	0.13	7.4	1.1	5.6	0.004	268	20	1.3	6.9	0.2	119	7.1	62.7	30.6	526	109	21
	st. dev.	6.31	0.38	0.72	1.65	1.24	0.69	10.1	4.1	44	4.7	2.3	0.1	3.3	0.3	2.6	0.004	100	9	0.6	4.2	0.18	62	4.8	72.2	44	540	213	20
329	n	15	15	15	15	15	15	15	15	15	15	15	15	15	15	15	15	15	15	15	15	15	15	15	15	15	15	15	15
	mean	5.51	0.91	0.13	0.2	0.94	0.297	91.3	10.9	57	2.5	7	0.1	11.2	1	4.1	0.003	348	37	1.3	6.5	0.08	131	12.1	42.7	14.9	346	68	10
	st. dev.	5.78	0.95	0.32	0.21	1.26	0.65	297.5	31.6	28	3.9	2.2	0.17	18.6	0	2.1	0.004	118	69	1	8.4	0.07	161	25	90	12.2	642	165	8
330	n	19	19	19	19	19	19	19	19	19	19	19	19	19	19	19	19	19	19	19	19	19	19	19	19	19	19	19	19
	mean	6.14	3.36	0.39	1.56	0.77	0.325	8.4	2.5	57	5.8	7.5	0.18	10.9	1.2	18.6	0.009	374	35	1.4	24.5	0.15	122	10.2	22.9	14.5	139	262	25
	st. dev.	6.26	3.45	0.59	1.73	1.15	0.553	14.6	1.7	28	14.3	7.2	0.21	10.6	0.4	52.6	0.012	163	49	0.8	81.8	0.17	56	7.5	20.4	12.5	113	774	25
301	n	70	70	70	70	70	70	70	70	70	70	70	70	70	70	70	70	70	70	70	70	70	70	70	70	70	70	70	70
	mean	7.71	7.8	0.46	1.02	1.27	0.092	6	3.4	127	2	5.2	0.3	13.8	2.3	3.3	0.06	52	88	1.2	4.7	0.25	146	10.1	74.9	15.3	207	164	15
	st. dev.	7.62	12.63	1.54	1.62	2.02	0.113	12.6	8.5	110	3.7	0.8	1.18	29.1	3.5	6.1	0.118	44	152	1.3	7.3	0.3	176	9.7	363.8	28.5	335	498	21
302	n	33	33	33	33	33	33	33	33	33	33	33	33	33	33	33	33	33	33	33	33	33	33	33	33	33	33	33	33
	mean	8.97	2.66	1.72	1.7	2.77	0.32	17.8	37.9	162	14025	25	0.04	69.3	1.3	64.6	0.012	26	27	0.8	7.5	0.12	86	10.2	30.5	53.5	104	174	11771
	st. dev.	5.26	6.63	3.86	2.21	2.86	0.636	27	196.1	285	79883.2	75.1	0.04	296.5	1.6	329.3	0.023	19	53	0.6	16	0.13	58	13.1	29.1	92.6	139	197	66825
303	n	21	21	21	21	21	21	21	21	21	21	21	21	21	21	21	21	21	21	21	21	21	21	21	21	21	21	21	21
	mean	8.23	2.06	0.14	1.97	1.54	0.177	11	2.1	131	1.5	6	0.04	17.9	1	8	0.007	49	56	1	93.3	0.21	102	11.9	34.5	12.5	118	197	34
	st. dev.	7.69	2.36	0.18	2.53	1.64	0.187	22.6	1.9	177	1.2	2.8	0.04	21.4	0.2	17.5	0.012	53	74	1.1	326.6	0.24	60	14.6	45	10.9	139	276	43
304	n	13	13	13	13	13	13	13	13	13	13	13	13	13	13	13	13	13	13	13	13	13	13	13	13	13	13	13	13
	mean	6.67	1.55	0.68	3.59	1.22	0.206	8.4	1.9	45	2	6	0.06	11	1	2.7	0.011	266	41	1	18.2	0.15	96	7.2	24.7	9.8	231	328	19
	st. dev.	6.85	1.67	2.05	6.68	2.26	0.414	17	2.4	25	1.9	3.6	0.07	13.3	0	2.8	0.023	211	85	1.6	49.1	0.22	81	6.2	24.7	7.4	283	671	22
305	n	14	14	14	14	14	14	14	14	14	14	14	14	14	14	14	14	14	14	14	14	14	14	14	14	14	14	14	14
	mean	10.92	2.64	1.11	1.62	2.36	1.147	11	6.5	68	158.3	10.3	0.08	19.1	1	3.6	0.016	126	37	0.7	7	0.28	141	29.8	36	18.4	192	487	89
	st. dev.	5.98	2.21	1.54	1.56	1.47	1.461	9.1	9	59	346	13.1	0.05	18.2	0	6	0.018	124	42	0.4	9.2	0.2	254	68.6	21.6	19	139	611	151
306	n	18	18	18	18	18	18	18	18	18	18	18	18	18	18	18	18	18	18	18	18	18	18	18	18	18	18	18	18
	mean	7.2	1.56	0.61	1.19	1.23	0.656	15.9	5	67	317.3	6.5	0.07	15.1	1	3.7	0.009	192	39	0.8	5.2	0.2	108	11.1	27	14.5	195	242	177
	st. dev.	7.9	1.04	1.21	2.21	1.73	1.528	20.4	9	55	870	5.6	0.08	18.1	0	5.4	0.018	184	59	0.9	5.1	0.23	96	19.5	24.7	17.6	271	512	450
307	n	23	23	23	23	23	23	23	23	23	23	23	23	23	23	23	23	23	23	23	23	23	23	23	23	23	23	23	23
	mean	6.63	2.2	1.13	1.47	1.42	0.438	7.9	2.8	69	10.5	5.1	0.08	28.3	1.1	7.3	0.028	203	53	0.5	10.1	0.29	114	13.4	22.8	13.3	176	207	32
	st. dev.	6.76	3.28	2.8	2.53	2.25	1.001	15.9	4.6	60	33.6	0.3	0.12	41.6	0.3	12.4	0.068	211	88	0.7	22.7	0.39	97	15.5	32.4	27.5	185	504	57
308	n	28	28	28	28	28	28	28	28	28	28	28	28	28	28	28	28	28	28	28	28	28	28	28	28	28	28	28	28
	mean	11.66	2.15	0.1	4.11	1.4	0.207	9.5	15.1	160	2	5.1	0.08	15.4	1.1	12	0.002	133	176	2.2	7.7	0.41	169	15.5	54.3	27.8	152	207	46
	st. dev.	8.62	3.59	0.14	4.91	1.12	0.187	11.2	43.8	189	1.9	1.1	0.12	11.4	0.4	13.6	0.002	142	184	1.8	10	0.33	114	15.1	57.7	62.2	175	203	72
13	n	0	0	0	0	0	0	1	1	0	1	0	0	1	0	1	1	0	1	0	0	0	0	0	0	0	1	1	1
	mean	-	-	-	-	-	-	45	5	-	1	-	-	30	-	65	39	-	20	-	-	-	-	-	-	-	150	1195	50
	st. dev.	-	-	-	-	-	-	-	-	-	-	-	-	-	-	-	-	-	-	-	-	-	-	-	-	-	-	-	-
15	n	0	0	0	0	0	0	1	1	0	1	0	0	1	0	1	1	0	1	0	0	0	0	0	0	0	1	1	1
	mean	-	-	-	-	-	-	59	9	-	1	-	-	15	-	50	205	-	20	-	-	-	-	-	-	-	75	195	70
	st. dev.	-	-	-	-	-	-	-	-	-	-	-	-	-	-	-	-	-	-	-	-	-	-	-	-	-	-	-	-
18	n	0	0	0	0	0	0	1	1	0	1	0	0	1	0	1	1	0	1	0	0	0	0	0	0	0	1	1	1
	mean	-	-	-	-	-	-	52	3	-	2	-	-	35	-	50	118	-	20	-	-	-	-	-	-	-	135	1580	50
	st. dev.	-	-	-	-	-	-	-	-	-	-	-	-	-	-	-	-	-	-	-	-	-	-	-	-	-	-	-	-
19	n	0	0	0	0	0	0	7	7	0	7	0	0	7	0	7	7	0	7	0	0	0	0	0	0	0	7	7	7
	mean	-	-	-	-	-	-	26	2.1	-	2.1	-	-	118	-	63	1059	-	1.32E+02	-	-	-	-	-	-	-	231	1361	154
	st. dev.	-	-	-	-	-	-	14	2.1	-	1.3	-	-	87	-	8	969	-	1.03E+02	-	-	-	-	-	-	-	182	862	84
20	n	0	0	0	0	0	0	2	2	0	2	0	0	2	0	2	2	0	2	0	0	0	0	0	0	0	2	2	2
	mean	-	-	-	-	-	-	45	14	-	2.5	-	-	60	-	55	308	-	50	-	-	-	-	-	-	-	182	565	62
	st. dev.	-	-	-	-	-	-	21	0	-	2.1	-	-	71	-	7	103	-	42	-	-	-	-	-	-	-	11	368	39
21	n	0	0	0	0	0	0	1	1	0	1	0	0	1	0	1	1	0	1	0	0	0	0	0	0	0	1	1	1
	mean	-	-	-	-	-	-	50	10	-	1	-	-	70	-	50	380	-	50	-	-	-	-	-	-	-	380	480	100
	st. dev.	-	-	-	-	-	-	-	-	-	-	-	-	-	-	-	-	-	-	-	-	-	-	-	-	-	-	-	-
22	n	0	0	0	0	0	0	1	1	0	1	0	0	1	0	1	1	0	1	0	0	0	0	0	0	0	1	1	1
	mean	-	-	-	-	-	-	10	1	-	3	-	-	35	-	35	320	-	320	-	-	-	-	-	-	-	50	1010	45
	st. dev.	-	-	-	-	-	-	-	-	-	-	-	-	-	-	-	-	-	-	-	-	-	-	-	-	-	-	-	-
23	n	0	0	0	0	0	0	1	1	0	1	0	0	1	0	1	1	0	1	0	0	0	0	0	0	0	1	1	1

Table 2 (cont.d')

	mean	-	-	-	-	-	-	30	0	-	1	-	-	150	-	60	805	-	120	-	-	-	-	-	-	-	340	1760	35
	st. dev.	-	-	-	-	-	-	-	-	-	-	-	-	-	-	-	-	-	-	-	-	-	-	-	-	-	-	-	-
25	n	0	0	0	0	0	0	2	2	0	2	0	0	2	0	2	2	0	2	0	0	0	0	0	0	0	2	2	2
	mean	-	-	-	-	-	-	48	6.5	-	3	-	-	90	-	52	3605	-	130	-	-	-	-	-	-	-	200	100	440
	st. dev.	-	-	-	-	-	-	25	2.1	-	0	-	-	21	-	11	4236	-	99	-	-	-	-	-	-	-	212	0	368
30	n	0	0	0	0	0	0	2	2	0	2	0	0	2	0	2	2	0	2	0	0	0	0	0	0	0	2	2	2
	mean	-	-	-	-	-	-	55	4.5	-	3.5	-	-	25	-	58	38	-	20	-	-	-	-	-	-	-	68	690	78
	st. dev.	-	-	-	-	-	-	35	0.7	-	2.1	-	-	14	-	32	29	-	0	-	-	-	-	-	-	-	11	28	18
31	n	0	0	0	0	0	0	1	1	0	1	0	0	1	0	1	1	0	1	0	0	0	0	0	0	0	1	1	1
	mean	-	-	-	-	-	-	75	5	-	2	-	-	20	-	65	31	-	20	-	-	-	-	-	-	-	170	1230	30
	st. dev.	-	-	-	-	-	-	-	-	-	-	-	-	-	-	-	-	-	-	-	-	-	-	-	-	-	-	-	-
33	n	0	0	0	0	0	0	1	1	0	1	0	0	1	0	1	1	0	1	0	0	0	0	0	0	0	1	1	1
	mean	-	-	-	-	-	-	45	2	-	2	-	-	25	-	60	96	-	20	-	-	-	-	-	-	-	50	200	20
	st. dev.	-	-	-	-	-	-	-	-	-	-	-	-	-	-	-	-	-	-	-	-	-	-	-	-	-	-	-	-
35	n	0	0	0	0	0	0	2	2	0	2	0	0	2	0	2	2	0	2	0	0	0	0	0	0	0	2	2	2
	mean	-	-	-	-	-	-	48	1	-	2	-	-	42	-	62	67	-	20	-	-	-	-	-	-	-	250	972	35
	st. dev.	-	-	-	-	-	-	11	1.4	-	1.4	-	-	32	-	18	41	-	0	-	-	-	-	-	-	-	177	180	14
36	n	0	0	0	0	0	0	1	1	0	1	0	0	1	0	1	1	0	1	0	0	0	0	0	0	0	1	1	1
	mean	-	-	-	-	-	-	35	2	-	2	-	-	50	-	50	310	-	30	-	-	-	-	-	-	-	290	1260	35
	st. dev.	-	-	-	-	-	-	-	-	-	-	-	-	-	-	-	-	-	-	-	-	-	-	-	-	-	-	-	-
38	n	0	0	0	0	0	0	2	2	0	2	0	0	2	0	2	2	0	2	0	0	0	0	0	0	0	2	2	2
	mean	-	-	-	-	-	-	42	3	-	2	-	-	65	-	75	402	-	72	-	-	-	-	-	-	-	190	812	45
	st. dev.	-	-	-	-	-	-	39	0	-	1.4	-	-	64	-	35	472	-	74	-	-	-	-	-	-	-	14	329	7
41	n	0	0	0	0	0	0	1	1	0	1	0	0	1	0	1	1	0	1	0	0	0	0	0	0	0	1	1	1
	mean	-	-	-	-	-	-	35	1	-	4	-	-	70	-	35	315	-	20	-	-	-	-	-	-	-	185	1840	45
	st. dev.	-	-	-	-	-	-	-	-	-	-	-	-	-	-	-	-	-	-	-	-	-	-	-	-	-	-	-	-
45	n	0	0	0	0	0	0	1	1	0	1	0	0	1	0	1	1	0	1	0	0	0	0	0	0	0	1	1	1
	mean	-	-	-	-	-	-	50	5	-	1	-	-	50	-	50	53	-	20	-	-	-	-	-	-	-	150	920	15
	st. dev.	-	-	-	-	-	-	-	-	-	-	-	-	-	-	-	-	-	-	-	-	-	-	-	-	-	-	-	-
47	n	0	0	0	0	0	0	1	1	0	1	0	0	1	0	1	1	0	1	0	0	0	0	0	0	0	1	1	1
	mean	-	-	-	-	-	-	30	1	-	1	-	-	70	-	35	300	-	60	-	-	-	-	-	-	-	400	1850	30
	st. dev.	-	-	-	-	-	-	-	-	-	-	-	-	-	-	-	-	-	-	-	-	-	-	-	-	-	-	-	-
74	n	0	0	0	0	0	0	6	6	0	6	0	0	6	0	6	6	0	6	0	0	0	0	0	0	0	6	6	6
	mean	-	-	-	-	-	-	43	1.5	-	1.2	-	-	58	-	68	353	-	72	-	-	-	-	-	-	-	211	1468	31
	st. dev.	-	-	-	-	-	-	30	0.5	-	0.4	-	-	54	-	21	467	-	93	-	-	-	-	-	-	-	50	729	34
75	n	0	0	0	0	0	0	3	3	0	3	0	0	3	0	3	3	0	3	0	0	0	0	0	0	0	3	3	3
	mean	-	-	-	-	-	-	47	1.7	-	1.3	-	-	72	-	57	367	-	63	-	-	-	-	-	-	-	350	1307	13
	st. dev.	-	-	-	-	-	-	25	0.6	-	0.6	-	-	55	-	6	275	-	75	-	-	-	-	-	-	-	44	652	6
S1	n	21	21	21	21	21	21	21	21	21	21	21	21	21	21	21	21	21	21	21	21	21	21	21	21	21	21	21	21
	mean	7.98	0.97	0.87	1.73	1.3	0.054	174	9.1	68	447	13.4	0.05	8671.3	31.7	135.8	0.042	107	45	1.6	37.6	0.27	171	21.8	40.4	24.6	169	30	181
	st. dev.	6.91	1.17	3.62	2.1	1.13	0.048	472.2	12.3	54	2005.6	28.6	0.04	39256.8	134.3	568.3	0.175	98	32	1.6	138.8	0.22	84	21.7	34.1	18.6	101	24	607
S2	n	24	24	24	24	24	24	24	24	24	24	24	24	24	24	24	24	24	24	24	24	24	24	24	24	24	24	24	24
	mean	13.76	3.53	0.21	4.75	1.14	0.087	3.6	3.3	82	1.5	5.8	0.15	12.9	1	8.8	0.015	178	111	2.6	9.1	0.66	135	13.3	32.2	11	83	38	79
	st. dev.	7.35	3.18	0.38	5.88	0.95	0.081	3.7	3.1	77	1.4	1.3	0.29	10.6	0.2	11.5	0.019	93	154	2.6	6.6	0.77	68	16.8	40.7	10.2	103	67	96

Table 3

Correlation matrix for geochemical analyses of samples from localities 301 to 331 (Table 2) in the study area, based on 15 512 analyses of 554 samples[1]

	Pb	U	B	As	Mo	Zn	Cd	Co	Cr	V	Be	Cu	Zr	Y	La	Th	Sr	Ba	Ni	Al	Fe	Ca	Mg	K	Na	P	Mn	Ti
Pb	1.000	0.218	0.057	0.111	0.103	0.154	-0.031	0.117	0.017	0.070	0.139	0.027	0.174	0.165	0.112	0.074	0.335	0.116	0.111	0.071	-0.025	-0.031	-0.004	0.152	0.106	0.047	0.010	0.021
U	0.218	1.000	0.048	0.968	0.824	0.878	-0.017	0.953	-0.051	0.082	0.081	0.009	0.026	0.097	0.012	0.044	0.024	-0.014	0.968	0.011	-0.022	0.018	-0.001	-0.004	-0.023	0.048	-0.004	4.237E-4
B	0.057	0.048	1.000	0.016	0.013	0.011	0.049	0.007	-0.154	0.081	0.067	-0.016	0.256	0.125	0.120	0.086	0.320	-0.167	0.016	0.132	0.010	-0.115	-0.005	0.113	-0.168	0.021	-0.030	0.107
As	0.111	0.968	0.016	1.000	0.846	0.896	-0.009	0.982	-0.048	0.012	0.015	0.012	-0.018	0.023	-0.013	0.025	-0.025	-0.021	10.000	-0.030	-0.017	0.018	-0.002	-0.028	-0.023	-0.010	-0.004	-0.033
Mo	0.103	0.824	0.013	0.846	1.000	0.761	0.005	0.860	-0.055	0.073	0.039	0.048	-0.016	0.019	0.004	0.030	-0.025	-0.018	0.846	-0.013	0.025	-0.005	0.168	-0.026	-0.036	-0.010	-0.007	-0.021
Zn	0.154	0.878	0.011	-0.896	0.761	1.000	0.044	0.908	0.013	0.256	0.289	0.049	0.007	0.072	0.109	0.019	-0.032	0.074	0.897	0.069	0.065	0.061	0.006	0.053	0.084	-0.002	0.008	0.117
Cd	-0.031	-0.017	0.049	-0.009	0.005	0.044	1.000	0.002	-0.103	0.473	0.183	-0.010	0.076	0.068	0.050	0.024	0.235	-0.048	-0.009	0.039	0.901	0.043	0.038	-0.044	-0.025	0.123	0.138	0.059
Co	0.117	0.953	0.007	0.982	0.860	0.908	0.002	1.000	-0.038	0.096	0.088	0.026	-0.001	0.045	0.010	0.028	-0.032	0.007	0.982	0.017	0.027	0.029	0.029	-0.012	-2.659E-4	-0.004	0.001	0.062
Cr	0.017	-0.051	-0.154	-0.048	-0.055	0.013	-0.103	-0.038	1.000	-0.008	0.097	0.005	-0.028	-0.026	-0.057	-0.039	-0.015	-0.051	-0.048	-0.143	-0.109	-0.021	0.011	-0.112	-0.008	-0.070	-0.025	-0.053
V	0.070	0.082	0.081	0.012	0.073	0.256	0.473	0.096	-0.008	1.000	0.707	0.036	0.115	0.136	0.099	0.002	0.096	0.015	0.014	0.220	0.571	0.006	0.146	0.022	-0.015	0.100	0.071	0.426
Be	0.139	0.081	0.067	0.015	0.039	0.289	0.183	0.088	0.097	0.707	1.000	0.043	0.241	0.209	0.182	0.182	0.109	0.115	0.016	0.380	0.269	-0.008	0.024	0.199	0.160	0.096	0.026	0.425
Cu	0.027	0.009	-0.016	0.012	0.048	0.049	-0.010	0.026	0.005	0.036	0.043	1.000	-0.013	-0.002	-0.002	-0.012	-0.029	0.123	0.012	0.026	0.021	-0.008	0.076	0.032	0.060	-0.010	0.002	0.044
Zr	0.174	0.026	0.256	-0.018	-0.016	0.007	0.076	-0.001	-0.028	0.115	0.241	-0.013	1.000	0.300	0.242	0.485	0.428	0.074	-0.018	0.219	0.074	-0.135	0.021	0.158	-0.024	0.065	0.034	0.388
Y	0.165	0.097	0.125	0.023	0.019	0.072	0.068	0.045	-0.026	0.136	0.209	-0.002	0.300	1.000	0.124	0.143	0.294	0.035	0.024	0.208	0.074	0.017	-0.002	0.085	0.027	0.449	0.029	0.314
La	0.112	0.012	0.120	-0.013	0.004	0.109	0.050	0.010	-0.057	0.099	0.182	-0.002	0.242	0.124	1.000	0.229	0.217	0.062	-0.013	0.162	0.058	-0.050	-0.005	0.121	0.018	0.070	0.019	0.289
Th	0.074	0.044	0.086	0.025	0.030	0.019	0.024	0.028	-0.039	0.002	0.182	-0.012	0.485	0.143	0.229	1.000	0.313	0.083	0.025	0.175	0.026	-0.097	-0.010	0.177	0.035	0.061	0.055	0.215
Sr	0.335	0.024	0.320	-0.025	-0.025	-0.032	0.235	-0.032	-0.015	0.096	0.109	-0.029	0.428	0.294	0.217	0.313	1.000	-0.015	-0.025	0.169	0.159	-0.087	-0.021	0.061	-0.041	0.161	0.003	0.235
Ba	0.116	-0.014	-0.167	-0.021	-0.018	0.074	-0.048	0.007	-0.051	0.015	0.115	0.123	0.074	0.035	0.062	0.083	-0.015	1.000	-0.021	0.334	0.024	0.020	0.041	0.683	0.608	-0.020	0.060	0.188
Ni	0.111	0.968	0.016	1.000	0.846	0.897	-0.009	0.982	-0.048	0.014	0.016	0.012	-0.018	0.024	-0.013	0.025	-0.025	-0.021	1.000	-0.029	-0.017	0.019	-0.001	-0.028	-0.023	-0.010	-0.004	-0.032
Al ppm	0.071	0.011	0.132	-0.030	-0.013	0.069	0.039	0.017	-0.143	0.220	0.380	0.026	0.219	0.208	0.162	0.175	0.169	0.334	-0.029	1.000	0.068	-0.100	0.039	0.442	0.350	0.033	0.022	0.477
Fe ppm	-0.025	-0.022	0.010	-0.017	0.025	0.065	0.901	0.027	-0.109	0.571	0.269	0.021	0.074	0.074	0.058	0.026	0.159	0.024	-0.017	0.068	1.000	0.040	0.059	-0.034	0.003	0.151	0.155	0.240
Ca ppm	-0.031	-0.018	-0.115	0.018	-0.005	0.061	0.043	0.029	-0.021	0.006	-0.008	-0.008	-0.135	0.017	-0.050	-0.097	-0.087	0.020	0.019	-0.100	0.040	1.000	-0.002	-0.083	0.090	0.163	0.021	-0.029
Mg ppm	-0.004	-0.001	-0.005	-0.002	0.168	0.006	0.038	0.029	0.011	0.146	0.024	0.076	0.021	-0.002	-0.005	-0.010	-0.021	0.041	-0.001	0.039	0.059	-0.002	1.000	0.013	-0.010	-0.009	0.002	0.056
K ppm	0.152	-0.004	0.113	-0.028	-0.026	0.053	-0.044	-0.012	-0.112	0.022	0.199	0.032	0.158	0.085	0.121	0.177	0.061	0.683	-0.028	0.442	-0.034	-0.083	0.013	1.000	0.515	-0.037	0.077	0.173
Na ppm	0.106	-0.023	-0.168	-0.023	-0.036	0.084	-0.025	-2.659E-4	-0.008	-0.015	0.160	0.060	-0.024	0.027	0.018	0.035	-0.041	0.608	-0.023	0.350	0.003	0.090	-0.010	0.515	1.000	-0.032	0.073	0.134
P ppm	0.047	0.048	0.021	-0.010	-0.010	-0.002	0.123	-0.004	-0.070	0.100	0.096	-0.010	0.065	0.449	0.070	0.061	0.161	-0.020	-0.010	0.033	0.151	0.163	-0.009	-0.037	-0.032	1.000	0.038	0.109
Mn ppm	0.010	-0.004	-0.030	-0.004	-0.007	0.008	0.138	0.001	-0.025	0.071	0.026	0.002	0.034	0.029	0.019	0.055	0.003	0.060	-0.004	0.022	0.155	0.021	0.002	0.077	0.073	0.038	1.000	0.023
Ti ppm	0.021	4.237E-4	0.107	-0.033	-0.021	0.117	0.059	0.062	-0.053	0.426	0.425	0.044	0.388	0.314	0.289	0.215	0.235	0.188	-0.032	0.477	0.240	-0.029	0.056	0.173	0.134	0.109	0.023	1.000

[1]All analyses in ppm

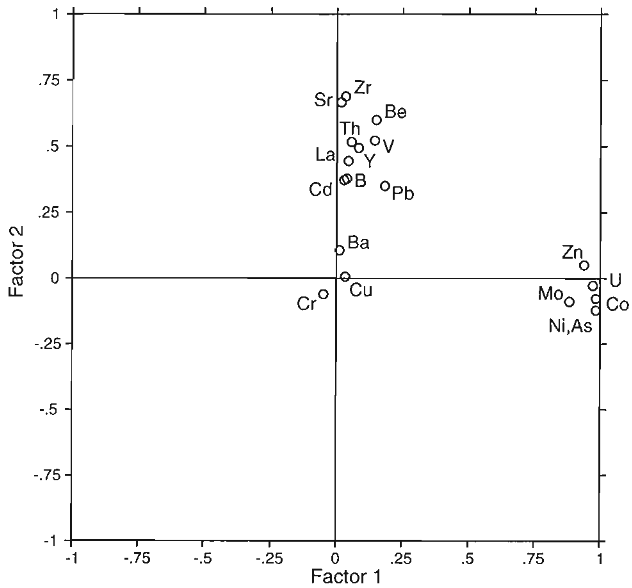

Figure 15. *Unrotated factor plot from factor analysis for 28 constituents in 554 samples from the study area.*

rammelsbergite ($Ni(Co)As_2$), pararammelsbergite ($NiAs_2$), gersdorffite (NiAs(Fe,Co)S), skutterudite ($(Co,Ni) As_3$) and nickeline (NiAs).

High correlation coefficients between U and Ni, U and Co, and U and As reflect the paragenetic association of these elements, which is typical for polymetallic unconformity deposits in the Saskatchewan part of the Athabasca Basin. The U and Ni association exhibits specific geochemical relationships within the entire sequence as demonstrated by bivariate regression plots (Fig. 16a–f). The degree of these associations are also numerically expressed by the coefficients of determination (R2), shown under the graphs:

(i) The U and Ni geochemical relationships in all rocks have R2 of 0.937 (Fig. 16a).

(ii) The U and Ni geochemical relationships in the basement rocks (Fig. 16b) are highly proportional (with R2 = 0.953) and reflect the common association of these elements in many uranium deposits hosted by metamorphic rocks elsewhere (e.g., in polymetallic vein deposits at Great Bear Lake, Canada, or at Jáchymov, Czech Republic).

(iii) The U and Ni geochemical relationships within the rocks of the Fair Point Formation, which is the basal formation of the Athabasca Group in the study area (Fig. 16c), are the highest ones within the sandstone cover rocks (with R2 = 0.449). They reflect the association of these two elements, which is typical for the polymetallic unconformity deposits (e.g., in deposits at Cigar Lake or Key Lake, Athabasca Basin, Canada). The lithostratigraphic position of the mineralization corresponds closely with the conceptual deposit model (location 2 in Fig. 6).

(iv) The U and Ni geochemical relationships in the rocks of the Manitou Falls Formation (Fig. 16d), which in the study area overlies the Fair Point Formation, have a very low coefficient of determination (with R2 = 0.053). This indicates that only weak mineralization processes took place at this distant place above the unconformity and monometallic rather than polymetallic fluids prevailed. This case resembles those cases found at a distance above the unconformity elsewhere within the Athabasca sequence (e.g., ''perched'' mineralization at Cigar Lake or at the Fond-du-Lac deposit). The lithostratigraphic position of the mineralization corresponds very closely with the conceptual deposit model (location 3 in Fig. 6).

(v, vi) The U and Ni geochemical relationships in the rocks of the Lazenby Lake Formation and in the Devonian rocks (Figs. 16e, f), which occupy the highest position in the sedimentary succession within the study area and occur only locally, display a minimal coefficient of determination (with R2 = 0.036 and R2 = 0.0004 respectively). This indicates that both uranium and nickel have their own independent and random distribution well away from zones of potential uranium monometallic or polymetallic mineralization.

Metallogenic features in the distribution of selected elements

The stratigraphic and regional distribution of selected elements was analyzed in order to investigate their metallogenic significance. A preference was given to those elements which are typical of the known unconformity deposits in the Athabasca Basin.

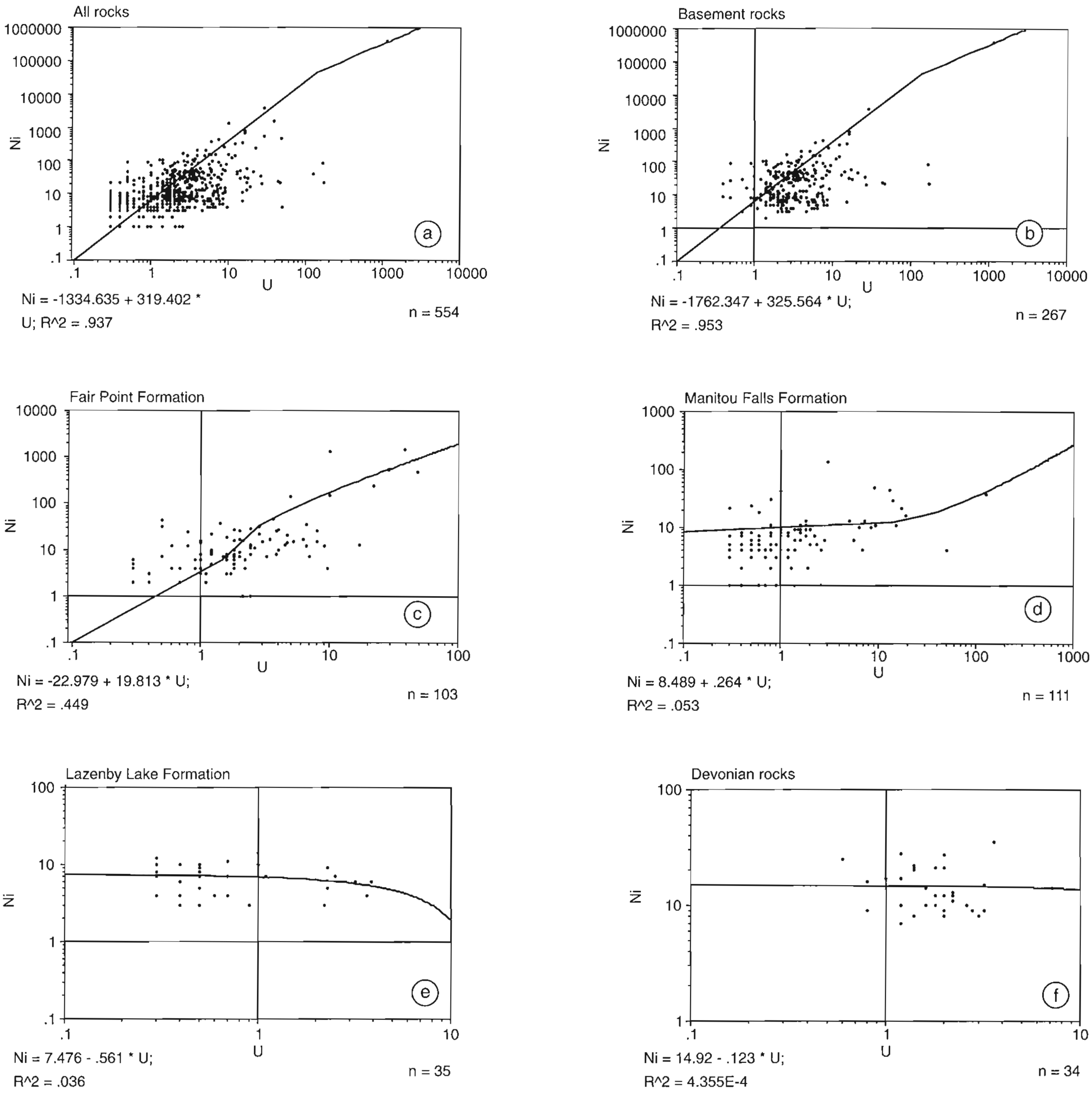

Figure 16. *Uranium and nickel contents in samples from selected units of the study area. Data are in ppm; n, number of samples analyzed. Scattergrams for:* ***a.*** *all rocks;* ***b.*** *basement rocks;* ***c.*** *rocks from Fair Point Formation;* ***d.*** *rocks from Manitou Falls Formation;* ***e.*** *rocks from Lazenby Lake Formation;* ***f.*** *Devonian rocks.*

Uranium

As indicated above, the basement rocks in the study area of Alberta, which include granitoid plutons (reactivated during the Hudsonian Orogeny) as well as Aphebian pyritic graphitic metapelites, contain an average of 5.9 times higher amounts of uranium than the average crustal rocks (clarke value). However, uranium contents in individual rock units vary greatly.

Geochemical analyses of uranium from a limited number of samples (n) from various basement units, as reported by Wilson (1986), were compiled, sorted according to rock units, and statistically analyzed. The analysis (Fig. 17) indicates that the highest (peak) contents (q) of uranium are associated with granitic rocks, particularly with alkali feldspar-rich granitoids (unit 'K' of Wilson; n = 18; q = 42 ppm U). All the remaining felsic units also contain elevated amounts of uranium, as follows: Fishing Creek granitoids (unit 'FC' of Wilson; n = 7; q = 14 ppm U); Grey Foliated Granitoids (unit 'GF' of Wilson; n = 9, q = 14 ppm U); Felsic Mylonite (unit 'FM' of Wilson; n = 6, q = 10 ppm U); and Wylie Lake granitoids (unit 'WL' of Wilson; n = 4, q = 9 ppm U). These data are compatible with the lithophile character of uranium and with its tendency to concentrate in late-stage felsic melts. During the present study, anomalous contents of uranium (as much as 1130 ppm U) have been found in granitoid basement rocks in a sample from drillhole 302 (Fig. 13; Table 4).

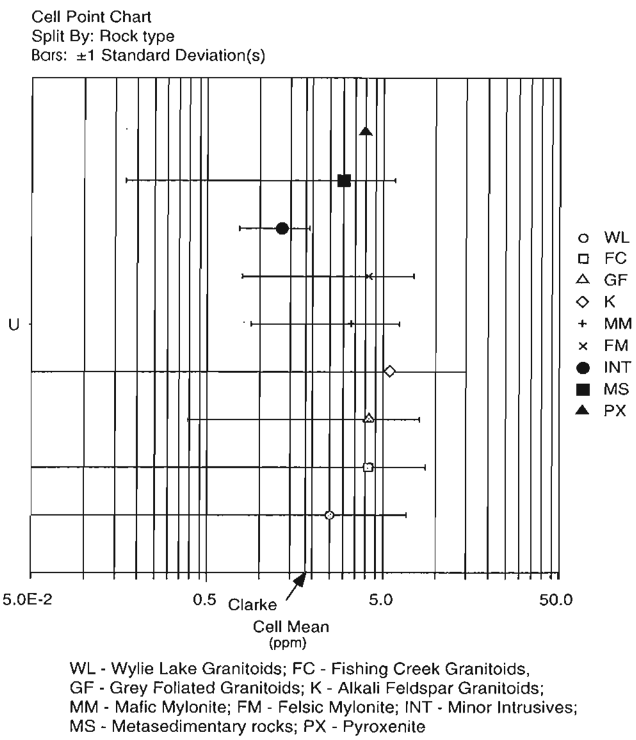

***Figure 17.** Uranium contents in various units of the basement rocks, northeastern Alberta. Analytical data after Wilson (1986).*

Table 4

Coordinates, dips and azimuths of selected drillholes in the study area. The depths, referred to in the text, are reported along the length of each drillhole

Drillhole	Longitude W	Latitude N	Elevation m ASL	Dip/ Azimuth	Length m
301	110°35′00″	58°17′00″	305	60°/250°	460.1
302	110°37′00″	58°08′30″	320	60°/250°	236.0
303	110°39′30″	58°11′30″	305	60°/250°	254.0
304	110°39′40″	58°12′15″	305	60°/270°	272.0
305	110°39′30″	58°12′15″	305	60°/250°	242.0
306	110°39′20″	58°12′15″	305	75°/270°	250.5
307	110°39′10″	58°12′15″	305	77°/270°	248.0
308	110°41′15″	58°07′00″	320	60°/250°	188.0
309	110°43′30″	58°07′30″	300	60°/045°	191.0
310	110°45′45″	58°10′30″	300	60°/045°	194.0
311	110°42′00″	58°08′45″	305	60°/045°	185.0
312	110°38′45″	58°06′00″	308	60°/045°	188.0
313	110°43′30″	58°07′30″	302	60°/045°	167.0
314	110°41′20″	58°07′45″	305	60°/045°	180.5
315	110°40′45″	58°08′00″	305	60°/045°	191.0
316	110°38′30″	58°09′00″	308	60°/045°	248.0
317	110°42′00″	58°08′00″	305	60°/045°	188.0
318	110°44′00″	58°09′15″	290	60°/045°	185.0
319	110°44′45″	58°09′45″	305	60°/045°	197.0
320	110°44′00″	58°10′10″	308	60°/045°	172.5
321	110°45′00″	58°10′45″	315	60°/045°	209.0
322	110°44′35″	58°09′55″	312	90°	197.0
323	110°43′00″	58°08′45″	312	60°/045°	164.0
324	110°40′00″	58°07′45″	300	60°/045°	192.0
325	110°40′30″	58°42′25″	305	60°/045°	170.0
326	110°43′00″	58°07′45″	303	60°/045°	182.0
327	110°38′30″	58°09′10″	307	60°/225°	179.0
328	110°38′00″	58°09′35″	312	60°/045°	226.6
329	110°38′00″	58°09′35″	312	75°/240°	207.5
330	110°38′45″	58°10′30″	310	60°/250°	260.0

As mentioned above, the uranium contents within the Athabasca Group rocks are controlled lithostratigraphically. The analysis of variance (ANOVA) interaction bar plot (Fig. 18a), which is based on geochemical analyses of 599 samples (554 from Alberta and 45 from Saskatchewan), indicates

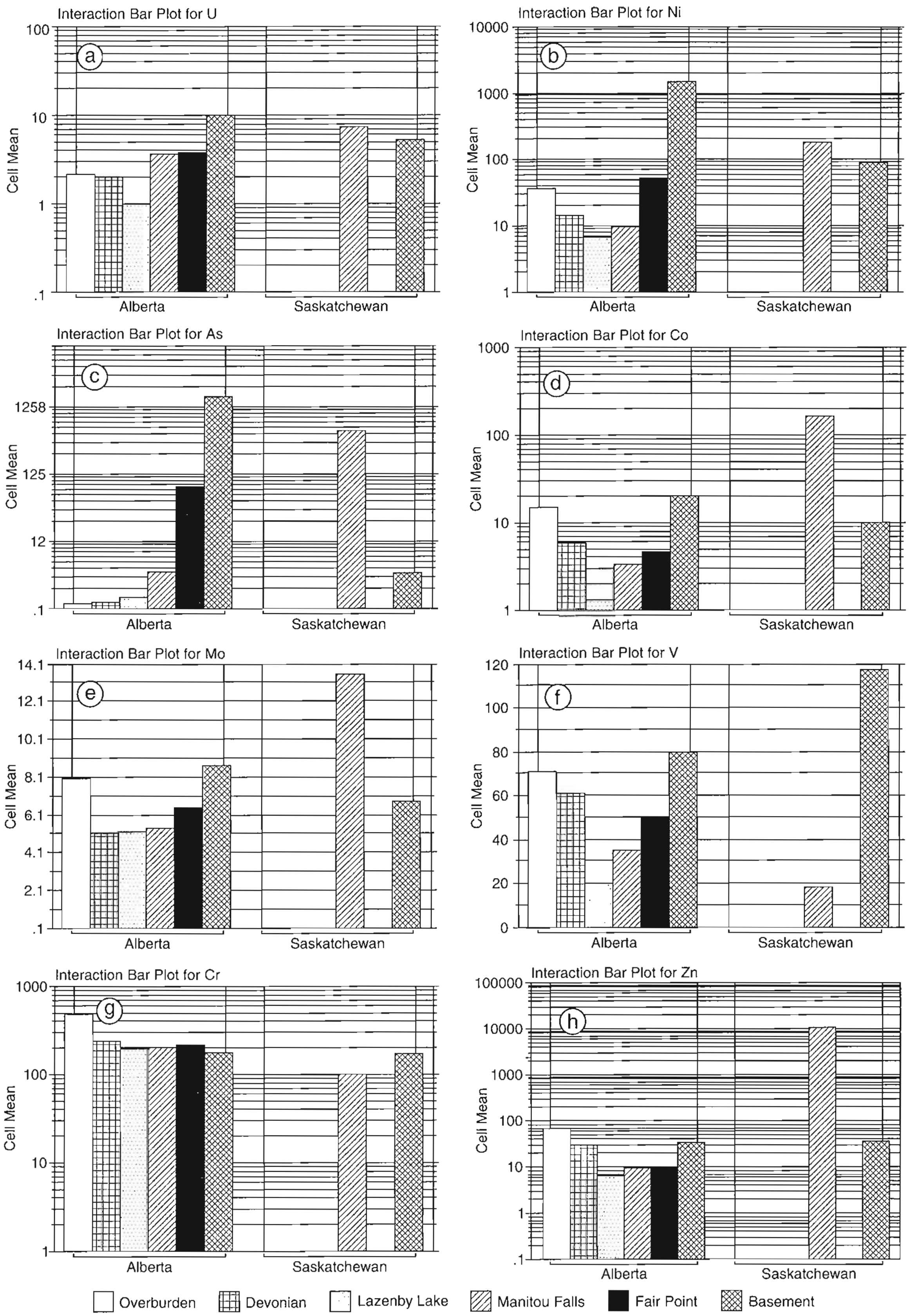

Figure 18. *Comparative ANOVA (analysis of variance) graphs for elemental content in samples from rock units of the study area in Alberta and the control areas in Saskatchewan. Data in ppm; n = 599 (554 from Alberta and 45 from Saskatchewan). Interaction bar plots for:* ***a.*** *uranium;* ***b.*** *nickel;* ***c.*** *arsenic;* ***d.*** *cobalt;* ***e.*** *molybdenum;* ***f.*** *vanadium;* ***g.*** *chromium;* ***h.*** *zinc.*

that the mean uranium content in the basal Fair Point Formation is 3.9 ppm U. However, a mineralized interval of altered sandstone from drillhole 306, which is located in the central part of the study area, contained 17.7% U over 5 m at a depth of 199 m (Orr et al., 1988). The mineralization consists of massive pitchblende, cubic uraninite, coffinite, galena, pararammelsbergite, rammelsbergite, gersdorffite, nickeline, apatite and traces of gold. The mineralized interval was not sampled in this study and the grade and thickness are not included in the analyses of 599 samples. However, several samples were collected from drillhole 306 from the vicinity of that uranium interval, and uraniferous zircons were identified in the samples. A sample collected from drillhole 306, about 3 m above a lens of massive pitchblende, contained uraniferous and thoriferous zircons intergrown with nickeline (Plates 2e, f, 3a, b). Occurrence of uraniferous zircons apparently indicates proximity to larger concentrations of uranium minerals in this area.

The other formations of the Athabasca Group, which are higher in the succession (i.e., farther above the unconformity) have mean uranium contents lower than the Fair Point Formation. For example the Lazenby Lake Formation has a mean uranium content of only 1.0 ppm U and a maximum content of only 3.9 ppm U. The mean values in the Devonian rocks, and particularly in the Quaternary deposits (2.0 and 2.2 ppm U, peaks 7.2 and 3.0 ppm U, respectively), slightly above background, appear to be related to remobilization and dispersion haloes.

In a three-dimensional view, uranium displays very specific distribution patterns, which are associated with lithologic, structural and geochemical controls, typical for unconformity deposits as suggested by the deposit model discussed above (Fig. 6). For example, in drillholes 305, 303 and 302 (Fig. 19), the highest concentrations of uranium within the Athabasca Group rocks are localized at the base of the sequence, in the Fair Point Formation, which indicates that the deposition of uranium was controlled by the unconformity. The basement rocks, which are considered as a source for uranium in the above-mentioned model, also contain high uranium anomalies (e.g., in drillhole 302; Fig. 13; Table 4). Typical polymetallic (U + Ni + As) mineralization associated with the sub-Athabasca unconformity has also been identified in some other drillholes (e.g., in drillhole 306; Fig. 20a).

Regional distribution of uranium is demonstrated by a three-dimensional graph (Fig. 22). A detailed examination of the locations of uranium anomalies reveals that their distribution is distinctly structurally and lithologically controlled. The structural and lithological controls correspond with those included in

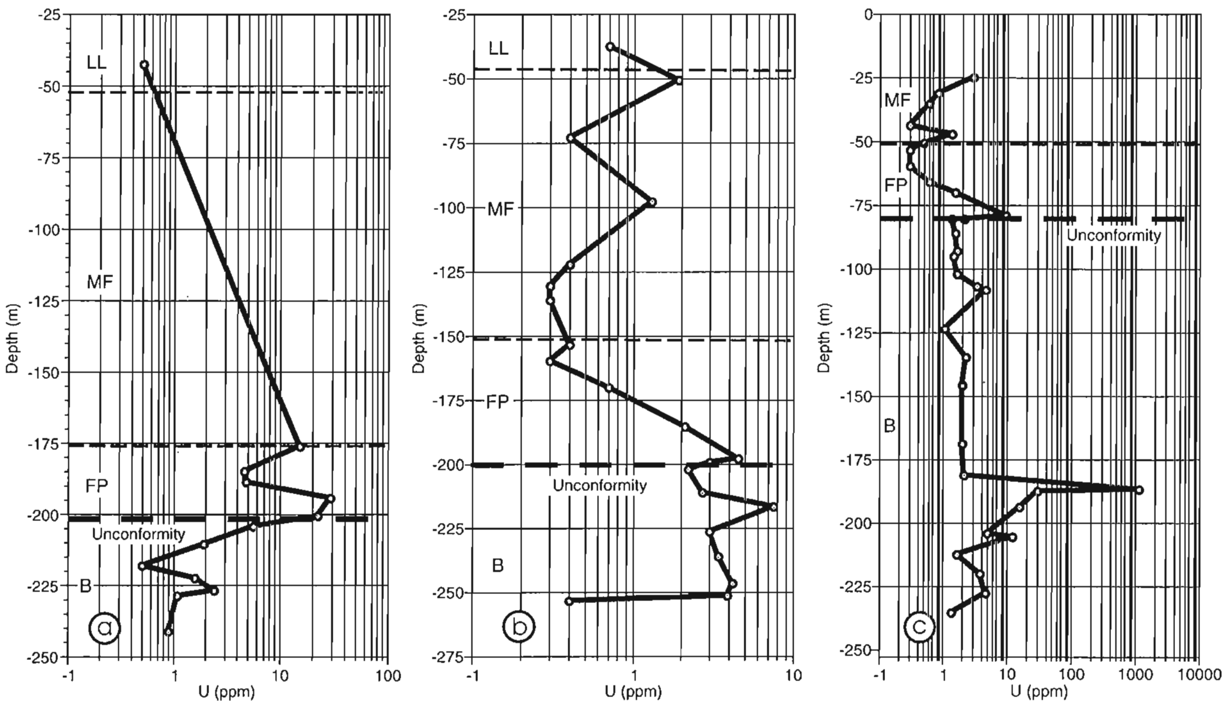

Figure 19. *Distribution of uranium in selected drillholes from the study area:* ***a.*** *drillhole 305;* ***b.*** *drillhole 303;* ***c.*** *drillhole 302. The graphs show distinct uranium enrichment of the sedimentary cover rocks at the sub-Athabasca unconformity and in some parts of the basement rocks. B, basement rocks; FP, Fair Point Formation; MF, Manitou Falls Formation; LL, Lazenby Lake Formation. Depths are along the drillholes (see Fig. 13 for locations of the drillholes and Table 4 for their dips).*

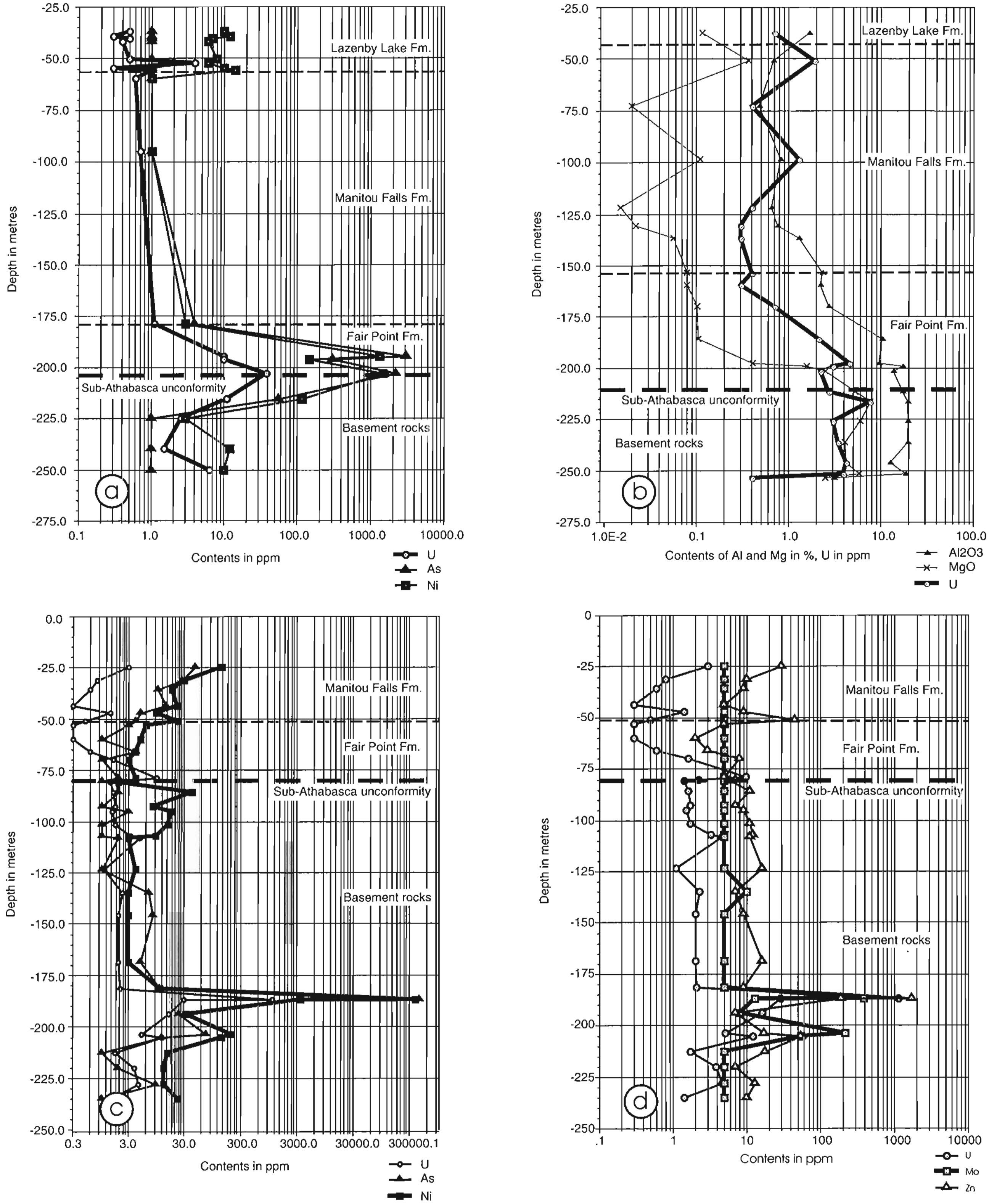

Figure 20. *Distribution of uranium and accompanying constituents in selected drillholes in the study area:* ***a.*** *uranium, arsenic and nickel in drillhole 306;* ***b.*** *uranium and aluminum and magnesium oxides in drillhole 303;* ***c.*** *uranium, arsenic and nickel in drillhole 302;* ***d.*** *uranium, molybdenum and zinc in drillhole 302. Depths are along the drillholes (see Fig. 13 for locations of the drillholes and Table 4 for their dips).*

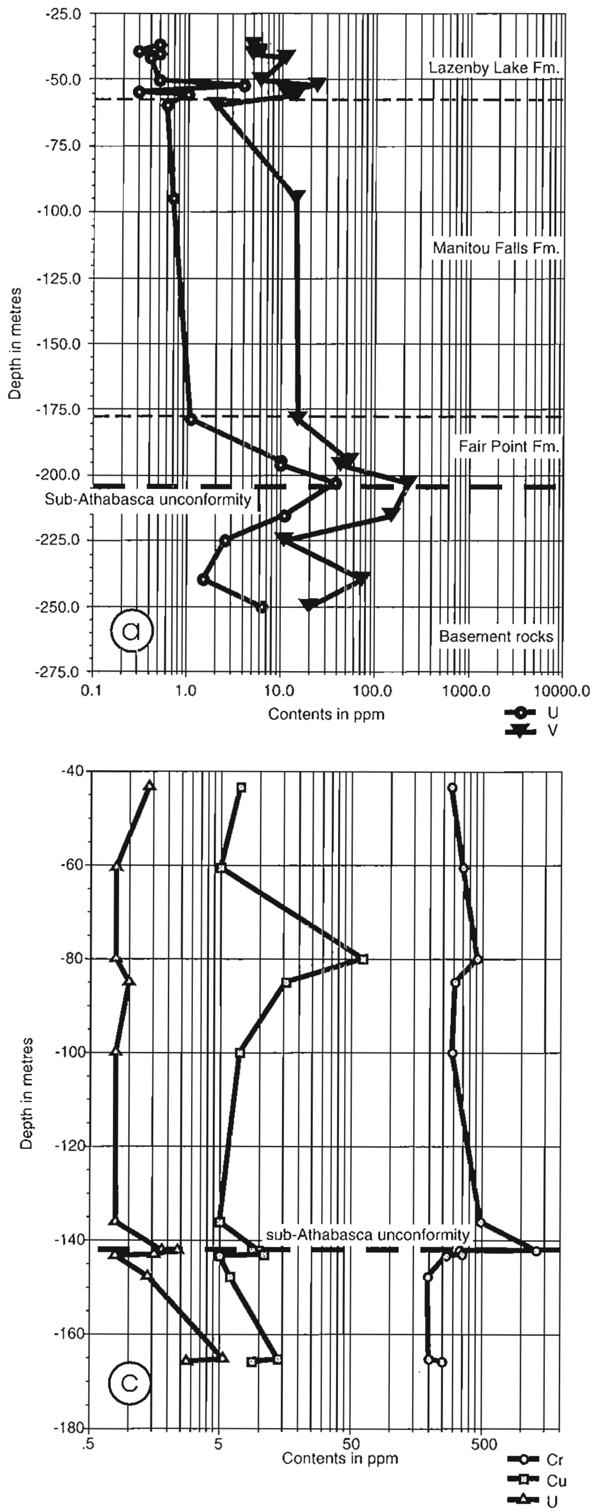

***Figure 21.** Distribution of uranium and accompanying elements in selected drillholes in the central part of the study area: **a.** uranium and vanadium in drillhole 306; **b.** uranium and chromium in drillhole 306; **c.** uranium, chromium and copper in drillhole 320. Depths are along the drillholes (see Fig. 13 for locations of the drillholes and Table 4 for their dips).*

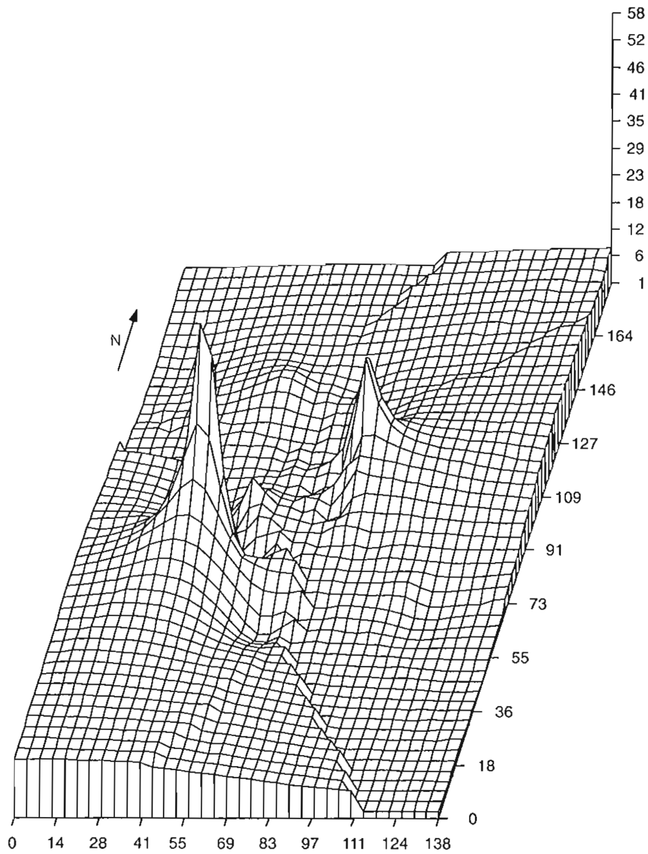

Figure 22. *Regional distribution of uranium in the study area. (Mean values are from drillhole samples. Data in ppm; n = 287.)*

the conceptual deposit model (Fig. 6). These controlling factors are, as a rule, regional faults, which, in turn, coincide with the presence of graphitic/pyritic metapelitic layers in the basement rocks. These layers typically have low electrical resistivity and thus can be detected by geophysical surveys.

The uranium anomalies represent concentrations of discrete uranium minerals, such as massive pitchblende, crystalline uraninite and coffinite (e.g., in drillhole 306). Uranium minerals are commonly accompanied by nickel arsenide and sulpharsenide minerals. The mineralization typically is surrounded by: alteration zones which consist of clay minerals; magnesian chlorite; sericite; and, locally, apatite and iron oxides. In addition to anomalies in the sedimentary rocks, anomalies also occur in basement rocks, particularly in chloritized graphitic-pyritic metapelite itself and in altered pegmatoids. Alteration of the host rocks is commonly associated with magnesium metasomatism, as is apparent on samples from drillhole 303, located in the central part of the study area (Fig. 20b).

Lithostratigraphic distribution of uranium in study area 'A' in Alberta was compared with the distribution in control areas 'B' and 'C' in Saskatchewan. The basement rocks in all three areas contain elevated amounts of uranium (Fig. 18a). Furthermore, concentration of uranium occurs in the lower parts of the Athabasca Basin sedimentary succession (i.e., in the Fair Point and Manitou Falls formations). In all three areas, the principal uranium mineral is pitchblende, which attests to epigenetic processes in its deposition. The mode of enrichment combined with the character of the mineralization testify to the operation of the same epigenetic processes that were involved in the formation of the unconformity deposits in all three areas. In Alberta, metallogenic features of area 'A' are compatible with the model for unconformity uranium deposits. Uranium mineralization in Alberta was identified in a geological environment similar to the one in which the known uranium unconformity deposits in Saskatchewan occur. However, the absence of discovered economic uranium deposits in Alberta (area 'A') is, apparently, related to the extent of exploration for uranium, which is much lower in Alberta than in the Saskatchewan part of the basin.

Nickel

Mean contents of nickel in various lithostratigraphic units within the study area ('A') and control areas ('B' and 'C') are apparent from the ANOVA interaction bar plot for nickel (Fig. 18b). The graph is based on geochemical analyses of 599 samples (554 from Alberta and 45 from Saskatchewan).

In study area 'A' the mean nickel content in 267 samples from basement rocks was 0.15% Ni. However, a sample of chloritized biotite gneiss from drillhole 302 (which is located in the central part of the study area), contains 38.4% Ni over 0.1 m at a depth of 186.8 m (Fig. 20c). In this sample, nickeline, gersdorffite, rammelsbergite, pararammelsbergite and annabergite are associated with pitchblende.

The sedimentary rocks of the Athabasca Group, the Devonian rocks and the Quaternary deposits contain an average of 26 ppm Ni in 287 samples. However, a mineralized interval within altered sandstone of the basal Fair Point Formation contains 7.1% Ni over 5 m. In addition to nickel minerals (pararammelsbergite, rammelsbergite, gersdorffite and nickeline), the mineralized interval contains uranium (see above), cobalt (0.17% Co), vanadium (0.27% V), molybdenum (0.08% Mo), lead (0.14% Pb), and 550 ppb of gold (Orr et al., 1988). Nickeline

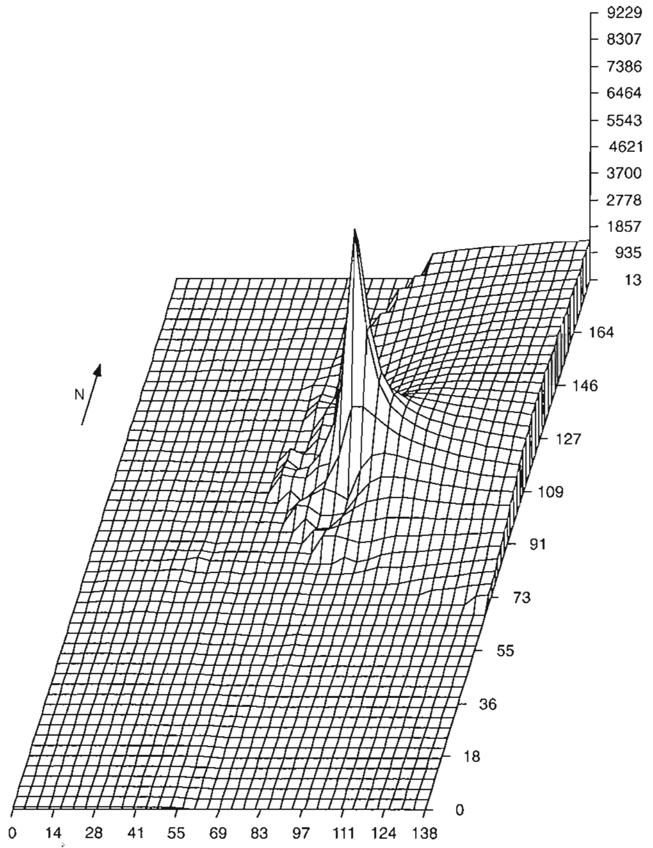

Figure 23. *Regional distribution of nickel in the study area. (Mean values are from drillhole samples. Data in ppm; n = 287.)*

disseminated in the sandstone and locally overgrowing pyrite has been identified in the vicinity of this mineralization (Plates 3c, d).

Regional distribution of nickel in the study area of Alberta is shown by a three-dimensional graph (Fig. 23). Examination of the distribution reveals that the main hosts of nickel are the basement rocks. In the sedimentary cover rocks, the nickel mineralization is commonly restricted to areas of uranium occurrences. In the study area, nickel typically occurs in arsenides, sulpharsenides and complex sulphides, particularly as rammelsbergite ($NiAs_2$), gersdorffite (NiAsS), nickeline (NiAs) and bravoite ((Ni,Co,Fe)S).

The mean nickel contents in samples from the basement rocks in the Alberta study area are higher than those in the Saskatchewan control areas (Fig. 18b). In the study area, the mean nickel contents of individual lithostratigraphic units within the Athabasca Group decrease in an upward direction. The Devonian rocks have slightly higher mean nickel values than those of the Athabasca Group. The relatively high nickel contents of the overburden are apparently related to its lithological composition derived from the basement rocks. In addition to basement rocks, the anomalous nickel contents in the Saskatchewan control areas are found in rocks of the Manitou Falls Formation, which are the principal host rocks for the unconformity deposits.

Arsenic

Arsenic is a significant constituent of the polymetallic unconformity deposits in the Athabasca Basin. In the study area, arsenic exhibits anomalous concentrations (mean = 852.8 ppm As; n = 554). The highest values are associated with the basement rocks (mean = 1736 ppm As, peak = 459 000 ppm As), whereas Athabasca Group and Devonian rocks, and Quaternary deposits contain lesser amounts (mean = 30.9 ppm As, peak = 3100 ppm As). Relative distribution of arsenic in the stratigraphic section is apparent from Figure 18c. The graph, which is based on geochemical analyses of 599 samples (554 from Alberta and 45 from Saskatchewan), also includes

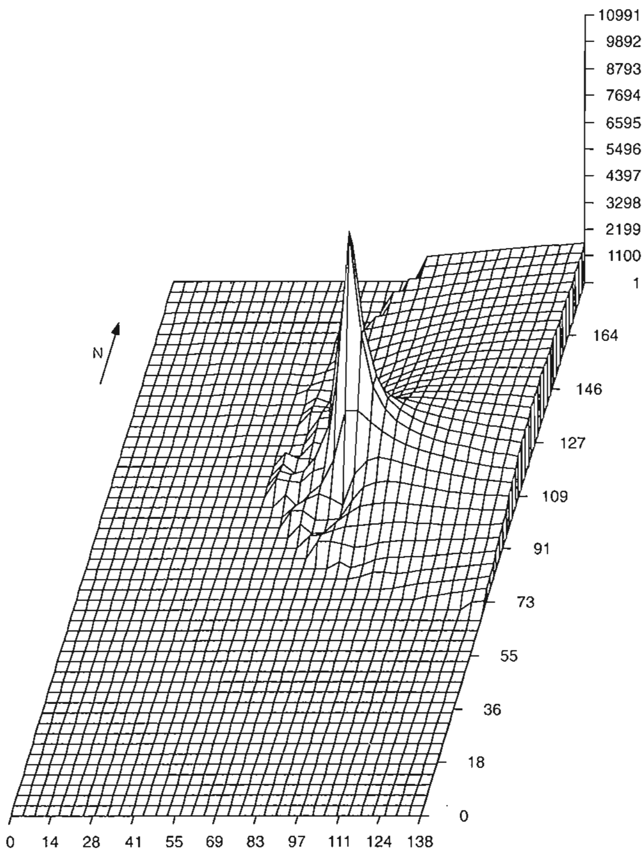

Figure 24. *Regional distribution of arsenic in the study area. (Mean values are from drillhole samples. Data in ppm; n = 287.)*

information on the control areas in Saskatchewan. Regional distribution of arsenic (Fig. 24) is almost identical to that of nickel. The most common occurrence of arsenic in the study area is in nickel and cobalt minerals, which are in turn frequently accompanied by uranium minerals. In addition to these assemblages, arsenic locally also occurs with gold. Arsenic enrichment of basement rocks in the Saskatchewan control areas is lower than in Alberta. However, the opposite situation is true for the rocks of the Manitou Falls Formation (Fig. 18c). In all the areas, observations on the distribution of arsenic complement those on the distribution of nickel.

Cobalt

The lithostratigraphic distribution pattern of cobalt in the study area is shown in Figure 18d. The graph, which is based on geochemical analyses of 599 samples (554 from Alberta and 45 from Saskatchewan), also includes information on the control areas in Saskatchewan. In spite of its paragenetic association with nickel, the mean content of cobalt in rocks in the study area is substantially lower than that of nickel, the Ni:Co ratios for individual rock units vary greatly, and the regional distribution differs from that for nickel. For example, the Ni:Co ratio is about 70:1 for the basement rocks, about 10:1 for the Fair Point Formation, about 3:1 for the Manitou Falls Formation, about 5:1 for the Lazenby Lake Formation, and about 2.5:1 for the Devonian rocks (cf. Figs. 18b, d). However, in rocks of the Manitou Falls Formation in the control areas in Saskatchewan (Fig. 18d), cobalt exhibits anomalous distribution and the Ni:Co ratios (mean values) in this formation are 1.1:1 and for all the rock units 1.9:1. This diversity is also apparent in the regional distribution of cobalt (Fig. 25), which differs not only from that of nickel (Fig. 23), but also from those for uranium (Fig. 22), arsenic (Fig. 24), vanadium (Fig. 26), chromium (Fig. 27) and zinc (Fig. 28). A part of a polymetallic aggregate of Co-Ni-As-Fe composition (spot 1 on Plate 3e) is intimately intergrown with a U-O-Ni-As-Co-Fe-S compound (spot 2 on Plate 3e).

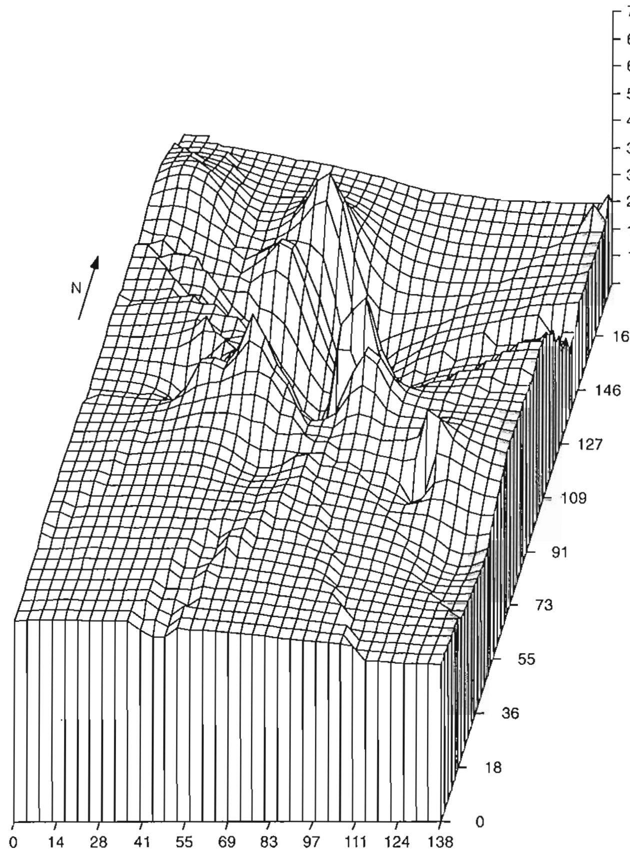

Figure 25. *Regional distribution of cobalt in the study area. (Mean values are from drillhole samples. Data in ppm; n = 287.)*

Molybdenum

Molybdenum is a typical metallic element accompanying uranium in the Athabasca Basin unconformity deposits (Ruzicka and LeCheminant, 1987). Relative distribution of molybdenum within the stratigraphic section of the study area is apparent from Figure 18e. The graph, which is based on geochemical analyses of 599 samples (554 from Alberta and 45 from Saskatchewan), also includes information on the control areas in Saskatchewan. Mean content for molybdenum in the rocks of the whole area is almost equal to that of uranium, but its peak value is lower (mean = 7.2 ppm Mo, peak = 388 ppm Mo). Elevated values of molybdenum were found in association, particularly with altered granitoid rocks (e.g., in drillholes 302, 309, 329 and 330). In drillhole 302 (Fig. 20d), molybdenum (388 ppm Mo over 1 m) occurs in strongly altered granite pegmatite in an assemblage with zinc, uranium, nickel and arsenic (cf. Fig. 20c). Molybdenum also occurs in chloritized graphitic metapelites (e.g., in drillholes 319 and 330). In some areas, elevated molybdenum values were also found in the Athabasca Group and Devonian rocks (e.g., in drillholes 309, 319 and 328). Mean values of molybdenum in rocks of the Manitou Falls Formation in the Saskatchewan control areas are higher than those in the rocks of the study area in Alberta (Fig. 18e). Molybdenum occurs mainly in molybdenite (Plate 3f) and in secondary minerals ilsemanite and jordisite.

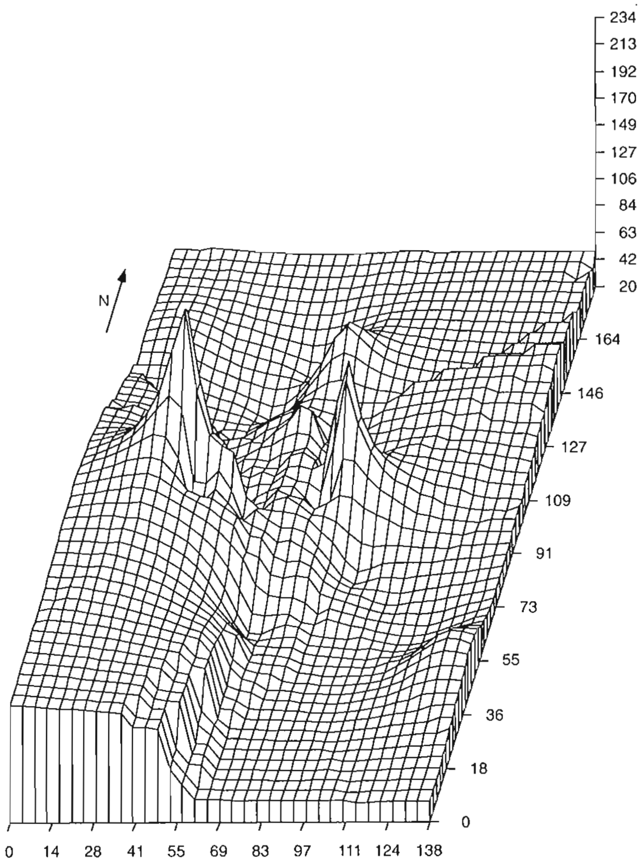

Figure 26. *Regional distribution of vanadium in the study area. (Mean values are from drillhole samples. Data in ppm; n = 287.)*

Vanadium

The highest content of vanadium (1352 ppm V) in the study area in Alberta was found in a sample of Devonian rocks. However, in all rock units the mean contents of vanadium are below its crustal abundance (Fig. 18f), but locally the peak contents exceed the average crustal abundance (clarke values) by as much as 9.7 times in the Alberta study area. Wilson (1985) reported an average content of 163 ppm V in seven samples of "mafic mylonite" collected from drillholes 4, 19, 23, 25 and 38, which are located in the southwestern part of the study area. He described the mafic mylonite as "dark gray to greenish gray rocks containing chlorite, biotite, epidote and clay groundmass with grains of pyrite and streaks of graphite" (Wilson, 1985). This unit is, apparently, equivalent to the metapelitic layer, which lithologically controls mineralization in the unconformity deposits in the Saskatchewan part of the basin. Vanadium correlates with uranium (cf. drillhole 306; Fig. 21a) and titanium in some areas. Regional distribution of vanadium is apparent from a three-dimensional graph (Fig. 26). The vanadium anomalies are confined to the central part of the study area, but in the southeastern and northernmost parts of the area, the vanadium contents in the rocks are substantially below its crustal abundance. The basement rocks in the control areas in Saskatchewan contain more vanadium than those in the study area in Alberta (Fig. 18f). This difference is probably related to more frequent presence of metapelitic rocks in areas 'B' and 'C' than in Alberta.

Chromium

In the study area, chromium has specific distribution patterns. The mean values in samples from all the stratigraphic units within the study area (Fig. 18g) exceed its clarke value, which amounts to 110 ppm Cr. The graph, which is based on geochemical analyses of 599 samples, also includes information on the control areas in Saskatchewan. Anomalous values of chromium have been found in samples from the Lazenby Lake Formation, but the highest concen-

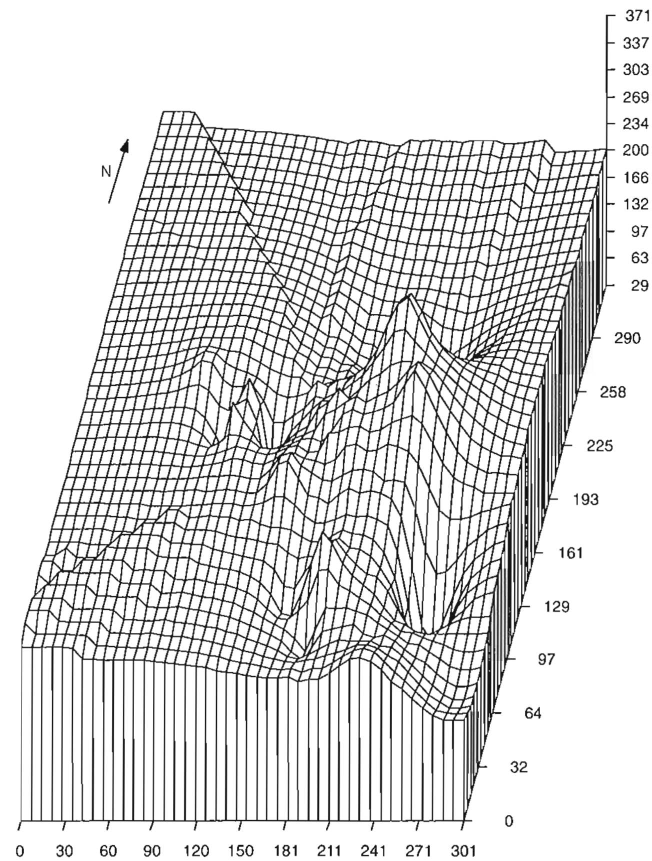

Figure 27. *Regional distribution of chromium in the central part of the study area. (Mean values are from drillhole samples. Data in ppm; n = 554.)*

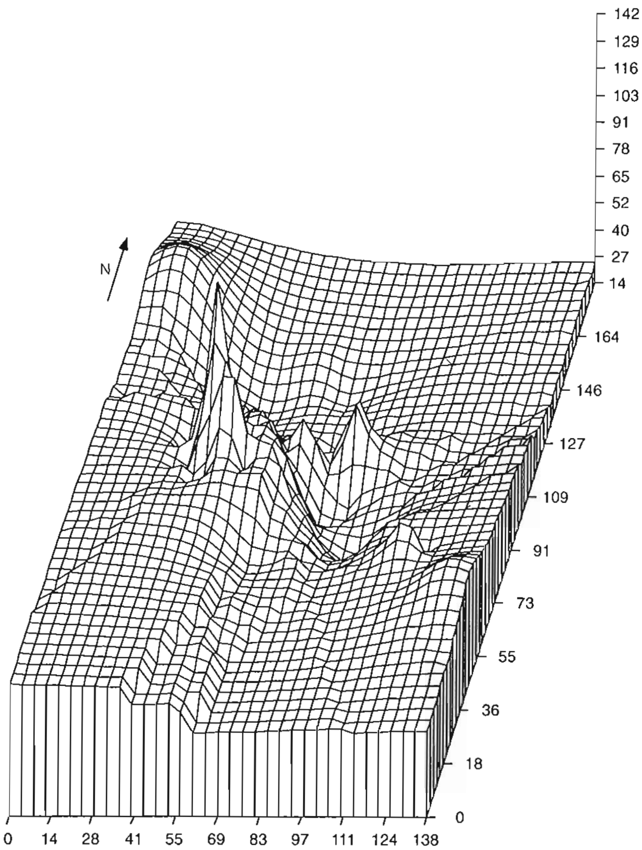

Figure 28. *Regional distribution of zinc in the study area. (Mean values are from drillhole samples. Data in ppm; n = 287.)*

tration of chromium (1328 ppm Cr) has been found in a sample from the altered basal part of the Fair Point Formation, in the central part of the study area. Anomalous contents of chromium in the Quaternary glacial deposits are a significant feature in the distribution pattern for chromium in Alberta. A three-dimensional diagram shows the regional distribution of chromium within the central part of the study area (Fig. 27). Mean contents of chromium in samples from the Saskatchewan control areas are substantially lower than those in the corresponding geological units in Alberta. In spite of this difference, elevated values of chromium have been identified in other parts of the Athabasca Basin. For instance, M. Fayek and K.T. Kyser (pers. comm., 1994) found distinct chromium mineralization in the Athabasca Group rocks in the Maw REE deposit between the Key Lake and P2 North deposits.

The chromium mineralization occurs, apparently, in two modes: (i) as sedimentary-syngenetic occurrences, and (ii) as epigenetic/diagenetic concentrations.

(i) As is apparent from the log of the drillhole 306 (Fig. 21b), chromium is enriched in the Lazenby Lake Formation. In this drillhole, the mean chromium contents in samples from the Lazenby Lake Formation exceed its average crustal abundance (clarke values) by as much as 4.7 times. Chromium tends to be distributed inversely to uranium (Fig. 21b) suggesting that it was deposited by different processes (apparently sedimentary syngenetic) than uranium. Conversely, the distribution pattern of uranium, the site of its concentration at the unconformity and its mineral form as pitchblende and coffinite, indicate that its deposition took place at a redox front from metalliferous brines by epigenetic processes, and therefore the mineralization is compatible with the model for unconformity deposits discussed above. The diverse models for uranium and chromium mineralization are also supported by the results of factor analyses. An unrotated factor plot for selected constituents from 548 samples from the study area indicates that uranium, cobalt, nickel, arsenic, zinc and molybdenum form one group of related variables, whereas chromium is in an entirely different group and closely spatially related to copper and barium (Fig. 15).

(ii) The second mode of chromium occurrence in the study area was observed in several drillholes, for example, in parts of drillholes 320 (Fig. 21c), 303 and 307. In these locations, anomalous values of chromium occur in the altered sedimentary cover or basement rocks directly at the sub-Athabasca unconformity. At the unconformity, the distribution pattern of chromium resembles that of uranium.

The chromium-bearing Athabasca sandstone might be comparable, to a certain degree, to some chromiferous deposits that occur in the eastern Ugui Graben in the Olekma-Vitim province in Russia (Bogdanov and Berlyand-Kozhevnikov, 1990). The copper and chromium mineralization occurs in lenses, several kilometres long and tens of metres thick, within sandstone of the 100 m thick Precambrian Pravdinskaya Formation. The deposits are associated with a redbed–greybed transition zone of the sandstone. The deposits occur as: (i) chromite-bearing concentrations, which are only of a limited extent; and (ii) copper- and chromium-bearing glauconite orebodies, which prevail. Buried coastal-marine placers, which occur elsewhere within the Pravdinskaya Formation, are considered as a source for the copper-and chromium-bearing glauconite mineralization. Chromium contents in the glauconite series minerals are as high as 14% Cr_2O_3.

In the samples collected from the study area, chromium is extremely finely disseminated in the rocks. Some chromium is associated with nonmetallic minerals, particularly potassium micas (muscovite). More studies of chromium distribution are necessary in order to determine its source and its metallogenic significance.

Zinc

The distribution pattern of zinc within the stratigraphic units of the study area is shown in Figure 18h. In spite of its common association with uranium, its regional distribution is more complex (Fig. 28). The mean content of zinc in rocks of all the units combined is about four times lower than its crustal abundance. Elevated concentrations of zinc have been found in rocks within the western part of the study area. Zinc exhibits anomalous values in the Manitou Falls Formation of the Saskatchewan part of the basin, but relatively uniform distribution in all stratigraphic units of area 'A' in Alberta (Fig. 18h).

Gold

Distribution of gold was investigated in 342 samples from the central part of the study area. In about 10 per cent of the samples, gold was present in elevated amounts in both the basement and in the Athabasca

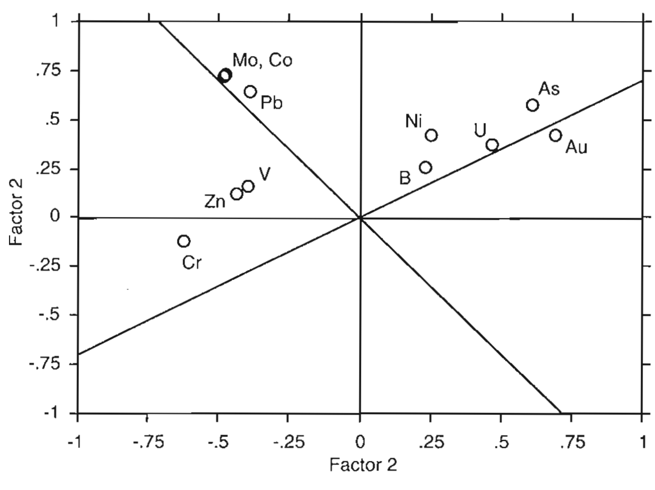

Figure 29. Oblique Factor Plot from factor analysis for 28 constituents in 554 samples from the study area.

Group rocks. The highest values (as much as 550 ppb Au) are associated with the rocks of the Fair Point Formation, which is the basal formation of the Athabasca Group in the study area. The above-mentioned peak value of gold occurs in proximity to uranium mineralization. Gold has the highest correlation coefficient with arsenic (0.974), but a factor analysis of gold contents in samples from the study area indicates that in addition to arsenic, uranium, nickel and boron are statistically related to gold more closely than to the other elements (Fig. 29). In the Cluff 'D' orebody, which was mined for uranium in the Carswell Structure about 15 km east of the anomaly, gold was confined to the basal part of the Athabasca Group rocks and intimately associated with high-grade uranium ore.

POTENTIAL FOR MINERAL DEPOSITS IN THE ATHABASCA BASIN, NORTHEASTERN ALBERTA

Ores of the polymetallic deposits in the Athabasca Basin, such as the Key Lake, Cigar Lake, Collins Bay 'B' zone, and Midwest, in addition to several generations of pitchblende and coffinite, consist of arsenides and sulpharsenides of nickel and cobalt; sulphides of nickel, copper, lead, molybdenum, iron and zinc; and oxides and hydroxides of iron. Silver, gold and platinum group elements occur locally. Chlorite, illite, kaolinite and siderite are the most common gangue minerals. Ores of the monometallic deposits in the basin, such as Rabbit Lake and Eagle Point, consist of pitchblende (in massive, globular, and sooty forms), coffinite and, locally, secondary minerals, such as boltwoodite, sklodowskite and kasolite. Carbonates (calcite, dolomite, siderite), sericite, chlorite, clay minerals (illite, kaolinite), celadonite, and tourmaline (dravite) are common gangue minerals.

Elemental assemblages constituting these polymetallic and monometallic ores in Saskatchewan are also typical of the basement and cover rocks of the Alberta part of the Athabasca Basin, as demonstrated by a factor analysis of elemental constituents in 554 samples from study area 'A' in Alberta (Fig. 15). Distribution of these assemblages in Alberta is commonly structurally controlled by the sub-Athabasca unconformity. Furthermore, the lithostratigraphic distribution of indicator elements such as uranium, nickel, cobalt, arsenic, molybdenum and zinc in Alberta resembles, to a certain degree, that of the control areas in Saskatchewan.

Observations in the Alberta part of the Athabasca Basin confirm that both the regional and conceptual deposit models established for the Saskatchewan world-class unconformity deposits are also applicable to Alberta. The Archean granitoids, which were reactivated during the Hudsonian Orogeny, represent a source of uranium and other lithophile elements, whereas the mafic and ultramafic basement rocks are a source of siderophile elements, such as nickel, cobalt and platinum group elements. Weathering processes preceding the formation of the Athabasca Basin and leading to the formation of a thick regolith (or saprolith) facilitated liberation of the metals from the basement rocks and their availability in the vast reservoir of the Athabasca Basin. Ore-forming processes, which were controlled structurally by the unconformity and fault or fracture systems and lithologically by the reducing basement rocks and oxidized basinal rocks, took place at redox fronts. The observations in Alberta yield evidence of interaction among the basement, basinal and 'retrograde' (derived from meteoric waters) fluids. Locally intensive alteration of the host rocks, which was associated with the circulating fluids, protected the mineralization from dispersion.

Observations of metallogenic features of the Alberta part of the Athabasca Basin confirm that the possibility for discovery of the unconformity-type deposits in northeastern Alberta exists. Apparently, the absence of identified economic uranium deposits in Alberta is related to the limited extent of past exploration for uranium and less efficient methods at the time of past exploration activities.

RECOMMENDATIONS FOR EXPLORATION

As concluded above, the Alberta part of the Athabasca Basin is favourable for discoveries of mineral deposits, particularly those associated with the sub-Athabasca unconformity. Therefore exploration for this deposit type should take into account the following criteria:

(i) Exploration targets should include terranes with basement rocks, including Archean granitoid rocks which have been reactivated during the Hudsonian Orogeny. The basement rocks should contain reductants, such as carbonaceous/graphitic or pyrite-bearing pelitic units. Because of the high conductivity of these zones, electromagnetic geophysical methods are an efficient tool for their detection, even at depths exceeding 500 m below the surface.

(ii) The structural pattern of the targets selected should include faults or fracture zones. The paleosurface of the bedrock below the overburden may exhibit the effects of glacial scouring in areas occupied by these faults or fracture zones. These features also may be identified by geophysical surveys.

(iii) Zones of alteration associated with mineralization may have a low density and be detectable by detailed gravity surveys.

(iv) Radiometric anomalies may be present, although they may be weak, particularly those with a high U/Th ratio. However, negative results of ground radiometric surveys (using Geiger-Müller counters, scintillometers or gamma-ray spectrometers) do not preclude the possible existence of uranium mineralization at depth.

(v) Geochemical anomalies of uranium and/or associated elements, such as arsenic, nickel, cobalt, molybdenum, zinc, lead, copper, bismuth and boron may be present and detectable by selective geochemical surveys.

(vi) During geological and radiometric logging of drillcore, particular attention should be paid to argillized (illitized/kaolinized) and chloritized rocks, and to ratios between their components (such as Al, Mg, K, Na and Fe). Important features are: the recognition and observation of the unconformity and intersecting faults and fracture zones along it; limonite/hematite alteration; dilational and hydrothermal effects associated with the mineralization process; presence of collapse structures; vugs filled with euhedral quartz and silicification aureoles within the clastic sedimentary cover rocks; and depletion of graphite in pelitic layers in the basement. Percival et al. (1993) and others have shown that alteration halos, extending tens of metres into enveloping rocks, may be present and detectable in association with polymetallic deposits such as the Cigar Lake deposit in the Saskatchewan portion of the Athabasca Basin.

(vii) Lithogeochemical sampling of drillcore is not only for the detection of the indicator elements (particularly U, Ni, Co, As, Mo and Zn), but also for the determination of their regional and stratigraphic distribution patterns, mutual relationships and behaviour as demonstrated in this study.

RECOMMENDATION FOR CONTINUING RESEARCH

The Athabasca Basin is one of the most important uranium/polymetallic metallogenic provinces of the world. The Saskatchewan part of the basin has been subject to extensive research on the regional and local features of uranium mineralization. Although the Alberta part represents only about 10 per cent of the total area of the basin, its favourable metallogenic features require continuing research, particularly in these directions:

(i) Updating of isopach maps of individual formations of the Athabasca Group and Phanerozoic rocks.

(ii) Detailed geophysical mapping of the structural pattern of the area.

(iii) Detailed geophysical mapping of the metapelitic (conductive) layers in the basement rocks.

(iv) Determination of the regional extent of regolith and the nature of processes participating in the formation of the regolith.

(v) Determination of fluid compositions/ generations and fluid flows from isotope analyses of the host rocks, alteration haloes and mineralization.

(vi) Determination of geochronology of the mineralization events, particularly through Pb-U-Th isotope analyses.

(vii) Particular attention to determination of the source rocks for chromium and their relationships to the distribution of chromiferous indicator minerals in context with the distribution of kimberlite pipes.

(viii) Distribution of gold and platinum group elements (PGE) in the context of epigenetic/diagenetic mineralization associated with the unconformities.

Acknowledgments

This study has been conducted under the Canada-Alberta Agreement on Mineral Development in cooperation with the geologists of the Alberta Geological Survey, particularly Wylie Hamilton, Dixon Edwards and Douglas Boisvert. Scanning electron microscope analyses were made by David Walker of the Geological Survey of Canada. Critical reading of the paper by Ian Jonasson and Roger Macqueen of the Geological Survey of Canada is gratefully acknowledged. Leadership of the Alberta MDA program by Roger Macqueen of the Geological Survey of Canada, Calgary, is greatly appreciated.

REFERENCES

Andrade, N.
1989: The Eagle Point uranium deposit, northern Saskatchewan, Canada. *In* Uranium Resources and Geology of North America, Proceedings of a Technical Committee Meeting, Saskatoon, 1987, International Atomic Energy Agency, IAEA-TECDOC-500, Vienna, p. 455-490.

Appleyard, E.C.
1984: The origin of plagioclasite in the vicinity of the Rabbit Lake uranium deposit. *In* Summary of Investigations 1984, Saskatchewan Geological Survey, Saskatchewan Energy and Mines, Miscellaneous Report 84-4, p. 68-71.

Ashton, K.E.
1988: Precambrian Geology of the southeastern Amer Lake area (66H/1), near Baker Lake, N.W.T. Unpublished Ph.D. thesis, Queen's University, Kingston, 335 p.

Baadsgaard, H.
1965: Geochronology. Meddelelser fra Dansk Geologisk Forening, Bind 16, p. 1-48.

Battey, G.C., Miezitis, Y., and McKay, A.D.
1987: Australian uranium resources. Australia, Bureau of Mineral Resources and Geophysics, Resource Report 1, Canberra, 67 p.

Bickford, M.E., Collerson, K.D., Lewry, J.F., van Schmus, W.R., and Chiarenzelli, J.R.
1990: Proterozoic collisional tectonism in the Trans-Hudson orogen, Saskatchewan. Geology, v. 18, p. 14-18.

Bogdanov, Yu.V. and Berlyand-Kozhevnikov, P.V.
1990: Cupriferous and chromiferous Precambrian deposits in Olekma-Vitim Province, U.S.S.R. *In* Program with Abstracts, 8th IAGOD Symposium, August 12-18, 1990, Ottawa, Canada, p. A223.

Cameron, A.E.
1930: Report on progress on mineral explorations in the Precambrian. Alberta Research Council Report 25, Tenth Annual Report, 1929, p. 34-39.

Cramer, J.J.
1986: A natural analog for a fuel waste disposal vault. *In* Proceedings of the Second International Conference on Radioactive Waste Management. Canadian Nuclear Association, p. 679-702.

Cumming, G.L. and Krstic, D.
1992: The age of unconformity-related uranium mineralization in the Athabasca Basin, northern Saskatchewan. Canadian Journal of Earth Sciences, v. 29, p. 1623-1639.

Cumming, G.L., Krstic, D., and Wilson J.A.
1987: Age of the Athabasca Group, northern Alberta. *In* Geological Association of Canada/Mineralogical Association of Canada, Program with Abstracts, v. 12, p. 35.

Cumming, G.L. and Rimsaite, J.
1979: Isotopic studies of lead-depleted pitchblende, secondary radioactive minerals and sulphides from the Rabbit Lake uranium deposit, Saskatchewan. Canadian Journal of Earth Sciences, v. 16, p. 1702–1715.

Davidson, G.I. and Gandhi, S.S.
1989: Unconformity-related U-Au mineralization in the Middle Proterozoic Thelon Sandstone, Boomerang Lake Prospect, Northwest Territories, Canada. Economic Geology, v. 84, p. 143–157.

de Carle, A.
1986: Geology of the Key Lake deposits. *In* Uranium deposits of Canada, E.L. Evans (ed.). The Canadian Institute of Mining and Metallurgy, Special Volume 33, p. 170–177.

Dudas, F.O., LeCheminant, A.N., and Sullivan, R.W.
1991: Reconnaissance and isotopic study of granitoid rocks from the Baker Lake region, District of Keewatin, N.W.T., and observations on analytical procedures. *In* Radiogenic Age and Isotopic Studies: Report 4. Geological Survey of Canada, Paper 90-2, p. 101–112.

Edwards, W.A.D., Richardson, R.J.H., and Fildes, B.J.
1991: Geology and mineral potential of northeastern Alberta. Alberta Research Council, Open File Report 1991-6, 70 p.

Ey, F., Piquard, J.P., Baudemont, D., and Zimmerman, J.
1992: The Sue uranium deposits, Saskatchewan, Canada. *In* New Developments in Uranium Exploration, Resources, Production and Demand, Proceedings of a Technical Committee Meeting, jointly organized by the International Atomic Energy Agency and the Nuclear Energy Agency of the OECD and held in Vienna, 26–29 August, 1991. International Atomic Energy Agency IAEA-TECDOC-650, Vienna, p. 189–213.

FIGNR
1989: Activity Report 1987/88. Federal Institute for Geosciences and Natural Resources, Hannover, p. 43.

Fouques, J.P., Fowler, M., Knipping, H.D., and Schimann, K.
1986: The Cigar Lake uranium deposit: discovery and general characteristics. *In* Uranium Deposits of Canada, E.L. Evans (ed.). The Canadian Institute of Mining and Metallurgy, Special Volume 33, p. 218–229.

Fuchs, H. and Hilger, W.
1989: Kiggavik (Lone Gull): An unconformity related uranium deposit in the Thelon Basin, Northwest Territories, Canada. *In* Uranium Resources and Geology of North America, Proceedings of a Technical Committee Meeting, Saskatoon, 1987, International Atomic Energy Agency, IAEA-TECDOC-500, Vienna, p. 429–454.

Godfrey, J.D.
1958: Mineralization in the Andrew, Waugh and Johnson Lakes area, northeastern Alberta. Alberta Research Council, Report 58-4, 17 p.

1960: Northeast corner of Alberta and adjacent area: its development and mineral potential. The Canadian Institute of Mining and Metallurgy, Transactions v. 63, p. 162–171.

1961: Geology of the Andrew Lake, north district, Alberta. Alberta Research Council, Report 58-3, 32 p.

Godfrey, J.D. and Peikert, E.W.
1963: Geology of the St. Agnes Lake district, Alberta. Alberta Research Council, Report 62-1, 31 p.

1964: Geology of the Colin Lake district, Alberta. Alberta Research Council, Report 62-2, 28 p.

Godfrey, J.D. and Watanabe, R.Y.
1964: The mineralogical composition of an area of Precambrian Shield in northeastern Alberta. Proceedings of the 22nd International Geological Congress, 1964, New Delhi, India, p. 300–328.

Henderson, J.R., Henderson, M.N., Pryer, L.L., and Cresswell, R.G.
1991: Geology of the Whitehills-Tehek area, District of Keewatin: an Archean supracrustal belt with iron-formation-hosted gold mineralization in the central Churchill Province. *In* Current Research, Part C. Geological Survey of Canada, Paper 91-1C, p. 149–156.

Hoeve, J. and Quirt, D.H.
1984: Mineralization and host-rock alteration in relation to clay mineral diagenesis and evolution of the Middle Proterozoic Athabasca Basin, Northern Saskatchewan, Canada. Saskatchewan Research Council, Technical Report No. 187, 187 p.

Hoeve, J. and Sibbald, T.I.I.
1978: On the genesis of Rabbit Lake and other unconformity-type uranium deposits. Economic Geology, v. 73, p. 1450–1473.

Jackson, D.G and Andrew, R.L.
1990: Kintyre uranium deposit. *In* Geology of the Mineral Deposits of Australia and Papua, New Guinea, F.E. Hughes (ed.). Australian Institute of Mining and Metallurgy, Melbourne, p. 653–658.

Knipping, H.D.
1974: The concepts of supergene versus hypogene emplacement of uranium at Rabbit Lake, Saskatchewan, Canada. *In* Formation of Uranium Deposits, International Atomic Energy Agency, Vienna, p. 531–548.

Koeppel, V.
1968: Age and history of the uranium mineralization of the Beaverlodge area, Saskatchewan. Geological Survey of Canada, Paper 67-31, 111 p.

Kotzer, T.
1992: Origin and geochemistry of fluid events in the Proterozoic Athabasca Basin. Unpublished Ph.D. thesis, University of Saskatchewan, 329 p.

1993: Fluid history of the Proterozoic Athabasca Basin. Ph.D. thesis, University of Saskatchewan, University Microfilms, Ann Arbor, Michigan, 310 p.

Kotzer, T.G. and Kyser, T.K.
1990a: Fluid history of the Athabasca Basin and its relation to uranium deposits. *In* Summary of Investigations 1990, Saskatchewan Geological Survey, Saskatchewan Energy and Mines, Miscellaneous Report 90-4, p. 153-157.

1990b: The use of stable and radiogenic isotopes in the identification of fluids and processes associated with unconformity-type uranium deposits. *In* Modern Exploration Techniques, L.S. Beck and T.I.I. Sibbald (eds.). Saskatchewan Geological Society, Special Publication 9, p. 115-131.

Kotzer, T.G., Kyser, T.K., and Irving, E.
1992: Paleomagnetism and the evolution of fluids in the Proterozoic Athabasca Basin, Northern Saskatchewan, Canada. Canadian Journal of Earth Sciences, v. 29, p. 1474-1491.

Krogh, T.E. and Clark, L.A.
1987: Zircon dating of sub-Athabasca granitoid rocks, Saskatchewan. *In* Geological Association of Canada/ Mineralogical Association of Canada, Annual Meeting, Saskatoon, Program with Abstracts, v. 12, p. 64.

Kyser, T.K., Kotzer, T.G., and Wilson, M.R.
1989: Isotopic constraints on the genesis of unconformity uranium deposits. *In* Geological Association of Canada/Mineralogical Association of Canada, Program with Abstracts, v. 14, p. A120.

Lainé, R., Alonso, D., and Svab, M. (eds.)
1985: The Carswell Structure Uranium Deposits, Saskatchewan. Geological Association of Canada, Special Paper 29, 230 p.

Langford, F.F.
1986: Geology of the Athabasca Basin. *In* Uranium deposits of Canada, E.L. Evans (ed.). The Canadian Institute of Mining and Metallurgy, Special Volume 33, p. 123-133.

LeCheminant, A.N. and Heaman, L.M.
1989: Mackenzie igneous events, Canada: Middle Proterozoic hotspot magmatism associated with ocean opening. Earth and Planetary Science Letters, v. 96, p. 38-49.

LeCheminant, A.N. and Roddick, J.C.
1991: U-Pb zircon evidence for widespread 2.6 Ga felsic magmatism in the central District of Keewatin, N.W.T. *In* Radiogenic Age and Isotopic Studies, Report 4. Geological Survey of Canada, Paper 90-2, p. 91-99.

Lewry, J.F. and Sibbald, T.I.I.
1980: Thermotectonic evolution of the Churchill Province in northern Saskatchewan. Tectonophysics, v. 68, p. 45-82.

Macdonald, C.
1985: Mineralogy and geochemistry of the sub-Athabasca regolith near Wollaston Lake. *In* Geology of Uranium deposits, T.I.I. Sibbald and W. Petruk (eds.). The Canadian Institute of Mining and Metallurgy, Special Volume 32, p. 155-158.

Marlatt, J., McGill, B., Matthews, R., Sopuck, V., and Pollock, G.
1992: The discovery of the McArthur River uranium deposit, Saskatchewan, Canada. *In* New Developments in Uranium Exploration, Resources, Production and Demand, Proceedings of a Technical Committee Meeting, jointly organized by the International Atomic Energy Agency and the Nuclear Energy Agency of the OECD and held in Vienna, 26-29 August, 1991. International Atomic Agency IAEA-TECDOC-650, Vienna, p. 118-127.

Miller, A.R.
1983: A progress report: uranium-phosphorous association in the Helikian Thelon Formation and sub-Thelon saprolite, central District of Keewatin. *In* Current Research, Part A. Geological Survey of Canada, Paper 83-1A, p. 449-456.

Miller, A.R., Blackwell, J.D., Curtis, L., Hilger, W., McMillan, R.H., and Nutter, E.
1984: Geology and discovery of Proterozoic uranium deposits, Central District of Keewatin, Northwest Territories, Canada. *In* Proterozoic unconformity and stratabound uranium deposits, J. Ferguson (ed.). International Atomic Energy Agency, IAEA-TECDOC-315, Vienna, p. 285-312.

Miller, A.R., Cumming, G.L., and Krstic, D.
1989: U-Pb, Pb-Pb and K-Ar isotopic study and petrography of uraniferous phosphate-bearing rocks in the Thelon Formation, Dubawnt Group, Northwest Territories, Canada. Canadian Journal of Earth Sciences, v. 26, p. 867-880.

NEA/IAEA
1994: Uranium, 1993 Resources, Production and Demand. A joint report by the OECD Nuclear Energy Agency and the International Atomic Energy Agency. Nuclear Energy Agency, Organization for Economic Co-operation and Development, Paris, 311 p.

Needham, R.S.
1988: Geology of the Alligator Rivers Uranium Field, Northern Territory. Bureau of Mineral Resources, Geology and Geophysics, Canberra, Australia, 96 p.

NRCan
1994: Uranium in Canada, 1994, Assessment of supply and requirements. Uranium Division, Electricity Branch of Natural Resources Canada (NRCan), Public information, Ottawa, 10 p.

Olson, R.A., Dufresne, M.B., Freeman, M.E., Eccles, D.R., and Richardson, R.J.H.
1994: Regional metallogenic evaluation of Alberta. Alberta Geological Survey, Open File Report 1994-8, 240 p.

Orr, R.G., Tan, B., Koegler, K., and Robertshaw, P.
1988: Project 71-42: Maybelle River Seasonal Report, Period January to July 31, 1988. Uranerz Exploration and Mining Limited, unpublished assessment report.

Percival, J.B.
1989: Clay mineralogy, geochemistry, and partitioning of uranium within the alteration halo of the Cigar Lake uranium deposit, Saskatchewan, Canada. Unpublished Ph.D. thesis, Carleton University, Ottawa, Ontario, Chapter 5.

Percival, J.B., Bell, K., and Torrance, J.B.
1993: Clay mineralogy and isotope geochemistry of the alteration halo at the Cigar Lake uranium deposit. Canadian Journal of Earth Sciences, v. 30, p. 689-704.

Percival, J.B. and Kodama, H.
1989: Sudoite from Cigar Lake, Saskatchewan. Canadian Mineralogist, v. 27, p. 633-641.

Ramaekers, P.
1981: Stratigraphy and tectonic history of the Athabasca Group (Helikian) of Northern Saskatchewan. *In* Summary of Investigations 1981, Saskatchewan Geological Survey, Saskatchewan Mineral Resources, Miscellaneous Report 81-4, p. 99-106.

1990: Geology of the Athabasca Group (Helikian) in Northern Saskatchewan. Saskatchewan Geological Survey, Report 195, 49 p.

Ray, G.E.
1977: The geology of Highrock Lake - Key Lake vicinity, Saskatchewan. Saskatchewan Geological Survey, Report 197, 29 p.

Rickwood, P.C.
1983a: Appendix 1 - Crustal abundance, distribution, and crystal chemistry of the elements. *In* Handbook of Exploration Geochemistry, Volume 3, Rock Geochemistry in Mineral Exploration, G.J.S. Govett (ed.). Elsevier Scientific Publishing Company, Amsterdam, p. 347-387.

1983b: Appendix 3 - Probability table for required number of samples. *In* Handbook of Exploration Geochemistry, Volume 3, Rock Geochemistry in Mineral Exploration, G.J.S. Govett (ed.). Elsevier Scientific Publishing Company, Amsterdam, p. 395.

1983c: Appendix 4 - List of deposits and mineralized districts and source of references for geochemical data. *In* Handbook of Exploration Geochemistry, Volume 3, Rock Geochemistry in Mineral Exploration, G.J.S. Govett (ed.). Elsevier Scientific Publishing Company, Amsterdam, p. 397-403.

Robinson, S.C.
1955: Mineralogy of uranium deposits, Goldfields, Saskatchewan. Geological Survey of Canada, Bulletin 31, 128 p.

Ruhrmann, G. and von Pechmann, E.
1989: Structural and hydrothermal modification of the Gaertner uranium deposit, Key Lake, Saskatchewan, Canada. *In* Uranium Resources and Geology of North America, Proceedings of a Technical Committee Meeting, Saskatoon, 1987. International Atomic Energy Agency, IAEA-TECDOC-500, Vienna, p. 363-377.

Ruzicka, V.
1984: Unconformity-related uranium deposits in the Athabasca Basin region, Saskatchewan. *In* proterozoic unconformity and stratabound uranium deposits, J. Ferguson (ed.). International Atomic Energy Agency, Vienna, IAEA-TECDOC-315, p. 219-267.

1989: Monometallic and polymetallic deposits associated with the sub-Athabasca unconformity in Saskatchewan. *In* Current Research, Part C. Geological Survey of Canada, Paper 89-1C, p. 67-79.

1992: Uranium in Canada, 1991. *In* Current Research, Part D. Geological Survey of Canada, Paper 92-1D, p. 49-57.

1993a: Comparative metallogenic studies of the Alberta and Saskatchewan parts of Athabasca Basin. *In* Current Research, Part E. Geological Survey of Canada, Paper 93-1E, p. 175-184.

1993b: Unconformity-type uranium deposits. *In* Mineral Deposit Modeling, R.V. Kirkham, W.D. Sinclair, R.I. Thorpe, and J.M. Duke (eds.). Geological Association of Canada, Special Paper 40, p. 125-149 (published 1995).

1995: Unconformity-associated uranium. *In* Geology of Canadian Mineral Deposit Types, O.R. Eckstrand, W.D. Sinclair, and R.I. Thorpe (eds.). Geological Survey of Canada, Geology of Canada, no 8 (also Geological Society of America, The Geology of North America, v. P-1), 640 p., p. 197-210 (published 1996).

Ruzicka, V. and LeCheminant, G.M.
1986: Developments in uranium geology in Canada, 1985. *In* Current Research, Part A. Geological Survey of Canada, Paper 86-1A, p. 531-540.

1987: Uranium investigations in Canada, 1986. *In* Current Research, Part A. Geological Survey of Canada, Paper 87-1A, p. 249-262.

Sibbald, T.I.I.
1976: Uranium metallogenic studies: Rabbit Lake. *In* Summary of Investigations, 1976, by the Saskatchewan Geological Survey, J.E. Christopher and R. Macdonald (eds.). Province of Saskatchewan, Department of Mineral Resources, p. 115-123.

1978: Uranium metallogenic studies: Rabbit Lake, geology. *In* Summary of Investigations, 1978, Saskatchewan Geological Survey, J.E. Christopher and R. Macdonald (eds.). Saskatchewan Mineral Resources, Miscellaneous Report 78-10, p. 56-60.

Sibbald, T.I.I., Quirt, D.H., and Gracie, A.J.
1990: Uranium deposits of the Athabasca Basin, Saskatchewan [Field Trip 11]. 8th IAGOD Symposium Field Trip Guidebook. Geological Survey of Canada, Open File 2166, 56 p.

Sopuck, V.J., de Carle, A., Wray, E.M., and Cooper, B.
1983: Application of lithogeochemistry to the search for unconformity-type uranium deposits in the Athabasca Basin. *In* Uranium Exploration in Athabasca Basin, E.M. Cameron (ed.). Geological Survey of Canada, Paper 82-11, p. 192-205.

Tremblay, L.P.
1982: Geology of the uranium deposits related to the sub-Athabasca unconformity, Saskatchewan. Geological Survey of Canada, Paper 81-20, 56 p.

Wallis, R.H., Saracoglu, N., Brummer, J.J., and Golightly, J.P.
1986: The geology of the McClean uranium deposits, northern Saskatchewan. *In* Uranium Deposits of Canada, E.L. Evans (ed.). The Canadian Institute of Mining and Metallurgy, Special Volume 33, p. 193-217.

Ward, D. M.
1984: Uranium geology, Beaverlodge Area. *In* Proterozoic Unconformity and Stratabound Uranium Deposits, J. Ferguson (ed.). International Atomic Energy Agency, IAEA-TECDOC-315, Vienna, p. 269-284.

Wilson, J.A.
1985: Geology of the Athabasca Group in Alberta. Alberta Research Council, Bulletin no. 49, 78 p.

1986: Geology of the basement beneath the Athabasca Basin in Alberta. Alberta Research Council, Bulletin no. 55, 61 p.

1987: The geology and economic potential of the Athabasca Basin in Alberta. The Canadian Institute of Mining and Metallurgy, Bulletin 80 (898), p. 29-36.

Worden, J.M., Cumming, G.L., and Baadsgaard, H.
1985: Geochronology of host rocks and mineralization of the Midwest uranium deposit, northern Saskatchewan. *In* Geology of Uranium Deposits, T.I.I. Sibbald and W. Petruk (eds.). The Canadian Institute of Mining and Metallurgy, Special Volume 32, p. 67-72.

PLATES 1–3

Plate 1

1a. Graphite (C) and pyrite (light grey) in metamorphosed pelitic basement rocks just below the sub-Athabasca unconformity and below a uranium anomaly (S.E.M. image). Drillhole 302/204.1 m, Athabasca Basin, Alberta (Fig. 13; Table 4).

1b. Distribution of graphite (C) and pyrite (Fe, S) in pelitic gneiss (S.E.M. image). Drillhole 302/204.1 m, Athabasca Basin, Alberta (Fig. 13; Table 4).

1c. S.E.M. image of a ferruginous carbonate in sandstone with two zones: an inner zone with high Ca and Mg contents, and an outer zone with low Ca and Mg contents. Drillhole 306/41.7 m, Athabasca Basin, Alberta (Fig. 13; Table 4).

1d. S.E.M. immage of a cavity in sandstone (Lazenby Lake Formation, drillhole 306/41.7 m) filled with authigenic (diagenetic) carbonates, which display variable Fe/Mg/Ca/O ratios (normalized to 100%):

	Fe	Mg	Ca	O
spot [1]	48.80	3.92	8.1	43.18
spot [2]	36.97	8.79	13.06	41.18
spot [3]	50.59	0.50	5.07	43.84
spot [4]	42.72	6.35	5.49	45.44

1e. Apatite grains disseminated in pelitic gneiss (S.E.M. image). Drillhole 307/207.9 m, Athabasca Basin, Alberta (Fig. 13; Table 4).

1f. Zoned zircon (Zr, Si, O) associated with yttrium phosphate (Y, P, O) in pelitic gneiss (S.E.M. image). Drillhole 308/115.4 m, Athabasca Basin, Alberta (Fig. 13; Table 4).

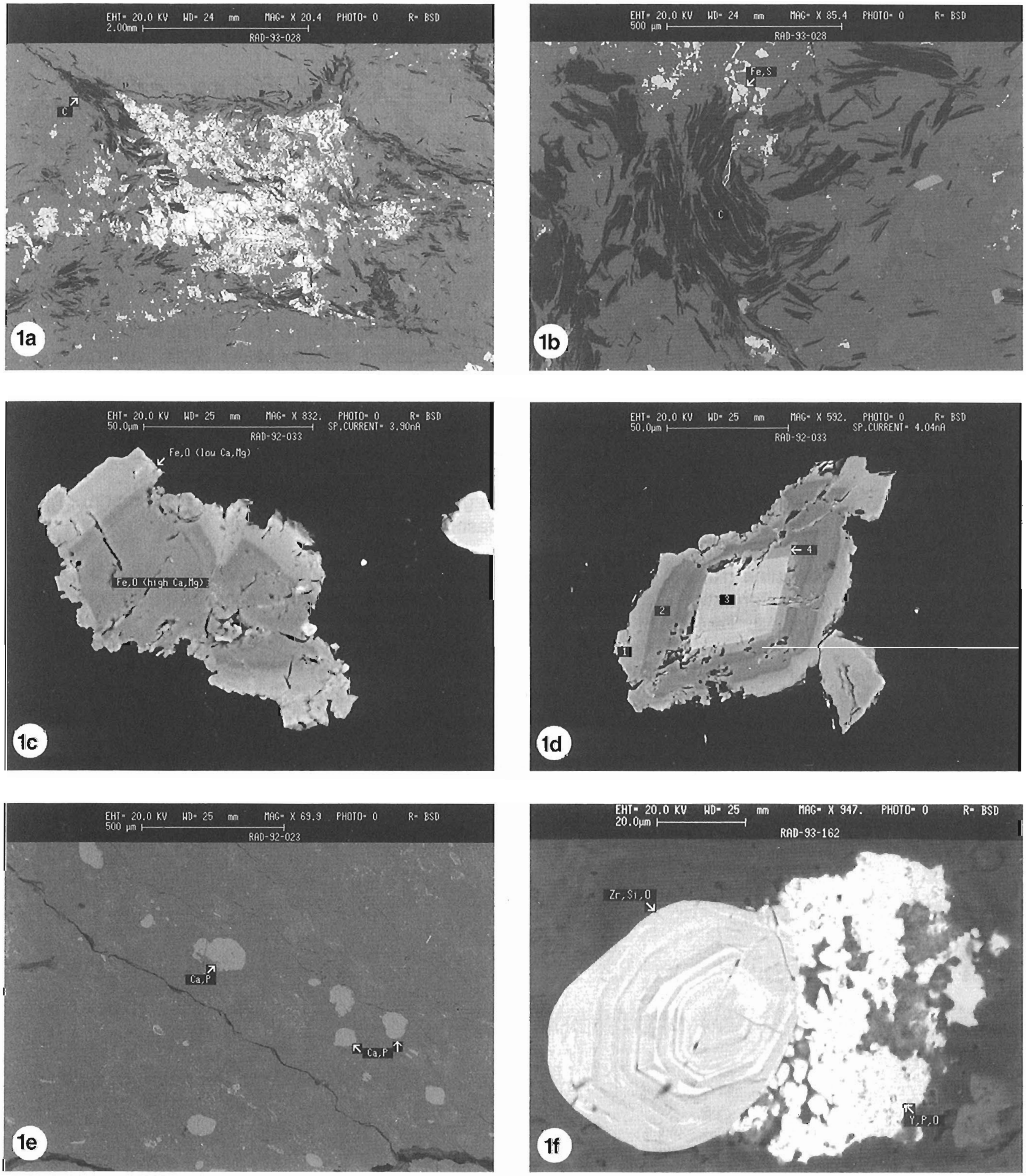
EHT= 20.0 KV WD= 24 mm MAG= X 20.4 PHOTO= 0 R= BSD
2.00mm
RAD-93-028
C
1a
EHT= 20.0 KV WD= 24 mm MAG= X 85.4 PHOTO= 0 R= BSD
500 µm
RAD-93-028
Fe,S
C
1b
EHT= 20.0 KV WD= 25 mm MAG= X 832. PHOTO= 0 R= BSD
50.0µm
RAD-92-033
SP.CURRENT= 3.90nA
Fe,O (low Ca,Mg)
Fe,O (high Ca,Mg)
1c
EHT= 20.0 KV WD= 25 mm MAG= X 592. PHOTO= 0 R= BSD
50.0µm
RAD-92-033
SP.CURRENT= 4.04nA
4
3
2
1
1d
EHT= 20.0 KV WD= 25 mm MAG= X 69.9 PHOTO= 0 R= BSD
500 µm
RAD-92-023
Ca,P
Ca,P
1e
EHT= 20.0 KV WD= 25 mm MAG= X 947. PHOTO= 0 R= BSD
20.0µm
RAD-93-162
Zr,Si,O
Y,P,O
1f

Plate 2

2a. Monazite (Ce, La, P) intimately intergrown with chalcopyrite (Fe, Cu, S) in altered pelitic gneiss (S.E.M. image). Drillhole 303/226.1 m, Athabasca Basin, Alberta (Fig. 13; Table 4).

2b. Native (radiogenic) lead (Pb) in graphitic and pyritic metamorphosed pelitic rock (S.E.M. image). Drillhole 302/204.1 m, Athabasca Basin, Alberta (Fig. 13; Table 4).

2c. Lead oxide (Pb, O) filling a fracture in graphitic and pyritic gneiss (S.E.M. image). Drillhole 302/204.1 m, Athabasca Basin, Alberta (Fig. 13; Table 4).

2d. Nickeline (Ni, As) associated with anhydrite (Ca, S, O) in sandstone of the Fair Point Formation (S.E.M. image). Drillhole 306/203.1 m, Athabasca Basin, Alberta (Fig. 13; Table 4).

2e. Uraniferous and thoriferous zircon (Zr, Si, O; U, Th, Ca) intergrown with nickeline (Ni, As) in altered sandstone of Fair Point Formation (S.E.M. image). Drillhole 306/196.0 m, Athabasca Basin, Alberta (Fig. 13; Table 4).

2f. Uraniferous, thoriferous and nickeliferous zircon (Zr, Si, O; U, Th, Ca, As, Ni) intergrown with nickeline (Ni, As) in altered sandstone of Fair Point Formation (S.E.M. image). Drillhole 306/196.0 m, Athabasca Basin, Alberta (Fig. 13; Table 4).

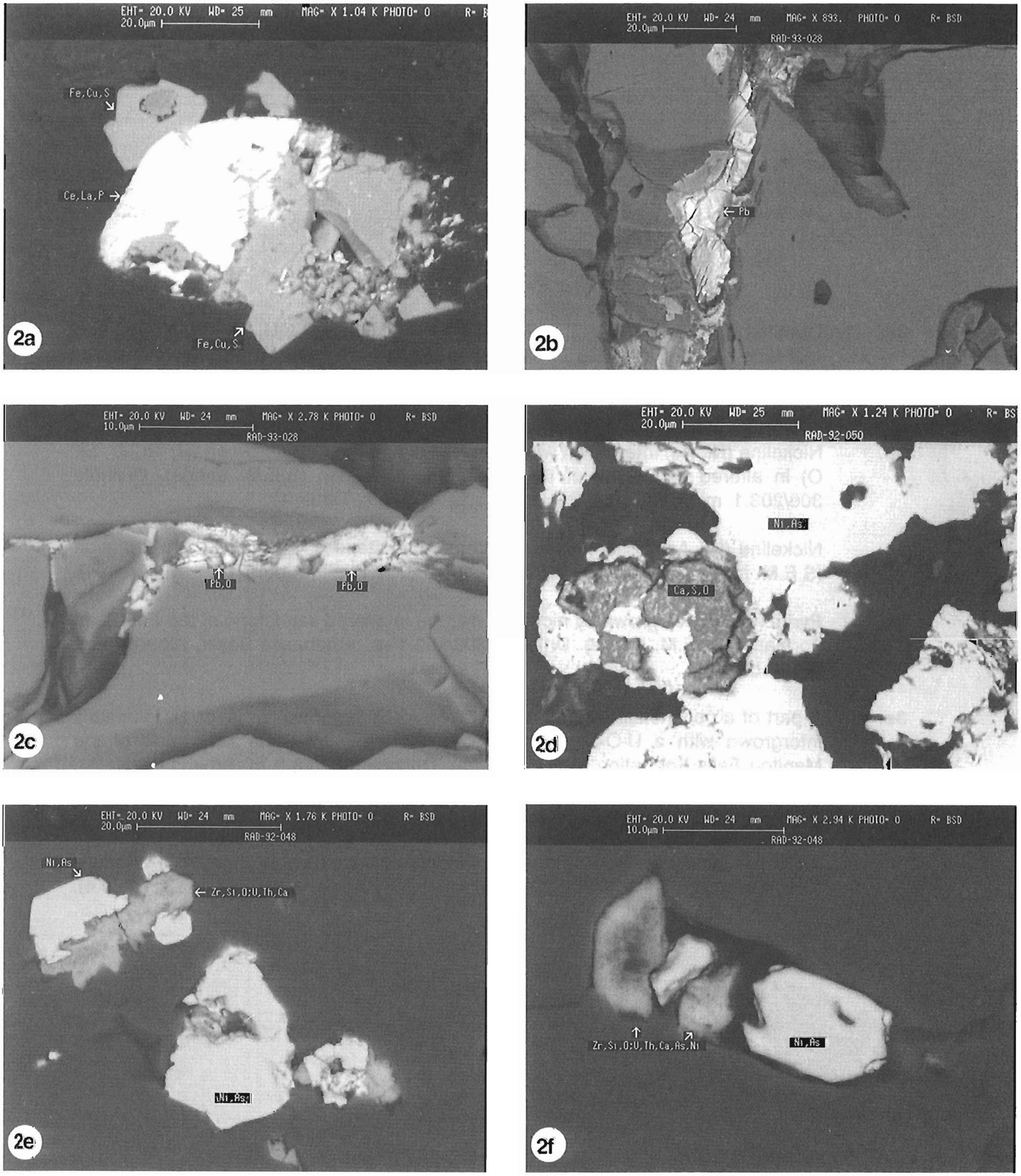
EHT= 20.0 KV WD= 25 mm MAG= X 1.04 K PHOTO= 0
20.0µm
Fe,Cu,S
Ce,La,P
Fe,Cu,S
2a
EHT= 20.0 KV WD= 24 mm MAG= X 893. PHOTO= 0 R= BSD
20.0µm
RAD-93-028
Pb
2b
EHT= 20.0 KV WD= 24 mm MAG= X 2.78 K PHOTO= 0 R= BSD
10.0µm
RAD-93-028
Pb,O
Pb,O
2c
EHT= 20.0 KV WD= 25 mm MAG= X 1.24 K PHOTO= 0
20.0µm
RAD-92-050
Ni,As
Ca,S,O
2d
EHT= 20.0 KV WD= 24 mm MAG= X 1.76 K PHOTO= 0 R= BSD
20.0µm
RAD-92-048
Ni,As
Zr,Si,O:U,Th,Ca
Ni,As
2e
EHT= 20.0 KV WD= 24 mm MAG= X 2.94 K PHOTO= 0 R= BSD
10.0µm
RAD-92-048
Zr,Si,O:U,Th,Ca,As,Ni
Ni,As
2f

Plate 3

3a. Uraniferous, thoriferous and nickeliferous zircon (Zr, Si, O; U, Th, Ca, Ni, As) and nickeline (Ni, As) in a vug in sandstone of the Fair Point Formation, about 3 m above uranium mineralization (S.E.M. image). Drillhole 306/196.0 m, Athabasca Basin, Alberta (Fig. 13; Table 4).

3b. Nickeline (Ni, As) intergrown with uraniferous and thoriferous zircon (U, Th, Zr, Si, O) in altered sandstone of the Fair Point Formation (S.E.M. image). Drillhole 306/203.1 m, Athabasca Basin, Alberta (Fig. 13; Table 4).

3c. Nickeline (Ni, As) disseminated in altered sandstone of the Fair Point Formation (S.E.M. image). Drillhole 306/203.1 m, Athabasca Basin, Alberta (Fig. 13; Table 4).

3d. Pyrite (Fe, S) overgrown by nickeline (Ni, As) in altered sandstone of the Fair Point Formation (S.E.M. image). Drillhole 306/203.1 m, Athabasca Basin, Alberta (Fig. 13; Table 4).

3e. A part of a polymetallic aggregate of Co-Ni-As-Fe composition (spot 1), intimately intergrown with a U-O-Ni-As-Co-Fe-S compound (spot 2) in sandstone of the Manitou Falls Formation (S.E.M. image). Drillhole 307/98.0 m, Athabasca Basin, Alberta (Fig. 13; Table 4).

3f. Molybdenite (Mo, S) associated with pyrite (light grey) in metapelitic basement rocks just below the sub-Athabasca unconformity and below a uranium anomaly (S.E.M. image). Drillhole 302/204.1 m, Athabasca Basin, Alberta (Fig. 13; Table 4).

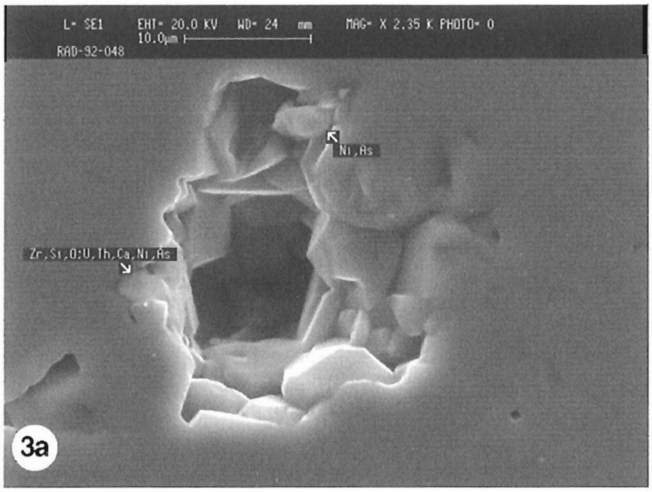
L= SE1 EHT= 20.0 KV WD= 24 mm MAG= X 2.35 K PHOTO= 0
10.0µm
RAD-92-048
Ni,As
Zr,Si,O;U,Th,Ca,Ni,As
3a

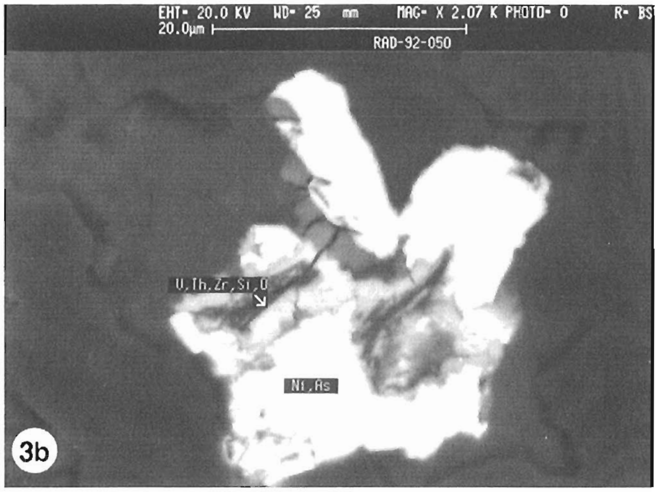
EHT= 20.0 KV WD= 25 mm MAG= X 2.07 K PHOTO= 0
20.0µm
RAD-92-050
U,Th,Zr,Si,O
Ni,As
3b

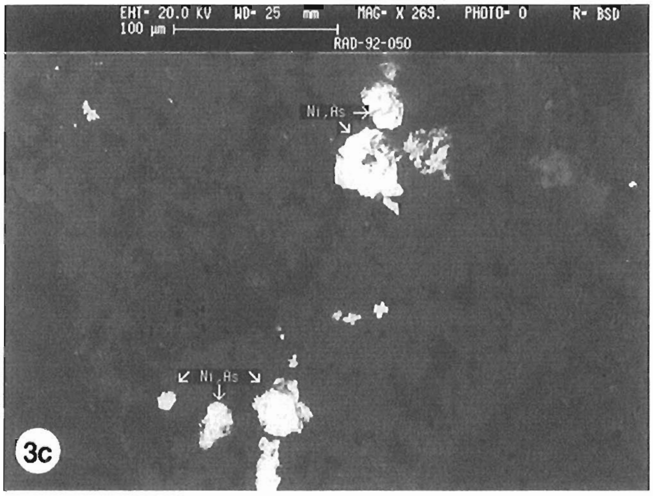
EHT= 20.0 KV WD= 25 mm MAG= X 269. PHOTO= 0 R= BSD
100 µm
RAD-92-050
Ni,As
Ni,As
3c

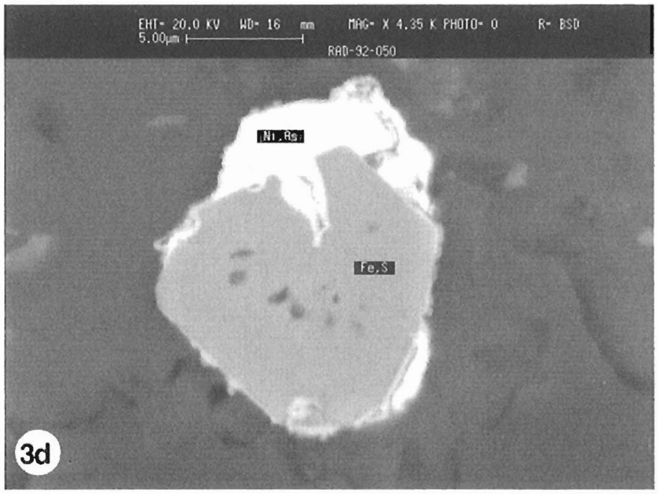
EHT= 20.0 KV WD= 16 mm MAG= X 4.35 K PHOTO= 0 R= BSD
5.00µm
RAD-92-050
Ni,As
Fe,S
3d

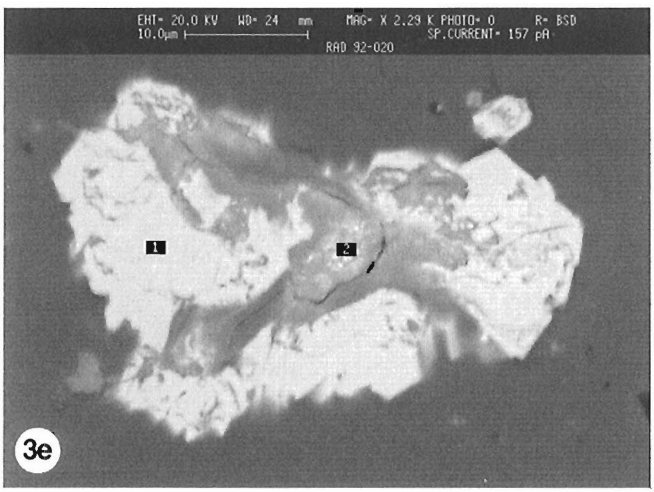
EHT= 20.0 KV WD= 24 mm MAG= X 2.29 K PHOTO= 0 R= BSD
10.0µm
SP.CURRENT= 157 pA
RAD 92-020
1
2
3e

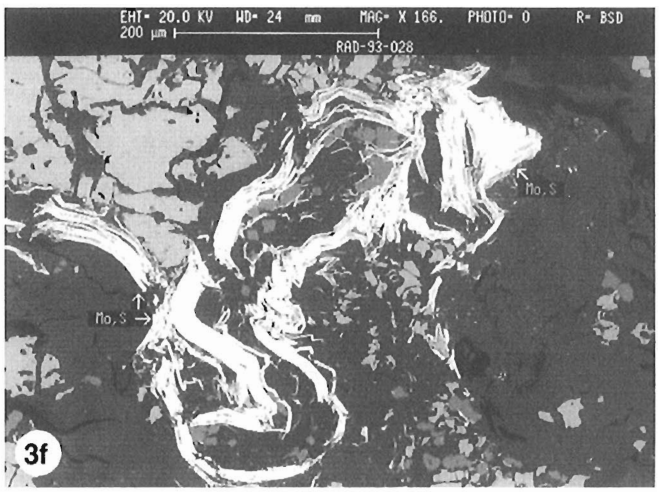
EHT= 20.0 KV WD= 24 mm MAG= X 166. PHOTO= 0 R= BSD
200 µm
RAD-93-028
Mo,S
Mo,S
3f

QUATERNARY GEOLOGY ALONG THE SHIELD MARGIN, NORTHEASTERN ALBERTA[1]

Jan M. Bednarski
Terrain Sciences Division, Calgary

Abstract

The exposed Precambrian shield in northeastern Alberta is sparsely covered by glacial deposits, although the area was extensively scoured during the last glaciation. This contrasts with areas underlain by Paleozoic sedimentary rocks west of the Slave River, where extensive deltaic and lacustrine deposits of postglacial age and thick lacustrine and glacial sediments occur.

During the glacial maximum, the dominant ice-flow over the area was from the northeast. As the ice thinned during deglaciation, a distinct ice lobe developed within the Lake Athabasca trough in the southern part of the area. The Athabasca lobe flowed to the west, converging along a lateral margin with the ice to the north. The lateral contact between the ice masses is marked by converging striae and a broad east-west band of glacial outwash and lake deposits.

When the ice front retreated to the east and northeast, glacial Lake McConnell inundated the Slave River lowlands and Lake Athabasca basin up to ±305 m above sea level. A major stillstand produced the Slave moraine, an extensive north-south moraine system, correlative with the 10 000 BP Cree Lake Moraine of northeastern Saskatchewan. Further ice front retreat across the Shield diverted meltwater along the ice margin, creating numerous ephemeral lakes and extensively redistributing drift.

Some 336 glacial drift samples were analysed for grain size, carbon content and a suite of elements. The distributions of As, Au, Co, Cr, Cu, Fe, Ni, Pb, U and Zn, in the silt and clay fractions are compared for 251 samples. Statistically derived contour maps describe the spatial distribution of elements in glacial drift.

Résumé

Le Boulier précambrien affleurant dans le nord-est de l'Alberta est recouvert ici et là de dépôts glaciaires, même si la région a été considérablement décapée durant la dernière glaciation. Ce paysage contraste avec les régions de roches sédimentaires paléozoïques à l'ouest de la rivière Slave, où l'on trouve de vastes dépôts deltaïques et lacustres d'âge post-glaciaire de même que d'épais sédiments lacustres et glaciaires.

Durant le maximum glaciaire, la provenance dominante de l'écoulement glaciaire dans la région était le nord-est. Un lobe glaciaire distinct s'est formé dans la cuvette du lac Athabasca, dans la partie méridionale de la région, à mesure que la glace s'amincissait durant la déglaciation. Le lobe d'Athabasca a flué vers l'ouest, convergeant en bordure de la marge latérale avec le glacier se trouvant au nord. Le contact latéral entre les masses glaciaires est marqué par des stries convergentes et une large bande est-ouest de dépôts d'épandage fluvioglaciaire et de sédiments lacustres.

Lorsque le front glaciaire a reculé vers l'est et le nord-est, le lac glaciaire McConnell a inondé les basses terres de la rivière Slave et le bassin du lac Athabasca jusqu'à une hauteur de ±305 m au-dessus du niveau de la mer. Une importante période stationnaire a produit la moraine de Slave,

[1]Canada-Alberta Agreement on Mineral Development, Project C1.13

vaste réseau morainique nord-sud corrélatif de la Moraine de Cree Lake (10 000 BP), dans le nord-est de la Saskatchewan. Un recul ultérieur du front glaciaire à travers le bouclier a détourné les eaux de fonte le long de la marge glaciaire, créant de nombreux lacs éphémères et redistribuant considérablement les débris glaciaires.

On a analysé quelque 336 échantillons de sédiments glaciaires pour en déterminer la granulométrie ainsi que la teneur en carbone et en d'autres éléments. Les distributions de divers éléments (As, Au, Co, Cr, Cu, Fe, Ni, Pb, U et Zn) dans les fractions silteuse et argileuse de 251 échantillons sont comparées. Les cartes d'isoteneurs établies statistiquement figurent la distribution spatiale des éléments dans les sédiments glaciaires.

INTRODUCTION

Continental ice sheets affected most of Canada and caused extensive physical removal, transport and mixing of rock during past glaciations. In the past two decades there has been an increased understanding of glacial dispersal of distinctive rocks. This has led to geochemical surveys that have traced the source of indicator minerals in glacial till, and tills have become important indicators of mineralization rather than obscurers of economic mineral deposits. To use till as a prospecting medium, an understanding of the glacial history of an area is essential. This includes a knowledge of flow directions, patterns of erosion and deposition, and fluctuations of glaciers, including the number and extent of past glaciations.

This paper describes the main results of the Canada-Alberta Mineral Development Agreement program undertaken in northeastern Alberta (NTS 74M and part of 74L; Fig 1) to map surficial geology and inventory till (drift) composition and geochemistry. Prior to this program, much of the Canadian Shield within Alberta remained unmapped and only reconnaissance information was available for other parts of the area. The objective of the project was to assist and stimulate mineral exploration in the area by providing detailed information on the genesis and distribution of surficial materials, including chemical and mineral variations within till to establish background values for element concentrations in glacial deposits of the area.

The study area encompasses the exposed Canadian Shield north of Lake Athabasca and the lowlands underlain by Paleozoic rocks along the Peace and Slave rivers, a total area of about 15 200 km^2. The research procedure consisted of interpreting 1:40 000 and 1:60 000 airphotos with ground verification conducted during field seasons in 1992, 1993 and 1994. Till and other surficial materials were sampled during the traverses on the Canadian Shield with an average density of one sample per 30 km^2, however, the greatest sampling density occurs around the larger lakes (Fig. 2). All information was entered into digital databases and compiled onto digital maps. A detailed 1:100 000 map of surficial geology is currently in preparation. Outputs to date include a preliminary description of the Quaternary history of the area (Bednarski, 1993a), 1:50 000 GSC Open File maps (Bednarski, 1995a, b) and Open File reports on till geochemistry of the northern part of the study area (Bednarski, 1993b, 1996). This paper summarizes the surficial geology, Quaternary history, glacial dispersal, and drift geochemistry and composition for the entire area.

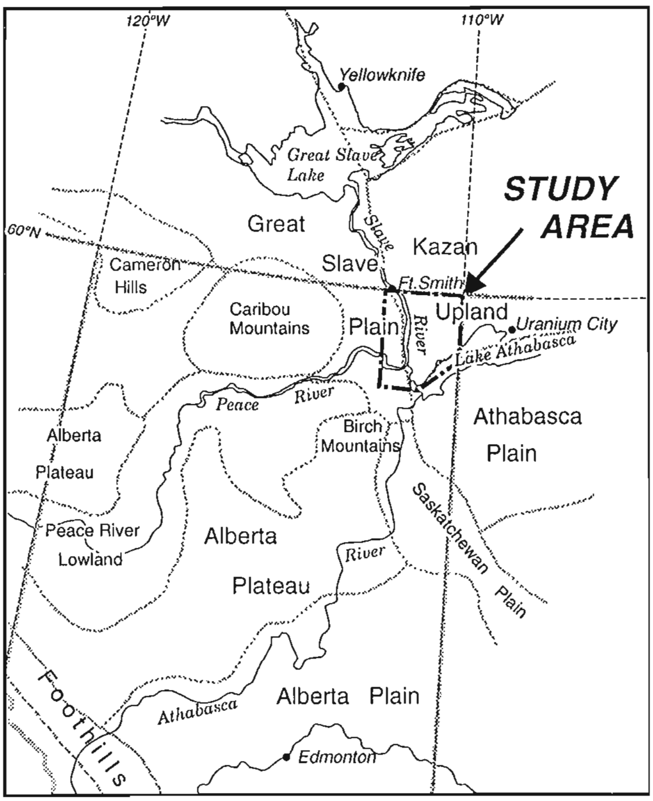

Figure 1. Location of the study area and physiographic regions of Alberta (after Bostock, 1970).

REGIONAL SETTING

Physiography

The preglacial physiography influenced the Quaternary history of northeastern Alberta by affecting glacial flow and decay of the Laurentide Ice Sheet. Elements of regional topography and underlying bedrock structure were used by Bostock (1970) to define three physiographic regions that are found in the study area (Fig. 1). The principal region, covering most of the study area north of Lake Athabasca and east of the Slave River, is the Kazan Upland, a large area of crystalline Precambrian basement consisting of exposed volcanic and sedimentary rocks of Archean and Early Proterozoic age (Godfrey, 1986). The Upland rises gently from ~215 m above sea level (asl) along the Slave River, to >400 m asl along the Saskatchewan border, forming a broadly rolling surface. The surface is etched by ridges, valleys, and

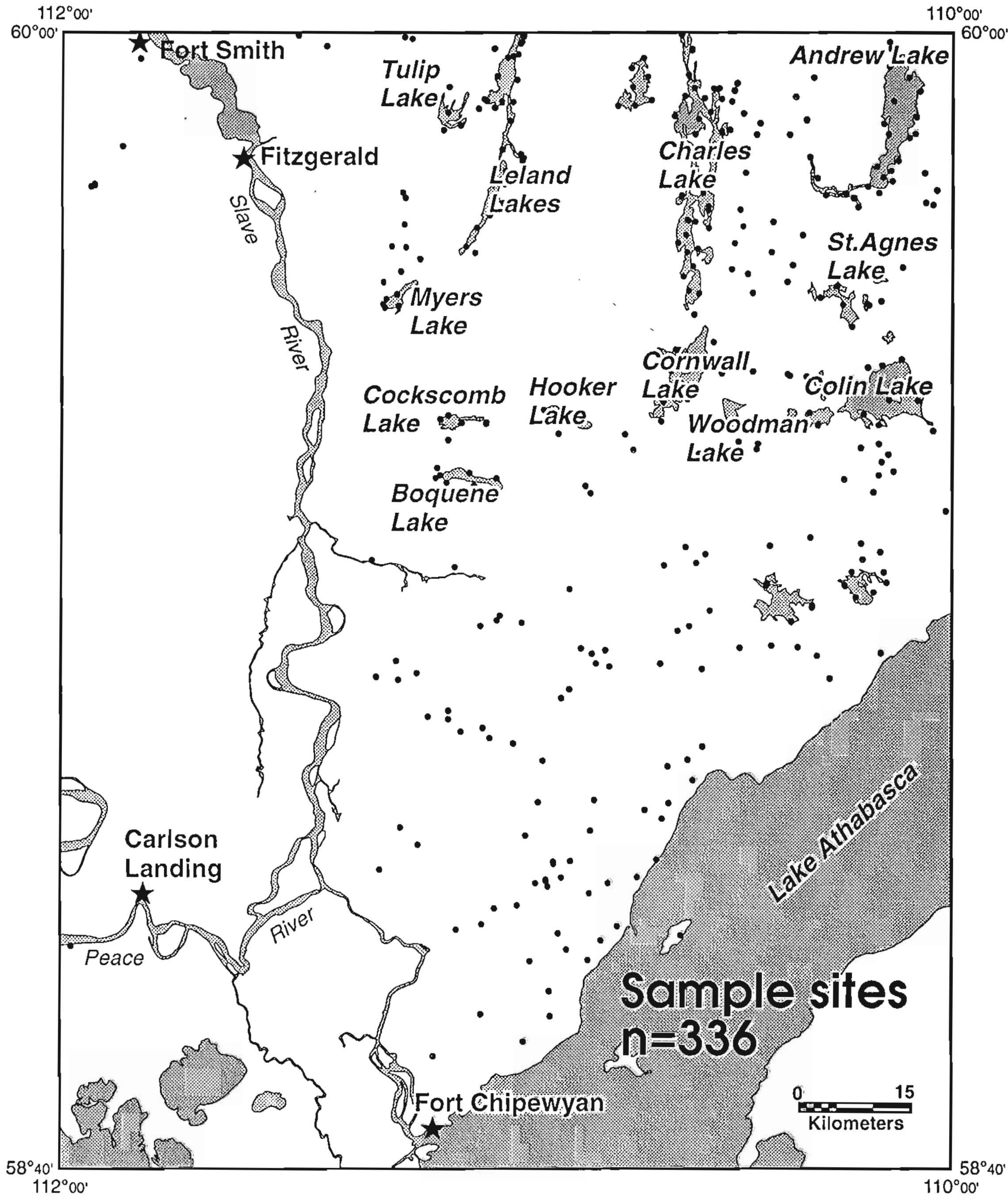

__Figure 2.__ Location of 336 sample sites and place-names.

shallow basins controlled by folding and fracturing of the rock, and by differential erosion of various bedrock units. The structures produce a general northeast-southwest topographic trend, with local relief usually less than 100 m.

The surficial cover over the Kazan Upland is very thin and drainage patterns are strongly influenced by bedrock structure. Main streams parallel the structure, whereas crosscutting joints and weaknesses in the bedrock are exploited by secondary channels that intersect the main streams at sharp angles. Similarly, larger lakes also have angular shorelines defined by the bedrock structure. Smaller depressions are poorly drained and perched lakes and bogs abound. Currently, the Kazan Upland drains either south, into Lake Athabasca and out the Slave River system, or west, directly into the Slave River. A small amount of runoff in the northeast drains northward into Great Slave Lake via the Tethul/Taltson River system. Drainage patterns during retreat phases of the Laurentide Ice Sheet were significantly different from those of the present.

The Athabasca Plain, the second major physiographic element in the study area, forms a large embayment into the western part of the Kazan Upland. This part of the Precambrian shield is composed of thick, unmetamorphosed Middle Proterozoic sedimentary rocks (Athabasca Group) that unconformably overlie the basement. Nearly flat-lying conglomerates and sandstones, with clay and silt interbeds, comprise the base of the Group which outcrops along the northern shore of Lake Athabasca (Wilson, 1985). Lake Athabasca (210 m asl) lies along the northern margin of the Athabasca Plain and defines the southern limit of the study area. Prior to glaciation, the Athabasca Group likely extended farther north onto the crystalline basement, but these rocks were extensively eroded back by continental glaciation. Large volumes of glacially transported sand within the study area probably were derived from these recessive rocks. The topographic depression that Lake Athabasca currently occupies is likely a glacially-eroded trough, however, Lake Athabasca has a maximum depth of only 81 m in Saskatchewan. Westward, in Alberta, the maximum depth is only ~16 m, shallowing to a few metres on its western end at the delta. In contrast, glacial erosion was extensive in the eastern bays of Great Slave Lake, located to the north in the Northwest Territories. Erosional troughs in Great Slave Lake are greater than 700 m deep, more than 550 m below sea level.

The Kazan Upland is bounded to the west by the Great Slave Plain where the Precambrian basement is covered by flat-lying Middle Devonian rocks, forming a lowland of ~245 m asl maximum elevation. The Slave River, draining Lake Athabasca, flows northward into Great Slave Lake (156 m asl) along this Paleozoic/Precambrian contact. The southern part of the Great Slave Plain is covered by the Peace/Athabasca Delta, a flat expanse of Pleistocene to Holocene deltaic and lacustrine sediment.

West of the Slave River, the drainage of the Great Slave Plain is poorly integrated and swampy and muskeg-covered terrain is common. Local relief is only 15 to 20 m along sandy beach ridges and dunes. The southwest part of the area, north of Peace River, is covered by part of the Wood Buffalo Sand Hills, an extensive stabilized dune field (David, 1977). Karst topography and salt pans are common in the extreme western parts of the study area (Bayrock, 1972b; Tsui and Cruden, 1984).

Beyond the study area, the Great Slave Plain is bound by the Caribou Mountains to the west and Birch Mountains to the southeast (Fig. 1). These uplands controlled the pattern of deglaciation and directed glacial meltwater diversion within the region. The Great Slave Plain forms a contiguous lowland with the Peace River Lowland in the west. Together these lowlands channelled large volumes of nonglacial runoff and meltwater which flowed into the study area from the west.

Glaciation of northern Alberta: Overview

Although continental glaciers probably overrode northeastern Alberta during previous glacial cycles, most of the evidence for earlier glaciations was obscured by the last glaciation (Late Wisconsin; Fulton, 1989). During the last glaciation, which began about 30 ka BP, the Laurentide Ice Sheet flowed southwestward out of the District of Keewatin, northeast of the study area. At the height of glaciation (~18 ka BP), the ice sheet consisted of a complex of thick ice domes, saddles and lobes capable of advancing against the regional slope. During this time, the Canadian Shield of northern Alberta was intensively scoured by the southwest flowing ice. The Laurentide Ice Sheet crossed the Interior Plains and may have contacted the eastward flowing Cordilleran Ice Sheet, causing major diversions in drainage (Mathews, 1980). Nonetheless, some workers suggest that the two ice sheets may not have coalesced during the Late Wisconsinan (cf. Bobrowsky and Rutter, 1992).

During deglaciation, large proglacial lakes formed along the ice margin as it retreated northeastward (Lemmen et al., 1994; Fig. 3). Moreover, as the ice

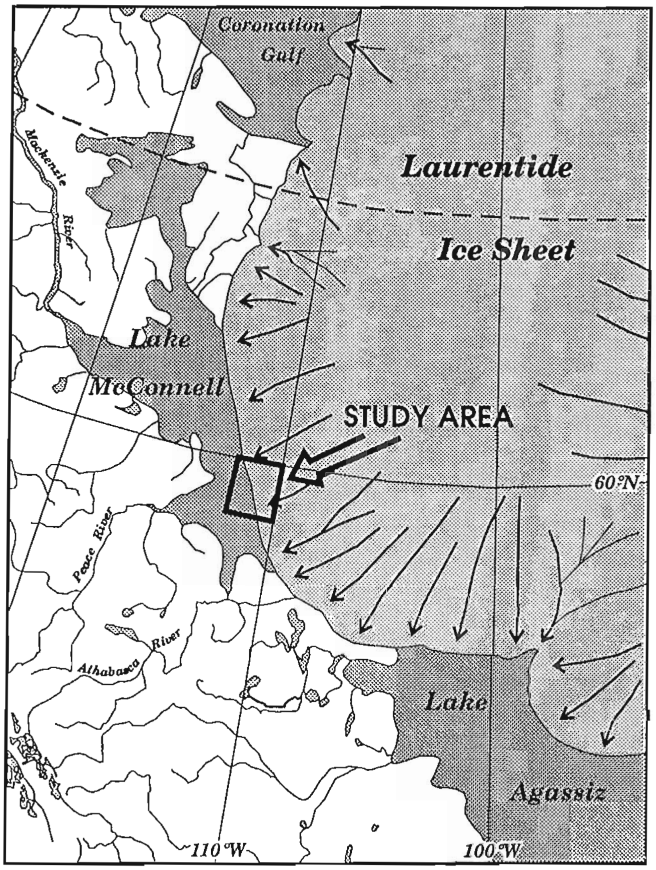

Figure 3. Paleogeography of the Laurentide Ice Sheet ~10 ka BP. Glacial Lake McConnell dominates the margin of the ice sheet in the study area (after Dyke and Prest, 1987).

sheet thinned, the underlying topography asserted greater control on ice-flow patterns, resulting in pronounced lobes along its margin. At ~11 ka BP, when ice still covered the study area, a lobe of Laurentide ice extended down the Peace River Lowland, but the Caribou Mountains to the north and the Birch Mountains to the south were ice free (Fig. 4). Regional drainage was blocked by the ice and a late phase of glacial Lake Peace contacted the front of the lobe within the lowland (Dyke and Prest, 1987), whereas glacial Lake McMurray occupied the Athabasca River valley to the south (Fisher, 1993; Lake Tyrrell, Taylor, 1960). In the far north, the retreating ice front led to the development of an early phase of glacial Lake McConnell that occupied part of present Great Bear Lake (Lemmen et al., 1994).

A chronology based on radiocarbon dates and correlation of water planes indicates that from 11 ka BP to ~9 ka BP the Laurentide ice front retreated eastward across the entire study area. During this time, glacial lake Peace rapidly expanded into the Lake Athabasca basin, forming glacial Lake Athabasca (Schreiner, 1984), collectively termed Lake Tyrrell (Taylor, 1960). Concurrently, glacial Lake McConnell expanded southward into Great Slave Lake basin and down Great Slave Plain, and radiocarbon dates suggest that, prior to 10 ka BP, glacial Lake McConnell coalesced with Lake Tyrrell. At its height, glacial Lake McConnell covered >215 000 km^2 and was the second largest Pleistocene lake in North America (Fig. 3; Lemmen et al., 1994). The lake reached this size because it exploited the crustal depression along the margin of the Laurentide Ice Sheet (Craig, 1965). Consequently, the lake was short-lived because, as the ice sheet decayed, postglacial rebound was continuously decanting the lake out the Mackenzie River system. Lake levels fell rapidly and by ~8.5 ka BP Lake McConnell separated into present-day Great Bear, Great Slave and Athabasca Lakes.

In summary, the sequence of events outlined above indicates that the immediate impact of Late Wisconsinan glaciation in northeastern Alberta lasted over a relatively short interval (~30 ka to 8.5 ka BP). During this period, major erosion and dispersal of the bedrock substrate and any previously accumulated glacial material occurred, but deposition of till was very sparse on the Kazan Upland. However, large volumes of glacial drift were transported by meltwater from the decaying ice sheet and the drift was concentrated as glaciofluvial sediment along former ice

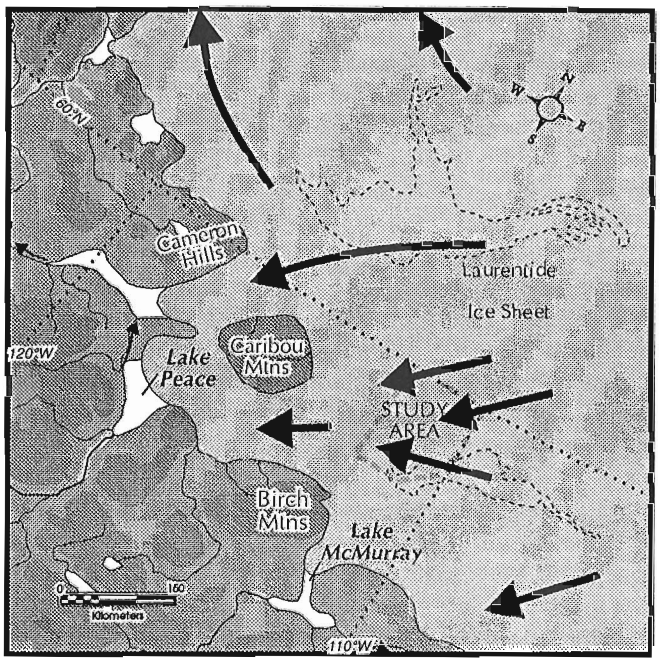

Figure 4. Regional glacial cover at ~11 ka BP. Note the meltwater diversions and ponded lakes along the margin of the Laurentide Ice Sheet. Arrows on the ice indicate major directions of glacial flow (after Lemmen et. al., 1994).

margins and in numerous proglacial lakes. Much of this sediment was redeposited during postglacial time as proglacial lakes drained and new networks developed. Further dispersal of sediment took place on the barren postglacial landscape by intensive wind erosion. These patterns of ice retreat, glacial sedimentation and drainage evolution will be detailed in the following sections.

SURFICIAL GEOLOGY

Glacial erosion

The exposed Kazan Upland has been scoured extensively by glaciers. Differential erosion of the bedrock produced much of the local relief. Generally, metasedimentary rocks are most recessive, whereas, granites tend to form the hills and mylonitic rocks form prominent ridges. Furthermore, when glacial flow was parallel to bedrock structural orientation, the topography was enhanced because local ice streams formed within the bedrock troughs and accelerated abrasion. A number of the larger lakes on the Kazan Upland are glacially eroded troughs. Conversely, resistant ridges that lay across the direction of former ice flow underwent little glacial erosion.

Numerous ice-flow indicators of varying scales are found on the Kazan Upland (Fig. 5). The most common are striations, formed by rock or mineral fragments being dragged along the sole of the glacier. The cumulative effect of this abrasion is to smooth and polish the bedrock surface, often sculpting the bedrock into streamlined bedrock knobs whose long axis is oriented in the direction of ice movement, several hundred metres long. Often the upstream side of ice-moulded bedrock knobs is gently inclined, rounded and striated, whereas the downstream side is steep and blocky, the result of glacial plucking enhanced by subglacial freezing of meltwater. Streamlined bedrock forms are prevalent in the northeastern parts of the study area and indicate strong glacial scour from the northeast.

Glacial meltwaters were effective in eroding the bedrock by cutting subglacial and proglacial channels. The meltwaters effectively exploited weaknesses along bedrock lineaments on the Kazan Upland. Often these channels connect with glaciofluvial deposits in successive valleys, and many are now dry or occupied by misfit streams.

For further discussion of glacial erosion see the following section on *Till*.

Ice-flow directions

Features of glacial-erosion usually provide unequivocal evidence of ice-flow direction and put definite constraints on the former configuration of the ice sheet. This is important in deducing glacial history and till provenance, but it must be noted that directional features are not recorded everywhere, and usually only the final flow direction of the decaying ice sheet is recorded.

When the Laurentide Ice Sheet covered the entire region during the last glacial maximum, the ice flowed southwest from the Keewatin Ice Divide (Dyke and Prest, 1987). Northeast–southwest ice-flow features are most common on the Kazan Upland, in the northern part of the study area, but are less common in the south, where the strongest flow recorded was approximately east–west (Fig. 5). The northern southwest flow gradually changes to a dominantly westward flow as the southern zone is approached. This boundary coincides with a belt of thick surficial sediments, informally named the Colin Lake Interlobate Moraine, that is mapped along an east–west transect from Colin Lake, to south of Cornwall Lake, to Cockscomb Lake (Fig. 5).

The westerward flow on southern Kazan Upland is thought to have developed during deglaciation when the ice sheet thinned and a lobe of the Laurentide Ice Sheet occupied the Lake Athabasca trough. This lobe likely developed downstream of Lake Athabasca within the Peace River Lowland (Fig. 4). There, the Caribou and Birch Mountains on either side of the lowlands were the first to become ice-free as the ice sheet thinned. Consequently, the flanking mountains deflected the ice sheet in a westward direction which can be traced upstream to Lake Athabasca.

Converging striae on the Kazan Upland indicate that the northern area continued to be dominated by southwest-flowing ice from the Keewatin Ice Divide during the same time. During subsequent retreat of the ice fronts, the northern lobe retreated earlier than the Lake Athabasca lobe. This is indicated by the pattern of meltwater diversion discussed in a following section.

As the ice thinned further, the local topography imparted greater control on ice flow. For example, minor striae oriented along the north shore of Lake Athabasca crosscut the more dominant westward flow. Similarly, in the northern part of the study area, the dominant southwestward striae are crosscut by secondary striae along valley bottoms and lake shores.

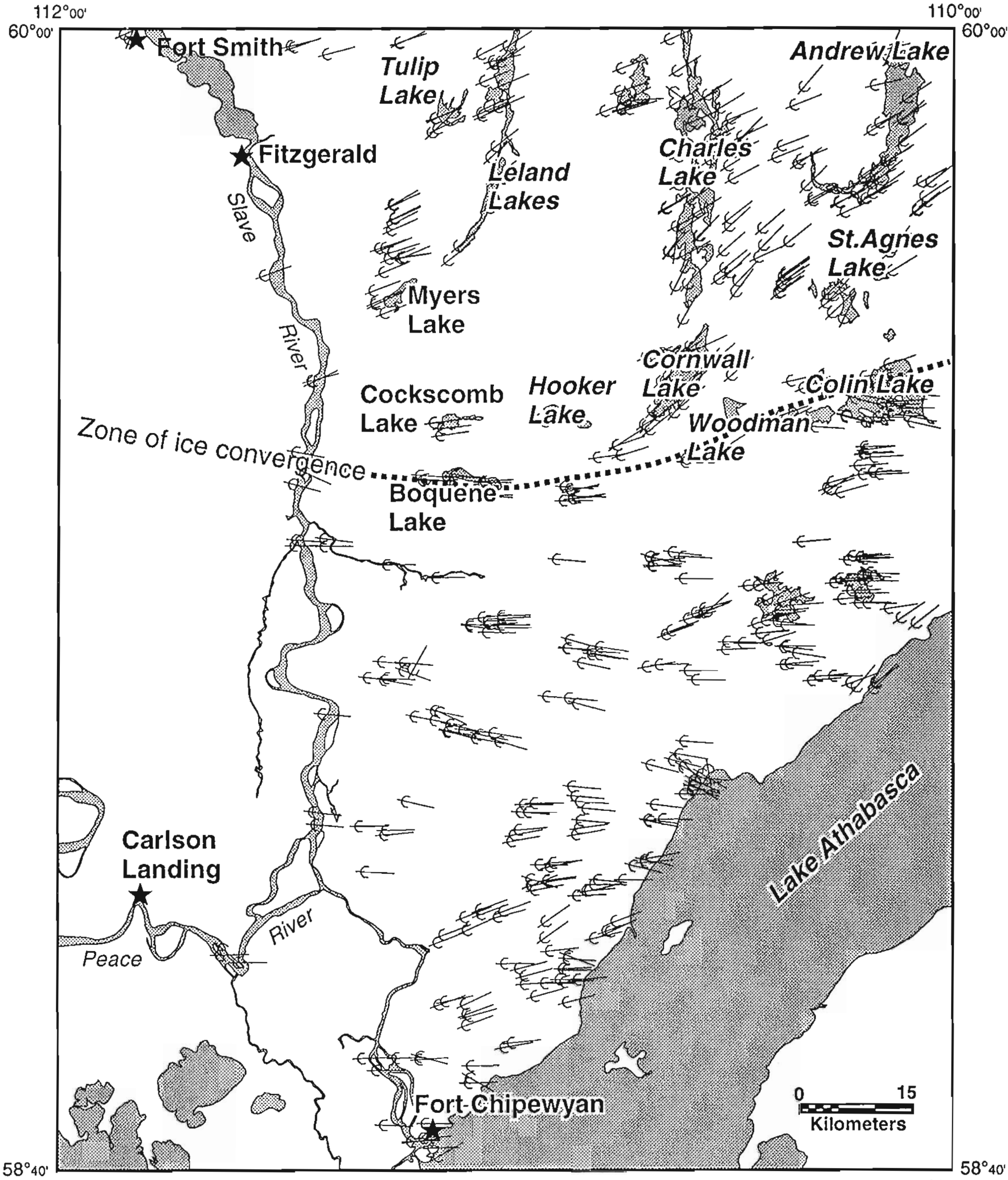

Figure 5. Glacial striations in the study area. Note the dominant flow from the northwest converging with predominantly westward flow in the southern part of the area.

Ice-flow patterns could be traced only as far west as the Precambrian/Paleozoic contact along the Slave River. Outcrops west of the Slave River are rare and lithologies are not conducive to preservation of striae. Nonetheless, Tsui and Cruden (1984) reported striae bearing 210 along Salt River in the northwest part of the study area. This implies that the prevailing flow pattern of the northern sector extended onto the Great Slave Plain (Fig. 5). Lemmen (pers. comm.) demonstrates similar flow directions north of the study area, in the Northwest Territories.

Glacial sediments

Two main categories of sediment were deposited in the study area in immediate contact with glacier ice: till and ice-contact glaciofluvial sediment.

Till

Till, representing the eroded products of glacial action, is very sparse on the Kazan Upland. Since the bulk of basal till is usually transported less than 10 km from its source (Puranen, 1988), the average amount of glacial erosion over the upland is likely to have been small. This being the case, any drift prospecting program in the study area must consider secondary transport processes that may have concentrated glacigenic sediment.

Glacial ice was very effective in eroding the sediments of the Athabasca Group, in contrast to rocks of the crystalline basement. Large sandstone erratics, several metres in diameter, and thick sand bodies are common several kilometres north of the contact along Lake Athabasca. Glacial erosion was also more effective on the Paleozoic substrate underlying the Great Slave Plain. A limited number of exposures show a till blanket overlying the bedrock.

Till is produced by sediment that is deposited directly by glacial melting or by basal lodgement. The latter produces the densest till with a strong clast fabric oriented in the direction of former glacial flow. This contrasts with the till on the Kazan Upland, which generally forms a thin discontinuous veneer of unconsolidated drift with a coarse sandy matrix. These characteristics indicate an ablation till facies, laid down during stagnant ice wastage. The till has a very similar texture to colluvium or coarse outwash diamictons, however, it can be distinguished by the relative abundance of erratics and striated clasts.

Dense basal till, particularly lodgement till (cf. Dreimanis, 1990), is uncommon in the study area. Glacial scour dominated the Kazan Upland, although basal till is occasionally found on the lee side of prominent outcrops. Locally, till forms a tapered tail on the downstream side of a bedrock knob (crag and tail features). Streamlined drift features such as drumlins or flutings are rare in the study area. Till was commonly reworked by glacial meltwater and it is often found interbedded with glaciofluvial gravel along former ice margins. The Slave Moraine is a good example of this (Fig. 6; see *Slave Moraine* below).

Local till derived from basement rocks is usually sandy (Fig. 7), containing angular to subangular igneous and metamorphic clasts and multimodal grain size. In the southern part of the study area, till derived from the Athabasca Group is very sandy, with uniform matrix and pinkish colour. Pebble analysis of 150 till samples reflects the diversity of lithologies on the Canadian Shield, but no clear distinctions of provenance could be made. Most of the till is composed of local bedrock, however, far-travelled lithologies are also present. For example, a volcanic erratic from the Keewatin (Pitz Formation), found in till north of Bocquene Lake (Fig. 5), indicates a transport distance of approximately 800 km from the northeast. In the southern parts of the Kazan Upland, large sandstone erratics are common 10 to 20 km north of the basement contact. West of the Slave River, till derived from the Paleozoics is more indurated and has a silty matrix and carbonate clasts in addition to the Canadian Shield lithologies.

Glaciofluvial sediment

Glaciofluvial sediment is divided into two types: ice-contact glaciofluvial sediment, and outwash deposited away from the immediate ice front as proglacial sediment. The glaciofluvial sediment found on the Kazan Upland is usually very coarse and unconsolidated sand. It contains subrounded to well-rounded pebbles to boulders and rudimentary bedding. Given that glaciofluvial sediment was usually concentrated along meltwater conduits within the ice sheet and along the ice margin, most of the sediment is probably farther travelled than local till. The greatest volumes of glaciofluvial sediment are found in a zone extending from Colin Lake to Boquene Lake (Fig. 5), within the Colin Lake Interlobate Moraine, described in the next section. A second large glaciofluvial body lies along Lake Athabasca, northeast of Fort Chipewyan (Fig. 6).

Large volumes of ice-contact gravel found within the moraines, eskers and kame terraces contain stratified drift. However, eskers are relatively rare in the study area and restricted to short segments in some valley bottoms. The lack of coherent esker networks in the study area implies that glacial retreat was too rapid for their development. A major esker zone lies ~75 km northwest of the study area, in the Northwest Territories (Aylsworth and Shilts, 1989; Prest et al., 1968). The eskers record radial outflow of meltwater from the Keewatin ice divide along an orientation subparallel to the ice-flow direction, and clearly show a large influx of glacial meltwater to the study area from hundreds of kilometres away. Schreiner (1984) felt that the eskers in northern Saskatchewan formed when the ice mass was bounded by the Cree Lake Moraine, and that most of the esker formation occurred when the ice front retreated 35 to 40 km north from the moraine.

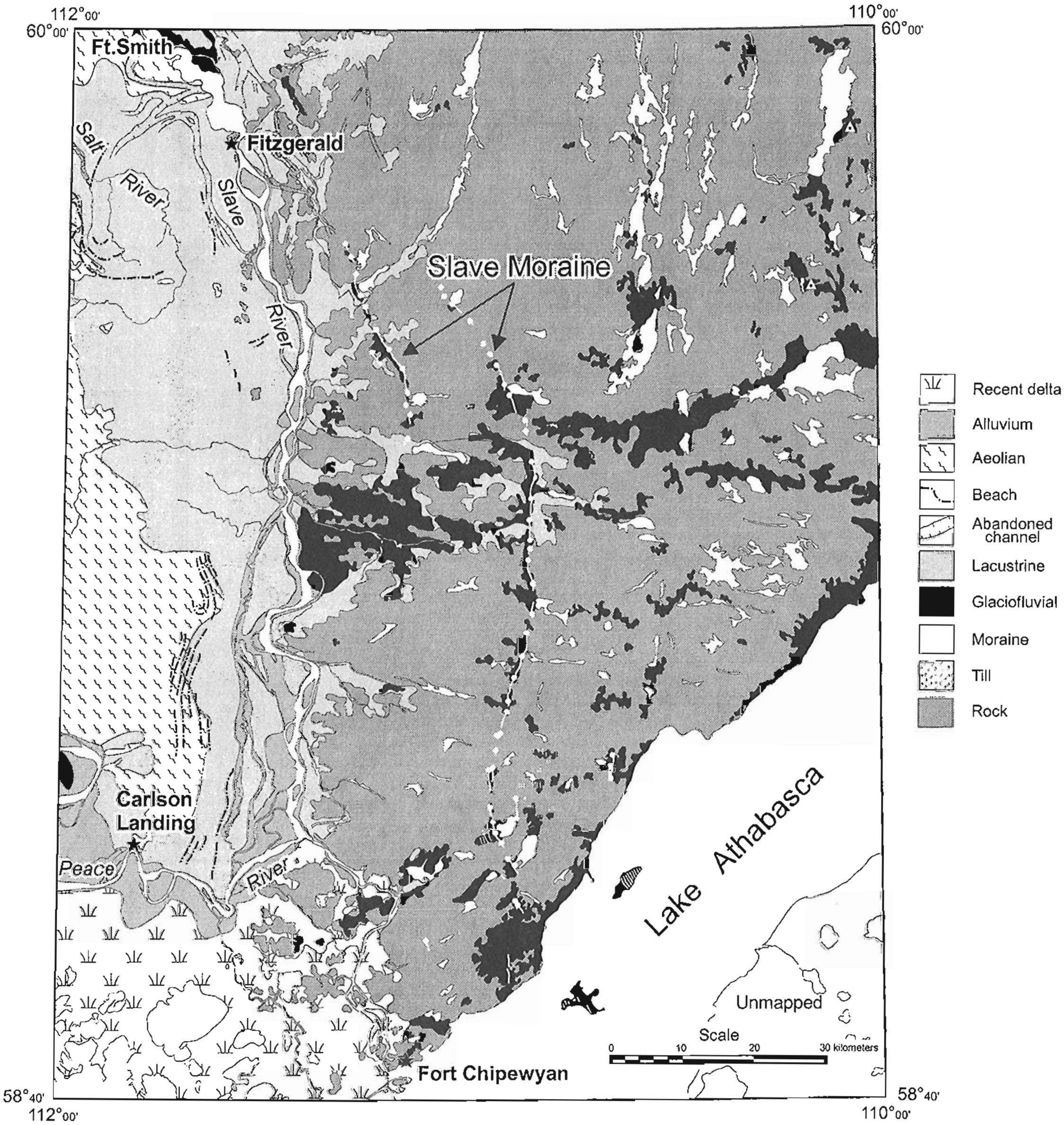

Figure 6. *Generalized surficial geology of the study area. Note the sparse surficial cover overlying the Kazan Upland: the extensive moraine system east of the Slave River which marks a major stillstand of the retreating Laurentide Ice Sheet (Slave Moraine) and the accumulation of thick glacial drift along an east–west belt marking the Colin Lake Interlobate Moraine. The Great Slave Plain, west of Slave River, is covered by thick glaciolacustrine and glaciodeltaic sediment, and recent deltaic sediment south of Peace River. Prominent raised beaches mark the regression of Lake McConnell. Thick surface till is limited to the southwestern part of the study area in the vicinity of Salt River.*

Glacial landforms

Colin Lake interlobate moraine

Two lobes of ice within the Laurentide Ice Sheet covered the study area. In the northern part of the study area, southwestward flowing ice over the Kazan Upland converged with the westward flowing Athabasca lobe, forming a contact zone of thick glacial drift from Colin Lake to Boquene Lake (Fig. 5), the greatest concentration of glacigenic sediments on the Kazan Upland. Colin Lake Interlobate Moraine is used

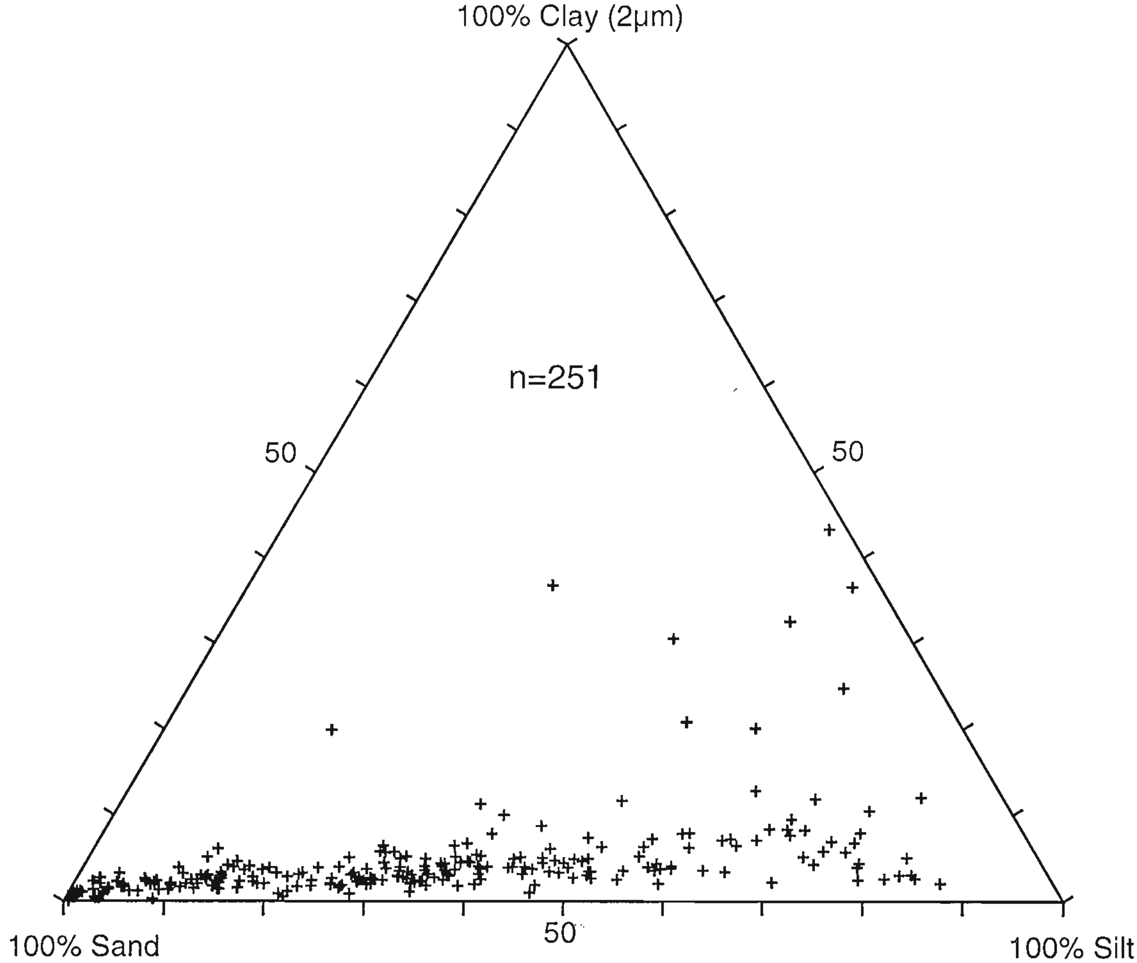

Figure 7. *Sand, silt and clay ratios for 251 glacial drift samples.*

as a collective term to describe the suite of sediments deposited along this lateral contact zone. Morphologically this zone comprises extensive kame terraces forming a broad east-west band, especially around Colin Lake and south of Woodman Lake (Fig. 5), and coincides with the band of glaciofluvial sediments shown in Fig. 6. Kame terraces are perched features that accumulated subaerially along the sides of hills when glacier ice occupied lowlands. Some terrace surfaces are pitted with steep-sided kettles that formed when isolated remnants of buried glacial ice subsequently melted out.

Generally, kame terraces in the study area are very sandy and can be tens of metres thick. Because all known exposures in the area show either glaciofluvial gravel or glaciolacustrine sand, it is not known how much of the Colin Lake Moraine is compresed of till. Nonetheless, bouldery gravel on the sides of numerous kettles suggests deposition by ice ablation.

Slave Moraine

Till and ice-contact gravels accumulated along the margin of the ice sheet when the ice front temporarily stabilized or readvanced during overall retreat. These accumulations usually form narrow ridges of sediment draped over bedrock, thus outlining the former ice margin. The Slave Moraine, on the Kazan Upland, is the most prominent of these ridges and can be traced in two segments for 120 km, from Lake Athabasca to southeast of Fort Smith (Fig. 6). The moraine forms a sharp-crested ridge, typically 50 m high and 500 m wide, located 7 to 35 km east of Slave River. The Slave Moraine frequently dams westward-trending valleys, forming lakes on the eastern side, but it is occasionally breached by former spillways and modern streams. In some cases the Slave Moraine crosscuts meltwater channels, suggesting that the channels were initially subglacial in origin.

The Slave Moraine is composed of stratified sands and gravels interbedded with thick diamicton lenses. A 22 m exposure in a borrow pit west of Myers Lake (Fig. 5) shows gravelly diamicton lenses dipping southwest at 20 to 30°. The diamictons contain numerous lithologies of cobbles to large boulders supported in a sandy matrix, and have a strong fabric (bearing 239°). Some of the material probably has been transported great distances; for example, there are very resistant quartzite boulders that are well rounded with numerous percussion marks. Slumping structures within the diamicton and gravel beds are common in a downslope, westward direction. Generally, clast size decreases upward in the section and sorting improves. The uppermost part of the section contains ~50 varves overlain by littoral gravel related to glacial Lake McConnell. Strandlines are common on either flank of the Slave Moraine.

The makeup of the Myers Lake section indicates till and gravel sloughing off the ice front in a subaqueous environment. As will be discussed in a following section, the Slave Moraine lies below the maximum elevation of glacial Lake McConnell and was the grounding line of the ice sheet.

The Cree Lake Moraine of northern Saskatchewan was traced to the southern shore of Lake Athabasca (Prest et al., 1968; Dyke and Prest, 1987). The Slave Moraine is thought to be the northern extension of the Cree Lake Moraine which is also associated with glaciofluvial complexes (Schreiner, 1984). Given the validity of this correlation, the Slave Moraine dates approximately 10 ka BP.

Minor moraines

Several short segments of end moraine, with similar characteristics to the Slave Moraine, are found throughout the Kazan Upland. These likely represent local pauses in recession of the ice front as deglaciation proceeded generally eastward. A second type of moraine, usually restricted to low-lying areas, is found in the vicinity of Lake Athabasca. These moraines were described as crevasse fillings by Bayrock (1972a), who mapped tens of square kilometres of them south of Lake Athabasca. Schreiner (1984) mapped them as DeGeer moraines, an interpretation that is supported by this study. Generally, they form short parallel ridges of glaciofluvial gravel and boulders that are no more than a few tens to hundreds of metres long. The spacing is very regular, usually ~150 m, with a maximum of 5 m relief. DeGeer moraines formed along a calving ice front when the ice sheet was retreating in contact with standing water. They are thought to be annual features that formed when the ice front became buoyant during the ablation season. The DeGeer moraines mapped here are found on either side of the Slave Moraine and are associated with glacial Lake McConnell.

Proglacial landforms and sediments

The environment peripheral to the ice sheet was dominated by deposition of glacial outwash, glacial lake sediment, and to a lesser extent, aeolian sediment. The proglacial zone migrated eastward as the ice front retreated, hence, proglacial sediments decrease in age eastward. Glacial outwash is usually composed of medium to coarse sand with minor amounts of gravel. Glacial lake deposits on the Kazan Upland are similar to outwash sand, except with an absence of pebbles and a slight increase in silt content. In contrast, glacial lake sediments in the western part of the area are more clay rich. Most aeolian sand was derived from outwash and glaciolacustrine and deltaic sand, and is medium grained. Sediments derived from the Athabasca Group (Wilson, 1985) are all texturally similar, thus complicating genetic interpretations, especially where extensive reworking by meltwater and wind occurred during deglaciation. Parts of the region are dominated by aeolian sand sheets and dunes. These formed during early Holocene time when strong adiabatic winds, blowing off the Laurentide Ice Sheet, remobilized sediment on recently exposed lake bottoms (David, 1977).

Glacial Lake McConnell

The greatest volume of glacial lake sediment is found on the Great Slave Plain and underlying the Peace/Athabasca delta where it forms flat, poorly-drained terrain. Most of this sediment was deposited in glacial Lake McConnell (Craig, 1965) when the ice front contacted the Slave Moraine. Sections along the Peace and Slave rivers expose dark clay and silt overlain by coarser deltaic sand. Glacial Lake McConnell sediment onlaps the western edge of the Kazan Upland, thinning out on the proximal (east) side of the Slave Moraine. Glacial lake sediments on the Kazan Upland in the eastern part of the study area have little clay and tend to be mostly fine sand and silt. As noted above, glaciolacustrine varves onlap the Slave Moraine at Myers Lake (Fig. 2). Lake McConnell varves were also found on the proximal side of the Slave Moraine, north of Lake Athabasca and in the Fort Chipewyan area (Fig. 2). The thickest set of varves were found at the Fort Chipewyan site where at least 170 rhythmic couplets were counted. Farther east, glacial lake sediment is patchy and confined to the valley bottoms and depressions. Most of this sediment was deposited in ephemeral lakes that formed along the retreating ice front, and not as part of Lake McConnell. These lakes were at least 15 m higher in elevation than the maximum elevation of Lake McConnell (320 m asl). The maximum elevation of raised shorelines indicates that in the vicinity of Lake Athabasca, glacial Lake McConnell reached a level of at least 305 m asl; south of Great Slave Lake, the highest level of glacial Lake McConnell was ~310 m asl (Lemmen 1990a, b).

Strandlines marking the regression of Lake McConnell are found throughout the area. On the west side of the Slave River, northeast of Carlson Landing (Figs. 2, 6), individual berms, providing 15 to 20 m of relief, can be traced for 50 km at 221 to 244 m asl. They appear to be made entirely of medium to coarse sand. On the east side of the Slave River, flights of well-developed beaches can be found on either side of the Slave Moraine (Fig. 6). These beaches are more gravelly than the western strandlines because they were built from underlying glaciofluvial material. The beaches commonly extend to the crest of the Slave Moraine because Lake McConnell overtopped the moraine as the ice front withdrew eastward. The maximum elevation of beaches on the Slave Moraine is 244 m asl, 25 km southeast of Fort Smith, to 305 m asl in the vicinity of Hooker Lake (Fig. 5). In the south, well-developed beaches lie along the north shore of Lake Athabasca up to ~305 m asl. Schreiner (1984) suggested that glacial Lake Athabasca, the south-eastern extension of glacial Lake McConnell, had an areal extent defined by the 305 m contour, including fluvial deltas near Uranium City, Saskatchewan, near the easternmost part of present Lake Athabasca. Although the maximum elevation of glacial Lake Athabasca was similar along its entire length, the maximum lake level must be time-transgressive because it took >1 ka for the ice sheet to completely vacate the lake basin (Dyke and Prest, 1987). The raised beaches along the north shore of Lake Athabasca are usually comprised of well-sorted pinkish sand derived from Athabasca Group lithologies.

When Lake McConnell separated into Great Slave Lake and Lake Athabasca, a large volume of deltaic sand was deposited over glaciolacustrine sediment on the Great Slave Plain (Fig. 1). The deltaic plain extends to the Caribou Mountains in the west while to the east and south it is bound by the Slave and Peace rivers that have incised up 30 m into the sediments near Carlson Landing (Fig. 6). Younger alluvium and delta sediment have been inset into the older delta by the Peace and Slave rivers. Several large channels were cut within the Slave River valley as lake drainage progressed. These channels are now abandoned or occupied by misfit streams (Fig. 6).

Lemmen et al. (1994) reconstructed a lake level curve describing the fall of Lake McConnell throughout postglacial time (Fig. 8). It is based on the elevations of published radiocarbon dates, along a transect from Great Slave Lake to the Peace River delta. The form of the curve is very similar to postglacial emergence curves from the Arctic that were caused by glacioisostatic rebound (cf. Bednarski, 1995c). The lake level curve provides a means of dating many features in the study area and will be referred to in a following section.

Proglacial outwash

Like glacial lake deposits, proglacial outwash decreases in age eastward. Most of the glaciofluvial sediment was deposited laterally along the ice margin, within spillways, and as coarse deltaic material prograded into glacial lakes. Continuous rearrangement of the drainage network took place as the ice front retreated eastward. The result is that, now, the outwash is found scattered throughout the area at various elevations. The material is composed of unconsolidated, coarse sand and gravel, containing many lithologies. Bedding is rarely visible. The interlobate zone from Colin Lake to Hooker Lake (Fig. 5) contains large volumes of proglacial outwash in close association with ice-contact material. In the northeastern part of the study area large spillways record southward flowing rivers that were diverted to the west by glacial ice that persisted in the south. One particular channel can be traced for >15 km to a prominent braided outwash delta east of St. Agnes Lake (mapped as glaciofluvial material on Fig. 6). A second outwash delta in the study area lies east of Andrew Lake (Fig. 6). Both of these deltas record lake levels of >320 m asl. The braid patterns on the outwash clearly show that the direction of outflow was to the west, despite the southern regional slope of the land.

Aeolian sediment

Throughout the study area, drainage of proglacial lakes during postglacial time exposed large plains of lacustrine and deltaic sand that was scoured by intense wind action, consequently, wind blown sediment and dune fields are found throughout the area. The western edge of the study area includes the Wood Buffalo Sand Hills, an area of particularly large dunes up to 30 m high (Fig. 6; David, 1977), formed by an abundance of well-sorted deltaic sand. On the Kazan Upland (Fig. 1),

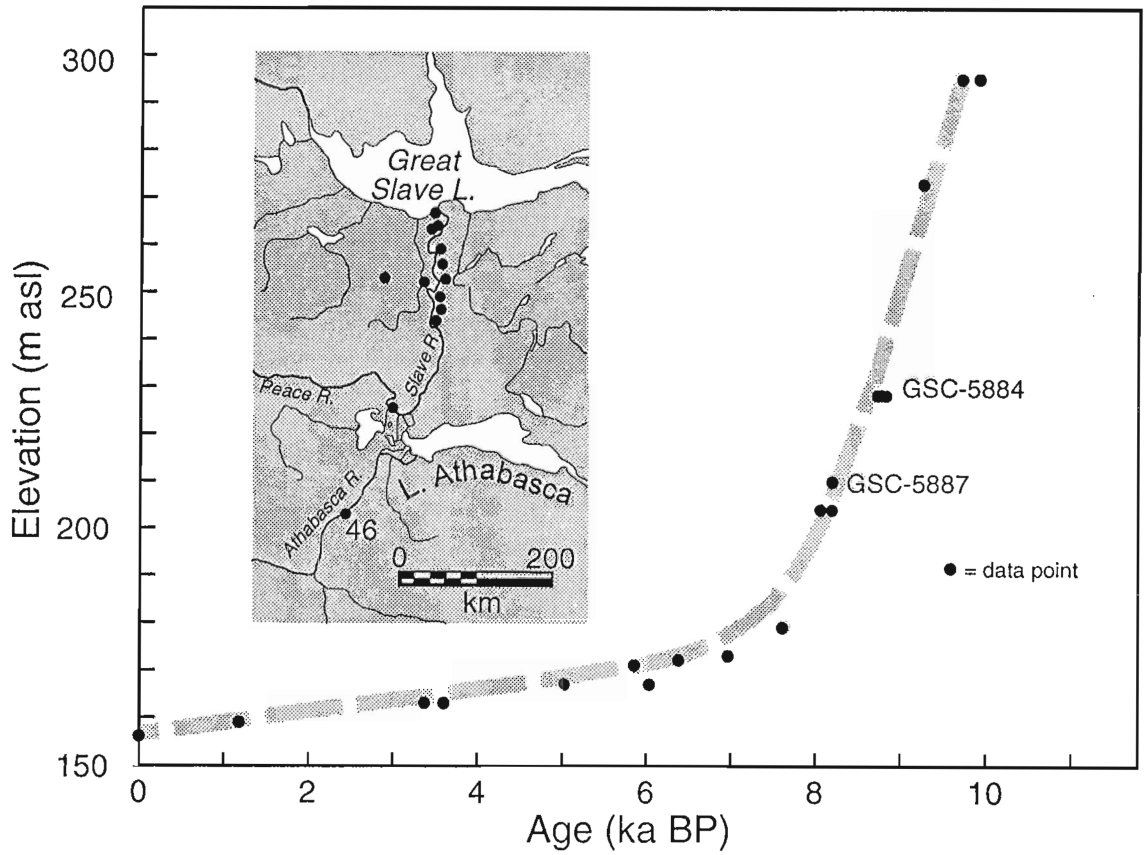

Figure 8. *Lake level curve depicting the history of Lake McConnell and Great Slave Lake from a transect along the Slave and Athabasca Rivers (from Lemmen et al., 1994), with the addition of GSC 5884 (8720±80 BP) and GSC 5887 (8070±100 BP).*

deltaic and lacustrine sediment is more localized and aeolian blankets are rare. Loess deposition is evident as 10 to 20 cm of silt layers overlying till in numerous hollows on the upland. Most dunes on the Kazan Upland are northwest of Hooker Lake and south of Woodman Lake, within the zone of the Colin Lake Interlobate Moraine (Fig. 5). These dunes are of the parabolic type (David, 1977), similar to the "Cree Lake" dune type described by David (1981). They are usually elongated in a downwind direction and they advanced downwind as long as there was a ready source of sediment. On the Kazan Upland, the dunes commonly advanced onto nonaeolian sediment or bedrock as thin sand ridges extending up to 3 km beyond any apparent sediment source. The dunes form ~5 m of relief and are usually steeper on the north side. The shape and surface texture of dune sands making up the dunes is not appreciably different from the source material. At present, the dunes appear to have been stabilized by vegetation, except for shallow blowouts near the tops of some ridges.

The predominant direction of dune elongation is to the northwest, implying strong surface winds from the southeast. This direction is diametrically opposite to strong present-day winds that tend to blow out of the northwest, as indicated by modern deflation hollows along the southern shore of Lake Athabasca. This indicates that the dunes likely date from early postglacial time when a persistent anticyclone was centred over the Laurentide Ice Sheet and dominated the regional circulation (COHAP Members, 1988). Consequently, the age of the dunes can be bracketed because they formed in a zone peripheral to the ice sheet. The demise of the ice sheet allowed Arctic air masses to penetrate southward causing an abrupt shift in the dominant wind direction. Rapid colonization by vegetation in early Holocene time (MacDonald, 1987) further stabilized aeolian deposits.

Postglacial sediments

Alluvium

The postglacial environment is typified by the development of contemporary drainage patterns following the separation of Lake McConnell in early

Holocene time. Without the input of glacial meltwater, fluvial activity greatly declined on the Kazan Upland, and currently, only minor redistribution of pre-existing glacigenic sediment takes place. Modern alluvium is restricted to narrow deposits along the Peace and Slave rivers and some of their larger tributaries. The alluvium is composed of fine grained sand and silt with small pockets of coarser gravel. Distinct scroll bars are commonly expressed on the surface. Except for the major river valleys, most valley bottoms throughout the study area are occupied by misfit streams meandering through organic-rich sediments, with no appreciable sediment transport.

Organic terrain

Poorly drained depressions abound on the Kazan Upland. They are usually filled with silt, clay, peat and other organic material of modern origin. Where the organic matter is ≥1 m thick, the substrate is often frozen throughout the summer. The study area lies within the zone of discontinuous permafrost (Brown, 1967) and landforms attributed to the growth of ground ice, such as peat plateaus and palsas, are common where the insulative layer is thick (Zoltai and Tarnocai, 1975). Peat plateaus, the larger of the two features, cover only a few hundred square metres where they occur, and may be tree covered. The areas underlain by permafrost are very sensitive to disturbance. Once the insulative layer is disrupted, the surface rapidly subsides as the ground ice melts. During the summers of 1992, 1993 and 1994, numerous peat plateaus were seen to be degrading because the edges of the plateaus are slumping and surface trees have a "drunken" appearance, tilting in every direction. This recent degradation has been reported on a regional scale and may signify recent climatic warming and resultant melting of ground ice (Vitt et al., 1994).

Deltaic sediment

The greatest volume of recent sediment was deposited by progradation of the Peace River Delta into Lake Athabasca (Recent delta, Fig. 6). The elevation of the Peace River Delta is usually 15 to 30 m lower than the Lake McConnell deltaic sediments. The flat surface is etched with a myriad of levees from constantly shifting channels. Historically, the modern delta underwent seasonal flooding when large volumes of silt and fine grained sand were deposited. However, diminished discharge of the Peace River over the last few decades has led to the drying of large areas of the delta, and most contemporary sedimentation occurs along distributary channels and smaller deltas within the overall deposit. Comparing airphotos from 1955 with those from 1982 and 1984 clearly shows the changes.

Littoral and lacustrine sediment

Modern littoral processes are most prevalent along the northern shore of Lake Athabasca, particularly where there is a lot of sandy sediment supplied by thick drift. The shoreline is affected by wind driven currents from both the northeast and southwest, forming prominent beach ridges and spits. The beaches often have large dunes, over 10 m high, behind them. Most of the dunes appear partly stabilized by vegetation, but active blowouts are common. It is possible that some of these dunes were partly derived from pre-existing raised beaches which are also common along the shore. In smaller lakes, littoral processes are minor and are restricted to outcrops of sandy drift or glaciofluvial material. High concentrations of erratic boulders are occasionally found along the shorelines of lakes on the Kazan Upland. The boulders can form prominent ridges of clast-supported material, but most are submerged 1 to 2 m. For example, on the east side of a large island in Cornwall Lake (Fig. 5), a boulder ridge about 3 m above the lake overlies bedrock at the shore. The boulders are typically angular, but some are subrounded and may be glaciofluvial deposits that were winnowed out as the lake level fell. Conversely, many of these features may have been formed by the ploughing action of lake ice during periods of colder climate. Ice-pushed ridges called "boulder barricades" are common along Arctic lake shores and coastlines (Bird, 1967).

Most of the currently exposed lacustrine sediment dates from early postglacial time when drainage systems were still plugged with glacial sediment or buried glacial ice. As integrated drainage systems developed with time, the lake levels dropped and lacustrine sediment was exposed. Generally, this sediment is thin and indistinguishable from unvarved proglacial lake sediment deposited earlier. In addition, many of the larger lakes on the Kazan Upland are bordered by prominent terraces up to 10 m above present levels (e.g., south end of Charles Lake, Fig. 5). The uniform height of these terraces above the lakes suggests that lake levels have dropped because of Holocene climatic change.

Colluvium

Significant mass wasting is restricted to cutbanks of the Peace and Slave rivers. A particularly large earthflow and slump is located at Carlson Landing on the Peace River (Fig. 6) involving at least 30 m thickness of material. Other large slumps occur on the west shore of Slave River, north of Fitzgerald. In each of these cases, slumping was enhanced because thick deltaic sediment overlies impermeable silts and clays. Rockfalls occur along brittle fault zones on the Kazan Upland where there is significant vertical relief involving angular blocks, several metres in diameter. The material does not look particularly weathered and is probably postglacial in age.

Aeolian sediment

Aeolian sedimentation during postglacial time declined abruptly with the decay of the Laurentide Ice Sheet and consequent shifts in regional wind patterns. Moreover, even by early Holocene time, vegetation migrated into the area, stabilizing the substrate (MacDonald, 1987). Small active blow-outs are found on the crests of some dunes and on sandy lacustrine deposits along the north shore of Lake Athabasca and on the sandy deltaic deposits west of the Slave River. As noted above, the direction of deflation is predominantly to the southeast, directly opposite to the regional winds of the early Holocene.

QUATERNARY HISTORY

Stratigraphy

The sporadic till deposition that occurred on the Kazan Upland makes stratigraphic correlations of till impractical, especially since the number of stratigraphic exposures throughout the region is very few. Moreover, the lithological composition of till on the upland is highly variable and distinct lobes could not be determined based on till composition. The greatest difference occurs between sandy till on the Canadian Shield and calcareous till derived from Paleozoic rocks west of the Slave River. The best exposure of till on the Kazan Upland is found in the Myers Lake section described previously, but in this case, the till is discontinuous and interbedded with glaciofluvial material. Good exposures of till derived from Paleozoic rocks are found along the Salt River in the northwest part of the area (Fig. 6). Natural sections through glaciofluvial sediments are usually very rare because of the loose nature of the sediment. A particularly good exposure is found in the Fort Chipewyan gravel pit, located south of the airport. This section records a glaciofluvial to glaciolacustrine succession, overlain by a regressive sequence. Extensive sections are found along the Peace and Slave rivers. The thicker sections record deltaic progradation over glaciolacustrine sediment, including frequently shifting channels recorded by cut-and-fill sequences.

The age of deltaic progradation along the Peace River was determined by radiocarbon dating of detrital organic matter deposited within the sediments. A spruce log extracted from organic-rich, foreset beds along the river yielded a date of 8720±80 BP (GSC 5884), providing maximum age on deposition, and a good age estimate on the ~215 m asl shoreline of glacial Lake McConnell. The apparent age of this shoreline corresponds with the lake level curve (Fig. 8) reconstructed by Lemmen et al. (1994). A second organic sample was collected from crossbedded sands at 210 m asl, just south of the Fort Smith townsite, where twigs and wood fragments yielded a radiocarbon age of 8110±100 BP (GSC 5887). This provides a good estimate for the age of the 210 m asl shoreline of Lake McConnell (Fig. 8).

Overview

Late Wisconsinan glaciation was responsible for much of the glacial geomorphology and all of the glacial stratigraphy found in the study area. The glacial maximum was achieved sometime after ~27 ka BP, based on the age of subtill organics found southwest of the study region (Liverman et al., 1989), and was maintained until ~18 ka BP (Dyke and Prest, 1987), when the Laurentide ice sheet inundated the area with strong flow from the northeast. Two convergent ice-flow patterns on the Kazan Upland, north of Lake Athabasca, were formed by two lobes of ice emanating from the ice sheet. These lobes probably developed during deglaciation (~11 ka BP) when uplands to the west and south emerged above the ice. The retreating ice front crossed the entire study area over a very short period (~11-9 ka BP), but the effects of glaciation on meltwater drainage lasted for at least another 1 ka. As the ice margin withdrew, glacial Lake McConnell, a huge ice-marginal lake, inundated all land below 305 m asl, and extensive lake sediment was deposited over the lowlands in the west (Fig. 9).

The retreat of the ice margin was marked by stillstands or minor readvances recorded by local accumulations of glacial sediments. The most significant pause in retreat occurred at ~10 ka BP, when the ice front was 10 to 30 km east of the Slave River and the Slave Moraine was formed. This 120 km long moraine is thought to be the northern extension of the Cree Lake Moraine of northern Saskatchewan (Prest et al., 1968). The Cree Lake Moraine marks a margin of the Laurentide Ice Sheet that extended

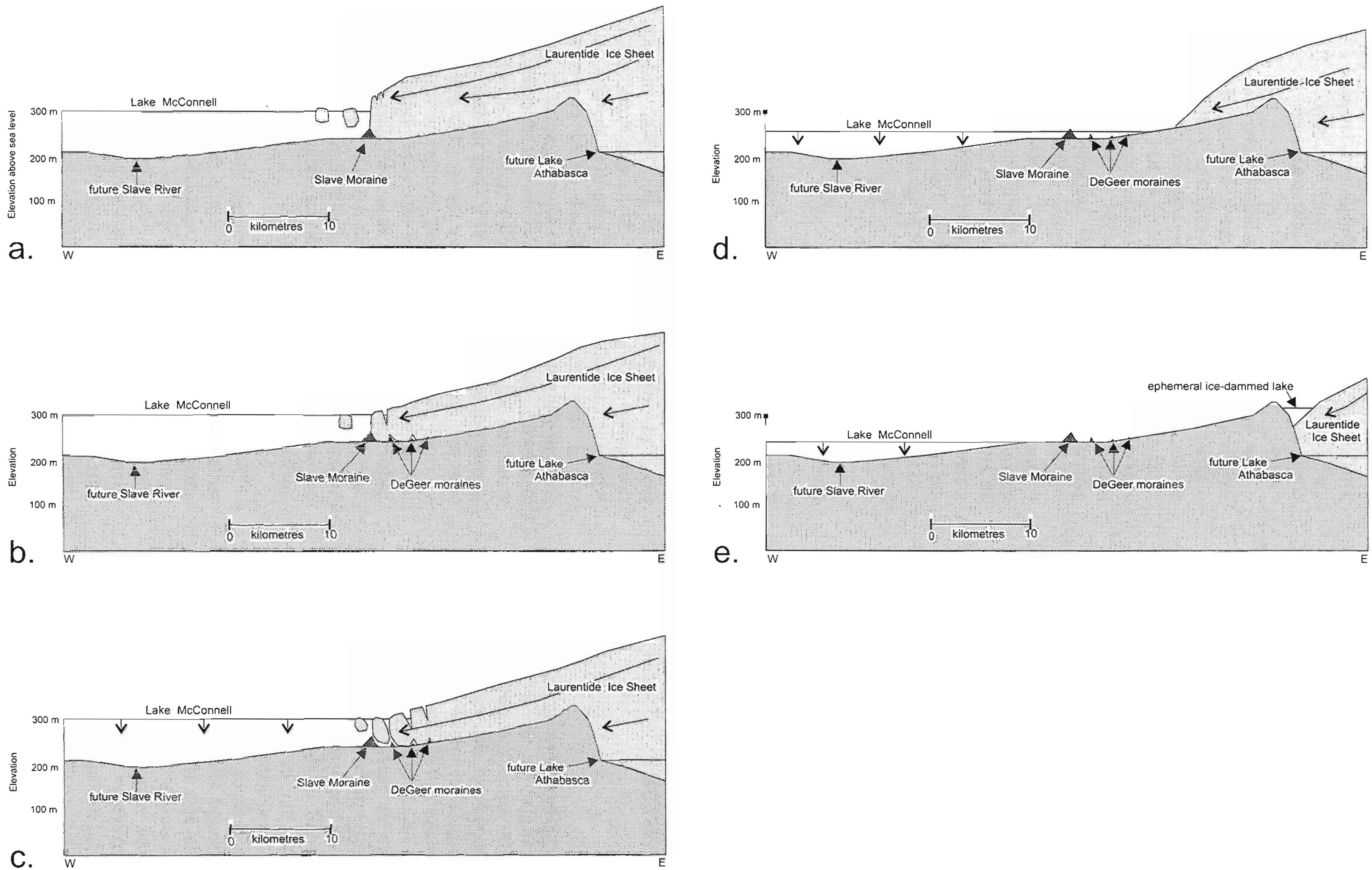

Figure 9. *Schematic profile of the Laurentide Ice Sheet and Lake McConnell during deglaciation (about latitude 59°03′N).* ***a.*** *At 10 ka BP the ice margin built the Slave Moraine subaqueously when Lake McConnell inundated deglaciated lowlands below 305 m asl.* ***b.*** *The ice sheet eventually thinned along the margin to the extent that ice-marginal crevasses formed and calving took place.* ***c.*** *The thinning margin became buoyant to the extent that very rapid retreat of the ice margin occurred and a series of DeGeer-type moraines formed beneath the ice.* ***d.*** *Eventually the margin of the Laurentide Ice Sheet retreated east of the Slave Moraine and Lake McConnell inundated the east (proximal) side of the moraine, but, because the level of Lake McConnell was continually dropping, the maximum elevation of the lake was not recorded on the deglaciated land east of the Slave Moraine.* ***e.*** *When the margin of the Laurentide Ice Sheet retreated within the Lake Athabasca trough, several lakes formed between the ice margin and higher ground to the north and west.*

across northern Saskatchewan to Manitoba. The Slave Moraine was deposited subaqueously, and subsequent retreat of the ice front caused Lake McConnell to overtop the moraine and inundate proximal lowlands to the east. The most rapid initial withdrawal of the ice front from the Slave Moraine occurred in the Lake Athabasca basin where water depths were greatest and glacial calving took place (Fig. 9). The level of Lake McConnell fell rapidly because of glacioisostatic rebound and free drainage through the Mackenzie river system, consequently, extensive regressive shorelines were built on the Slave Moraine and along the north shore of Lake Athabasca. As the level of Lake McConnell fell, the Slave Moraine blocked many westward flowing valleys and numerous smaller lakes persisted until the moraine was breached by spillways. Several present-day lakes are still dammed by the Slave Moraine.

Numerous ephemeral lakes were created when the ice front retreated eastward across the Canadian Shield (Fig. 9). Impounded by ice-blocked drainage, these lakes were filled with sandy glaciolacustrine sediments. Elsewhere, meltwater scoured channels in bedrock and deposited outwash. Ice sheet thinning exposed the Colin Lake Interlobate Moraine that was formed where the northern and southern ice lobes converged. This interlobate zone accumulated thick glaciofluvial and glaciolacustrine sediment. Patterns of meltwater diversion suggest that after initial ice front retreat from the Slave Moraine, the northern part of the study area became ice free prior to the southern part. In the southern part of the study area, the Lake Athabasca lobe continued to occupy the Lake Athabasca trough. The lobe ponded meltwater along its margin on the Kazan Upland and thick accumulations of glacio-lacustrine sand were deposited. By the time the ice front vacated the study area, most lakes drained and large expanses of sandy sediment were exposed to strong southeasterly winds, leading to the formation of parabolic dunes throughout the region. These winds were a late-glacial feature caused by a persistent anticyclone over the remaining Laurentide Ice Sheet.

By ~8.7 ka BP, ice retreating from the Lake Athabasca trough opened an embayment in Lake McConnell, termed glacial Lake Athabasca by Schreiner (1984). As lake levels dropped, the Peace River formed a delta over the Great Slave Plain, and eventually Lake Athabasca separated from Lake McConnell along a prominent bedrock sill near Fort Smith (Craig, 1965). By ~8.2 ka BP, ancestral Great Slave Lake (a remnant of Lake McConnell) receded north of Fort Smith with a water level of about 204 m asl (Vanderburgh and Smith, 1988; Lemmen et al., 1994). The Slave River entrenched large channels into the plain as Lake McConnell receded northward. On the Kazan Upland, most lake levels continued to decline throughout the Holocene as the modern integrated drainage patterns developed.

DRIFT GEOCHEMISTRY

A sampling program for the study area was designed to characterize bulk properties of the regional drift cover, with the hope that regional background levels for trace elements will identify areas that may warrant a more detailed drift prospecting scheme. The geochemistry data coupled with information on the distribution of surficial cover complements the survey of modern lake-sediment geochemistry (Friske et al., 1994). Within the scope of this paper, only selected measured elements are discussed. The complete data set will be released in a GSC Open File 3348.

Sampling procedures

The primary sampling medium was till, but because till is absent in parts of the area, several other genetic types of material were sampled to characterize the surficial cover. These included glaciofluvial, glacial lake and some aeolian sediments. Special consideration must be made when assessing these sediments because their dispersal paths are distinctly different than those of the till. The location of 336 drift sample sites is shown on Figure 2. Usually, 2 kg samples were retrieved by hand auger or shovel, below any pedogenic or oxidized horizons. Ten larger samples of ~25 kg were processed for heavy minerals. Most of the till samples were collected from isolated deposits in hollows and depressions in the bedrock. Sample stations were located by averaged GPS readings and/or fixed on 1:40 000 aerial photographs and 1:50 000 topographic maps.

Analytical procedures

Grain size was analyzed by sieving and sedimentation into: granules >2 mm, sand (2 mm to 63 μm), silt (2 μm to <63 μm), and clay (<2 μm) fractions. Sand, silt and clay ratios for 251 samples are presented in Figure 7. Carbonate content was analyzed by the Leco method (Fig. 10).

Two analytical techniques were used to determine the geochemical composition of the samples: inductively coupled plasma/atomic emission spectroscopy (ICP) and instrumental neutron activation analysis (INAA). ICP analysis was

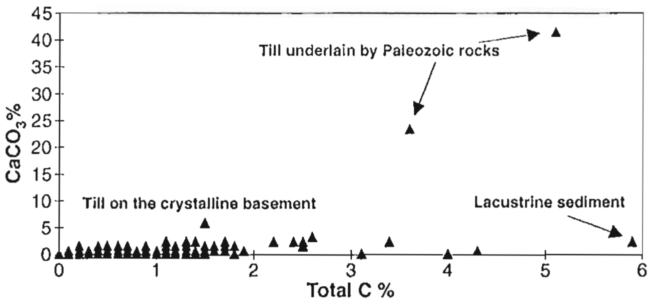

Figure 10. Scatter plot of per cent total carbon versus per cent $CaCO_3$ for 251 samples.

performed by Chemex Labs Ltd., Mississauga, Ontario, for 32 trace elements. Two grain size fractions (clay and silt plus clay) were analyzed separately, because trace metals can concentrate in the clay fraction (Shilts, 1992). In the ICP-32 analysis, a 1.0 g aliquot was digested using a concentrated nitric-aqua regia solution for two hours. The solution was then diluted to 25 ml with demineralized water and analyzed with a Jarrell Ash 1100 plasma spectrometer. The accuracy of the geochemical technique was checked by submitting 10 duplicate samples for each of the clay and silt-plus-clay runs and an "in house" GSC till standard (SBA) was inserted into the analytical batch to monitor the accuracy. INAA analysis was performed on the till matrix by Actlabs Ltd., Ancaster, Ontario. The analysis covered 35 elements, including gold and rare earth elements.

Results

Eleven elements determined by INAA and ICP (silt and clay) analyses on 251 samples generated three data sets that are compared in frequency polygons (Fig. 11). The resulting element distributions are usually positively skewed as is typical for spatial surveys (log-normal distribution; Levinson, 1974). Generally, the ICP analysis on the clay fraction (<2 μm) yielded higher maximum concentrations, with a higher mode, than values from the silt and clay fraction (<63 μm). The <63 μm fraction tends to have many more values below the level of detection. It is clear that the elements are concentrated in the clay fraction. Except for a few elevated values within the clay fraction, most values for elements fall within ranges typical for soils (Levinson, 1980). The distribution derived from INAA is usually intermediate between the two ICP derived distributions. A statistically derived spatial distribution of the 10 elements and per cent calcium carbonate is depicted as a series of contour maps in Figure 12. The contours were calculated by semivariance analysis, followed by kriging interpolation of gridded values. All the contour maps, except for gold (n = 222), describe the elemental distribution measured by ICP analysis of the clay fraction (n = 251).

Arsenic

Arsenic is a useful pathfinder for gold (Levinson, 1980). The distributions of the three data sets for arsenic are similar (Fig. 11a), with the highest number of readings below the level of detection. The clay fraction yielded the highest values, with a range of 1.9 to 86 ppm, a mean of 6.1 ppm, and the 75th percentile at 8 ppm. The highest values are found immediately south of Andrew Lake, in the northeast part of the study area (Fig. 2, 12a), with values above the typical range for soils (1–50 ppm, Levinson, 1980). Drift from the southern half of the study area appears to have depressed values when compared to the northern half. This difference may be related to the distinct ice lobes described in previous sections.

Cobalt

The level of cobalt is highest in the clay fraction measured by ICP, with a range from 2 to 36 ppm and a mean of 12.7 ppm (Fig. 11b). The data from the clay fraction approximates a normal distribution, with values typical for soils (Levinson, 1980). The spatial distribution is shown in Figure 12b.

Copper

Copper is one of the most commonly used elements in exploration geochemistry (Boyle, 1974). The data for copper is only from ICP analysis of clay and silt fractions. Values in the clay fraction range from 5 to 93 ppm, with a mean of 26, which is typical for soils (Levinson, 1980; Fig. 11c). The highest concentrations of copper are found about 15 km southwest of Colin Lake and west of northern Charles Lake (Fig. 2), and concentrations fall off to the west on the Great Slave Plain (Fig. 12c).

Figure 11. (right) Frequency polygons for 10 selected elements comparing INAA and ICP analysis for silt and clay fractions from glacial drift. Note that greatest concentrations occur in the clay fraction measured by ICP. For INAA, n = 137; for gold, n = 222; for ICP, n = 251.

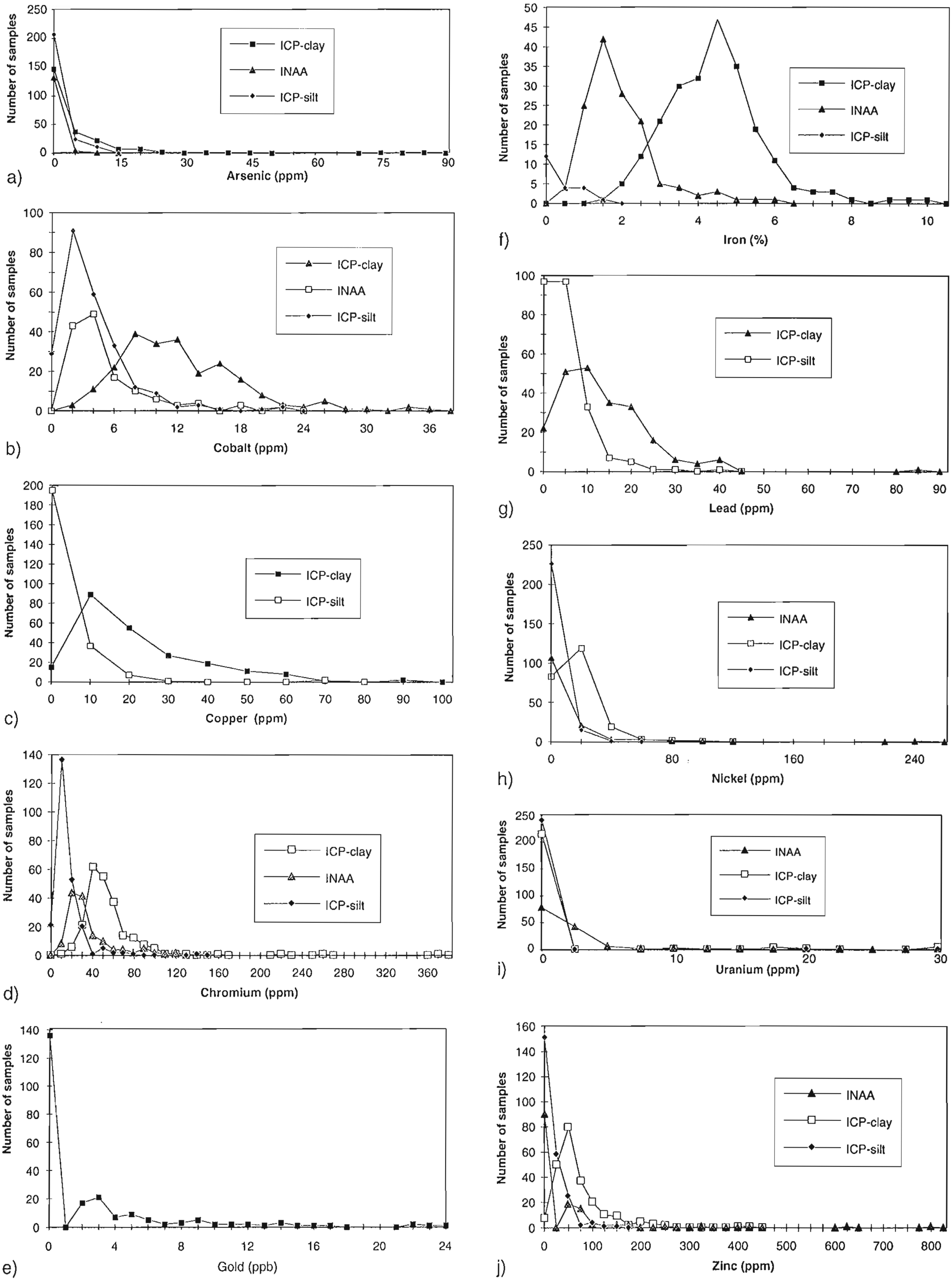

a)
Arsenic (ppm)
b)
Cobalt (ppm)
c)
Copper (ppm)
d)
Chromium (ppm)
e)
Gold (ppb)
f)
Iron (%)
g)
Lead (ppm)
h)
Nickel (ppm)
i)
Uranium (ppm)
j)
Zinc (ppm)
Number of samples
ICP-clay
INAA
ICP-silt

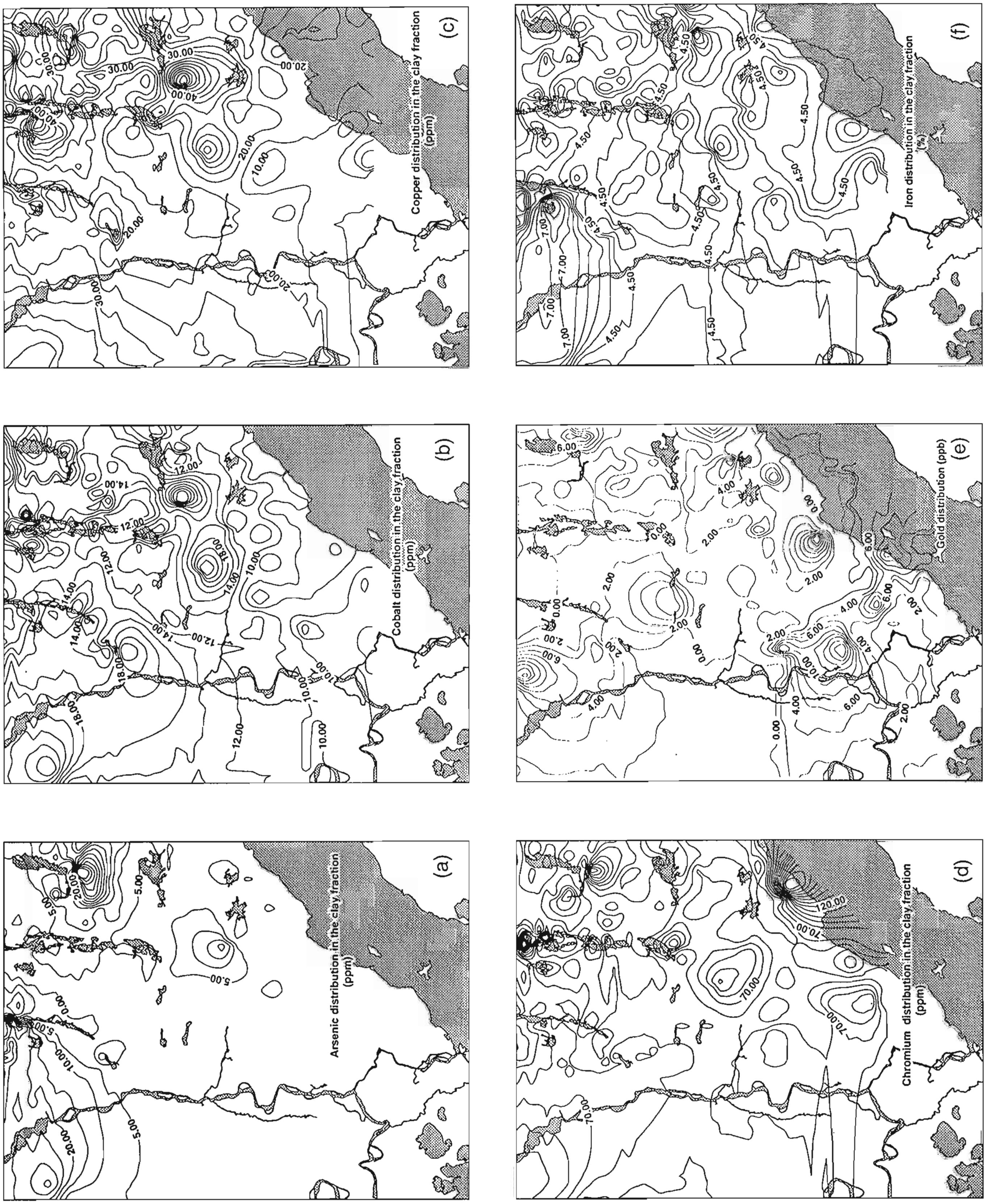
Arsenic distribution in the clay fraction (ppm)
(a)
Cobalt distribution in the clay fraction (ppm)
(b)
Copper distribution in the clay fraction (ppm)
(c)
Chromium distribution in the clay fraction (ppm)
(d)
Gold distribution (ppb)
(e)
Iron distribution in the clay fraction (%)
(f)

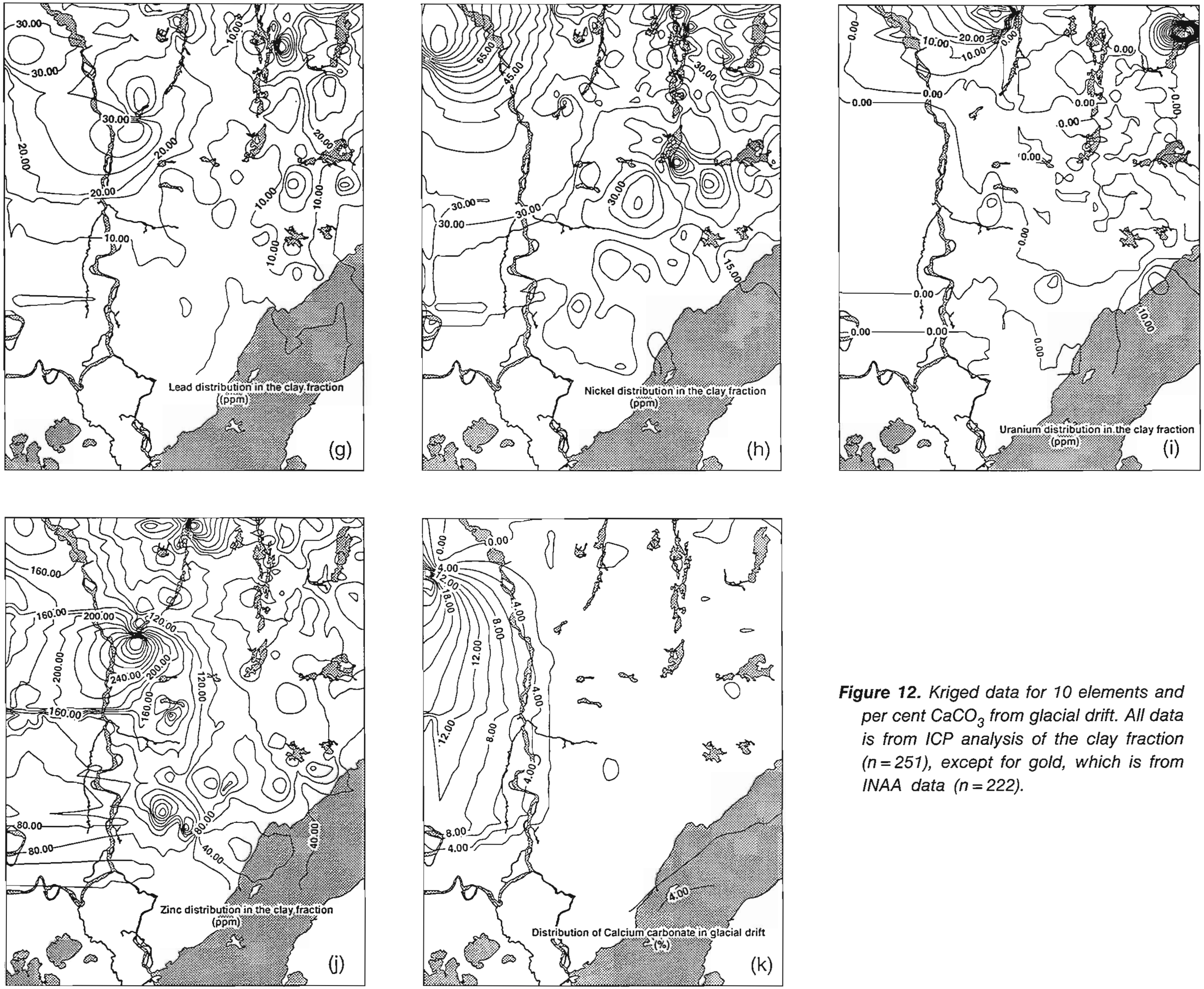

Figure 12. *Kriged data for 10 elements and per cent* $CaCO_3$ *from glacial drift. All data is from ICP analysis of the clay fraction (n = 251), except for gold, which is from INAA data (n = 222).*

Chromium

The highest concentrations of chromium are found on the crystalline basement of the Kazan Upland, with a string of highs along the Charles Lake Shear Zone (McDonough, 1997). The highest values occur on the northern end of Charles Lake, and a second high along the north shore of Lake Athabasca (Fig. 12d). Chromium has a mean of 40 ppm and a range of 16 to 370 ppm in the clay fraction. As is the usual pattern, the ICP values for the silt size fraction and the INAA values are significantly lower (Fig. 11d).

Gold

Gold concentrations were determined by INAA only, with a sample size of 222. The mean value of gold in the drift is 2.4 ppb, which is slightly elevated compared to typical values in soils (Levinson, 1980). Several anomalies of >16 ppb, with a maximum of 24 ppb, are indicated (Fig. 11e, 12e). A marked high in gold, contoured west of Tulip Lake, is located just west of a gold anomaly found in lake sediment by McCurdy and Friske (1996).

Iron

The per cent iron within the clay fraction of the drift closely approximates a normal distribution (Fig. 11f). Iron content ranges from 1.5 to 10 %, with a mean of 4.6 %. The highest levels tend to be found in the western part of the study area (Fig. 12f).

Lead

Lead data is available from ICP analysis only. Lead levels in the clay fraction ranged from 0 to 86 ppm, with an average of 15.4 ppm (Fig. 11g). Lead concentrations tend to be depressed in the southern part of the study area (Fig. 12g).

Nickel

ICP analysis detected nickel levels from 7 to 102 ppm, with a mean of 26 ppm, which is within usual soil values (Fig. 11h; Levinson, 1980). The INAA measured mean was 10 ppm, however, a single anomaly of 250 ppm was recorded near south Andrew Lake. The contoured data for the clay fraction indicates gradually rising values to the northwest (Fig. 12h).

Uranium

Unlike most other distributions, the ICP analysis on the clay and silt fraction gave similar results (Fig. 11i), nonetheless, the highest levels of uranium were still in the clay fraction. The range was from 0 to 120 ppm with a mean of 2.3 ppm, with most samples below the detection limit (<10 ppm). The INAA results gave a higher mean of 3.5 ppm, but with a maximum value of only 30 ppm (Fig. 11i). Contours on the clay-sized fraction generally show the highest values in the north (Fig. 12i).

Zinc

Zinc is a commonly determined element in geochemical exploration because it is mobile in most environments and forms extensive halos within surrounding soil and glacial drift (Levinson, 1980). In the clay fraction, zinc ranges from 8 to 430 ppm with a mean of 82.5 ppm, slightly higher than normal values for soils (Fig. 11j). The INAA showed two anomalies above 600 ppm near north Charles Lake. However, contours on the ICP data for the clay fraction show several highs forming a north–south ridge along the western edge of the Kazan Upland (Fig. 12j).

Carbonate contents

A scatter plot of per cent total carbon versus per cent calcium carbonate for 251 samples (Fig. 10) clearly distinguishes carbonate poor drift over the Kazan Upland from the till overlying the Paleozoic terrane. A sample of lacustrine silt from the Canadian Shield is discerned from the other samples by having higher total carbon content. Contouring the $CaCO_3$ content of glacial drift also shows the distinct difference in between the Precambrian/Paleozoic contact (Fig. 12k). The data clearly demonstrates that effective dilution of glacial sediment derived from the Shield occurred over a very short distance as the ice sheet flowed off the Kazan Upland and onto the carbonate terrain (Fig. 12k).

Heavy mineral analysis

The 10 large samples (~25 kg) were processed for heavy mineral concentrates at the Saskatchewan Research Council Sedimentary Laboratory. The following procedure was used: samples were disaggregated and the <1.7 mm grain-size fraction was preconcentrated on a shaker table. Ferromagnetic minerals were then removed from the reduced fraction with a hand magnet. The reduced fraction was then divided into specific gravities of 3.0 gcm^{-3} and 4.1 gcm^{-3} by a Magstream separator; all >0.25 mm grains of both fractions were submitted for hand picking. The heavy concentrates were further divided with a Frantz isodynamic separator and the weakly paramagnetic portion (>0.25 mm) was recovered for hand picking. Fifty-six grains suspected to have kimberlitic affinities were mounted and polished for electron microprobe analysis at the University of Calgary.

The bulk samples yielded 1.5 to 8.9 x 10^{-4}% heavy minerals by weight. Microprobe analysis of the 56 grains with possible kimberlite affinities identified one chrome spinel with oxide values of 40.3 wt% for chromium, and 13.8 wt% for magnesium, considered to be a good diamond indicator (Fipke, 1989; B.A. Kjarsgaard, pers. comm., 1995). The chrome spinel comes from ice-contact glaciofluvial sediment sampled near Colin Lake (lat. 59°33′N, long. 110°19′W). The glaciofluvial sediment was concentrated along the northern margin of the southern ice lobe, and may have been transported a large distance from the east, nonetheless, processing other samples from the area for diamond indicator minerals may be warranted.

Discussion

The maps presented in Figure 12 provide an effective method of depicting spatial till geochemistry, but they should be compared to other data sets, especially bedrock geology, for interpretation. The broad-scale patterns for many elements described above reflect the underlying bedrock, particularly the Phanerozoic/Precambrian contact along Slave River. They also reflect Pleistocene glacial Lake McConnell deposits in the southwestern part of the area. The main purpose of the maps is to show background trends in element concentrations from which abnormal chemical patterns reflecting mineralization may be discovered.

The mode or median of a distribution is often used as a measure of background value (Levinson, 1974), however, if trends or multiple populations exist in the data set, this may not be a valid procedure. Determining anomalously high concentrations is also not straightforward, because the presence of regional trends imparted by bedrock or dilution by surficial material must first be subtracted. Criteria that have been used to estimate threshold values to define an anomaly include: twice the background value, the mean plus two standard deviations, residuals after subtracting trend surfaces, or values occurring with a probability of 1:40 (Davis, 1986; Levinson, 1974). Thus, preliminary background levels can be obtained from the frequency polygons in Figure 11, however, these plots also show a fundamental problem with till analysis because the values vary between coarse and fine particle-size fractions.

In summary, in ultimately finding the source of mineral indicators, the net direction and distance vectors of sediment transport must be known. For glacial drift this means an understanding of glacial processes and Quaternary history.

SUMMARY

1. The exposed Precambrian shield of northeastern Alberta was extensively scoured by the Laurentide Ice Sheet during the last glaciation, but glacial deposits on the shield are rare. At the maximum extent of the last glaciation, the dominant ice flow was from the northeast and some rock debris was transported as far as 800 km by the ice sheet.

2. During deglaciation, a westward flowing ice lobe dominated the southern part of the study area as it flowed out of the Lake Athabasca trough. This ice lobe converged with the southwest-flowing ice, in the northern part of the study area, along a lateral zone that is traced from Colin Lake, near the Saskatchewan border, to the Slave River, near the latitude of Boquene Lake. This zone, termed the Colin Lake Interlobate Moraine, is characterized by ice-contact glaciofluvial gravels and sandy glaciolacustrine deposits overlying the bedrock.

3. Between about 11 000 and 10 000 BP, the margin of the Laurentide Ice Sheet retreated eastward, and all land below ~305 m in elevation, in the Slave River lowlands and Lake Athabasca trough, was inundated by glacial Lake McConnell. Extensive deltaic and lacustrine deposits of postglacial age were deposited in the Slave River lowlands during the existence of Lake McConnell.

4. A major stillstand or readvance of the ice margin produced the Slave moraine, an extensive moraine ridge running approximately parallel to the east side of the Slave River valley. The Slave Moraine is correlative with the 10 000 BP Cree Lake Moraine of northeastern Saskatchewan.

5. The distributions of As, Au, Co, Cr, Cu, Fe, Ni, Pb, U and Zn, measured by INAA and ICP in the silt and clay fractions of glacial drift, indicate enrichment in the clay fraction. Statistically derived contour maps describe the spatial

distribution of elements and delimit several anomalies. Some anomalies correspond with anomalies recorded in lake sediments (McCurdy and Friske, 1996).

6. Heavy mineral analysis of ten drift samples found one kimberlite indicator mineral from a glaciofluvial deposit near Colin Lake.

RECOMMENDATIONS FOR FUTURE WORK

Gold anomalies in the study area and the presence of a kimberlite indicator mineral near Colin Lake warrant future research. A denser sampling program in the anomalous areas should determine the extent of glacial dispersal and narrow the target zone. In the case of the kimberlite indicator mineral, the meltwater system along the Colin Lake Moraine should be sampled in detail, however, given the nature of the sediment, the mineral may have travelled tens of kilometres from the northeast.

Acknowledgments

Field assistance for the 1992, 1993, and 1994 field seasons was provided by R. Gault, T. Glover, and S. Hinds, respectively. A thorough review by Dr. D. Lemmen, Terrain Sciences Division, was much appreciated.

REFERENCES

Aylsworth, J.M. and Shilts, W.W.
1989: Glacial features around the Keewatin Ice Divide: districts of Mackenzie and Keewatin. Geological Survey of Canada, Paper 88-24, 21 p.

Bayrock, L.A.
1972a: Surficial geology, Fort Chipewyan NTS 74L. Alberta Research Council, Map 141, scale 1:250 000 with marginal notes.

1972b: Surficial geology, Peace Point and Fitzgerald west of 111°20′, NTS 84P, 74M. Alberta Research Council, Map 145, scale 1:250 000 with marginal notes.

Bednarski, J.M.
1993a: Preliminary report of the Quaternary geology of the Canadian Shield of northeastern Alberta. *In* Current Research, Part E. Geological Survey of Canada, Paper 93-1E, p. 191-196.

1993b: Geochemistry of surficial deposits in northeastern Alberta. Geological Survey of Canada, Open File 2747.

1995a: Surficial geology, Andrew Lake, Alberta–Saskatchewan–Northwest Territories (74M/16). Geological Survey of Canada, Open File 2982, colour map, scale 1:50 000.

1995b: Surficial geology, Colin Lake, Alberta–Saskatchewan (74M/9). Geological Survey of Canada, Open File 3041, colour map, scale 1:50 000.

1995c: Glacial advances and stratigraphy in Otto Fiord and adjacent areas, Ellesmere Island, Northwest Territories. Canadian Journal of Earth Sciences, v. 32, p. 52–64.

1996: Geochemistry of surficial deposits of Northeastern Alberta (NTS 74M and Part of 74L). Geological Survey of Canada, Open File 3348.

Bird, J.B.
1967: The Physiography of Arctic Canada. The John Hopkins Press, Baltimore, Maryland, 336 p.

Brown, R.J.E.
1967: Permafrost in Canada. Geological Survey of Canada, Map 1246A.

Bobrowsky, P.T. and Rutter, N.W.
1992: The Quaternary geologic history of the Canadian Rocky Mountains. Géographie physique et Quaternaire, v. 46, p. 5–50.

Bostock, H.S.
1970: Physiographic regions of Canada. Geological Survey of Canada, Map 1254A, scale 1:5 000 000.

Boyle, R.W.
1974: Elemental associations in mineral deposits and indicator elements of interest in geochemical prospecting. Geological Survey of Canada, Paper 74-45, 40 p.

COHAP Members,
1988: Climatic changes of the last 18,000 years: observations and model simulations. Science, v. 241, p. 1043–1052.

Craig, B.G.
1965: Glacial Lake McConnell, and the surficial geology of parts of Slave River and Redstone River map-areas, District of MacKenzie. Geological Survey of Canada, Bulletin 122, 33 p.

David, P.P.
1977: Sand dune occurrences of Canada. National Parks Branch, Canada, Department of Indian and Northern Affairs, Contract Report 74-230, 118 p.

1981: Stabilized dune ridges in northern Saskatchewan. Canadian Journal of Earth Sciences, v. 18, p. 286–310.

Davis, J.C.
1986: Statistics and data analysis in geology. John Wiley and Sons, New York, 646 p.

Dreimanis, A.
1990: Formation, deposition, and identification of subglacial and supraglacial tills. *In* Glacial Indicator Tracing, R. Kujansuu, and M. Saarnisto (eds.). A.A.Balkema, Rotterdam, p. 35–59.

Dyke, A.S. and Prest, V.K.
1987: Late Wisconsinan and Holocene history of the Laurentide Ice Sheet. Géographie physique et Quaternaire, v. 41, p. 237-263.

Fipke, C.E.
1989: The development of advanced technology to distinguish between diamondiferous and barren diatremes: a review of geological material relevant to diamond exploration and a summary of results. Geological Survey of Canada, Open File 2124.

Fisher, T.G.
1993: Glacial Lake McMurray, northeastern Alberta. *In* Program and Abstracts, Geological Association of Canada/Mineralogical Association of Canada, p. A-30.

Friske, P.W.B., McCurdy, M.W., Day, S.J., Gross, H., Balma, R.G., Lynch, J.J., and Durham, C.C.
1994: National Geochemical Reconnaissance lake sediment and water data, northeastern Alberta (Parts of NTS 74E, 74L, and 74M). Geological Survey of Canada, Open File 2856.

Fulton, R.J.
1989: Forword to the Quaternary Geology of Canada and Greenland. *In* Quarternary Geology of Canada and Greenland, R.J. Fulton (ed.). Geological Survey of Canada, Geology of Canada, no. 1, p. 1-11.

Godfrey, J.D.
1986: Geology of the Precambrian Shield in northeastern Alberta. Alberta Research Council, Map 1986-11, scale 1:250 000.

Lemmen, D.S.
1990a: Surficial materials associated with glacial Lake McConnell, southern District of MacKenzie. Current Research, Part D. Geological Survey of Canada, Paper 90-1D, p. 79-83.

1990b: Surficial geology of the Great Slave Lake region, N.W.T.: evolution of the central basin of glacial Lake McConnell. Canadian Association of Geographers, 1990 Annual Meeting, Program and Abstracts, p. 141.

Lemmen, D.S., Duk-Rodkin, A., and Bednarski, J.M.
1994: Late glacial drainage systems along the northwestern margin of the Laurentide ice sheet. Quaternary Science Reviews, v. 13, p. 805-828.

Levinson, A.A.
1974: An Introduction to Exploration Geochemistry. Applied Publishing Ltd., Wilmette, Illinois. 612 p.

1980: An Introduction to Exploration Geochemistry. The 1980 Supplement. Applied Publishing Ltd., Wilmette, Illinois.

Liverman, D.G.E., Catto, N.R., and Rutter, N.W.
1989: Laurentide glaciation in west-central Alberta: a single (Late Wisconsinan) event. Canadian Journal of Earth Sciences, v. 26, p. 266-274.

MacDonald, G.M.
1987: Postglacial vegetation history of the Mackenzie river basin. Quaternary Research, v. 28, p. 245-262.

Mathews, W.H.
1980: Retreat of the last ice sheets in northeastern British Columbia and adjacent Alberta. Geological Survey of Canada, Bulletin 331, 22 p.

McCurdy, M.W. and Friske, P.W.B.
1996: Elemental distributions for selected elements over Precambrian rocks in norhteastern Alberta (NTS 74E, 74L, and 74M). Geological Survey of Canada, Bulletin.

McDonough, M.R. (*this volume*)
1997: Structural controls and age constraints on sulphide mineralization, southern Taltson magmatic zone, northeastern Alberta. *In* Exploration for Minerals in Alberta: Geological Survey of Canada Geoscience Contributions, Canada-Alberta Agreement on Mineral Development (1992-1995), R.W. Macqueen (ed.). Geological Survey of Canada, Bulletin 500, p. 13-29.

Prest, V.K., Grant, D.R., and Rampton, V.N.
1968: Glacial map of Canada. Geological Survey of Canada, Map 1253A, scale 1:5 000 000.

Puranen, R.
1988: Modelling of glacial transport of basal tills in Finland. Geological Survey of Finland, Report of Investigation 81, 36 p.

Schreiner, B.T.
1984: Quaternary geology of the Precambrian Shield, Saskatchewan. Saskatchewan Geological Survey, Report 221, 106 p.

Shilts, W.W.
1992: Geological Survey of Canada's contributions to understanding the composition of glacial sediments. Canadian Journal of Earth Sciences, v. 30, p. 333-353.

Taylor, R.S.
1960: Some Pleistocene lakes of northern Alberta and adjacent areas (revised). Journal of the Alberta Society of Petroleum Geologists, v. 8, p. 167-185.

Tsui, Po C., and Cruden, D.M.
1984: Deformation associated with gypsum karst in the Salt River escarpment. Canadian Journal of Earth Sciences, v. 21, p. 949-959.

Vanderburgh, S. and Smith, D.G.
1988: Slave River delta: geomorphology, sedimentology, and Holocene reconstruction. Canadian Journal of Earth Sciences, v. 25, p. 1990-2004.

Vitt, D.H., Halsey, L.A., and Zoltai, S.C.
1994: The bog landforms of continental western Canada in relation to climate and permafrost patterns. Arctic and Alpine Research, v. 26, p. 1-13.

Wilson, J.A.
1985: Geology of the Athabasca Group in Alberta. Alberta Research Council, Bulletin, No. 49, 78 p.

Zoltai, S.C. and Tarnocai, C.
1975: Perennially frozen peatlands in the western Arctic and subarctic of Canada. Canadian Journal of Earth Sciences, v. 12, p. 28-43.

AIRBORNE GAMMA SPECTROMETER-MAGNETIC-VLF SURVEY OF NORTHEASTERN ALBERTA[1]

B.W. Charbonneau, P.B. Holman and R.J. Hetu
Mineral Resources Division, Ottawa

Abstract

The survey (10 000 km^2) presented at 1:250 000 scale, based on 1 km flight line spacing comprises 12 colour geophysical maps, a geological/mineral occurrence map, and a set of 146 stacked multiparameter profiles. The digitally recorded survey is ideal for integration with other data sets acquired during this MDA and for geophysical modelling.

The radioelement distribution patterns provide significant information over the peraluminous igneous rocks. The thorium and uranium/thorium ratio map patterns are controlled by monazite which hosts most of the thorium and is generally accompanied by zircon. Uraninite hosts most of the uranium. The more thoriferous magmatic rocks are less evolved (lower differentiation index) and have greater amounts of biotite, monazite and zircon. The more evolved magmatic rocks (more felsic) generally have lower thorium concentrations, which correspond to less monazite and zircon. Areas of high potassium (with a low Th/K ratio) commonly relate to evolved granitoids although some anomalies may indicate potassium alteration.

Magnetic patterns relate to magnetite/ilmenite with some hematization of magnetite. The magnetic maps are particularly useful in outlining geological structure and faulting. VLF patterns correlate with fractures and high-grade metasedimentary bands and in places indicate sulphide-rich conductors.

Geophysical signatures have often been linked to processes which point to mineralization and potential exists for U, Mo, Cu, Sn, W, REE and Au. In northeastern Alberta, such linkages are not currently recognized with the exception of VLF anomalies coincident with certain sulphide-rich metasedimentary bands and uranium anomalies relating to some uranium occurrences. However, with further investigation of observed geophysical patterns, correlations with mineralized systems may be recognized.

Résumé

Le présent levé (10 000 km^2) a été mis en carte à une échelle de 1:250 000 et effectué selon un espacement des lignes de vol de 1 km; il a donné lieu à 12 cartes géophysiques en couleurs, à une carte de la géologie et des indices minéralisés de même qu'à une série de 146 représentations en relief de plusieurs paramétres. Le levé, enregistré sous forme numérique, est idéal pour être intégré avec d'autres ensembles de données acquis dans le cadre de cette entente sur l'exploitation minérale et pour réaliser des modélisations géophysiques.

Les configurations de distribution des éléments radioactifs renseignent sur les roches ignées hyperalumineuses. Les configurations cartographiées du thorium et des rapports uranium/thorium dépendent de la présence de monazite, un minéral qui renferme la majeure partie du thorium et est généralement associé au zircon. L'uraninite recèlent la presque totalité de l'uranium. Les roches magmatiques plus thorifères sont moins évoluées (indice de différenciation inférieur) et contiennent plus de biotite, de monazite et de zircon. Les roches magmatiques plus évoluées (plus felsiques) présentent en général des concentrations moins élevées de thorium, ce qui correspond à une quantité moindre de monazite et de zircon. Les zones à forte teneur en potassium (rapport ThK

[1]Canada–Alberta Agreement on Mineral Development, Project C1.14

faible) sont habituellement liées à des granitoïdes évolués, bien que certaines anomalies puissent témoigner d'une altération en potassium.

Les configurations magnétiques reflètent la présence de magnétite et d'ilménite, la magnétite étant quelque peu hématisée. Les cartes magnétiques sont particulièrement utiles pour faire ressortir la structure géologique et les failles. Les configurations VLF sont liées à des fractures et à des bandes sédimentaires fortement métamorphisées et, par endroits, indiquent la présence de conducteurs riches en sulfures.

Les signatures géophysiques ont souvent été liées à des processus qui permettent d'identifier les zones minéralisées; ainsi, il existe un potentiel pour les éléments suivants : U, Mo, Cu, Sn, W, ÉTR et Au. Dans le nord-est de l'Alberta, il n'a pas été possible d'établir de telles relations, à l'exception d'anomalies VLF coïncidant avec certaines bandes métasédimentires riches en sulfures et d'anomalies d'uranium apparentées à certains indices d'uranium. Cependant, en poussant les travaux sur les configurations géophysiques observées, il se peut qu'on réussisse à établir des corrélations avec des systèmes minéralisés.

INTRODUCTION

The Canada-Alberta Agreement on Mineral Development (1992–95) (MDA) is comprised of a wide range of geoscience projects. The Northeastern Minerals Subprogram, which covers the Precambrian Shield portion of northeastern Alberta, involved six projects. Three of the projects — quaternary geology/ geochemistry (Bednarski, 1993, 1997; Bednarski et al., 1993); lake sediment geochemistry (Friske et al., 1994); and airborne multiparameter geophysics (gamma-ray spectrometry gamma-magnetics-VLF-EM) (Charbonneau et al., 1994) — provide an integrated set of geoscience surveys which will be invaluable in assessing the mineral potential of the area.

The scope of this paper is to provide a brief overview of the geophysical data with interpretation, thus refining the previous geophysical studies in the area; and to offer interpretations that will aid in relating the airborne geophysical patterns to various aspects of the regional geology and to the mineral exploration potential of the region.

The federal government has previously published geophysical surveys of the area for aeromagnetics at one-half mile (0.8 km) line spacing (Geological Survey of Canada, 1964a, b), reconnaissance gravity at 10 km stations (Walcott and Boyd, 1971), and reconnaissance gamma-ray spectrometry at 5 km line spacing (Geological Survey of Canada, 1977a, b). This data set was interpreted by Sprenke et al. (1986). The 1993 airborne geophysical survey flown as a contribution to the Canada-Alberta MDA can be regarded as a significant upgrading of this database with much improved sample density, the addition of VLF, and the added advantage that all of the geophysical data is now available digitally.

To assess the geological and exploration potential of the survey data, field investigations were conducted in 15 selected areas during July 1994 and the results are presented in this study. Field investigations consisted of in situ gamma-ray spectrometry, magnetic susceptibility measurements and bedrock sample collection for subsequent lithogeochemical and petrographic investigation.

Airborne geophysical surveys

The 1993 airborne geophysical survey flown by the Geological Survey of Canada (Fig. 1) combined gamma-ray spectrometric, total field magnetic, and VLF-EM sensors over an area of approximately 10 000 km^2. The survey data were published by Charbonneau et al. (1994). The survey data consists of a set of 12 maps at 1:250 000 scale and a set of stacked profiles for each flight line (1000 m line spacing). The gamma-ray spectrometric data consist of eight colour maps, ternary radioelement, exposure rate, μR/h potassium (pct K), equivalent uranium (eU, ppm) and equivalent Thorium (eTh, ppm) concentrations, and maps of the ratios eU/eTh, eU/K, and eTh/K. The aeromagnetic data are represented as colour maps of total field (nT) and calculated magnetic vertical gradient. The VLF-EM data consists of a total field colour map and a quadrature profile map. A geological compilation at 1:250 000 scale showing mineral occurrences accompanies the geophysical maps. The stacked profiles depict radar altimeter, seven gamma ray spectrometric parameters, magnetic total field, and VLF total field and quadrature components for each flight line. All of the above data is available digitally as grids (excluding VLF quadrature) and/or line data accompanied by "SurView" a viewing program published by Grant (1993). Details of the survey parameters are published with the survey.

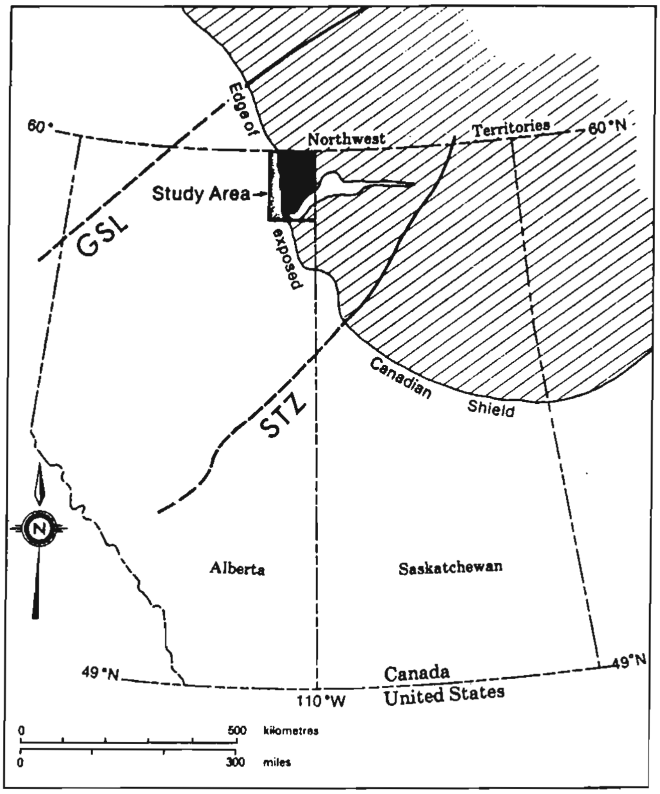

Figure 1. Northeastern Alberta project area showing Great Slave Lake shear zones (GSL), and Snowbird Tectonic Zone (STZ).

Geological overview including mineral occurrences

Information on the geology of the Precambrian Shield of northeastern Alberta, which is part of the Churchill province of the Canadian Shield, is summarized in Edwards et al. (1991) and McDonough et al. (1993, 1995), based on extensive work by Godfrey (1986a, b). Bostock and Loveridge (1988) have reviewed the geology of the Fort Smith belt to the north which is geologically continuous with northeastern Alberta. A compilation map by Hoffman and Hall (1993) gives an overview of the geology of the area to the north in the Northwest Territories, at a scale of 1:1 000 000. The study area in Alberta is part of the Taltson magmatic zone. The generalized geology of northeastern Alberta, including the Fort Smith belt to the north, is shown on Figure 2a, compiled from Bostock and Loveridge (1988), Edwards et al. (1991) and McDonough et al. (1993).

Edwards et al. (1991) summarized the geology of northeastern Alberta in the following manner:

> The basement migmatitic gneissic belt consists of granitic gneisses with minor components of small granitoid bodies, high-grade metasediments and amphibolite. This basement complex probably represents multiple cycles of sedimentation, intrusion, deformation and metamorphism, all rock units have been affected by ductile or brittle deformation.
>
> The granitoid complex west of the gneissic belt is dominated by the Slave and Arch Lake Granitoids and includes the LaButte Granodiorite and Francis Granite. It appears that the granitoids are ultrametamorphic partial-melt derivatives from the protolithic granite gneisses. The major contact between the granitoids and the gneissic belt is intrusive, with gneissic wall wedges protruding into the granitoids.
>
> Granitoids east of the gneissic belt include the Wylie Lake and Colin Lake Granitoids. This large band of relatively homogeneous porphyroblastic biotite granites overlies the granite gneiss complex. These rocks are metamorphic equivalents of highly deformed, low-grade metasedimentary and metavolcanic rocks in the Waugh Lake area.

Langenberg et al. (1993), however, indicated that the age relationship between Colin Lake granite and Waugh lake sediments and volcanics is uncertain. The Wylie Lake and Colin Lake granites are mineralogically similar to the Slave and Arch Lake granites but contain some hornblende which is rare in the Arch and Slave granites.

Goff et al. (1986) have noted that all of the granitoid units are peraluminous, or at least on the peraluminous-metaluminous boundary. The major granitoid units in northeastern Alberta, the Slave Lake and Arch Lake granitoids, are correlated with the Slave and Konth granites to the north in the Fort Smith belt. These granitoids are Aphebian (approximately 1955 m.y. and 1935 m.y. respectively) although McDonough et al. (1993) have postulated that Slave granite may be in part younger than Arch Lake granite. The eastern granites in the Rae Province (Colin and Wylie lakes) are broadly similar in age to the granites of the Taltson magmatic zone. McDonough et al. (1993) suggested that the Colin Lake granite may be similar in age to the Natael muscovite granite in the Northwest Territories (1935 m.y.), although they also postulated that the phase just east of Andrew Lake may be somewhat older.

The Andrew Lake phase contains a substantial amount of hornblende (McDonough et al., 1995) and may depart somewhat from the peraluminous nature of the other granitoids such as those at Slave, Arch,

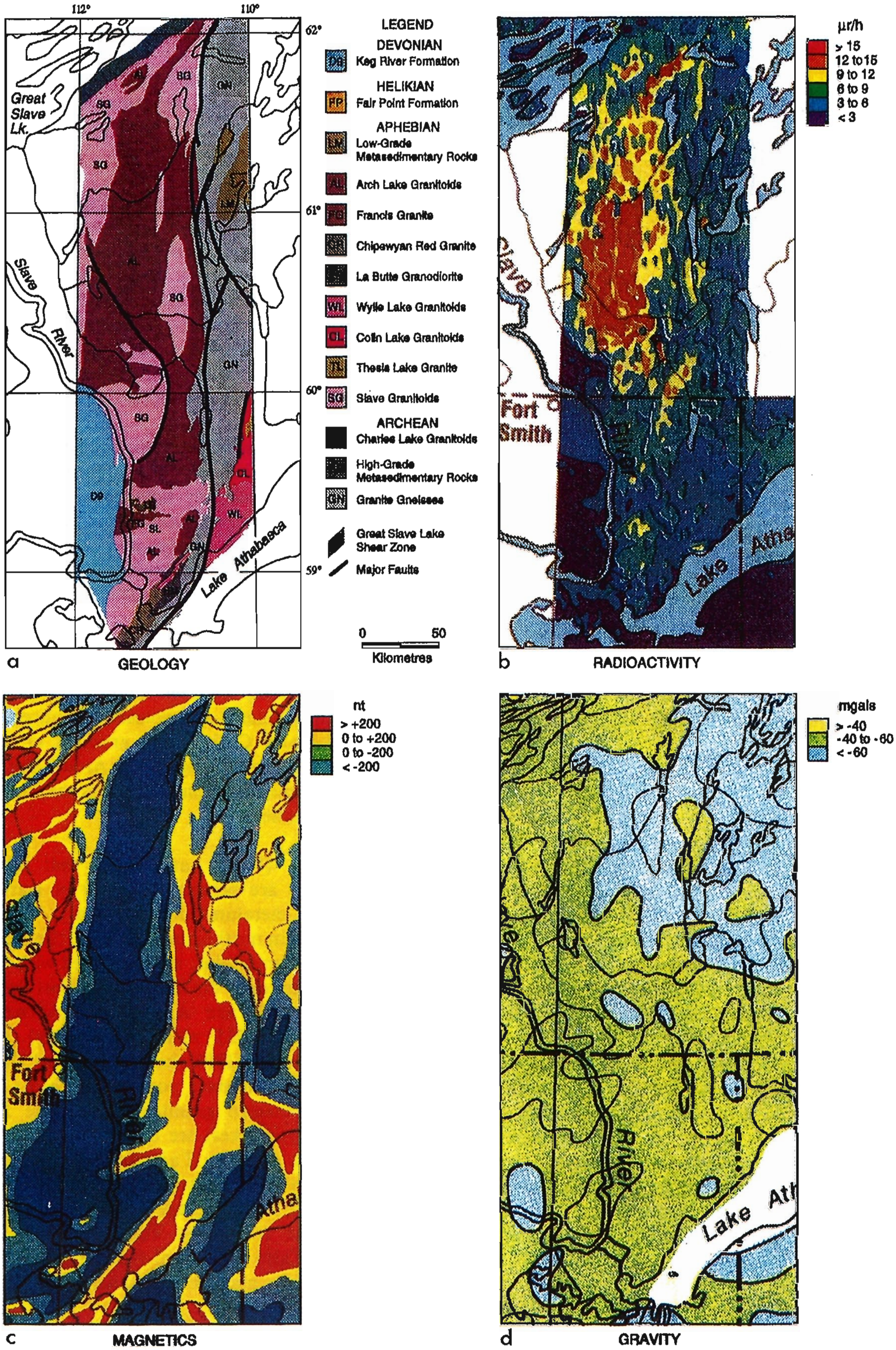

Figure 2. *Maps showing the **a)** geology, **b)** radioactivity, **c)** magnetics, and **d)** gravity of the Taltson magmatic belt in northeastern Alberta and adjacent Northwest Territories.*

Wylie, and Colin lakes. In this regard the Wylie Lake granite contains considerable hornblende but still plots dominantly (lithochemically) as peraluminous (see Goff et al., 1986; Fig. 3). The granitoids of northeastern Alberta also tend to contain magnetite which is not usually characteristic of peraluminous "S" type granites, to be discussed later.

The major structural subdivision in the area is the boundary between the Rae Province to the east and Taltson basement complex to the west. The contact is inferred (McDonough et al., 1993) to trend north-south through Andrew Lake, although, as they note, this is a considerable distance to the east of the position of the contact in the Fort Smith area to the north. Three major north-south oriented shear zones transect the southern Taltson magmatic zone in northeastern Alberta and are shown on Figure 2a. From west to east these are the Leland Lake, Charles Lake and Andrew Lake shear zones. The Rae–Taltson boundary is approximately at the Andrew Lake shear zone. The Leland Lake shear zone connects with the Warren shear zone in the Northwest Territories and the Charles Lake shear zone connects with the Allan shear zone in the Northwest Territories (McDonough et al., 1993).

Recent reviews of the mineral occurrences of the area have been published by Godfrey (1986b), Edwards et al. (1991), Langenberg et al. (1993), Olson et al. (1994), and McDonough (1997). There are a wide range of mineral occurrences known in northeastern Alberta in a variety of geological settings although the overall mineral potential is rated as low (see Edwards et al., 1991). Nevertheless, many occurrences of U, Au, Mo, Cu, W, and REE are documented in the above references. Most of the sulphide occurrences are gossans in narrow bands of high-grade metasedimentary rocks in the northeastern part of the survey. Uranium occurs in Slave, Colin Lake, and Wylie Lake granites and at the Athabasca unconformity near Lake Athabasca. Molybdenum is reported from the granites (mainly the Slave granite), but it is difficult to differentiate from graphite. Molybdenum also occurs in the granite gneisses southwest of Andrew Lake and in Colin Lake granites. Copper occurrences are noted in Paleozoic rocks along the Slave River and in shear zones in granite gneiss. A wide range of metal concentrations have been noted and/or postulated to occur in the area to the north (Bostock and Thompson 1983; Charbonneau, 1980, 1991; Charbonneau and Harris, 1993). Figure 3 is taken from Edwards et al. (1991) and summarizes the main mineral occurrences known in the area by 1990. Figure 3 is also useful for referencing geographical locations discussed later in the paper (i.e., Andrew Lake, Tulip Lake, Flett Lake, etc.).

Utilization of airborne geophysical data to recognize the signature of a mineralized area is a significant part of the interpretative process, but one should always keep an open mind about mineralization possibilities and use geophysics and geochemistry to recognize processes which may be related to unrecognized mineralization (i.e., processes of magmatic differentiation, potassium alteration, oxidation of magnetic rocks). Integration of the geophysical data with the other available data sets in the area (i.e., lake sediment geochemistry, till geochemistry) is, of course, of primary importance.

Overviews of the geophysics of the area (Sprenke et al., 1986), and of the lithogeochemistry (Goff et al., 1986) provide two extensive studies on which to base much of the present interpretation in this paper. The geophysical data utilized in Sprenke et al. (1986) was composed of aeromagnetic data summarized in Geological Survey of Canada (1964a, b); reconnaissance gamma ray spectrometry at 5 km line spacing (Geological Survey of Canada, 1977a, b); and gravity measurements at approximately 10 km station spacing (Walcott and Boyd, 1971).

Interpretation of regional geophysics

Figure 2 presents an overview of the geophysical patterns of the Fort Smith, Northwest Territories, and northeastern Alberta portions of the Taltson magmatic zone, showing the geology (Bostock and Loveridge, 1988; Edwards et al., 1991; McDonough et al., 1993), gravity (Department of Energy, Mines and Resources, 1980), total radioactivity (Darnley et al., 1986) and regional aeromagnetic signature (Morley et al., 1968). The geophysical patterns for part of this area were described by Charbonneau (1980, 1991). It is important to understand these patterns as they relate to the extension of the Taltson magmatic zone (TMZ) into northeastern Alberta in order to place northeastern Alberta into a regional context.

The core of the TMZ is underlain by Konth granite rocks which are equivalent to Arch Lake granite of northeastern Alberta. They exceed 15 μR/h on the total radioactivity map. Bedrock concentrations actually average ~80 ppm eTh with extensive areas exceeding 200 ppm eTh (Charbonneau, 1980, 1991). High uranium/thorium ratio anomalies (not shown) are peripheral to the high thorium rocks and correlate with portions of the Konth granite itself (more differentiated) and with border zones of older Slave granite and/or marginal gneisses which have been enriched with uranium. The central thorium-rich area is located within a north-south low magnetic anomaly.

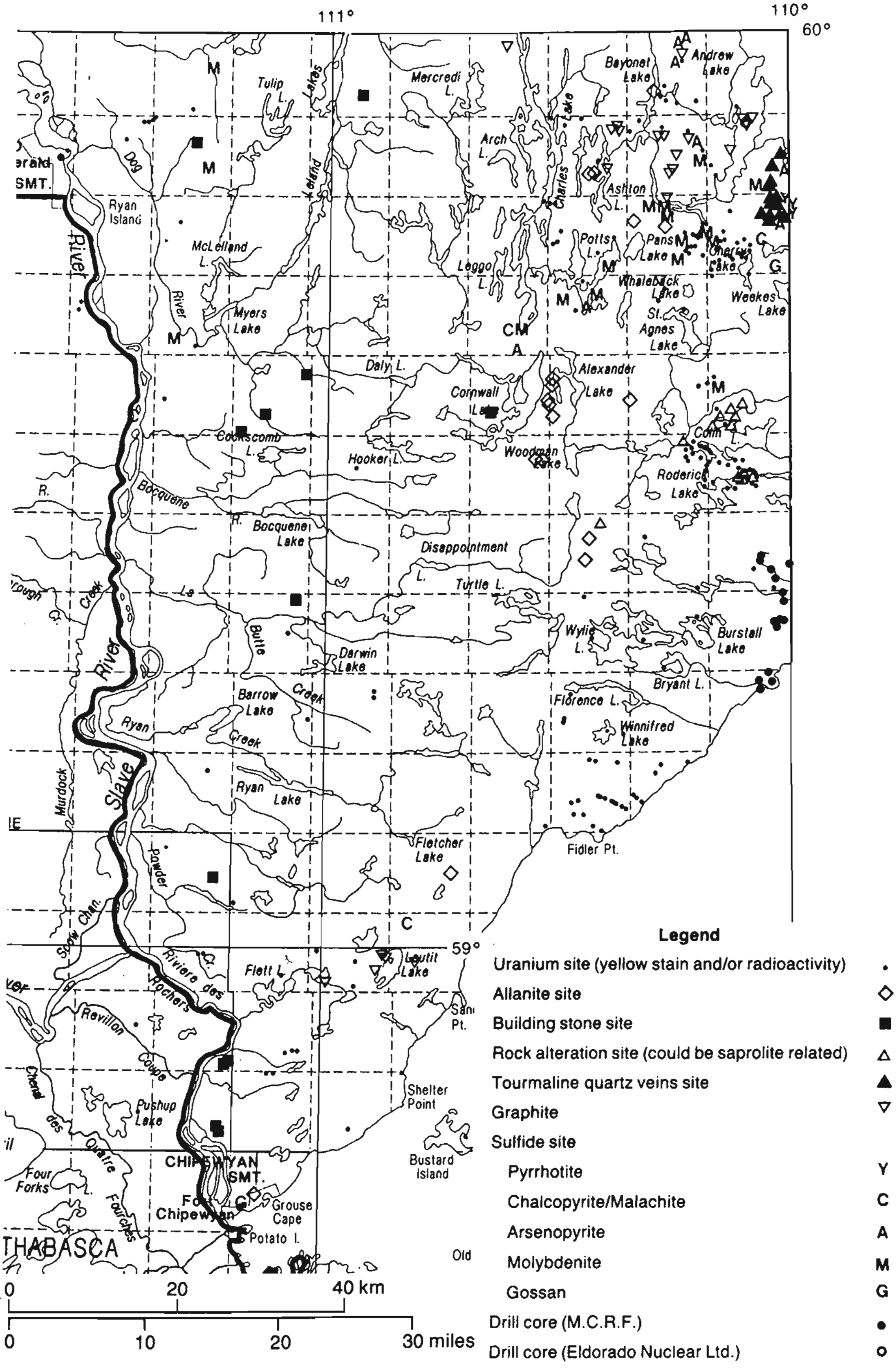

Figure 3. Mineral occurrences of Northeastern Alberta discovered before 1990 (from Edwards et al., 1991).

The explanation for the low magnetic anomaly is that the opaque oxides in this part of the Konth granite are mainly ilmenite with specks of hematite which may be remnants of oxidized magnetite (Charbonneau, 1991).

As shown on Figure 2, rock units in the Northwest Territories correlate with the units in northeastern Alberta. Geophysically, the Arch Lake granite of northeastern Alberta correlates with a band of low total radioactivity in the Northwest Territories situated east of the strongly radioactive central portion of the Konth granite. In addition, this belt of granite is magnetic whereas the central thorium-rich part of the Konth granite in the Northwest Territories lies within the magnetic low. Therefore, although the Arch Lake granite in northeastern Alberta correlates geophysically with Konth granite in the Northwest Territories, it correlates, not with the main body of highly radioactive (thorium) low magnetic Konth granite, but with an eastern belt separated somewhat from the main body of Konth granite and quite different geophysically (i.e., showing only moderate radioactivity and positive magnetic character). Gravity patterns in the area are quite subdued with only a slight low relating to part of the Konth granite. Slave granite in the Northwest Territories is magnetic along the western boundary in Figure 2c and variably magnetic and non-magnetic in northeastern Alberta as discussed below.

Database for interpretation

In addition to the literature referenced earlier and used in the present interpretation, one month (July 1994) of ground fieldwork was carried out in the area. In addition, insight gained during several years of fieldwork in the Northwest Territories to the north, concerning the geophysical patterns (Charbonneau, 1980, 1991), have been integrated into this study.

Crushed standard samples, which were collected during geological mapping by the Alberta Geological Survey and utilized in the geophysical study by Sprenke et al. (1986) and the geochemical study by Goff et al. (1986), were obtained from the Alberta Geological Survey. These samples had been analyzed for mineralogy, major chemistry, some trace elements, and certain geophysical parameters (magnetic susceptibility, specific gravity) but they had not been analyzed for the majority of the trace elements, which are of interest in interpreting the geophysical and geochemical patterns in the area. A gold plus 33 element neutron activation package (INAA) plus atomic absorption (AA) was completed on the samples. All of this new trace element data was integrated into the data file. We thus have potassium, uranium, and thorium values plus all the other traces and other parameters mentioned above for all the samples. This enables one to correlate the radioelements and their ratios with other elements and geophysical parameters.

Certain of the elements which had been analyzed by XRF during the previous work of Sprenke et al. (1986) and Goff et al. (1986) were re-analyzed by INAA and AA during this study and afforded a comparison of the two sets of analyses, for such elements as Na, Ba, Sr, Rb, and Zn. Figure 4 illustrates the excellent degree of correlation for 273 granitoid samples. Unfortunately the older samples had been crushed with tungsten carbide and a number of elements of potential significance were not useable (i.e., W, Co). However, many of the elements were not affected, including those that are of particular significance in evaluating magmatic processes (i.e., U, Th, Ce, La). These new lithogeochemical analyses are being prepared for a separate release at a later date.

In addition to the lithogeochemistry on the Alberta Geological Survey sample set, 100 samples of 15 anomalies were taken during field work in 1994 and their analyses are incorporated into this study.

Interpretation of airborne geophysical data acquired over northeastern Alberta during this study

Results of the 1993 multiparameter airborne geophysical survey are shown in Figures 5, 6, and 7. Charbonneau et al. (1994) contains these maps at a

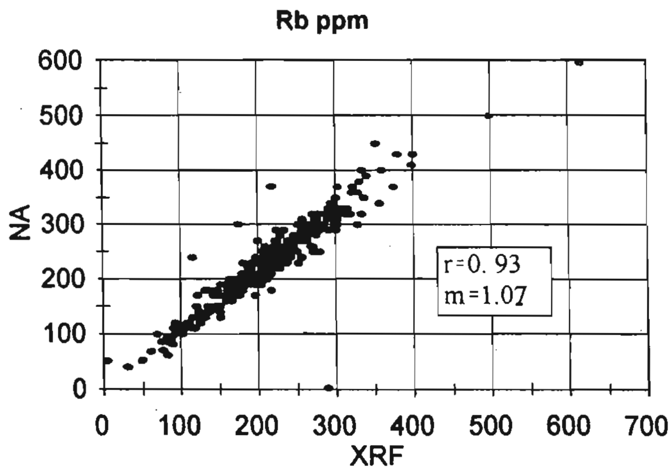

Figure 4. Plot of Rb ppm analyzed by neutron activation (NA) in this study verus Rb ppm analyzed by X-Ray fluorescence (XRF) for Alberta Geological Survey lithogeochemical standard samples analyses.

TERNARY RADIOELEMENT MAP

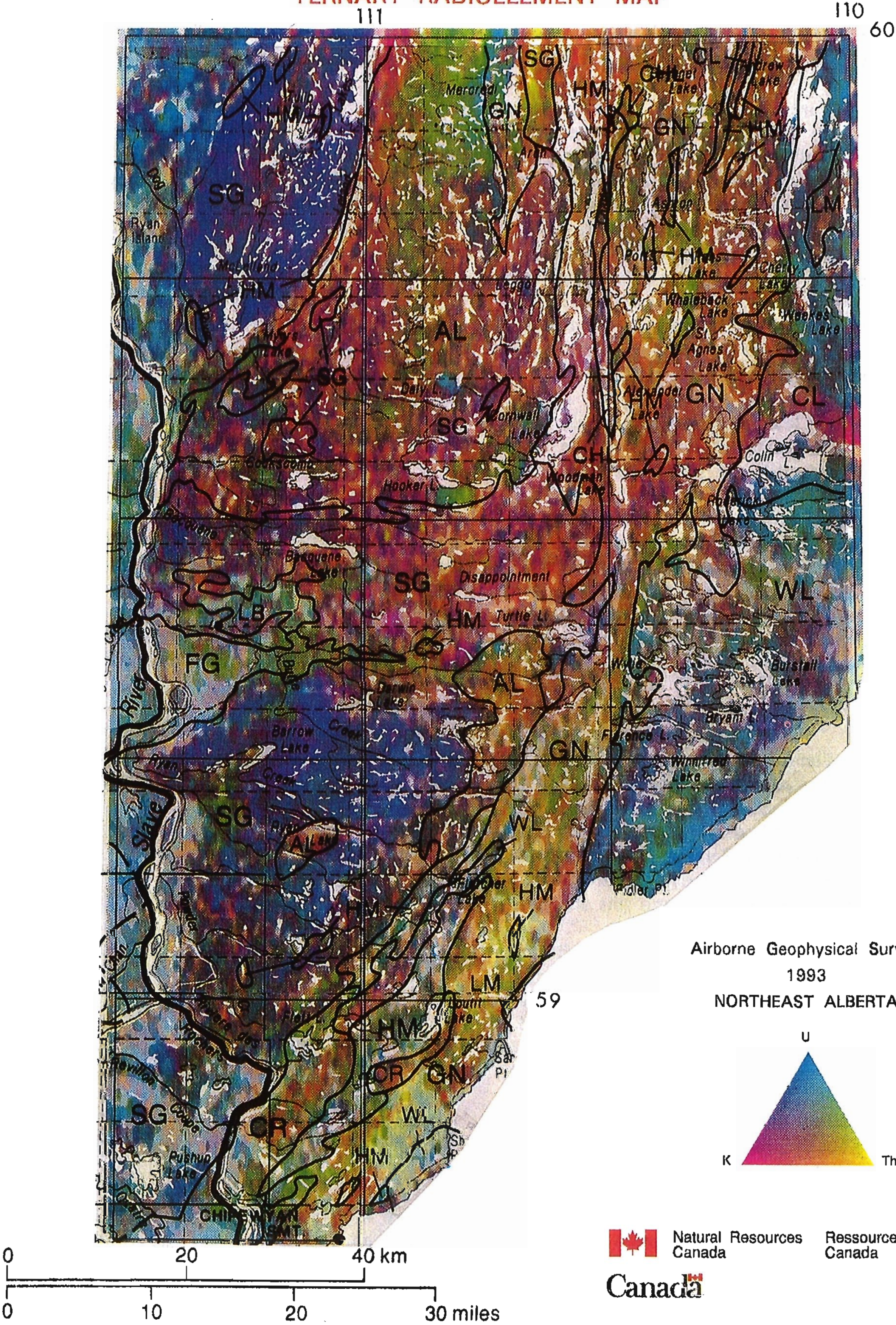

Natural Resources Canada
Ressources naturelles Canada
Canada

1:250 000 scale, as well as two total field VLF maps (one with total field VLF profile data superimposed, and one with quadrature VLF profile data superimposed), and additional maps showing (a) calculated vertical magnetic gradient, (b) total radioactivity, and (c) mineral occurrences on a geological compilation base. This publication also contains a complete set of stacked profiles from which the geophysical maps which cover the survey area were derived.

Briefly, the airborne geophysical data correlates well with the bedrock geology. The ternary radioelement map with geology overlay (Fig. 5) best illustrates the correlation of the radioelement patterns with the overall geology. In the ternary map presentation, potassium, uranium, and thorium are all plotted on the same map (potassium - red, uranium - blue, thorium - yellow), with varying combinations of the three radioelements being depicted by different "hues" of colour. The intensity of the colour on the ternary map is modulated by the total radioactivity. This technique has been described by Broome et al. (1987).

Slave granites (SG) along the western boundary of the survey are clearly demarcated from Arch Lake (AL) and related granitoids. Colin Lake (CL) and Wylie Lake (WL) granitoids in the Rae Province along the eastern margin of the survey are similarly delineated. The Slave, Colin Lake and Wylie Lake granites are relatively high in uranium (bluish on the ternary map; Fig. 5). The area of Slave granite in the central part of the map differs from the masses to the northwest and southwest in that the central body has a low uranium/thorium ratio with moderate potassium.

The gneiss belt (GN) which separates the eastern and western granitoids is also clearly recognized on the ternary map. Internal variations within the major granitoid units are obvious, for example the Arch Lake granite (AL) varies from bluish (uranium-rich) to greenish (more thorium enriched) to reddish (predominantly potassium) going from east to west in the northern part of the Arch Lake granite near the Northwest Territories/Alberta border. The Wylie Lake (WL) granite has a highly uranium-rich phase relative to thorium and potassium near Lake Athabasca. Many other variations are evident on the map (Fig. 5).

__Figure 5.__ Ternary radioelement map of Northeastern Alberta with geology overlay (for geology legend see Fig. 6a).

Airborne geophysical patterns: Slave–Arch Lake granite terrain

The geological mapping capability, which is best exemplified by the ternary radioelement map (Fig. 5), is one application of this type of survey. Applications to mineral exploration for a variety of commodities is equally if not more important. Figures 6 and 7 illustrate, in detail, variations that may indicate geological processes that may relate to mineralization. To illustrate a mineral exploration application, the following discussion focuses mainly on the Slave–Arch Lake granitoid suite which occupies approximately one half of the survey area.

The Slave and Arch Lake granites have been described by McDonough et al. (1993), and the following descriptions are paraphrased from that publication.

Slave granites comprise medium to coarse grained, massive to moderately foliated, quartz monzogranites, monzogranites, and granites that vary in colour from white to pink. Major minerals are potassium feldspar, plagioclase and quartz. The grain size is medium to coarse, often megacrystic. Small clots of mafic minerals are reported to be assemblages of garnet, biotite, hercynite (spinel), and cordierite (Nielsen et al., 1981). Locally, western Slave granites along the western margin of the study area have abundant rafts of pelitic and quartzose paragneisses.

A small pluton of massive to weakly foliated, medium to coarse grained granite, distinguished by feldspar phenocrysts in an equigranular matrix, and termed the "raisin granite" or eastern phase of the Slave granites by Godfrey and Langenberg (1986), outcrops west of Charles Lake (Fig. 3). The pluton contains approximately 30 to 40% equant (1-4 cm) K-feldspar phenocrysts within a fine to medium grained matrix of quartz, feldspar, and biotite. Garnet is abundant where significant quantities of paragneiss xenoliths are present. Eastern Slave granites contain xenolithic rafts of banded basement rocks, paragneisses, and amphibolite, and clearly intrude banded Taltson basement complex gneisses.

A large pluton of variably deformed megacrystic K-feldspar syenogranite to granite called the Arch Lake plutonic suite (Godfrey and Langenberg, 1986) underlies the central part of the area. The Arch Lake granitoids comprise a suite of foliated K-feldspar augen gneiss to weakly foliated K-feldspar megacrystic biotite ± hornblende granite with 30 to 50% lenticular, 1 x 3 cm K-feldspar crystals contained in a matrix of biotite, quartz, feldspar, and garnet.

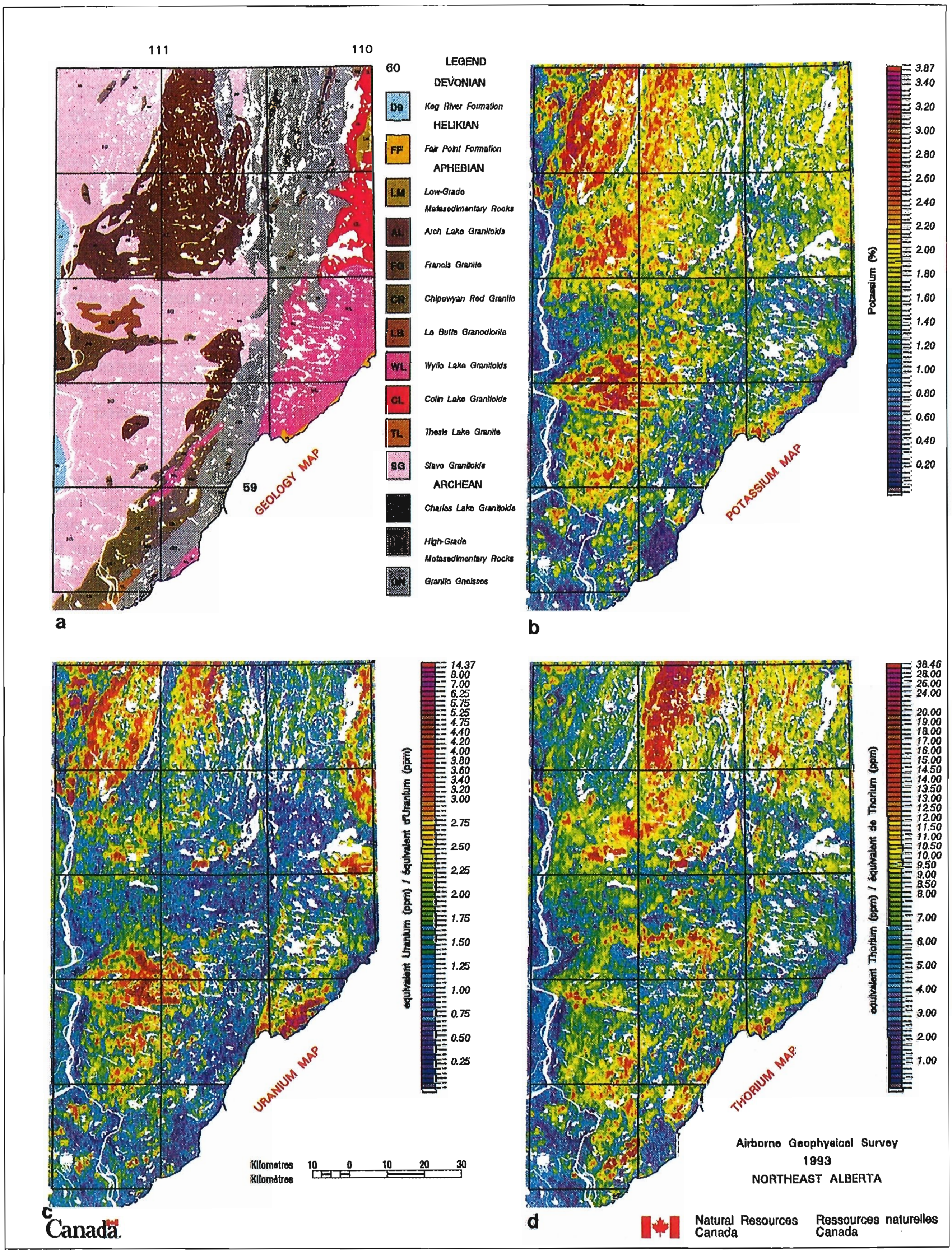

Figure 6. *Maps showing the **a)** geology, **b)** potassium, **c)** uranium, and **d)** thorium of northeastern Alberta.*

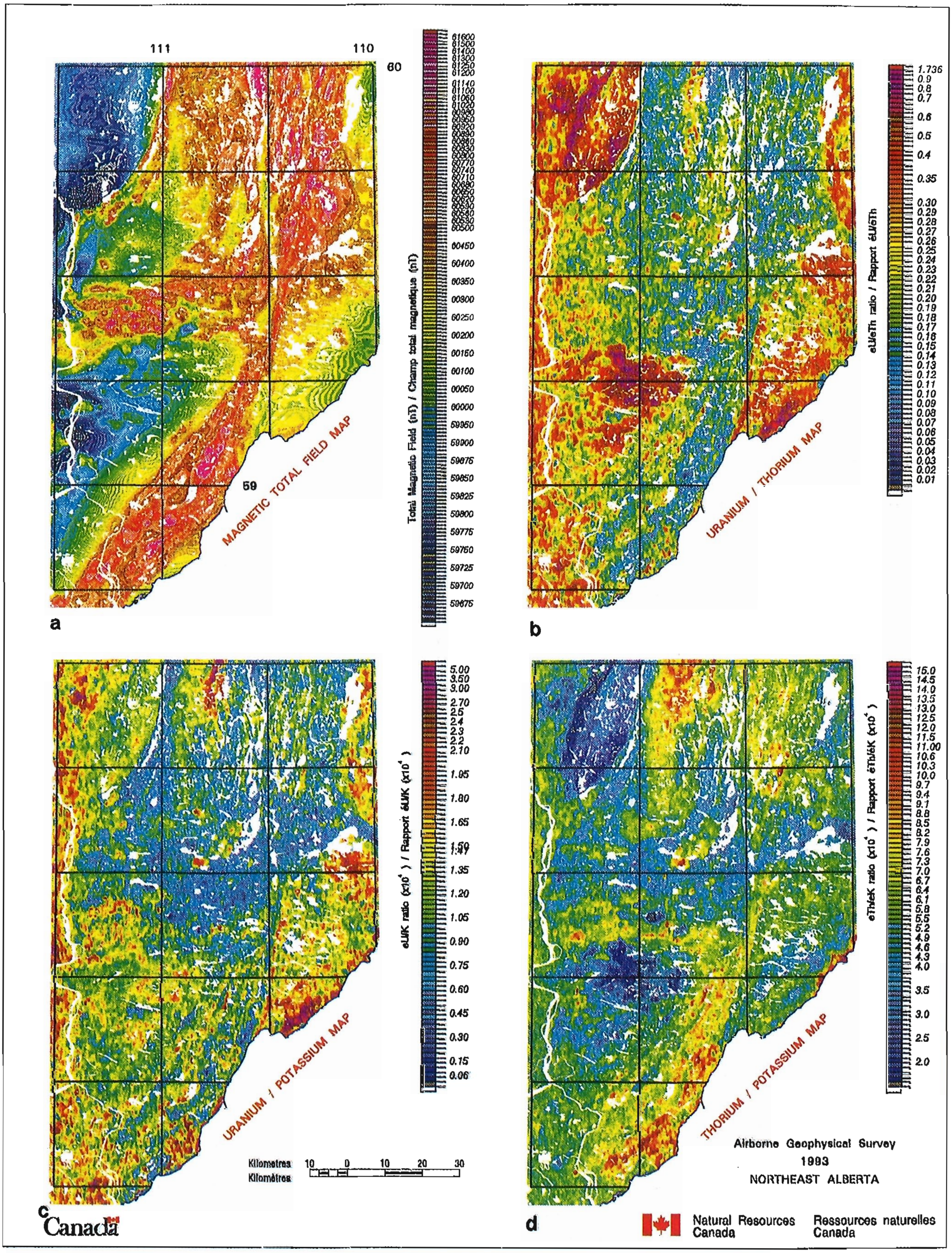

Figure 7. *Maps showing the **a)** magnetic total field, **b)** uranium/thorium ratio, **c)** uranium/potassium ratio, and **d)** thorium/potassium ratio of northeastern Alberta.*

In addition to the mineralogy described above, the Slave and Arch Lake granites contain a wide range of accessory minerals at the trace level that control the radioelement and magnetic geophysical anomaly patterns, these include monazite, zircon uraninite (thorium-rich uraninite-uranothorianite), magnetite, and ilmenite, to be discussed later.

The metamorphic grade of the Slave granites is classified as granulite facies because of the presence of some hypersthene whereas the Arch Lake granite, because of the presence of almanandine-hornblende, is placed in the amphibolite facies. In places the alteration of biotite to chlorite indicates greenschist facies retrograde metamorphorism (Godfrey, 1984).

The following comments relate to the geophysical patterns shown on Figures 6 and 7. Interpretation of regional geophysics, geology and geochemistry by Goff et al. (1986) and Sprenke et al. (1986) were based on earlier geophysical surveys noted above, and on lithogeochemical analyses of a sample set collected by personnel of the Alberta Geological Survey. Interpretations presented here are based on these earlier studies, the 1993 airborne geophysical survey (Charbonneau et al., 1994), additional lithogeochemical analyses of the Alberta Geological Survey sample set as noted above, and analytical data from the 15 anomalies examined in the field in 1994.

There are three main lobes of Slave granite: the northern near Tulip Lake, a central area near Cockscomb Lake, and a southern body near Ryan Lake. The northern and southern lobes are anomalous in potassium and uranium whereas the central area is low in uranium and thorium but has a moderate amount of potassium. The northern and southern lobes of Slave granite have low Th/K ratios and a high U/Th ratio. The northern and southern lobes of Slave granite are low in aeromagnetic signature but the central mass is high.

Geophysical patterns over the Arch Lake granite are quite different than over the Slave granite. The western part of the main Arch Lake granite body is high in potassium with a low magnetic signature. The eastern part of this body is higher in uranium content and has a higher uranium/thorium ratio as noted earlier in the discussion of the ternary map (Fig. 5).

In both the Slave granite and the Arch Lake granite, a number of very sharp, strong anomalies can be seen on the profiles (to be discussed later). These anomalies can also be seen on the contour maps as small anomalies (i.e., near Hooker Lake). The lake sediment geochemical pattern for uranium (Friske et al., 1994) gives a pattern (Fig. 8) which is almost identical to the airborne gamma spectrometry pattern for uranium and illustrates the coherence of the two data sets.

The general relationship between uranium and thorium concentration processes and the various petrochemical types of granitoids has been discussed by Maurice and Charbonneau (1987). In peraluminous granites it is usually observed that uranium increases somewhat with differentiation along with silica, whereas thorium decreases as does CaO, FeO and TiO_2. This tendency has been explained mineralogically — uranium and thorium occur in different mineral phases in these rocks, uraninite and monazite respectively, which have different magmatic control so that uranium and thorium show no positive correlation. The zircon tends to correlate with the monazite. Since monazite and zircon have low saturation in peraluminous magma (Pagel, 1982), the rocks with a high amount of thorium and a low uranium/thorium ratio are usually less evolved (differentiated), and conversely, the granitoids with a higher uranium/thorium ratio are more evolved (differentiated). The monazite and zircon tend to occur with biotite which contains most of the FeO and TiO_2 and with more Ca-rich plagioclase. This theme has been observed in many studies of peraluminous granites in Canada (e.g., Chatterjee and Muecke, 1982; Ford and O'Reilly, 1985; Charbonneau, 1991; Legault and Charbonneau, 1993).

Figure 9 shows the locations of 591 regional reference samples collected by Alberta Geological Survey personnel. In addition, 69 aggregate samples were also collected from metasedimentary bands within Slave, Arch Lake, Wylie Lake, and Colin Lake granites, which were obtained from the Alberta Geological Survey. The following observations of the granites of northeastern Alberta have been noted, based on trace element lithogeochemical analyses of 273 of these samples.

Airborne and ground radioelement concentrations correlate well for the granites, in other words the peak modal values for the Slave, Arch Lake, Wylie Lake and Colin Lake granites (Fig. 10) are all about 5 ppm in uranium. The values tend to be lower on the airborne maps because of the effect of surface conditions (i.e., overburden, witness, vegetation). Thus the peak map values are closer to 3 ppm uranium. This is a well known tendency and results from the fact that overburden, surface wetness, and vegetation will reduce radiometric count rates from bedrock, thereby reducing the absolute concentrations, whereas with ratios, both numerator and denominator are reduced and the values stay much closer to bedrock levels (Charbonneau et al., 1976).

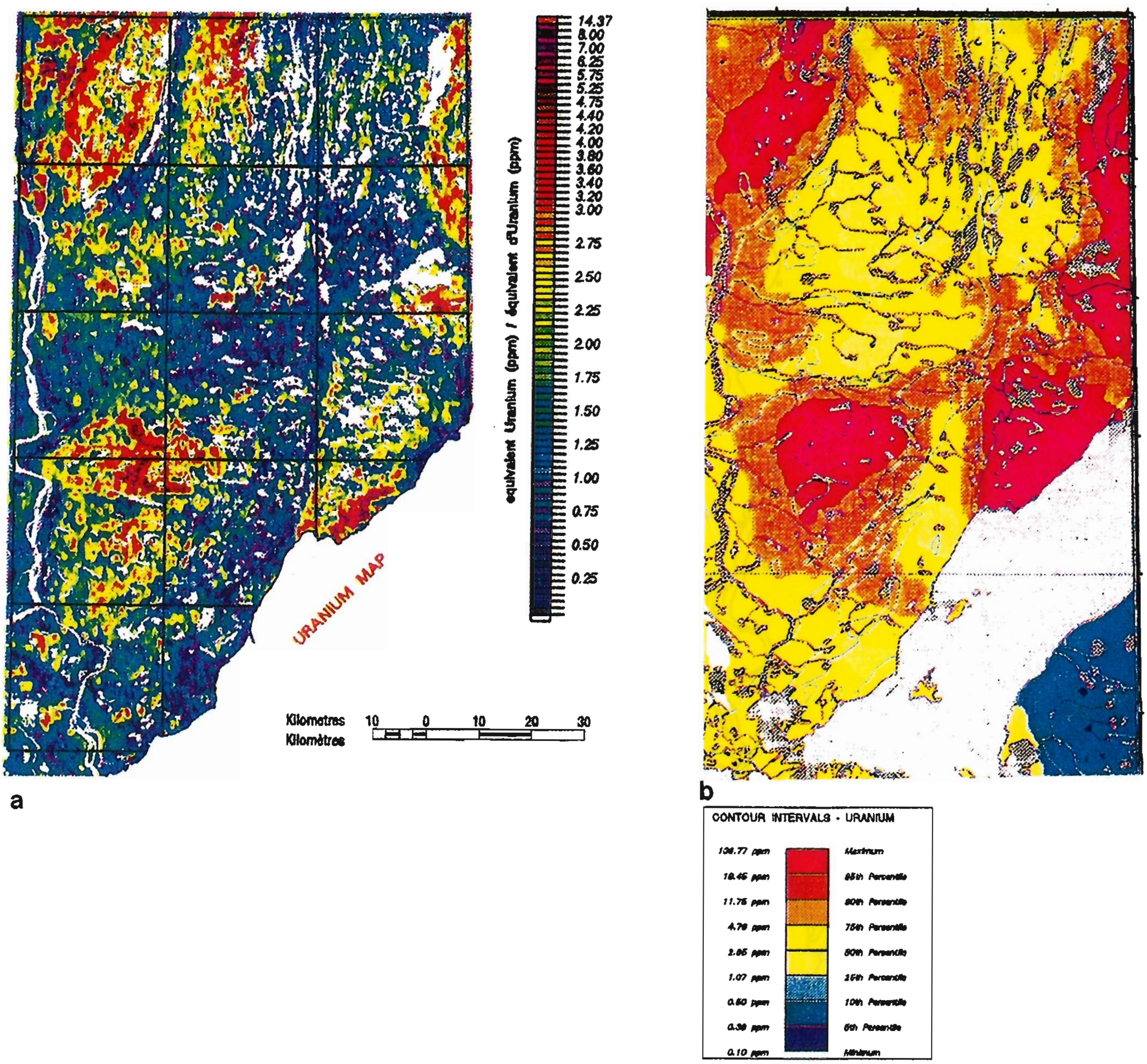

Figure 8. *Comparison of* ***a)*** *airborne gamma spectrometry uranium with* ***b)*** *lake sediment uranium.*

Figure 11 is a plot of Ce+La versus Th, Ce+La versus Zr, and Zr versus TiO_2 for the Slave granite. The Ce+La is contained mainly within monazite and correlates directly with thorium. The Ce+La also correlates with Zr, indicating that zircon is located with the monazite. The plot of Zr versus TiO_2 indicates that the monazite and zircon are located near biotite in these rocks since most of the TiO_2 is in biotite. Rocks showing higher levels of thorium/monazite and zircon are less evolved magmatically; they tend to have higher $FeO+TiO_2+MgO$ and have a lower differentiation index and less SiO_2. A table published by Goff et al. (1986, p. 20) shows major chemistry of Slave and Arch Lake granites at 5% SiO_2 intervals, including Differentiation Index (DI). Zircon is included in their table and is clearly higher in the rocks with lower SiO_2 and higher TiO_2. The Ce+La levels correlate with the higher TiO_2 rocks as already shown above. Similar observations can be made for Arch Lake granite and most of the other granitoids of northeastern Alberta.

The peraluminous granites of northeastern Alberta relate to the "S" type of Chappel and White (1974). Ishihara (1977) classified granites into the magnetite (magnetic) and ilmenite (nonmagnetic) series according

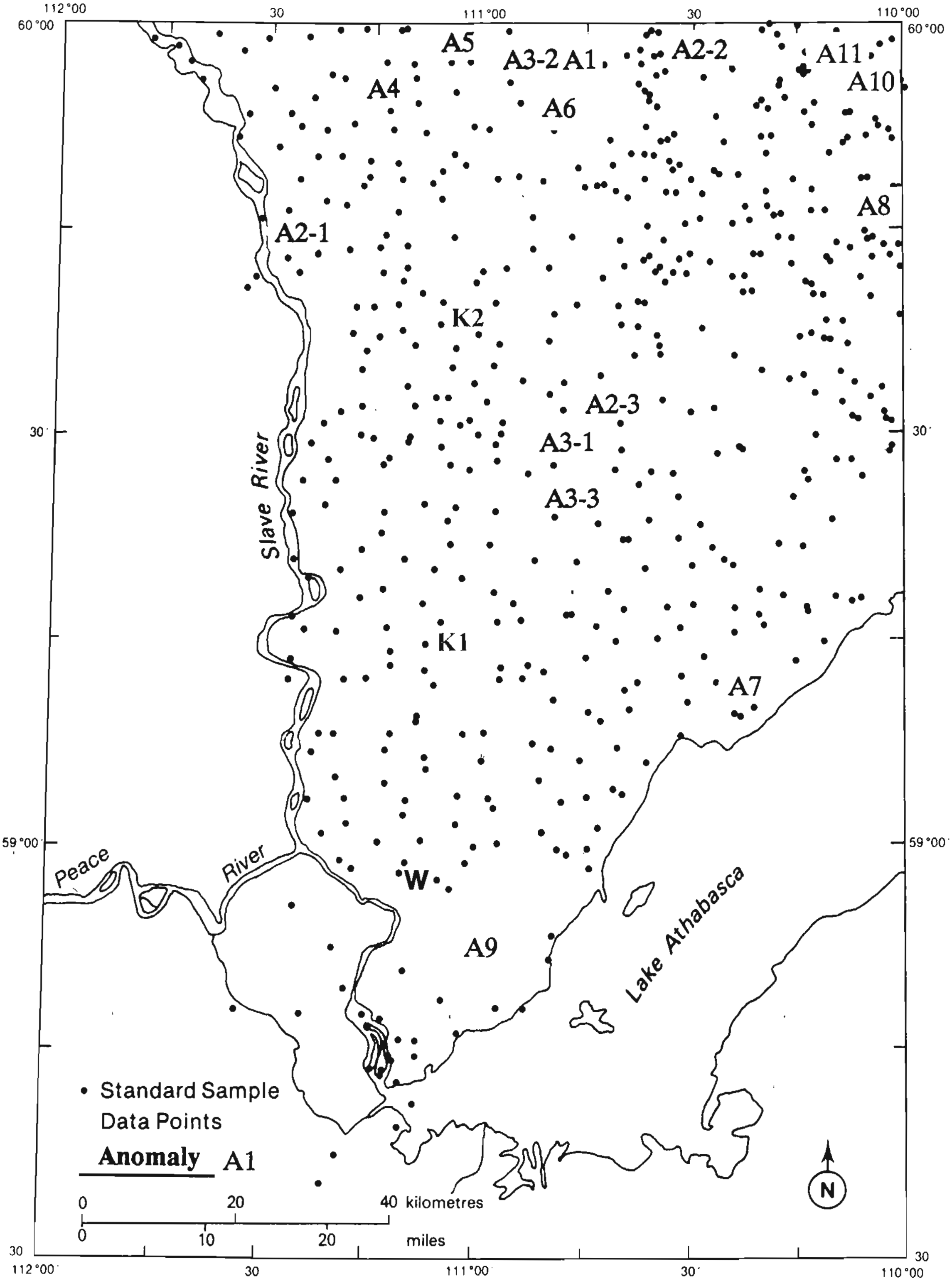

Figure 9. Lithogeochemical sample locations for Alberta Geological Survey samples (unnumbered) and anomaly locations for Geological Survey of Canada ground investigations (A1, etc.).

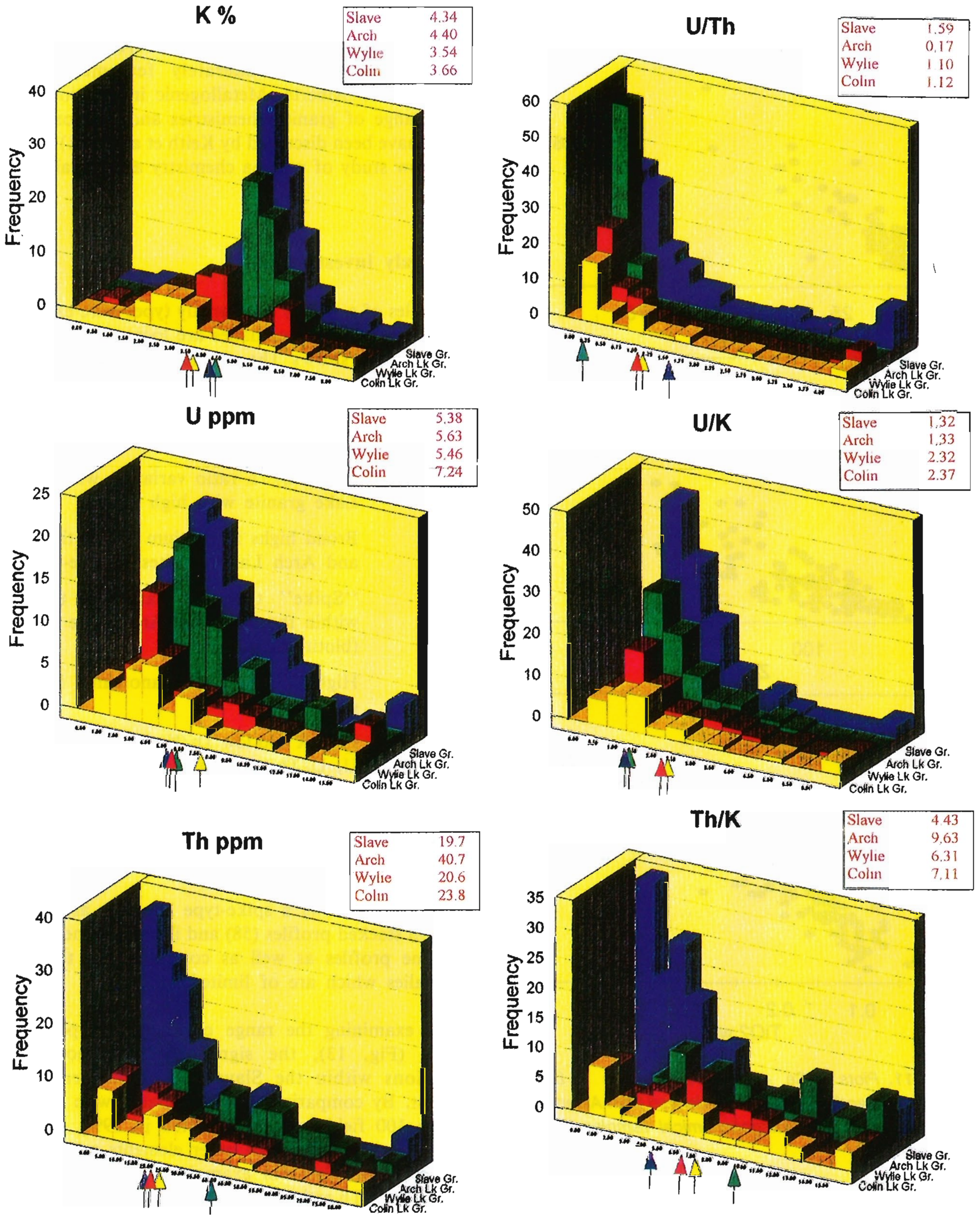

Figure 10. *Histograms of lithogeochemical sample radioelement values for major granitoid units in northeastern Alberta.*

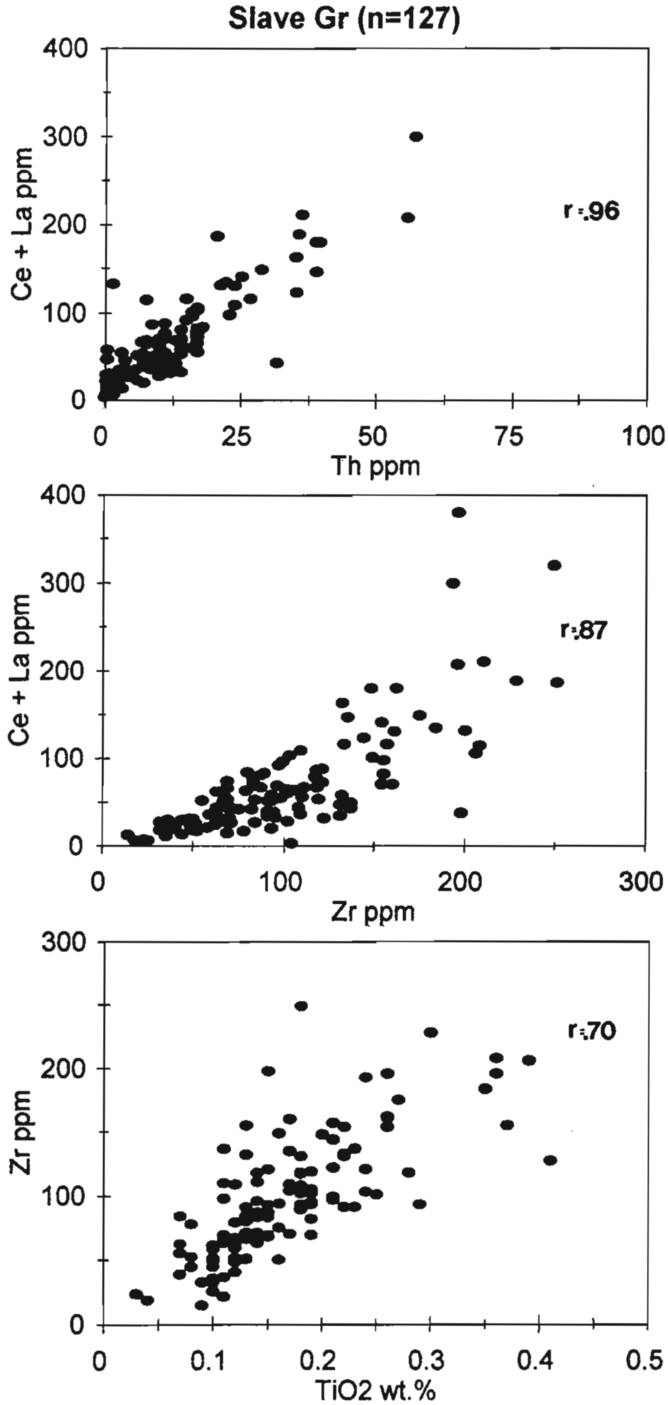

Figure 11. Plots of Ce + La versus Th, Ce + La versus Zr, and Zr versus TiO_2, derived from Alberta Geological Survey lithogeochemical samples.

to their magnetic and/or nonmagnetic character. These series correspond more or less to the "I" (igneous) and "S" (sedimentary) types of Chappel and White (1974). Depending on the conditions of crystallization, peraluminous granites can occasionally be ferromagnetic (i.e., magnetite-bearing), and of course "I" type granites that are very low in iron or have all the iron in silicate minerals such as biotite could be very low in magnetic susceptibility. The Arch Lake and Slave granites are moderately ferromagnetic in northwestern Alberta. Metallogenic implications of a wide range of granite chemistries and iron oxidation states have been discussed by Keith et al. (1991) in their overview study of magma chemistry and metallogeny.

Anomaly investigations

Examples of a variety of anomaly types were examined in the field. These anomalies are located in Figure 9, which also shows the distribution of regional lithogeochemical samples discussed earlier (refer to the geophysical patterns on Figs. 6, 7).

A1	Broad U/Th ratio variation within Arch Lake granite with high U, Th.
A2	Broad highs in thorium within the Slave and Arch Lake granites (biotite-rich).
A3	"Spike" type anomalies in thorium within the Slave and Arch Lake granites (biotite-rich).
A4	High U, U/Th ratio anomalies in Slave granites.
A5	High K and low Th/K with accompanying U, U/Th ratio in Slave granites.
A6	Magnetic highs in Arch Lake granites.
A7 to A11	Anomalies in other rock types described below.

Figure 12 shows a spike-type anomaly at A3-1 as seen on stacked profiles (58) and illustrates the need to examine profiles as well as contour maps to reveal anomalies which are of limited size.

By examining the range of anomaly types listed above (Fig. 13), the significance of geophysical variations within the Slave–Arch Lake granites is evident. By comparing those anomalies with analyses of the 100 field samples collected in 1994, one can determine whether or not other elements might relate to these anomalies. For example, it is often the case that high U/Th ratios in peraluminous granites may be associated with high concentrations of Sn, W.

The character of these anomalies and the mineralogy and radioelement concentrations found at each of the 15 sites are summarized on Figure 13. As

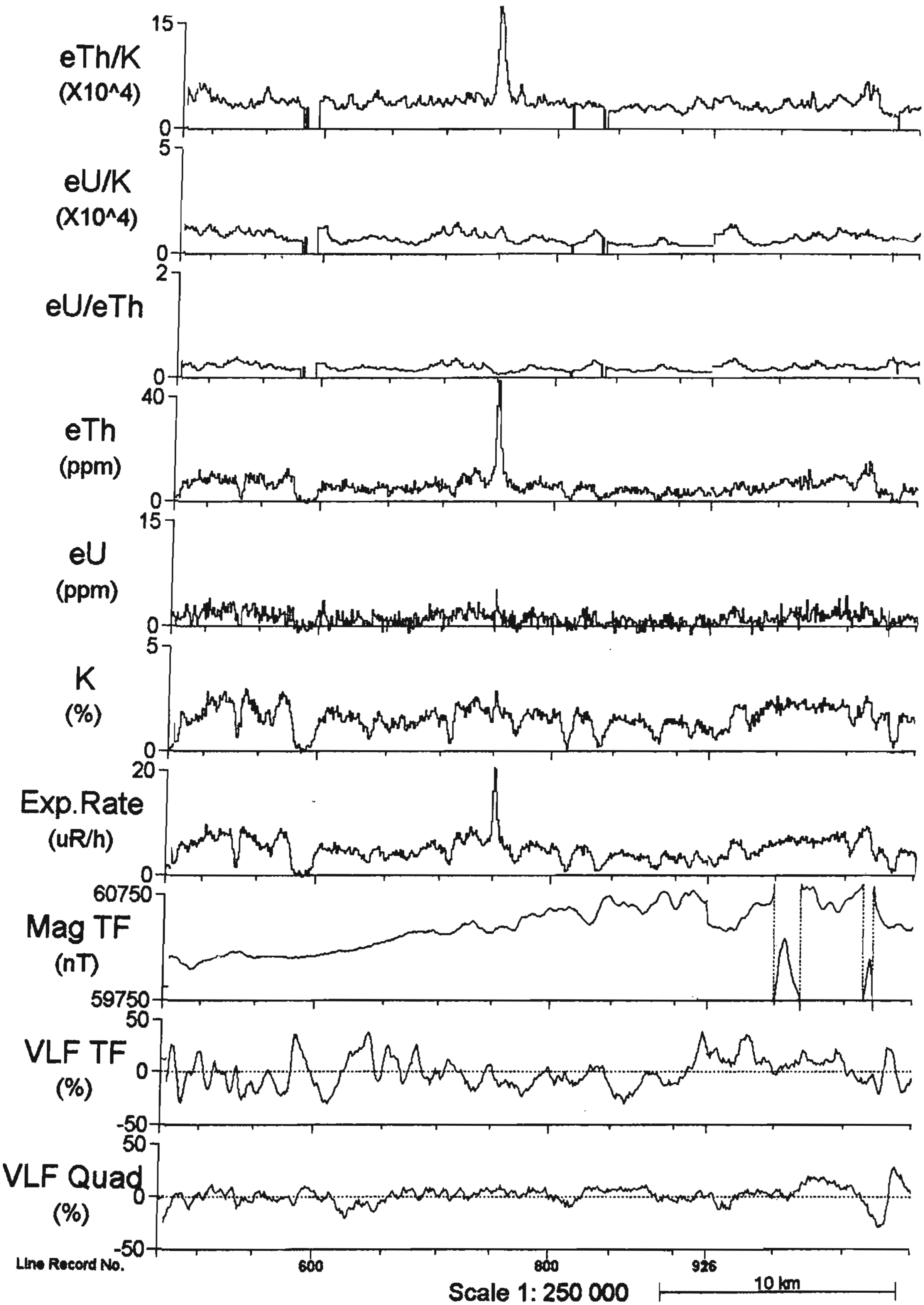

__Figure 12.__ Stacked airborne geophysical profile showing the nature of the stacked profiles and a spike anomaly at A3-3.

Anomaly	Anomaly type	Rock type	Sample no.	Radioelement concentration	Radioactive magnetic mineralogy
A1	U, Th, U/Th	Arch Lake Gr	CZ-11-94	U 19.0, Th 54.2, U/Th 0.35	Monazite, zircon, Th-uraninite, magnetite ilmenite
A2-1	Th	Slave Gr	CZ-55A-94	U 16.0, Th 191.0	Monazite, zircon, magnetite, ilmenite
A2-2	Th	Eastern Slave Gr	CZ-29A-54	U 3.2, Th 132.0	Monazite, zircon, magnetite, ilmenite
A2-3	Th	Arch Lake Gr	CZ-40A-94	U 6.5, Th 284.0	Monazite, zircon, magnetite, ilmenite
A3-1	Th spike	Slave Gr	CZ-38-94	U 7.1, Th 2239.0	Monazite, zircon, magnetite, ilmenite
A3-2	Th spike	Arch Lake Gr	CZ-20-94	U 5.2, Th 353.0	Monazite, zircon, magnetite, ilmenite
A3-3	Th spike	Slave Gr	CZ-4-94	U 4.2, Th 409.0	Monazite, zircon, magnetite, ilmenite
A4	U, U/Th	Slave Gr	CZ-46-94	U 18.0, Th 19.0, U/Th 0.95	Trace monazite, trace zircon, uraninite
A5	K, low Th/K U, U/Th	Slave Gr	CZ-59-94	K 7.1%, U 17.0 m Th 17.0, U/Th 1.0	Trace monazite, zircon
A6	Mag	Arch Lake Gr	CZ-28C-94	U 6.3, Th 170, Mag 10	Monazite, zircon, magnetite, ilmenite
A7	U, U/Th	Wylie Lake Gr	CZ-36-94	U 16.0, Th 23.3, U/Th 0.7	Trace monazite, zircon, Th-uraninite, magnetite, ilmenite
A8	U, U/Th	Colin Lake Gr	CZ-61B-94	U 1320, Th 19.0, U/Th >70	Uraninite
A9	Th	Ft. Chipeywan Belt Gr	CZ-48-94	U 6.1, Th 71.5	Monazite, zircon, magnetite, ilmenite
A10	Mag	Andrew Lake Gr	CZ-63-94 high CZ-64-94 low	mag 30 mag 1	Magnetite, hematite
A11	VLF	Metased	CZ-60E-94	Au 19 ppb	

Figure 13. *Table of results of mineralogy and radioelement geochemistry of 15 anomalies investigated in northeastern Alberta.*

described above, data relating to anomalies in Arch Lake and Slave granites are indicated by A1 to A6, and anomalies in other lithologies (i.e., Wylie Lake granite, Colin Lake granite, Chipeywan granite, granite gneiss, and metasediments) are indicated by A7 to A11. The locations of these anomalies are indicated in Figure 9. Photomicrographs of mineralogy from four of these anomalies are shown on Figure 14 and described in the figure caption. The character and mineralogy of the anomalies at A1 to A6 are clearly in accord with the geochemical variations described previously in this paper.

Uranium and thorium anomalies and possible economic implications

Uranium and thorium characteristics of the granitic lithologies in northeastern Alberta are controlled primarily by the varying amount of monazite in the rocks, which controls the thorium concentration, and by the presence of uraninite, and Th-uraninite, which controls the concentration of uranium. Zircon is usually present and is often associated with monazite in the rocks but has a very low concentration of uranium and thorium.

Various examples of uranium enrichment are shown by the anomalies at A1 to A5. Anomalies at A1, A2, and A3 are of the style described earlier in the paper where higher levels of monazite and zircon, containing higher concentrations of uranium and thorium, correlate with more mafic biotite-rich phases of the granites. Anomalies at A4 and A5 relate to more evolved granite with higher uranium content, lower thorium content, and a high U/Th ratio. Anomalies at A4 and A5 may relate to primary magmatic processes and may be of metasomatic origin.

It is highly unlikely that these granitic styles of uranium mineralization could ever form economic grades under modern market conditions, especially given the styles of uranium mineralization now known to exist (i.e., unconformities etc.).

It has been shown elsewhere that several granophile elements such as Li, Be, F, Rb, Cs, Sn, and W often increase with increasing U, and U/Th ratio and decreasing Th in peraluminous granites (Collins et al., 1981; Chatterjee and Muecke, 1982; Yeates, 1982; Webster, 1984; Ford and O'Reilly, 1985). Unfortunately, the Alberta lithogeochemical samples were not useable for W or Sn because of con-

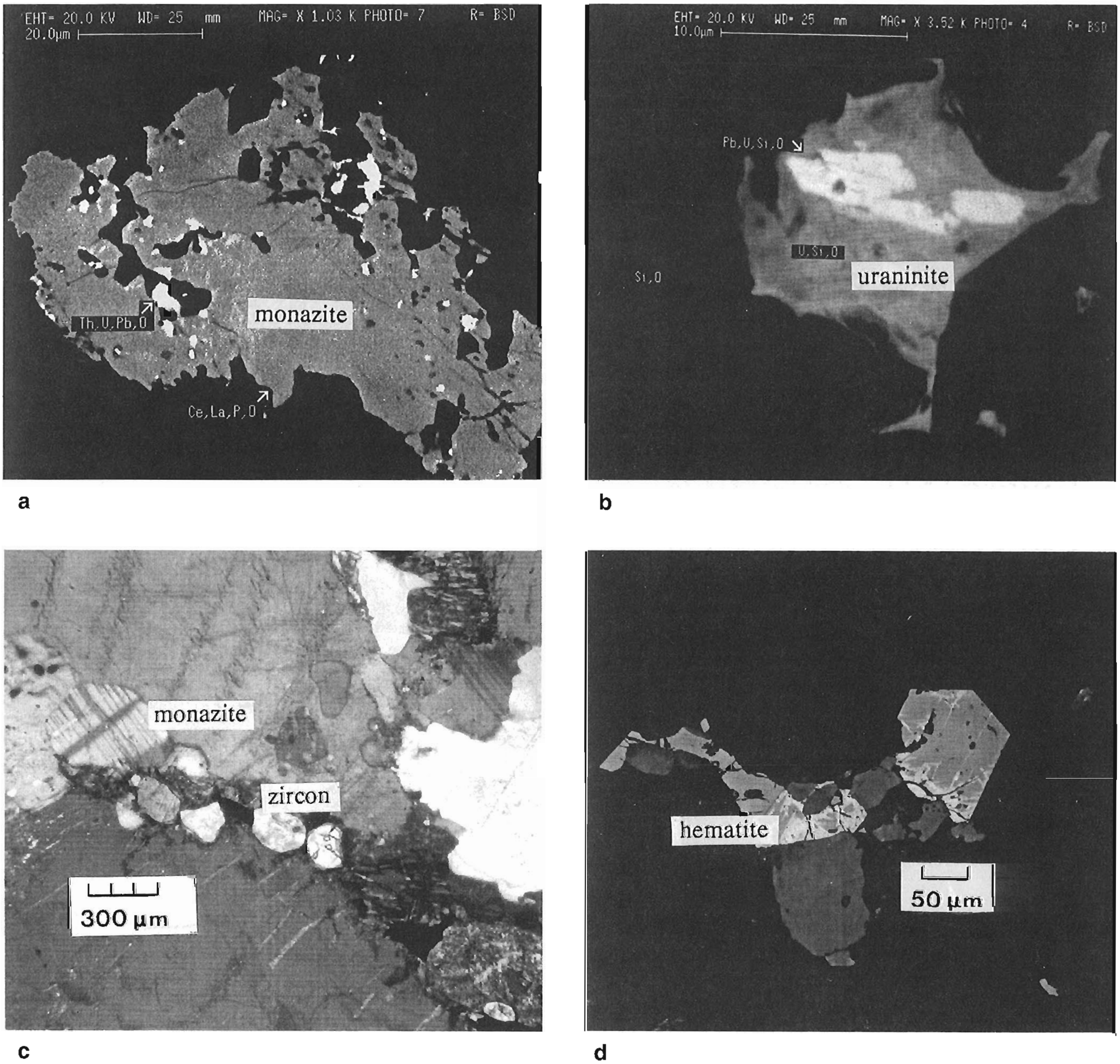

Figure 14. *Scanning electron microprobe **(a, b)** and transmitted light microscopy **(c, d)** of rock samples from four anomalies from northeastern Alberta: **a)** monazite with areas of uranothorianite in Arch Lake granite A; **b)** uraninite in Slave granite anomaly A4; **c)** monazite and zircon in the spike anomaly at A3-3 in Slave granite; and **d)** magnetite altering to hematite in granite gneiss west of Andrew Lake.*

tamination in the crushing process; thus possible correlations of these elements with U and Th were not assessable from that data set.

Of the 100 field samples collected during this study, only two samples were enriched in tungsten, one to 17 ppm (a granite at A5) and the other to 39 ppm (a metasediment near Flett Lake located (W) on Fig. 3). Granites at both these localities have a high uranium/thorium ratio. Tungsten occurrences have been noted in association with a high U/Th ratio in Arch Lake (Konth) granites to the north (Bostock and Thompson, 1983). Tin analyses were made on the 100 field samples taken during this study but showed no obvious increase relating to the anomalies studied. Tin analyses on 25 samples of Konth (Arch Lake) and Slave granites from the Fort Smith area to the north averaged only 4 ppm with a maximum value of 15 ppm

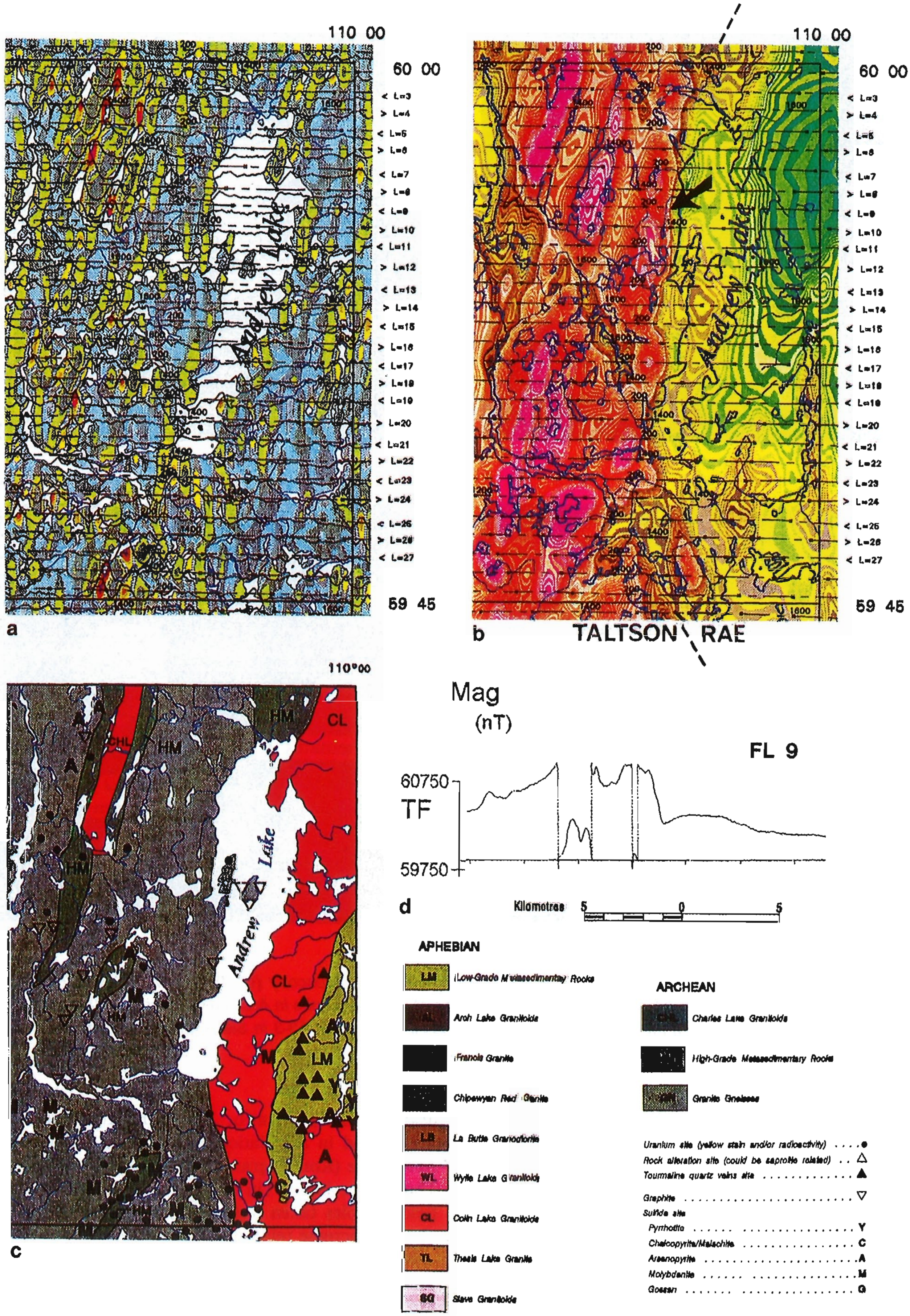
110 00
60 00
59 45
a
b
TALTSON
RAE
Andrew Lake
110°00
c
Mag
(nT)
FL 9
60750
TF
59750
d
Kilometres
5
0
5
APHEBIAN
LM
Low-Grade Metasedimentary Rocks
Arch Lake Granitoids
Francis Granite
Chipewyan Red Granite
LB
La Butte Granodiorite
WL
Wylie Lake Granitoids
CL
Colin Lake Granitoids
TL
Thesis Lake Granite
SG
Slave Granitoids
ARCHEAN
Charles Lake Granitoids
High-Grade Metasedimentary Rocks
Granite Gneisses
Uranium site (yellow stain and/or radioactivity)
Rock alteration site (could be saprolite related)
Tourmaline quartz veins site
Graphite
Sulfide site
Pyrrhotite
Y
Chalcopyrite/Malachite
C
Arsenopyrite
A
Molybdenite
M
Gossan
G

(Charbonneau, 1991). The average levels are close to crustal average in granites. The lake sediment geochemical patterns (Friske et al., 1994) show no obvious tungsten or other element anomalies correlatable with the radioelement patterns on the airborne gamma spectrometric maps aside from the possible correlation of increased F with portions of the Slave granite which have high K, U, and U/Th ratios. This could be a magmatic or metasomatic phenomenon. Nevertheless, high U/Th ratio granites remain of exploration interest in the area and deserve further exploration.

Potassium anomalies

While the foregoing discussion has focused on uranium and thorium variations, prominent anomalies in potassium are also of interest in the area (Fig. 6). The most prominent areas of elevated potassium levels occur in the extreme northwest portion of the survey area near Tulip Lake, in the west-central part near Cockscomb Lake, and in the southwestern part near Ryan Lake (see Fig. 3 for locations).

The areas of high potassium near Tulip Lake, A5, and Ryan Lake, K_1 (>3% K airborne) are marked by low Th/K ratios (<2.5 x 10^{-4}), whereas the high potassium area near Cockscomb Lake, K_2 (>3% K airborne) has an average Th/K ratio of about 4 x 10^{-4}. As discussed earlier, ratios are especially valuable in studying radioelement patterns on airborne surveys because ratios are not much affected by surface conditions (Charbonneau et al., 1976), and in addition, while radioelement values (K, U, Th) can range quite widely in various lithologies, ratios tend to be quite fixed (Galbraith and Saunders, 1983).

The area of high K with "normal" crustal Th/K ratio (i.e., Cockscomb Lake) is due to a simple increase in K, U and Th in the Arch Lake granite. The other two areas of high potassium (i.e., Tulip Lake and Ryan Lake) are quite different. These latter two situations have unusual ratios, especially low Th/K and high U/Th, suggesting unusual processes have operated in these rocks. These latter two anomalies are in Slave granite.

*Figure 15. Maps showing **a)** VLF, **b)** aeromagnetics, **c)** geology, and **d)** aeromagnetic profile around gold occurrences. In b, the arrow shows an aeromagnetic break west of Andrew Lake. In c, A indicates arsenopyrite at Pythagoras Lake west of Andrew Lake.*

The correlation of high K in granitoid rocks with low Th/K (especially in peraluminous granites) can indicate a high degree of magmatic evolution with attendant thorium depletion, or a situation of potassium addition (alteration) without attendant thorium addition. Thorium is relatively immobile during potassium alteration. Many examples of the radiometric signal relating to potassium alteration are presented in Shives et al. (1995) and Hoover and Pierce (1990). The correlation of high F with the two anomalous areas in Slave granite could have a primary magmatic explanation or it could relate to a metasomatic phenomenon.

Potassium alteration is a feature of many deposits of metals including Au, Ag porphyry systems involving Au, Cu, and Mo; and volcanogenic massive sulphide (VMS) systems including Cu, Pb, Zn etc. (Hoover and Pierce, 1990; Shives et al., 1995). Following from the above discussion, it is usually possible to separate out areas of possible potassium alteration (high potassium, low Th/K ratio) from areas of primarily high potassium (high potassium, crustal average Th/K). This rationale was used in selecting the areas of potassium alteration (enrichment) in northeastern Alberta. Field examination took place in the northerly anomaly west of Tulip Lake (see anomaly 5, Fig. 9).

The Slave granite in the core of the northern potassium anomaly at A5 (Fig. 9) averages about 7.1% (8.5% K_2O), although some measurements in the projection of this anomaly in the area to the north in the Northwest Territories are greater than 10% K_2O (Charbonneau, 1980). The rock at A5 is composed of potassium feldspar, plagioclase, quartz, biotite, and muscovite (sericite). Much of the feldspar is altered. However, no increase in elements of potential economic interest (aside from one tungsten value of 17 ppm) has been noted in the geochemical analysis of samples from this area in both the 100 rock samples taken in this study and the Alberta Geological Survey lithogeochemistry. In addition, the lake sediment geochemistry in the vicinity of the potassium anomalies does not reveal any anomalies in metals of interest (i.e., Au, Ag, Cu, Mo, etc.) (Friske et al., 1994).

Although these two major potassium anomalies near Tulip Lake and near Ryan Lake are not known to relate to mineralization, they should remain of exploration interest as they are high in K and low in Th/K, similar to anomalies that do relate to economic mineralization (Shives et al., 1995). The correlation of increased F with these features is of interest. One difference in these anomalies, when compared to the majority of potassium anomalies in the above references that do relate to mineralization, is the increase in U which correlates with the increase in K (see Goff et al., 1986). This suggests that these anomalies are different in temperature of formation when compared with potassium alteration of economic significance. Accordingly, these anomalies may be more of a broad scale magmatic-metasomatic type that may be barren of mineralization. Nevertheless, these potassium anomalies may warrant further investigation.

Anomalies in other lithologies

A brief summary of some anomalies examined that are in lithologies other than Slave Lake or Arch Lake granite can be seen on Figure 13 (A7, A8, A9). A7 is marked by a high U, U/Th ratio in Wylie Lake granite near Lake Athabasca. The Cherry Lake "U" occurrence in Colin Lake granite is located at A8, and the Fort Chipeywan red granite belt which is anomalous in thorium is located at A9. The mineralogy is consistent with the geological signature as the anomaly at A7 contains monazite, zircon, uraninite-uranothorianite, magnetite, and ilmenite, the anomaly at A8 is uraninite rich, and the rocks underlying the anomaly at A9 contain monazite, zircon and magnetite.

High molybdenum values on the lake sediment geochemical maps (Friske et al., 1994), in the northeastern part of the area near Andrew Lake, are not obviously correlated with geophysical anomalies, although in places (i.e., near Cherry Lake) high U/Th ratios appear to correlate to molybdenum in uraniferous phases of the Colin Lake granite. This correlation was noted by Bennett (1971) based on an older geophysical survey by industry in the area.

A prominent discontinuity is seen in the aeromagnetic pattern at A10 (Figs. 9, 15). The magnetic break at A10, shown on the magnetic map in Figures 6 and 15, is an interesting feature on the ground. This break which is just west of the western shore of Andrew Lake is shown on the ground by a reddened zone which marks the contact between magnetite bearing rocks and oxidized hematized rocks to the east. Within the granite gneiss, a photomicrograph in Figure 14d shows the nature of the alteration (hematization of magnetite). This contact is near the Rae Province–Taltson magmatic zone boundary of McDonough et al. (1993), which is postulated to be located to the east under Andrew Lake. The contact is structurally a west-dipping thrust as indicated by McDonough et al. (1993). The magnetic profile flight line 9 from the airborne survey is also shown on Figure 15. This profile shows the advantage of the detailed digital geophysical traces now available. This anomaly is consistent with the west-dipping thrust interpretation of McDonough et al. (1993). The exact position of the contact between these two provinces can now be postulated to extend to the south based on the aeromagnetic map. This contact is indicated on Figure 15.

The VLF total field and quadrature data show many anomalies that correlate well with the known fault systems in the area. In many places these are accentuated because the fault zones are occupied by conductive material occupying drainage systems. Many anomalies may relate to conductive sulphide mineralization (Fig. 9). Figure 15 shows such an anomaly pattern in the Pythagoras Lake area where metasedimentary rocks are enriched in gold (A). Control over the sulphide mineralization in this area and in northeastern Alberta in general has been discussed by McDonough (1996). Many other anomalies of potential interest are found on the VLF maps.

CONCLUSIONS

The detailed airborne geophysical survey in northeastern Alberta shows patterns which provide significant information relating to the geology and mineral potential of the area. Because the survey was acquired digitally, it is an ideal format for interpretation and integration with other data sets (e.g., lake sediment geochemistry).

The thorium and U/Th ratio map patterns are controlled by monazite (thorium) with accompanying zircon and uraninite/uranothorianite (uranium) which correlates with magmatic processes. Areas of high potassium (with accompanying low Th/K ratio) relate to magmatically evolved granites and/or alteration. In northeastern Alberta, these areas are also high in uranium. Magnetitic patterns relate to presence or absence of magnetite (ilmenite) and in places hematization. VLF patterns correlate with fractures and high-grade metasedimentary bands, and in places may indicate sulphide-rich conductors.

All of the above processes potentially can be linked to a wide range of mineralization, but at present, such a linkage (except for the VLF anomalies over certain metasedimentary bands such as in Fig. 15) has not been recognized in northeastern Alberta, although further investigation of the processes suggested in this paper may eventually lead to such recognition.

Acknowledgments

The authors would like to thank the personnel of Loon Air, Fort Smith, Northwest Territories, and Chris Kozuskanich for their assistance in the field. The paper was critically reviewed by K.L. Ford and R.W. Macqueen of the Geological Survey of Canada.

REFERENCES

Bednarski, J.M.
1993: Geochemistry of surficial deposits in northeastern Alberta. Geological Survey of Canada, Open File 2747.

1997: (*this volume*) Quarternary geology along the shield margin, northeastern Alberta. *In* Exploring for Minerals in Alberta: Geological Survey of Canada Geoscience Contributions, Canada-Alberta Agreement on Mineral Development (1992-1995), R.W. Macqueen (ed.). Geological Survey of Canada, Bulletin 500, p. 81–105.

Bednarski, J.M., Charbonneau, B.W., Chung, C.-J.F., Friske, P.W., McDonough, M.R., and Rencz, A.N.
1993: Northeastern Alberta MDA project, an Integrated GSC study: Highlights of proposed work for 1993-94. Canadian Institute of Mining Bulletin, v. 86, no. 968, p. 69.

Bennett, R.
1971: Exploration for hydrothermal mineralization with airborne gamma-ray spectrometry. *In* Canadian Institute of Mining, Special Volume 11, p. 475–478.

Bostock, H.H. and Loveridge, W.D.
1988: Geochronology of the Taltson Magmatic Zone. *In* Radiogenic Age and Isotopic Studies: Report 2. Geological Survey of Canada, Paper 88-2, p. 59–65.

Bostock, H.H. and Thompson, D.L.
1983: Fluorescent minerals from the Fort Smith area, District of Mackenzie. *In* Current Research, Part B. Geological Survey of Canada, Paper 83-1B, p. 401–402.

Broome, J., Carson, J.M., Grant, J.A., and Ford, K.L.
1987: A modified ternary radioelement mapping technique and its application to the south coast of Newfoundland. Geological Survey of Canada, Paper 87-14.

Chappell, B.W. and White, A.J.R.
1974: Two contrasting granitic types. Pacific Geology, v. 8, p. 173–174.

Charbonneau, B.W.
1980: The Fort Smith radioactive belt, Northwest Territories. *In* Current Research, Part C. Geological Survey of Canada, Paper 80-1C, p. 45–57.

1991: Geophysical signature, geochemical evolution and radioactive mineralogy of the Forth Smith radioactive belt, Northwest Territories, Canada. *In* Primary Radioactive Minerals (The textural patterns of radioactive mineral paragenetic associations). Theophrastus Publications, Athens, Greece, p. 21–48.

Charbonneau, B.W. and Harris, D.C.
1993: Cu-Ni-Mo-PGE-Au rich mafic inclusions in the Forth Smith (Konth) granite Northwest Territories. *In* Current Research, Part C. Geological Survey of Canada, Paper 93-1C, p. 53–59.

Charbonneau, B.W., Holman, P.B., and Hetu, R.J.
1994: Airborne geophysical survey of northeastern Alberta NTS 74L/14, 15, 74M/11-3, 6-11, 14-16. Geological Survey of Canada, Open File 2807.

Charbonneau, B.W., Killeen, P.G., Carson, J.M., Cameron, G.W., and Richardson, K.A.
1976: The significance of radioelement concentration measurements made by airborne gamma-ray spectrometry over the Canadian Shield. *In* Proceedings of the International Symposium on Exploration for Uranium Deposits, Proceedings Series, International Atomic Energy Agency, Vienna, p. 35–54.

Chatterjee, A.K. and Muecke, G.K.
1982: Geochemistry and the distribution of uranium and thorium in the granitoid rocks of the Southern Mountain Batholith, Nova Scotia: some genetic and exploration implications. *In* uranium in granites, Y.T. Maurice (ed.). Geological Survey of Canada, Paper 81-23, p. 11–17.

Collins, P.L.F., Wyatt, B.W., and Yeates, A.N.
1981: A gamma-ray spectrometer and magnetic susceptibility survey of Tasmanian granitoids. Tasmanian Department of Mines Report 1981/41.

Darnley, A.G., Richardson, K.A., Grasty, R.L., Carson, J.M., Holman, P.B., and Charbonneau, B.W.
1986: Radioactivity Map of Canada. Geological Survey of Canada, Map 1600A, 1st edition, 1:5 000 000.

Department of Energy, Mines and Resources Canada
1980: Gravity map of Canada. Department of Energy, Mines and Resources, Earth Physics Branch, Gravity Map Series, map 80-1, scale 1:5 000 000.

Edwards, W.A.D., Richardson, R.J.H., and Fildes, B.J.
1991: Geology and metallic mineral potential of northeastern Alberta. Geological Survey of Alberta, Alberta Research Council, Open File 1991-6.

Ford, K.L. and O'Reilly, G.A.
1985: Airborne gamma ray spectrometric surveys as an indicator of granophile element specialization and associated mineral deposits in the granitic rocks of the Meguma Zone of Nova Scotia, Canada. *In* High Heat Production (HHP) Granites, Hydrothermal Circulation and Ore Genesis. The Institute of Mining and Metallurgy, London, England, p. 113–133.

Friske, P.W.B., McCurdy, M.W., Day, S.J., Gross, H., Balma, R.G., Lynch, J.J., and Durham, C.C.
1994: Regional lake sediment and water geochemical reconnaissance data, northeastern Alberta (parts of 74E, L, M). Geological Survey of Canada, Open File 2856.

Galbraith, J.H. and Saunders, D.F.
1983: Rock classification by characteristics of aerial gamma-ray spectrometry. Journal of Geochemical Exploration, v. 18, p. 49–73.

Geological Survey of Canada
1964a: Aeromagnetic map no. 7161G, Fitzgerald area, NTS 14M, scale 1:250 000.

1964b: Aeromagnetic map no. 7159G, Fort Chipewyan, NTS 74L, scale 1:250 000.

1977a: Fitzgerald 74M airborne gamma-ray spectrometric map no. 36374G, scale 1:250 000.

1977b: Fort Chipewyan 74L, airborne gamma-ray spectrometric map no. 336274G, scale 1:250 000.

Godfrey, J.D.
1984: Geology of the Ryan-Fletcher lakes district, Alberta. Alberta Research Council, Earth Sciences Report 84-2, 28 p.

1986a: Geology of the Precambrian Shield in northeastern Alberta, NTS 74M and NTS 74L. Alberta Research Council, Map EM-180.

1986b: Mineral showings of the Precambrian Shield in Northeastern Alberta, NTS 74L and NTS 74M. Alberta Research Council, Map EM-182.

Godfrey, J.D. and Langenberg, C.W.
1986: Geology of the Fitzgerald, Tulip-Mercedes-Charles lake district, Alberta. Alberta Research Council, Earth Sciences Report 84-7, 32 p.

Goff, S.P., Godfrey, J.D., and Holland, J.G.
1986: Petrology and geochemistry of the Canadian Shield of northeastern Alberta. Alberta Research Council, Bulletin 511, 60 p.

Grant, J.A.
1993: SurView - a Microsoft Windows 3.1 application to view geophysical survey data [line, grid, contour and stacked profiles]. Geological Survey of Canada, Open File 2661.

Hoffman, P. and Hall, L.
1993: Geology, Slave craton and environs, District of Mackenzie, Northwest Territories. Geological Survey of Canada, Open File 2559, scale 1:1 000 000.

Hoover, D.B. and Pierce, H.A.
1990: Annotated bibliography of gamma-ray methods applied to gold exploration. U.S. Geological Survey, Open File 90-203.

Ishihara, S.
1977: The magnetite series and ilmenite series granitic rocks. Mining Geology, v. 27, p. 293-305.

Keith, S.B., Laux, D.P., Maughan, G., Schwab, K., Ruff, S., Swan, M.M., Abbott, E., and Friberg, S.
1991: Magma series and metallogeny: a case study from Nevada and environs. Field Trip Number 8 Guidebook Compendium, Great Basin symposium on Geology and Ore Deposits of the Great Basin, Reno, Nevada, April 1-5, 1990, co-sponsored by the U.S. Geological Survey and the Geological Survey of Nevada.

Langenberg, W., Solat, H., Turner, A., and Eccles, R.
1993: Evaluation of the economic mineral potential in the Andrew Lake-Charles Lake area of northeast Alberta. Alberta Research Council, Open File 1993-08.

Legault, M.I. and Charbonneau, B.W.
1993: Geophysical, geochemical and petrological study of Contwoyto Batholith, Lupin Gold Mine area, Northwest Territories. *In* Current Research Part E. Geological Survey of Canada, Paper 93-1E, p. 207-218.

McDonough, M.R. (*this volume*)
1997: Structural controls and age constraints on sulphide mineralization, southern Taltson magmatic zone, northeastern Alberta. *In* Exploring for Minerals in Alberta: Geological Survey of Canada Geoscience Contributions, Canada-Alberta Agreement on Mineral Development (1992-1995), R.W. Macqueen (ed.). Geological Survey of Canada, Bulletin 500, p. 13-29.

McDonough, M.R., Grover, T.W., McNicoll, V.J., and Lindsay, D.D.
1993: Preliminary report of the geology of the southern Taltson magmatic zone, northeastern Alberta. *In* Current Research, Part C. Geological Survey of Canada, Paper 93-1C, p. 221-232.

McDonough, M.R., McNicoll, V.J., and Schetselaar, E.M.
1995: Age and kinematics of crustal shortening and escape in a two-sided oblique-slip collisional and magmatic orogen, Paleoproterozoic Taltson magmatic zone, northeastern Alberta. *In* Alberta Basement Transects Workshop, Lithoprobe Report #47, G.M. Ross (ed.). Lithoprobe Secretariat, University of British Columbia, p. 264-308.

Maurice, Y.T. and Charbonneau, B.W.
1987: U and Th concentration processes in Canadian granitoids, their detection by airborne gamma ray spectrometry and their relationship to granophile mineralization. *In* Revista Brasileira de Geociências, v. 17, no. 4, p. 644-646.

Morley, L.W., MacLaren, A.S., and Charbonneau, B.W.
1968: Magnetic anomaly map of Canada, 1st edition, scale 1:5 000 000. Geological Survey of Canada, map 1255A.

Nielsen, P.A., Langenberg, C.W., Baadsgaard, H., and Godfrey, J.D.
1981: Precambrian metamorphic conditions and crustal evolution, Northeastern Alberta, Canada. *In* Precambrian Research, v. 16, p. 171-193.

Olson, R.A., Dufresne, M.B., Freeman, M.E., Richardson, R.J.H., and Eccles, R.
1994: Regional metallogenic evaluation of Alberta. Alberta Research Council, Open File 1994-08.

Pagel, M.
1982: The mineralogy and geochemistry of uranium, thorium, and rare-earth elements in two radioactive granites of the Vosges, France. *In* Mineralogical Magazine, v. 46, no. 339, p. 149-161.

Shives, R.B.K., Ford, K.L., and Charbonneau, B.W.
1995: Applications of gamma ray spectrometric-magnetic-VLF-EM surveys. Geological Survey of Canada, Open File 3061.

Sprenke, K.F., Wavra, C.S., and Godfrey, J.D.
1986: Geophysical expression of the Canadian Shield of northeastern Alberta. Alberta Research Council, Bulletin 52, 54 p.

Walcott, R.I. and Boyd, J.B.
1971: The gravity field of northern Alberta, and part of Northwest Territories and Saskatchewan. Department of Energy, Mines and Resources, Earth Physics Branch, Gravity Map Series, maps 103-111.

Webster, S.S.
1984: Comments on the use of gamma-ray spectrometry for tin prospecting. *In* Exploration Geophysics 1984(15), p. 611-63.

Yeates, A.N.
1982: Radioelement characteristics of tin and tungsten granitoids in the New England Batholith and other granitoid provinces of southeast Australia. *In* New England Geology: Proceedings of a Symposium on the Geology of the New England region held in Armidale in July 1982 in honour of Emeritis Professor Aa.H. Voisayj, P.G. Floral and B. Runnegar (eds.). Department of Geology, University of New England, Avondale, N.S.W., p. 301-311.

INTERPRETATION OF GEOCHEMICAL DATA FROM LAKE SEDIMENTS AND WATERS OVER PRECAMBRIAN ROCKS IN NORTHEASTERN ALBERTA (NTS 74E, 74L, 74M)[1]

Martin W. McCurdy
Mineral Resources Division, Ottawa

Abstract

A lake sediment and water geochemical survey was carried out in 1994 in northeastern Alberta (parts of NTS 74E, L, and M) under the Canada–Alberta Agreement on Mineral Development (1992–1995). Over an area of 22 100 km^2, samples were collected from 1160 sites. Analytical results for 35 elements were published in a Geological Survey of Canada Open File.

Data for six economic metals (uranium, molybdenum, gold, zinc, nickel, and copper) and two "pathfinder" elements (arsenic and antimony) were contoured and plotted over a topographic base. The results, in conjunction with structural, bedrock and surficial geology, were used to determine areas where detailed studies or follow-up exploration are warranted.

South of Lake Athabasca, in areas of thick overburden, glacial processes played a major role in the geochemical signature of the elements examined. North of Lake Athabasca, where overburden is thin or nonexistent, bedrock geology is the prime factor affecting geochemical results.

A number of areas have potential for further exploration. Particularly interesting is an area in the northwest where a number of east-trending faults intersect a north-trending fault. Uranium and gold values are high in lake sediments over this area of granitoids and high-grade metasediments. South of Lake Athabasca, there are a number of areas that should be explored for the possibility of placer gold deposits, particularly along the Athabasca River and along the south shore of Lake Athabasca. An area of granitoid and mylonitic rocks in the southern part of the survey is recommended for follow-up work for gold based on an unusually high antimony value.

Résumé

En 1994, un levé géochimique des sédiments et des eaux lacustres a été réalisé dans le nord-est de l'Alberta (parties des feuillets 74E, L et M du SNRC), dans le cadre de l'Entente Canada–Alberta sur l'exploitation minérale (1992-1995). On a prélevé des échantillons à 1 160 sites différents sur une superficie de 22 100 km^2. Les résultats d'analyse de 35 éléments ont été publiés dans un dossier public de la Commission géologique du Canada.

On a tracé les courbes d'isovaleurs de six métaux économiques (uranium, molybdène, or, zinc, nickel et cuivre) et de deux éléments marqueurs (arsenic et antimoine) sur un fond topographique. Les résultats, conjugués aux données sur la géologie structurale, la géologie du substratum rocheux et les dépôts superficiels, ont servi à déterminer les zones où il était justifié d'entreprendre des études détaillées ou de poursuivre l'exploration.

Au sud du lac Athabasca, dans des zones de morts-terrains épais, les processus glaciaires ont joué un rôle majeur dans la signature géochimique des éléments analysés. Au nord du lac Athabasca, où les morts-terrains sont minces ou inexistants, la géologie du substratum est le principal facteur influant sur les données géochimiques.

[1]Canada–Alberta Agreement on Mineral Development, Project C1.15

Un certain nombre de zones méritent d'être explorées plus en détail. Une zone particulièrement intéressante se trouve dans le nord-ouest de la région, là où de nombreuses failles d'orientation est entrecoupent une faille d'orientation nord. Les teneurs en uranium et en or sont élevées dans les sédiments lacustres de cette zone de granitoïdes et de sédiments fortement métamorphisés. Au sud du lac Athabasca, de nombreuses régions devraient être explorées en raison de leur potentiel en placers aurifères, en particulier le long de la rivière Athabasca et de la rive sud du lac Athabasca. Il est recommandé de poursuivre l'exploration dans une zone de roches granitoïdes et mylonitiques dans le sud du secteur à l'étude, compte tenu d'une concentration inhabituellement élevée d'antimoine qui indiquerait la présence d'or.

INTRODUCTION

A centre-lake sediment and water geochemical survey was carried out in 1993 under the supervision of the Geological Survey of Canada (GSC) in northeastern Alberta (Fig. 1) over mainly Precambrian rocks. The project was funded by the Canada–Alberta Agreement on Mineral Development (1992-1995). Analytical results for 35 elements, loss-on-ignition in sediments, and uranium, fluoride, and pH values for lake waters at 1160 sites were published in Friske et al. (1994a). A digital version of this open file with field and analytical data was released at the same time. Average sampling density over the 22 100 km^2 area was one sample per 19 km^2.

Regional lake sediment and water data are useful for evaluating economic mineral potential and providing environmental baseline data over large areas, but the geochemical profile of an individual lake sediment is influenced by a number of factors. The main factors are bedrock geology and glacial processes; others are mineralization, climate, physiography, and vegetation, along with geochemical character (i.e., mobility) of individual elements under different conditions such as pH or the presence or absence of other elements.

The purpose of this paper is to discuss the major influences on elemental distributions in lake sediments and waters for selected elements and groups of elements in the study area and suggest areas where further investigations may be warranted.

Bedrock geology

Most of the lake survey sites sampled are located on granitic gneiss intruded by granitoid batholiths, high-grade metasediments, and amphibolite of the Precambrian Churchill Structural Province of the Canadian Shield, north of Lake Athabasca (Edwards et al., 1991; Fig. 2). South of Lake Athabasca, sandstones of the Athabasca Basin form the bedrock (Ruzicka, 1997; *this volume*). In the Marguerite River area, Precambrian granitoids and mylonites outcrop (Charbonneau et al., 1994; McDonough, 1997; *this volume*). Along the western margins of the survey area, Cretaceous and Devonian sedimentary rocks bound the Precambrian rocks, including clastic, carbonate, and evaporitic sedimentary rocks. East- and northeast-trending faults and shear zones are extensive in Precambrian rocks north of Lake Athabasca (Edwards et al., 1991; Fig. 3), and faults delineate the margins of the Athabasca Basin. Radial faults are noted around the margins as well (Wilson, 1985).

Surficial geology

The Laurentide Ice Sheet advanced in a southwestward direction out of the District of Keewatin (Bednarski, 1997; this volume). The southern section of the survey area (NTS 74E, northeast quarter) is overlain by extensive outwash deposits of sand and gravel, surrounding a central 'island' of exposed granitoid rocks (Fig. 4). A belt of glaciofluvial deposits consisting of end moraines, eskers, kames, and other deposits from a retreating glacier, in turn, surrounds the outwash deposits (Bayrock, 1971).

The central part of the survey area (NTS 74L) contains considerable volumes of aeolian sands east of the Athabasca River and south of Lake Athabasca. Extensive glaciofluvial deposits occur east of the aeolian sands. South and west of Lake Athabasca, deltaic sand, silt, and clay occur. Bayrock (1972) noted a calcareous composition in these deltaic sediments. North of Lake Athabasca, exposed rock, in places with a thin covering of drift, predominates. Remaining areas are covered by outwash deposits of sand and gravel (Fig. 4).

The northern section of the survey area (NTS 74M) is characterized by bare or thinly covered granitic or metasedimentary rock, and glaciofluvial deposits of sand and gravel (Fig. 4). Glaciolacustrine sand, silt, and minor clay, usually overlain by organic deposits, are found along the Slave River and in the west-central part of the area (Bednarski, 1997; this volume).

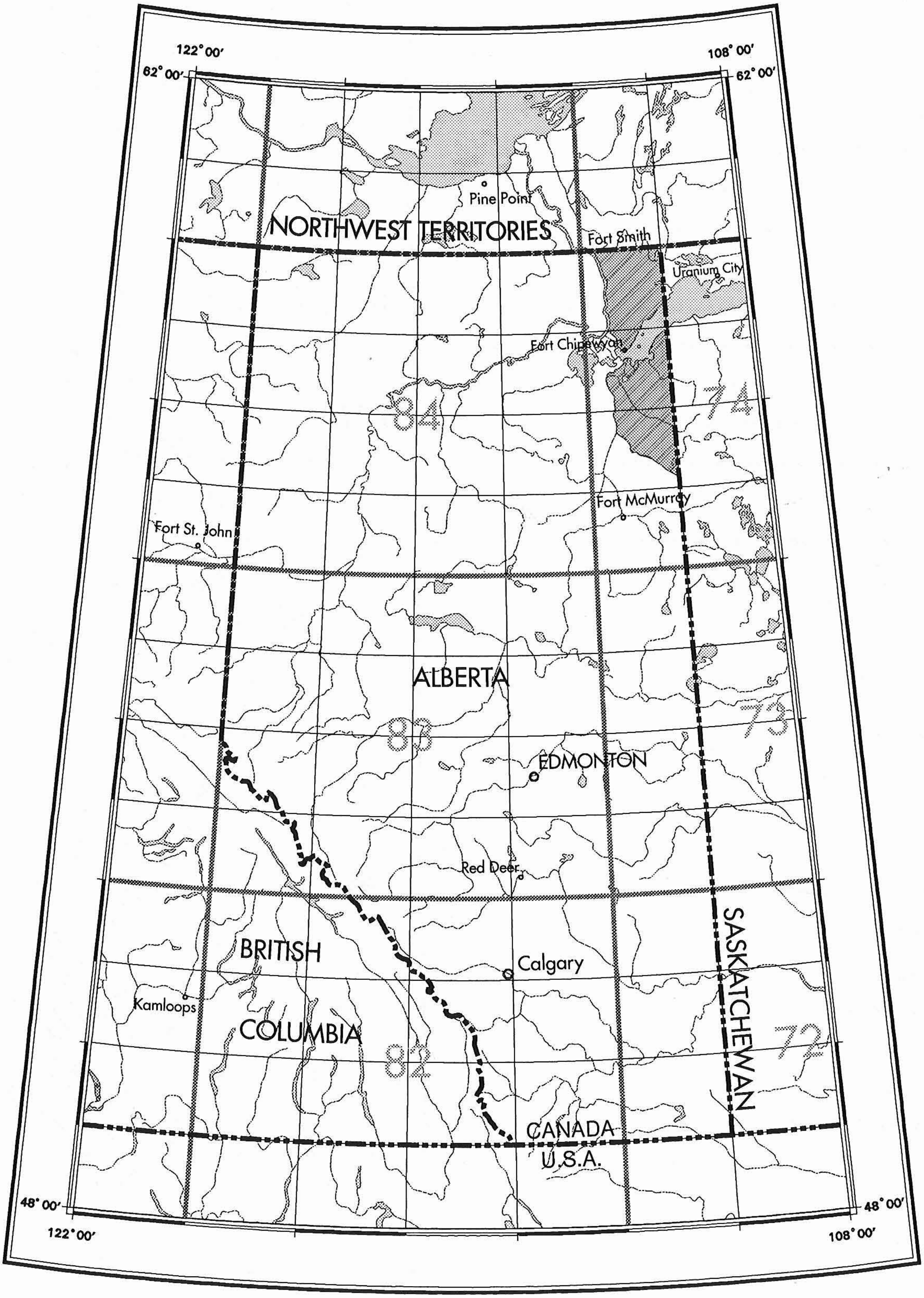

Figure 1. Location of the northeastern Alberta study area, shown in grey with diagonal lines.

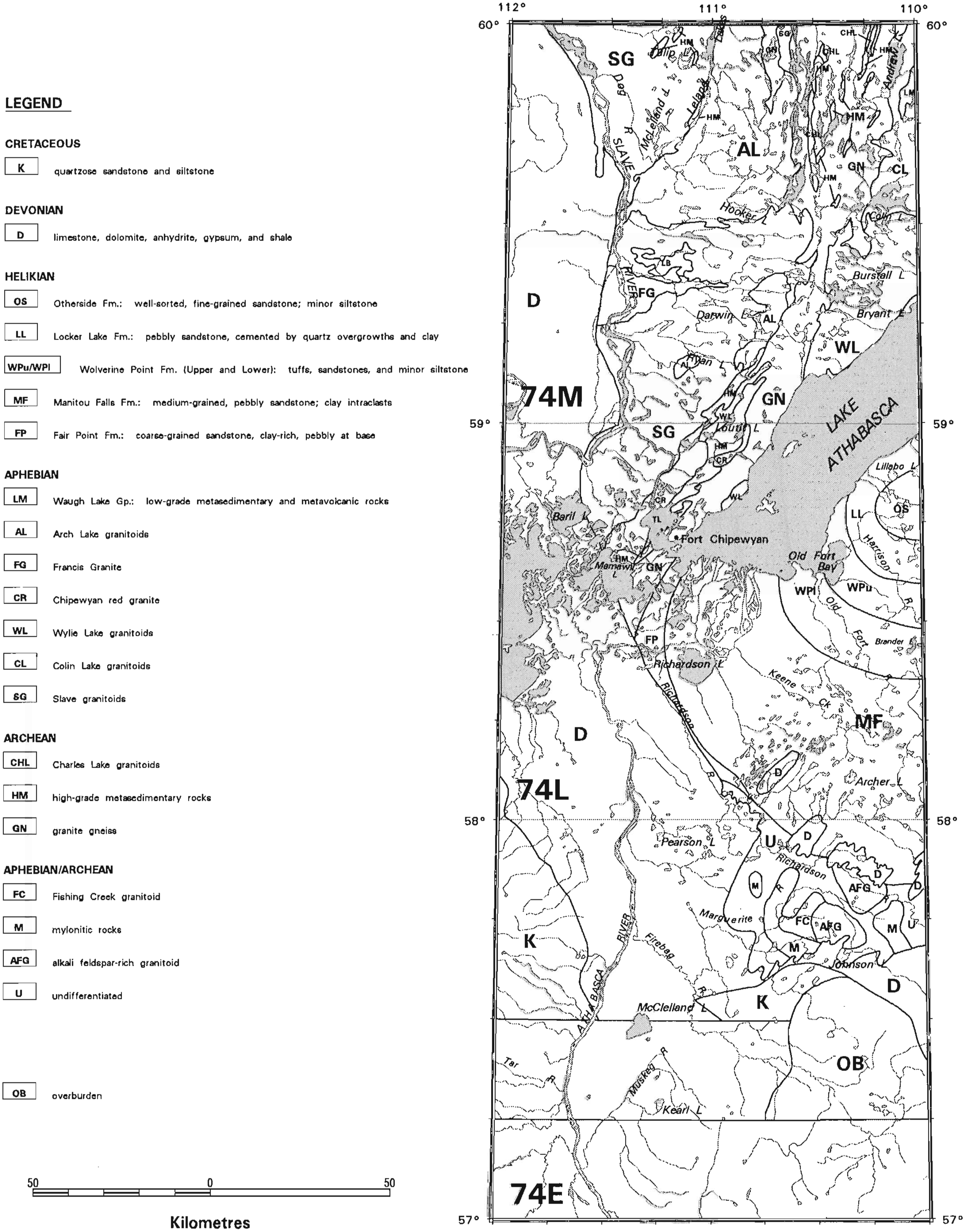

Figure 2. *Geology of northeastern Alberta (after Charbonneau et al., 1994).*

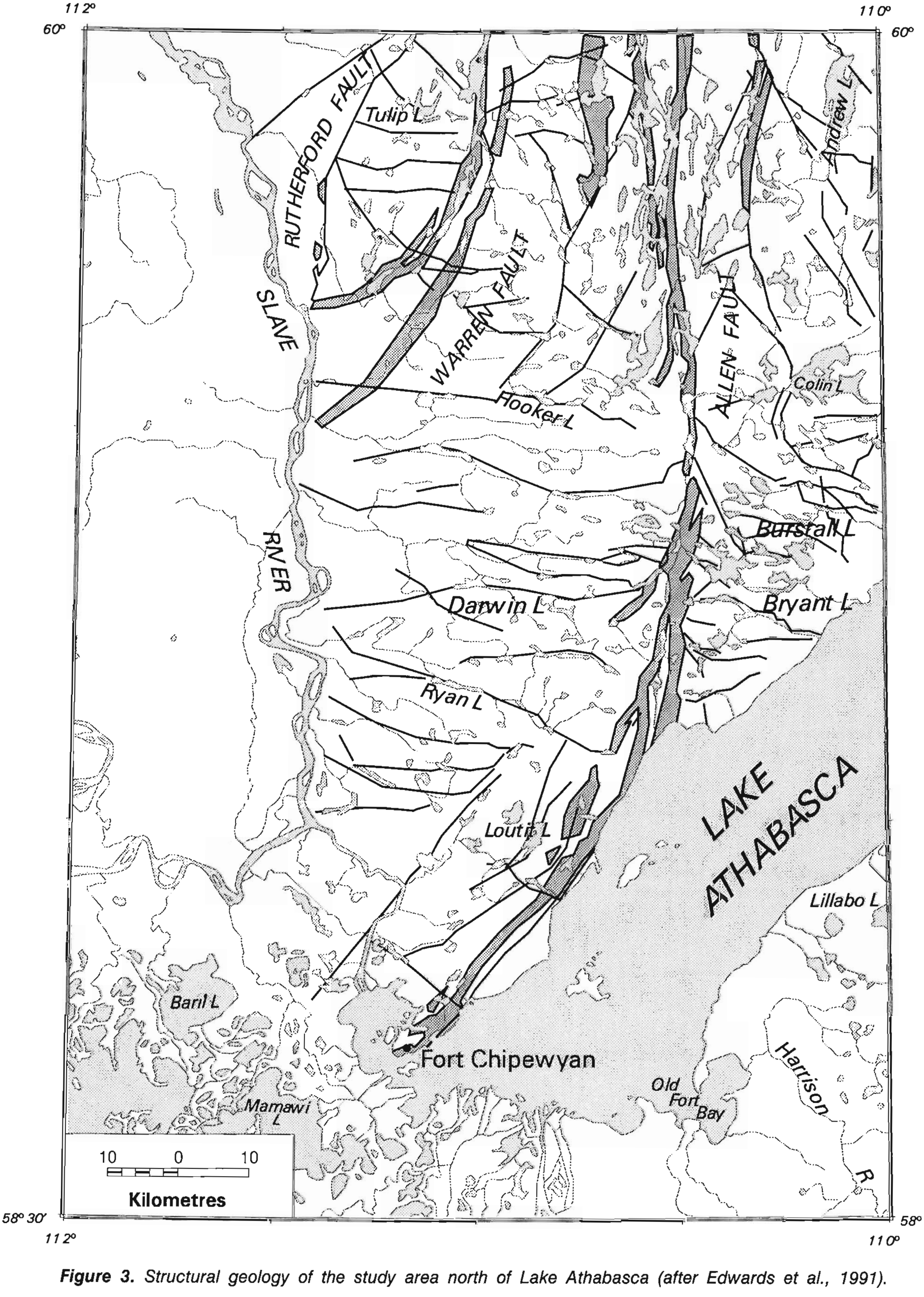

Figure 3. *Structural geology of the study area north of Lake Athabasca (after Edwards et al., 1991).*

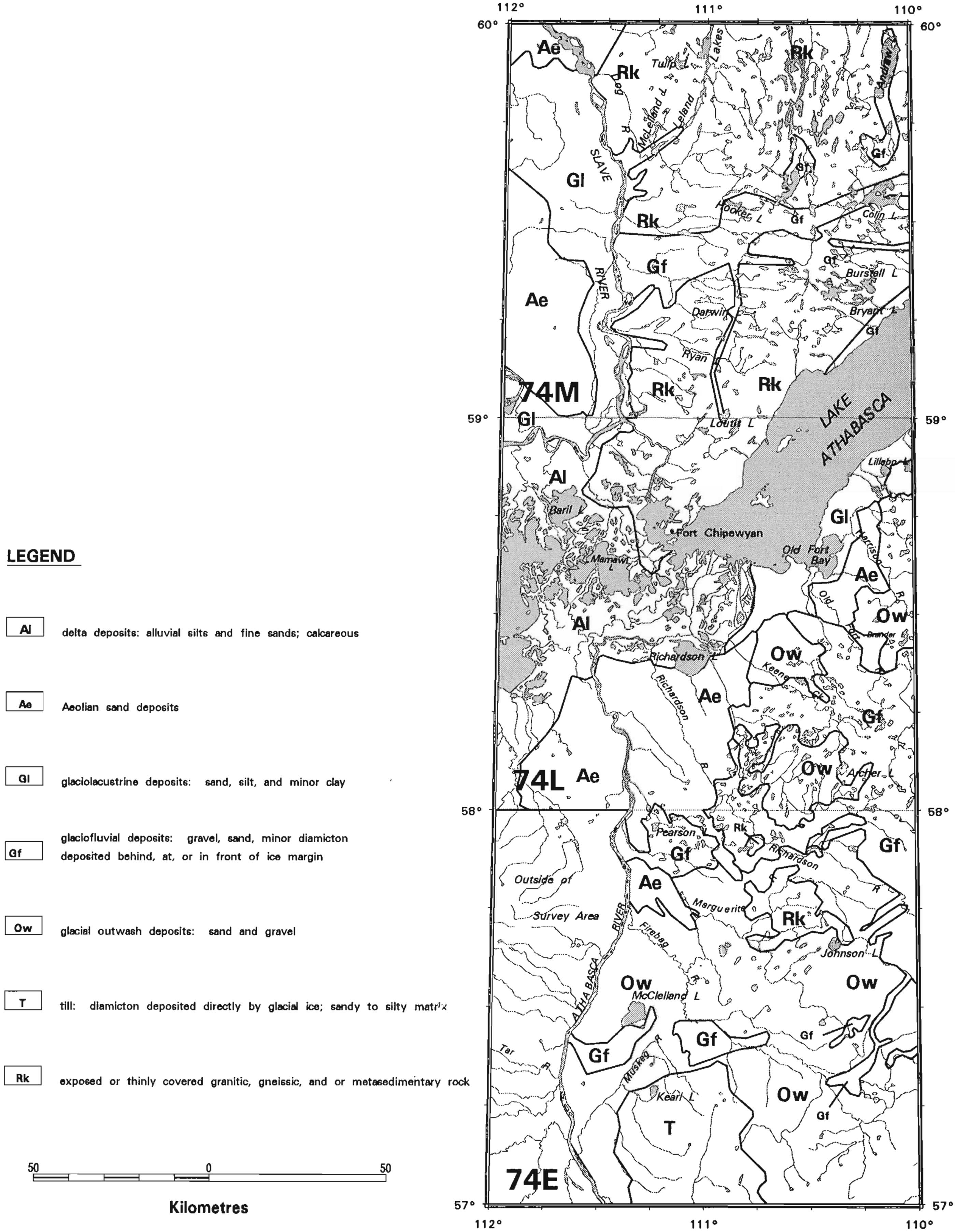

Figure 4. Generalized surficial geology of northeastern Alberta (after Bayrock, 1971, 1972; Bednarski, 1994).

Economic geology

The survey area lies west of uranium deposits at Cluff Lake and Uranium City (see Ruzicka, 1997, for details), but no mines, now or in the past, have operated in the area. Evidence of mineralization consists mainly of uranium staining, molybdenite, and graphite occurrences in the granitic and metasedimentary gneiss north of Lake Athabasca, and sulphides, including chalcopyrite, noted in Paleozoic rocks overlying Proterozoic rocks. Minor gossans in high-grade metasedimentary rocks yield elevated values of copper, nickel, silver, and gold (Edwards et al., 1991).

Sample collection and analysis

The GSC, under the National Geochemical Reconnaissance Program (NGR), has been collecting and analyzing lake and stream sediments and waters since 1973, when the first major lake sediment geochemical survey was carried out in Saskatchewan. The goal of the program has been, and continues to be, to build a national geochemical database that can be used for resource assessment, mineral exploration, geological mapping, and environmental studies. Data are available for over 200 000 sites, covering about 2.5 million square kilometres of Canada at a sampling density of about one sample per 13 km^2 (Friske and Hornbrook, 1991). Coverage to date is confined mainly to areas of Precambrian or Cordilleran exposures.

A bottom-valved, hollow-pipe sampler is used to collect 1 kg or so of wet lake sediment. The sampler is vented at the top, allowing the top few centimetres of sediment to escape so that possible contamination in the upper levels of sediment can be avoided. A modern lake sediment from a Shield lake will normally consist of varying amounts of organic gels, organic sediments and inorganic sediments (Timperley et al, 1973). Typically, 1 kg of the organic gel, the preferred collection material, is about 95% water, and once dried, about 50 g of material remains for analysis.

Sediments are normally analyzed for 35 elements, plus loss-on-ignition, which gives an approximation of the per cent organic material in samples. At each site, 250 ml of water are collected and analyzed for pH, fluoride, and uranium. Data returned by laboratories are checked for accuracy and precision. Listings and statistics are generated and two types of maps are prepared. A sample location map includes background geology, and smaller maps illustrate, with symbols, relative concentrations of elements in the survey area. This information is released as a GSC Open File approximately one year after sample collection. Digital data are also made available, which includes field and analytical data with UTM location coordinates.

DIGITAL DATA

Spatial data in an ASCII comma-delimited format was imported into Microsoft Excel, a spreadsheet package. A suitable ASCII comma-delimited file containing sample numbers, Universal Transverse Mercator (UTM) coordinates, and analytical data was created and imported into the Arc/Info geographic information system. Data were converted to $\log_{10}$ values using the Info module, an elementary relational database management system. Digital background geology was derived from Charbonneau et al. (1994). A basemap was obtained from the 1:1 000 000 scale vector Digital Chart of the World (DCW) for Arc/Info, available from the Environmental Systems Research Institute (ESRI), Redlands, California.

Using the Arc/Info Grid module and $\log_{10}$ data, contour maps of elemental abundance were created, using eight classes based on percentiles for selected elements and using an inverse distance-weighted interpolation. To highlight anomalous data, a power of 0.8 was used, giving relatively more influence to elevated values within the search radius of 10 km. The number of input sample points was set at 25 on the assumption that all sample points within a 10 km search radius would be included in the interpolation. Output was in the form of a Postscript file.

After examining the contoured data for the elements selected, statistics were generated for the data set using Excel for Windows. Statistical data for the data set includes Pearson product-moment correlation coefficients, cumulative probability plots (Garrett, 1991), and scatterplots.

Observations[1]

Uranium/Molybdenum

Anomalous uranium values in lake sediment are noted north of Ryan Lake, within the Wylie Lake granitoids south of Bryant Lake and at the contacts of the Wylie Lake and Colin Lake granitoids (Figs. 2, 5). North and west of McLelland Lake, in the southern part of the

[1]Unless otherwise stated, the term 'anomalous' is used to described high elemental concentrations at or above the 95th percentile of the data set.

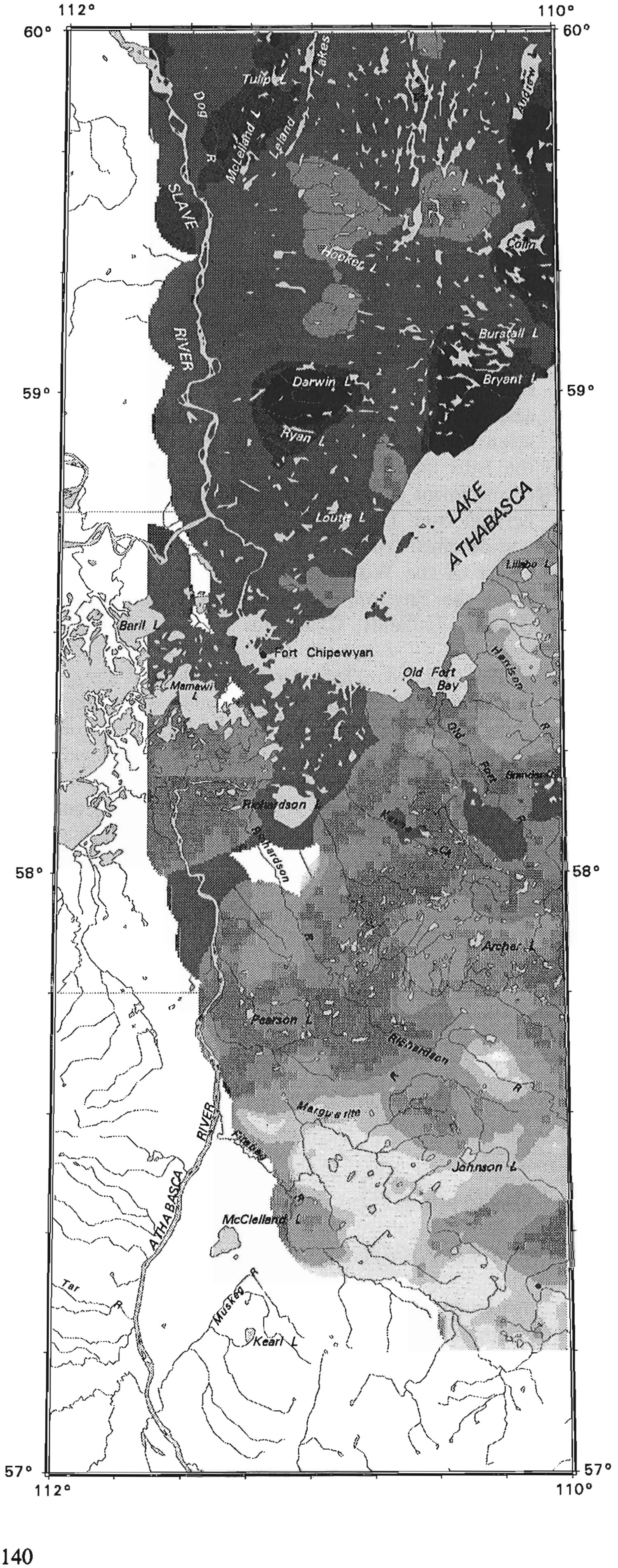

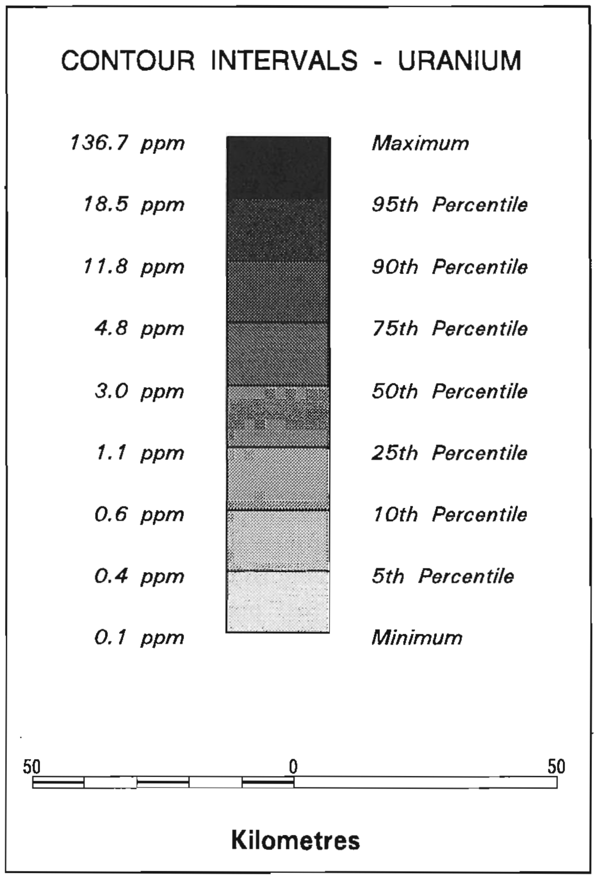

Figure 5. *Map showing relative concentrations of uranium in lake sediments, with contoured log_{10} data divided into percentile-based classes.*

area, elevated values are observed. Anomalous uranium in waters associated with elevated fluoride is centred over a Paleozoic outlier on the contact between Athabasca Group sandstones and Proterozoic rocks west of Johnson Lake, also in the southern part of the area (Fig. 5). This anomaly is not observed in lake sediments.

Molybdenum (Fig. 6), which tends to be associated with uranium in Saskatchewan Precambrian Shield rocks, particularly around Black Lake, does not show as strong an association within the current survey area. Anomalous values occur over and adjacent to the Colin Lake granitoids (Figs. 2, 6). An interesting anomaly appears east of Pearson Lake in granitoids and mylonitic rocks near the Richardson River.

Gold

Anomalous gold values are isolated except along the Paleozoic–Proterozoic contact (Figs. 2, 7). Point occurrences are found in lake sediments within areas of glaciofluvial sands and gravels near the contacts of the Wolverine Point Formation with upper and lower units of the Athabasca Group sandstones, notably west of Old Fort Bay (Figs. 2, 4, 7). Anomalous gold values occur southwest of Richardson Lake in Paleozoic limestones and dolomites along the Athabasca River. The Warren Fault, a shear zone between Arch Lake and Slave granitoids (Edwards et al., 1991; Fig. 3), and the Allen Fault (Fig. 3) are delineated by anomalous (at or above the 75th percentile of the data set) gold values, and elevated values are noted around contacts between low-grade metasediments and Colin Lake granitoids (Figs. 2, 7).

Zinc, Arsenic, Antimony, Nickel, Copper

Anomalous values for these elements are clustered along the Paleozoic–Proterozoic contact traced roughly by the Slave River (Figs. 2, 8-12). Zinc appears to represent, in area, the most extensive anomalous pattern of this group, and also appears in elevated concentrations in Manitou Falls Formation sandstones, centred around Pearson Lake, in the southern part of the area (Figs. 2, 8). South of Johnson Lake, in an area of drumlins and glaciofluvial deposits (Fig. 4, 8), high values are noted.

Arsenic and antimony show patterns similar in distribution to zinc: concentrations decrease east of the Palaeozoic–Proterozoic contact. Anomalous arsenic values (at or above the 75th percentile of the data set) are associated with elevated gold in an area of Lower Wolverine Point sandstones and siltstones around Brander Lake (Figs. 2, 9), and antimony and gold are both anomalous in Manitou Falls Formation sandstones southwest of the same area (Figs. 2, 10).

Nickel and copper exhibit a relatively restricted pattern of anomalous distribution, confined to the area immediately east of the Paleozoic–Proterozoic contact (Figs. 2, 11, 12). Elevated copper values are also associated with low-grade metasedimentary and metavolcanic rocks of the Waugh Lake Group within Colin Lake granitoids (Figs. 2, 12).

Discussion

Unconsolidated sediments are derived from two primary sources: the underlying bedrock and glacial deposits. Lake sediments reflect differences in the types and compositions of these source materials within individual catchment basins, as well as variations in the chemical and mechanical dispersion processes that move the material from source to sampling site. Other factors which can affect the distribution of elements include the presence of mineralization, scavenging by organic material or hydrous iron and manganese oxides, and contamination by air- and water-borne substances. Generally, the chemical signature of the underlying bedrock is observed in the analytical results, but locally, overlying glacial deposits or mineralization may dominate or overprint the bedrock response.

Although the size of a mineral occurrence might be small in relation to a catchment basin, it can exert a considerable influence on the sediment composition of a nearby lake because elements such as copper, lead, zinc, silver, and molybdenum usually occur in mineralization in concentrations several orders of magnitude greater than those of the surrounding bedrock. Most of the areas in Canada covered by geochemical lake sediment surveys have been glaciated and are covered to some extent by glacial deposits, of which till is the most common. Usually, till has been transported only a short distance from the source (Shilts, 1991). However, on a local scale, considerable down-ice dispersion of glacial debris can take place, and materials from a point source such as mineralization commonly will be smeared over several catchment basins (Friske, 1991). While this increases the size of the exploration target, the source is more difficult to pinpoint. Certain types of glacial deposits, such as lacustrine clays, outwash, and aeolian deposits, can mask geochemical response from the underlying bedrock, but post-depositional processes such as ground-water movement, uptake by vegetation, or erosion can result in anomalous concentrations in these areas.

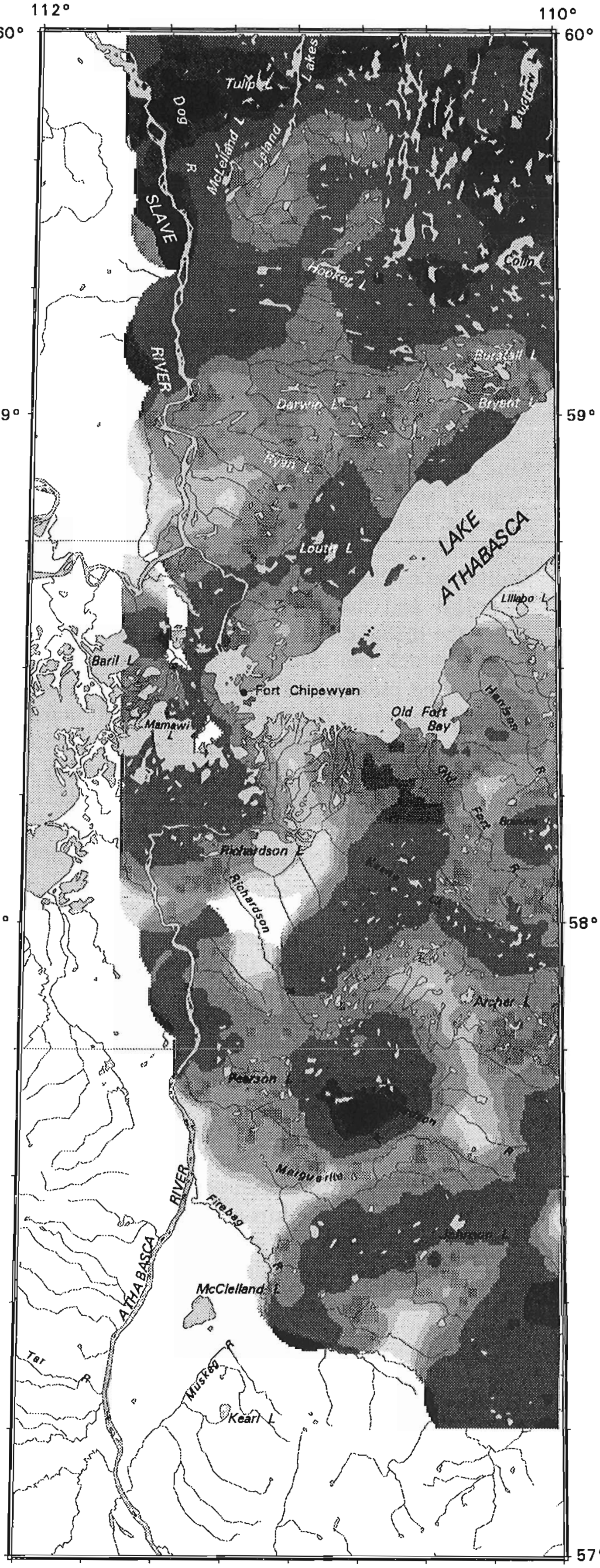

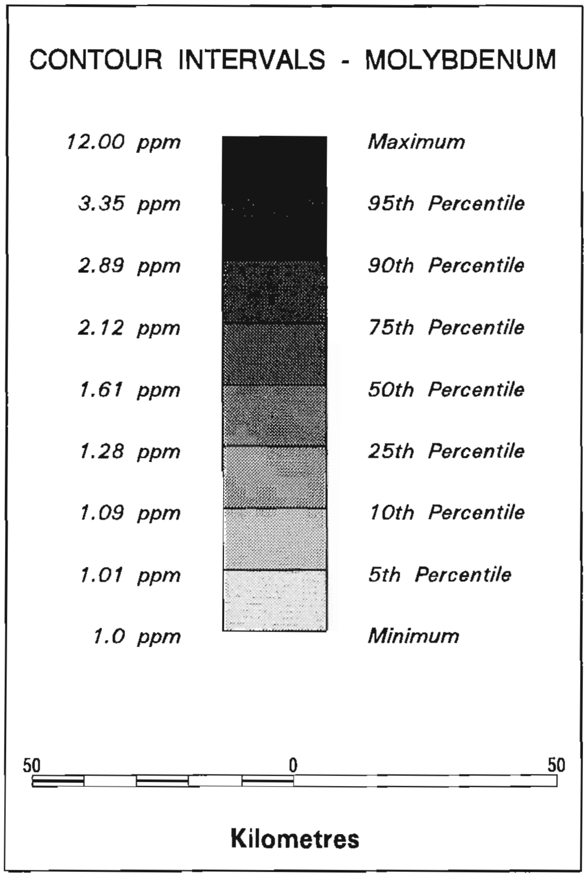

Figure 6. *Map showing relative concentrations of molybdenum in lake sediments, with contoured $\log_{10}$ data divided into percentile-based classes.*

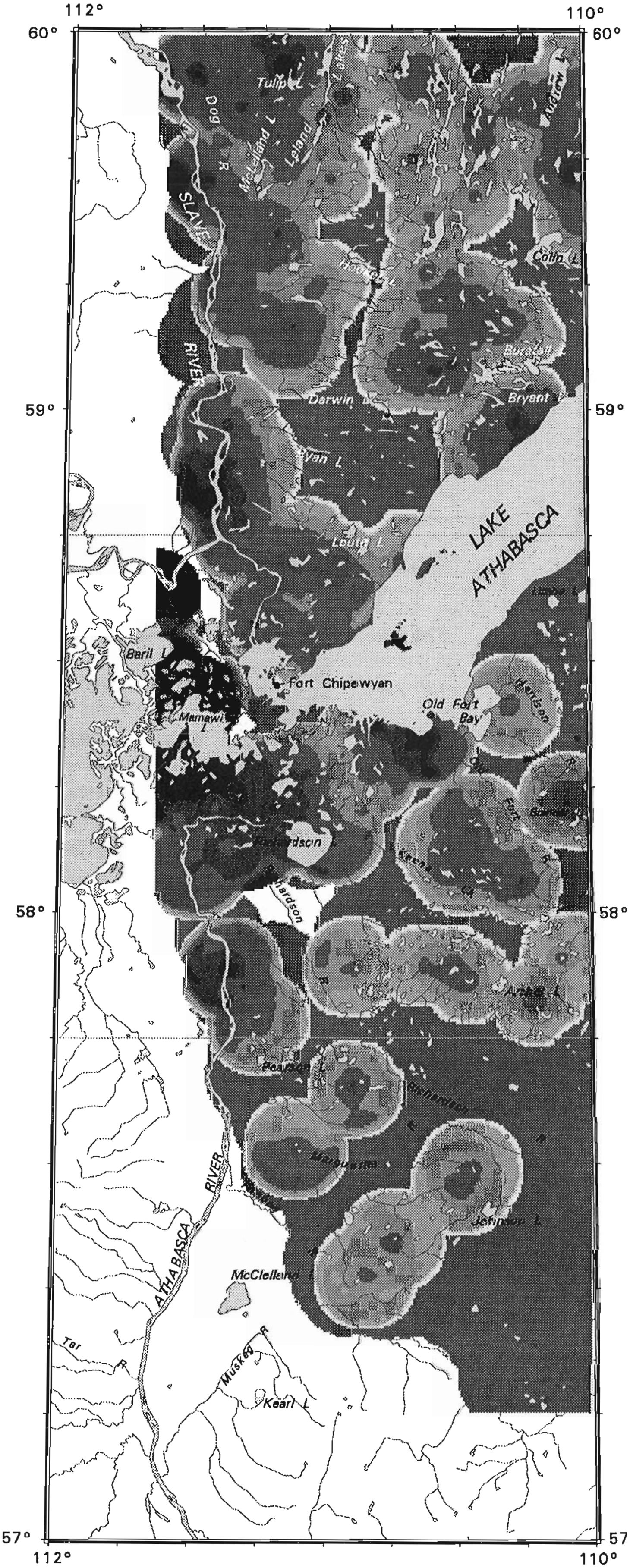

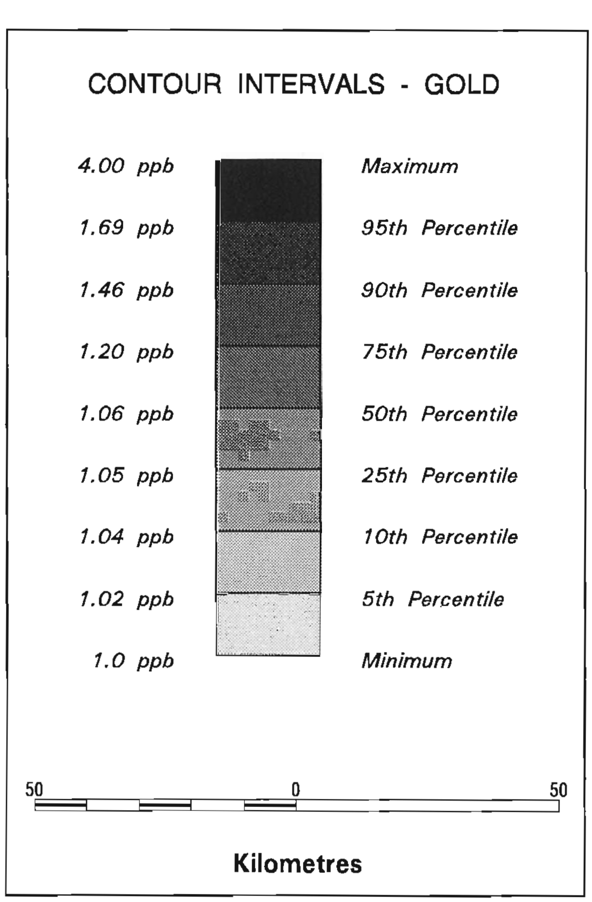

Figure 7. *Map showing relative concentrations of gold in lake sediments. Circular patterns of distribution result from the inverse distance weighted method with a 10 km search radius used to contour gold data that commonly have isolated high values.*

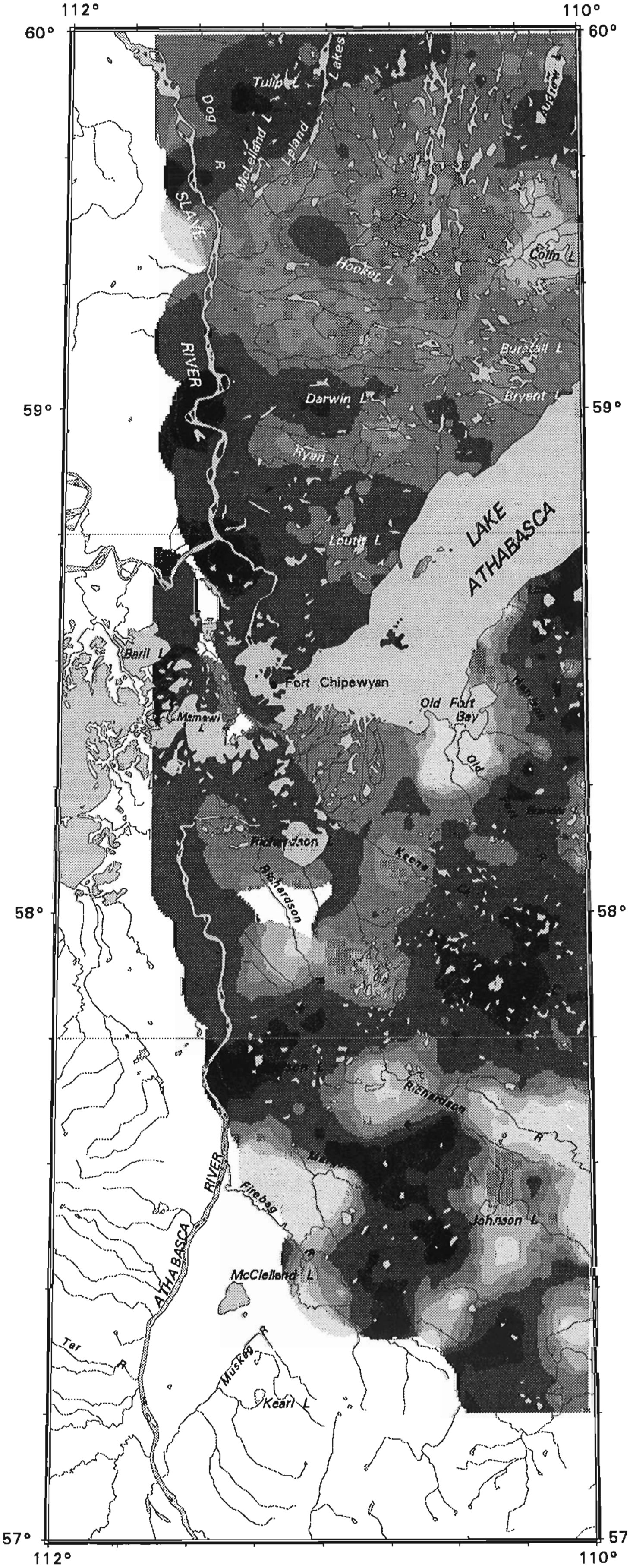

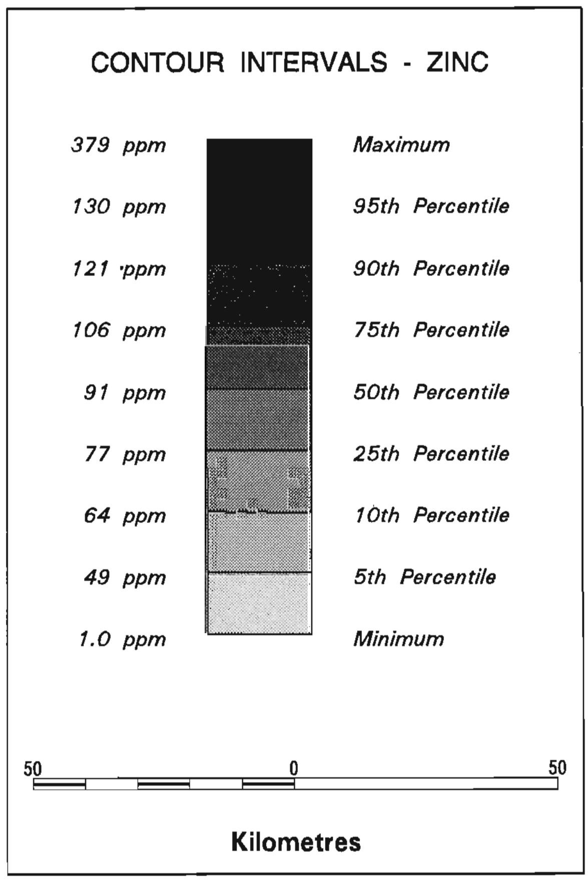

Figure 8. *Map showing relative concentrations of zinc in lake sediments, with contoured log_{10} data divided into percentile-based classes.*

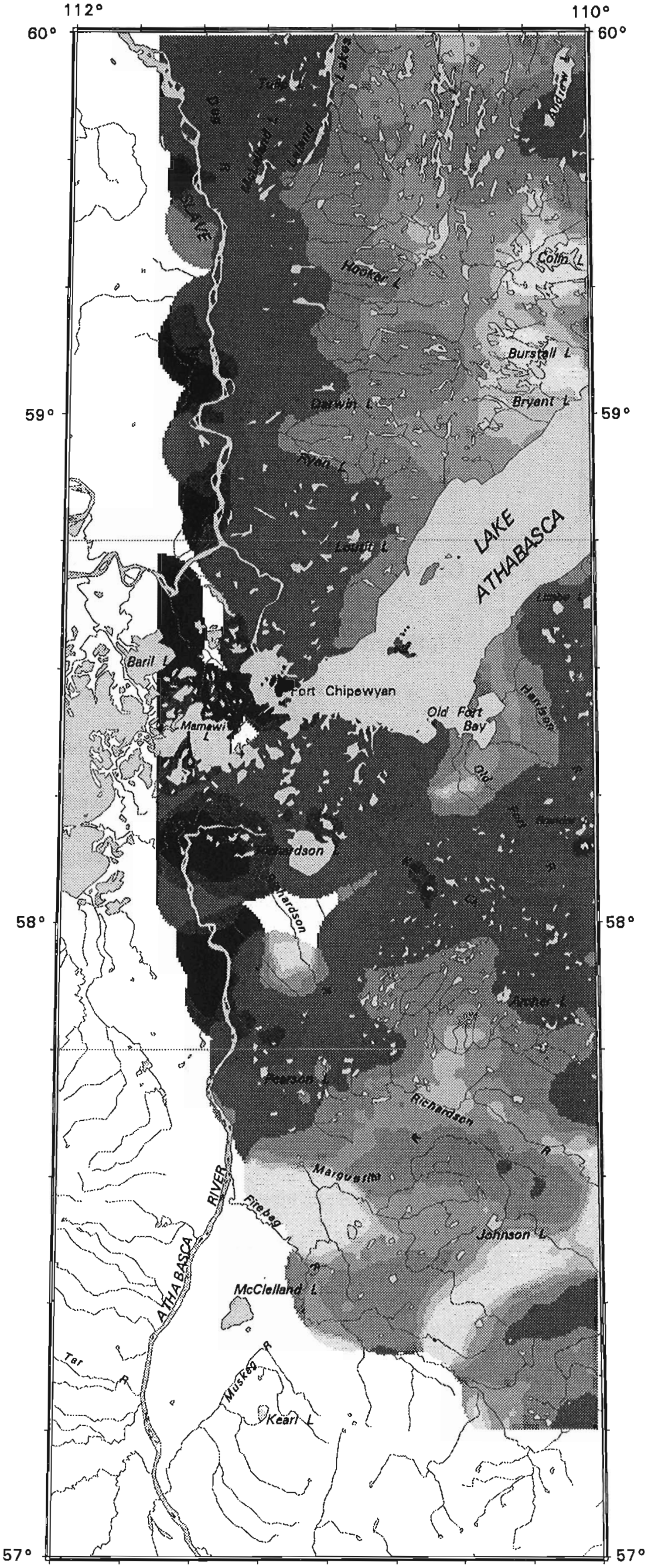

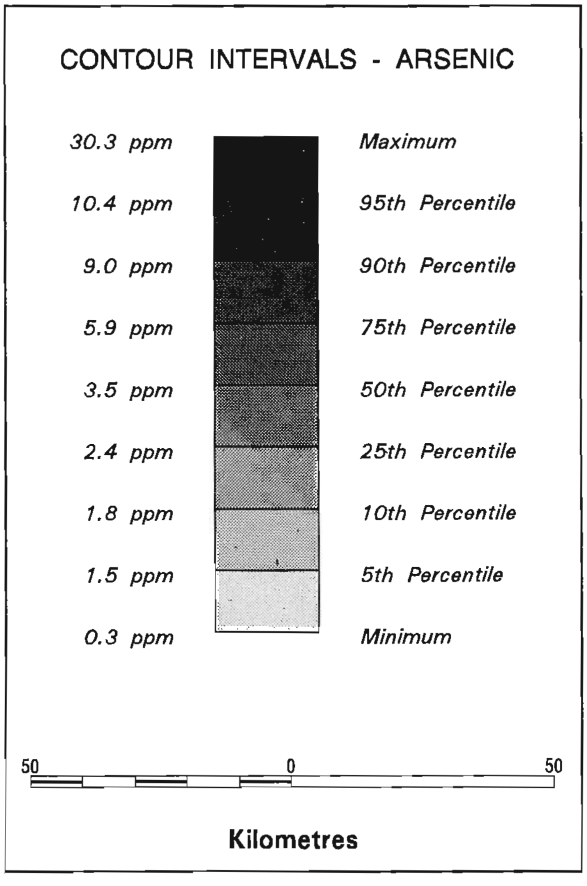

Figure 9. *Map showing relative concentrations of arsenic in lake sediments, with contoured log_{10} data divided into percentile-based classes.*

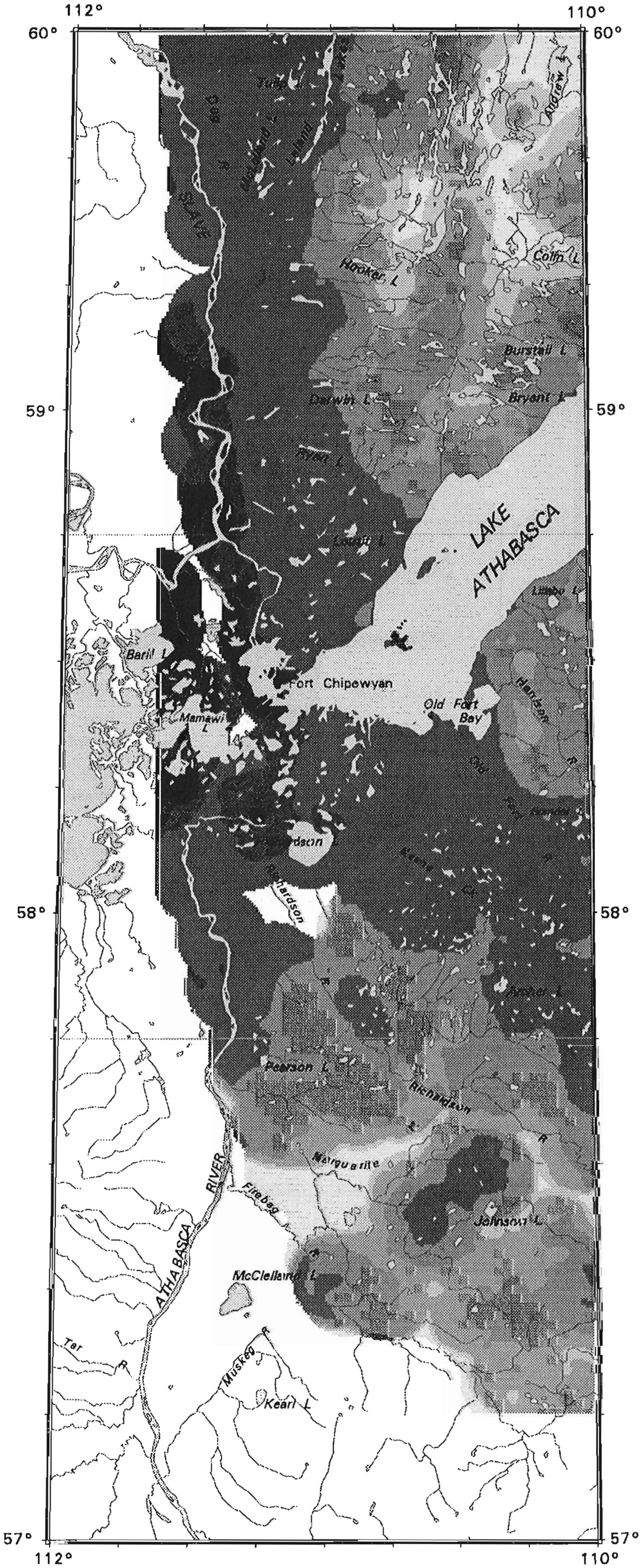

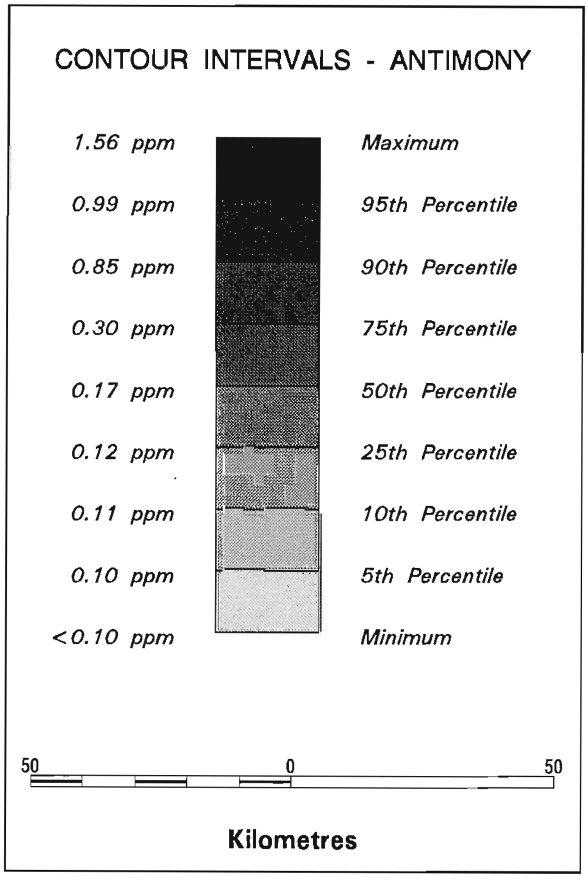

Figure 10. *Map showing relative concentrations of antimony in lake sediments, with contoured log_{10} data divided into percentile-based classes.*

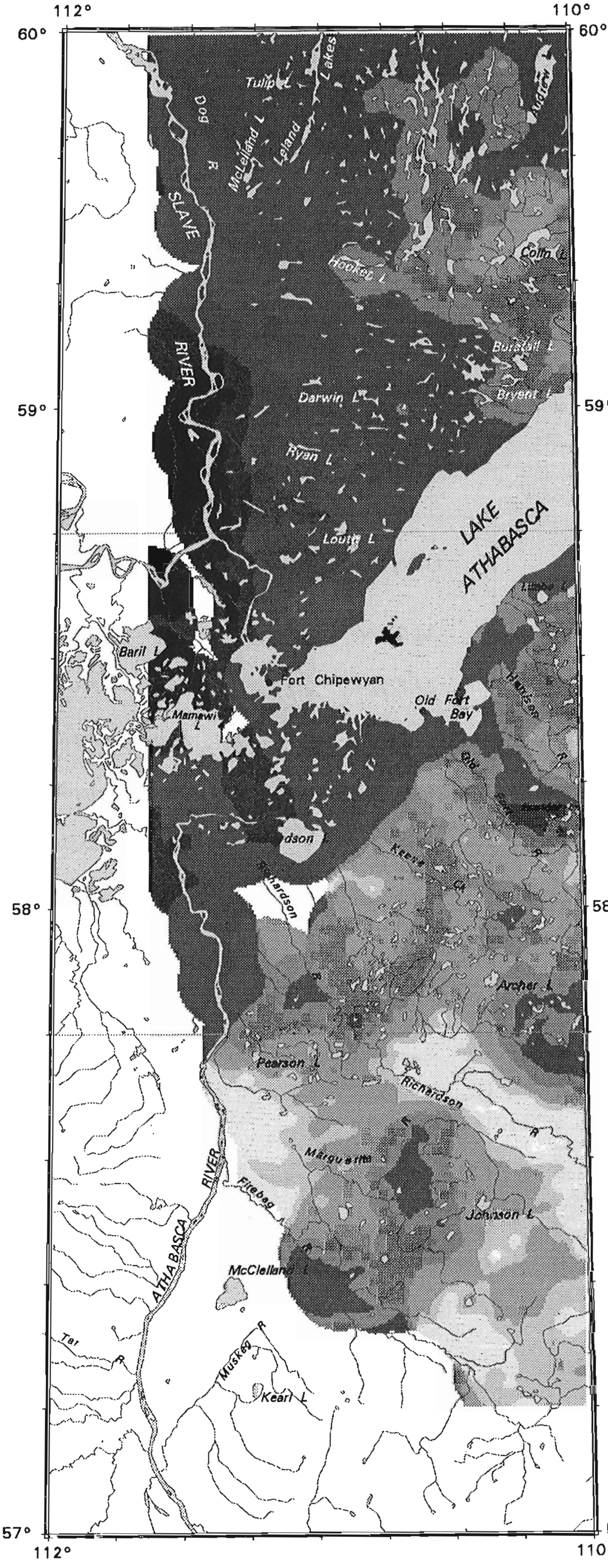

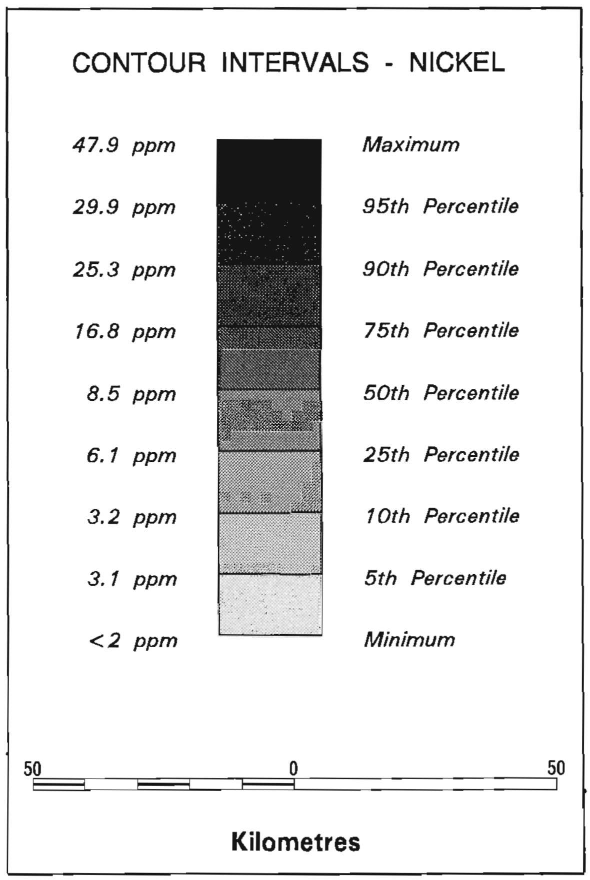

Figure 11. *Map showing relative concentrations of nickel in lake sediments, with contoured log_{10} data divided into percentile-based classes.*

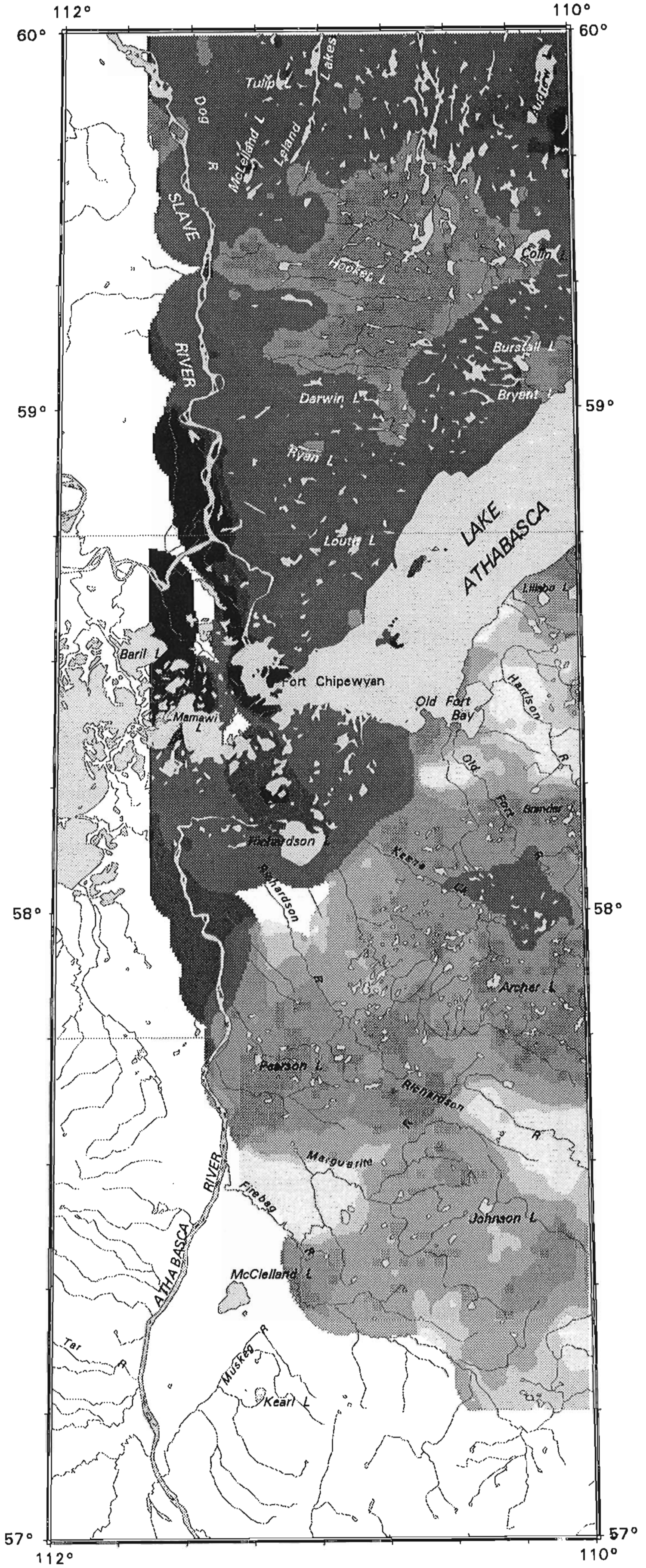

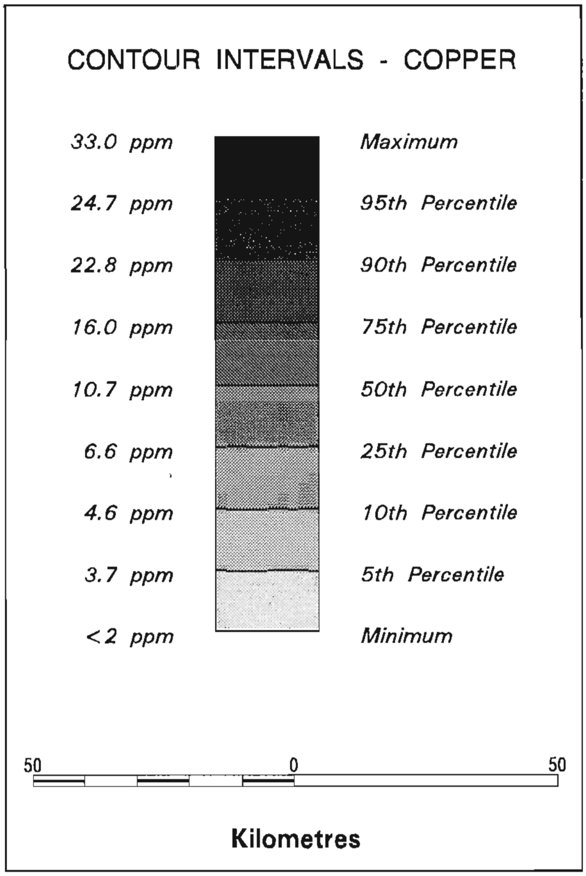

Figure 12. *Map showing relative concentrations of copper in lake sediments, with contoured log_{10} data divided into percentile-based classes.*

Chemical dispersion of elements, that is, the ability of an element to travel in solution, is affected by such factors as pH, organic content of the sediments, and the presence of hydrous metal oxides. As a rule of thumb, under oxidizing conditions and a pH between 5 and 8, molybdenum is the most mobile element and iron the least (Friske, 1991). The distribution of anomalous concentrations can be used as a guide to the proximity of the source, with less mobile elements such as lead, mercury, and silver producing more compact anomalous zones than zinc, cadmium, or copper. A few elements can show a related response. Mercury is commonly associated with an abundance of organic material in the sediment, and high cobalt values usually appear with above-average values for iron and manganese. Gold, tungsten, copper, lead, nickel, and antimony usually show no distinct trends or associations in lake sediments over Precambrian Shield rocks (Friske, 1985a).

Uranium/Molybdenum

Both uranium and molybdenum are more soluble in alkaline waters (Friske, 1985b): over the sedimentary rocks south of Lake Athabasca and the deltaic areas west of Lake Athabasca, this relationship appears to conform well with pH variation (Fig. 13), especially for molybdenum. In the region south and west of Lake Athabasca, regional variation is probably the result of differences in pH resulting either from the presence of calcareous overburden (alkaline), no overburden (acidic), or aeolian sand or sand deposits (acidic).

North of Lake Athabasca, over gneissic and metasedimentary rocks thinly covered with overburden, bedrock and structural geology appear to be the main factors controlling elemental concentrations of uranium and molybdenum in lake sediments. Values above about 77 ppm uranium in lake sediments shown on a cumulative probability plot for uranium (Fig. 14) are all located within the granitoids and metasediments north of Lake Athabasca. Highest mean values are found in lakes over the Colin Lake granitoids (Fig. 2), but the highest value, 153 ppm, is located in high-grade metasediments north of Tulip Lake near the Alberta–Northwest Territories border, near the intersection of the Rutherford Fault and a northwest-trending fault (Figs. 3, 5). High uranium values appear to be associated with the northeast-trending fault system, with highest values clustered around areas where these faults intersect with east- or northeast-trending faults.

Gold

South of Lake Athabasca, at least two dispersal trains can be traced by elevated gold values, both down-ice of areas mapped by Bayrock (1971) as exposed Archean mylonites and granitoids (Figs. 2, 4, 7). The direction of ice advance for the most part determines the dispersal pattern and the subsequent pattern of anomalous values away from the source in lake sediments. It is interesting to note that an unusually high antimony value (61.6 ppm) occurs in the same area north of Johnson Lake as anomalous gold values. Antimony, which is one of a number of elements commonly associated with Archean lode gold deposits in Ontario (Colvine et al., 1988), can also be traced down-ice (Fig. 10) from this point.

Elevated values of gold delineate the glaciofluvial sands and gravels south of Lake Athabasca. However, weathering effects on glaciofluvial sediments may lead to enhancement of labile minerals in lake sediments, resulting in geochemical anomalies not related to provenance (Shilts, 1993). Fine material derived from weathering processes washed into lakes from glaciofluvial sediments (eskers, kames, outwash, etc.) and supraglacial tills, both of which have little or no primary fine fraction (Shilts, 1993) and which may contain material from distant sources, could result in lake sediment gold values that are less representative of underlying bedrock.

Elevated gold values around Old Fort Bay on Lake Athabasca (Fig. 7) may represent alluvial concentration of gold from till and glaciofluvial deposits.

North of Lake Athabasca, elevated gold values trace the line of the north-trending Allen, Rutherford, and Warren faults (Figs. 3, 7). Colvine et al. (1988) noted that in Ontario, deformation zones associated with Archean lode gold deposits are formed by large-scale crustal movement or emplacement of plutons and batholiths. In Ontario, faults and shear zones formed by large scale crustal movement or shortening host most of the significant gold deposits. Thus in Ontario, at least, the absence of greenstones does not preclude the presence of gold. In Ontario, clastic metasediments within Archean subprovinces host proportionally the same frequency of mineralization as mafic and ultramafic volcanic and intrusive rocks (Colvine et al., 1988).

As with copper, nickel, and a number of other elements, elevated gold values mark the Proterozoic–Paleozoic boundary.

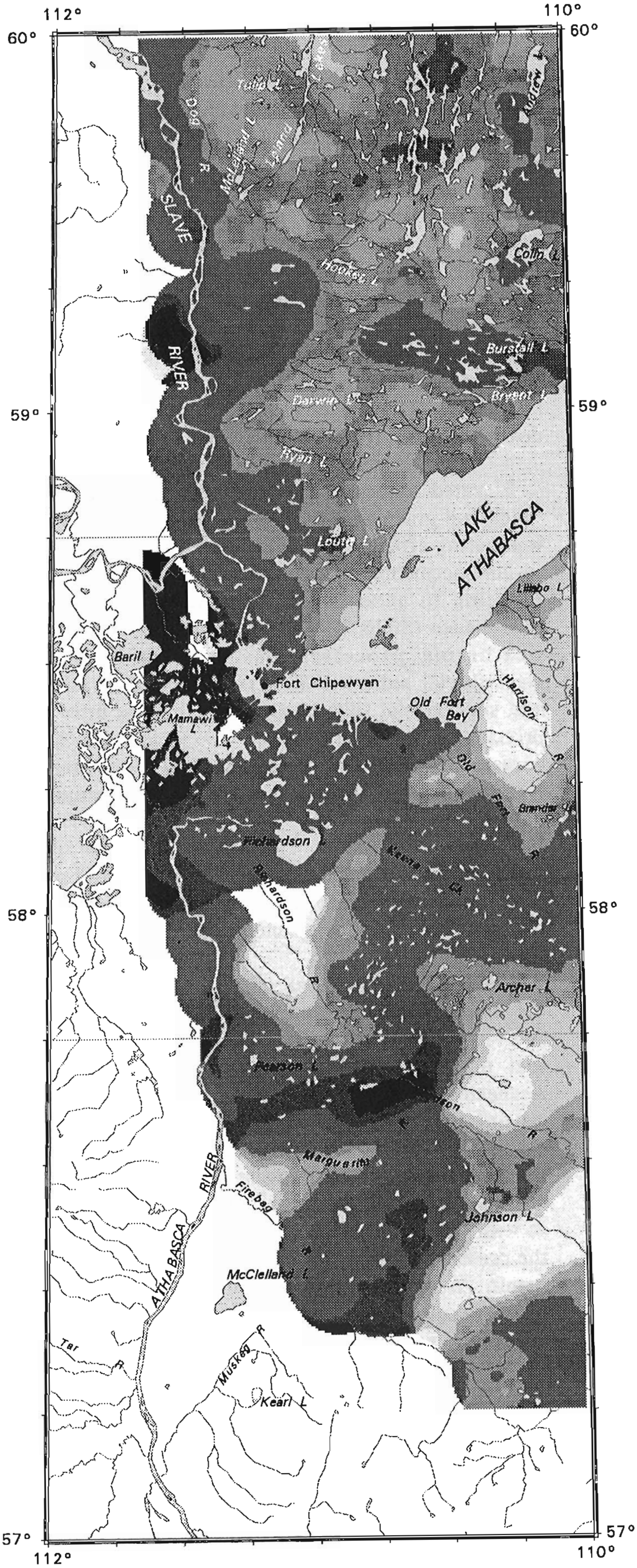

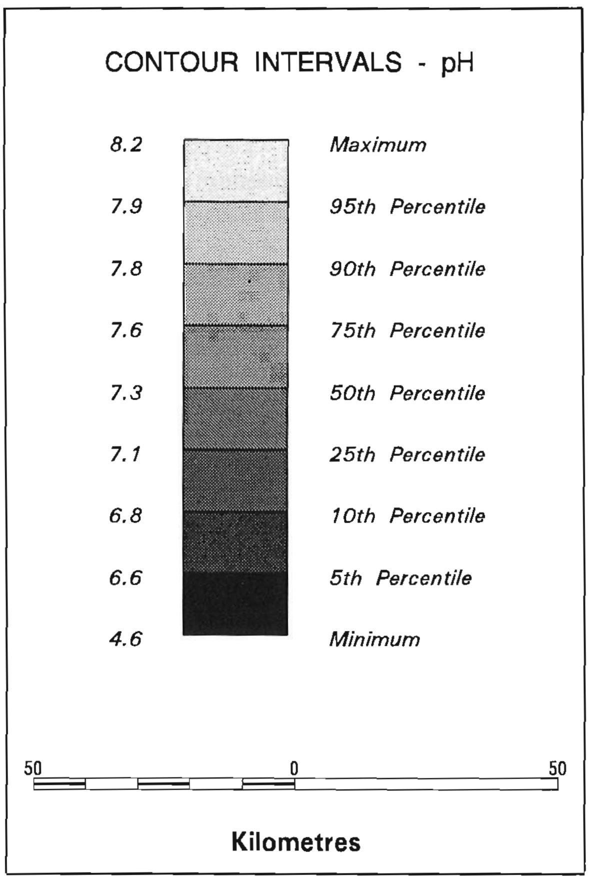

Figure 13. *Map showing relative pH values in lake waters, with contoured log_{10} data divided into percentile-based classes.*

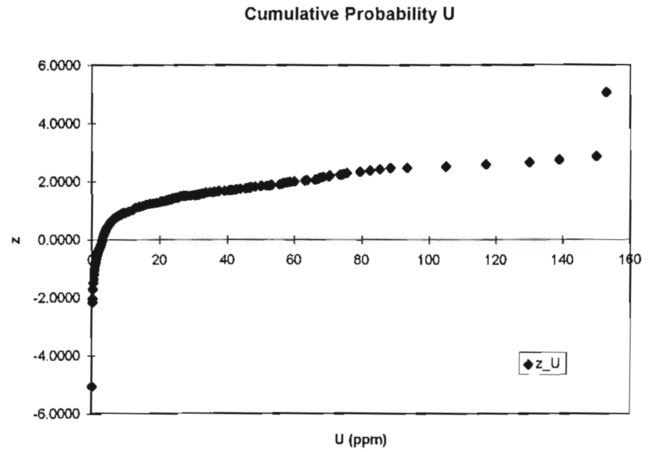

Figure 14. *Cumulative probability plot showing uranium concentrations in lake sediments on the x-axis versus cumulative probability (z) on the y-axis.*

Zinc, Antimony, Arsenic, Nickel, Copper

South of Lake Athabasca, there appears to be a relationship between zinc and loss-on-ignition (LOI) (Figs. 8, 15). The Pearson correlation coefficient (*r*) of these two variables equals 0.56. Garrett and Hornbrook (1976) noted that zinc values increased below 12% LOI, decreased slowly from 12% to 50% LOI, and decreased at an accelerating rate over 50% LOI in lake sediment samples from east-central Saskatchewan. They suggested that the 12% to 50% range represents the values over which there is insufficient zinc to maintain a sympathetic relationship, while above 50% LOI the decrease of the curve is probably the result of dilution.

North of Lake Athabasca, the zinc–LOI relationship is less clear ($r = 0.12$). A number of anomalous areas occur along the Paleozoic–Proterozoic contact and may be related to stratiform mineralization in Paleozoic dolomite immediately overlying a regolith developed in Precambrian Shield rocks, described by Edwards et al. (1991). Two areas of elevated zinc values in lake sediments appear to be associated with the intersection of faults. An area southwest of Tulip Lake is located where the southwest-trending Rutherford fault intercepts an east–west fault (Fig. 3). The line of the Rutherford Fault can be traced for some distance south by the high zinc values. West of Darwin Lake, where a northwest-trending fault intercepts a northeast-trending fault, a cluster of relatively high zinc values occurs (Figs. 3, 8).

As noted above, an unusually high antimony value (61.6 ppm) occurs in the same area north of Johnson Lake as anomalous gold values (Figs. 7, 10). The value of the mean for the entire data set is 0.297 ppm, which is characteristic for antimony values in lake sediments across northern Saskatchewan (Friske et al., 1994b). The anomaly may be fault-related, as it is centred over the intersection of a northeast–southwest fault with a northwest–southeast fault (Fig. 3; Edwards et al., 1991). Further investigation is highly recommended.

North of Lake Athabasca, arsenic appears to be associated with nickel. The nickel–arsenic association is a common one in in both massive sulphide deposits and unconformity-hosted uranium deposits (Levinson, 1980). The Paleozoic–Proterozoic contact, particularly where it follows the course of the Slave River, is well defined by anomalous nickel and copper values in lake sediments. Similar but more restricted than the distribution pattern of high zinc values, anomalous nickel and copper values may be related to stratiform mineralization noted by Edwards et al. (1991) in Paleozoic dolomite above a Precambrian regolith. One other area of elevated nickel and copper values in lake sediments occurs along the northeast-trending section of the Rutherford Fault, in Slave granitoids, at the intersection with a number of east-trending faults (Fig. 3). Although the highest mean value for copper is from lake sediments overlying the Colin Lake granitoids, interestingly enough, the highest individual value is located over Manitou Falls Formation sandstones, in an area mapped by Bayrock (1972) as glaciofluvial sands and gravels. Nickel values are somewhat elevated in this area, in the 80th to 90th percentile range. As noted above in the discussion on gold, these anomalies may be the result of selective weathering of these elements from the generally coarse glaciofluvial and supraglacial overburden, rather than a reflection of the underlying bedrock.

CONCLUSIONS

Regional lake sediment surveys are used to quickly and economically evaluate the mineral potential of large areas of the Canadian Shield. As the focus narrows to specific areas, however, a higher degree of interpretation is required to evaluate geochemical results. There are no universal rules that can be applied to interpret geochemical results from different areas. The nature of the overburden and the geology, mineralogy, topography and chemistry of a lake basin can all play major roles affecting the concentration and distribution of an element within a catchment basin.

Within the survey area, the interpretation of analytical results varies considerably north and south of Lake Athabasca. North of Lake Athabasca, the

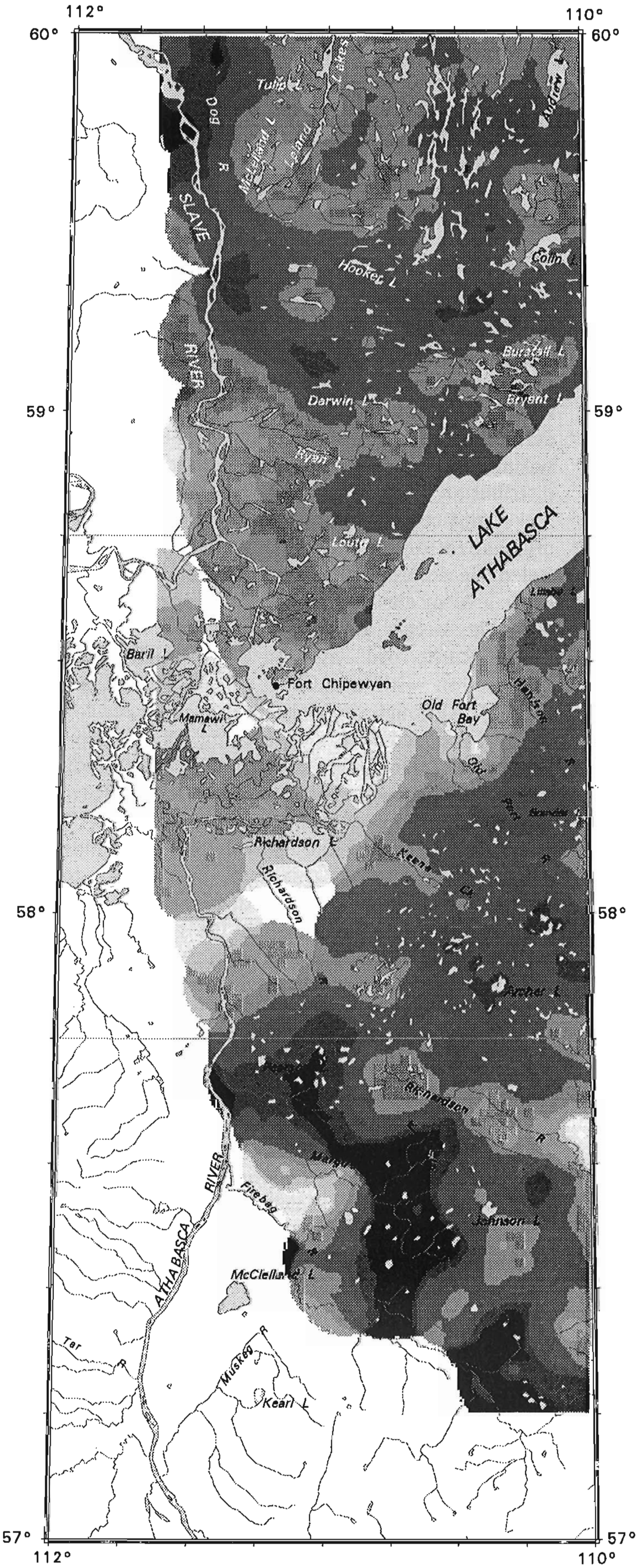

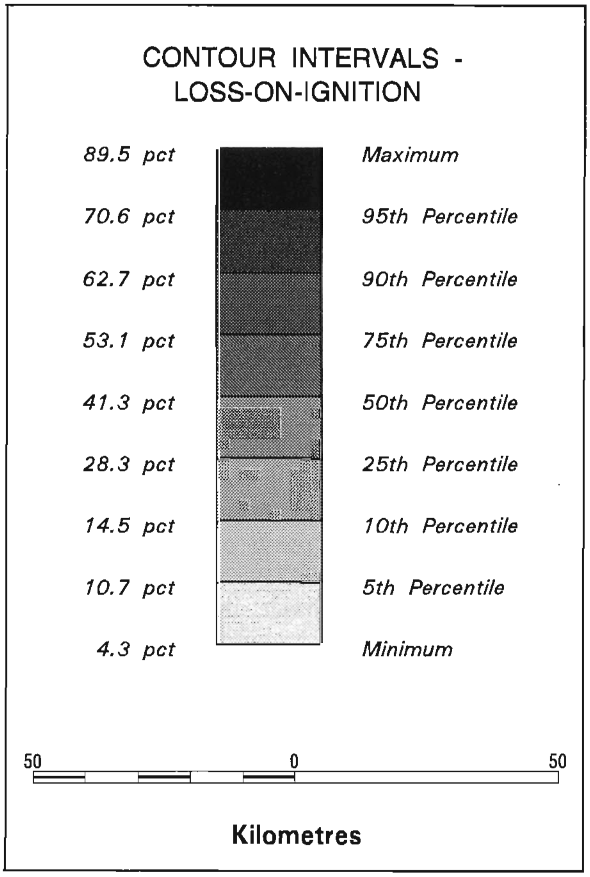

Figure 15. *Map showing relative loss-on-ignition values in lake sediments, with contoured log_{10} data divided into eight percentile-based classes.*

major features of the landscape controlling geochemical results are the bedrock and structural geology. In the south, glacial processes have a significant effect on analytical values and subsequent interpretation of the results.

Based on geochemical profile, the uranium potential in the survey area is moderate. The areas of particular interest are at fault intersections in Slave granitoids and high-grade metasediments.

There is some potential for gold, including the possibility of placer deposits over areas of Athabasca sandstone. Shear zone-hosted gold in northern parts of the survey area is suggested by above-average gold values in some areas. Finally, a closer examination of the granitoid rocks north of Johnson Lake is recommended, based on an unusually high antimony value and an associated gold anomaly.

Only eight of the 35 elements determined for Friske et al. (1994a) have been examined in this report: all elements, as well as uranium and fluoride in waters, could be useful to the prospector seeking to outline areas for detailed exploration. Alone, lake sediment geochemical data can be used to outline broad regional trends; with related geological data, the search can be narrowed to specific areas. As a result of the Canada–Alberta Agreement on Mineral Development (1992–1995), a wealth of geochemical, geological, and geophysical information has been made available for mineral exploration in northeastern Alberta, considerably improving the prospects of an economic discovery.

Acknowledgments

The author thanks P.W.B. Friske for providing valuable comments and suggestions, and S.J.A. Day, H. Gross, R. Balma, J.J. Lynch, and C.C. Durham for assistance with the preparation of Friske et al. (1994a). Sample collection for Friske et al. (1994a) was carried out by Northway Map Technology, Limited, Don Mills, Ontario. Lake sediment samples were prepared by Bondar-Clegg and Company Limited, Gloucester, Ontario. Lake sediments were analyzed by Becquerel Laboratories, Mississauga, Ontario, and Bondar-Clegg and Company Limited. Lake waters were analyzed by CanTech Laboratories, Calgary, Alberta. The lake sediment and water regional geochemical reconnaissance survey was carried out under the auspices of the Canada–Alberta Mineral Development Agreement (1992–1995).

REFERENCES

Bayrock, L.A.

1971: Surficial geology, Bitumount NTS 74E. Alberta Research Council, Map 34, scale 1:250 000 with marginal notes.

1972: Surficial geology, Fort Chipewyan NTS 74L. Alberta Research Council, Map 141, scale 1:250 000 with marginal notes.

Bednarski, J.M.

1994: Generalized Surficial Geology of Northeastern Alberta (NTS 74M and 74L North). Abstract presented at MEG, Calgary Mining Forum, April 1994.

1997: (*this volume*) Quaternary geology along the shield margin, northeastern Alberta. *In* Exploring for Minerals in Alberta: Geological Survey of Canada Geoscience Contributions, Canada–Alberta Agreement on Mineral Development (1992–1995), R.W. Macqueen (ed.). Geological Survey of Canada, Bulletin 500, p. 81–105.

Charbonneau, B.W., Holman, P.B., and Hetu, R.J.

1994: Airborne Geophysical Survey, Northeast Alberta, 1994. Geological Survey of Canada, Open File 2807.

Colvine, A.C., Fyon, J.A., Heather, K.B., Marmont, S., Smith, P.M., and Troop, D.G.

1988: Archean Lode Gold Deposits in Ontario. Ontario Geological Survey, Mines and Minerals Division, Miscellaneous Paper 139, 136 p.

Edwards, W.A.D., Richardson, R.J.H., and Fildes, B.J.

1991: Geology and Metallic Mineral Potential of Northeastern Alberta. Alberta Research Council, Open File 1991-6.

Friske, P.W.B.

1985a: Regional geochemical reconnaissance: interpretation of data from the north shore of Lake Superior. Geological Survey of Canada, Paper 84-21, 38 p.

1985b: Regional geochemical reconnaissance: interpretation of data from the Rainy Lake-Quetico area, northwestern Ontario. Geological Survey of Canada, Paper 84-20, 24 p.

1991: The application of lake sediment geochemistry in mineral exploration. *In* Exploration Geochemistry Workshop, Geological Survey of Canada, Open File 2390.

Friske, P.W.B. and Hornbrook, E.H.W.

1991: Canada's National Geochemical Reconnaissance Program. *In* Transactions of the Institution of Mining and Metallurgy, Section B, Volume 100, p. 47–56.

Friske, P.W., McCurdy, M.W., Day, S.J., Gross, H., Balma, R.G., Lynch, J.J., and Durham, C.C.

1994a: National Geochemical Reconnaissance lake sediment and water data, northeastern Alberta (Parts of NTS 74E, 74L, and 74M). Geological Survey of Canada, Open File 2856.

1994b: National Geochemical Reconnaissance lake sediment and water data, northwestern Saskatchewan (Parts of NTS 74N and 74O). Geological Survey of Canada, Open File 2858.

Garrett, R.G.
1991: The management, analysis and display of exploration geochemical data. *In* Exploration Geochemistry Workshop, Geological Survey of Canada, Open File 2390.

Garrett, R.G. and Hornbrook, E.H.
1976: The relationship between zinc and organic content in centre-lake bottom sediments. Journal of Geochemical Exploration, v. 5, p. 31-38

Levinson, A.A.
1980: Introduction to Exploration Geochemistry, Second Edition. Applied Publishing Limited, Wilmette, Illinois, 924 p.

McDonough, M.R. (*this volume*)
1997: Structural controls and age constraints on sulphide mineralization, southern Taltson magmatic zone, northeastern Alberta. *In* Exploring for Minerals in Alberta: Geological Survey of Canada Geoscience Contributions, Canada-Alberta Agreement on Mineral Development (1992-1995), R.W. Macqueen (ed.). Geological Survey of Canada, Bulletin 500, p. 13-29.

Ruzicka, V. (*this volume*)
1997: Metallogenic features of the uranium-polymetallic mineralization of the Athabasca Basin, Alberta, and a comparison with other parts of the basin. *In* Exploring for Minerals in Alberta: Geological Survey of Canada Geoscience Contributions, Canada-Alberta Agreement on Mineral Development (1992-1995), R.W. Macqueen (ed.). Geological Survey of Canada, Bulletin 500, p. 31-79.

Shilts, W.W.
1991: Principles of glacial dispersal and sedimentation *In* Exploration Geochemistry Workshop, Geological Survey of Canada, Open File 2390.

1993: Geological Survey of Canada's contributions to understanding the composition of glacial sediments. Canadian Journal of Earth Sciences, v. 30, p. 333-353.

Timperley, M.H., Jonasson, I.R., and Allan, R.J.
1973: Sub-aquatic organic gels: A medium for geochemical prospecting in the southern Canadian Shield. Geological Survey of Canada Report of Activities, Paper 73-1, Part A, p. 58-62.

Wilson, J.A.
1985: Geology of the Athabasca Group in Alberta. Alberta Research Council, Alberta Geological Survey, Bulletin No. 49, 78 p.

DATA INTEGRATION STUDY FOR MINERAL POTENTIAL MAPPING IN NORTHEASTERN ALBERTA[1]

C-J. Chung, A.N. Rencz, and A. Zhang
Mineral Resources Division, Ottawa

Abstract

A preliminary data integration study was conducted for a part of the Canadian Shield in northeastern Alberta to produce mineral potential maps. Digital data sets of geology, geophysics, geochemistry, mineral occurrences and remote sensing information were compiled and registered to a common coordinate system, thus forming a number of discrete layers of digital data. Several modelling procedures were developed to integrate the data to produce mineral potential maps. One of these procedures is the logistic discriminant function model. The application of this model involves using statistical correlations among data layers and gold occurrences at the locations of known gold occurrences in the study area to predict the potential for unknown gold occurrences elsewhere in the study area. A training area was used to construct a statistical relationship among 27 of the 36 known gold occurrences in the area and the 14 layers of input data. The statistical relationship derived from the training area was then applied to the entire area. Application of the discriminant function model over the entire area successfully predicts the occurrence of more than 75% of the known gold occurrences in the area.

Résumé

Afin de produire des cartes du potentiel minéral d'une portion du Bouclier Canadien dans le nord-est de l'Alberta, on a réalisé une étude sur l'intégration de données provisoires. On a procédé à la compilation et à la conversion, dans un système de coordonnées commun, des ensembles de données sur la géologie, la géophysique, la géochimie et les indices minéralisés de même que de l'information obtenue par télédétection; il en a résulté plusieurs couches distinctes de données numériques. De nombreux procédés de modélisation ont été élaborés pour intégrer les données et ainsi produire des cartes du potentiel minéral. L'un de ces procédés est le modèle de fonction discriminante logistique. L'application de ce modèle consiste à établir des corrélations statistiques entre les couches de données et les indices connus de minéralisation aurifère dans la région à l'étude, afin de prévoir le potentiel d'y découvrir d'autres indices. Une aire d'apprentissage a servi à établir une relation statistique entre 27 des 36 indices d'or de la région et les 14 couches des données d'entrée. La relation en question a ensuite été extrapolée à l'ensemble de la région. Le modèle de fonction discriminante appliqué à toute la région a pu prédire plus de 75 % des indices connus de minéralisation aurifère.

INTRODUCTION

As a part of the Canada-Alberta Agreement on Mineral Development (1992-1995), Northeastern Minerals Subprogram, a spatial data integration study for mineral potential mapping in northeastern Alberta was initiated. The study had three objectives:

(i) compile data from a variety of data sources into a common coordinate system;

(ii) provide these data in image and digital format; and

(iii) develop and illustrate a methodology of resource assessment.

The study area covers most of map sheet 74M. In this area, data were compiled and integrated into a database consisting of the following five parts, shown diagrammatically in Figure 1.

[1]Canada-Alberta Agreement on Mineral Development, Project C1.16

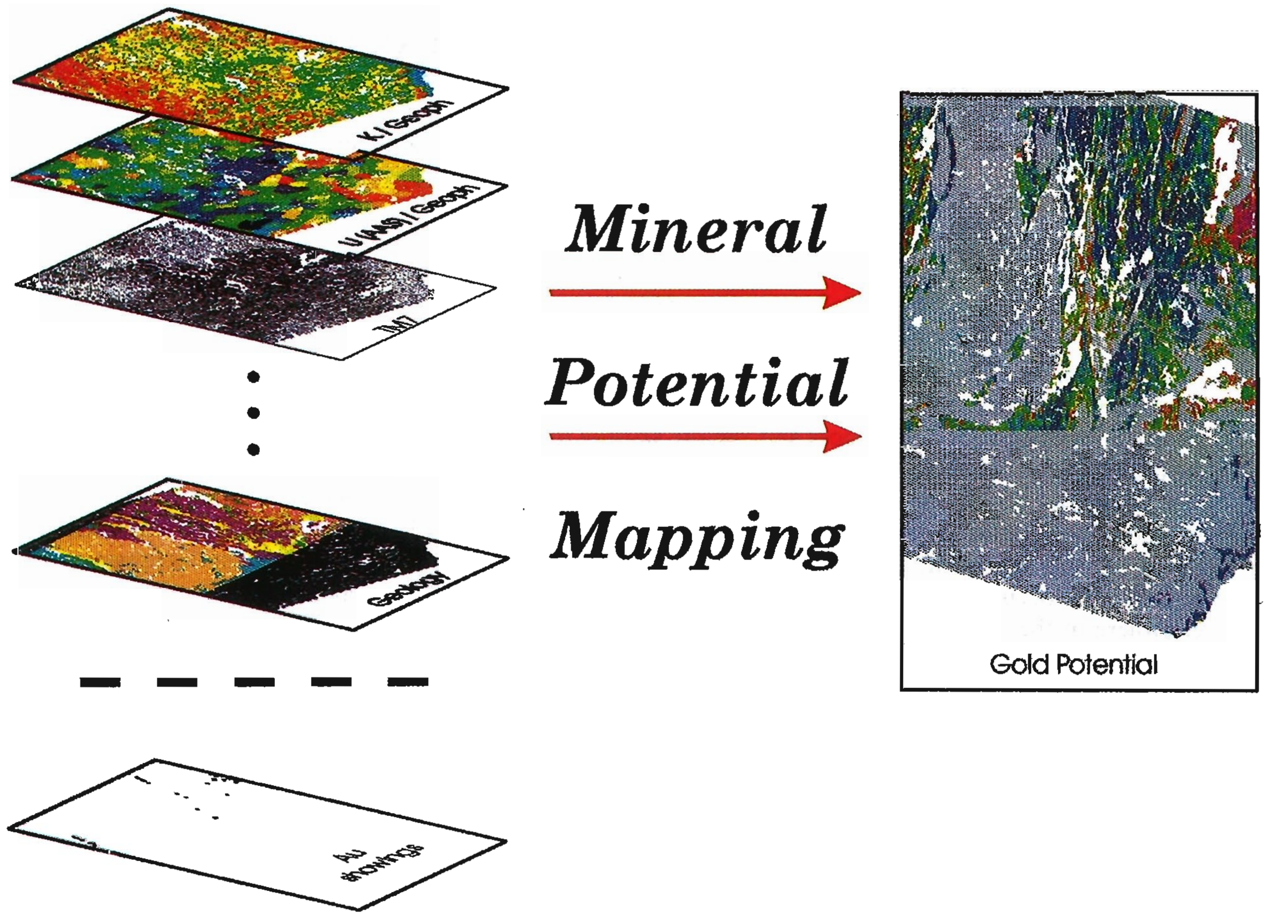

Figure 1. Schematic representation of the process of making potential maps.

(i) Remotely sensed (satellite) data
- seven channels of LANDSAT TM (thematic mapper) data
- one channel of ERS-1 SAR (synthetic aperture radar) data

(ii) Geophysical data (airborne geophysics)
- Radiometric survey (total count, K, eU, eTh, eTh/eK, eU/eK, eU/eTh)
- E-M (total field VLF) and aeromagnetic survey

(iii) Mineral occurrence data (Au, Cu, Mo, U, graphite and granite)
- Locations and descriptions of mineral occurrences

(iv) Lithological data
- Bedrock lithology

(v) Geochemical data
- 634 lake sediment samples (35 elements)

A GSC Open File covering the first two objectives of the study as noted above is being prepared for publication (C.F. Chung, pers. comm., 1995). It will contain the above database on CD-ROM and software for viewing the data using a PC.

As a part of the study, several quantitative data integration techniques are being developed for mineral potential mapping. One of the techniques has been applied to obtain the gold potential maps shown in Figures 2 and 3.

INPUT DATA

Remotely sensed data

LANDSAT TM data

Seven bands of LANDSAT TM data acquired on September 13, 1989, were used. The spatial and spectral characteristics of the data are presented in Table 1.

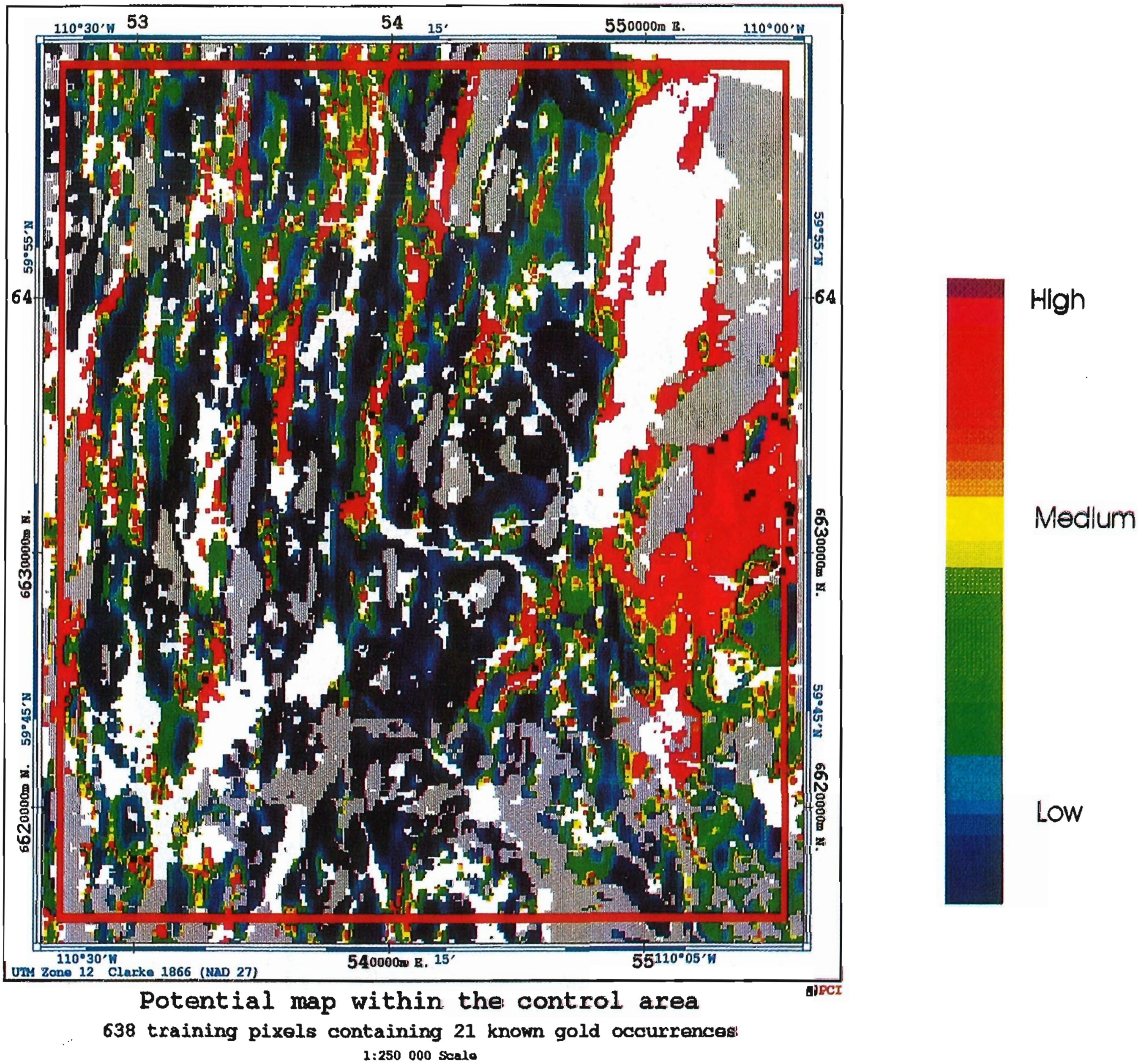

Figure 2. *The training area, showing the results of logistic discriminant analysis.*

ERS-1 SAR data

The radar data used herein were acquired on November 7, 1992. Their radiometric and spatial characteristics are listed in Table 2.

Geophysical data

Radiometric data and magnetic data

The original data were released by Charbonneau, Holman, and Hetu (1994). These data include three maps of the ground concentration of potassium (K), equivalent uranium (eU) and equivalent thorium (eTh), three ratio maps (eU/eTh, eU/K and eTh/K), the total field, a VLF map, magnetic total field map, and calculated magnetic vertical gradient maps. The data cover 74M and part of 74L.

The integrated data include a subset of the data mentioned above: 7 channels of radiometric data, total count, potassium (K), equivalent thorium/potassium (RTK), equivalent uranium/potassium (RUK), equivalent uranium/thorium (RUT), equivalent thorium (Th), equivalent uranium (U), one channel of

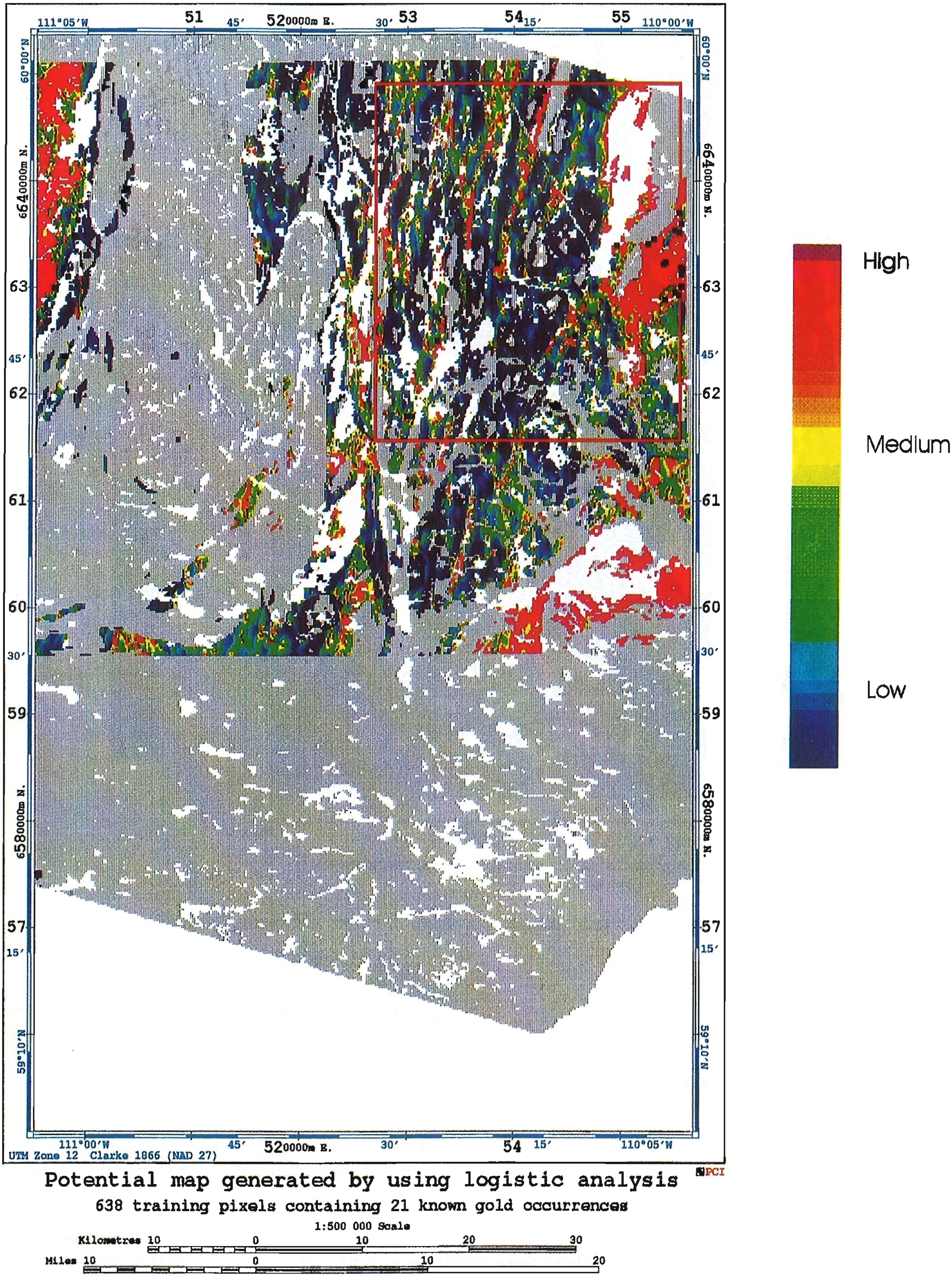

Figure 3. *The whole study area, showing the overall predictions.*

Table 1

Spatial and spectral characteristics of LANDSAT TM Channels.

LANDSAT TM CHANNEL	Wavelength (*nm*)	Pixel size original/resampled (*m*)
Channel 1	450–520	30/30
Channel 2	520–600	30/30
Channel 3	630–690	30/30
Channel 4	760–900	30/30
Channel 5	1550–1750	30/30
Channel 6	10 300–12 500	120/30
Channel 7	2080–2035	30/30

Table 2

Spatial and radiometric characteristics of ERS-1 data.

Parameter	
Wavelength (cm)	5.66cm
Polarization	VV
Pixel size (m)	30 m ground resolution
Incidence Angle (degrees)	23.0 3.0

VLF data, and one channel of magnetic data. The 8 bit (0–255) data presented were derived from the original 16 bit (0–32768) data for radiometrics and the 32 bit real numbers for magnetics by rescaling the minimum and maximum values to 0 and 255 respectively. Therefore each channel contains only 256 possible gray levels.

Mineral occurrence data

Mineral occurrences were classified into six types according to the principal element or commodity contained: gold, copper, uranium, granite, graphite, and molybdenum. These data, obtained from Price, Hamilton, and Fildes (1993), contain 36 gold, 4 copper, 107 uranium, 19 granite, 18 graphite, and 17 molybdenum occurrences.

Lithological data

Geological maps

For the Northeastern Minerals Subprogram, six geological maps were prepared at a scale of 1:50 000 by McDonough et al. (1994a–e, 1995), and the original linework was provided in digital form by M.R. McDonough (pers. comm.). The six maps were then compiled into one coverage using Arc/Info.

Geochemical data

The lake sediment geochemical data previously released by Friske et al. (1994) include 35 elements plus LOI in sediments, and uranium, fluoride and pH in waters based on analysis of 1160 samples taken in 1993.

In the area selected for the integration study, there are 634 samples with results on 35 elements plus pH and LOI (these 634 samples came from the original 1160 samples). Using the 634 sample points, the study area was divided into nonoverlapping Voronoi polygons and then rasterized into 2052 x 3421 pixels of the unit size 30 m x 30 m. Voronoi interpolation implies that the nearest neighbor pixels were assigned the same value as the closest sample point. The original observed measurements were converted to percentile values by reordering the 634 values for each element. As an example, 634 observed measurements for As (arsenic) were reordered by decreasing value. Samples with the highest 6 (1% of 634) values were assigned "99" (above 99%), the next highest 7 (2% of 634 minus the first 6) were assigned "98" (between 98% and 99%), and so on. The data in the map were these percentile values, from 1 to 99. All sample values below the analytical detection limit were assigned "0", however.

All the layers were co-registered using the projection shown in Table 3 and illustrated in Figure 1. The database contains 55 channnels. The file is 2052 pixels by 3421 lines.

Table 3

Geographic projection for the data.

Projection	Universal Trans-Mercator
Ellipsoid	Clarke 1866
NAD	NAD 27
Scale	0.9996
Zone	12
Pixel size	30 m
Min. Easting	495206
Max. Easting	556739
Min. Northing	6550999
Max. Northing	6653599

EXAMPLE OF MINERAL POTENTIAL MAPPING

The construction of mineral potential maps (Fig. 1) using quantitative methods is based on two fundamental assumptions:

(i) The quantitative models used can adequately characterize genetic models of mineral deposit types using the input data.

(ii) Such models can be constructed based on statistical relationships between known mineral deposit types and the input data.

One of the data integration techniques developed for mineral potential mapping in this study was the logistic discriminant function (C.F. Chung, pers. comm., 1995). The mineral potential model applied here utilized some of the data described above: airborne geophysics, lake sediment geochemistry, and lithologic maps. In this model, the location and observed measurements of these data layers at known gold occurrences were used to predict the potential for undiscovered gold occurrences.

For this preliminary study, we used several processing steps to construct the model. We sampled only one pixel for every 4 x 4 (16) pixels in order to reduce computational complexity. This procedure implies that each pixel in this study indirectly represents a 120 m x 120 m area. From our previous experience (C.F. Chung, pers. comm., 1995), such sampling appears adequate to develop quantitative models.

As a first step in the construction of the model, we selected only three of the 35 geochemical layers: Au, As and Sb. Quantifying thematic maps, such as geological maps, is one of the difficulties in applying quantitative models for mineral potential mapping. For this preliminary study, the 26 lithological units in the geological map were numbered from 1 to 26 in an order determined by statistical relationships between the 36 known gold occurrences and the 26 lithological units. The ordered numbers were used for the quantitative model. It is also possible to apply geological knowledge of the gold occurrences to reorder the ordered numbers before using them for the quantitative analysis.

All nine geophysical layers were selected: seven radiometric, one VLF, and one aeromagnetic. For the remotely sensed data, only ERS-1 SAR data was selected for the analysis. The 14 layers discussed and 36 known gold occurrences as shown in Figure 1, were used as input data.

A training area in the northeast corner of the study area containing 240 x 280 pixels (30 km x 33.6 km) is shown in Figure 2. Within this training area, 11 pixels contain the known 27 gold occurrences and represent a "gold occurrence area". Outside of the 118 pixels, 520 pixels were randomly selected and they represent a "no gold occurrence area". Logistic discriminant analysis was performed on these 638 pixels (118 + 520) to determine statistical relationships between the known gold occurrences (21 of the 36 occurrences) and the 14 layers of input data. The results of logistic discriminant classification modelling (C.F. Chung, pers. comm., 1995) for gold based on the 21 gold occurrences in the training area are shown in Figure 2. The pixels have been divided roughly into four classes: reddish, yellowish, greenish and bluish colours. Reddish coloured pixels represent very high potential for gold mineralization, whereas bluish colours represent the lowest potential. As can be seen in Figure 2, all except two known occurrences (out of 21) are located in reddish, high potential areas.

We extended this logistic model from the training area to the whole study area. The overall predictions are shown in Figure 3. The high potential area, illustrated by reddish coloured pixels, occupies only 2.3% of the whole study area, but contains 30 of the 36 known gold occurrences (over 80% of the known gold occurences). The prediction in the training area (the northeast corner) of Figure 3 is, of course, identical to that of Figure 2. There are 15 known gold occurrences (seen in Figure 2) outside the training area which were not used to construct the logistic model. Of these 15 outside occurrences, 11 are located in the high potential reddish area shown in Figure 3.

In this example, a logistic discriminant model has not only adequately characterized the gold mineralization in the training area from SAR, geophysical, geochemical, and geological data, but also accurately (73%: 11 out of 15) predicted the known occurrences in the area outside of the training area.

Technical aspects of the logistic discriminant analysis and other quantitative modelling procedures and results will be the focus of future papers.

Acknowledgments

We wish to thank D.F. Garson of the Geological Survey of Canada who produced Figure 1 and C.W. Jefferson and R.W. Macqueen of the Geological Survey of Canada who read an earlier draft of the manuscript and provided many useful comments.

REFERENCES

Charbonneau, B.W., Holman, P.B., and Hetu, R.J.
1994: Airborne Geophysical Survey: Northeast Alberta. Geological Survey of Canada, Open File 2807.

Friske, P.W., McCurdy, M.W., Day, S.J., Gross, H., Balma, R.G., Lynch, J.J., and Durham, C.C.
1994: Regional lake sediment and water geochemical data, northeastern Alberta (Parts of 74E, 74L and 74M). Geological Survey of Canada, Open File 2856.

McDonough, M.R., Cooley, M.A., and Schetselaar, E.M.
1994a: Geology, Hay Camp (74M/11), Alberta. Geological Survey of Canada, Open File 2832.

McDonough, M.R., Grover, T.W., McNicoll, V.J., Cooley, M.A., Schetselaar, E.M., and Robinson, N.N.
1994b: Geology, Cornwall Lake (74M/10), Alberta. Geological Survey of Canada, Open File 2896.

McDonough, M.R., Grover, T.W., McNicoll, V.J., Cooley, M.A., Schetselaar, E.M., Robinson, N.N., and Bednarski, J.
1995: Geology, Colin Lake (74M/9), Alberta-Saskatchewan, scale 1:50 000. Geological Survey of Canada, Open File 3047.

McDonough, M.R., Grover, T.W., McNicoll, V.J., Lindsay, D.D., Kelly, K.L., and Guerstein, P.G.
1994c: Geology, Tulip Lake (74M/14), east-half, Alberta-Northwest Territories. Geological Survey of Canada, Open File 2820.

1994d: Geology, Mercredi Lake (74M/15), Alberta-Northwest Territories. Geological Survey of Canada, Open File 2904.

1994e: Revised geology, Andrew Lake (74M/16), Alberta-Saskatchewan-Northwest Territories. Geological Survey of Canada, Open File 2905.

Price, M., Hamilton, W., and Fildes, B.
1993: Alberta Mineral Deposits and Occurrences. Alberta Geological Survey, Open File Report 1991-17.

PETROLOGY AND ECONOMIC GEOLOGY OF THE CROWSNEST VOLCANICS, ALBERTA[1]

T.D. Peterson, K.L. Currie, E.D. Ghent[2], N.J. Bégin[2], and R.E. Beiersdorfer[3]
Continental Geoscience Division, Ottawa

Abstract

The Crowsnest Volcanics are lower Cretaceous (ca. 100 Ma) epiclastic and volcanic rocks exposed in west dipping, Tertiary thrust stacks in southwestern Alberta. Nearly all of the volcanic rocks are mildly potassic trachytes and phonolites (average 1.4 wt% K_2O/Na_2O) with phenocrysts of sanidine, clinopyroxene, titanite, melanite, and analcite; apatite is abundant in some cumulate xenoliths. An unusual pyroclastic unit contains strongly potassic juvenile fragments rich in biotite, leucite (converted to potassium feldspar) and sulphides. In the phonolites, fresh analcite, up to 3 cm in diameter, has magmatic $\partial^{18}O$ (9.5‰), occurs as sealed inclusions in other phenocrysts, and has normal and reverse K and Fe zoning profiles that match associated sanidine phenocrysts. The analcite is interpreted as a primary high-pressure, low-temperature phenocryst phase (ca. 7 kbar, 700°C). Whole rock samples do not display geochemical patterns, such as negative Eu anomalies, that are consistent with crystal fractionation of alkali or transitional basalt. Rare earth element (REE) patterns are highly fractionated with flat heavy REE, consistent with equilibration with a garnet-rich residue. The markedly negative E_{Nd} composition and the bulk Earth-like Sr composition of Sr from the Crowsnest Volcanics resembles that of some strongly potassic rocks of the Churchill and Wyoming Archean provinces. The Crowsnest magmas probably originated by partial melting of moderately metasomatized lithosphere, near the crust-mantle boundary (25-30 km). Primary gold and base metal concentrations are noneconomic; low-grade metamorphism did not produce anomalous vein or stratiform concentrations.

Résumé

Les volcanites de Crowsnest sont des roches épiclastiques et volcaniques du Crétacé inférieur (vers 100 Ma), qui affleurent dans le sud-ouest de l'Alberta sous la forme d'empilements à pendage ouest résultant d'un épisode de chevauchement au Tertiaire. Presque toutes les volcanites sont des trachytes et des phonolites faiblement potassiques (moyenne de 1,4 % en poids de K_2O/Na_2O), contenant des phénocrisatux de sanidine, de clinopyroxène, de sphène, de mélanite et d'analcime; l'apatite abonde dans certains xénolites de cumulats. Une unité pyroclastique inhabituelle contient des fragments juvéniles fortement potassiques riches en biotite, en leucite (transformée en feldspath potassique) et en sulfures. Dans les phonolites, l'analcime inaltérée, mesurant jusqu'à 3 cm de diamètre, a une valeur de $\partial^{18}O$ (9,5‰) qui témoigne d'une source magmatique et se présente sous la forme d'inclusions scellées dans d'autres phénocristaux; les profils de zonation du potassium et du fer sont normaux et inverses, tout comme ceux des phénocristaux de sanidine associés. L'analcime est interprétée comme une phase primaire de formation de phénocristaux dans des conditions de pression élevée et de température basse (env. 7 kbar, 700°C). Les échantillons de roche totale ne présentent pas de tendances géochimiques, comme des anomalies négatives en Eu qui sont représentatives d'une différenciation magmatique des basaltes alcalins ou de transition. Les spectres des terres rares sont fortement différenciés, caractérisés par une portion de courbe plate au niveau des terres rares lourdes, ce qui correspond à un équilibre avec un résidu riche en grenat. Les valeurs de E_{Nd} nettement négatives et la teneur en strontium des volcanites de Crowsnest (semblable à la teneur globale en strontium de la Terre) s'apparentent à celles de certaines roches fortement potassiques des provinces archéennes de Churchill et de Wyoming. Les magmas de Crowsnest

[1]Canada-Alberta Agreement on Mineral Development, Project C1.21
[2]Department of Geology and Geophysics, The University of Calgary, Calgary, Alberta T2N 1N4
[3]Department of Geology, Youngstown State University, Ohio, USA, 44555-3612

résultent probablement de la fusion partielle d'une lithosphère modérément métasomatisée, près de la limite croûte-manteau (25-30 km). Les concentrations d'or et de métaux communs n'ont pas de valeur économique; le faible métamorphisme n'est pas à l'origine de concentrations anomales, sous la forme de gîtes filoniens ou stratiformes.

INTRODUCTION

The volcanogenic Crowsnest Formation (CNF) was first recognized and mapped by Dawson (1885). Outcrops are restricted to the area between the Highwood River and Mill Creek in southwestern Alberta, where east-verging thrust faults in the foothills expose Mesozoic formations rich in coal and subsurface gas and oil (Fig. 1). Excellent exposures of the volcanogenic rocks are located in the Blairmore area (NTS 82G) (Fig. 2), which lent its name to blairmorite (a.k.a. analcite phonolite), a rare rock type that is abundant in the formation. North of Coleman, the Crowsnest Formation reaches its greatest thickness of about 600 m and thins rapidly in all directions (Norris, 1964).

This region is celebrated for a legendary gold deposit (the Lost Lemon Mine) that was found, lost, found again, and re-lost. A recent report in a popular periodical (Johnson, 1989) suggested that the CNF may be locally rich in gold. The Crowsnest Formation itself has been controversial for decades. Petrologists and field geologists have mostly concluded that the large, euhedral analcite crystals are primary phenocrysts (e.g., Pearce, 1970; Ferguson and Edgar, 1978). More detached theoretical petrologists have argued that the physical conditions necessary to generate such phenocrysts are extreme, and that it is probable that the analcite is secondary after leucite (e.g., Karlsson and Clayton, 1991). Although this issue has been largely academic in the past, with the recent discovery of numerous primary diamond sources in western Canada, it has become important to establish whether or not the CNF was originally composed of ultrapotassic rocks. Ultrapotassic lamproites, which can be richly diamondiferous, often contain large amounts of leucite. Diamondiferous kimberlites erupted contemporaneously with the Crowsnest Formation (100 Ma) in a very similar floodplain environment at Fort a la Corne, Saskatchewan (B.A. Kjarsgaard and W. Davis, pers. comm., 1995).

Phonolitic rocks are commonly associated with carbonatites, which can be economic sources of numerous minerals. In addition, the CNF is known to have undergone low-grade regional metamorphism during faulting, introducing the potential of vein- or unconformity-hosted metal deposits. A reinvestigation of the CNF, with the purpose of resolving these issues, was made as part of the 1992–1995 Alberta MDA program. Igneous petrogenesis, volcanology, and primary mineralogy were studied by T. Peterson and K. Currie (GSC), and metamorphism and secondary mineralogy by E. Ghent, N. Bégin, and R. Beiersdorfer (University of Calgary). Detailed summaries of metamorphism and secondary mineralization are given by Bégin et al. (1995; pers. comm., 1995).

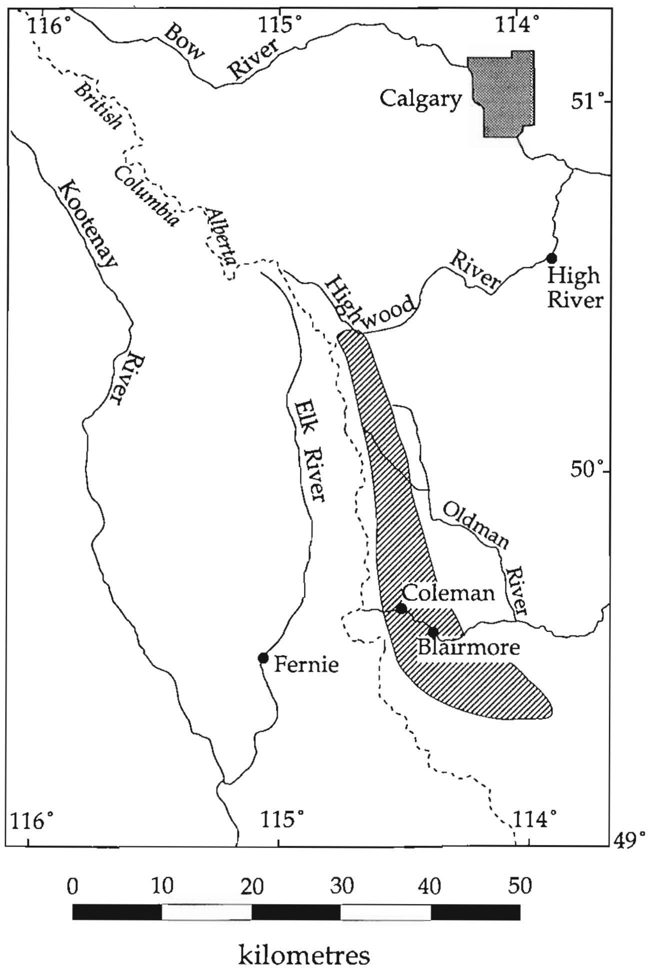

Figure 1. Location map of the area containing known outcrops of the Crowsnest Formation (ruled area).

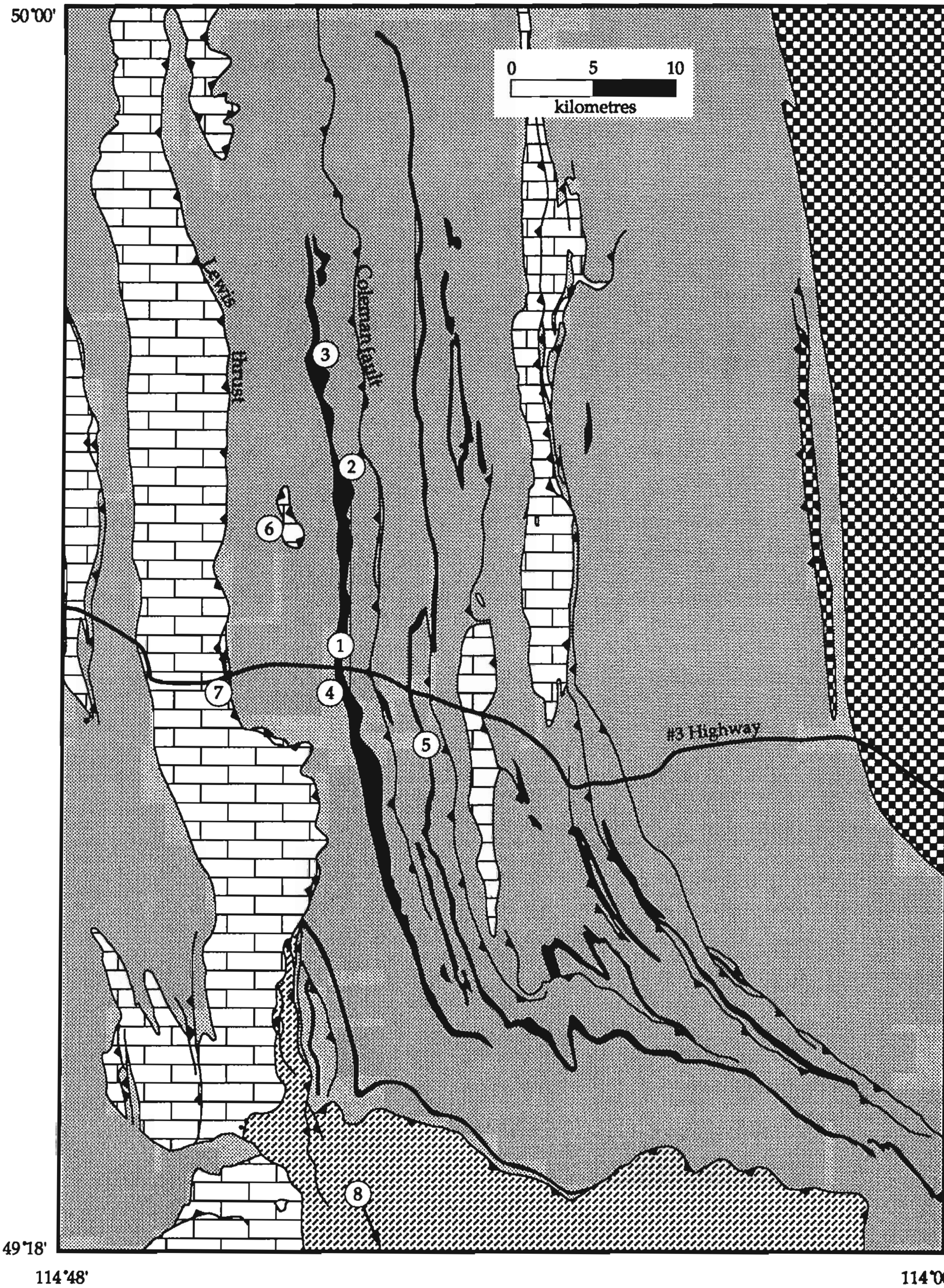

Figure 2. Geology of the Coleman–Blairmore area, Fernie map sheet (NTS 82G, west half). Adapted from Price (1962, pers. comm., 1993). Checkered, Tertiary rocks; shaded, Mesozoic rocks; brick pattern, Paleozoic rocks; dashed, Proterozoic rocks; black, Crowsnest Formation. Numbered circles refer to prominent outcrop sites: 1, Iron Ridge; 2, Ma Butte; 3, Racehorse Creek; 4, Star Creek; 5, Lynx Creek road; 6, Crowsnest Mountain dyke; 7, Crowsnest Lake dyke; and 8, Howell Creek (15 km in direction of arrow).

This study only addresses the potential for primary igneous and secondary (metamorphic) economic mineralization. Detrital gold, derived from contemporaneous unroofed plutons and metamorphic complexes to the west, may be present within the CNF and the underlying McDougall-Segur conglomerate (Norris et al., 1965; Leckie and Craw, 1996, in press).

REGIONAL GEOLOGY

The following descriptions are taken from Norris (1964) except where noted. The CNF conformably overlies the Blairmore Group. Interfingering of feldspar-rich, volcaniclastic sands and gravels with glauconitic or grey-green, silty sands and chert conglomerates is observed along the contact. The Blairmore Group consists of littoral marine and floodplain sediments that are often strongly calcareous. The basal Cadomin conglomerate of this group, and overlying crossbedded sandstones, have clasts and grains of chert, vein quartz, and quartzite, derived from Paleozoic limestones and Proterozoic siliciclastic rocks. The middle Blairmore Group has more feldspathic sandstone. Some conglomerates within the upper Blairmore Group contain about 10% igneous pebbles, which are mainly granites of uncertain provenance that do not resemble clasts within the CNF. However, some volcanic pebbles resembling trachytes of the CNF are present within the upper Blairmore Group (Norris et al., 1965).

In the Coleman area, the total thickness of Blairmore Group strata is about 700 m. Palinspastic reconstructions indicate an original thickness of over 2000 m about 50 km west of these exposures, and the sediment source was clearly an upland to the west and southwest. The environment was probably a floodplain, with lacustrine and braidplain deposition occasionally interrupted by swollen rivers arising in the western high ground. Chert-rich conglomerates that are especially prominent just below the Crowsnest Formation probably represent flood deposits.

Radiometric ages for the CNF and some correlated volcanic rocks range from 72 to 126 Ma. Folinsbee et al. (1957) reported a K-Ar age (sanidine) of 96 Ma for the CNF near Coleman. Amajour (1985) noted that the CNF is nearly isochronous with bentonites of the Viking Formation, which yield an average K-Ar age (biotite and sanidine) of 98 Ma (Tizzard and Lerbekmo, 1975). Norris et al. (1965) dated igneous pebbles from chert-quartzite conglomerates in the upper Blairmore Group, and from garnet-sanidine arkoses in the lower CNF. They obtained K-Ar ages of 113 to 174 Ma, somewhat older than other ages. The authors describe the pebbles as altered, and as being dacites and rhyodacites. Faunal studies indicate that the CNF is Albian (100–106 Ma) (Norris et al., 1965), and because 100 Ma is near the upper limit of radiometric ages of unaltered CNF and the Viking Formation, that is the assumed age in this study.

Trachytic dykes in the Flathead area yield K-Ar ages of 72 to 112 Ma, and are probably related to Crowsnest volcanism (Gordy and Edwards, 1962). An altered, porphyritic trachyte dyke 100 ft. below the top of Crowsnest Mountain yielded a whole-rock K-Ar age of 61 Ma. Carey (1991) described similar but undated dyke intruding Paleozoic limestone near the shore of Crowsnest Lake. In southeastern British Columbia, the trachytic Howell Creek intrusives cut strata as young as lower Blairmore Group. The age span of this regional igneous activity is not accurately known, but it is noteworthy that all of these rocks are uniformly trachytic in composition; no basaltic dykes or eruptive rocks have been recorded.

The CNF is disconformably overlain by shallow water marine black shales and siltstones of the Blackstone Formation. This represents a regional marine incursion, and Norris (1964) speculated that eruption of the Crowsnest volcanics occurred near the peak of uplift associated with the Columbian orogeny. The pre-Blackstone surface had modest relief (40 m?; Norris, 1964), consistent with additional uplift and erosion after deposition of the CNF.

FIELD DESCRIPTIONS

Previous field studies of the CNF have identified flows, domes, and various volcaniclastic and epiclastic rocks. In particular, Norris (1964) and Pearce (1967) interpreted locally thick accumulations within the formation as sites of enhanced flow activity. Two sites are prominent: Ma Butte, north of the Alberta #3 Highway; and Star Creek, south of the highway. These two sites encompass the range of rock types observed in this study (see also Peterson and Currie, 1993).

Ma Butte and Highway #3 outcrop (Iron Ridge)

The CNF is well exposed due north of Coleman along a series of peaks and ridges between the Lewis and Coleman thrust faults. West-dipping exposures begin at the highway and continue north to Racehorse Creek, where a spectacular cliff exposure of the formation is present. At Ma Butte, opposite (east of) Crowsnest Mountain, the CNF is about 450 m thick. The foot of Ma Butte is accessed by a fire road branching north from the highway, but the last 3 to 4 km are impassable by vehicle. The west slope of Ma Butte is parallel to the bedding near the upper contact of the formation; the rugged east slope gives an excellent cross-section through the formation down to its lower contact with a chert-pebble, nonvolcanogenic conglomerate at the top of the Blairmore Group.

Norris (1964) and Pearce (1970) interpreted this section as consisting mostly of sandy to silty crystal and lithic tuffs, with bombs of trachyte up to 10 cm, and rare flows. However, we recorded few lithologies, bed forms, or grain sorting features that were not compatible with fluvial erosion and redeposition of volcanic rocks. The exposures consist mainly of volcanogenic sandstone, conglomerate, and unsorted debris flows with both igneous clasts and silty to sandy intraclasts rich in sanidine and melanite. Locally, concentrations of very large trachyte boulders (up to 10 m) can give an impression of flows, particularly where exposures are 50% or less, but these could never be traced laterally to define continuous horizons (Fig. 3). Bed truncations, channel scours, caliche horizons, and synsedimentary faults are very common.

At the highway roadcut, an excellent outcrop of well-sorted, poorly indurated sandstone with distinctive pink (sanidine), black (melanite garnet), and green (matrix, clinopyroxene) grains, 0.5 to 3 mm in diameter, has weathered into loose sand grains. Bed forms are planar with little crossbedding, and typically persist for only a few meters before they are truncated by another sand bed or an unsorted debris flow. Similar outcrops, which could be mistaken for crystal tuffs, are very common in the area, particularly where they are rich in sand to pebble-sized clasts of fine grained trachyte.

Figure 3. *Tabular megablocks of trachyte in unsorted, trachyte-rich debris, Racehorse Creek. Although superficially resembling flows, the blocks cannot be traced horizontally. Person for scale.*

Unambiguous evidence for volcaniclastic, and especially pyroclastic rocks in this section is lacking, with one exception. On the south side of Highway 3, at the west edge of Coleman, a dark green-grey weathering outcrop contains rounded clasts of intrusive syenite, country rocks (mainly Blairmore Group siltstones), thin shards of coal, and flat, plastically deformed green-black volcanic fragments containing pyrite in a fine grained, schistose matrix. The matrix is rich in glassy lapilli (≈ 2 mm) with oxidized rims, and in angular grains of deformation-twinned carbonate and chert (the latter derived from Paleozoic limestones). We consider this to be a proximal volcanic deposit blanketed by trachytic sediments. This lithology extends north of the highway (Iron Ridge), where it overlies the trachyte sandstone, and the outcrop area extends southward down a slope into the outskirts of Coleman. This locale is the site of anomalous gold assays (Johnson, 1989).

In an environment where water-saturated, unconsolidated sediment is present (which was clearly the case for the CNF), primary volcanic deposits should be mainly phreatomagmatic deposits with vesicular tuffs, accretionary lapilli, and other characteristic features (Fischer and Schmincke, 1984). However, hydroclastic rocks and accretionary lapilli have never been described from the CNF. Nearly all igneous clasts are blocky and angular, consistent with erosion from thermally fractured domes and thin flows. Angular, glassy shards are rarely observed in sandstones and siltstones. In contrast, the common presence of intraclasts, and excellent sorting in many of the sandstones, are features consistent with erosion and redeposition in an alluvial fan setting or similar environment. We interpret the Ma Butte section as an assortment of fluvial deposits, mudstones, and matrix-supported debris flows with few volcanic features preserved. Some authors have interpreted the debris flows as lahars (e.g., Ricketts, 1982), but evidence for hot mud flows (such as steam-escape structures) was not noted.

Star Creek and Pipeline Road

The Star Creek and Pipeline Road localities are accessed by a road leading southwest from Coleman. A short walk of 100 m is necessary to reach Star Creek. A truck with excellent ground clearance is required on the Pipeline Road, which begins and ends with rutted dirt roads on steep inclines.

On Star Creek, a narrow gorge which ends in a cliff and waterfall exposes altered, massive analcite phonolite. The groundmass is pale green and clay-rich, and all analcite crystals are translucent white-orange to opaque white and green. Some green analcites are flattened or otherwise distorted. The outcrops are penetratively deformed by numerous microfaults with a spacing of about 0.1 to 1 m. Fine grained, 5 cm wide, grey-pink veins resembling felsite dykes are common; these are also faulted and have 10 cm alteration haloes. We interpret this outcrop as a phonolite dome displaying abundant hydrothermal alteration and synextrusive brittle faults.

Outcrops on the south side of the Pipeline Road consist of unsorted debris flows with angular clasts (0.01-3 m), mainly of analcite phonolite and reworked volcanogenic sandstone and conglomerate (Fig. 4). Fresh, dark green phonolite boulders contain resinous, transparent analcite. In slightly altered phonolites, large analcite crystals can be extracted by hand due to the formation of a thin, white, secondary rind on their surface. This locality provides the freshest igneous material available in the formation.

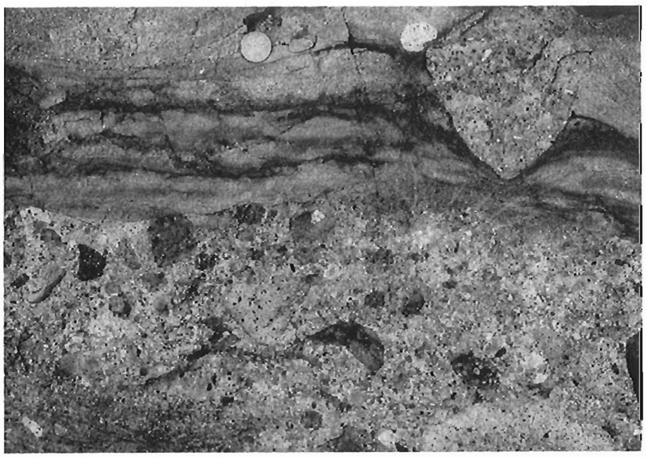

Figure 4. *Fine grained sandstone overlying unsorted, polymictic debris flow, Pipeline Road (near Star Creek). Clasts in the debris flow are dominantly of analcite-rich phonolite. The large block deforming the bedding in the sandstone is an intraclast nearly identical to the underlying debris and is not an igneous bomb. Penny for scale.*

PETROGRAPHY AND MINERALOGY

Primary igneous phases: trachytes and phonolites

Large blocks in the debris flows are excellent sources of fresh samples of volcanic rocks, which have a restricted mineral assemblage. Except for the melanocratic Iron Ridge tuffs, all of the samples collected contain phenocrysts of clinopyroxene (diopside-hedenbergite-aegirine solid solutions), melanite garnet, and sanidine. Titanite is a prominent accessory mineral in sanidine-rich samples, and euhedral analcite is very abundant in sanidine-poor samples. Rounded apatite phenocrysts are present in most samples. Euhedral magnetite is relatively rare and is restricted to the groundmass. Green-brown pleochroic biotite occurs as a late phase, partially replacing clinopyroxene, in some plutonic syenite clasts. The mineral assemblages indicate magma compositions ranging from trachyte to phonolite, with all liquids being close to critical silica saturation, or slightly undersaturated.

The phenocryst mineral assemblage was used to discriminate three rock types. Trachytes contain sanidine phenocrysts, with analcite very subordinate or absent. Blairmorites contain abundant analcite phenocrysts, with sanidine restricted to the groundmass and a small number ($<1\%$ by volume) of phenocrysts (Fig. 5). Analcite phonolites are intermediate between these extremes, with subequal analcite and sanidine.

Cumulate fragments consisting of clinopyroxene and melanite, and single macrocrysts of diopsidic clinopyroxene were found in two outcrops rich in tuffaceous rocks (Iron Ridge at Highway #3, and Lynx Creek road; Fig. 2). No evidence was found for the presence of mafic magmas containing olivine, hornblende, or phlogopite. The compositions of clinopyroxene and garnet are strikingly similar to those in phonolites from central nephelinite-phonolite volcanos (e.g., Peterson, 1989); however, the abundance of sanidine in the Crowsnest volcanics is high relative to these volcanos.

Clinopyroxene

Clinopyroxene is colourless to deep green in thin section and displays oscillatory zoning, with an overall trend to diopside-poor and aegirine-rich rims. Inclusions of all other phenocryst phases may be present, with apatite, melanite, and titanite inclusions most common. A 5 cm macrocryst from a pebble conglomerate (tuffaceous lag deposit?) which also contained melanite-clinopyroxene cumulates and crustal amphibolites, is the most magnesian pyroxene analyzed (Table 1).

Garnet

Euhedral melanite (titanian andradite) exhibits a range of 3.8 to 10.7% TiO_2 content (Table 1). Oscillatory

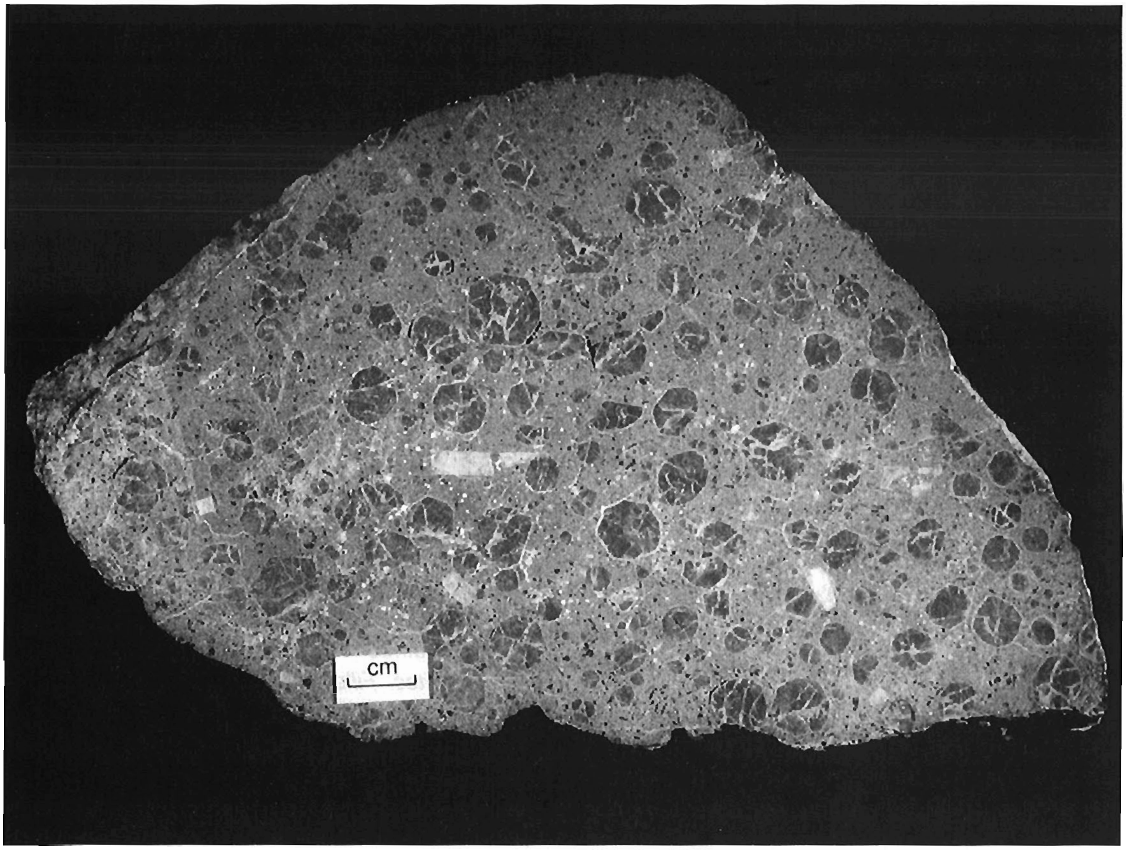

Figure 5. *Polished slab of blairmorite sample PHA-92-1006A. The reddish crystals are analcite; the pale wedge-shaped grain (left of center) is sanidine. The specimen is 17 cm wide. The sample is from the Pipeline Road locality.*

Table 1

Microprobe analyses of clinopyroxene and melanite phenocrysts.

Sample mineral	**1010B mel**	**1006B mel**	**1010B cpx***	**1010B cpx core**	**1010B →**	**1010B cpx rim**	**1006B cpx core**	**1006B cpx rim**	**1005E cpx****
SiO_2	34.09	30.38	51.57	54.21	51.09	51.57	49.79	49.50	54.42
TiO_2	3.80	10.73	0.30	0.03	0.23	0.37	0.35	0.72	0.29
Al_2O_3	2.30	0.88	0.45	0.17	0.94	0.50	0.83	1.30	0.72
FeO	23.73	23.39	17.88	8.81	16.79	18.90	15.55	19.23	3.71
MnO	0.39	0.47	0.43	0.48	0.69	0.58	0.55	0.52	0.08
MgO	0.34	0.38	7.04	12.76	7.94	6.32	8.22	6.32	16.73
CaO	32.34	31.30	19.12	22.32	20.26	18.04	20.25	18.81	24.69
Na_2O	0.02	0.20	3.54	1.84	2.80	3.94	1.98	3.06	0.21
K_2O	0	0	0.03	0.00	0.00	0.01	0.00	0.00	0.01
sum	97.09	97.91	100.41	100.82	100.91	100.22	97.52	99.57	100.95

*inclusion in analcite
**5 cm macrocryst

zoning is prominent, with an overall trend of lower Ti and higher Al toward the rim. Many melanocratic cumulate clasts consist of 75% or more of melanite, with subordinate apatite and clinopyroxene.

Sanidine

Analyzed sanidines have a compositional range of Or_{80} to Or_{90}. Phenocryst rims are enriched in Or relative to cores in most samples (Table 2), as has been reported elsewhere (e.g., Pearce, 1970; Goble et al., 1993). However, sample 1006A contains oscillatorily zoned sanidines with distinctly sodic rims. The sample has no other petrographic peculiarities, except for unusually deep green clinopyroxene. BaO ranges from 1 to 5%, and is negatively correlated with K_2O (Fig. 6). SrO, at about 0.5%, is not correlated with K_2O.

Analcite

Crystals up to 3 cm in diameter that exhibit the {211} cubic form occur in profusion in many phonolite samples. All of these now consist of analcite (Table 3). The colour, transparency, and inclusion content of the analcite varies considerably (e.g., Pearce, 1970). In the freshest phonolite samples, with dark green, flinty matrices, the analcite is tightly bonded to the matrix and is a transparent, pale yellow-brown with resinous reflectance and no internal fractures. In slightly altered samples, the matrix is a paler green and the analcites have a thin (ca. 100 μm) whitish rind which easily separates from the matrix. In thin section, these slightly altered analcites are seen to contain patches of oriented needles of exsolved hematite. With progressive alteration, the analcites become translucent white to orange-pink, with abundant hematite inclusions, then

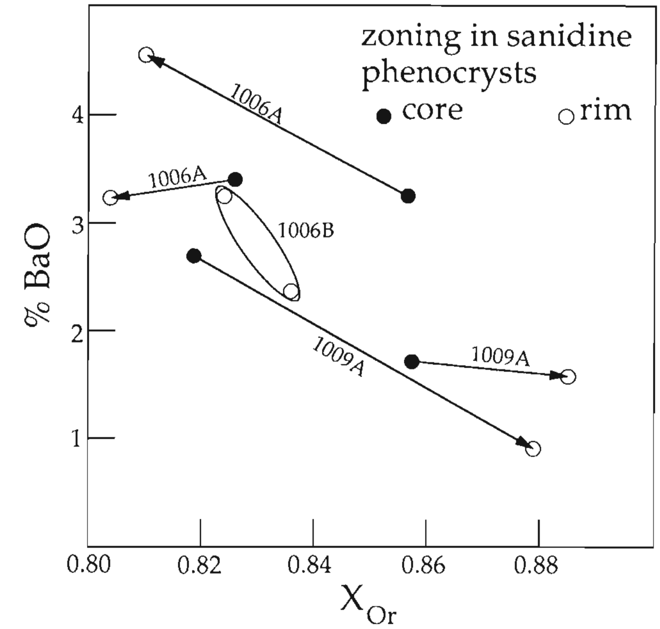

Figure 6. *Plot of %BaO versus X_{Or} for selected sanidines from analcite phonolites and blairmorites. Filled circles are phenocryst cores; open circles are phenocryst rims.*

opaque and pale green. Translucent analcites are commonly recrystallized and extensively twinned. Green analcites, commonly flattened or otherwise distorted, are prominent at the Star Creek locality, which is thought to be a dome with intense hydrothermal alteration. Extensively recrystallized analcite with wispy, bright green chlorite inclusions, but no hematite, was also noted at this locality.

Unaltered analcites contain prismatic inclusions of clinopyroxene about 1 μm long; some are large enough to be analyzed (Table 1). Armoured inclusions of

Table 2

Microprobe analyses of feldspar phenocrysts.

Sample notes	1006A core 1	1006A rim 1	1006A core 2	1006A rim 2	1006B mp	1006B mp	1009A core 1	1009A rim 1	1009A core 2	1009A rim 2	10.1* vein
SiO_2	61.52	60.59	61.76	61.71	62.03	62.72	62.31	63.35	62.72	62.69	68.95
Al_2O_3	18.93	18.89	19.09	18.79	18.73	18.66	18.92	18.00	18.60	18.31	19.65
Fe_2O_3	0.73	0.69	0.69	0.59	0.81	0.81	0.66	1.04	0.75	0.75	0.00
SrO	0.55	0.50	0.32	0.42	0.42	0.40	0.40	0.42	0.35	0.46	NA
BaO	3.25	4.54	3.40	3.23	3.24	2.36	2.69	0.90	1.71	1.57	NA
Na_2O	1.50	1.88	1.79	2.02	1.84	1.79	1.95	1.37	1.56	1.29	11.52
K_2O	13.63	12.19	12.93	12.63	13.13	13.82	13.34	15.06	14.28	15.06	0.08
sum	100.11	99.28	99.97	99.38	100.20	100.55	100.27	100.14	99.98	100.14	100.30
X_{Or}	85.66	81.02	82.6	80.4	82.41	83.6	81.87	87.9	85.74	88.5	0.00

mp, microphenocryst
* albite in secondary vein

Table 3

Microprobe analyses of analcite phenocrysts.

Sample location	1010B core	1010B rim	1010B core	1010B rim	1008E core	1008E rim	1008E core	1008E rim	1006A core	1006A rim	1006B core	1006B rim	3.2* vein
SiO_2	55.67	55.47	55.27	55.56	55.35	56.79	55.22	55.10	54.83	54.83	54.10	53.89	58.64
Al_2O_3	22.68	22.55	22.07	21.42	21.79	21.27	22.34	23.28	21.64	22.08	22.11	22.08	20.76
FeO	1.34	1.52	1.15	1.88	0.08	0.10	0.10	0.33	1.02	0.81	1.36	1.80	0.01
CaO	0.21	0.21	0.19	0.32	0.01	0.04	0.08	0.04	0.07	0.05	0.06	0.11	0.00
Na_2O	7.03	8.90	9.99	9.42	12.37	12.28	13.24	13.59	11.88	12.14	12.37	12.11	10.65
K_2O	0.09	0.45	0.30	0.93	0.02	0.04	0.08	0.08	0.39	0.36	0.64	0.78	0.65
BaO	0.08	0.18	0.00	0.00	0.09	0.00	0.00	0.00	0.00	0.06	0.04	0.01	NA
sum	87.10	89.27	88.96	89.53	89.72	90.51	91.05	92.42	89.83	90.35	90.68	90.77	90.71
Si/Al	2.08	2.09	2.13	2.20	2.16	2.27	2.10	2.01	2.15	2.11	2.08	2.07	2.40

*albite in secondary vein

analcite up to 2 mm occur in melanite and sanidine phenocrysts, but these are rare.

Microprobe analyses of Na, and the anhydrous weight total, are inaccurate due to volatilization of Na and H_2O during analysis, but Si/Al ratios (average 2:1) are close to the stoichiometric value (secondary vein analcite is more siliceous). Unaltered analcites have high Fe_2O_3 (up to 1.9%), but recrystallized analcite has low Fe_2O_3 ($\approx$0.2%; sample 1008E, Table 3). Weak oscillatory zoning in Fe_2O_3 was observed, but overall most phenocrysts are normally zoned with Fe-enriched rims (Fig. 7). The rims of fresh analcites are relatively enriched in K_2O (average 0.63%) compared to the cores (average 0.37%). The exception, as for sanidine, is sample 1006A. Ca, Ba, and Sr are negligible.

The degree of analcite alteration is strongly correlated with its framework oxygen ∂O^{18} (Fig. 8). Gem-quality analcite has $\partial O^{18} = 9.4$ ‰, whereas

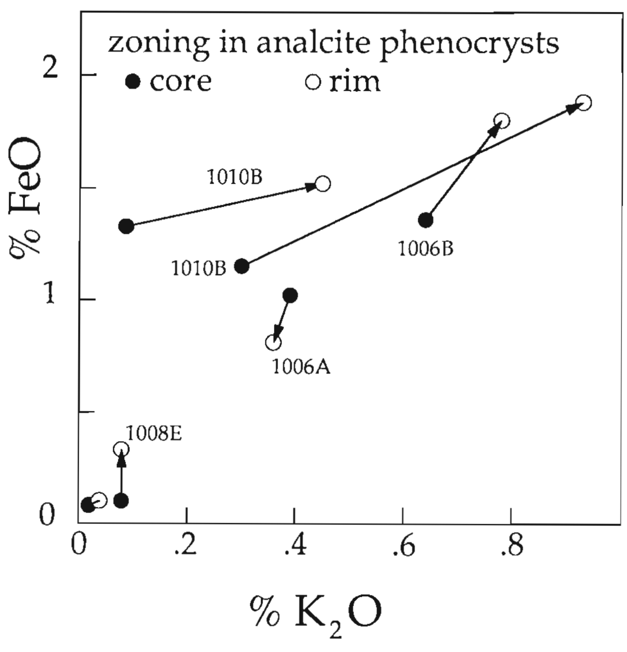

Figure 7. Plot of FeO versus K_2O for analcite phenocrysts. Note that in the strongly altered sample 1008E, in which the analcite is recrystallized to twinned, polycrystalline mosaics, both K_2O and FeO have been eliminated and all evidence of primary zoning has been destroyed. Filled circles are phenocryst cores; open circles are phenocryst rims.

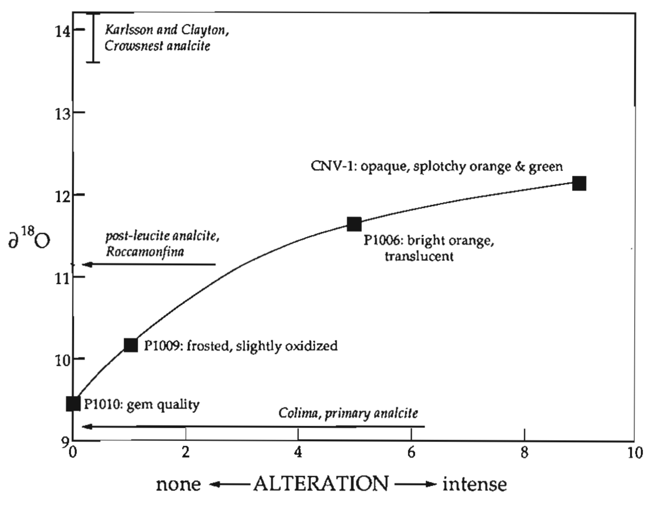

Figure 8. Plot of framework ∂O^{18} versus alteration index for four analcites from the Crowsnest Formation. The index was arbitrarily assigned before analysis, on the basis of clarity and degree of recrystallization. Hand-picked separates were heated to 375° to remove channel water. Other data sources: Roccamonfina: Taylor et al., 1979; Colima: Luhr and Kyser, 1989.

green-white, opaque analcite has $\partial O^{18} = 12.2$ ‰. Karlsson and Clayton (1991) measured a range in ∂O^{18} of 13.5 to 14.2 ‰ for analcite from the CNF, but the origin and optical properties of their material were not reported. The high ∂O^{18} values suggest that their samples were strongly altered or even secondary.

Origin of analcite

As indicated previously, some workers have considered analcite in the CNF to be secondary after leucite, which also typically crystallizes with a {211} cubic form. Direct precipitation of analcite from a melt and replacement of leucite by analcite are fundamentally different processes which should be readily distinguishable (Karlsson and Clayton, 1991). Prevailing published opinion, exemplified by Karlsson and Clayton, holds that analcite in the CNF is secondary after leucite. However, in our opinion, the elemental and isotopic composition of analcite, as well as textural relations of analcite with the groundmass and other phenocrysts, are inconsistent with the replacement hypothesis.

The replacement hypothesis implies original ultrapotassic magma with the assemblage melanite + leucite (+ others). Rocks with this mineral assemblage (or melanite + other K-rich felsic minerals, such as kalsilite) are rare (Mitchell and Bergman, 1991) and, to our knowledge, restricted mainly to Ca-rich, ultrabasic rocks containing melilite or wollastonite (compare to Lewis, 1982; and Tilley and Henry, 1952). The other known occurrence of blairmorite (Lupata Gorge, Mozambique: Woolley and Syme, 1976) is associated with feldspathoid-bearing trachytes (kenytes) very similar to the trachytes of the CNF. Mafic and potassic extrusive rocks or dykes also do not appear at this locality.

If leucite were converted to analcite by ion exchange with the surrounding matrix, K-rich cores should be locally preserved. However, the CNF analcites generally exhibit Na-rich cores, consistent with increasing K/Na in the crystallizing melt as indicated by K-rich rims on associated sanidine phenocrysts. The only exception is sample 1006A, in which both sanidine and analcite have Na-rich rims. The parallelism in K–Na zoning for sanidine and analcite is clearly consistent with co-crystallization from a melt, but not with alteration of leucite.

Much of the analcite shows alteration features, notably exsolution of iron oxide and recrystallization to twinned polycrystalline masses. These changes are clearly associated with increasing ∂O^{18} values for framework oxygen. Fresh analcite without visible alteration exhibits ∂O^{18} well within the range of primary lower crustal melts (Taylor, 1968). We question how leucite, on an outcrop scale, could be converted by alteration to gem-quality, Fe-rich analcite with igneous oxygen isotope ratios.

Some authors have suggested that blairmorite magma could not have contained enough water to stabilize primary analcite, since blairmorite samples do not contain other hydrous phases such as amphibole or biotite. However, the magmas were felsic and strongly depleted in Mg, Ca, and Ti. (Biotite is present in many syenite clasts, and in the mafic tuffs of Iron Ridge.) As deduced by Roux and Hamilton (1976), the bulk composition of the phonolite and trachyte magmas was outside the stability field of amphibole, and possibly also of biotite, but within the field of primary analcite. The pressure–temperature window for primary analcite is narrow, requiring a partial pressure of water greater than 4.5 to 5 kbars at temperatures of about 650°C in the system SiO_2–Al_2O_3–Na_2O–H_2O (Peters et al., 1966). Some authors consider these conditions unrealistic (Karlsson and Clayton, 1991), however they are well within the range of conditions deduced by geothermobarometry for lower crustal assemblages. Furthermore, the role of other volatile species in the melt (F, Cl), and of minor elements in analcite (Fe, K), on their co-stability has not been systematically studied. The numerous uncertainties make it unrealistic to claim that analcite phenocrysts cannot crystallize from magmas.

Primary igneous phases: Iron Ridge tuffs

The melanocratic Iron Ridge tuffs contain an unusual mineral assemblage dominated by Fe- and K-rich minerals. Juvenile volcanic clasts are dominated by biotite (extensively replaced by chlorite), which is aligned parallel to a presumed flattening plane, producing a schistose texture. Euhedral crystals of pyrite, ranging from 1 μm to 2 mm, are prominent (Fig. 9); these often occur in elongate clusters parallel to the schistosity. The largest pyrites usually contain some biotite inclusions. Euhedral, colourless crystals with a {211} cubic form are present at 0 to 20%. These now consist of pure potassium feldspar; some contain tiny (1–2 μm) inclusions of zircon and rutile. Also present are rounded, multiphase inclusions situated at the corners of an indeterminate cubic form.

Potassium feldspar also occurs in late segregations with chalcopyrite and galena (Fig. 10). The feldspar in these segregations has an elongated, euhedral habit, and is weakly zoned (rims richer in Na). Notable for

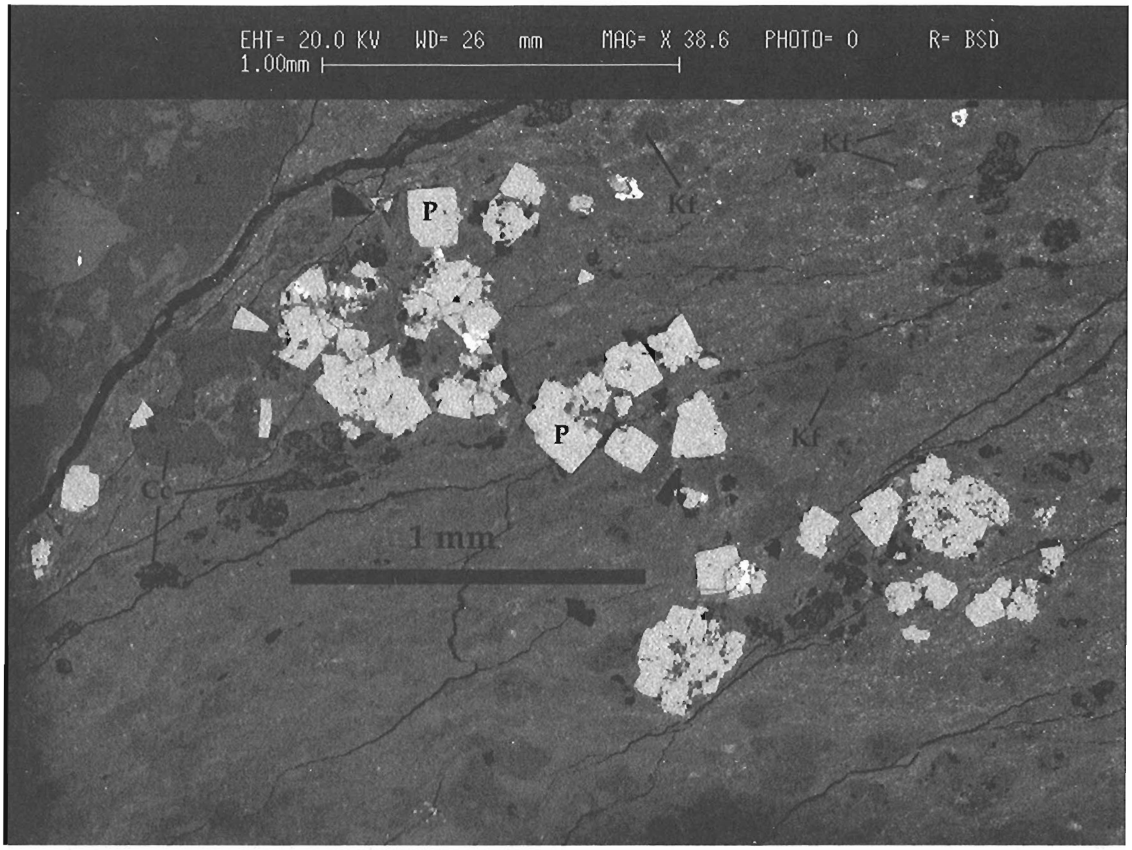

Figure 9. *Backscattered electron (BSE) image of a polished section of melanocratic tuff from Iron Ridge. The image is dominated by a biotite-rich juvenile volcanic fragment; matrix is visible in the top left corner. Note the abundance of euhedral pyrite (P) and equant grains of potassium feldspar (Kf), presumed to have originally crystallized as leucite. Calcite (Cc) is a late stage primary mineral. The bright areas adjacent to pyrite are galena + cerussite; the bright specks in the groundmass are various sulphides and monazite.*

their absence are clinopyroxene and melanite, which are prominent mafic phases in the trachytes and phonolites. Melanite is rarely observed in the tuffs, and only as fractured and highly resorbed grains which appear to be xenocrysts.

Calcite and monazite are prominent late stage minerals in the juvenile fragments. Although calcite occurs in profusion as a sand-sized contaminant in the matrix of the tuffs, it occurs as euhedral laths in the juvenile clasts. Monazite, sometimes closely associated with chalcopyrite, forms irregular masses comprised of thousands of minute grains (Fig. 11). Titanomagnetite is dispersed as tiny grains in the groundmass.

The juvenile clasts in the tuff appear to have been plastic, and perhaps partially molten, during eruption. Pyrite appears to have been a phenocryst phase, and the chalcopyrite–Kspar segregations have every appearance of crystallizing from a late stage melt. The melt which generated these clasts was apparently rich in H_2O, S, and CO_2. Although no analyses of the juvenile clasts are available, they are clearly strongly enriched in Fe, K, P, and rare earth elements relative to the trachytes and phonolites, and cannot be considered cumulates of the felsic magmas.

The colourless Kspar grains with {211} faces superficially resemble the analcites in the phonolites, but have some important differences. They lack the pale brown colour and Fe zoning prominent in the analcites, and contain the symmetry-controlled melt inclusions which are typical of leucite; inclusions in the analcites have no relation to the crystallographic form. The Kspar grains are interpreted as primary leucite converted to Kspar by liquid–solid reaction with cooling. This interpretation is substantiated by the presence of late primary potassium feldspar, with weak K–Na zoning, which presumably crystallized below the temperature where the reaction *leucite* + $SiO_{2(liq)}$ =

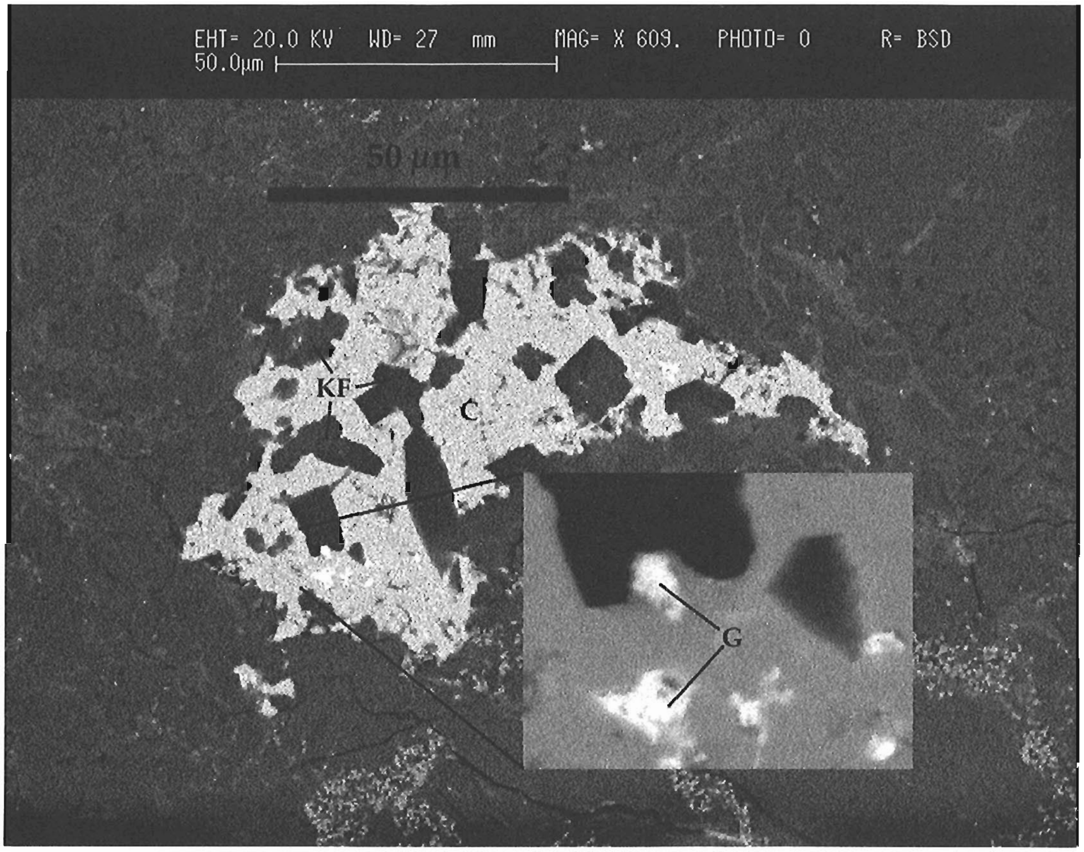

Figure 10. BSE image of a chalcopyrite (C)–potassium feldspar (KF) segregation in the Iron Ridge tuff. Galena (G) is a minor component.

Kspar occurs. This temperature is strongly controlled by $f(H_2O)$, which cannot be precisely determined in this case and which probably increased as crystallization progressed. However, the presence of pyrite crystals requires magma liquidus temperatures below 743°C (above this temperature, pyrite is unstable with respect to pyrrhotite + S_2 at all pressures; Toulmin and Barton, 1964). The leucite-Kspar reaction curve reaches an invariant point at 750°C and 8.4 kbar at $P_{H20} = P_{total}$; at higher pressures leucite is unstable (Scarfe et al., 1966). The reaction curve is at 470°C at 1 atm; crystallization must therefore have occurred between 470°C and 743°C, and below about 8.4 kbars pressure.

Secondary and metamorphic minerals

Many samples of the CNF exhibit incipient to weak metamorphic alteration. The most advanced degree of alteration occurs in finer grained epiclastic rocks where much of the matrix consists of metamorphic minerals such as calcite, chlorite and albite. With the exception of chlorite, albite, calcite and quartz, the metamorphic minerals described below have been identified in only one or two specimens.

For the metamorphic study, each thrust slice was sampled at several localities along strike; 105 hand samples were collected from 30 different localities (see Bégin et al., 1995, for sample locations). All of the sample preparations and analyses were performed at the Department of Geology and Geophysics, University of Calgary. During thin section preparation, the epoxy was cured slowly (one week) at low temperature (<50°C) to avoid any alteration of the zeolites present. Selected minerals in 15 samples were analyzed using an ARL-SEMQ electron microprobe equipped with nine wavelength dispersive spectrometers. Analytical conditions were 15 Kv accelerating potential and 0.15 Na beam current. Spot size was 1 µm for all minerals except analcite (spot size was 7 µm). Counting time per analysis was 20 seconds. Silicates were used as standards and the data were reduced using the methods of Bence and Albee (1968) and the programs outlined in Nicholls and Stout (1988).

Nineteen samples were chosen for X-ray diffraction studies (XRD). Each sample was broken into fragments of approximately 1 cm diameter with a hammer. Further crushing was done using a hand steel and crush cylinder. The crushed sample was sieved and a <2 µm fraction was separated by centrifuge methods. Samples

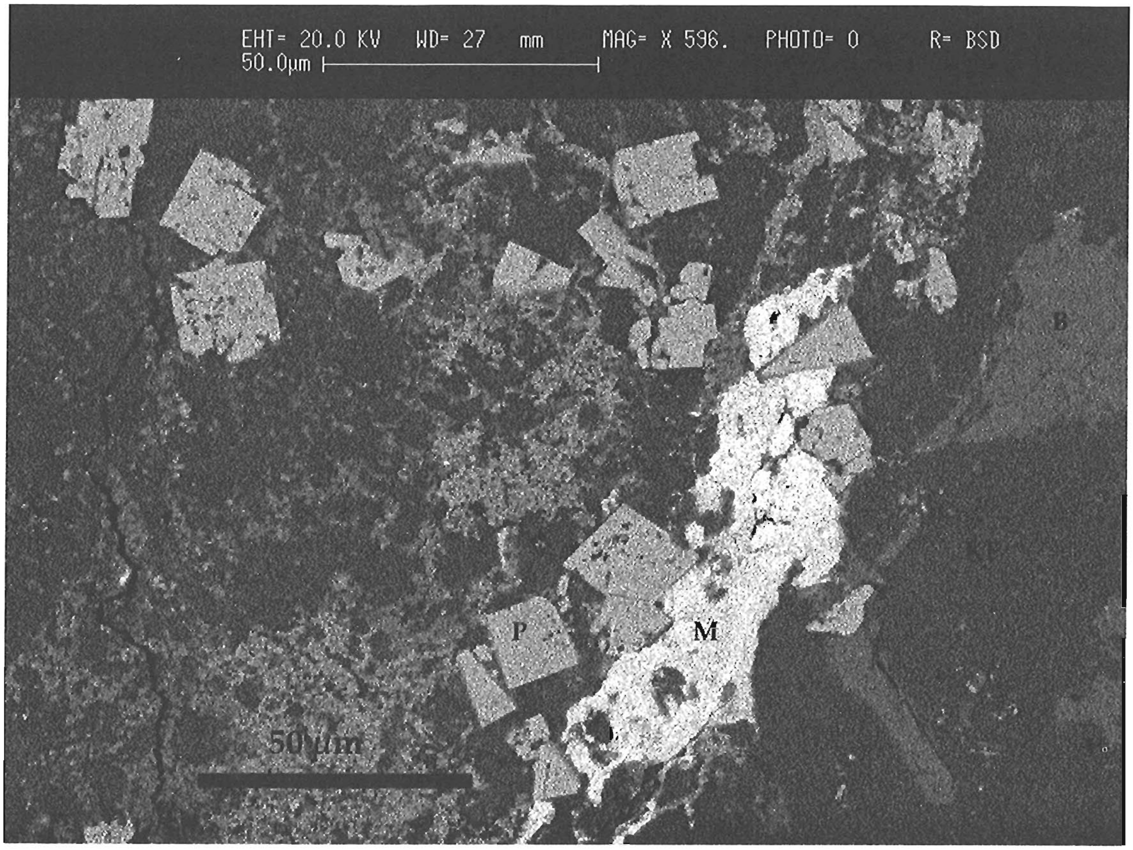

Figure 11. *BSE image of monazite (M) and pyrite (P) in the Iron Ridge tuff.*

were glycol solvated at 60°C for at least 12 hours and heat treated at 550°C for 30 minutes. A light mineral fraction (specific gravity <2.45) was separated from the 100 to 200 mesh sieved portion using heavy liquids. The XRD analysis was conducted on a Phillips-Norelco X-Ray Diffractometer with FeK radiation operated at 40 Kv accelerating potential and 20 Ma current.

Phyllosilicates

Chloritic phyllosilicates are ubiquitous throughout the CNF. They occur as cryptocrystalline aggregates throughout the matrix of clastic rocks and as a replacement of relict phases in the groundmass of some samples. Celadonite was identified by electron-microprobe analysis in one sample (27.1) (Table 4) where it occurs as olive-green to brown, cryptocrystalline aggregates replacing groundmass analcite. Average chlorite compositions from four samples are listed in Table 4. Chlorite formula units were recalculated assuming 14 oxygens per formula unit with all iron as Fe^{2+}. Calculated Si cations are equal to or greater than 3.0 per 14 oxygens, indicating the presence of smectite interlayers in the chlorite (Bettison and Schiffman, 1988). The proportion of chlorite (**X**) in a mixed layer smectite/chlorite can be calculated based on the number of noninterlayered cations (Si+

Table 4

Microprobe analyses of phyllosilicates.

Sample	22.1 prh	27.1 cel	3.2 chl	5.1 chl	19.1 chl	22.1 chl
SiO_2	44.56	54.76	28.28	26.05	27.64	30.69
Al_2O_3	20.30	18.53	19.21	16.30	18.66	17.83
FeO_T	4.13	9.60	35.01	39.71	34.17	31.50
MnO	0.09	0.11	0.60	1.16	1.00	1.38
MgO	0.02	2.72	6.21	6.47	7.40	7.90
CaO	26.19	0.14	0.10	0.07	0.17	0.25
Na_2O	0.10	0.67	0.00	0.00	0.00	0.00
K_2O	0.00	9.07	0.56	0.02	0.08	1.15
H_2O^a	4.28	4.36	10.89	10.70	10.87	11.21
sum	99.67	99.92	100.86	100.46	100.17	101.81
Number of atoms based upon 12 oxygens (O+OH) for prehnite, 11 oxygens for celadonite, and 14 oxygens for chlorite.						
Si	3.105	3.743	3.055	2.923	2.994	3.225
Al	1.667	1.493	2.447	2.156	2.408	2.210
Fe	0.217	0.550	3.164	3.727	3.096	2.774
Mn	0.005	0.006	0.055	0.110	0.092	0.123
Mg	0.002	0.278	1.000	1.082	1.195	1.241
Ca	1.956	0.010	0.011	0.008	0.019	0.028
Na	0.013	0.088	0.000	0.000	0.000	0.000
K	0.000	0.791	0.078	0.003	0.010	0.152

^aH_2O estimated from stoichiometry. prh, prehnite; cel, celadonite; chl, chlorite.

Al + Fe + Mn + Mg). An end-member chlorite (**X** = 1) would have 10 noninterlayered cations per 14 oxygens whereas an end-member smectite (**X** = 0) would have 8.91. The average proportion of chlorite in the CNF chloritic phyllosilicates have been interpolated between these two extremes. Values of **X** for chlorite analyses listed in Table 4 range from 0.61 to 0.91, indicating the presence of some proportion of smectite interlayers. Chlorite compositions are predominantly within the field of brunsvigite and exhibit relatively low Mg/(Mg + Fe) ranging from 0.23 to 0.31.

Quartz

Quartz occurs as radiating aggregates of bladed or columnar hypidioblastic crystals in the matrix, in veins of 100% quartz, and in the center of a vein that is lined with analcite. Quartz is also an abundant clastic mineral in some of the epiclastic rocks.

Feldspar

Albite occurs as microlaths in the matrix and in amygdules. It is also found as veins in two samples (4.2 and 10.1). Microprobe analysis for this albite is listed in Table 2. It is relatively pure albite, containing only trace amounts of K_2O (0.05 wt.%) and CaO (0.09 wt.%; note: the detection limits for these oxides is 0.01 wt.%). Albite also occurs as alteration patches within sanidine phenocrysts (Pearce, 1970).

Calcite

Calcite is commonly observed in the CNF, as veins, in the groundmass, as replacement of igneous phenocrysts and as poikiloblastic cement.

Analcite

In addition to its occurrence as phenocrysts, analcite was observed in veins in two samples (3.2 and 26.5). In one sample (3.2), analcite occurs as idioblastic equant isotropic crystals lining a vein with quartz in the center. Another sample (26.5) contains veins composed solely of colourless interlocking xenoblastic analcite that exhibits faint birefringence. The occurrence of this analcite in veins is interpreted as a product of late alteration (metamorphic), as opposed to a product of igneous crystallization. Similar distinct generations of analcite have recently been described by Goble et al. (1993) in an analcite phonolite sill from the Proterozoic Purcell Supergroup of southwestern Alberta. Microprobe analyses of analcite in veins are listed in Table 3. The compositions reported here for analcite in veins are slightly lower Al/(Al + Si) and Na/(Na + K) ratios than those in phenocrysts. These compositions overlap with those of analcite from burial metamorphic rocks (Coombs and Whetten, 1967).

Prehnite

Prehnite was observed in only two samples (18.2 and 22.1). It occurs as colourless, radiating aggregates of bladed or columnar hypidioblastic crystals, filling amygdules. Microprobe compositions of prehnite are listed in Table 4. Average X_{Fe} for this sample is 0.12 which is comparable to the X_{Fe} reported for other very low temperature metamorphic (e.g., zeolite facies) terrains (e.g., Cho et al., 1986; Bevins et al., 1991).

Laumontite and heulandite

Although not observed in thin section, laumontite was identified by XRD of the low specific gravity fraction (< 2.45) from a separate of sample 22.1, one of the prehnite-bearing samples in the study area. Laumontite, near end-member composition, has been described previously by Miller and Ghent (1973) and Ghent and Miller (1974) as a pore-filling cement in the nonmarine sandstones of the Blairmore Group, stratigraphically underlying the CNF. Norris (1964) reported heulandite from the CNF, but we were unable to independently verify this occurrence. Miller and Ghent (1973) and Ghent and Miller (1974) reported Ba–Sr-rich heulandite as a pore-filling cement in the Blairmore sandstones.

GEOCHEMISTRY

Whole-rock analyses of selected samples are given in Table 5. Analyses were by X-ray fluorescence (majors) and ICP-MS (trace elements and Nd–Sr isotopes).

Unaltered samples

Major elements

In a total alkalies–silica diagram, the compositions of Crowsnest volcanic rocks (CNV) plot around the point where the fields of phonolites, trachytes, tephriphonolites, and trachyandesites meet (Fig. 12). Compared to phonolites from central volcanos, the

Table 5

Whole-rock analyses.

Rock	1006C blmrt	1010B blmrt	1010E blmrt	1009A an phon	1010G an phon	1007B trachyte	1008J trachyte	1011B trachyte	1006B an phon
SiO_2	51.68	52.48	56.12	56.32	59.12	56.51	60.18	58.65	55.81
TiO_2	0.49	0.34	0.18	0.5	0.63	0.08	0.24	0.21	0.44
Al_2O_3	17.73	17.81	20.71	19.08	18.9	24.81	20.53	19.94	18.65
Fe_2O_3	5.37	8.65	5.42	6.19	6.48	1.36	3.3	3.07	5.27
MgO	0.72	1.39	1.62	1.04	1.44	0.75	0.31	0.43	0.4
MnO	0.27	0.27	0.2	0.21	0.22	0.08	0.12	0.08	0.16
CaO	8.64	3.84	3.01	3.07	4	2.43	2.35	1.43	2.99
Na_2O	6.48	6.65	3.95	5.26	2.83	5.71	2.91	7.54	7.61
K_2O	4.5	2.67	6.29	6.41	8.01	6.94	9.22	8.23	4.89
P_2O_5	0.07	0.11	0.03	0.05	0.14	0.01	0.03	0.02	0.05
sum	95.95	94.21	97.53	98.13	101.77	98.68	99.19	99.6	96.27
S	288	50	28	416	51	5954	89	464	61
Cl	68	117	35	97	38	214	42	52	26
Rb	199	202	214	322	196	307	385	178	84
Sr	1384	1361	1249	1903	2754	418	8482	1132	1452
Ba	2091	1090	2279	3368	3410	364	3001	2670	2215
Y	7.7	3.7	2.7	11.9	16.3	1.1	6.5	11.7	7
Zr	169	177	155	234	281	160	214	305	161
Hf	4.33	2.36	2.58	5.77	6.62	3.34	5.16	7.11	4.1
Nb	40	115	91	58	48	79	40	47	37
Ta	1.87	7.14	4.89	1.93	3.76	3.04	1.11	1.52	1.66
Cr	0	0	0	0	0	0	0	0	0
Ni	0	0	0	0	0	0	0	0	0
Cu	67	9	37	24	53	95	13	131	8
Zn	113	144	96	111	128	181	133	127	97
La	56	124	90	59	53	47	58	60	48
Ce	106	215	151	110	119	88	100	100	91
Pr	10.9	18.7	12.9	11.2	13.2	7.4	9.1	9	9.5
Nd	34.4	47.3	32.2	35.5	47.8	16	26.4	27.1	30.4
Sm	4.07	3.69	2.25	4.72	7.78	0.85	3.14	3.93	3.72
Eu	1.03	0.75	0.46	1.33	2.03	0.19	0.77	1.06	0.92
Gd	3.47	3.08	2.18	2.85	4.79	0.21	1.55	3.41	3.13
Tb	0.256	0.115	0.089	0.321	0.59	0.024	0.205	0.309	0.235
Dy	1.486	0.665	0.498	1.939	3.232	0.194	1.089	1.829	1.332
Ho	0.267	0.105	0.086	0.383	0.57	0.032	0.213	0.372	0.239
Er	0.815	0.288	0.248	1.069	1.612	0.085	0.659	1.169	0.661
Tm	0.112	0.04	0.039	0.165	0.216	0.011	0.098	0.183	0.098
Yb	0.749	0.249	0.248	1.076	1.394	0.134	0.671	1.249	0.682
Lu	0.118	0.047	0.041	0.173	0.214	0.016	0.101	0.198	0.105
Th	14.3	23.8	19.5	14.8	17.4	28.2	16.7	52.8	13.6
U	4.3	2.7	1.3	6.6	3.2	6.3	6.0	15.4	3.0
$^{87}Rb/^{86}Sr$	0.2851	0.473085	—	0.26876	—	3.00437	—	0.42609	—
$^{87}Sr/^{86}Sr$	0.704497	0.705105	—	0.70479	—	0.707664	—	0.71018	—
$^{147}Sm/^{144}Nd$	0.07173	0.51222	—	0.08395	—	0.03501	—	0.09477	—
$^{143}Nd/^{144}Nd$	0.51223	0.512156	—	0.512156	—	0.512006	—	0.511864	—

Trachyte sample PHA-93-21: $^{87}Rb/^{86}Sr = 0.188427$, $^{87}Sr/^{86}Sr = 0.7044495$, $^{147}Sm/^{144}Nd = 0.091945$, $^{143}Nd/^{144}Nd = 0.5120565$.

CNV are slightly richer in silica and slightly lower in alkalies. Those samples identified mineralogically as trachytes have higher average SiO_2, and higher K_2O/Na_2O; SiO_2 and K_2O/Na_2O are positively correlated (Fig. 13). All samples are markedly depleted in compatible elements, with MgO contents ($\approx 1\%$) only slightly greater than in many rhyolites.

Previous authors have attempted to relate the phonolites and trachytes by crystal fractionation schemes (e.g., Pearce, 1970). Strong depletions in Ti and P are consistent with fractionation of titanian andradite (melanite) and apatite phenocrysts. These phases plus clinopyroxene are also abundant in cumulate rocks. However, elemental patterns that might indicate the direction of fractionation [to silica enrichment (trachytes), or depletion (phonolites)?] are contradictory, and isotopic data (below) strongly indicate that differences in silica content result from differences in source region material, rather than crystal fractionation.

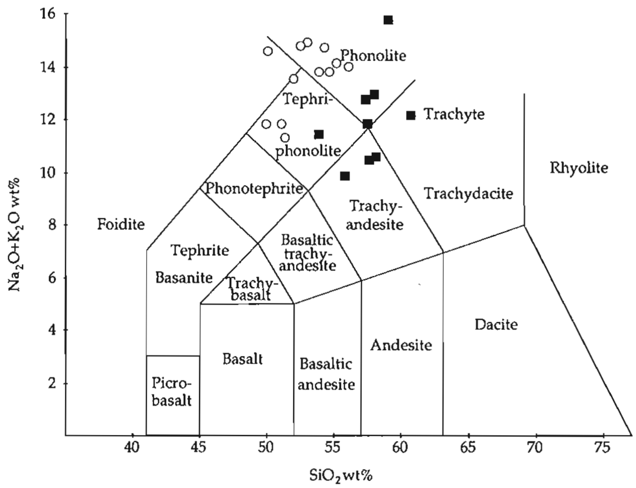

Figure 12. Positions of Crowsnest Formation volcanic rocks (filled squares), and for comparison, phonolite from a central nephelinite-phonolite volcano, East Africa (Shombole: Peterson, 1989; open circles), in a total alkalies-silica diagram. All analyses are recalculated to 100% volatile-free.

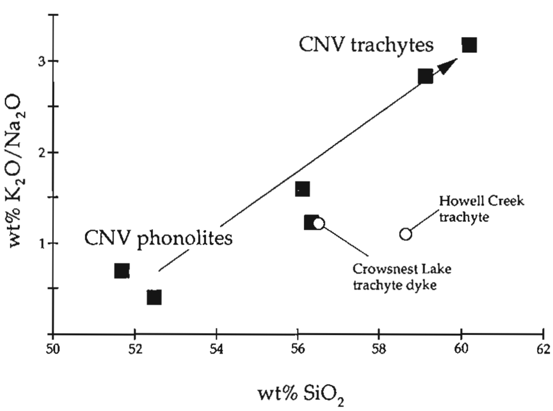

Figure 13. Plot of K_2O/Na_2O versus SiO_2 for analyzed volcanic rocks of the Crowsnest Formation, also showing Howell Creek trachyte and Crowsnest Lake trachyte dyke for comparison.

Trace elements

The CNV have simple REE (Fig. 14) and other trace element patterns (Fig. 15). They are light rare earth element (LREE)-enriched, with no Eu anomalies. The phonolites are slightly more enriched in LREE than the trachytes. All samples show an abrupt break at Dy, where a fractionated, linear LREE profile flattens to a linear heavy real earth element (HREE) profile of zero slope. This presumably reflects the presence of a residual phase or phases in the source region with high distribution coefficients for HREE.

Mid-ocean ridge basalt (MORB)-normalized trace element profiles show simple incompatible-element enrichment with strong negative anomalies in P and Ti. Aside from these, no other high field-strength elements (Nb, Zr, Hf) show anomalies (a small negative Ta anomaly probably reflects analytical errors). The Howell Creek trachyte and the Crowsnest Lake dyke strongly resemble the Crowsnest trachytes in their trace element patterns (neglecting unusual depletions in Sr and Ba in the Crowsnest dyke which may be due to carbonate-related alteration).

Nd, Sr isotopes

Isotopic data (Sm–Nd and Rb–Sr) were obtained for four whole rocks from the CNF, for one Howell Creek trachyte, and for the Crowsnest Lake dyke (Table 5). The Howell Creek trachyte is immediately separable from the CNV on the basis of its markedly radiogenic Sr composition (Fig. 16). The Crowsnest Lake dyke isotopically resembles the Crowsnest trachytes.

There is a strong correlation between rock type and E_{Nd}, though not E_{Sr}. With increasing SiO_2, E_{Nd} becomes increasingly negative (from -6 to -10), with depleted mantle model ages varying from 844 to 1370 Ma. Sr is close to bulk Earth in composition. The four CNF samples define an Rb-Sr isochron age of 158 Ma, but the assumption of equal initial $^{87}Sr/^{86}Sr$ required to obtain this age is almost certainly unwarranted.

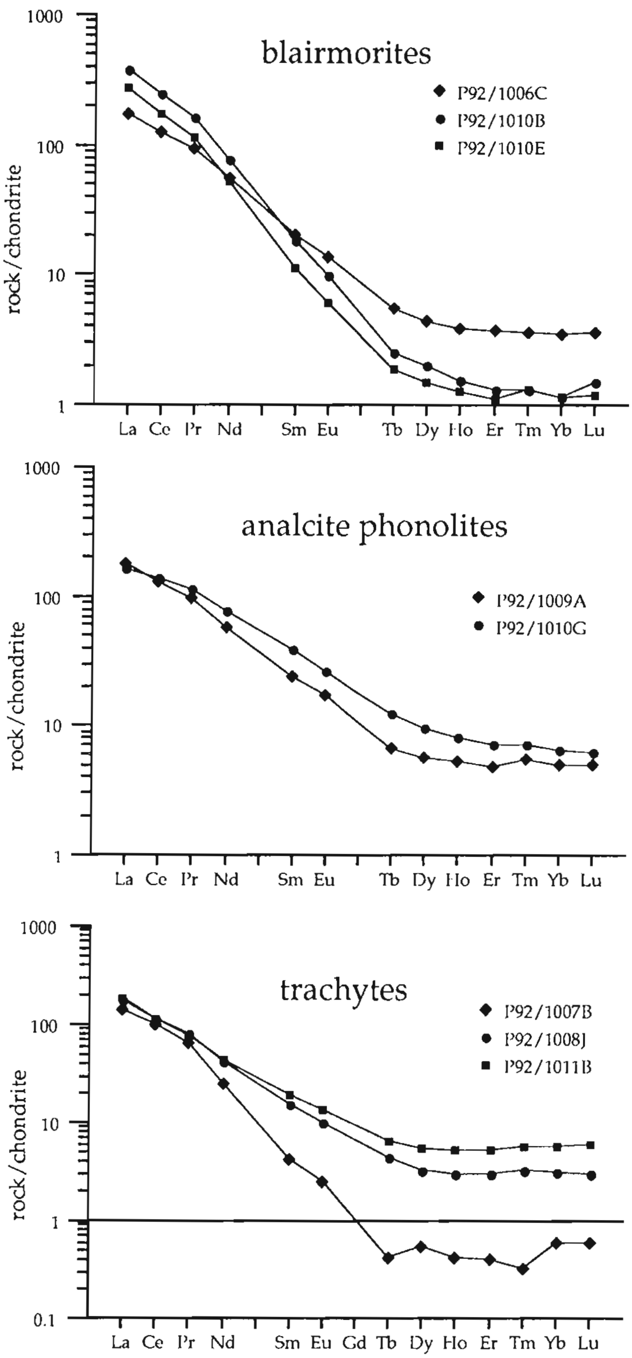

Figure 14. Plots of rare earth elements (REE) for the Crowsnest volcanics; also shows Howell Creek trachyte (sample 1011B) and Crowsnest Lake dyke (sample 1007B) for comparison.

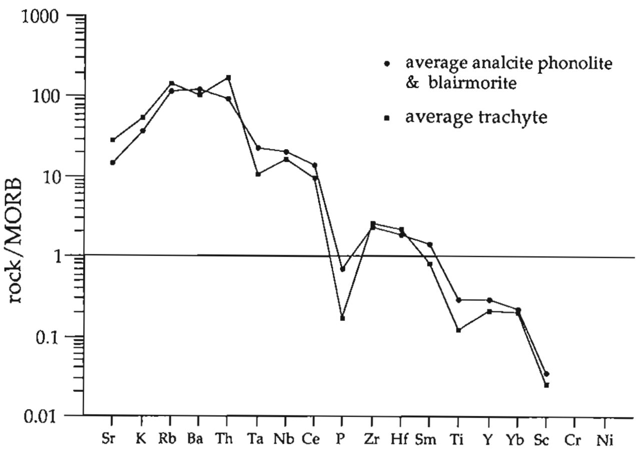

Figure 15. Mid-ocean ridge basalt (MORB)-normalized trace element diagram for average Crowsnest trachytes and analcite-rich rocks (blairmorites and analcite phonolites).

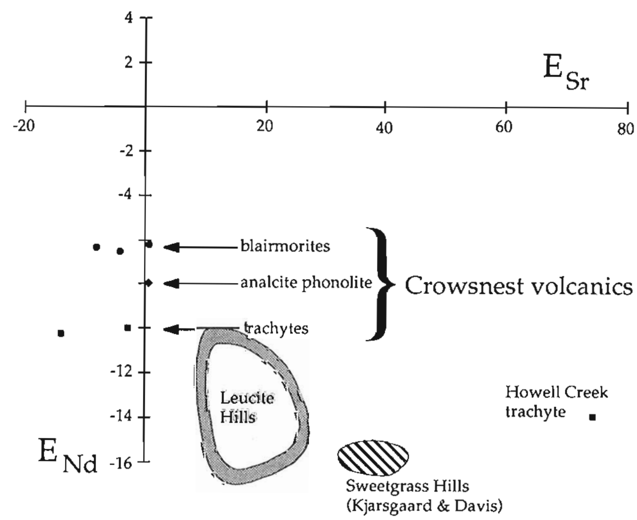

Figure 16. Plot of $E_{Nd,\ 100\ Ma}$, versus $E_{Sr,\ 100\ Ma}$ for all analyzed samples. Normalization values: for CHUR (Chondritic Uniform Reservoir), $^{143}Nd/^{144}Nd = 0.512638$; for bulk Earth, $^{87}Sr/^{86}Sr = 0.7045$. Data for Sweetgrass Hills from Kjarsgaard and Davis (in prep.; pers. comm., 1995).

The CNF samples have Nd–Sr compositions that are inconsistent with a nonenriched mantle source, or an uncontaminated crustal source. Rather, their markedly negative $E_{Nd,100\ Ma}$, and bulk Earth-like Sr, are most like some strongly potassic rocks of the Churchill and Wyoming Archean provinces (e.g., Peterson et al., 1994). Both the present location of the CNF rocks and palinspastic reconstructions indicate that the CNF magmas also erupted through Archean lithosphere that is part of the Churchill Province (specifically, the Medicine Hat block; Ross et al., 1991). The depleted mantle model ages indicate that enrichment may have occurred in the mid-Proterozoic.

Altered and metamorphosed samples

Visibly altered samples were also analyzed in an effort to identify mobilization patterns of various elements and determine if anomalous concentrations of metals were present. No significant variations in the concentration of metals were noted, and no secondary sulphide mineralization (e.g., chalcopyrite, bornite, galena) was observed. Whole rock compositions of altered samples are given by Bégin et al. (1995), and because these show no systematic differences from fresh samples, those data are not repeated in Table 5.

DISCUSSION

Origin of the Crowsnest magmas

From the data cited above, we identify certain restrictions on hypotheses regarding the origin of the Crowsnest trachytes and phonolites. These are:

(1) Derivation from mafic magmas such as alkali basalt is unlikely, since no such rocks occur within the CNF or as dyke rocks in the region, and Eu anomalies consistent with plagioclase fractionation are absent.

(2) The source region underwent K, incompatible element, and LREE enrichment during the Proterozoic. The source material was therefore older, and probably lithospheric. Mass balance models for partial melting indicate that "normal" mantle or lower crustal rocks could not have produced these magmas. An enrichment event is necessary and residual garnet and clinopyroxene are required to account for the REE profile.

(3) The presence of primary analcite phenocrysts indicates a relatively deep origin (ca. 20 km), and perhaps ponding in the middle lithosphere. All mineralogical indicators (analcite and pyrite phenocrysts, and leucite/liquid reaction) require low magmatic temperatures, consistent with limited partial melting and the absence of regional basaltic volcanism.

The simplest petrogenetic model that incorporates these constraints places the source region in moderately metasomatized upper lithospheric mantle, or lower crust, with small degrees of partial melting to produce moderately alkaline, compatible-element depleted magmas ranging from trachyte to phonolite in composition. The requirement of high water pressure to form analcite phenocrysts may indicate that melting was triggered by the migration of fluids, possibly as a consequence of faulting in the lower lithosphere during uplift in the later stages of the Columbian Orogeny. Fractionation of garnet and apatite (accompanied by clinopyroxene) occurred during ascent to produce strong negative anomalies in Ti and P.

The origin of the magma represented in the Iron Ridge tuff is unclear. The large quantity of deformation-twinned carbonate grains in the tuff matrix suggests that the magma erupted through, or from within, Paleozoic carbonate formations, but the possibility of eruption from the same depth as the analcite phonolites cannot be discounted. The ubiquity of sulphidic segregations, plus the high content of pyrite phenocrysts, permits speculation that the high Fe-K-S melt originated as an immiscible, sulphur-rich segregation from trachytic melts. However, it is conceivable that the melt acquired its unusual characteristics by absorbing S and CO_2 from carbonate wall rocks, and reacting with syenites in a plutonic complex. Either hypothesis is consistent with the very limited distribution of the Iron Ridge tuff.

Metamorphic pressure-temperature conditions

Although diagnostic, low-variance assemblages have not been observed in the CNV, the pressure and temperature of metamorphism can be estimated with the petrogenetic grid of Frey et al. (1991) for very low grade metamorphic rocks, and with the recent review of experimental studies by de Capitani and Liou (in press) for some Ca-zeolites. In addition, Ghent and Miller (1974) outlined pressure-temperature (P-T) constraints on the metamorphism of the underlying Blairmore sandstones. The P–T stability field of laumontite is limited by the following equilibria:

$$\text{Lmt} = \text{Wa} + 2\ H_2O \quad (1)$$
$$\text{Lmt} = \text{Lws} + 2\ \text{Qtz} + 2\ H_2O \quad (2)$$
$$\text{Stb} = \text{Lmt} + 3\ \text{Qtz} + 3\ H_2O \quad (3)$$
$$\text{Hul} = \text{Lmt} + 3\ \text{Qtz} + 2\ H_2O \quad (4)$$

Abbreviations are: Lmt, laumontite; Wa, wairakite; Lws, lawsonite; Qtz, quartz; Stb, stilbite; and Hul, heulandite.

Laumontite-bearing equilibria have been examined by de Capitani and Liou (in press). Because of the absence of stilbite and wairakite in the CNV, the stability of laumontite and quartz is restricted to 180 to 300°C at 1 to 3 kbar for $P_{H2O} = P_S$ (Fig. 17). Temperatures based on chlorite thermometry (Cathelineau and Viena, 1985) from matrix chlorite give scattered results in the range of 150 to 300°C. Geothermometry using chlorite compositions has been critically reviewed by deCaritat et al. (1993), who questioned the reliability of some of the calibrations. In addition, the presence of smectite interlayers would cast doubt upon the reliability of the estimates. The presence of prehnite and laumontite in sample 22.1 constrains the pressure for the metamorphism to between 0.9 and 2.9 kbar for a temperature range of 200 to 250°C (Frey et al., 1991). This range of pressure estimates is consistent with that of maximum burial depths, between 4.7 and 7.8 km, based upon structural–stratigraphic reconstruction (Ghent and Miller, 1974) for rocks of the Blairmore Group, which stratigraphically underlie the CNV rocks. Ghent and Miller (1974) documented the occurrence of laumontite + albite + quartz assemblages in the sandstones of the underlying Blairmore Group. They detected no analcite in these rocks. Vitrinite reflectance and coal rank in the Mesozoic sedimentary rocks underlying the CNV are consistent with laumontite + albite + quartz stability (see summary in Greenwood et al., 1992, p. 542, 543)

The occurrence of analcite and quartz in veins (sample 3.2) has been used to further constrain the P–T conditions of metamorphism. Experimental data of Liou (1971) show that the equilibrium:

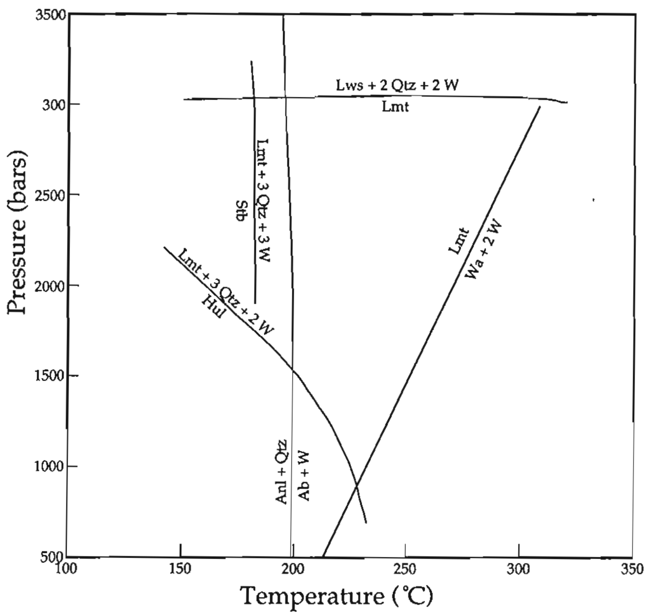

Figure 17. Pressure-temperature (P-T) diagram for mineral equilibria relevant to the metamorphism of the Crowsnest volcanic rocks. P-T curves were calculated using the program TWEEQU of Berman (1991). Thermodynamic properties of the phases in the system $CaO–Al_2O_3–SiO_2–H_2O$ are from de Capitani and Liou (1995, in press). Thermodynamic properties of analcite are discussed in the text. Anl, analcite; see text for other abbreviations.

$$\text{analcite} + \text{quartz} = \text{albite} + H_2O \qquad (5)$$

lies near 200°C and 1 kbar. We used the heat capacity and entropy of analcite calculated by Berman and Brown (1985) and adjusted the enthalpy ($\Delta H^o_{f,298}$ = -3 307 050 J) of analcite in equilibrium (5) until it passes through 200°C at 1 kbar, using the multiequilibrium program TWEEQU of Berman (1991). The presence of analcite and quartz together in veins, without albite, indicate an upper temperature limit of 200°C. The presence of laumontite + quartz and the absence of heulandite and lawsonite constrain the univariant assemblage Anl + Qtz + Ab to a pressure range of 1.5 to 3.0 kbar (Fig. 17). These estimates are in agreement with those stated above.

The minimum temperature of metamorphism is more difficult to constrain, particularly without independent estimates of a_{H2O}. In addition, experimental mineral reactions at low temperatures are generally unreversed: that is, the reactants are typically far outside of their pressure–temperature–fluid composition stability fields. The documented production of laumontite at temperatures of 100°C or less (Liou et al., 1987) is an example of this problem.

Metamorphic fluid composition

The presence of laumontite suggests that the fluids attending metamorphism were low in CO_2 (e.g., Ghent and Miller, 1974). The occurrence of extensive veining and amygdules in the CNV indicates the presence of an active fluid phase during metamorphism. Calculations of (a_{K+}/a_{Na+})-a_{SiO2} diagrams using the program TWEEQ suggest that analcite-bearing assemblages would be favored by low a_{SiO2} and lower values of (a_{K+}/a_{Na+}). Adularia–albite assemblages would be favored by higher a_{SiO2} and higher values of (a_{K+}/a_{Na+}). Variable SiO_2 and K^+/Na^+ activities for the fluids must have occurred throughout the metamorphic process, since both adularia-albite and analcite-bearing assemblages are observed in the CNV with no distinction on a regional scale.

ECONOMIC POTENTIAL OF THE CROWSNEST FORMATION

A review of this topic was given by Bégin et al. (1995), but we specifically address the question of gold mineralization and a possible association with carbonatites in this study. The Iron Ridge melanocratic tuff has been reported as containing "anomalous" gold concentrations. A 5 kg sample, rich in sulphides from this site, was analyzed for gold, yielding only 7 ppb. Additional recent analyses by other workers produced maximum Au concentrations of 50 ppb (W. Langenberg, Alberta Geological Survey, pers. comm., 1995). Samples of the tuff were carefully examined with a scanning electron microscope for evidence of gold grains. All grains with the appropriate mean atomic number turned out to be chalcopyrite. Our data indicate that primary Au and base metal concentrations are very low and were not concentrated by secondary processes, such as metamorphism or hydrothermal alteration.

No evidence was found for the presence of carbonatite. Although the rocks are potassic, and clearly continental, there is no indication that any magmas originated at depths sufficient to traverse diamond-bearing lithosphere.

Economic potential for the CNV may centre around industrial minerals. Analcite, which has a number of industrial uses owing to its ion-exchange properties, could be separated in large volume from some debris flows and sandstones. The quality would vary considerably, however, owing to iron contamination and alteration. Gem quality (unaltered and not fractured) analcite will have considerable attraction to mineral collectors. Some outcrops of fresh blairmorite have a striking appearance and an attractive, dark green colour, and thus may have some potential as decorative stone. Large blocks (>1 m), suitable for quarrying as bulding stone, are unfortunately uncommon; however, suitably sized blocks of porphyritic trachyte are relatively common (e.g., Racehorse Creek). Melanite garnet, locally comprising up to 10% by volume of some sandstones, is widely distributed and might be mined for its abrasive properties.

Acknowledgments

T. Peterson and K. Currie thank Tara Sagriff and Al Trigg for assistance in field studies.

REFERENCES

Amajour, L.C.
1985: Biotite grain size distribution and source area of the lower Cretaceous Viking bentonites, Alberta, Canada. Bulletin of Canadian Petroleum Geology, v. 33, p. 471-478.

Bence, A.E. and Albee, A.L.
1968: Empirical correction factors for the electron microanalysis of silicates and oxides. Journal of Geology, v. 76, p. 382-403.

Bégin, N.J, Ghent, E.D., and Beiersdorfer, R.E.
1995: Mineralogical and geochemical analyses and economic potential of the Crowsnest volcanics. *In* Current Research 1995-E, Geological Survey of Canada, p. 11-25.

Berman, R.G.
1991: Thermobarometry using multiequilibrium calculations: a new technique with petrological applications. Canadian Mineralogist, v. 29, p. 833-855.

Berman, R.G. and Brown, T.H.
1985: The heat capacity of minerals in the system K_2O-Na_2O-CaO-MgO-FeO-Fe_2O_3-Al_2O_3-SiO_2-TiO_2-H_2O-CO_2: representation, estimation and high temperature extrapolation. Contributions to Mineralogy and Petrology, v. 89, p. 168-183.

Bevins, R.E., Robinson, D., and Rowbotham, G.
1991: Compositional variations in mafic phyllosilicates from regional low-grade metabasites and application of the chlorite thermometer. Journal of Metamorphic Petrology, v. 9, p. 711-721.

Bettison, L.A. and Schiffman, P.
1988: Compositional and structural variations of phyllosilicates from the Point Sal ophiolite, California. American Mineralogist, v. 73, p. 62-76.

Cathelineau, M. and Viena, D.
1985: A chlorite solid solution geothermometer: The Los Azufres (Mexico) geothermal system. Contributions to Mineralogy and Petrology, v. 91, p. 235-244.

Carey, A.
1991: Petrography of an analcite-bearing trachyte dyke from Crowsnest Lake, southwestern Alberta. B.Sc. thesis, University of Calgary.

Cho, M., Liou, J.G., and Maruyama, S.
1986: Transition from the zeolite to prehnite-pumpellyite facies in the Karmutsen metabasites, Vancouver Island, British Columbia. Journal of Petrology, v. 27, p. 467-494.

Coombs, D.S. and Whetten, J.T.
1967: Composition of analcite from sedimentary and burial metamorphic rocks. Geological Society of America Bulletin, v. 78, p. 264-282.

Dawson, G.M.
1885: Preliminary report on the physical and geological features of that portion of the Rocky Mountains between latitudes 49° and 51°30′. Geological Survey of Canada, Annual Report Part B, 69 p.

de Capitani, C. and Liou, J.G.
in press: Thermodynamic analyses of some Ca-zeolites and Mg-Al pumpellyite. Geochimica et Cosmochimica Acta.

de Caritat, P., Hutcheon, I., and Walshe, J.L.
1993: Chlorite geothermometry: a review. Clays and Clay Minerals, v. 41, p. 219-239.

Ferguson, L.J. and Edgar, A.D.
1978: The petrogenesis and origin of the analcite in the volcanic rocks of the Crowsnest Formation, Alberta. Canadian Journal of Earth Sciences, v. 15, p. 69-77.

Fischer, R.V. and Schmincke, H.-U.
1984: Pyroclastic Rocks. Springer-Verlag, New York, 472 p.

Folinsbee, R.E., Ritchie, W.D., and Stansberry, G.F.
1957: The Crowsnest volcanics and Cretaceous geochronology. Alberta Society of Petroleum Geologists, Guidebook, 7th Annual Field Conference, September 1957, p. 20-26.

Frey, M., de Capitani, C., and Liou, J.G.
1991: A new petrogenetic grid for low-grade metabasites. Journal of Metamorphic Geology, v. 9, p. 497-509.

Ghent, E.D. and Miller, B.E.
1974: Zeolite and clay-carbonate assemblages in the Blairmore Group (Cretaceous) southern Alberta Foothills, Canada. Contributions to Mineralogy and Petrology, v. 44, p. 313-329.

Goble, R.J., Treves, S.B., and Ghazi, A.M.
1993: Comparison of the Rainy Ridge analcite phonolite sill and the Crowsnest volcanics, Lewis thrust sheet, Alberta, Canada. Canadian Journal of Earth Sciences, v. 30, p. 1644-1649.

Gordy, P.L. and Edwards, G.
1962: Age of the Howell Creek intrusives. Journal of the Alberta Society of Petroleum Geologists, v. 10, p. 369-372.

Greenwood, H.J., Woodsworth, G.J., Read, P.B., Ghent, E.D., and Evenchick, C.A.
1992: Metamorphism. *In* Geology of the Cordilleran Orogen in Canada, H. Gabrielse and C.J. Yorath (eds.). Geological Survey of Canada, Geology of Canada, v. 4, p. 533-570.

Johnson, T.
1989: The Lost Lemon lives again. Alberta Report, February 20, p. 989.

Karlsson, H.R. and Clayton, R.N.
1991: Analcite phenocrysts in igneous rocks: primary or secondary? American Mineralogist, v. 76, p. 189-199.

Leckie, D.A. and Craw, D.
1995: Westerly-derived Early Cretaceous gold paleoplacers in the western Canada Foreland Basin, southwestern Alberta: tectonic and economic implications. Canadian Journal of Earth Sciences, v. 32, p. 1079-1092.

1997: Anomalous gold occurrences in Cretaceous and Tertiary sediments of Alberta. *In* Exploring for Minerals in Alberta: Geological Survey of Canada Geoscience Contributions, Canada-Alberta Agreement on Mineral Development (1992-1995), R.W. Macqueen (ed.). Geological Survey of Canada, Bulletin 500, p. 331-344.

Lewis, R.
1982: Petrology and mineralogy of the monticellite alnoite associated with the Omaha oilfield, Gallatin County, Illinois. Geological Society of America, Abstracts with Programs, v. 14, p. 265.

Liou, J.G.
1971: Analcime equilibria. Lithos, v. 4, p. 389-402.

Liou, J.G., Maruyama, S., and Cho, M.
1987: Very low-grade metamorphism of volcanic and volcaniclastic rocks-mineral assemblages and mineral facies. *In* Low temperature metamorphism, M. Frey (ed.). Blackie, Glasgow, p. 59-113.

Luhr, J.F. and Kyser, T.K.
1989: Primary igneous analcite: the Colima minettes. American Mineralogist, v. 74, p. 216-223.

Miller, B.E. and Ghent, E.D.
1973: Laumontite and barian-strontian heulandite from the Blairmore Group (Cretaceous), Alberta. Canadian Mineralogist, v. 12, p. 188-192.

Mitchell, R.H. and Bergman, S.C.
1991: Petrology of Lamproites. Plenum Press, New York, 445 p.

Nicholls, J. and Stout, M.Z.
1988: Picritic melts in Kilauea-evidence from the 1967-1968 Halemaumau and Hiiaka eruptions. Journal of Petrology, v. 29, p. 1031-1057.

Norris, D.K.
1964: The Lower Cretaceous of the Southeastern Canadian Cordillera. Fourteenth Annual Field Conference Guide Book. Bulletin of Canadian Petroleum Geology, v. 12, p. 512-535.

Norris, D.K, Stevens, R.D., and Wanless, R.K
1965: K-Ar age of igneous pebbles in the McDougall-Segur conglomerate, southeastern Canadian Cordillera. Geological Survey of Canada, Paper 65-26, 11 p.

Pearce, T.H.
1967: The analcite-bearing volcanic rocks of the Crowsnest Formation. Ph.D. thesis, Queen's University, Kingston, Ontario.

1970: The analcite-bearing volcanic rocks of the Crowsnest Formation, Alberta. Canadian Journal of Earth Sciences, v. 7, p. 46-66.

Peters, T.J., Luth, W.C., and Tuttle, O.F.
1966: The melting of analcite solid solutions in the system $NaAlSiO_4$-$NaAlSi_3O_8$-H_2O. American Mineralogist, v. 51, p. 736-753.

Peterson, T.D.
1989: Peralkaline nephelinites. I. Comparative petrology of Shombole and Oldoinyo Lengai, East Africa. Contributions to Mineralogy and Petrology, v. 101, p. 458-478.

Peterson, T.D. and Currie, K.L.
1993: Analcite-bearing igneous rocks from the Crowsnest Formation, southwestern Alberta. *In* Current Research, Part B. Geological Survey of Canada, Paper 93-1B, p. 51-56.

Peterson, T.D., Esperança, S., and LeCheminant, A.N.
1994: Geochemistry and origin of the Proterozoic ultrapotassic rocks of the Churchill Province, Canada. Mineralogy and Petrology, v. 51, p. 251-276.

Price, R.A.
1962: Fernie map-area, east half, Alberta and British Columbia. Geological Survey of Canada, Paper 61-24, 65 p.

Ricketts, B.D.
1982: Laharic breccias from the Crowsnest Formation, southern Alberta. *In* Current Research, Part A. Geological Survey of Canada, Paper 82-1A, p. 83-87.

Ross, G.R., Parrish, R.R., Villeneuve, M.E., and Bowring, S.A.
1991: Geophysics and geochronology of the crystalline basement of the Alberta Basin, western Canada. Canadian Journal of Earth Sciences, v. 28, p. 512-522.

Roux, J. and Hamilton, D.L.
1976: Primary igneous analcite—an experimental study. Journal of Petrology, v. 17, p. 244-257.

Scarfe, C.M., Luth, W.C., and Tuttle, O.F.
1966: An experimental study bearing on the absence of leucite in plutonic rocks. American Mineralogist, v. 51, p. 726-735.

Taylor, H.P.
1968: The oxygen isotope geochemistry of igneous rocks. Contributions to Mineralogy and Petrology, v. 19, p. 1-71.

Taylor, H.P., Giannetti, B., and Turi, B.
1979: Oxygen isotope geochemistry of the potassic igneous rocks from the Roccamonfina Volcano, Roman Comagmatic region, Italy. Earth and Planetary Science Letters, v. 46, p. 81-106.

Tizzard, P.G. and Lerbekmo, J.F.
1975: Depositional history of the Viking Formation, Suffield area, Alberta, Canada. Bulletin of Canadian Petroleum Geology, v. 23, p. 715-752.

Tilley, C.E. and Henry, M.A.
1952: Latiumite (sulphatic potassium-calcium aluminium silicate), a new mineral from Albano, Latium, Italy. Mineralogical Magazine, v. 30, p. 39-45.

Toulmin, P., III and Barton, J.B., Jr.
1964: A thermodynamic study of pyrite and pyrrhotite. Geochimica et Cosmochimica Acta, v. 28, p. 641-671.

Woolley, A.R. and Syme, R.F.
1976: The analcite-phyric phonolites (blairmorites) and associated analcite kenytes of the Lupata Gorge, Mozambique. Lithos, v. 9, p. 9-15.

DIAMONDS IN ALBERTA: STUDIES OF POTENTIAL HOST ROCKS OF DEEP-SEATED ORIGIN AND APPLICATIONS OF INDICATOR MINERAL EXPLORATION TECHNIQUES[1]

B.A. Kjarsgaard
Continental Geoscience and Mineral Resources Divisions,
Geological Survey of Canada, Ottawa

Abstract

The recent identification of subsurface crystalline basement domains of Archean and Paleoproterozoic age in Alberta is geologically favourable for the occurrence of kimberlite- or lamproite-hosted diamond deposits. Throughout Alberta, diamonds and indicator minerals have been recovered from various Quaternary glacial deposits and modern drainage systems, largely as a result of intensive diamond exploration prospecting since 1990. Recently, pipes containing crater-facies rocks have been discovered in the Grande Prairie area. These pipes, together with strongly potassic igneous rocks exposed in the Milk River area, constitute the only currently known occurrences in Alberta of magmatic rocks of deep-seated origin that have the potential to be diamond-bearing. The "Sweet Grass Intrusives" outcrop as hypabyssal intrusive rocks (dykes, plugs) as well as extrusive rocks in the Milk River area. Combined whole-rock major- and trace-element chemistry, and isotopic studies, coupled with petrographic studies and mineral chemistry, demonstrate that these rocks are minettes, which were derived from a veined, lithospheric mantle source region at >100 km depth (i.e., P >30 kb; garnet-bearing peridotite assemblages). Major- and trace-element chemistry of Cr-spinels from the Sweet Grass minettes indicate that existing classification and discrimination diagrams do not separate minette Cr-spinels from kimberlite or lamproite Cr-spinels. This is important, as Cr-spinel is used commonly in surficial diamond indicator mineral exploration programs in Alberta. Both the Hinton (central Alberta) and Legend (southern Alberta) areas, suggested to have high diamond potential, have complex sedimentological histories (multiply recycled indicator minerals), and the primary source(s) of the diamonds and indicator minerals are still unknown.

Résumé

En Alberta, l'identification récente, au niveau du substratum rocheux, de domaines cristallins d'âge archéen et paléoprotérozoïque est le signe, du point de vue géologique, qu'il pourrait y avoir des gisements de diamants dans des kimberlites ou des lamproïtes. Partout en Alberta, des diamants et des minéraux indicateurs ont été récupérés des divers dépôts glaciaires quaternaires et des réseaux de drainage modernes, principalement dans le cadre des travaux d'exploration intensifs menés depuis 1990 dans le dut de découvrir des gisements de ce type. Récemment, des pipes composées de roches de cratère ont été découvertes dans la région de Grande Prairie. Ces pipes, ainsi que les roches ignées fortement potassiques affleurant dans la région de la rivière Milk, constituent les seules occurrences actuellement connues en Alberta de roches magmatiques d'origine profonde qui présentent un potentiel en diamants. Les intrusifs de Sweet Grass affleurent sous la forme de roches intrusives hypabyssales (dykes, culots) et de roches effusives dans la région de la rivière Milk. Des études sur roche totale d'éléments majeurs et traces ainsi que d'isotopes, conjuguées à des analyses pétrographiques et minérales, ont permis de classer ces roches dans la catégorie des minettes, étant issues d'une région filonienne dans le manteau lithosphérique à >100 km de profondeur (par ex. pressi on >30 kb; assemblage de lherlozite à grenat). Des analyses des éléments majeurs et traces de spinelles chromifères extraits des minettes de Sweet Grass indiquent

[1]Canada-Alberta Agreement on Mineral Development, Project C1.13

que les diagrammes de classification et de discrimination ne permettent pas de séparer les spinelles chromifères provenant de minettes de ceux provenant de kimberlites ou de lamproïtes. Ce fait est important puisque, en Alberta, les spinelles chromifères sont souvent utilisés dans les programmes d'exploration en surface à l'aide des minéraux indicateurs dans le but de découvrir des gisements de diamants. Tant dans la région de Hinton que dans celle de Legend, respectivement dans le centre et le sud de l'Alberta et toutes deux reconnues pour leur grand potentiel en diamants, on note une histoire sédimentologique complexe (minéraux indicateurs recyclés plusieurs fois), ce qui explique pourquoi la(les) source(s) primaire(s) des diamants et des minéraux indicateurs n'a(n'ont) toujours pas été identifiée(s).

INTRODUCTION

Recently the province of Alberta has been the site of intensive prospecting for diamonds. The activity started with Monopros Ltd. claiming ground in the Peace River area in 1988. Changes in the procedure for the staking of metallic mineral permits (diamond staking falls within metallic mineral permitting), and the general high level of interest in diamond exploration across the country led to a staking rush in Alberta. By March 1, 1994, 60 to 75 per cent of the total crown land in Alberta was staked, with approximately 85 per cent of this area the focus of diamond exploration (Dufresne et al., 1994, 1996). Large tracts of ground claimed in the foothills area by a DiaMet/Cameco joint venture lent credence to the Alberta diamond exploration play, as both of these companies had significant involvement in diamond plays in other parts of Canada (DiaMet in the Lac de Gras area, N.W.T.; Cameco in central Saskatchewan). Consequently, the majority of the province has been staked for diamond exploration (Fig. 1) by a variety of junior and senior exploration companies.

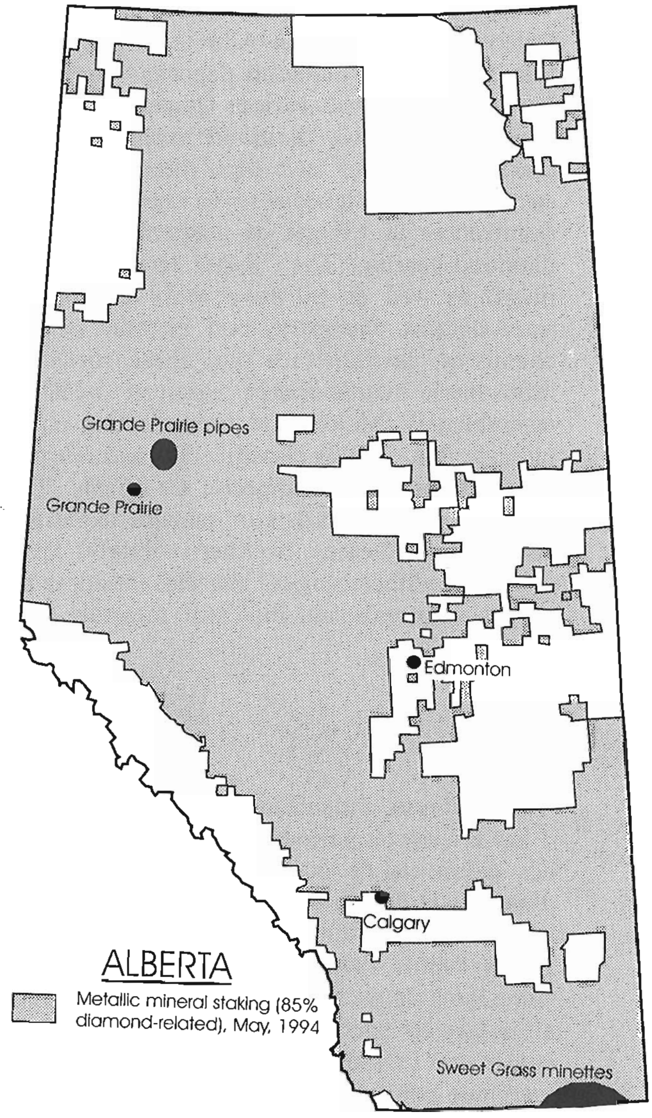

Figure 1. Extent of staking in Alberta, also showing the Sweet Grass minettes and the region in which ultramafic lamprophyre/kimberlite pipes have been discovered in northwestern Alberta. Note that metallic mineral staking includes diamonds, and approximately 85% of the area shown as staked in this figure is related to diamond exploration (modified from Dufresne et al., 1994).

Recent scientific advances in understanding the buried (and exposed) Precambrian basement in Alberta (Ross et al., 1991; Villeneuve et al., 1993; McDonough et al., 1993; McNicholl et al., 1994; McDonough, 1997) have provided an important framework for selecting prospective areas for diamond exploration. Ross et al. (1991) and Villeneuve et al. (1993) utilized U-Pb ages and Nd model ages on core samples from the subsurface basement (acquired from industry hydrocarbon drilling), coupled with regional geophysical data to interpret the geology of the crystalline basement (Fig. 2). Basement domains of Archean and Paleoproterozoic age, as identified by Ross et al. (1991), are geologically favourable for the occurrence of diamondiferous kimberlite and lamproite pipes.

Recognition that economic kimberlites are found in areas underlain by Archean basement ("Clifford's Rule"; Janse, 1994) suggests that most of southern Alberta is prospective for diamondiferous kimberlites (Fig. 2). Archean domains of the Churchill Province include the Loverna block, Eyehill high, Matziwin high and Vulcan low (Villeneuve et al., 1993). The Archean Medicine Hat block (U-Pb zircon ages range from 2612-3278 Ga; Villeneuve et al., 1993) is somewhat enigmatic in that it is not yet clear if this domain is part of the Churchill Province or the Wyoming Craton. Additional regions underlain by Archean basement include the Nova domain in northwestern Alberta, and the Rae subprovince (of the Churchill Province) in northeastern Alberta. Although all these areas are prospective for kimberlites, they can be further subdivided into "stable" Archean domains, and those overprinted by younger thermal and/or collisional events. It has been suggested that Paleoproterozoic titanite ages for the Vulcan low (Villeneuve et al., 1993) and the Medicine Hat block (Davis et al., 1995) record a Proterozoic collisional event in these two domains. Furthermore, Davis and Kjarsgaard (1994) and Davis et al. (1995) have suggested that the lower crust in the Medicine Hat block was thermally reworked in the Paleoproterozoic, synchronous with a metasomatic event in the mantle. In the Loverna block, a biotite granite with a zircon age of 1.78 Ga has been tentatively correlated with the rocks of the Swift Current anorogenic province to the east (Villeneuve et al., 1993), indicating that part of this block has also been subject to a late Paleoproterozoic thermal event.

In contrast to kimberlites, economic lamproites usually occur at the margins of Archean cratons in mobile belts formed during Archean to Proterozoic accretion/orogenesis (Mitchell and Bergman, 1991). From this perspective, the central and northern areas of Alberta, in which the crystalline basement (exposed and subsurface) is predominantly of Paleoproterozoic age, is prospective for diamondiferous lamproites. Prospectivity for diamond-bearing kimberlites in

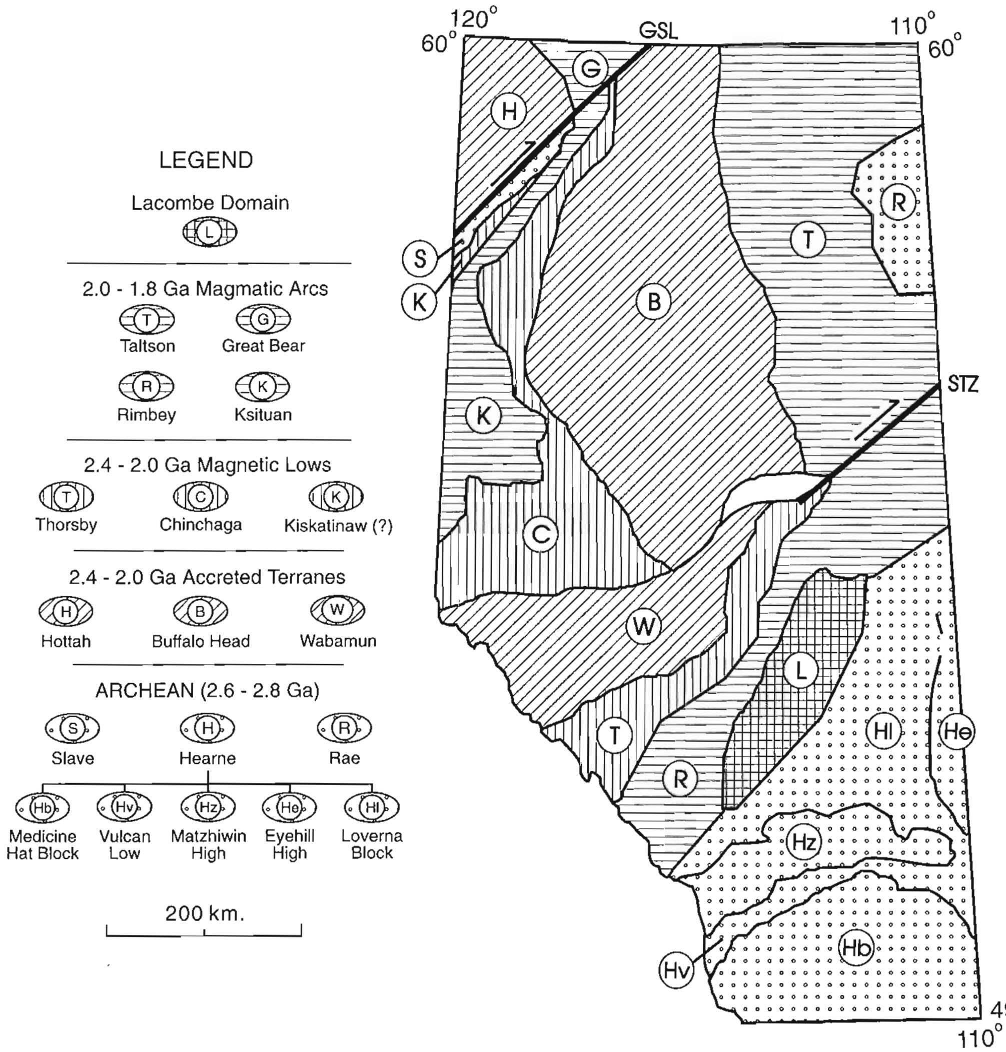

Figure 2. *Age domain map of exposed and subsurface basement terranes in Alberta based on geophysical properties and U-Pb zircon and monazite age data in Villeneuve et al. (1993). Arrows show a relative sense of displacement along the Great Slave Lake shear zone (GSL) and the Snowbird Tectonic Zone (STZ). From Ross et al. (1991).*

northern Alberta cannot be ruled out. Sm-Nd systematics infer an inherited Archean component for a number of the northern Alberta domains. Thériault and Ross (1991) have suggested that the Buffalo Head terrane (a region of complex crustal growth) has scattered initial epsilon Nd values due to the mixing of juvenile and evolved sources during the Paleoproterozoic amalgamation of small Archean crustal blocks. Additional information on diamond prospectivity in Alberta can be found in Dufresne et al. (1994) who discussed the relationships between crystalline basement geology and important structural elements (e.g., Snowbird tectonic zone) and provided an analysis of areas of high diamond potential.

Figure 3. Map of Alberta, Sakatchewan, southern Northwest Territorries, eastern British Columbia and northern Montana showing the location of all diamondiferous and potentially diamondiferous magmatic rocks of deep-seated origin. Localities are as follows: 1, Lac de Gras kimberlite field; 2, Cross Lake kimberlite cluster; 3, Dry Bones bay kimberlite; 4, Grande Prairie pipes; 5, central Saskatchewan (Fort à la Corne and Candle Lake) kimberlite fields; 6, Columbia Icefields/Golden pipes; 7, Bull River pipes and Crossing Creek kimberlite; and 8, Montana alkaline province (minette, alnöite, kimberlite, lamproite).

Importantly, there is no *a priori* reason to suggest that diamond-bearing host rocks will not be found within Alberta. Igneous rocks of deep-seated origin occur near Milk River and Grande Prairie and in general, basement geology is favourable. In addition, a number of different types of potassic rocks of high pressure origin (some diamond-bearing) are found in adjacent areas surrounding Alberta (Fig. 3). These include the kimberlites in central Saskatchewan to the east (Fort à la Corne and Candle Lake fields; Kjarsgaard, 1995), the kimberlite, lamproite, minette and ultramafic lamprophyre of the Montana alkaline province to the south (Hearn, 1989), kimberlites at Crossing Creek, and the alkaline ultrabasic diatremes at Bull River, Golden, Ospika and Kechika River in eastern British Columbia (Pell, 1994), and the Dry Bones Bay kimberlite (Pell, 1995) and other Slave Province kimberlites to the north (Kjarsgaard, 1996).

PETROLOGICAL STUDIES

Sweet Grass minettes, Milk River area

Introduction

Large areas of land in southern Alberta, including the Milk River area, were staked for diamond exploration commencing in 1990. This area is particularly interesting because potassic rocks known as the "Sweet Grass Intrusives" outcrop locally and the regional geologic setting (Archean basement of the Medicine Hat Block; Ross et al., 1991) is, at first approximation, favorable for diamonds. Early geological studies in the 1870s to 1920s considered the Sweet Grass Intrusives to be 'mica traps', or minettes (Dawson, 1884; Weed and Pirsson, 1895; Kemp and Billingsley, 1921). More recently, Currie (1976) described a sample from Black Butte (locality 6, Fig. 4). The mineral assemblage observed (biotite + augite + potash feldspar + olivine) and the lamprophyric texture noted, is consistent with that of a minette (Currie, 1976). Preliminary petrological studies reported by Kjarsgaard (1994) support the interpretation that the Sweet Grass intrusives are, in fact, minettes.

Geology

Potassic rocks outcrop in six areas in southern Alberta (Fig. 4), forming 1 to 3 m wide dykes, larger ovoid shaped plugs and a vent complex (Kjarsgaard, 1994). Recent high-resolution geophysical surveys are strongly suggestive of the presence of related dykes intruding the Phanerozoic sedimentary cover sequence (Ross et al., 1994, 1996). The region of potassic magmatism may therefore extend northward to the Lethbridge area. At present, however, the verified northern limit of the Montana alkaline province (69-27 Ma; Marvin et al., 1980) is defined by outcrops in the vicinity of Milk River (Fig. 4).

A Rb-Sr phlogopite/whole-rock isochron age of 50.3±0.5 Ma reported for an olivine minette dyke from the Coulee 29 locality (Davis and Kjarsgaard, 1994) is identical, within error, to a previously

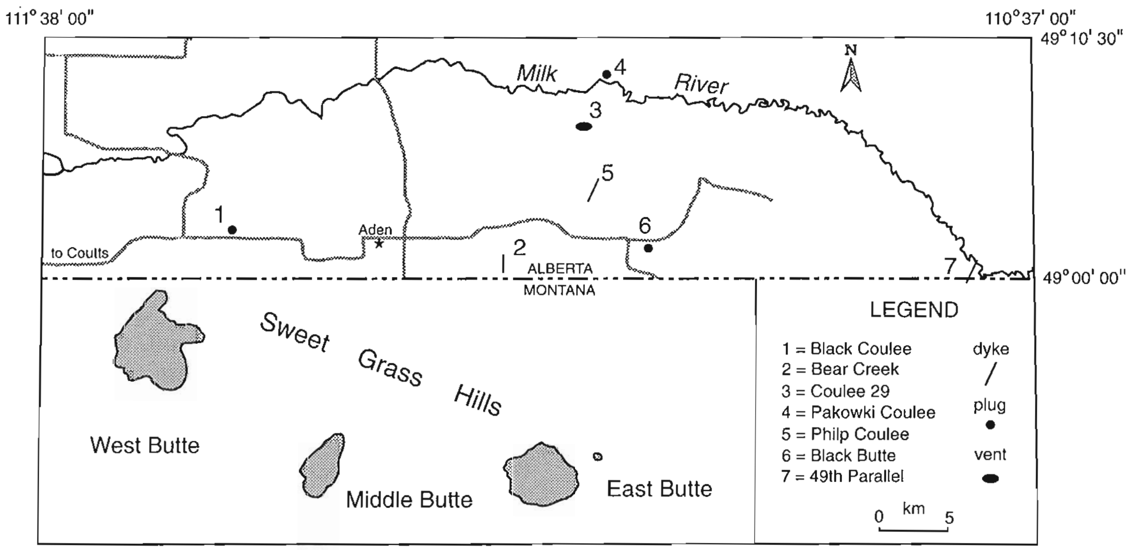

Figure 4. Location map of the Sweet Grass intrusives in the Milk River area of southern Alberta in relation to the Sweet Grass Hills igneous complex (grey hatching) in Montana (adapted from Davis and Kjarsgaard, 1994).

published K-Ar age of 49.2 ± 2.5 Ma (recalculated) for a minette from Black Butte (Baadsgaard et al., 1961). These data confirm an Eocene emplacement age for the Sweet Grass minettes in southern Alberta and are within error of the 50-54 Ma age determined by Marvin et al. (1980) for rocks from the Sweet Grass Hills in Montana. This magmatism is synchronous with the peak of magmatic activity occurring in the Montana alkaline province (Missouri Breaks, Eagle Buttes, Sweet Grass Hills, and the Bearpaw and Highwood mountains) at 49 to 55 Ma (Davis and Kjarsgaard, 1994; Marvin et al., 1980).

The Sweet Grass rocks in Alberta are subdivided into six distinct types (andesite, mixed andesite/minette, and four variants of minette), based on combined petrography, mineralogy and geochemistry. The four types of minette include:

1) alkali olivine minette, consisting of olivine + phlogopite + diopside + Cr-spinel phenocrysts in a groundmass of mica (phlogopite-biotite$_{ss}$) + salite + sanidine + titanomagnetite + apatite + calcite ± analcime;

2) phlogopite minette, consisting of phlogopite (cumulate-rich) + diopside + olivine + Cr-spinel phenocrysts in a groundmass of mica (phlogopite-biotite$_{ss}$) + salite + sanidine + titanomagnetite + apatite + calcite ± analcime;

3) alkali minette, consisting of phlogopite + augite + Cr-spinel (± rare olivine) phenocrysts in a groundmass of mica (phlogopite-biotite$_{ss}$) + salite + sanidine + titanomagnetite + apatite + calcite ± analcime; and,

4) peralkaline minette, consisting of rare phlogopite + salite phenocrysts in a groundmass dominated by phlogopite- biotite$_{ss}$ mica and sanidine with calcite + apatite + NaK-Ti amphibole + aegirine augite + titanomagnetite ± analcime.

Mafic minerals in the minettes exhibit lower magnesium numbers ($Mg\# = Mg/Mg + Fe^{2+}$) in the sequence alkali olivine minette ≈ phlogopite minette > alkali minette > peralkaline minette. In all minettes, phlogopite and clinopyroxene phenocrysts are strongly zoned, showing normal, reverse and oscillatory zoning. Alkali olivine minette, phlogopite minette and alkali minette are gradational into each other and are related by crystal fractionation/accumulation processes; however, the mineralogy of the peralkaline minettes suggests that processes such as variation in degree of partial melting was important in their genesis.

Two other rock types are also observed. Andesite (diorite porphyry) is found at Black Coulee (Fig. 4) and consists of plagioclase + hornblende phenocrysts in a matrix of feldspar + hornblende + Fe-Ti spinel ± quartz. "Mixed" andesite/minette occurs at Coulee 29 (Fig. 4; the tan vent breccia) and forms Sill 39 at Middle Butte (Sweet Grass Hills, Montana; Kemp and Billingsley, 1921). These rocks contain phenocrysts of hornblende + plagioclase feldspar + diopside + salite + phlogopite + biotite phenocrysts in a fine grained groundmass of feldspar + diopside + salite + biotite + spinel.

Coarse grained xenoliths (clinopyroxenite, phlogopite clinopyroxenite, and glimmerite) occur at all localities (with the exception of the 49th Parallel locality; Fig. 4) and have varying modal proportions of mica (phlogopite or biotite), clinopyroxene (diopside–augite) and apatite (±K-feldspar ± dolomite). The mineralogy is similar to the host minettes (except that dolomite occurs in the xenoliths versus calcite in the minettes). Minerals in the xenoliths show minor or no compositional zoning, in contrast to those in the minettes.

Mineralogy

Phlogopite-biotite mica

A ubiquitous phase in the Sweet Grass minettes and associated cognate xenoliths, exhibits a wide compositional range. Microprobe analyses of zoned mica phenocrysts (core to rim) and homogeneous groundmass crystals from minette, mica from coarse grained cognate xenoliths, and mica from glomerophyric clusters (associated with olivine and Cr-spinel) are illustrated in Figures 5a and b. The salient points to be observed on these two diagrams are: 1) compositions of mica from xenoliths overlap those from the core and middle of zoned phenocrysts from minettes, although Al_2O_3 contents are slightly higher in mica from phlogopite clinopyroxenite and clinopyroxenite xenoliths; 2) zoning trends show increasing FeO_{total} and TiO_2 at constant to decreasing Al_2O_3; and 3) most, but not all, compositions fall in the known range for micas from minettes (c.f. Mitchell and Bergman, 1991). Importantly, a subset of samples have alumina levels which are similar to those observed in some lamproites (Fig. 5a, b). However, it should be noted that FeO_{total}-TiO_2-Al_2O_3 ternary relations of micas from lamproites and the Sweet Grass minettes are not similar, thus allowing discrimination of these two rock types. The core to rim trend of decreasing Al_2O_3 in the Sweet Grass micas is suggested here to be typical of alkaline and peralkaline minettes; it is also observed, but not well developed, in other highly

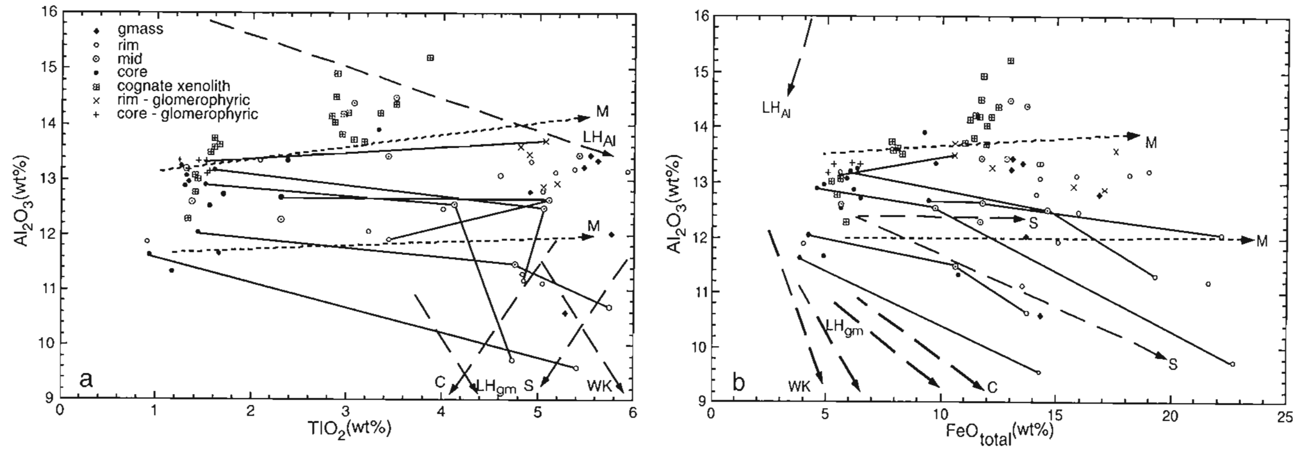

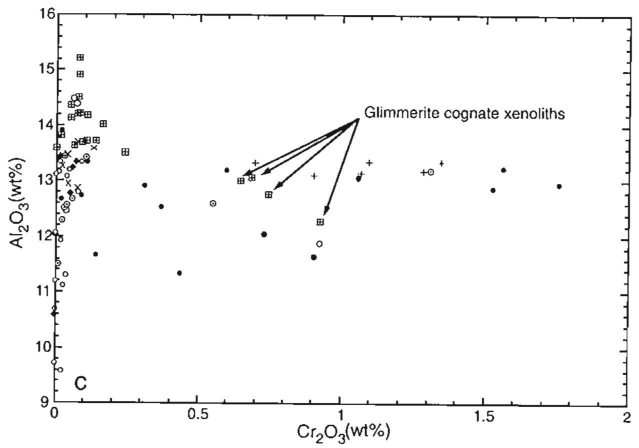

Figure 5. Microprobe analysis of micas from the Sweet Grass minettes: **a.** *Al_2O_3 versus TiO_2;* **b.** *Al_2O_3 versus FeO total;* **c.** *Al_2O_3 versus Cr_2O_3. All diagrams are wt%. Symbol legend for Figures 5a, b, and c is shown on Figure 5a. Solid lines join analyses from zoned phenocrysts. The minette differentiation trend (Mitchell, 1986) is indicated by short dashed lines labelled M. Representative lamproite differentiation trends (Mitchell and Bergman, 1991) are indicated by long dashed lines labelled as follows: WK, West Kimberley; C, Chelima; S, Sisimiut; LH_{gm}, Leucite Hills groundmass; LH_{Al}, Leucite Hills aluminous biotite high pressure phenocrysts.*

alkaline minettes (e.g., Bohemian alkali minettes; Mitchell and Bergman, 1991).

Spinel

Petrographic studies illustrate that Cr-rich spinels in the Sweet Grass minettes are commonly observed in glomeroporphyritic clusters comprised of Cr-spinel, olivine and phlogopite. Microprobe analyses of cores of phlogopite from this association reveal a Cr-rich composition, similar to cores of phlogopite in minettes, and Cr-rich phlogopite in glimmerite xenoliths (Fig. 5c). In contrast, phlogopite in phlogopite clinopyroxenite and clinopyroxenite xenoliths is generally Cr-poor (Fig. 5c), consistent with co-existing spinel being Ti- and Fe-rich. Mineral chemistry, combined with petrographic observations suggest that the Cr-rich spinels are an early formed, high pressure minette liquidus phase, and the Ti- and Fe-rich spinels are a later formed lower pressure liquidus phase. The variation in the spinel chemistry is best displayed in two dimensions by utilizing a plot of *Mg#* versus Ti/Ti + Cr + Al (the front face of the reduced spinel prism; Mitchell, 1986). Figure 6 illustrates the compositional

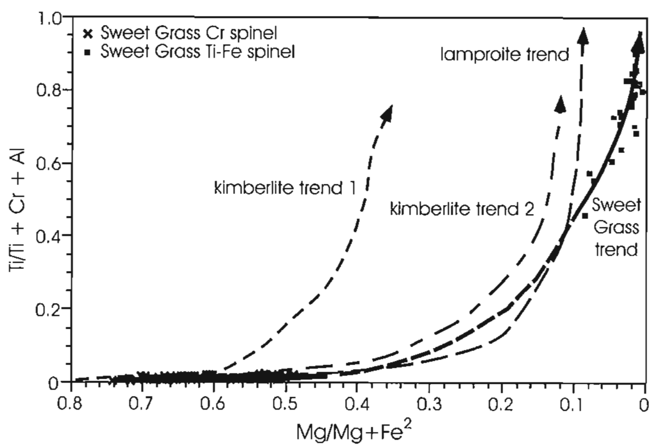

Figure 6. The front face of the reduced spinel prism, comparing the compositional trend of magmatic spinels from the Sweet Grass minettes with kimberlite magmatic spinel trends 1 and 2 and the lamproite magmatic spinel trend. Kimberlite and lamproite magmatic spinel trends are from Mitchell (1986).

trend of spinels from the Sweet Grass Intrusives, and for comparison magmatic spinel trends observed in kimberlite, lamproite, and a variety of ultrabasic rock types.

Heavy mineral concentrates

Heavy mineral concentrates from two Sweet Grass minette samples did not contain any diamonds, however, Cr-pyrope "G9" garnets, with compositions typical of garnet from garnet lherzolite (Fig. 7) were recovered, along with olivine (Fo_{89-91}) and abundant Cr-spinel. Unfortunately, no polymineralic aggregates or xenoliths containing Cr-pyrope + olivine + enstatite ± Cr-diopside were found, thus it was not possible to execute pressure-temperature (P–T) calculations to constrain the minimum depth of origin of the Sweet Grass minette magmas. However, the recognition of Cr-pyrope garnet does provide a minimum depth constraint for these minette magmas at >30 kb (based on the spinel to garnet lherzolite transition; e.g., Wyllie, 1984).

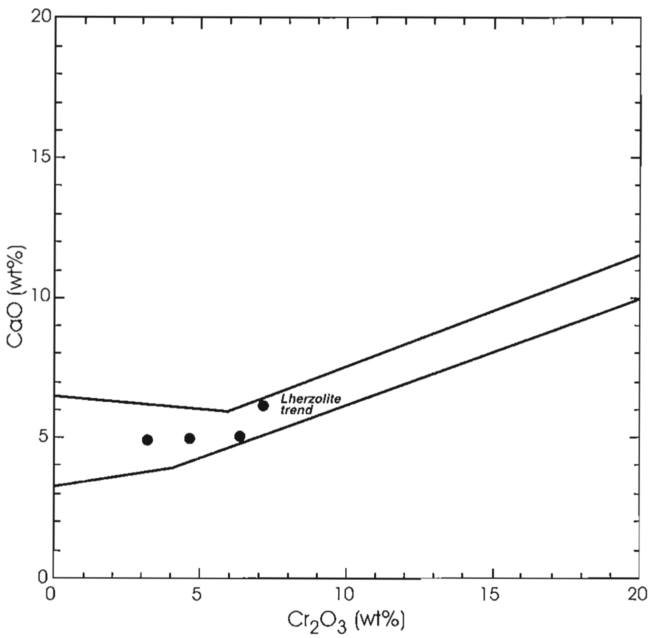

Figure 7. Microprobe analyses of Cr-rich pyrope garnet from concentrate, Sweet Grass Hills, southern Alberta, plotted on the CaO versus Cr_2O_3 discriminant diagram. The lherzolite trend is from Sobolev (1974).

Geochemistry

Revised (from Kjarsgaard, 1994) and new whole-rock major, trace and stable element isotopic chemistry from each locality is presented in Figures 8 through 14.

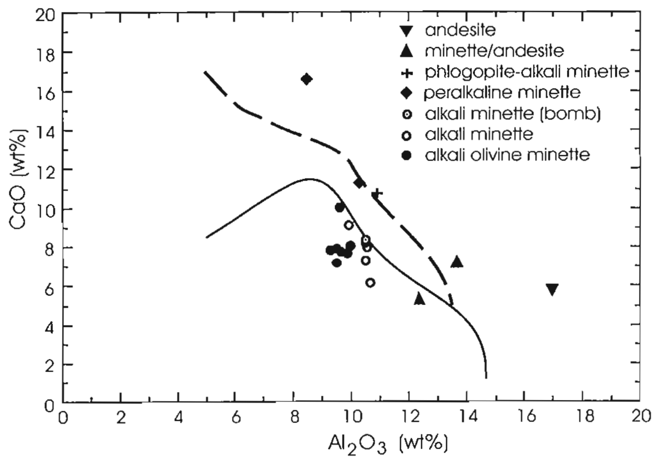

Figure 8. Plot of CaO versus Al_2O_3 (wt%) for rocks from the Sweet Grass area, southern Alberta. The lines indicate discriminant boundaries separating lamproites from other potassic rocks after Foley et al. (1987; solid line) and Mitchell and Bergman (1991; dashed line).

Major and trace element analytical methods are outlined in Kjarsgaard (1994); stable isotope analyses were performed at the University of Ottawa utilizing standard techniques. The abundance of CaO and Al_2O_3 in the Sweet Grass minettes, as shown in Figure 8, illustrates that the majority of the samples fall within the lamproite field as defined by Foley et al. (1987) or Mitchell and Bergman (1991). However, application of the CaO versus Al_2O_3 discriminant diagram alone is not supported by other data; mineral chemistry (see previous) and trace element abundances in Sweet Grass rocks are inconsistent with those observed in lamproites. Figure 9 illustrates this inconsistency with a Pearce type spiderdiagram (sample/MORB normalized) which compares element abundances from Leucite Hills, Wyoming and Smoky Butte, Montana, lamproites with average Sweet Grass alkali olivine minette, alkali minette and peralkaline minette. Compared to the Sweet Grass minettes, the lamproite samples have higher levels of K, Sr, Ba, LREE (light rare earth elements), Th, Ta, Hf, Nb, Zr, P and Ti. The REE (rare earth elements) data are shown on a separate spiderdiagram (Fig. 10) for greater clarity. Plots of Sm versus La/Yb_{cn} ratio (Fig. 11), Hf versus Ta (Fig. 12), and Nb versus Zr (Fig. 13) also illustrate that the lamproites have higher abundances of these trace elements than the Sweet Grass minettes. Figures 9 to 13 demonstrate that the lower trace element levels in the Sweet Grass rocks, which preclude their classification as lamproites.

Peralkaline minettes from the 49th Parallel locality (Fig. 4) have higher levels of K, Rb, Sr, Ba, Th, Hf, Ta, Nb, Zr, LREE, P and Ti than other Sweet Grass

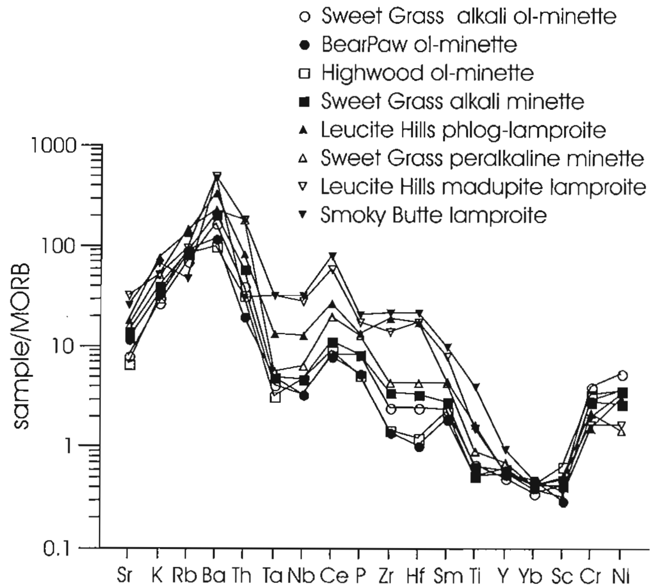

Figure 9. *Pearce spiderdiagram comparing element level abundances for average Sweet Grass alkali olivine minette, alkali minette and peralkaline minette (this study) with olivine minette from the Bearpaw (Macdonald et al., 1992) and Highwood Mountains (O'Brien et al., 1989), Montana. Lamproites from the Leucite Hills, Wyoming, and Smoky Butte, Montana, are also shown for comparison (data from Mitchell and Bergman, 1991). MORB (mid-ocean ridge basalt) normalization values are from Pearce (1983).*

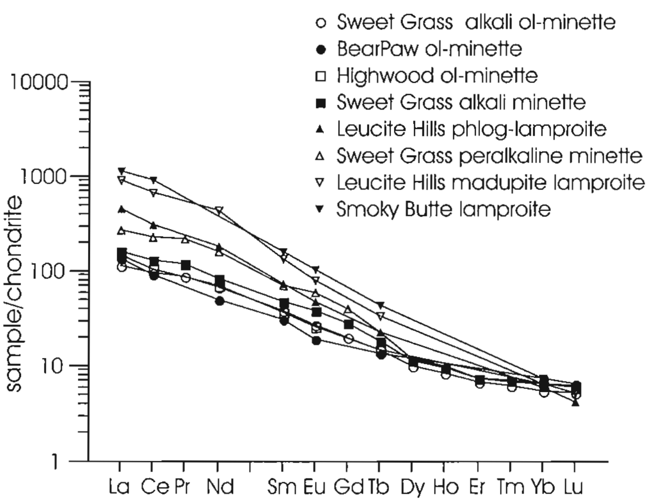

Figure 10. *REE abundances in average Sweet Grass alkali olivine minette, alkali minette and peralkaline minette. Olivine minette from the Bearpaw and Highwood Mountains, and lamproites from the Leucite Hills and Smoky Butte are shown for comparison. Data sources are the same as for Figure 9. Chondrite normalization values from Nakamura (1974).*

minettes, and show some geochemical similarity to trace element-poor lamproites (Figs. 9-13). However, in terms of major element chemistry (Fig. 8), these peralkaline minettes do not plot in the lamproite field, owing to their high CaO. Elevated CaO (plus CO_2 and P_2O_5) is consistent with the high modal proportions of calcite and apatite observed by petrography. Stable isotopic analyses of calcite and dolomite for selected minette and cognate xenolith samples are shown in Figure 14. The isotopic compositions of the carbonates fall outside the known range of values for both mantle

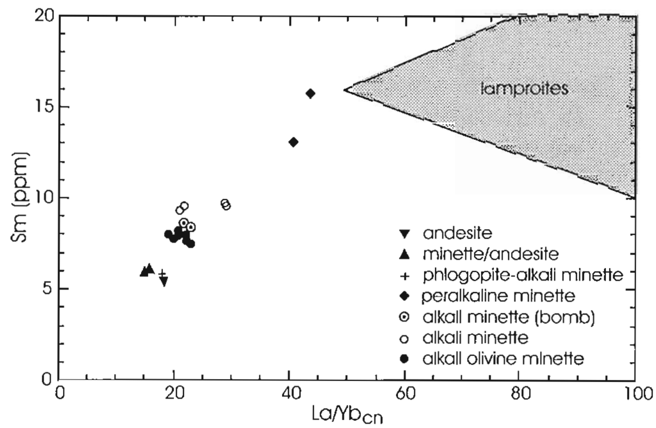

Figure 11. *Sm (ppm) versus La/Yb$_{cn}$ trace element diagram for minette/lamproite discrimination. Sweet Grass data are from this study; main field of lamproite compositions are from Mitchell and Bergman (1991).*

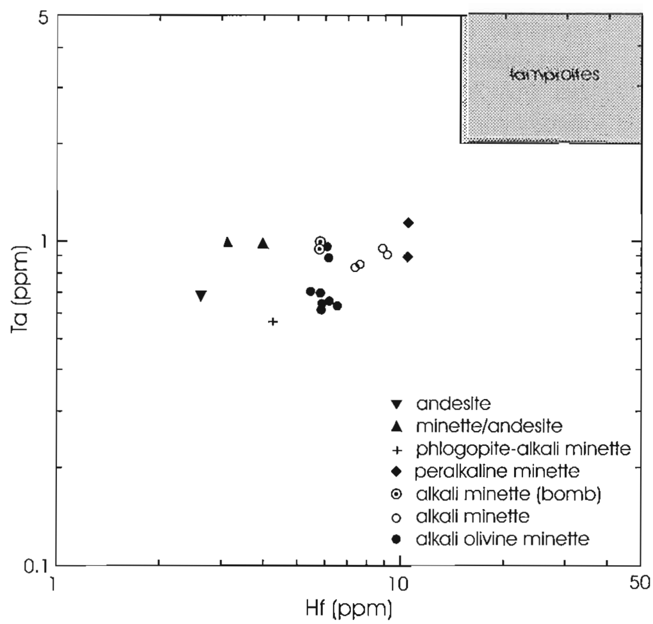

Figure 12. *Hf versus Ta (ppm) trace element diagram for minette/lamproite discrimination. Data sources are the same as for Figure 11.*

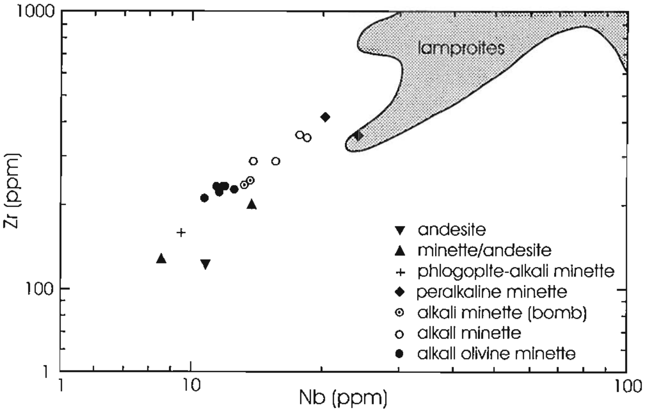

Figure 13. *Nb versus Zr (ppm) trace element diagram for minette/lamproite discrimination. Data sources are the same as for Figure 11.*

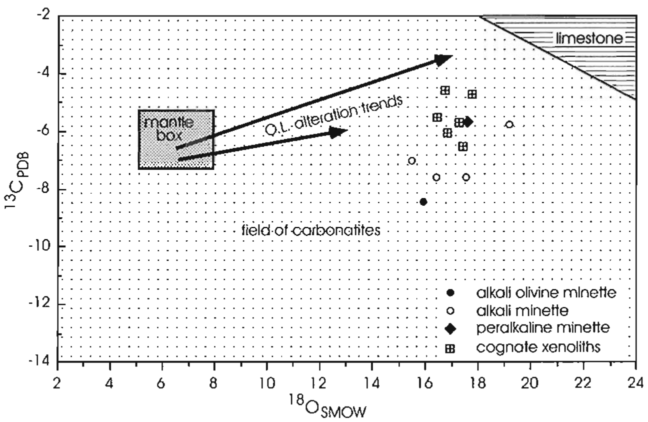

Figure 14. *$^{13}C_{PDB}$ versus $^{18}O_{SMOW}$ for calcite (from minettes) and dolomite (from cognate xenoliths) from selected Sweet Grass Hills samples. Mantle box from Kyser (1986), carbonatite and limestone fields from Bell and Dawson (1995). O.L., Oldoinyo Lengai alteration trend (Keller and Hoefs, 1995).*

carbonates and crustal limestone, but are similar to those from carbonatites (many of which are interpreted to have undergone some post-emplacement alteration). Calcite and dolomite in the Sweet Grass minettes is interpreted to be of magmatic origin (i.e., mantle derived C and O), with the isotopic signature shifted as a result of interaction with meteoric water.

INTERPRETATION

Similar to other potassic (and alkali-rich) magmas, the Sweet Grass magmas are interpreted to have formed from variable degrees of partial melting of lithospheric mantle which was veined as a result of an earlier metasomatic event (e.g., Meen et al., 1989; Foley, 1992; at a pressure of >30 kb). In this interpretation, peralkaline minette magmas originated by low degrees of partial melting, with the melts dominated by low melting temperature vein minerals (amphibole-carbonate-apatite-phlogopite). Olivine minette magmas originated from higher degrees of partial melting, with the "vein component" of the melt subordinate to that generated from the peridotite wall rock. The olivine minettes are notable for containing xenoliths. Multiple lines of evidence (see below) suggest that these xenoliths are of cognate origin, in the sense that they are comprised of minerals precipitated (and accumulated) from the minette magma in deep crustal and/or lithospheric mantle magma chamber(s). In contrast, cognate xenoliths are not observed in peralkaline minettes, suggesting that minimal ponding of magma occurred during ascent from the source region enroute to the surface.

The absence of zoning in minerals from cognate xenoliths is consistent with their formation as cumulates in ponded magma. The occurrence of magmatic dolomite (and not calcite) in the xenoliths suggests a minimum pressure of ≈15 kb (Dalton and Wood, 1993), that is, magmatic ponding is suggested to have occurred at the base of thick crust or at deeper levels within the lithospheric mantle. In clinopyroxene-rich cognate xenoliths, the Cr_2O_3 content of phlogopite is low (<0.25 wt%; Fig. 5c), suggesting precipitation from a fractionated melt. However, in glimmerite xenoliths, phlogopite is simmilar in composition (0.60–1.50 wt% Cr_2O_3; Fig. 5c) to that observed in the Cr-spinel - olivine - phlogopite glomeroporphyritic clusters, suggesting early phlogopite fractionation and accumulation to form the glimmerites at high pressure. This suggests the cognate xenoliths formed over a range of pressure (>30 kb to ≥15 kb).

Compositions of spinel are bimodal; early, primitive high pressure Cr- and Mg-rich spinel occur in glomeroporphyritic clusters while late, fractionated lower pressure Ti- and Fe-rich spinel is present in both cognate xenoliths (containing low Cr-phlogopite) and the minette groundmass. Spinels of intermediate composition rarely occur as thin reaction rims on spinels. The Sweet Grass minette spinel trend is similar to magmatic spinel trend 2 (also seen in kimberlite and lamproite; Mitchell, 1986), which supports the interpretation that this mineral is both an early and late liquidus phase in these rocks. The compositional gap observed at intermediate *Mg#* (Fig. 6), however, suggests that spinel is not a liquidus phase throughout the course of crystallization. This may be a result of the spinel liquidus volume decreasing with pressure (as observed in simple basaltic experimental systems; e.g., Presnall et al., 1978), but remains unproved.

The occurrence of andesite (diorite porphyry), as well as rocks containing phenocryst assemblages from both andesite and minette (e.g., Sill 39, tan vent breccia at Coulee 29), indicates that a second discrete magma-type (andesite) existed in addition to minette magma. Rocks from Sill 39 and the tan vent breccia at Coulee 29 are interpretated to have resulted from the mixing of andesite and minette magmas. The origin of the andesite magma is not well understood, due to a restricted number of samples. However, they are suggested to have a large remelted lower crustal component, related to the latent heat of crystallization of ponded olivine minette magma at the base of the crust.

Economic significance

The diamond potential of minette, in general, is inferred to be low to nonexistent, because these rocks are considered to have been generated at pressures below the stability of diamond for normal shield geotherms (<30 kb; e.g., Mitchell, 1991). However, the Akluilak ultrapotassic lamprophyre (minette) dyke in the Churchill Province, N.W.T., is richly diamondiferous (McRae et al., 1995, 1996). Furthermore, minette from The Thumb, New Mexico, although non-diamondiferous, contains garnet lherzolite xenoliths sampled from ≈ 150 km depth (46 kb, Ehrenburg, 1982) the pressure at which a typical diamond is stable for a typical shield geotherm. Classification of the "Sweet Grass Intrusives" as minette (more specifically, alkali and peralkaline minette) and the observation that these melts were generated at pressures of Cr-pyrope garnet stability (exact pressures unknown, but >30 kb) warrants examination for diamond potential. Interestingly, there are a number of mineralogical and geochemical similarities between the diamondiferous Akluilâk lamprophyre and 49th Parallel, dykes. In both rocks, mineralogy is dominated by biotite + K-feldspar + apatite + calcite.

Geochemical analyses illustrate similar major element abundances, for example both the Akluilak and 49th Parallel rocks have low SiO_2 and MgO, and high TiO_2, Al_2O_3, K_2O, P_2O_5, and CO_2. In addition, many trace elements in both of these rocks have similar abundances. Furthermore, when compared to their associated rocks (Christopher Island Formation minettes or the Sweet Grass minettes, respectively), both the Akluilak lamprophyre and 49th Parallel dykes have anomalous geochemistry. The geochemical and mineralogical similarity between the diamondiferous Akluilak and 49th Parallel dykes, coupled with the interpretation that the 49th Parallel dykes did not undergo significant fractionation or ponding in the crust enroute to the surface (as indicated by the lack of cognate xenoliths), suggests that these dykes could have the highest diamond-bearing potential of all the Sweet Grass rocks. Diamond recovery was not attempted on these samples; heavy mineral concentrates were only made from two alkali minettes. It was previously noted that the Archean Medicine Hat Block was reworked by Proterozoic tectonothermal and metasomatic events (Davis, 1994; Davis et al., 1995; Villeneuve et al., 1993). This event could have affected the preservation of the underlying mantle root (and diamonds), and might explain why diamonds have not been recovered from the Sweet Grass minettes, nor from bulk sampling of kimberlite and alnöite in the Missouri Breaks area to the south in Montana (Hausel, 1995).

Potential exists for other types of economic deposits associated with minettes. Rock (1991) summarized the available data, and suggested a relationship exists between gold deposits and lamprophyres. Specifically of interest are the gold deposits at Middle and East Buttes, Sweet Grass Hills, Montana (Gavin, 1991). Kjarsgaard (1994), however, presented results from neutron activation analysis for 17 minette samples for silver, gold and iridium (used as an indicator for platinium group elements), which indicated low abundances of these elements in the samples analysed.

Grande Prairie pipes

Pipes with crater facies material have been identified northeast of Grande Prairie (Fig. 1). They are similar to those at Fort à la Corne, Saskatchewan (B.H. Scott-Smith, oral presentation, CIM Meeting, Vancouver, 1994). The basement geology in this region consists of Paleoproterozoic gneissic rocks of the Chinchaga Domain (a prominent gravity low), formed at 2.17 to 2.08 Ga (U-Pb zircon; Villeneuve et al., 1993). Nd model ages range from 2.46 to 2.68 Ga (Thériault and Ross, 1991; Villeneuve et al., 1993), indicating juvenile and Archean components in the Chinchaga rocks. Preliminary studies suggest that the Grande Prairie pipes are either of kimberlite or ultramafic lamprophyre affinity. The classification difficulty arises because the single sample (courtesty of Monopro Ltd.) studied by the author was altered and contaminated by crustal material. Whole rock trace element geochemistry of the sample indicates crustal contamination (e.g., Mitchell, 1986), as shown in

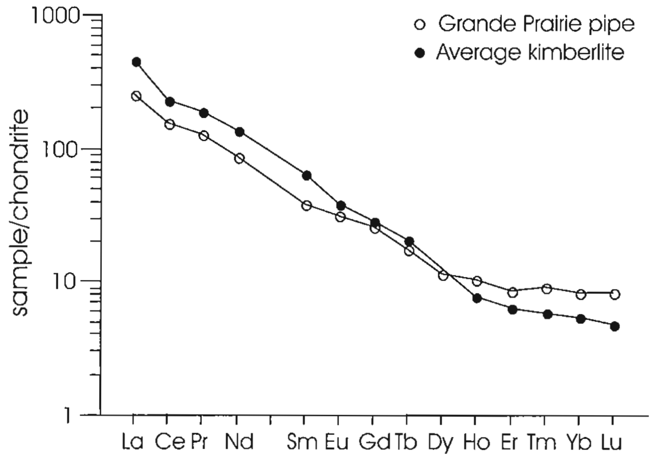

Figure 15. *REE abundances for Grande Prairie pipe as compared to average kimberlite (Mitchell, 1986). Chondrite normalization values are from Nakamura (1974).*

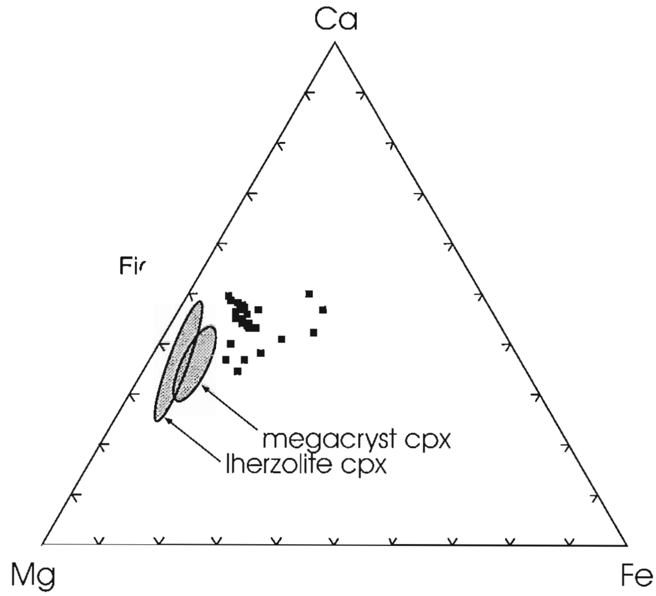

Figure 16. *Compositions of clinopyroxene (mol%) from the Grande Prairie pipe as compared to the fields for clinopyroxenes from the kimberlite megacryst suite (Schulze, 1987) and mantle lherzolite (Nixon, 1987).*

Figure 15 by the low La/Yb_{cn} ratio and high HREE (heavy rare earth element) abundances. The major element geochemistry also suggests contamination using varies contamination indices (*in* Mitchell, 1986). For example, Clement's Contamination Index = 3.82 (where > 1-1.5 is contaminated); Si/Mg Contamination Index = 2.50 (where > 1.2 is contaminated); *Mg#* = 82 (where < 85 is contaminated). Compared to typical, uncontaminated kimberlites, the Grande Prairie sample studied has higher abundances of Sc and V, a higher Ba/Sr ratio ($\approx$ 18), and lower Ni/Cr (0.66) and MgO/CaO (5.58) ratios. These differences are suggested to be a result of contamination (MgO/CaO ratio) and post-emplacement alteration (Ba/Sr and MgO/CaO ratios), although the variation in Sc and V abundance and Ni/Cr ratio is interpretated to be a primary feature.

The Grande Prairie sample is petrographically classified as an olivine-rich juvenile lapilli tuff. The euhedral to anhedral olivine is completely altered to clay minerals and serpentine. The lapilli consist of devitrified vesicular glass and microphenocrysts with crystals of altered olivine and usually fresh clinopyroxene. The lapilli matrix consists of devitrified glass, clinopyroxene, spinel, rutile, perovskite and apatite with very minor carbonate. Broken plagioclase feldspar crystals that are assumed to result from contamination during emplacement are also present. Three distinct populations of clinopyroxene are defined on the basis of shape and colour: 1) dark green euhedral to subhedral crystals with a grain size of 0.5 to 1.5 mm; 2) light green, 1 to 2 mm long acicular crystals, and 3) 0.5 to 1 mm pale green blocky crystals. In the Grande Prairie pipe, clinopyroxene is Ca- and/or Fe-rich as compared to clinopyroxene from mantle xenoliths or the kimberlite megacryst suite (Fig. 16). The three types of clinopyroxenes (i.e., diopside, augite, and salite) are suggested to be liquider phases which have rims showing extenisve solid solution toward aegirine.

Results from whole rock geochemistry, petrography and mineralogy suggest that the Grande Prairie pipes may be of ultramafic lamprophyre affinity, rather than bonafide kimberlites. The presence of liquidus clinopyroxene (and associated high Sc and V in whole rock trace element chemistry), in particular, supports this interpretation. The morphology and chemistry (e.g., augite and salites) of the clinopyroxenes are quite different from microcrystalline diopside which forms in contaminated kimberlites (e.g., Mitchell, 1986). Additional studies on a larger suite of uncontaminated samples, however, is required to properly classify the Grande Prairie pipes as either ultramafic lamprophyres or kimberlites. To address this problem, a detailed investigation of the Grande Prairie pipes is currently underway by a Geological Survey of Canada - Alberta Geological Survey joint venture. Sampling has been completed, consisting of drilling two cores, one from each of the north and south bodies. Investigations in progress include sedimentology and stratigraphy, volcanology, geochemistry, radiometric geochronology, glaciology, indicator mineral studies, micropaleontology, and palynology of these associated rocks. These studies are similar in scope to those done on the Smeaton, Fort à la Corne, Saskatchewan, kimberlite drill core (Kjarsgaard et al., 1995).

DIAMOND EXPLORATION TECHNIQUES

Compositional trends of minette spinels: implications for diamond exploration

Cr-spinel is an important mineral utilized in stream sample sediment and till sample prospecting for diamond deposits (kimberlites and lamproites; e.g., Thorleifson and Garrett, 1996). This mineral is also used in follow-up studies because spinels of specific chemistry have been recognized to be intimately associated with diamond (Gurney, 1989). A number of detailed studies have been published in the past five years specifically dealing with the major and trace element composition of spinel and application to diamond exploration (Griffin and Ryan, 1993; Fipke, 1994; Griffin et al., 1994; Fipke et al., 1995; Schulze, 1996). The most commonly applied spinel mineral chemistry plot utilized is a MgO-Cr_2O_3 major element discrimination diagram, in which a well-defined field of Mg- and Cr-rich spinel compositions derived from diamond inclusion studies is known (Moore and Gurney, 1989; Fipke et al., 1995). Figure 17 compares

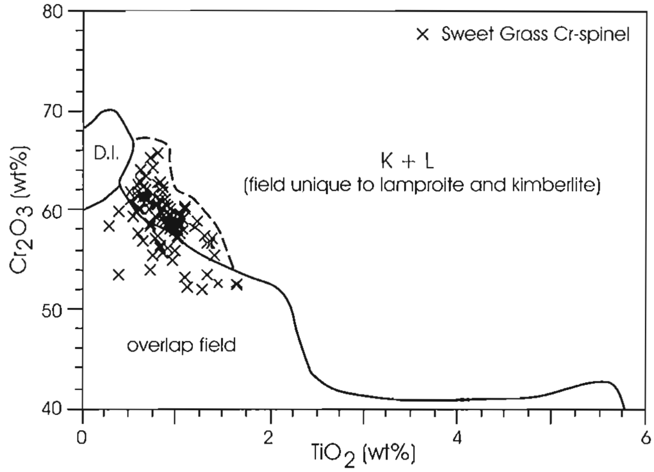

Figure 18. *The TiO_2 versus Cr_2O_3 (wt%) spinel discrimination plot of Fipke (1994). Solid lines separate: D.I., diamond inclusion spinels; K+L, spinels unique to kimberlite and lamproite; and overlap field, spinels from kimberlite plus lamproite and various other rocks. Note that approximately half the Sweet Grass Cr-spinels fall into the field of spinels suggested to be unique to kimberlite or lamproite. The heavy dashed line is the recommended revision to the empirical discriminant line of Fipke (1994) separating spinels equal to kimberlite plus lamproite from the spinels in the overlap field. See text for further details.*

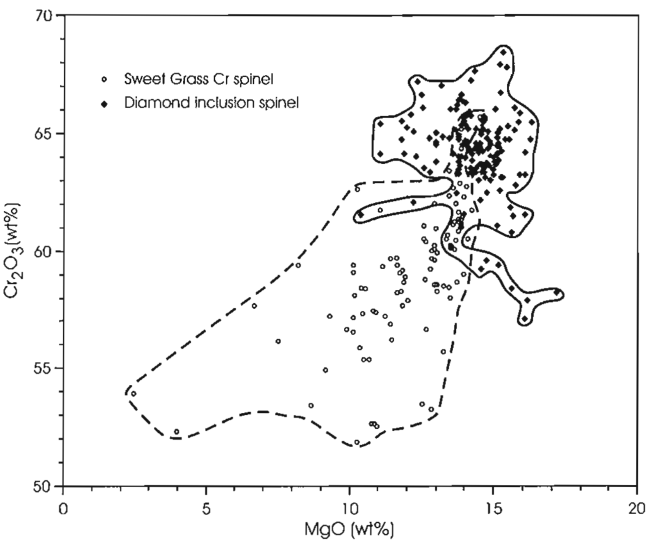

Figure 17. *Plot of MgO versus Cr_2O_3 (wt%) for Cr-rich spinels from the Sweet Grass Hills minettes (area enclosed by a dashed line; data from this study) versus diamond inclusion Cr-spinels (area enclosed by a solid line; data are from Moore and Gurney, 1989).*

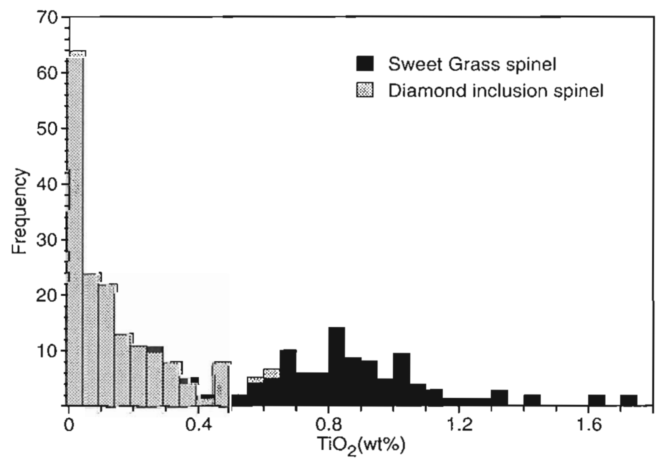

Figure 19. *Histogram comparing the frequency distribution of TiO_2 (wt%) in diamond inclusion Cr-spinels (data are from Moore and Gurney, 1989) with Cr-rich spinels from the Sweet Grass minettes (data from this study).*

the composition of Cr-spinels from the Sweet Grass minettes with those from diamond inclusions (Moore and Gurney, 1989; Fipke et al., 1995); note that a subset of the Sweet Grass Cr-spinels falls into the "diamond inclusion" field.

Further major element discrimination of spinel can be made utilizing plots of TiO_2 versus Cr_2O_3 (Fig. 18), with diamond inclusion spinels having high-Cr_2O_3 and low-TiO_2 (Fipke, 1994; Fipke et al., 1995). Note that the Sweet Grass spinels do not fall into the "diamond inclusion" field on the basis of their high TiO_2 contents (Fig. 18). This is evident in Figure 19, which compares the frequency distribution of TiO_2 in diamond inclusion Cr-spinels with the Sweet Grass Cr-spinels. The TiO_2–Cr_2O_3 plot (Fig. 18) can also be utilized to discriminate kimberlite- and lamproite-derived spinels (e.g., spinels from prospective diamond host rocks) from spinels derived from kimberlite, lamproite and other rocks such as lamprophyres and basalts (the latter are considered to be nonprospective for diamonds; Fipke et al., 1995). However, as is apparent from Figure 18, more than half of the spinel population from the Sweet Grass minette heavy mineral concentrates falls into the field "unique to kimberlite and lamproite." Since the Sweet Grass spinels are minette-derived, this suggests that the empirical discrimination line (Fipke, 1994), which separates spinels from kimberlite and lamproite from rocks in the overlap field, requires modification (see Fig. 18). Furthermore, it is apparent that there is considerable overlap amongst spinels from various sources, and even with revision of the discrimination line (Fig. 18), the validity of using this diagram for application to diamond prospecting may be tenuous.

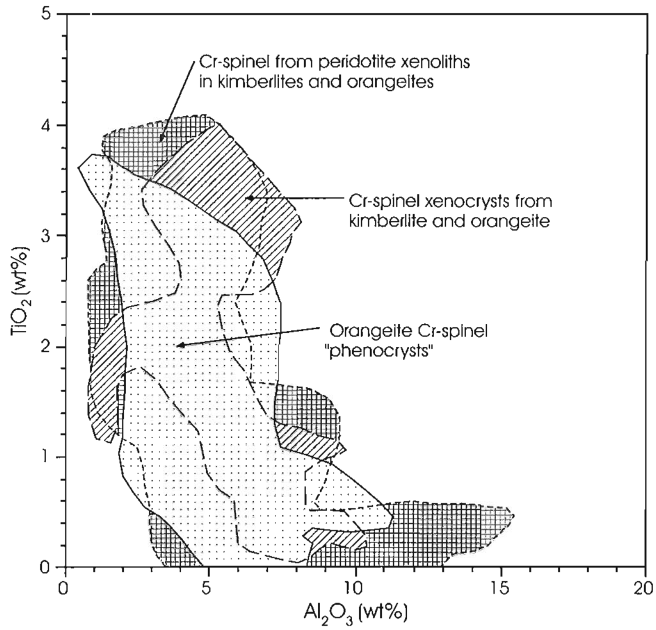

Figure 20. Comparison of orangeite Cr-spinel "phenocrysts" (the "P2" population of Griffin et al., 1994) with Cr-spinel xenocrysts and Cr-spinels from peridotite xenoliths (derived from kimberlite and orangeite; Schulze, 1996) in TiO_2 versus Al_2O_3 (wt%) space. Note the high degree of overlap amongst the three fields, consistent with Schulze's observation that the "P2" Cr-spinels (previously interpreted by Griffin et al., 1994, as high pressure orangeite phenocrysts) were actually derived from disaggregated Cr-spinel peridotites. These three fields are considered to represent only one spinel population (see text and Fig. 21).

Griffin et al. (1994) also discussed major element discrimination methods for kimberlite-, lamproite- and orangeite-derived Cr-spinels. Note that orangeites (Mitchell, 1995) are defined as a group of diamond-bearing rocks found only in South Africa that have geochemical, isotopic and mineralogical characteristics that show some similarities to lamproites, but are clearly distinct from kimberlites. Griffin et al. (1994) utilized a classification and regression tree analysis procedure to distinguish four populations of spinel (P1, P2, P3, and P4). They suggested the origins of the four groups of Cr-spinels to be: P1 spinels, derived from high-pressure mantle peridotites found in kimberlite and orangeite; P2 spinels, TiO_2-rich, high-pressure phenocrysts from orangeite; P3 spinels, high-pressure phenocrysts found in lamproite; and P4 spinels, derived from low-pressure mantle peridotites which are found in lamproite. However, a recent study by Schulze (1996) on Cr-spinel-bearing peridotite xenoliths (from kimberlite and orangeite) noted quite variable TiO_2 content in the spinels. Schulze (1996) concluded that both the P1 and P2 Cr-spinel populations of Griffin et al. (1994) are derived from the disaggregation of Cr-spinel from peridotite xenoliths (Fig. 20). Schulze (1996) also noted good congruence between compositions of Cr-spinel xenocrysts with Cr-spinels from peridotite xenoliths from the same pipe (Fig. 20).

TiO_2-rich spinels in lherzolite xenoliths from kimberlite and orangeite were also previously documented by Hervig et al. (1980), Haggerty (1983), and Schulze (1989), supporting the notion that the P2 population of Cr-spinel macrocrysts (Griffin et al., 1994) are in fact derived from disaggregated spinel-bearing mantle xenoliths. One can conclude, therefore, that the P1, P2 and P4 groups of Griffin et al. (1994) are a single spinel population, derived from the disaggregation of TiO_2-bearing spinels from peridotite xenoliths which had equilibrated at high to

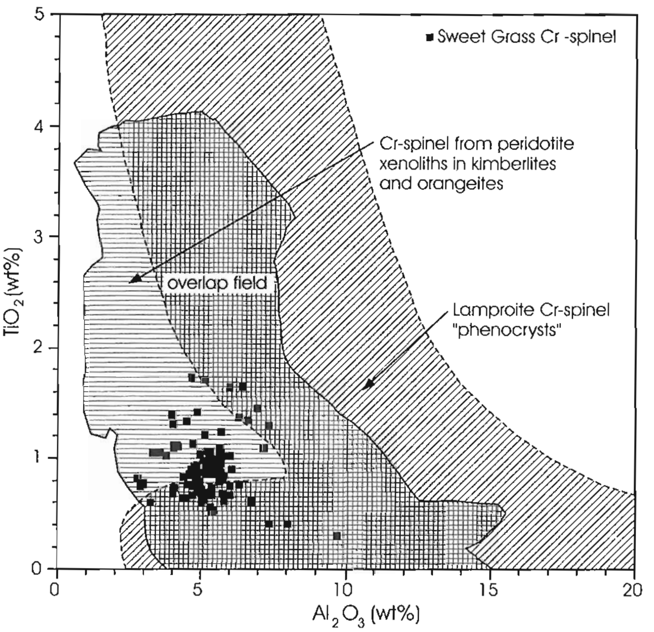

Figure 21. Comparison of compositions of Sweet Grass Cr-spinel phenocrysts with Cr-spinels from disaggregated peridotites (see text, this field combines data from the three fields shown in Fig. 20) and as "phenocrysts" in lamproites ("P3" population of Griffin et al., 1994) in TiO_2 versus Al_2O_3 (wt%) space. Note that the Sweet Grass Cr-spinel phenocrysts fall completely in the field of spinels from disaggregated peridotite (hachured area enclosed by a solid line), and partly in the lamproite "phenocryst" field (hachured area enclosed by a dashed line).

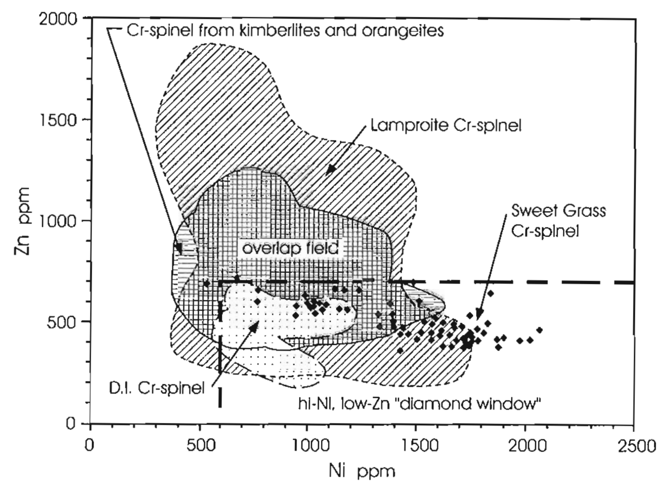

Figure 22. Comparison of Zn versus Ni concentration for Sweet Grass Cr-spinels (filled diamonds). D.I., diamond inclusion. Long/short dashed lines enclose an area of low Zn and high Ni, termed the "diamond window"; Griffin et al. (1994) considered Cr-spinels with Zn and Ni abundances in this region to be good indicators of diamond. Note that most Sweet Grass minette Cr-spinel phenocrysts fall in the kimberlite + orangeite or lamproite fields, a subset also in the diamond inclusion field. Data for lamproite, diamond inclusion, and combined kimberlite plus orangeite (see text for details) fields are from Griffin et al. (1994).

low pressure. This spinel population is sampled by kimberlite, lamproite and orangeite, plus potentially a host of other igneous rocks of deep seated origin (e.g., ultramafic lamprophyres, minettes). A second population of spinel, the P3 group of Griffin et al. (1994) is interpreted as phenocrysts from lamproite, however, there is overlap with peridotite-derived (and other) Cr- spinels (Fig. 21).

The Sweet Grass Cr-spinels fall within the ranges for Cr-spinels from peridotite xenoliths (i.e., the P1 + P2 + P4 population as defined in this study) and "lamproite" (P3 population) on the Al_2O_3 versus TiO_2 discriminant plot (Fig. 21). The Sweet Grass Cr-spinels are high-pressure minette phenocrysts (see above), and these Cr-spinels were not derived from disaggregated peridotite xenoliths, nor are they phenocrysts from a lamproite magma. The chemistry of the Sweet Grass minette spinels illustrates the potential difficulty in applying minor element mineralogical discriminant plots for diamond prospecting purposes in isolation (i.e., without ancillary observations).

Application of trace element discrimination diagrams for spinels is also problematic. On the Ni versus Zn diagram (Fig. 22), more than 75 per cent of the Sweet Grass minette Cr-spinels plot in the field of peridotite (obtained by combining the kimberlite + orangeite fields of Griffin et al., 1994; see previous rationale outlined) or lamproite-derived Cr-spinels. A subset of the Sweet Grass Cr-spinels has Ni and Zn abundances within the range of diamond inclusion Cr-spinels. Furthermore, the majority of these Cr-spinels have low (<700 ppm) abundances of Zn, consistent with conditions of diamond formation (Griffin et al., 1994).

However, application of Zn in spinel thermometry to predict whether Cr-spinel equilibrated at conditions of diamond stability (Griffin and Ryan, 1993) is suggested to have various shortcomings (for discussion see Canil, 1994; Kjarsgaard, 1995; Fipke et al., 1995). For Zn in spinel thermometry, a number of assumptions need to be made (e.g., spinel was in equilibrim with olivine and garnet) and uncertainties in pressure estimates arise if the geothermal gradient is not constrained by other methods (a problem previously noted for the Ni in garnet thermometer; Kjarsgaard, 1992). Furthermore, the Zn thermometer is an empirical calibration, based on the contentious calibration of the Ni in garnet thermometer (for discussion see Kjarsgaard, 1992; Canil, 1994; Campbell et al., 1996). The Zn thermometer incorporates any error in the Ni thermometer, as well as inherent errors in the Zn thermometer itself (Canil, 1994; Kjarsgaard, 1995; Fipke et al., 1995), thus its applicability for diamond exploration is suggested to be, at present, limited.

The Sweet Grass minette spinel mineral chemistry has been utilized to illustrate the complexity of utilizing spinel discriminant diagrams in diamond exploration programs. Utilizing the classification programs developed by Griffin et al. (1994) and Fipke et al.

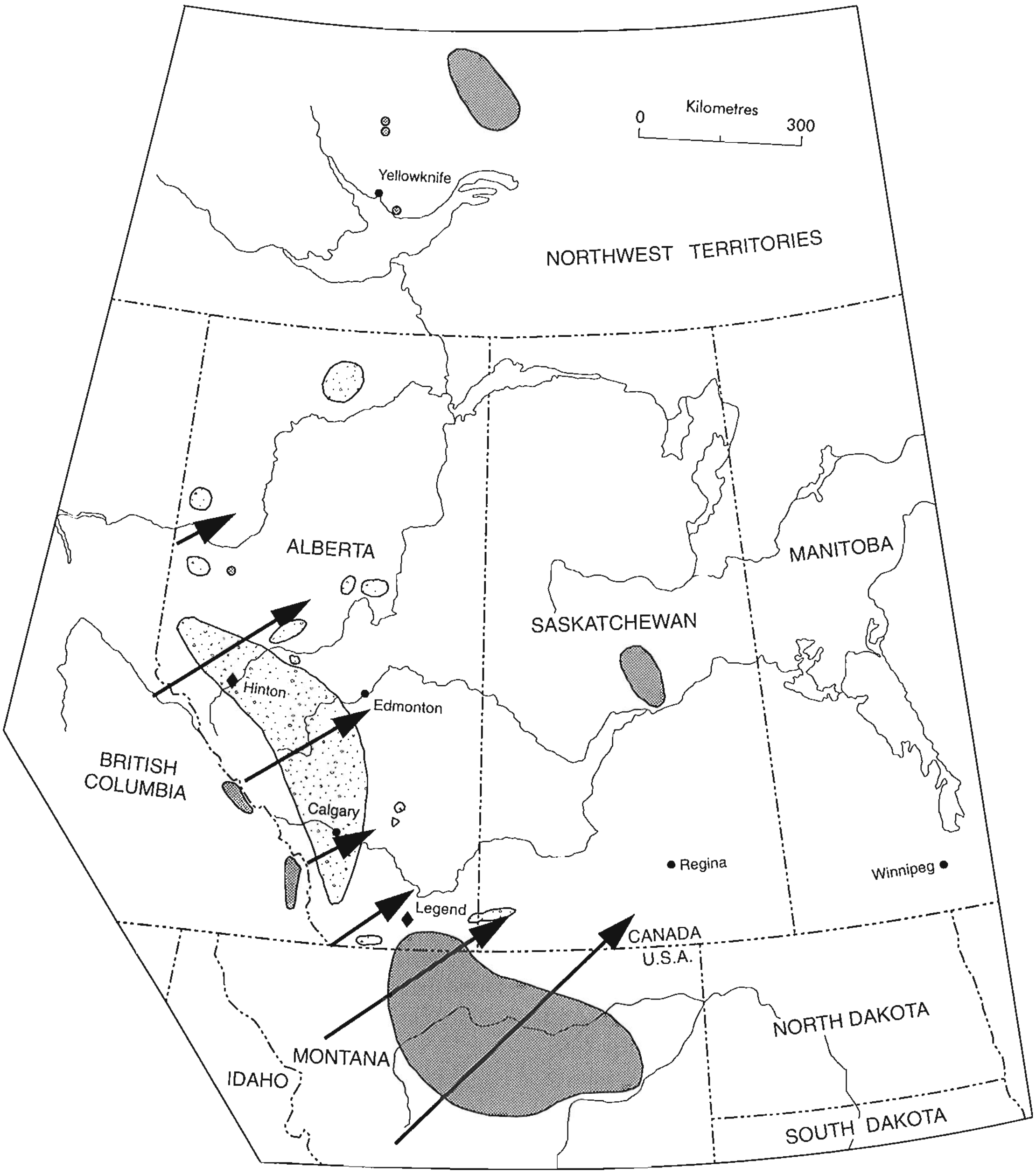

Figure 23. *Tertiary gravels (stippled areas) in Alberta and Saskatchewan (from Leckie and Cheel, 1989). Heavy arrows represent paleocurrent directions (thalwegs from Vonhof, 1969), indicating the source regions. The locations of rocks of deep seated origin are shown in grey. The Hinton and Legend diamond locations are indicated by filled diamonds.*

(1995), the Sweet Grass minette spinels would be interpreted as being related to lamproite or kimberlite, which is not the case. Furthermore, application of trace element criteria (Griffin et al., 1994) to the Sweet Grass Cr-spinels data set suggests moderate diamond potential, but this conclusion does not seem warranted. Fipke et al. (1995) point out that there are many practical problems in spinel classification, specifically that many Cr-spinels cannot be uniquely classified by major (and trace) element chemistry. Since the application of Cr-spinel major- and trace-element geochemical data for diamond exploration purposes is fraught with difficulties (Fipke, et al., 1995; Schulze, 1996; this study), results should be interpreted with caution.

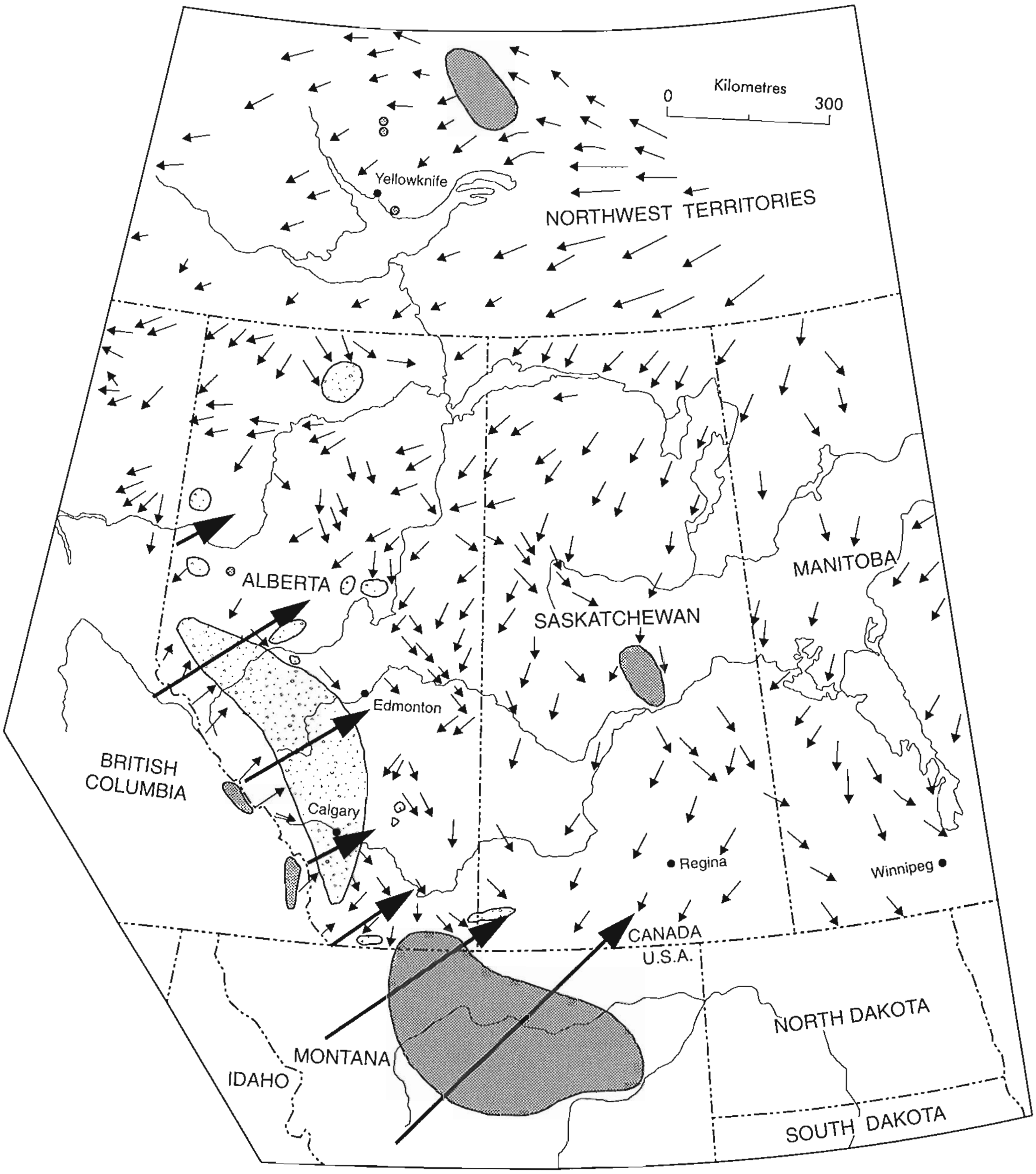

Figure 24 *Quaternary ice flow directions in Alberta (adapted from Klassen, 1989) and surrounding regions (adapted from Prest et al., 1967) overlain with the locations of Tertiary gravels plus rocks of deep-seated origin (Fig. 23), indicating the potential complexity of interpreting diamond exploration indicator minerals from glacial till and modern stream sediments.*

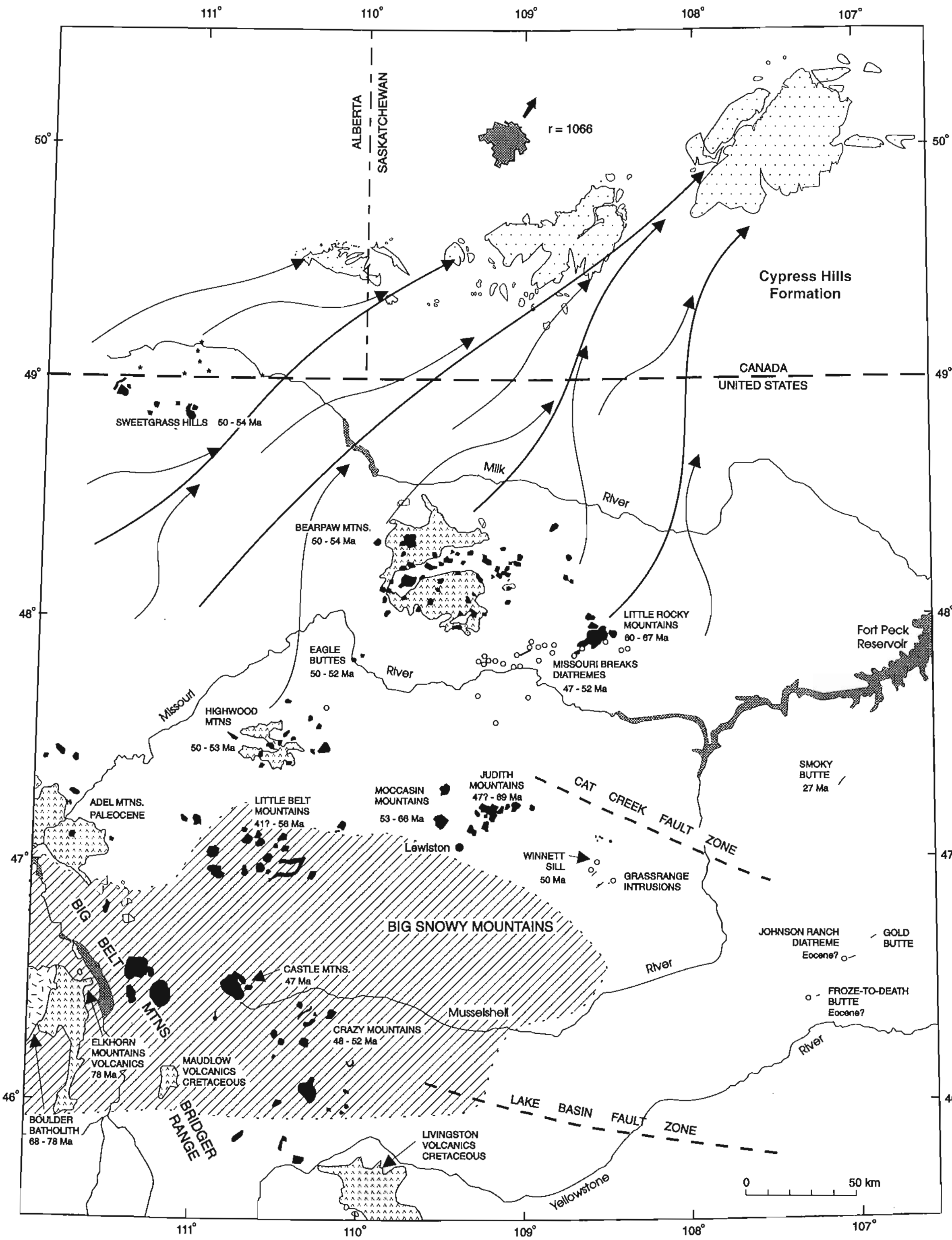

Figure 25. *Southern Saskatchewan and Alberta, and northern Montana paleogeographical reconstruction illustrating source regions for northeast-trending (paleoflow) braided river systems which deposited the Cypress Hills Formation during the Late Eocene and Oligocene. Paleodrainage braided river networks are based on Tertiary gravel paleocurrent data and clast plus heavy mineral provenance data from Leckie and Cheel (1989), Vonhof (1969), and Kjarsgaard (unpublished data). Montana alkaline province geology is from Hearn (1989), symbols are as follows: solid fill, intrusive rocks; v fill, volcanic rocks; open circles, diatremes; hatched pattern, extent of Belt Supergroup; dotted fill, Tertiary formations. Note that the Sweet Grass Hills, Bearpaw and Highwood Mountains, and Eagle Buttes are dominantly minettes and related rocks; Missouri Breaks diatremes are kimberlites and alnoites.*

Provenance of indicator minerals in Alberta tills: multiple recycling problems

Diamond exploration pathfinder minerals are resistant to weathering. Resistance to weathering is a double-edged sword, however, and minerals of the indicator suite may be multiply recycled within the geological environment. Thus diamond exploration utilizing indicator mineral methods may be hindered by complex sedimentological histories. In this respect, Alberta contains and is surrounded by a variety of occurrences of different rocks of deep-seated origin (Fig. 3), all of which may contain indicator minerals. Indicator mineral transport histories in Alberta are potentially very complex (Figs. 23, 24), owing to the combined transport effects of Jurassic to Tertiary and younger fluvial systems and their deposits, Quaternary glaciation, and modern drainage systems. Diamonds and indicator minerals have been found throughout Alberta in various Quaternary glacial deposits and modern drainage systems (e.g., Morton et al., 1993), but the source of these minerals remains enigmatic. Diamond finds at Etzikom Coulee in southern Alberta and in the Hinton area of west-central Alberta (Fig. 23; Dufresne et al., 1994) are of high interest. These regions are examined in greater detail because the sediment movement patterns since the Triassic are quite complex, making identification of the diamond source a real challenge.

Recent till sampling programs for kimberlite minerals in the prairies have discovered variable concentrations in southern Alberta (Thorleifson and Garrett, 1996) and two diamonds have been recovered from Etzikom Coulee (Dufresne et al., 1994). The concentrations of indicator minerals in southern Alberta, while higher than background levels, are not as anomalous as those observed in southern Saskatchewan (Garrett and Thorleifson, 1995). The southern Saskatchewan till anomalies are proximal to Miocene gravels/conglomerates of the Wood Mountain Formation (Kjarsgaard, 1995; Garrett and Thorleifson, 1995). Indicator mineral chemistry is similar for samples from till from the Wood Mountain Formation conglomerates, and from rocks of deep-seated origin from the Montana Alkaline Province (Kjarsgaard, 1995). This led Kjarsgaard (1995) to suggest that the indicator minerals found in till were multi-stage recycled, originally from the Montana Alkaline Province.

In contrast, in southern Alberta there is not a highly distinctive till anomaly adjacent to the Eocene Cypress Hills Formation. However, indicator minerals (spinel, clinopyroxene, garnet) are found in Cypress Hills Formation conglomerates. These are visually indistinguishable from concentrate derived minerals from Montana alkaline province rocks (Kjarsgaard, 1995; and unpublished data). Analyses of clasts and heavy mineral concentrates in the Cypress Hills Formation are consistent with fluvial transport of minette, alnöite and kimberlite (plus many other) clasts and particles from northern Montana to southern prairies during Tertiary time (Vonhof, 1969; Leckie and Cheel, 1989; Kjarsgaard, 1995; see Fig. 25). Although indicator minerals are common in Cypress Hills conglomerates, the adjacent till anomaly is not particularly anomalous, consistent with these rocks being nunataks during Pleistocene glaciation (Klassen, 1989). That is, the Cypress Hills Formation provided little, if any, source material for the local Pleistocene deposits.

In the Hinton area, the presence of diamonds and diamond indicator minerals in modern stream sediments has been problematic because the source rocks are still unknown. Potentially the diamonds and indicator minerals are glacially derived from pipes in either the Grande Prairie area or the Columbia Icefields/Golden area of British Columbia (see Fig. 24). These latter pipes, two of which are reported to be diamond-bearing (Pell, 1994), mainly occur in the Western and Main ranges of the Rocky Mountains, to the east of the Rocky Mountain Trench, situated in the present day Pacific watershed. This poses a problem with respect to fluvial transport of indicator minerals (and diamonds) across the drainage divide. However, prior to the beginning of the Laramide Orogeny in the late Cretaceous, sediments deposited in the Rocky Mountain trough (western Alberta/eastern British Columbia) were interpreted by Stott (1984) to be in part derived from the west (i.e., the Columbia Icefields/Golden area) during the Late Jurassic (ca. 175 Ma) to Cretaceous (ca. 110 Ma). If exposed during this time period, the Columbia Icefields pipes (emplaced at 391 to 469 Ma; Pell, 1994), could be a source for indicators in Late Jurassic to Cretaceous sediments in Western Alberta.

Further eastward transport and recycling of indicator minerals by subsequent erosion of the Rocky Mountain trough sediment pile is possible during uplift associated with Laramide orogenesis and formation of Tertiary clastic sequences. From this standpoint, diamonds and indicator minerals conceivably could be found in the Hinton area in modern stream sediments, glacial deposits and Tertiary to Upper Jurassic clastic sequences. Although the source of the diamonds and indicator minerals could be local (e.g., from kimberlite or lamproite), the potential in this area for multiply recycled indicator minerals hinders the search for local primary sources. The complexity of recycling (Tertiary drainage, Quaternary glaciation, and modern drainage) in relation to potential sources of indicator minerals is illustrated in Figure 24.

Acknowledgments

I would like to thank John Stirling of the electron microprobe lab (GSC Ottawa) for assistance, and Jake Jakop for help with figure preparation. Discussions with Bill Davis, Gerry Ross, Dale Leckie, Harvey Thorleifson, Bob Garrett, and Mike Dufresne about various aspects of the geology of Alberta have been of great assistance. The author, however, is solely responsible for the interpretations and conclusions. The preliminary study of the Grande Prairie pipe would not have been feasible without sample access courtesy of Monopros Ltd. Tony LeCheminant and John Henderson kindly reviewed earlier drafts of the manuscript. Roger Macqueen is thanked for reviewing, and editing numerous drafts of the manuscript, and for his patience while waiting for the final version.

REFERENCES

Baadsgaard, H., Burwash, R.A., and Lipson, J.
1961: Potassium-argon dates of biotites from Cordilleran granites. Geological Society of America Bulletin, v. 72, p. 689–702.

Bell, K., and Dawson, J.B.
1995: An assessment of the alleged role of evaporites and saline brines in the origin of natrocarbonatite. *In* IAVCEI Proceedings in Volcanology v. 4, Carbonatite Volcanism of Oldoinyo Lengai - Petrogenesis of Natrocarbonatites, K. Bell and J. Keller (eds.). Springer, Berlin, p. 137–147.

Canil, D.
1994: An experimental calibration of the "Nickel in Garnet" geothermometer with applications. Contributions to Mineralogy and Petrology, v. 117, p. 410–420.

Campbell, J.L., Teedale, W.J., Kjarsgaard, B.A., and Cabri, L.J.
1996: Micro-PIXE analysis of silicate reference standards for trace Ni, Cu, Zn, Ga, Ge, As, Rb, Sr, Y, Zr, Nb, Mo and Pb, with emphasis on Ni for application of the Ni-in-garnet geothermometer. Canadian Mineralogist, v. 34, p. 37–84.

Currie, K.L.
1976: The alkaline rocks of Canada. Geological Survey of Canada, Bulletin 239, 228 p.

Dalton, J.A. and Wood, B.J.
1993: The composition of primary carbonate melts and their evolution through wallrock reaction in the mantle. Earth and Planetary Science Letters, v. 119, p. 511–525.

Davis, W.J.
1994: U-Pb geochronology of crustal xenoliths from the Archean Medicine Hat Block, Northern Montana and Southern Alberta: Early Proterozoic granulite metamorphism in the lower crust. EOS abstracts, Transactions, American Geophysical Union, v. 75, no. 44, p. 691.

Davis, W.J. and Kjarsgaard, B. A.
1994: A Rb-Sr phlogopite-whole rock isochron age for olivine minette from the Milk River area, southern Alberta. *In* Radiogenic Age and Isotopic Studies: Report 8. Geological Survey of Canada, Current Research 1994-F, p. 11–14.

Davis, W.J., Berman, R., and Kjarsgaard, B.A.
1995: U-Pb geochronology and isotopic studies of crustal xenoliths from the Archean Mèdicine Hat Block, northern Montana and southern Alberta: Paleoproterozoic reworking of the lower crust. *In* Lithoprobe Alberta Basement Transects Workshops, April 10-11, 1995, G.M. Ross, (ed.). Lithoprobe Report no. 47, Lithoprobe Secretariat, University of British Columbia, p. 330–335.

Dawson, G.M.
1884: Geological Survey of Canada, Report of Progress 1882-83-84, part C, p. 16–17 and 45–47.

Dufresne, M.B., Olson, R.A., Schmitt, D.R., McKinstry, B., Eccles, D.R., Fenton, M.M., Pawlowicz, J.G., Edwards, W.A.D., and Richardson, R.J.H.
1994: The diamond potential of Alberta: a regional synthesis of the structural and stratigraphic setting, and other preliminary indications of diamond potential. Alberta Research Council, Open File no. 1994-10, 401 p.

Dufresne, M.B., Eccles, D.R., McKinstry, B., Schmitt, D.R., Fenton, M.M., Pawlowicz, J.G., and Edwards, W.A.D.
1996: The Diamond Potential of Alberta. Alberta Geological Survey, Bulletin 63, 158 p.

Ehrenburg, S.N.
1982: Petrogenesis of garnet lherzolite and megacrystalline nodules from the Thumb, Navajo volcanic field. Journal of Petrology, v. 23, p. 507–547.

Fipke, C.
1989: The development of advanced technology to distinguish between diamondiferous and barren diatremes. Geological Survey of Canada, Open File 2124, 621 p.

1994: Significance of chromite, ilmenite, G5 Mg-almandine garnet, zircon and tourmaline in heavy mineral detection of diamond-bearing lamproite. *In* Proceedings of the Fifth International Kimberlite Conference, Brazil, v. 2, Diamonds: Characterization, Genesis and Exploration, H.O.A. Meyer and O.H. Leonardos (eds.). Comphania de Pesquisa de Recursos Minerais, Special Publication 1B, p. 215–235.

Fipke, C., Gurney, J.J., and Moore, R.O.
1995: Diamond exploration techniques emphasizing indicator mineral geochemistry and Canadian examples. Geological Survey of Canada, Bulletin 423, 86 p.

Foley, S.F.
1992: Vein plus wall-rock melting mechanisms in the lithosphere and the origin of potassic magmas: partial melting in veined, lithospheric mantle. Lithos, v. 28, p 435-453.

Foley, S.F., Venturelli, G., Green, D.H., and Toscani, L.
1987: The ultrapotassic rocks: characteristics, classification and constraints for petrogenetic models. Earth Science Reviews, v. 24, p. 81-134.

Garrett, R.G. and Thorleifson, L.H.
1995: Kimberlite indicator mineral and till geochemical reconnaissance, southern Saskatchewan. *In* Investigations completed by the Saskatchewan Geological Survey and the Geological Survey of Canada under the Geoscience Program of the Canada-Saskatchewan Partnership Agreement on Mineral Development (1990-1995), D. Richardson (ed.). Geological Survey of Canada, Open File 3119, p. 227-254.

Gavin, B.
1991: Precious-metal mineralization in the Sweet Grass Hills, north-central Montana. *In* Central Montana Alkalic Province Guidebook, D.W. Baker and R.B. Berg (eds.). Montana Bureau of Mines and Geology, Special Publication no. 100, p. 55-62.

Griffin, W.L. and Ryan, C.J.
1993: Trace elements in garnets and chromites: evaluation of diamond exploration targets. *In* Diamonds: exploration, sampling and evaluation, P.A. Sheahan and A. Chater (eds.). Short Course Proceedings, Prospectors and Developers Association of Canada, Toronto, p. 187-211.

Griffin, W.L., Ryan, C.J., Gurney, J.J., Sobolev, N.V., and Win, T.T.
1994: Chromite macrocrysts in kimberlites and lamproites: geochemistry and origin. *In* Proceedings of the Fifth International Kimberlite Conference, Brazil, v. 1, Kimberlites, related rocks and mantle xenoliths, H.O.A. Meyer and O.H. Leonardos (eds.). Comphania de Pesquisa de Recursos Minerais, Special Publication 1A, p. 366-377.

Gurney, J.J.
1989: Diamonds. *In* Proceedings of the Fourth International Kimberlite Conference, v. 1. Kimberlites and Related Rocks: Their Composition, Occurrence, Origin and Emplacement, J. Ross (ed.). Geological Society of Australia, Special Publication 14, Blackwell Scientific Publications, Oxford, p. 935-965.

Haggerty, S.
1983: The mineral chemistry of new titanites from the Jagersfontein kimberlite, South Africa: implications for metasomatism in in the upper mantle. Geochimica et Cosmochimica Acta, v. 47, p. 1833-1854.

Hausel, W.D.
1995: Diamonds, kimberlites, lamproites and related rocks in the United States. Exploration and Mining Geology, v. 4, no. 3, p. 243-270.

Hearn, B.C., Jr.
1989: Montana high-potassium igneous province. *In* Field trip guidebook T346, 28th International Geological Conference. American Geophysical Union, p. 1-5.

Hervig, R.L., Smith, J.V., Steele, I.M., and Dawson, J.B.
1980: Fertile and barren Al-Cr-spinel harzburgites from the upper mantle: ion and electron probe analyses of trace elements in olivine and orthopyroxene and relations to lherzolites. Earth and Planetary Science Letters, v. 50, p. 41-58.

Janse, A.J.A.
1994: Is Clifford's rule still valid? Affirmative examples from around the world. *In* Proceedings of the Fifth International Kimberlite Conference, Brazil, v. 2, Diamonds: Characterization, Genesis and Exploration, H.O.A. Meyer and O.H. Leonardos (eds.). Comphania de Pesquisa de Recursos Minerais, Special Publication 1B, p. 215-235.

Keller, J. and Hoefs, J.
1995: Stable isotopic characteristics of Recent natrocarbonatites from Oldoinyo Lengai. *In* IAVCEI Proceedings in Volcanology, v. 4, Carbonatite Volcanism of Oldoinyo Lengai - Petrogenesis of Natrocarbonatites, K. Bell and J. Keller (eds.). Springer, Berlin, p. 70-86.

Kemp, J.F. and Billingsley, P.
1921: Sweet Grass Hills, Montana. Geological Society of America Bulletin. v. 32, p. 437-478.

Kjarsgaard, B.A.
1992: Is Ni in chrome pyrope garnet a valid diamond exploration tool? *In* Current Research, Part E. Geological Survey of Canada, Paper 92-1E, p. 315-322.

1994: Potassic magmatism in the Milk River area, southern Alberta: petrology and economic potential. *In* Current Research, 1994-B. Geological Survey of Canada, p. 59-68.

1995: Research on kimberlites and applications of diamond exploration techniques in Saskatchewan. *In* Investigations completed by the Saskatchewan Geological Survey and the Geological Survey of Canada under the Geoscience Program of the Canada-Saskatchewan Partnership Agreement on Mineral Development (1990-1995), D. Richardson (ed.). Geological Survey of Canada, Open File 3119, p. 167-181.

1996: Slave Province kimberlites, N.W.T. *In* Searching for diamonds in Canada, A.N. LeCheminant, R. DiLabio, and K.L. Richardson (eds.). Geological Survey of Canada, Open File 3228, p. 55-60.

Kjarsgaard, B.A. and Davis, W.J.
1994: Eocene magmatism in the Sweet Grass Hills and its tectonic significance. *In* Lithoprobe Alberta Basement Transects Workshops, February 14-15, 1994, G.M. Ross (ed.). Publication no. 37, Lithoprobe Secretariat, University of British Columbia, p. 234-237.

Kjarsgaard, B.A., Leckie, D., Bloch, J., McIntyre, D., McNeil, D., Stasiuk, L., and Haggart, J.W.
1995: Smeaton kimberlite drill core, Fort à la Corne field, Saskatchewan. Geological Survey of Canada, Open File 3170, 57 p.

Klassen, R.W.
1989: Quaternary geology of the southern Canadian Interior Plains. *In* Chapter 2 of Quaternary geology of Canada and Greenland, R.J. Fulton (ed.). Geological Survey of Canada, Geology of Canada, no. 1, p. 138-166.

Kyser, T.K.
1986: Stable isotope variations in the mantle. *In* Stable isotopes in high temperature geological processes, J.W. Valley (ed.). Reviews in Mineralogy, v. 16. Mineralogical Society of America, Washington, D.C., p. 141-164.

Leckie, D.A. and Cheel, R.J.
1989: The Cypress Hills Formation (Upper Eocene to Miocene): a semi-arid braidplain deposit resulting from intrusive uplift. Canadian Journal of Earth Science, v. 26, p. 1918-1931.

Leckie, D.A. and Smith, D.G.
1992: Regional setting, evolution, and depositional cycles of the western Canada Foreland Basin. In Foreland Basins and Fold Belts, R.W. Macqueen and D.A. Leckie (eds.). American Association of Petroleum Geologists, Memoir 55, p. 9-46.

Macdonald, R., Upton, B.G.J., Collerson, K.D., Hearn, B.C., Jr., and James, D.
1992: Potassic mafic lavas of the Bearpaw Mountains, Montana: mineralogy, chemistry, and origin. Journal of Petrology, v. 33, p. 305-346.

MacRae, N.D., Armitage, A.E., Miller, A.R., Roddick, J.C., Jones, A.L., and Mudry, M.P.
1996: The diamondiferous Akluilak lamprophyre dyke, Gibson Lake area, N.W.T. *In* Searching for diamonds in Canada, A.N. LeCheminant, R. DiLabio, and K.L. Richardson (eds.). Geological Survey of Canada, Open File 3228, p. 101-107.

Marvin, R.F., Hearn, B.C., Jr., Mehnert, H.H., Naeser, C.W., Zartman, R.E., and Lindsay, D.A.
1980: Late Cretaceous-Paleocene-Eocene igneous activity in north central Montana. Isochron West, v. 29, p. 5-25.

McDonough, M.R. (*this volume*)
1997: Structural controls and age constraints on sulphide mineralization, southern Taltson magmatic zone, northeastern Alberta. *In* Exploring for Minerals in Alberta: Geological Survey of Canada Geoscience Contributions, Canada-Alberta Agreement on Mineral Development (1992-1995), R.W. Macqueen (ed.). Geological Survey of Canada, Bulletin 500, p. 13-29.

McDonough, M.R., Grover, T.W., McNicholl, V.J., and Lindsay, D.D.
1993: Preliminary report of the geology of the southern Taltson magmatic zone, northeastern Alberta. *In* Current Reserach, Part C. Geological Survey of Canada, Paper 93-1C, p. 221-232.

McNicholl, V.J., McDonough, M.R., and Grover, T.W.
1994: U-Pb geochronological studies in the southern Taltson magmatic zone, northern Alberta. *In* Lithoprobe Alberta Basement Transects Workshops, February 14-15, 1994, G.M. Ross (ed.). Lithoprobe Report no. 37, Lithoprobe Secretariat, University of British Columbia, p. 270-273.

Meen, J.K., Ayers, J.C., and Fregau, E.J.
1989: A model of trace element metasomatism by carbonated alkaline melts: trace element and isotopic compositions of mantle source regions of carbonatite and other continental igneous rocks. *In* Carbonatites: Genesis and Evolution, K. Bell (ed.). Hyman and Unwin, London, p. 464-499.

Mitchell, R.H.
1986: Kimberlites. Plenum Press, New York, 442 p.

1991: Kimberlites and lamproites: primary sources of diamond. Geoscience Canada, v. 18, no. 1, p. 1-16.

1995: Kimberlites, orangeites, and related rocks. Plenum Press, New York, 410 p.

Mitchell, R.H. and Bergman, S.C.
1991: Petrology of lamproites. Plenum Press, New York, 447 p.

Moore, R.O. and Gurney, J.J.
1989: *In* Fipke, C. The development of advanced technology to distinguish between diamondiferous and barren diatremes. Geological Survey of Canada, Open File 2124, v. 1, p. 1-90.

Morton, R.D., Stewart, J.P., and Day, R.G.
1993: A Review of Diamond Occurrences and Potential in Alberta. *In* Mid-Continent Diamonds, K.P.E. Dunne and B. Grant (eds.). Geological Association of Canada - Mineralogical Association of Canada Symposium Volume, p. 101-104.

Nakamura, N.
1974: Determination of REE, Ba, Mg, Na and K in carbonaceous and ordinary chondrites. Geochimica et Cosmochimica Acta, v. 38, p. 757-775.

Nixon, P.H.
1987: Kimberlite xenoliths and their cratonic setting. *In* Mantle Xenoliths, P.H. Nixon (ed.), J. Wiley and Sons, Toronto, p. 215-240.

O'Brien, H.E., Irving, A.J., and MacCallum, I.S.
1989: Eocene Potassic magmatism in the Highwod mountains, Montana: petrology, geochemistry, and tectonic implications. Journal of Geophysical Research, v. 96, p. 13,237-13,260.

Pearce, J.
1983: Role of the sub-continental lithosphere in magma genesis at active continental margins. *In* Continental Basalts and mantle xenoliths, C.J. Hawkesworth and M.J. Norry (eds.). Shiva Publishing Limited, Cheshire, p. 230-249.

Pell, J.
1994: Carbonatites, nepheline syenites, kimberlites and related rocks in British Columbia. British Columbia Ministry of Energy, Mines and Petroleum Resources, Bulletin 88, 135 p.

1995: NWT kimberlite database. Department of Indian and Northern Affairs, Yellowknife, NWT, Open File no. EGS95-2.WB1.

Presnall, D.C., Dixon, S.A., Dixon, J.R., O'Donnell, T.H., Brenner, N.L., Schock, R.L., and Dycus, D.W.
1978: Liquidus phase relations on the join diopside-forsterite-anorthite from 1 atm to 20 kbar: their bearing on the generation and crystallization of basaltic magma. Contributions to Mineralogy and Petrology, v. 66, p. 203-220.

Prest, V.K., Grant, D.R., and Rampton, V.N.
1967: Glacial map of Canada. Geological Survey of Canada, Map 1253A, 1:5 000 000 scale.

Rock, N.M.S.
1991: Lamprophyres. Blackie & Son Ltd., Glasgow, 285 p.

Ross, G.M., Parrish, R.R., Villeneuve, M.E., and Bowring, S.A.
1991: Geophysics and geochronology of the crystalline basement of the Alberta basin, western Canada. Canadian Journal of Earth Science, v. 28, p. 512-522.

Ross, G.M., Mariano, J., and Dumont, R.
1994: Was Eocene magmatism widespread in the subsurface of southern Alberta? Evidence from new aeromagnetic anomaly data. *In* Lithoprobe Alberta Basement Transects Workshops, February 14-15, 1994, G.M. Ross (ed.). Lithoprobe Report no. 37, Lithoprobe Secretariat, University of British Columbia, p. 240-249.

Ross, G.M., Mariano, J., Dumont, R., Kjarsgaard, B.A., and Teskey, D.
1996: Was Eocene magmatism widespread in the subsurface of southern Alberta? Evidence from new aeromagnetic anomaly data. (this volume).

Schulze, D.J.
1987: Megacrysts from alkalic volcanic rocks. *In* Mantle Xenoliths, P.H. Nixon (ed.). J. Wiley and Sons, Toronto, p. 433-442.

1989: Green garnets from south African kimberlites and their relationship to wehrlites and crustal uvarovites. *In* Proceedings of the Fourth International Kimberlite Conference, v. 2, Kimberlites and Related Rocks: Their mantle/crust setting, diamonds and diamond exploration, J. Ross (ed.). Geological Society of Australia, Special Publication 14, Blackwell Scientific Publications, Oxford, p. 820-826.

1996: Cr-spinel macrocrysts from southern African kimberlites: mantle xenolith sources and post-diamond re-equilibration. Africa Geoscience Review (in press).

Sobolev, N.V.
1974: Deep seated inclusions in kimberlites and the problem of the composition of the uper mantle. American Geophysical Union, Washington, 279 p.

Stott, D.F.
1984: Cretaceous sequences of the foothills of the Canadian Rocky Mountains. *In* The Middle Mesozoic of North America, D.F. Stott and D.J. Glass (eds.). Canadian Society of Petroleum Geologists, Calgary, p. 85-107.

Thériault, R.J. and Ross, G.M.
1991: Nd isotopic evidence for for crustal reycling in the 2.0 Ga subsurface of western Canada. Canadian Journal of Earth Science, v. 28, p. 1140-1147.

Thorleifson, L.H., and Garrett, R.G. (*this volume*)
1997: Kimberlite indicator mineral and geochemical reconnaissance of southern Alberta. *In* Exploring for Minerals in Alberta: Geological Survey of Canada Geoscience Contributions, Canada-Alberta Agreement on Mineral Development (1992-1995), R.W. Macqueen (ed.). Geological Survey of Canada, Bulletin 500, p. 209-233.

Villeneuve, M.E., Ross, G.M., Thériault, R.J., Miles, W., Parrish, R.R., and Broome, J.
1993: Tectonic subdivision and U-Pb geochronology of the crystalline basement of the Alberta basin, western Canada. Geological Survey of Canada, Bulletin 447, 86 p.

Vonhof, J.A.
1969: Tertiary gravels and sands in the Canadian Great Plains. Unpublished Ph.D. thesis, University of Saskatchewan, 170 p.

Weed, W.H. and Pirsson, L.V.
1895: On the igneous rocks of the Sweet Grass Hills, Montana. American Journal of Science, Third Series, v. L, no. 298, p. 309-313.

Wyllie, P.J.
1984: Constraints imposed by experimental petrology on possible and impossible magma sources and products. Transactions of the Royal Society London, v. A310, p. 439-456.

KIMBERLITE INDICATOR MINERAL AND GEOCHEMICAL RECONNAISSANCE OF SOUTHERN ALBERTA[1]

L.H. Thorleifson[2] and R.G. Garrett[3]
Geological Survey of Canada, Ottawa

Abstract

An indicator mineral and geochemical survey designed to examine diamond and metallic mineral potential, glacial sediment transport history, and both exploration and environmental geochemistry, was carried out in southern Alberta in 1992. Sampling sites were randomly selected prior to field work, with two sites in 40 x 40 km cells designated for the sampling of till (unsorted glacial sediments) and soil, and additional sites designed to define local variability of soils. At 252 sites, a 25 ℓ sample of till was collected from 1 to 2 m depth from surface exposures, mainly road cuts. Soil samples from the A and C horizons were obtained from 352 sites randomly distributed on all parent materials. Processing of the till samples, followed by mineralogical and chemical analysis, resulted in the confirmation of an average of one indicator mineral per two samples. Several areas where favourable kimberlite indicator mineral results are clustered were defined. Additional lithological, mineralogical, and geochemical analyses of till were used to provide evidence of the bedrock source of the sediment. Sediment consisting of material transported generally southwestward by Pleistocene glaciation radiating from the Canadian Shield can be distinguished from Pleistocene sediments north and south of Calgary which contain abundant material glacially transported from the Cordillera. The soil geochemical data are of less direct application to mineral exploration than the till data, owing to variable texture and greater modification by pedological processes, but these data provide useful information of relevance to environmental and agricultural issues.

Résumé

En 1992, un levé géochimique et un échantillonnage de minéraux indicateurs ont été réalisés dans le sud de l'Alberta. Ces travaux visaient à analyser le potentiel en diamants et en minéraux métalliques de cette région, à reconstituer l'histoire du transport des sédiments glaciaires et à recueillir des données utiles en géochimie de l'exploration et de l'environnement. Les sites d'échantillonnage ont été choisis au hasard avant les travaux sur le terrain. Il y avait d'abord des sites désignés pour échantillonner le till (sédiments glaciaires non triés) et le sol, au nombre de deux par cellule de 40 km de côté, mais aussi des sites additionnels définis pour déterminer la variabilité locale des sols. Ainsi, dans les matériaux de surface de 252 sites, surtout dans des tranchées routières, on a prélevé un échantillon de 25 litres de till à une profondeur de 1 à 2 m. On a aussi recueilli des échantillons de sol dans les horizons A et C de 352 sites répartis au hasard parmi tous les matériaux mères. Le traitement des échantillons de till, suivi de leur analyse minéralogique et chimique, a permis de confirmer la présence d'un minéral indicateur par deux échantillons en moyenne. Plusieurs zones où l'on a observé le regroupement de minéraux indicateurs (de la présence de kimberlite) ont été définies. D'autres analyses lithologiques, minéralogiques et géochimiques du till ont été utilisées pour en savoir plus sur l'origine des sédiments dans le substratum. Les sédiments composés de matériaux transportés généralement vers le sud-ouest par une glaciation pléistocène rayonnant à partir du Bouclier canadien se distinguent des sédiments pléistocènes au nord et au sud de Calgary, qui contiennent d'abondantes quantités de matériaux transportés par les glaciers à partir de la Cordillère. Les données géochimiques sur le sol ont une application moins directe en exploration minière que les données sur le till, étant donné la texture

[1]Canada-Alberta Agreement on Mineral Development, Project C1.32
[2]Terrain Sciences Division, Ottawa
[3]Mineral Resources Division, Ottawa

application moins directe en exploration minière que les données sur le till, étant donné la texture variable des sols et leur modification accrue par les processus pédologiques. Cependant, ces données fournissent des informations utiles en environnement et en agriculture.

INTRODUCTION

Rationale, scope, and objectives

Much of Canada is underlain by geological terrane which has a high potential for the presence of diamond-bearing rocks. Early diamond exploration focussed on the Great Lakes region (Brummer, 1978), but shifted west in recent years (Fipke et al., 1995). In 1988, kimberlite discoveries in central Saskatchewan were announced (Lehnert-Thiel et al., 1992; Scott-Smith, 1995), and in 1991, a dramatic increase in diamond exploration activity occurred in Alberta (Dufresne et al., 1994). In 1992, the Northwest Territories became the most active area of diamond exploration in Canada. This exploration activity, including the processing of sediment for indicator minerals, geophysical surveys, and drilling, was accompanied by a recognition of the need for regional government surveys that would place detailed industry data into context.

The work in Alberta summarized here is part of a survey covering the entire Canadian prairie region (Garrett and Thorleifson, 1995). The objectives of the work were: to map regional trends in indicator mineral frequency and chemistry; to seek evidence for the presence of gemstone and metallic mineral deposits; to demonstrate and compare various mineralogical and geochemical exploration methods; to map glacial sediment composition as an indicator of its transport history; and, to map regional soil geochemistry as an aid to exploration and environmental applications. Soil geochemical sampling was extended southward 100 km into the USA, in cooperation with the United States Geological Survey (USGS), in order to provide correlation to US regional surveys. The survey in Alberta was limited to contiguous agricultural land in the southern part of the province (Fig. 1), where road access permitted relatively inexpensive systematic coverage.

The prairie survey evolved from a 1990 proposal for a survey of southern Saskatchewan. In 1991, an orientation set of till and soil samples was collected at 40 to 50 km intervals along an orientation transect from Winnipeg to Calgary, and from Edmonton back to Winnipeg. Processing of these samples led to refinement of laboratory procedures and indicated that well-defined regional trends could be mapped by ultra-low density sampling. In 1992, the southern Alberta survey was authorized, and coverage was extended across southern Manitoba as a cooperative effort with Manitoba Energy and Mines. All sampling for the regional survey was completed in 1992, and laboratory work progressed in stages over the ensuing three years.

Data obtained from the orientation samples were released in 1993 (Garrett and Thorleifson, 1993). Electron microprobe data for indicator minerals obtained from the regional survey, as well as till matrix geochemistry, were released later that year (Thorleifson and Garrett, 1993), prior to the release of proton microprobe indicator mineral data by Thorleifson et al. (1994).

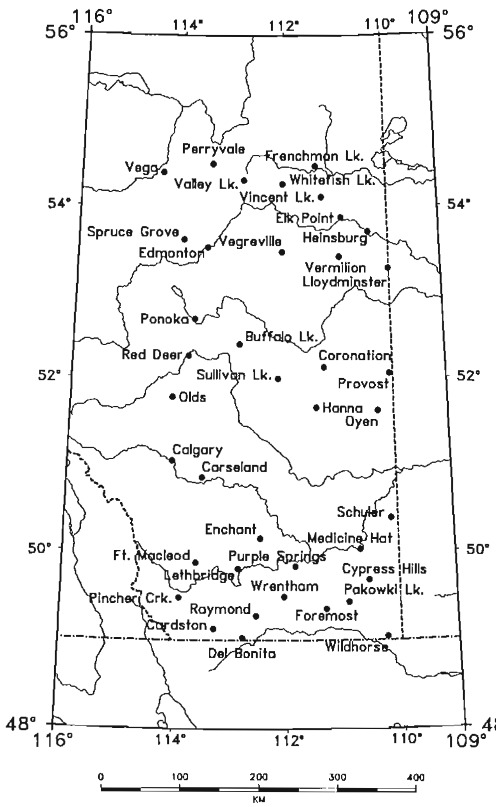

Figure 1. Location of geographic features discussed in the text.

Regional geology

The prairie region of southern Alberta is underlain by extensive Cretaceous to Paleocene sandstones, mudstones and coal, isolated occurrences of Oligocene, Miocene and early Pleistocene gravels, and, in southeasternmost Alberta, several small intrusions of Tertiary age (Dawson et al., 1994; Stott et al., 1993; Mossop and Shetsen, 1994). Outcrops of these pre-Quaternary deposits are generally limited to river valleys and areas of high relief. Northeast of the study area, in northeasternmost Alberta and to the east in Saskatchewan and Manitoba, are Precambrian igneous and metamorphic rocks of the Canadian Shield, as well as Paleozoic carbonate rocks which occur along the shield margin, mainly in Alberta and Manitoba. To the west in the Cordillera are extensive carbonate, metasedimentary, and other sedimentary rocks.

The oldest rocks that underlie the Quaternary sediments or outcrop in the study area are Cretaceous in age. They are the shale-dominated Milk River Formation, which outcrops along the Montana border southeast of Lethbridge, and Lea Park shale, northeast of the North Saskatchewan River. Sedimentary rocks which overlie the Milk River Formation elsewhere include the deposits of four progradational cycles of sand-dominated sedimentation associated with uppermost Cretaceous to Paleocene Laramide orogenesis: the Cretaceous Belly River, Horseshoe Canyon, and lower Scollard units, as well as the Paleocene Paskapoo and equivalent strata. Each of these sandstone units is underlain by mudstone and coal-dominated units, the Pakowki, Bearpaw, Battle, and upper Scollard strata respectively (Dawson et al., 1994).

Thermal maturity of coals and the elevation of the uppermost gravels indicate that the regional unconformity at the top of the Cretaceous–Tertiary sequence resulted from the removal, over most of the area, of 1 to 3 km of sediment by subaerial and glacial processes in post-Eocene time (Nurkowski, 1984; Bustin, 1992; Dawson et al., 1994). The subcrop pattern produced by this erosion generally consists of north–south belts. The Paskapoo sandstone dominates the western portion of the study area, extending from Calgary nearly to Edmonton (Mossop and Shetsen, 1994). The subcrop of the Horseshoe Canyon Formation, which underlies the City of Edmonton, is to the east. The Bearpaw shale is the next major subcropping or outcropping unit to the east, underlying a large area which bulges to the Saskatchewan border between Medicine Hat and Lloydminster. Northeast and southeast of the Bearpaw shale, the Lloydminster and Medicine Hat regions are underlain by the Belly River Formation. Southeasternmost Alberta is underlain by Bearpaw shale, whereas the northeastern corner of the study area extends to the subcrop of Lea Park shale.

Most of the post-Eocene erosion which occurred in the area resulted from the action of eastward- and northeastward-flowing braided streams (Leckie and Cheel, 1989). Deposits of sand and gravel transported by these streams have been preserved across southern Alberta and Saskatchewan. The oldest preglacial gravels rest on the highest uplands, such as the Cypress Hills, and the youngest, deposits immediately preglacial in age such as the Empress Formation, fill in buried valleys. This succession of sand and gravel deposits can be divided into four groups (Dawson et al., 1994): 1) the Upper Eocene to Miocene Cypress Hills Formation and equivalents such as the Porcupine Hills Formation, which rest at an elevation close to the pre-existing surface indicated by coal maturity (Nurkowski, 1984; Bustin, 1992); 2) the Miocene to Pliocene Handhills Formation and equivalents on Del Bonita Upland and Wintering Hills, as well as on Wood Mountain in Saskatchewan; 3) Upland gravels, including the Willowbrook and Bredenbury Formation; and 4) the early Pleistocene Saskatchewan Gravels as well as the associated Grimshaw Gravels and the Empress Formation.

Throughout most of the area, pre-Quaternary deposits are overlain by Pleistocene glacial sediments. At the surface, and to a lesser extent in the subsurface, other Quaternary deposits such as glaciolacustrine clay and glaciofluvial sand and gravel also occur (Gravenor and Bayrock, 1961; Shetsen, 1987a, b). According to Fenton et al. (1994), sediments across most of the study area are less than 50 m thick, considerably thinner than values commonly exceeding 100 to 200 m which occur across southern Saskatchewan. Sediment exceeding 50 m in thickness occurs intermittently along the Alberta/Saskatchewan border and along the Montana border. The greatest thicknesses in the study area, over 100 m, occur between Medicine Hat and the Cypress Hills (Fig. 1), and midway between Calgary and the Montana border.

The complex Quaternary history of the study area may be summarized as three major glacial events of somewhat uncertain age: 1) an early, extensive Cordilleran ice advance; 2) a subsequent extensive advance of Laurentide ice which radiated outward from the Canadian Shield and overrode the glacial deposits of the earlier flow; and, 3) a less extensive coalescent Cordilleran and Laurentide ice flow which deposited a train of Cordilleran erratics along the foothills, passing through Calgary (Stalker, 1976; Stalker and Harrison, 1977; Jackson, 1980; Rutter, 1984; Fenton, 1984; Fulton et al., 1984; Bobrowsky and Rutter, 1992; Stalker and Vincent, 1993; Young et al., 1994; Evans and Campbell, 1995; Little, 1995).

The Quaternary stratigraphy of adjacent southern Saskatchewan has been described by Christiansen (1968), Whitaker and Christiansen (1972), Christiansen (1968, 1979), Schreiner (1990), Christiansen (1992), and Klassen (1992, 1994). The oldest tills are the Sutherland Group, consisting of the Mennon, Dundurn and Warman formations, of pre-Illinoian age. These are overlain by younger sediments of the Saskatoon Group, comprising the Floral and Battleford formations. The lower part of the Floral Formation is of Illinoian age, whilst the Upper Floral and Battleford Formations are Early and Late Wisconsinian age. In the Saskatoon area, where this stratigraphy was described by Christiansen (1992), at least six separate glacial events can be distinguished on the basis of till carbonate content. Varying composition at least implies unroofing of sources progressively lower in the bedrock stratigraphy, if not variation in distance as well as direction of transport. According to Schreiner (1990), ice flow directions ranging from westward to southeastward are indicated by the composition of Saskatchewan tills.

Survey design

The project originally was designed as an ultra-low density soil geochemical reconnaissance meant to define broad regional trends in geochemical baselines. Similar ultra-low density surveys based on 100 x 100 km grids have been carried out by the USGS (Severson and Tidball, 1979; Severson and Wilson, 1990) and are becoming increasingly applied elsewhere (Darnley et al., 1995). The sampling design for the present project, for which both soil and till would be sampled, had to fulfill two contrasting needs (Garrett, 1983). From the point of view of kimberlite/lamproite exploration, sample spacing had to be sufficient to intersect the glacial dispersal patterns from any significant clusters of kimberlites in the study area. With respect to estimating baseline levels, in order to characterize the different till units exposed at the surface, an essentially evenly distributed (i.e., random) sampling is required that gives all till and soil localities an equal chance of being selected (Garrett, 1994).

The sampling grid was designed using the 10 km UTM grid printed on 1: 250 000 topographic maps. The 80 x 80 cells stepped out both westward and eastward from the central meridian of each UTM zone. The southern boundary of the southernmost 80 x 80 km cell was at UTM northing 5 340 000 m. This procedure led to some partially populated 80 x 80 cells at the UTM zone boundaries, however, the logistical convenience of this procedure was considered to outweigh this disadvantage.

The preferred site for soil sampling was the edge of agricultural land along a road allowance in or near the target cell. Inaccessible targets were relocated within the same 10 km cell if possible, or elsewhere in the same 20 km cell, or in one of the unsampled 20 km cells, if necessary. If only one 20 km cell within a 40 km cell was accessible, only one site was sampled. No preference for parent material or topographic position was permitted in soil sampling, except for avoidance of narrow stream valleys and sites inundated by water or peat. The objective was to collect an unbiased statistical sample of the soils in the study area. This would lead to a data subset, and subsequent statistics, weighted by the spatial frequency of the various till and soil environments across the study area, and so provide a valid basis for geochemical baseline level estimation.

All sites, including supplementary sites designed to characterize the variability of soil geochemistry on a hierarchy of scales, were to be sampled for A horizon and C horizon soil. Till, if present in the 40 km cell, was to be sampled at a nearby exposure such as a road cut at two sites per 40 km cell only.

Field procedures

Orientation sampling was carried out by the authors during August 1991. Survey sampling was completed on a contract basis by professional staff of the Alberta Research Council, during summer 1992. Sampling in the northeastern part of the area was completed in autumn 1992 by the first author.

The A and C horizons were chosen as the sampling media for soil geochemistry. The A horizon was readily identifiable as the blackish horizon at surface, typically a ploughed Ap horizon. The C horizon was sampled below the A horizon, and the B horizon, if present.

At 26 orientation transect sites and 352 survey sites, A horizon samples were obtained from an interval which ranged on average from 3 to 18 cm below surface, and C horizon samples from depths of 40 to 66 cm below surface. The A horizon sample was collected by making a small excavation through the entire A horizon with a shovel. After A horizon material was cleared from the pit, the C horizon sample was recovered with a Dutch auger. Soil samples were 1 to 2 ℓ in size. Steel sampling tools were sand-blasted at the start of the survey to remove coatings that could have contaminated sampled material. No contact of sample material with jewelry was permitted.

Till, unsorted Pleistocene glacial sediment, was chosen as the indicator mineral sampling medium, rather than more easily and inexpensively sampled and processed fluvial or glaciofluvial sediments. Till has a simpler transport history, more extensive occurrence, more uniform composition, and greater usefulness in the study of sediment provenance. A sampling depth below 0.8 m below surface was preferred in order to obtain material in which carbonate was less likely to have been precipitated or leached due to weathering. Till can be recognized in the field as a silty to sandy sediment which contains scattered pebbles and a clayey matrix. In the study area, the presence of very coarse sand grains in a silty matrix is diagnostic. These unsorted sediments are diamicts, regarded in most cases to be till, sediment deposited directly by glacial ice. No preference for any particular till type or stratigraphic affinity was applied. Such distinctions generally can only be made at large vertical exposures or in drill core.

Till samples were obtained at 16 orientation transect sites and 252 survey sites. In order to avoid laborious excavation from the surface, existing exposures, such as road cuts near the soil sites, were sampled. The exposure was cleared of a few tens of centimetres of material in order to sample undisturbed sediment. Rare deeper exposures, where unoxidized material might be exposed, were avoided in order to obtain till samples from which most or all of the sulphide fraction had consistently been lost to oxidation, thus simplifying the interpretation of heavy mineral geochemistry. Sand-blasted steel shovels and picks were used, and samples were homogenized in large plastic pans. Two samples, 2 and 3 ℓ in size, weighing about 2 and 3 kg and intended for geochemical analysis and as a reserve respectively, were taken in plastic bags. A 25 ℓ sample, which weighed 25 to 30 kg, from which heavy mineral and pebble fractions were to be recovered, was then placed in a plastic pail.

Most of the C horizon samples consist of oxidized till, however, many were derived from several other parent materials. Definitions of soil vary from the tendency of engineers to refer to all sediment as soil, to the view that only the A and B horizons are soil and the C horizon is sediment acting as parent material. Oxidation has had a profound effect on the geochemical behaviour of the near-surface glacial sediments by destroying virtually all sulphide mineral grains occurring above the water table (Shilts and Kettles, 1990; Thorleifson and Kristjansson, 1993). Here, however, this material is referred to as till, rather than soil, in order to distinguish it from the A horizon and C horizon sets.

Field data were recorded at each site, and the actual sampling sites plotted on 1:250 000 topographic maps for later digitizing or manual UTM coordinate recovery. The field data provide information on the general sampling environment and observations on the colour, texture, moisture content, and composition of the soil and till.

Indicator mineral methods

Introduction

Indicator mineral tracing involves the sampling of sediments dispersed from bedrock sources by earth surface processes, the classification of mineral grains (in most cases by density and/or magnetic methods), and the recognition of mineral grains which indicate the presence of mineral deposits in the area from which the sediments were derived. Examples of indicator minerals include garnets, pyroxenes and oxides associated with potentially diamond-bearing kimberlites and lamproites, visible gold grains, sulphides in unoxidized sediments collected below the water table, and scheelite.

In Canada, the most common sediment available for indicator mineral sampling is till, which has, at least, been transported by glacial processes. In some cases, glacially transported mineral grains may also have been transported by fluvial action in preglacial or interglacial time, and material may have undergone multiple phases of glacial transport. Glaciofluvial sediments such as eskers, as well as fluvial sediments in modern rivers, have undergone an even more complex transport history involving the reworking of till and other sediments.

Ideally, indicator mineral analyses are used in three phases of diamond exploration, two using sediment and one using rock:

1. Following the selection of a region which is favourable for diamond potential with respect to tectonic context, sediment sampling at spacing on the order of 10 km is used to narrow the area of interest. Fluvial and glaciofluvial sediments, rather than till, may in some cases be favoured on the basis of ease of sampling and processing. Areas of interest on the order of 100 km across are

designated on the basis of elevated frequency and more favourable chemistry of recovered indicator minerals.

2. Geophysical surveys are conducted in the selected area. In areas where relatively thin till outcrops, sampling of till at spacing on the order of 100 m along several lines down-ice from the target and oriented perpendicular to ice flow may be used to test geophysical targets with respect to their lithology and indicator mineral chemistry.

3. Geophysical targets where the most favourable indicator mineral chemistry is obtained are chosen for drilling. A small sample of the intrusion, such as a diamond drill core, is processed for indicator mineral and petrological studies. Ideally, it is only on the basis of promising indicator mineral chemistry that a decision to extract an expensive bulk sample for diamond grade assessment would be made.

Most published literature on minerals derived from kimberlite relates to work on kimberlites themselves. Relatively little literature is available regarding the size, shape, and surface textures of minerals dispersed from kimberlite sources. Furthermore, clearly defined methods for the differentiation of likely-kimberlitic minerals from background minerals have not been published. Useful general discussions on the use of glacial sediments in mineral exploration programs have been presented by Shilts (1982, 1984), DiLabio (1989), Hirvas and Nenonen (1990) and Saarnisto (1990).

Kimberlite indicator minerals include: certain types of pyrope and almandine from the garnet group of silicate minerals; chrome-bearing forms of the relatively common pyroxene mineral diopside; and magnesian examples of the oxide minerals ilmenite and spinel. All of these minerals have specific chemical compositions which relate to conditions during crystallization in kimberlite or rocks such as peridotite or eclogite which were transported by the kimberlite. Perhaps the best known kimberlite indicator mineral is purplish Cr-pyrope garnet. In most cases, these garnets are derived from disaggregated peridotite xenoliths, which are the principal source of diamond in kimberlite (Deer et al., 1982; Fipke, 1989; Gurney and Zweistra, 1995). Dawson and Stephens (1975, 1976) and Gurney (1984) established protocols for the classification of kimberlitic garnets, with names derived from arbitrarily sequenced group numbers. For example, subcalcic to calcic, non-titanian Cr-pyropes were classified as Groups 10, 9, and 7 (respectively G10, G9, G7), and were attributed to harzburgites, lherzolites, and wehrlite respectively. Titanian Cr-pyropes, of a distinctive rich orange to purple-orange colour, were classified as G1 and G2, on the basis of increasing TiO_2 content, and G11 in the case of pyropes rich in both TiO_2 and Cr_2O_3. Pyropes with very high chrome content were classified as G12. Eclogite xenoliths, which also supply abundant diamonds to some kimberlites, contain titanian, calcic, and magnesian orange-coloured almandine garnets, which were classified as G3, G4, G6, and G8 by Dawson and Stephens (1975, 1976), on the basis of TiO_2 and CaO content. Crustal almandine garnets have the composition of the G5 group defined by these authors.

Diopsides with >0.50% Cr_2O_3 commonly occur in kimberlite (Deer et al., 1982; Fipke, 1989), as well as various other rocks. Hence the degree to which kimberlite indicator minerals are exclusive to kimberlite varies. From the oxide group of minerals, Mg-ilmenites with >6% MgO and Cr-spinels with >60% Cr_2O_3 and >12% MgO are also used as kimberlite indicators (e.g., Gurney and Moore, 1993).

Sample size is a critical issue in indicator mineral tracing (Craigie, 1993; Davison, 1993; Gregory and White, 1989; Clifton et al., 1969). The fundamental requirement is for a sufficient number of grains to be present in each sample, in areas where such grains occur, for regional trends in indicator mineral frequency to be mapped. A 25 ℓ sample size was chosen for the orientation transect and confirmed for the survey on the basis of advice received regarding current activity in the region, as well as experience in northern Ontario (Thorleifson and Kristjansson, 1993). This sample size was considered marginally acceptable, but appropriate due to the logistical challenge and expense of larger samples.

Mineral processing methods: orientation

In the case of the orientation samples collected in 1991, experiments in the refinement of preconcentration procedures at the Saskatchewan Research Council (SRC) were followed by processing at CF Mineral Research of Kelowna, British Columbia. The till, washed of clay and fine silt, was separated at 2.96 specific gravity using tetrabromoethane. The >2.96 specific gravity fraction was subsequently separated at a specific gravity of 3.2 using methylene iodide (MI) diluted with acetone. The MI concentrate was screened at 0.25 mm (60 mesh) and 0.063 mm (230 mesh). Ferromagnetic minerals, mainly magnetite, were removed using a Carpco top feed roll separator. The almandine and ferro-ilmenite rich paramagnetic fraction was removed using a Carpco bottom-feed separator, followed by Frantz isodynamic separation at low amperage. A higher amperage Frantz pass was then used to remove the nonmagnetic fraction from the weakly paramagnetic fraction, which was subsequently visually examined for potential kimberlitic indicator minerals.

A total of 3457 grains, or an average of about 70 mineral grains per sample, were selected from the orientation samples, mounted, and polished by CF Minerals staff. About 75% of these mounted grains were regarded as potential eclogitic almandine garnets. Black opaque grains, considered possible Mg-ilmenites and Cr-spinels, as well as potential lamproitic tourmalines, each make up about 10%. The remaining grains were green clinopyroxenes, potentially Cr-diopsides, and a total of 6 purplish grains considered likely to be peridotitic garnets. Of the 3457 grains which were picked as potential indicator minerals, about 70% of the grains were from the 0.25 to 2.0 mm fraction. The remainder were recovered from the 0.063 to 0.25 mm fraction of five samples in order to test the viability of using this fraction. The grains, mounted and polished in four 25 mm epoxy cylindrical mounts, were analyzed by CF Minerals using multi-element EDS mapping followed by quantitative EDS analysis of selected grains. These grains were subsequently re-analyzed by electron microprobe at the GSC in order to test analytical procedures being developed for this application.

At the GSC, a reference set of non-kimberlitic grains which occur in abundance in all samples was selected from the orientation samples and analyzed to obtain comparative data for non-kimberlitic minerals in the area. A total of 1378 grains were mounted from four sites. Two of these sites were located in Alberta, near Suffield and Vegreville. The remaining two sites were located near Lanigan, Saskatchewan, and River Hills, Manitoba. The grains were mounted and polished in two 25 mm araldite cylindrical mounts. The grains were selected on the basis of the following preliminary visual identifications: 160 pink garnets, 160 orange garnets, 160 clinopyroxenes, 80 hornblendes, 80 orthopyroxenes, 50 epidotes, 10 barites, 20 rutiles, 160 black opaques, 80 grey ilmenites, 80 magnetites, 40 hematites, 10 goethites, 10 tourmalines, 10 apatites and gahnites, 10 leucoxenes, 40 staurolites, 40 sphenes, 30 weakly paramagnetic garnets, 30 weakly paramagnetic clinopyroxenes, 28 weakly paramagnetic black opaques, 30 paramagnetic garnets, 30 paramagnetic clinopyroxenes, and 30 paramagnetic black opaques.

Mineral processing methods: survey

The 25 ℓ till samples collected for the 1992 regional survey were processed at the SRC. The material was disaggregated in a cement mixer with the aid of a sodium hexametaphosphate (calgon) solution (Fig. 2). In a few cases, repeated washings were required to prevent flocculation of sulphate- and carbonate-rich samples. The disaggregated till was screened at 10 mesh to remove the >2 mm fraction which was washed, dried, screened at 4, 8, and 16 mm, and weighed.

The -10 mesh (<2 mm) fraction was preconcentrated at SRC by passing it over a shaker table twice to obtain large heavy mineral preconcentrates which were then transferred to Overburden Drilling Management in Nepean, Ontario. The concentrates were renumbered and randomized in order to avoid uncertainty in distinguishing trends related to spatial distribution from those related to analysis order. The material was screened at 0.5 mm and all >0.5 mm material was submitted directly to heavy liquid separation. The <0.5 mm fractions were inspected for visible gold on a shaker table. Samples in which three or more gold grains were seen were panned in order to count and size the gold. Following panning, the gold was returned to the table concentrate which was dried and further concentrated using methylene iodide diluted with acetone to 3.2 specific gravity. The ferromagnetic fraction, averaging 4 g in the Alberta samples, was removed using a hand magnet. The concentrates were then also screened at 0.25 mm in preparation for indicator mineral analysis.

The coarse heavy mineral concentrates were returned to the SRC and examined for potential indicator minerals under a stereoscopic microscope. An average of 15 minutes were spent examining an average of 3 g of 0.5 to 2.0 mm nonferromagnetic concentrate from each sample. The 0.25 to 0.50 mm nonferromagnetic fraction, which averaged 5 g in total mass, was sorted by magnetic susceptibility using a Frantz isodynamic separator. The strongly paramagnetic fraction, rich in ferro-ilmenite, was not examined. The moderately paramagnetic fraction, which in this area contains abundant Fe-rich almandine garnet, was visually scanned for Mg-ilmenite and Cr-spinel. The weakly paramagnetic to nonmagnetic fraction was visually scanned for indicator garnets and pyroxenes. An average of 20 minutes were spent examining each 0.25 to 0.50 mm fraction.

All visually selected grains, an average of 30 per site, were subsequently re-examined by the mineralogical staff of Consorminex Inc. of Gatineau, Quebec, and unwanted minerals such as staurolite and

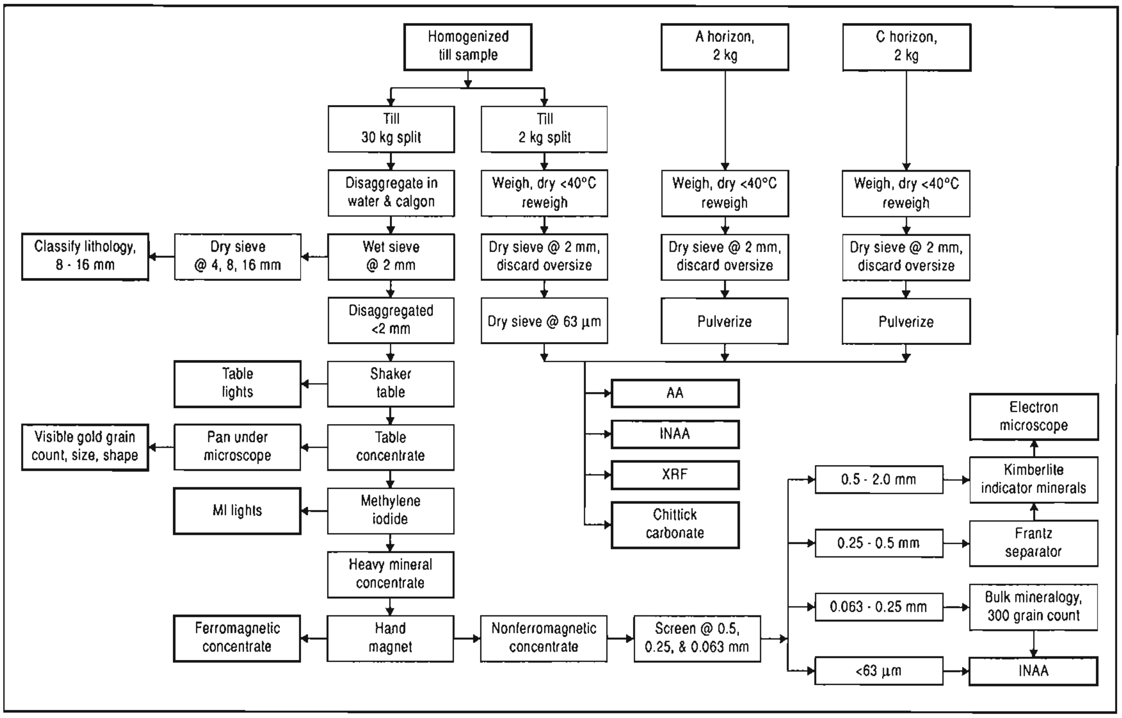

Figure 2. *Sample processing flow-sheet.*

hornblende were removed on the basis of properties such as birefringence. An average of 8 grains per sample, averaging 4 from the 0.25 to 0.50 and 4 from the 0.25 to 0.50 mm fraction, were selected for analysis.

Minerals were mounted in 25 mm cylindrical araldite mounts, with grains arranged in rows within 9 cells per mount. Grains from the 0.5 to 2.0 mm fraction were arranged in 5 rows of 6 grains per cell, to yield a total of 270 grains per mount. Grains from the 0.25 to 0.5 mm fraction were placed in 8 rows of 10 in each cell, resulting in a total of 720 grains per mount. The mounts were polished using diamond paste. Maps recorded the site number and identification number of each grain.

Microprobe analysis

In the case of the orientation sampling, coordinates of points to be analyzed were entered using an optical microscope. One point in the core of each grain was analyzed at the GSC, with care to avoid inclusions, fractures, or pits. A second point was analyzed at the end of the batch for one grain in every 20, in order to assess analytical variability. In order to make possible the analysis of a very large number of grains, high amperage (200 nA, 20 kv) and short counting times were used. Values reported for potassium and sodium by this method are of low reliability. Background counts were included in the routine for each element. Detection limits were estimated by calculation to be about 0.01 wt. % for SiO_2, Al_2O_3, CaO, FeO, MgO, Cr_2O_3, TiO_2, Na_2O, and K_2O; 0.02 wt. % for MnO, NiO, ZnO, and CoO; 0.04 wt. % for Nb_2O_5; and 0.05% for V_2O_3.

Chemical analyses of a total of 7813 grains from the 1992 regional survey samples were carried out in the Canada Centre for Mineral and Energy Technology (CANMET) laboratories in Ottawa, using a JEOL 8900 electron microprobe operating at 40 nA and 20 kV. Peak counting times of 10 seconds were used for Na_2O, K_2O, CaO, total Fe as FeO, MgO, Al_2O_3, MnO, and SiO_2, and 40 seconds for TiO_2 and Cr_2O_3. Calibration was confirmed at the beginning and end of each batch. In order to reduce machine time, background determinations were made on every 50th grain and used for the 50 grains which followed. Hence detection limits were elevated above the levels normally used in research work. The analyses were completed in 11 automated runs which were driven by a set of x-y-z coordinates for one point per grain, selected to avoid inclusions, fractures or pits. At the end of each batch, every 45th grain, on average, was re-analyzed at another similar point to monitor precision related to grain heterogeneity, calibration drift, or unusual background measurements. These replicates indicate good reproducibility at levels above 0.1% for all elements, with a few exceptions attributed to heterogeneity.

Subsequent to the initial microprobe analyses, a total of 156 eclogitic garnets and garnets which only marginally failed to surpass the definition being used for eclogitic garnets were re-analyzed at CANMET using detection limits which were reduced by the inclusion of background measurements with every analysis. These analyses were carried out to obtain acceptable Na_2O sodium data used to assess the potential association of eclogitic garnets with diamond (Gurney and Moore, 1993), and to enhance TiO_2 data which were being used for the recognition of eclogitic garnets. A total of 233 Cr-pyropes and 136 Cr-spinels were analyzed by proton microprobe at the University of Guelph for Ni and several other elements in order to utilize classification methods developed by Griffin and Ryan (1993). Nickel temperatures were calculated for Cr-pyropes using the equation presented by Griffin et al. (1989).

Geochemical methods

The <2 mm fraction of soil samples was utilized for geochemical analysis in order to conform with accepted agricultural and environmental analytical protocols. As has been done elsewhere for till geochemical studies (e.g., Eden and Bjorklund, 1995), the <0.063 mm fraction of till was prepared. This fraction, from which the silica-dominated sand fraction is excluded, provides a greater reflection of regional bedrock composition and hence provenance.

The 2 ℓ soil and till samples were air dried below 40°C, gently disaggregated, avoiding the crushing of rock and mineral grains, and screened using a 2 mm stainless steel sieve. The oversize was discarded. Approximately 50 g of the <2 mm soil was ground to <0.150 mm in an agate pestle and mortar and stored for analysis. In the case of till, enough of the retained <2 mm material was screened using a 0.063 mm stainless steel sieve to yield approximately 50 g of material that was stored for analysis. The remaining <2 mm soil and till was archived.

Prior to analysis, 33 quality assurance samples were added to the 252 field till samples to be analyzed. These quality assurance samples consisted of 22 randomly selected sample preparation duplicates (second cuts of 50 g of the <0.063 mm fraction) intended to monitor precision, as well as 11 aliquots of certified reference materials (coded as sample 7) intended to monitor accuracy. The soil samples, consisting of two sets of 352 A and C horizon soil samples, were augmented with 32 sample preparation duplicates consisting of material from code 5 sites split after preparation, the resulting sample being coded as sample 6. Sixteen control samples consisting of certified reference materials and material from bulk samples prepared as project references were added to each soil batch.

The A horizon, C horizon, and till sample sequences for the entire prairie survey were each randomized and renumbered prior to analysis in order to prevent the mistaken attribution of analysis order trends to spatial patterns.

All samples were submitted to Becquerel Laboratories, Inc., Mississauga, Ontario, for instrumental neutron activation analysis (INAA) which produced data for 34 elements. A fixed volume of prepared material, averaging 7.3 g (4.82 to 10.12 g), was encapsulated, sealed and irradiated with neutron flux monitors in a 2 MW pool-type reactor. Following a 7 day decay period, the samples were analyzed using a high-resolution Ge detector system. Gamma radiation was counted for approximately 500 seconds. Usable data were obtained for the elements indicated in Table 1.

Table 1

Elements for which geochemical data were obtained, with lower limit of detection indicated

INAA		AAS		XRF	
As	0.5 ppm	Ag	0.2 ppm	SiO_2	0.01%
Au	2 ppb	Cd	0.2 ppm	Al_2O_3	0.01%
Ba	50 ppm	Co	2 ppm	CaO	0.01%
Br	0.5 ppm	Cu	2 ppm	MgO	0.01%
Ce	5 ppm	Fe	0.02 %	Na_2O	0.01%
Cs	0.5 ppm	Hg	10 ppb	K_2O	0.01%
Co	5 ppm	Mn	5 ppm	Fe_2O_3	0.01%
Cr	20 ppm	Mo	2 ppm	MnO	0.01%
Eu	1 ppm	Ni	2 ppm	Cr_2O_3	0.01%
Fe	0.2 %	Pb	2 ppm	P_2O_5	0.01%
Hf	1 ppm	V	5 ppm	TiO_2	0.01%
La	2 ppm	Zn	2 ppm	LOI	0.01%
Lu	0.2 ppm			Ba	10 ppm
Na	0.02%			Nb	10 ppm
Rb	5 ppm			Rb	10 ppm
Sb	0.1 ppm			Sr	10 ppm
Sc	0.2 ppm			Y	10 ppm
Sm	0.1 ppm			Zr	10 ppm
Ta	0.5 ppm				
Tb	0.5 ppm				
Th	0.2 ppm				
U	0.2 ppm				
W	1 ppm				
Yb	1 ppm				

At Barringer (Alberta) Laboratories, Ltd., a 1 g aliquot from each of the same vials already subsampled for INAA was decomposed, with a fuming mixture of HF, $HClO_4$, and HNO_3, to near dryness on a hot plate. The residue was taken into solution with concentrated HCl and, following dilution to a 1 M concentration, was analyzed by flame atomic absorption spectrophotometry (AAS) for elements indicated in Table 1. Mercury was determined on a separate 0.5 g aliquot by flameless AAS after an aqua-regia dissolution.

The till and C horizon soil samples also were analyzed for major elements by X-Ray Fluorescence (XRF) following fused disk preparation at XRAL Laboratories, Don Mills, Ontario, for elements indicated in Table 1.

The <0.25 mm nonferromagnetic heavy mineral concentrates were screened at 0.063 mm in preparation for mineralogical as well as geochemical analysis. After a few milligrams of the 0.063 to .25 mm fraction were obtained for mineralogical analysis by coning and quartering, 0.063 to 0.25 mm fractions averaging 21 g and <0.063 mm fraction averaging 3 g were analyzed by nondestructive INAA at Becquerel Labs. The <0.25 mm concentrate was divided at 0.063 mm in order to permit the comparison of sand and silt sized material, including comparison of the geochemical data to visual mineralogical counts of the 0.063 to 0.25 mm fraction. The entire concentrate was analyzed. Data for samples split into multiple INAA vials were recombined by weighted average. Due to variable and frequently small sample sizes, detection limits vary. Data for the 0.063 to 0.25 mm and <0.063 mm fraction were retained separately, as well as being combined by calculation of a weighted average in order to obtain data for the <0.25 mm heavy mineral fraction.

Lithological methods

The texture of the <2 mm matrix of till samples collected along the orientation transect was determined by GSC staff using methods described by McDonald and Kelly (1968). A 50 g split was used for textural analysis. An additional 10 g sample was tested for moisture content. The subsample was disaggregated by freeze-drying and subsequently by treatment with 0.5N sodium hexametaphosphate. The sample was then mechanically mixed, heated to boiling, cooled, stirred and subjected to an ultrasonic probe for 20 seconds. Sand fractions were determined by dry sieving. The material finer than 0.063 mm was analyzed by pipette analysis.

The carbonate content of the <0.063 mm till matrix was analyzed using a technique for the Chittick gasometric apparatus described by Dreimanis (1962). Because of the contrasting reaction rates of calcite and dolomite in HCl, two readings of the amount of carbon dioxide produced by these reactions could be taken and the contributions of each of these minerals to total carbonate in the sample could be estimated.

The 8 to 16 mm fraction of till samples was classified with respect to lithology. The 4 to 8 mm and 2 to 4 mm fraction for selected samples were classified in order to compare fractions.

Bulk mineralogy of the 0.063 to 0.25 mm nonferromagnetic heavy mineral concentrates was determined by the staff of Consorminex Inc. on the basis of visual identification, under a stereoscopic microscope, of 300 grains in an araldite mount. This size fraction corresponds to that used in similar surveys elsewhere (Parfenoff et al., 1970; Karrow, 1976; Gwyn and Dreimanis, 1979; Paré, 1982; Peuraniemi, 1990), where the objective has been to determine the bedrock source of sediments.

KIMBERLITE INDICATOR MINERALS

The mean total moist weight of the 25 ℓ till samples from the prairie survey was 28 kg. The 2 ℓ till samples, which had been stored in sealed pails, were weighed before and after being air dried at <40°C. The resulting moisture content determinations averaged 10%, hence the mean air dry weight of the large till samples was 25 kg. The samples contained an average of 2 kg of gravel (>2 mm). The mean sand content of the <2 mm fraction of the orientation samples was found to be 35% (Garrett and Thorleifson, 1993), so the total amount of sand in the samples was about 8 kg. About 3 kg consisted of medium to very coarse sand, the fraction eventually used for indicator mineral analysis.

Electron microprobe data were used to assign mineral identifications. The data are considered clearly adequate for the recognition of Cr-pyrope, Mg-ilmenite, and Cr-spinel, adequate for the selection of Cr-diopsides, and marginally adequate for the distinction of eclogitic Ti-almandines (>0.2% TiO_2). Garnets were classified using a scheme based on those of Dawson and Stephens (1975, 1976), Gurney (1984), and Gurney and Zweistra (1995). Diopsides with >0.50% Cr_2O_3 were regarded as Cr-diopside (Deer et al., 1982; Fipke, 1989). Mg-ilmenites in every case contained well in excess of 6% MgO. Cr-spinels exceeding 60% Cr_2O_3 and 12% MgO were regarded as compositions comparable to those reported for diamond inclusions by Gurney and Moore (1993).

Among the 252 survey samples, a total of 148 mineral grains were judged to be kimberlite indicator minerals, which also serve as the principle indicator for lamproites, despite their lower abundance in the latter rocks. This frequency can be approximated as one indicator mineral in every second sample.

A total of 67 Cr-pyropes were recovered. The majority of these grains have non-titanian, peridotitic compositions. One grain is a calcium-rich G7, 33 are lherzolitic or G9, and one grain, recovered near Provost, at the Saskatchewan border in the east-central part of the area (Fig. 1; Table 2), was classified as a subcalcic G10. The remaining 32 Cr-pyropes are titanian in composition (G1, G2, G11). These pyropes show a nonrandom distribution (Fig. 3), with the

Table 2

G7, G9, G10, and G11 garnets recovered from till (approx 25 kg) in southern Alberta

Site	NTS sheet	Location name	UTM coordinates	Mineral ID	CaO %	Cr_2O_3 %	TiO_2 %	Temp C	Ni ppm	Zr ppm
5-2-2	83J	Vega	11 670100 6031800	G9	5.72	5.34	0.23	894	26	20
15-4-2	83H	Spruce Grove	12 305300 5946000	G9	5.01	4.34	0.26	1008	39	194
16-3-1	83A	Ponoka	12 316900 5842600	G9	6.05	4.95	0.03	781	16	5
16-3-1	83A	Ponoka	12 316900 5842600	G9	6.09	4.97	0.03	932	30	6
19-4-1	82I	Carseland	12 321900 5637500	G9	5.09	4.61	0.20	950	32	31
20-3-1	82H	Ft. Macleod	12 311900 5528700	G9	4.84	2.46	0.01	583	5	16
21-3-1	82H	Cardston	12 332900 5444200	G9	5.82	7.28	0.04	852	22	152
24-2-2	83I	Perryvale	12 344500 6042900	G9	5.75	5.94	0.07	na	na	na
24-4-2	83I	Valley Lake	12 383000 6020500	G9	5.44	5.44	0.22	1111	53	18
27-2-1	83A	Buffalo Lake	12 373500 5808500	G11	6.20	7.99	0.45	959	33	37
30-1-2	82H	Lethbridge	12 365700 5519600	G11	5.90	6.39	0.78	1323	88	112
30-4-2	82I	Enchant	12 394700 5557800	G9	6.20	7.79	0.17	1016	40	122
31-3-2	82H	Raymond	12 387800 5459500	G9	5.42	3.43	0.03	768	15	14
34-2-2	73L	Whitefish L	12 432900 6015000	G9	4.23	2.67	0.21	1131	56	13
34-3-1	73L	Vincent L	12 482000 5997300	G9	5.69	6.08	0.25	1008	39	47
34-4-2	73L	Frenchman L	12 475000 6037200	G9	4.57	2.79	0.19	1016	40	19
34-4-2	73L	Frenchman L	12 475000 6037200	G9	5.07	5.72	0.14	818	19	22
37-1-2	83A	Sullivan Lake	12 421600 5762700	G9	4.88	4.82	0.17	841	21	15
37-3-1	73D	Coronation	12 480900 5776800	G9	4.61	3.02	0.08	739	13	12
38-3-1	72M	Oyen	12 497200 5685900	G9	6.43	7.39	0.06	1039	43	7
38-4-1	72M	Hanna	12 470200 5724900	G9	4.60	2.51	0.30	1170	62	16
40-1-1	72E	Purple Springs	12 439300 5521600	G9	5.28	3.87	0.08	884	25	61
41-2-1	82H	Wrentham	12 424100 5483600	G9	5.36	2.89	0.04	400	0	18
41-4-2	72E	Foremost	12 478100 5467500	G9	5.97	6.56	0.24	984	36	34
44-1-1	73E	Vermilion	12 503200 5919400	G9	5.63	5.46	0.07	950	32	4
44-2-2	73E	Elk Point	12 506700 5970100	G9	4.79	3.73	0.00	794	17	42
44-4-2	73E	Heinsburg	12 541600 5951800	G9	4.52	2.67	0.22	950	32	23
46-3-2	73D	Provost	12 564900 5768200	G10	4.68	6.56	0.01	894	26	88
47-1-1	72M	Oyen	12 530300 5697100	G11	5.87	6.39	0.86	1295	83	112
47-1-1	72M	Oyen	12 530300 5697100	G11	6.14	6.95	0.86	1317	87	112
47-4-1	72M	Oyen	12 549100 5720100	G9	5.00	4.03	0.13	894	26	22
47-4-2	72M	Oyen	12 542600 5734200	G7	7.35	6.11	0.18	884	25	8
48-1-1	72L	Suffield East	12 535000 5581400	G9	4.83	3.78	0.18	806	18	20
48-3-1	72L	Schuler	12 562900 5582900	G9	4.53	3.08	0.18	806	18	22
48-3-1	72L	Schuler	12 562900 5582900	G11	5.92	6.09	0.89	1448	112	140
48-3-2	72L	Suffield East	12 552200 5590000	G9	6.39	7.89	0.08	830	20	1
49-1-1	72E	Cypress Hills	12 533900 5504000	G9	5.19	6.24	0.22	1350	93	68
50-2-1	72E	Pakowki Lake	12 507100 5475800	G9	5.00	4.27	0.03	781	16	22
50-3-2	72E	Wildhorse	12 555300 5432500	G9	4.55	3.46	0.22	1024	41	20
50-3-2	72E	Wildhorse	12 555300 5432500	G9	4.66	3.48	0.24	1016	40	23
50-3-2	72E	Wildhorse	12 555300 5432500	G11	5.83	7.58	0.43	923	29	32

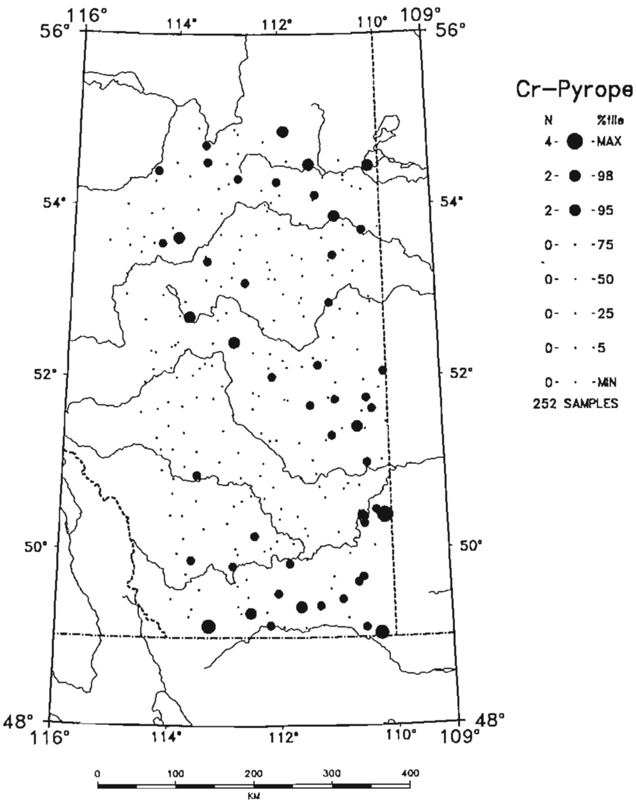

Figure 3. Cr-pyropes (0.25–2 mm) recovered from 25 ℓ till samples.

highest concentrations in the southern, east-central, and northern parts of the survey area. The most noteworthy cluster is located 50 km north of Medicine Hat, east of Canadian Forces Base Suffield.

Ni determinations by proton microprobe on a total of 40 garnets classified as G7, G9, G10, and G11 were used in a geothermometry study. Although there is some uncertainty regarding precision of the method and validity of the assumptions (e.g., Kjarsgaard, 1992, 1995), tentative conclusions may be made by assuming a 40 mW/m^2 geotherm (Griffin et al., 1989) and acceptable calibration to other instruments. On that basis, 12% of the garnets, mostly G11, report temperatures above the diamond stability field (>1250°C, >75 ppm Ni), 38% are in the diamond stability field (32–75 ppm Ni), and 50% are cooler (<950°C, <32 ppm Ni). The G10 at Provost reported a Ni concentration of 26 ppm, implying a low temperature of formation (~890°C). The grains indicating temperatures in the diamond stability field are scattered across the area. Six grains occur along a belt of Cr-pyrope occurrences across the northern part of the study area (Fig. 3), five in the central portion of the study area, and four in the south. Of the grains in the Griffin diamond window (950–1250°C, 32–75 ppm Ni), 87% contain <50 ppm Zr, a positive sign regarding diamond grade, according to Griffin and Ryan (1993) and Griffin et al. (1994a, b). Among the diamond stability field Cr-pyropes, only one in the central belt and one in the southern belt contained >50 ppm Zr.

Using a minimum TiO_2 value of 0.25%, Thorleifson and Garrett (1993) identified 4 titanian, calcic, and magnesian, hence eclogitic, almandines (G3, G4, G6) from the survey samples. At a lower cutoff of 0.2%, Thorleifson et al. (1994) reported the occurrence of 16 eclogitic garnets on the basis of re-analysis data. These grains were obtained from sites in the southeastern, east-central, and north-central portions of the area. None of these grains was found to contain anomalous concentrations of Na_2O.

A total of 51 Cr-diopsides were recovered from the survey samples (Fig. 4). These occurrences show a tendency toward east-west alignment, similar to the pattern shown by Cr-pyropes (Fig. 3). A cluster of occurrences north of Medicine Hat coincides with occurrences of Cr-pyropes (Fig. 3). Clusters in Cr-diopside frequency also are apparent near Oyen and Red Deer, as well as elevated frequency in the northern portion of the study area.

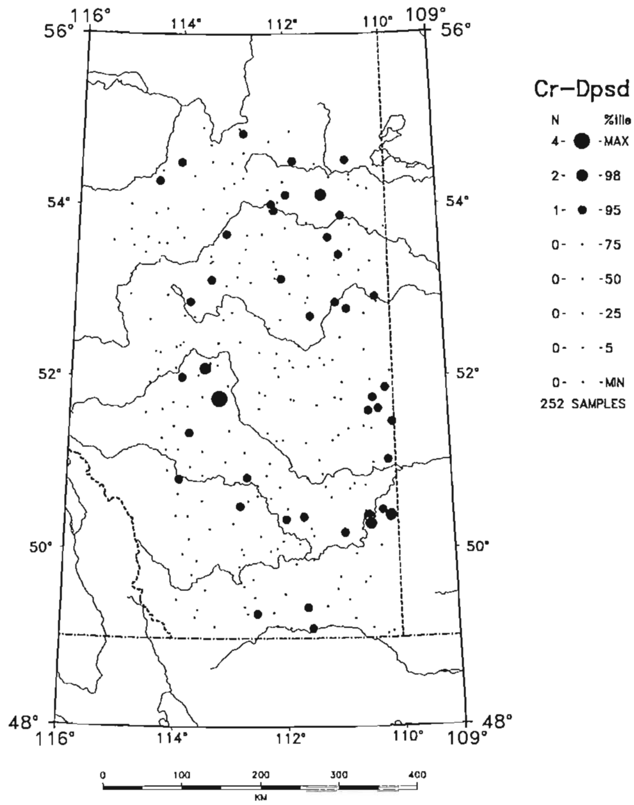

Figure 4. Cr-diopsides (0.25–2 mm) recovered from 25 ℓ till samples.

A total of 26 Mg-ilmenites were recovered from the survey samples (Fig. 5). Two were recovered from the sample that yielded a G10, near Provost. Occurrences of Mg-ilmenites also are relatively concentrated in the Red Deer area.

A total of 18 Cr-spinels were recovered from the Alberta survey samples (Fig. 6), with occurrences tending to occur in the western half of the area. None of these grains exceeds 60% Cr_2O_3 and 12% MgO, values characteristic of diamond inclusion spinels. The prairie-wide Cr-spinel data are readily divisible into two clusters separated at 53% Cr_2O_3. Above this value, Ni concentrations cluster between 200 and 800 ppm. This group is comparable to the P1 cluster from kimberlites reported by Griffin and Ryan (1993, 1995). Below 53% Cr_2O_3, Ni values are more variable, ranging from 200 to 2000 ppm. This compositional range is comparable to the P3 and P4 clusters of Griffin and Ryan (1993, 1995). High-Cr grains preferentially occur in the eastern half of the prairie region, including eastern Saskatchewan, whereas grains recovered in Alberta tend to be low-Cr grains.

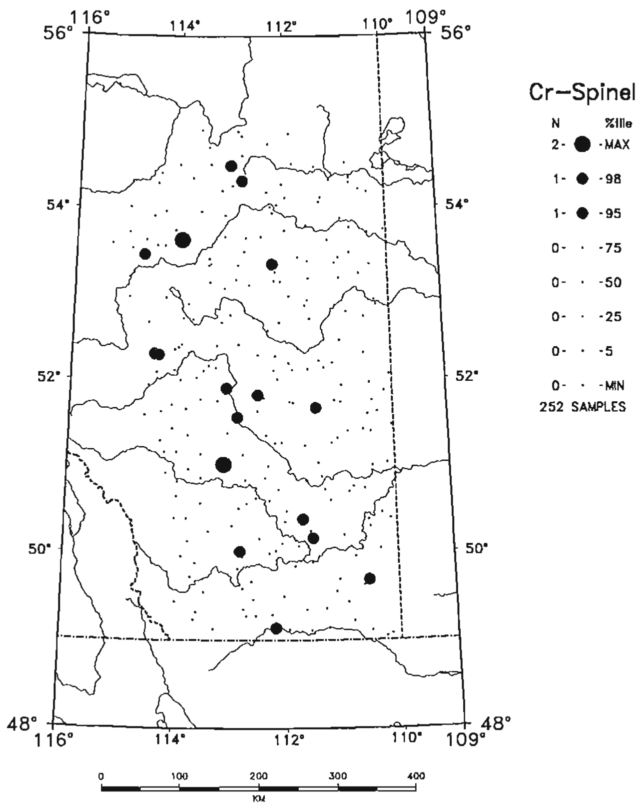

Figure 6. *Cr-spinels (0.25–2 mm) recovered from 25 ℓ till samples.*

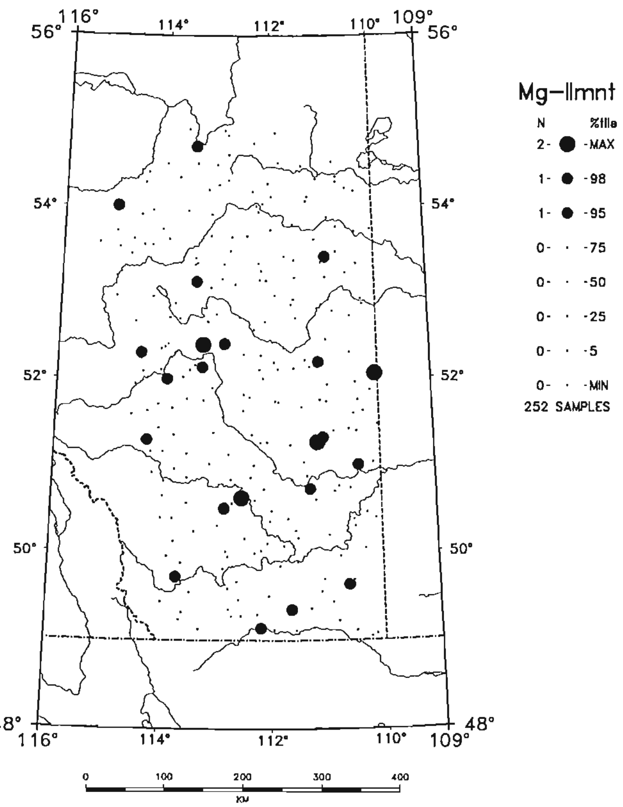

Figure 5. *Mg-ilmenites (0.25–2 mm) recovered from 25 ℓ till samples.*

VISIBLE GOLD

The 25 ℓ till samples contained as many as 19 visible gold grains per sample (Fig. 7). The highest counts were obtained in the Edmonton area, an area of former placer gold production (Halferdahl, 1965; Romaniuk, 1981; Giusti, 1986, 1987; Day and Fletcher, 1987; Edwards, 1990). At least one visible gold grain was recovered in 75% of the samples, and of these grains, approximately 70% are about 0.075 mm or smaller (i.e., silt sized). The remainder are sand-sized grains with dimensions exceeding 0.3 mm in only a few cases. In the opinion of the staff of Overburden Drilling Management Ltd., the majority of the grains exhibit characteristics typical of glacially transported gold, such as tool marks and folding. A few of the grains exhibit characteristics more typical of placer deposits, such as raised rims.

Provenance of the grains in Alberta is thought to be primarily from the Cordillera, by some combination of eastward fluvial transport in Cretaceous, Tertiary, or interglacial time, Cordilleran ice flow, and at least one phase of Laurentide glacial transport. In addition, intrusions penetrating the Phanerozoic sequence may be contributing visible gold (Harris and Ballantyne,

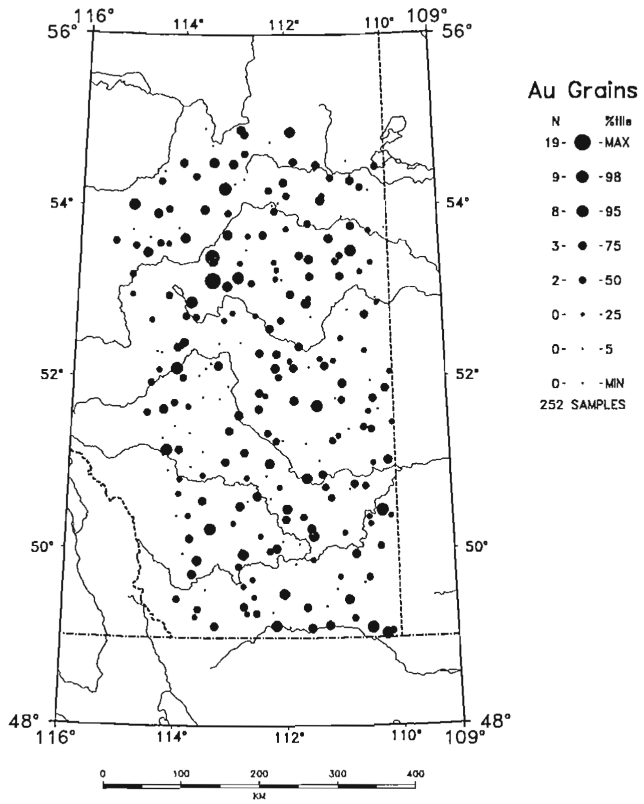

Figure 7. Visible gold grains recovered from 25 ℓ till samples.

1994; Ballantyne and Harris, 1997), and long distance transport from the Canadian Shield is likely the source for some of the grains. Paleoplacers in Early Cretaceous rocks of the Foothills Ranges, such as the McDougal-Segur conglomerate (Leckie and Craw, 1997), may be the source for some of the gold.

GEOCHEMISTRY

Till matrix geochemistry

As was previously documented by Bayrock and Pawluk (1967), geochemical data for the fine grained matrix of till across Alberta reveal broad-scale patterns that can be related to regional provenance. In addition, a number of elements exhibit patterns that may be related to mineral occurrences, even though they are of low geochemical contrast. The broadest division that can be delineated in the geochemical data is the distinction between an area extending north and south from Calgary and the remainder of the area. For example, As values in the <0.063 mm fraction are depressed around Calgary (Fig. 8), whereas Cd values are elevated (Fig. 9). In addition, As values are elevated in the south-central part of the study area, in the Brooks region, which may be due to an area of more metalliferous shale, perhaps the Bearpaw. A

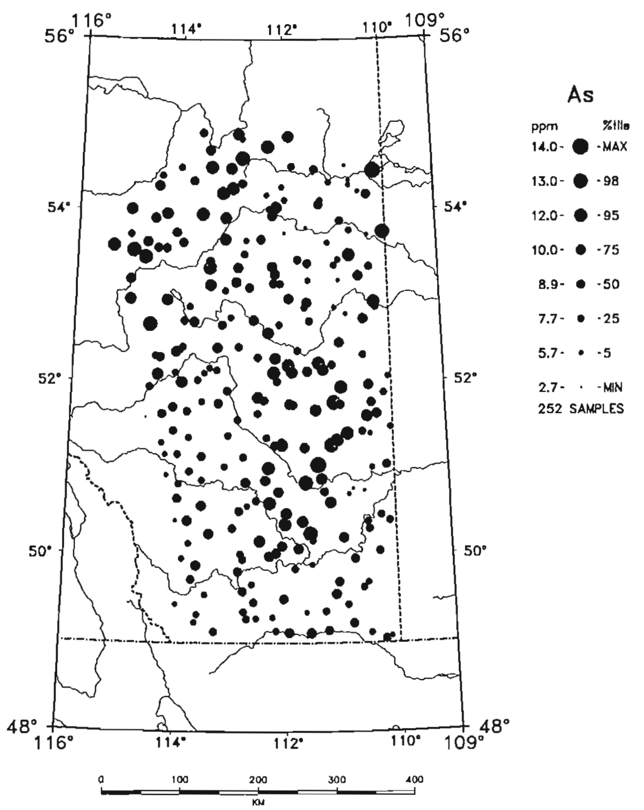

Figure 8. As in the <0.063 mm fraction of till.

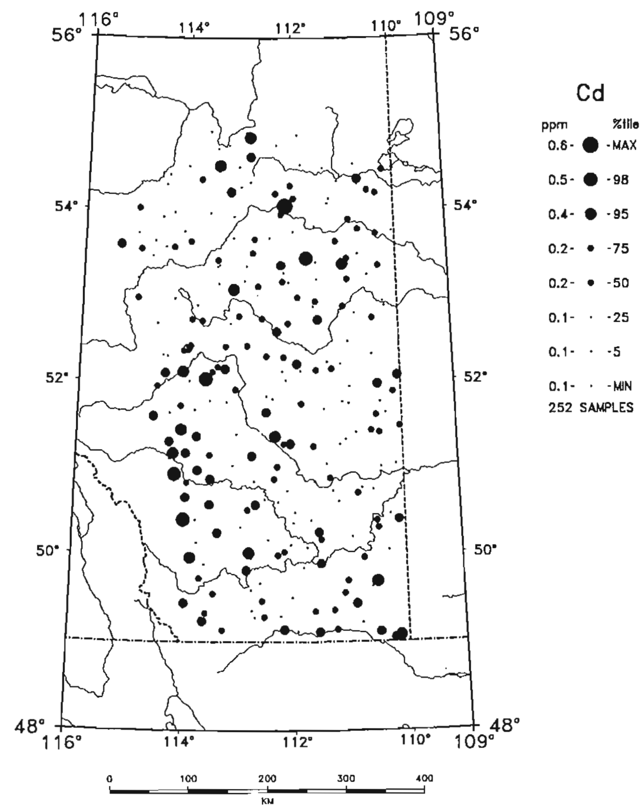

Figure 9. Cd in the <0.063 mm fraction of till.

number of elements increase in abundance to the northwest in Alberta relative to the area to the south [e.g., Fe, V, Cu (Fig. 10), Ni, Cr, Th, Sc, Rb and As]. This is likely a lithological control being exerted on the till composition. Shales are more widespread to the north and northwest in comparison to the Tertiary sandstones and Foothills carbonates in the west, which are likely poorer in trace elements. Some elements, such as Th (Fig. 11), are most abundant in the northeast, apparently reflecting proximity to the Canadian Shield.

The Calgary area, which has already been noted as being distinct with respect to trace elements, stands out as an area of elevated CaO (Fig. 12). As discussed below, this is attributed to carbonate derived by glacial transport from the Cordillera. Elevated values for P_2O_5 in the Calgary area (Fig. 13) raise the possibility that phosphatic rocks may play a role with respect to the elevated Cd levels in that area.

Heavy mineral concentrate geochemistry

Analyses of the <0.063 and 0.063 to 0.25 mm heavy mineral concentrates were combined into a composite <0.25 mm value. These data reveal many of the same

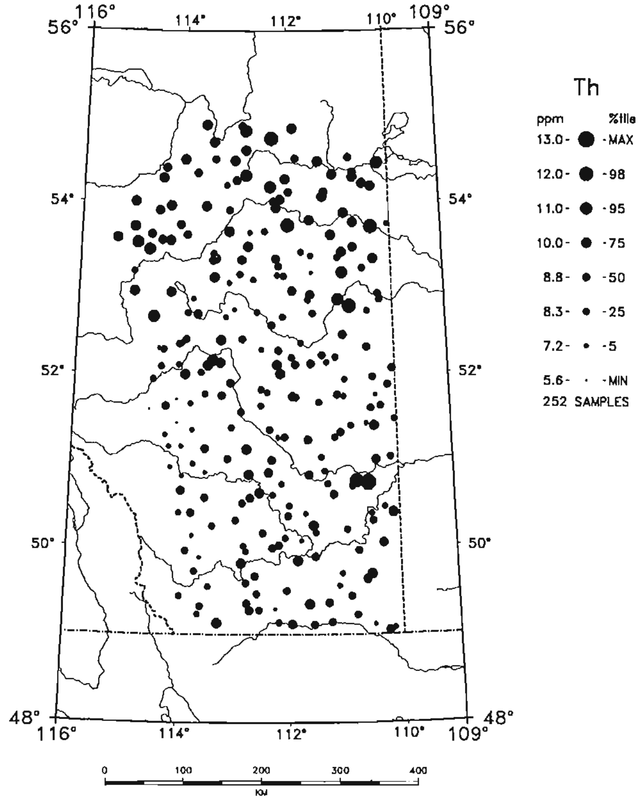

Figure 11. Th in the <0.063 mm fraction of till.

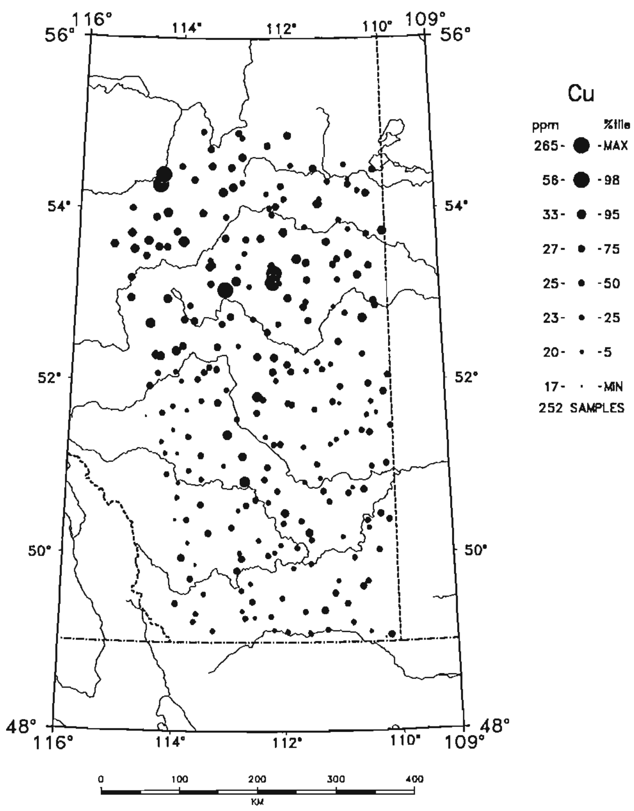

Figure 10. Cu in the <0.063 mm fraction of till.

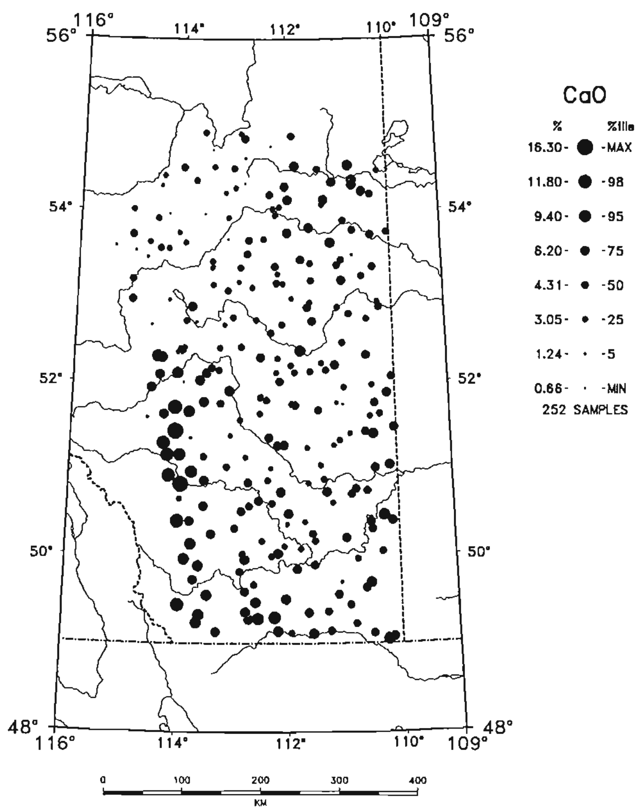

Figure 12. CaO in the <0.063 mm fraction of till.

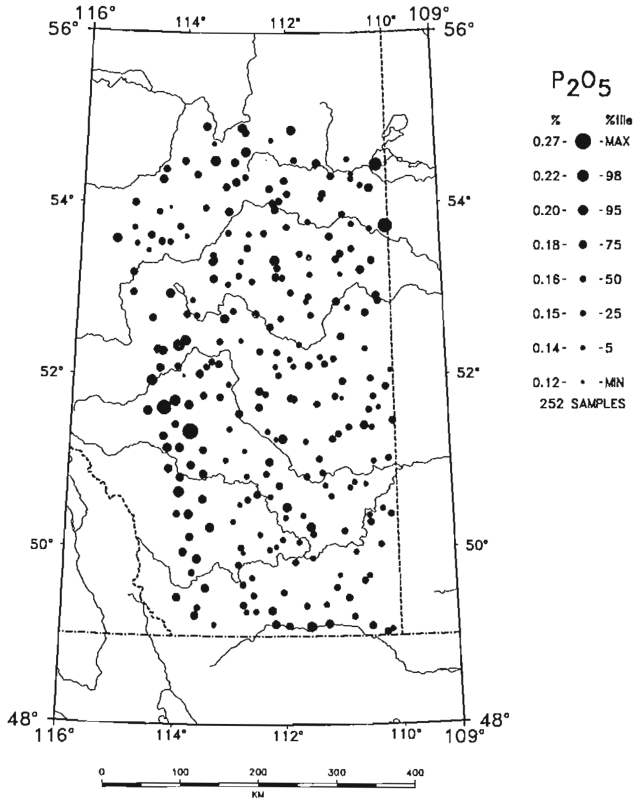

Figure 13. P_2O_5 *in the <0.063 mm fraction of till.*

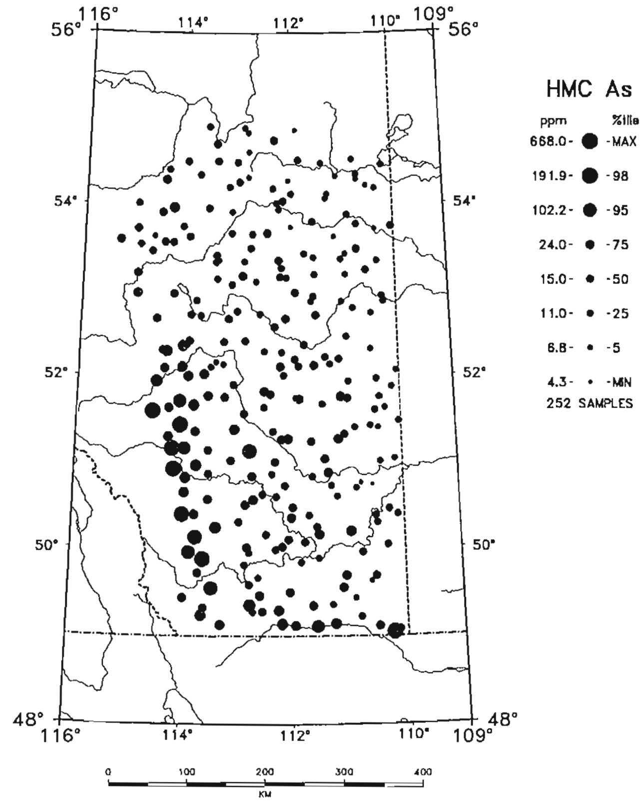

Figure 14. As in the <0.25 mm, nonferromagnetic, >3.2 specific gravity fraction of till.

features as the till matrix data that appear to divide the surface till data into two geochemical domains. In the Calgary area, As is elevated in the concentrates, (Fig. 14), the reverse of its behaviour in the <0.063 mm fraction (Fig. 8), perhaps reflecting dilution by abundant <0.063 mm carbonate material in the till matrix. However, Sc (Fig. 15) and Ta (Fig. 16), occur at concentrations in this fraction which are elevated to the northeast.

Soil geochemistry

The geochemical patterns in the soil data closely follow those observed for the tills. However, as soils were collected on all parent materials, some patterns relate to fluvial derivatives of till, such as quartz-rich fluvial and aeolian sand, and clay-sized material of glaciolacustrine sediments. These two groups are characterized by generally lower trace-element values in the case of coarse, quartz-rich sediments and higher values for many elements in fine grained parent materials. The A horizon samples have been influenced by pedological processes that have led to a modification of the C horizon patterns through concentration and depletion, with relationships varying between areas and soil regimes. For example, As is relatively concentrated in light brown chernozemic surface soils in the south of the survey area.

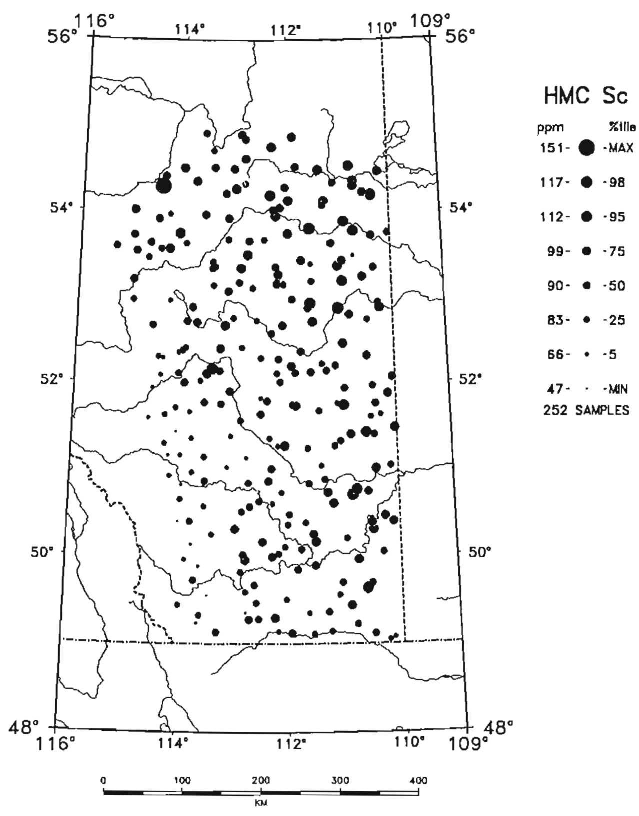

Figure 15. Sc in the <0.25 mm, nonferromagnetic, >3.2 specific gravity fraction of till.

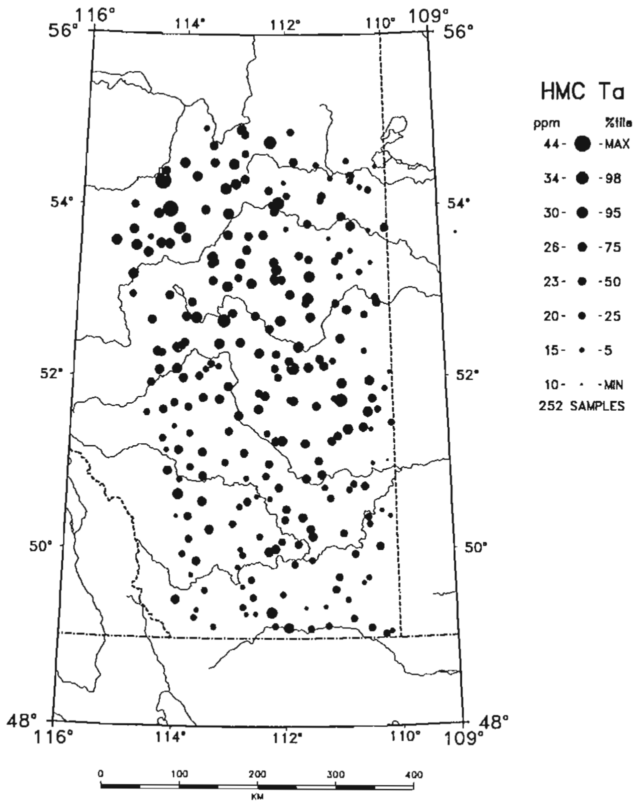

Figure 16. Ta in the <0.25 mm, nonferromagnetic, >3.2 specific gravity fraction of till.

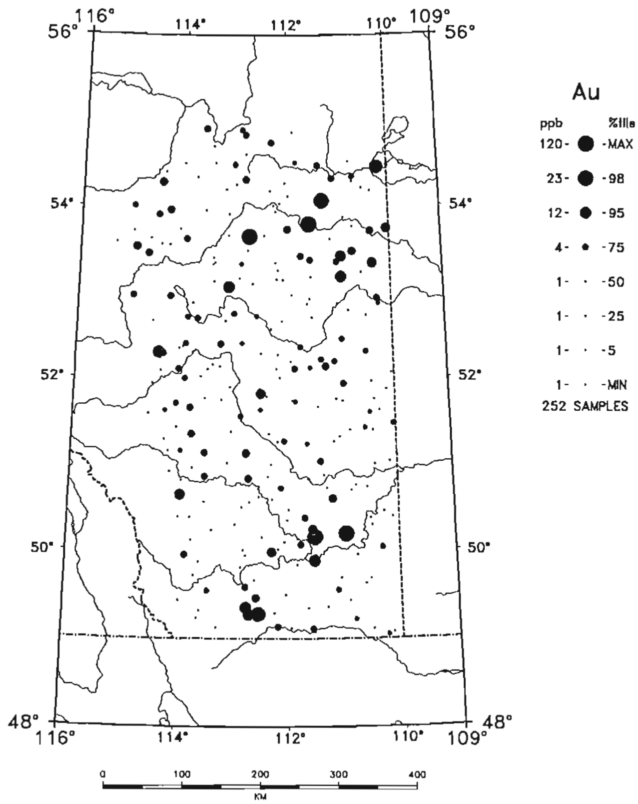

Figure 17. Au in the <0.063 mm fraction of till.

The distribution of Cd in the soils is of particular interest in environmental and agricultural studies because certain compounds of this element were regulated under the Canadian Environmental Protection Act (CEPA) in 1994. A discussion of the close relationship of the Cd data for A horizon soils to glacial sediment parent materials has been presented by Garrett (1994). Similarly, toxic Hg compounds are regulated in Canada, and a discussion of the distribution of Hg in surface and C horizon soils has been presented by Garrett and Thorleifson (1994). Again, the dominant controls on Hg distribution are the chemistry of the soil parent materials, glacial sediments, and in turn, their provenance.

Comparison of gold analyses

INAA analyses of the <0.063 mm fraction of the till samples indicate clusters of elevated Au values in the southern and northeastern portions of the study area (Fig. 17). This fraction seems to be responding to the presence of gold in silts and clays, the origin and significance of which differs from the visible gold grains and other gold detected in the heavy mineral concentrates. Perhaps this gold was chemically dispersed in shales. The highest count of visible gold grains, which does not take the mass of this gold into account, is in the Edmonton area (Fig. 7). However, INAA analyses of heavy mineral concentrates (Fig. 18), which do take the mass of the gold into account, but which are referred to as the mass of the concentrate, clearly show a pattern of elevated values parallel and adjacent to the Foothills.

Gold analyses for A and C horizon soil samples indicate lower concentrations and less systematic variability than the till data. This is attributed to dilution by sterile sand due to analysis of the <2 mm fraction, as well as to the fact that many of the samples were taken on glaciolacustrine and glaciofluvial clay and sand. Data for this size fraction are more susceptible to the nugget effect.

SEDIMENT TRANSPORT HISTORY

Introduction

Only till was processed for indicator minerals in this survey, so all the minerals reported here were transported by the continental ice sheet during the Pleistocene. These mineral grains may have undergone multiple phases of reworking by glacial processes, and may also have been transported by fluvial processes in interglacial and preglacial time.

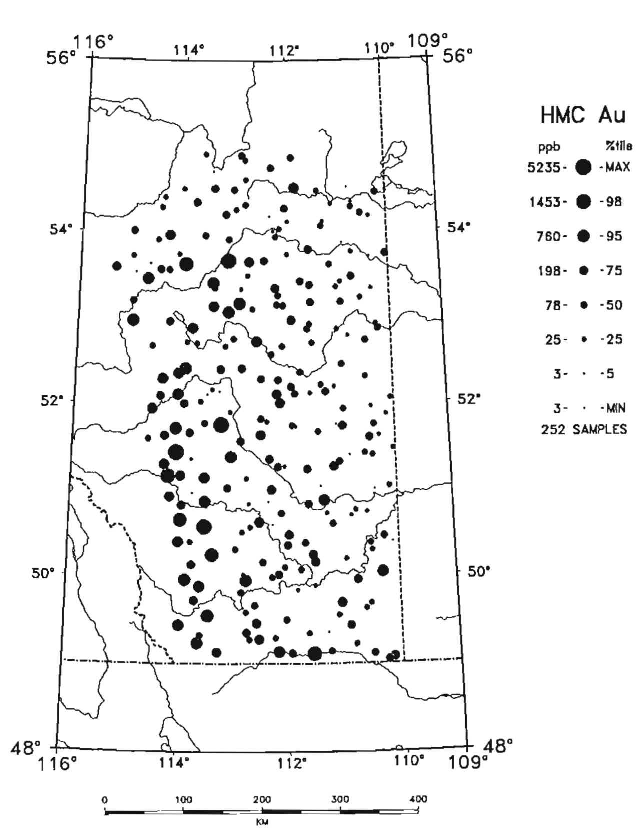

Figure 18. Au in <0.25 mm heavy mineral concentrates.

Furthermore, determination of the relative contributions of natural or anthropogenic processes to soil chemistry in environmental studies is dependent on an understanding of the transport history of a sediment. In southern Alberta, till is the most available sediment and the material with the greatest influence on soil geochemistry.

Hence the tracing of glacial transport history is required for the interpretation of data collected by this and other soil and till sampling surveys. Previous efforts to examine regional trends in the provenance of Alberta glacial sediments include work by Pawluk and Bayrock (1969).

Depositional processes

Previous research on processes of glacial sedimentation in the prairie region have focussed on landforms (e.g., Gravenor and Kupsch, 1959) and sedimentary structures in diamicts released from stagnant ice (Shaw, 1982). Discussion of sedimentation by active ice has been influenced by work elsewhere (e.g., Boulton, 1974) which emphasized high-stress lodgement of sediments from sliding ice. Recent research has indicated, however, that till sedimentation in areas of thick, extensive, fine grained till may be related to subglacial deformation, rather than entrainment in the ice. Seismic surveys of the bed of Ice stream B in the west Antarctic have indicated a 10 m thick sediment layer, the seismically determined shear strength of which is less than the shear stress exerted by the overriding ice (Alley et al., 1986, 1987a, b). The implied deformation and hence transport of the sediments is analogous to deformation observed in Iceland by Boulton and Jones (1979) and discussed by Boulton (1982, 1987) and Boulton and Hindmarsh (1987). Thick exotic diamicts of the prairie region, therefore, may represent deposits of sediments transported by shear below a very thin glacier (Mathews, 1974). In this context, preservation of carbonate clasts and indicator minerals susceptible to abrasion could be attributed to protection by the enclosing fine grained deforming matrix.

Texture

Processing of till samples for indicator minerals presented an opportunity to determine gravel content of till in the area. The mean gravel (>2 mm) content of air dry till in the study area was determined to be 5%. Values of 15 to 20% occur in the Calgary area. Only the orientation samples were processed for detailed textural analysis of the <2 mm fraction. Among these 14 samples, sand content ranged from 27 to 47% and averaged 37%, silt ranged from 31 to 58% and averaged 39%, and clay ranged from 14 to 32% and averaged 24%. A bimodal grain size distribution is consistently apparent, with modes centred on fine sand and medium silt. Whereas silt content of the <2 mm fraction was consistently between 30 and 40% for most of the samples, values well over 40% were obtained in the Calgary area, where several variables indicate the presence of material derived from the Cordillera.

Matrix carbonate content

The <0.063 mm fraction of the survey till samples contains, on average, 9% carbonate, as indicated by the Chittick gasometric method. This average composition is made up of near equal contributions of calcite and dolomite. Values range from less than 1% each to highs of 22% calcite and 19% dolomite. Several samples which clearly stand out as outliers at over 20% carbonate occur in the Calgary area, ranging from Olds in the north to Pincher Creek in the south.

Pebble lithology

Pebbles recovered in the 8 to 16 mm fraction were classified with respect to lithology. Till in the area contains an average of 10 g of 8 to 16 mm pebbles per kg of dry <16 mm till. On average, this amount is made up of about 2 g each of intrusive and high-grade metamorphic rocks ('granite'), quartz sandstone, and brown carbonate. At about 1 g or less each, on average, are grey carbonate, immature sandstone, quartzite, ironstone, and low grade metasedimentary and metavolcanic rocks. Small quantities of shale and coal are present in some of the samples.

The bedrock source of these rock types has been determined by previous work on gravel lithology in the area by Gravenor and Bayrock (1955, 1956), Stalker and Craig (1956), Rutter (1972), Metz (1968), Vonhof (1965, 1969), Whitaker (1980), Shetsen (1981, 1984), Shaw and Kellerhals (1982), and Little (1995). The Precambrian Shield is considered the source for virtually all of the intrusive and high-grade metamorphic rocks as well as the low-grade metasedimentary and metavolcanic rocks. Brown carbonate, in general, is attributed to long distance transport from the outcrops which occur along the shield margin in northeastern Alberta and Manitoba. Quartz sandstone was likely derived from the Cordillera as well as the Athabasca sandstone of northern Saskatchewan, grey carbonate from the Cordillera, immature sandstone from local Cretaceous and Tertiary bedrock, quartzite from Tertiary gravels and the Cordillera, and ironstone, shale and coal from local bedrock.

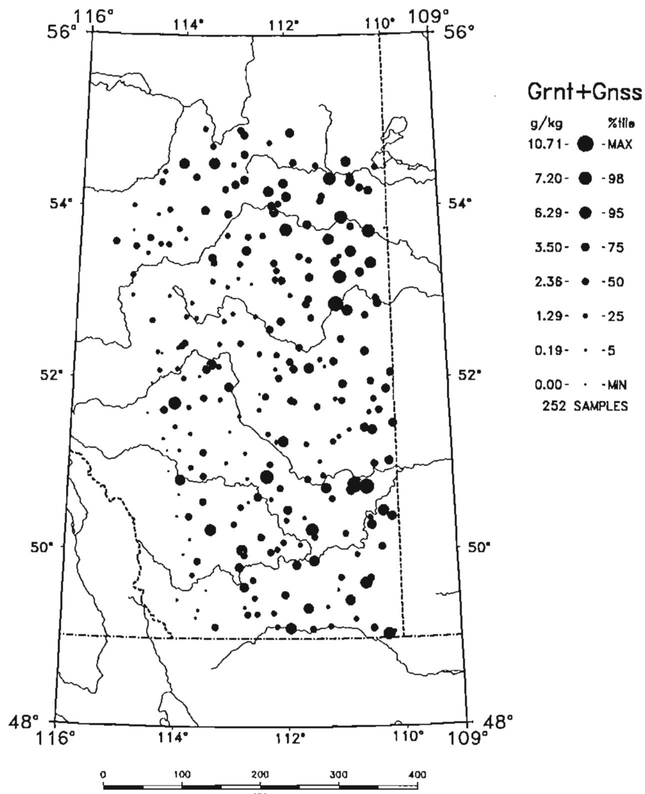

Figure 19. *Intrusive and high-grade metamorphic clasts in the 8 to 16 mm fraction of till.*

Concentrations of Precambrian rocks in general increase to the northeast (Fig. 19). Enhanced concentrations of low-grade metasedimentary and metavolcanic rocks in the southwesternmost portion of the area are attributed to Proterozoic rocks of the Waterton area.

Anomalous values for grey carbonate (Fig. 20) occur in an area extending north and south of Calgary. This area, which has already been noted as being distinctive with respect to geochemistry, texture, and carbonate, is the site of what has been referred to as the Foothills Erratics Train (Stalker, 1956; Mountjoy, 1958; Roed et al., 1967; Morgan, 1969; Tharin, 1969). This narrow zone extends from Jasper, west of Edmonton, along the mountain front, to the Montana border as a narrow strip of compositionally distinct till and large conglomeratic boulders. The train is attributed to coalescence of the Cordilleran and Laurentide ice sheets, and southward transport of material from the Athabasca valley along the mountain front.

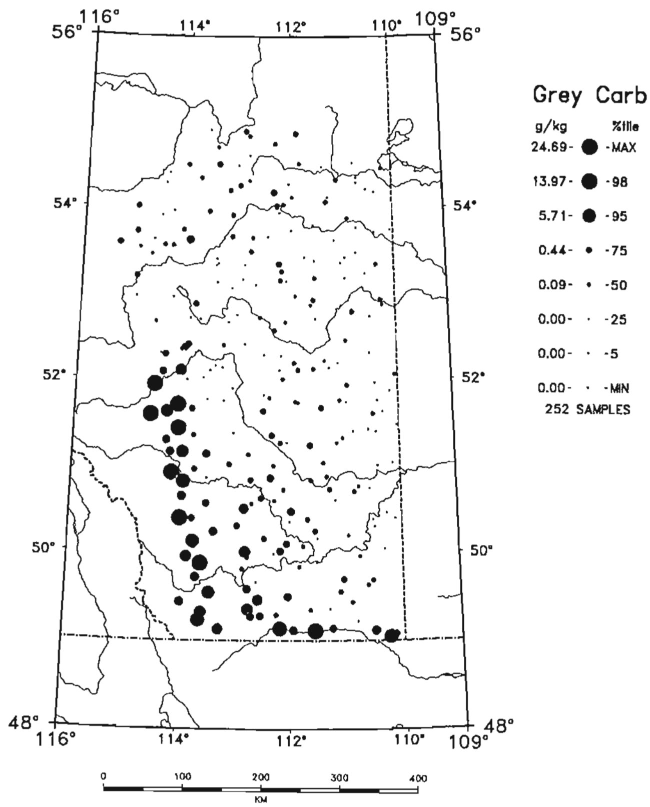

Figure 20. *Grey carbonate clasts in the 8 to 16 mm fraction of till.*

Quartzite is abundant in the Foothills Erratics Train (Fig. 21). Other areas where preglacial gravels have contributed quartzite to the till are apparent in the south-central and southern portion of the area. These abrupt increases in quartzite concentration are

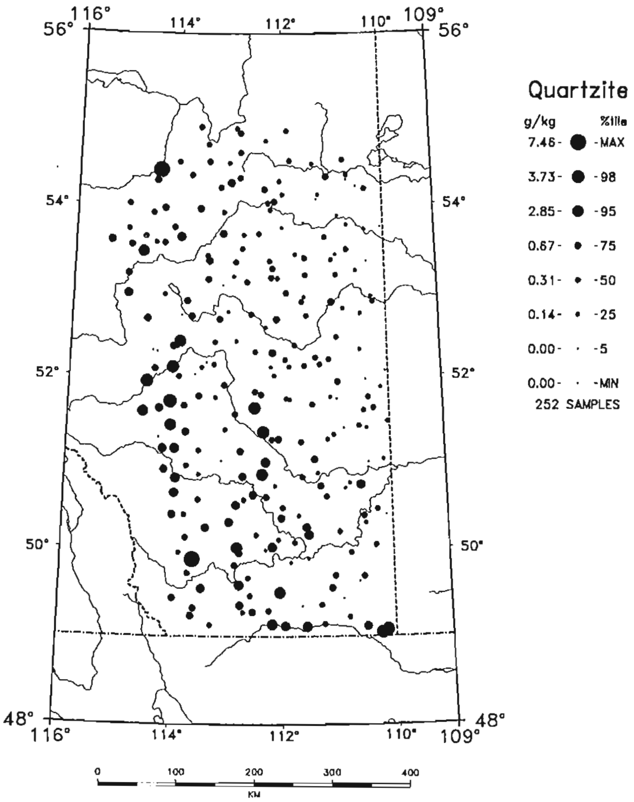

Figure 21. Quartzite clasts in the 8 to 16 mm fraction of till.

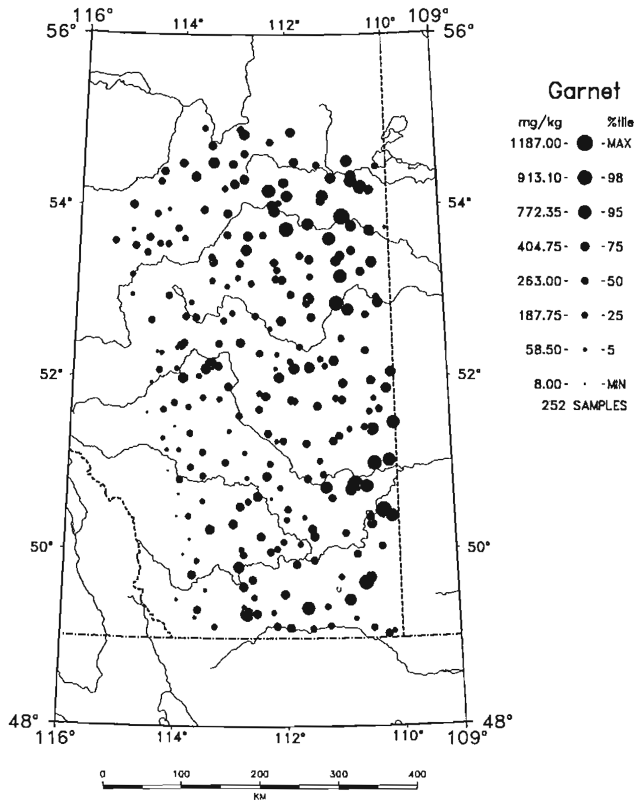

Figure 22. Garnet in the 0.063 to 0.25 mm, nonferromagnetic, >3.2 G fraction of till.

examples of a distinguishable local component, confirming that surface till provides information about nearby bedrock geology and, therefore, mineral potential.

Heavy minerals

The bulk mineralogy of heavy mineral concentrates provides another indicator of sediment transport history. For example, garnet (Fig. 22) increases in abundance to the northeast, probably indicating that the Canadian Shield is the principal source. Despite the presence of heavy minerals in local Cretaceous and Tertiary sandstones (Vonhof, 1965, 1969; Rahmani and Lerbekmo, 1975), Bayrock (1962) concluded that the vast majority of heavy minerals in surface till in east-central Alberta were derived from the Shield. In contrast, barite is more abundant to the southwest, implying a local, Cordilleran, or authigenic source (Fig. 23).

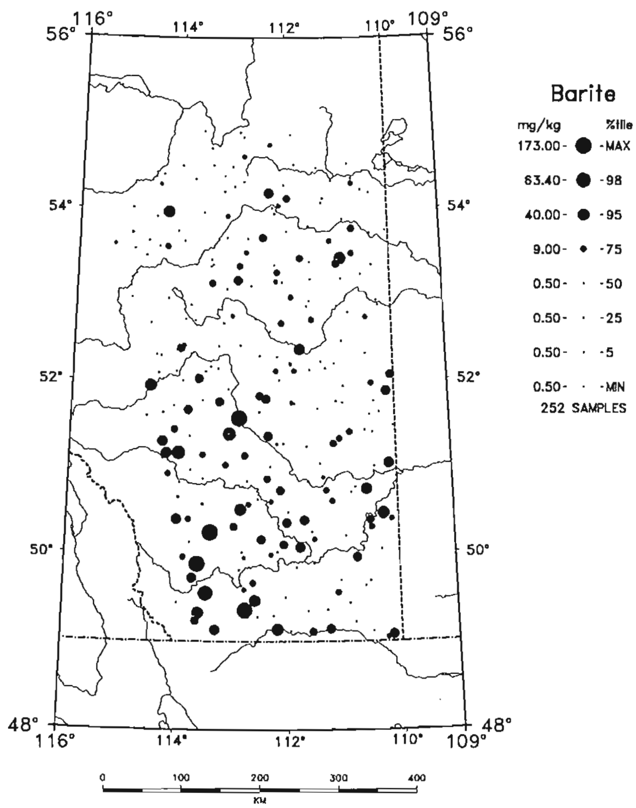

Figure 23. Barite in the 0.063 to 0.25 mm, nonferromagnetic, >3.2 G fraction of till.

CONCLUSIONS

This reconnaissance has provided the first systematic data on the distribution of till matrix, soil mineralogy, geochemistry, and kimberlitic and lamproitic indicator minerals in the region. It has demonstrated that:

1. Kimberlite indicator minerals, including Cr-pyrope, Cr-diopside, and Mg-ilmenite, as well as gold in various forms, are present in surface till of southern Alberta in a nonrandom distribution;

2. Till geochemistry, pebble lithology, and bulk mineralogy of heavy minerals vary systematically across the region, indicating derivation generally from the northeast over most of the area, but also from the Cordillera in the Calgary area; and

3. Ultra-low density soil geochemical data show patterns which are relevant to environmental and agricultural investigations.

Acknowledgments

We wish to acknowledge with appreciation the effort by a large number of people who contributed to this project: Walter Nassichuk and Roger Macqueen of GSC for coordination and facilitation of the project; colleagues Mark Fenton, Lionel Jackson, Erik Nielsen, Rudy Klassen, Bryan Schreiner, and Archie Stalker for discussions on the Quaternary history of the region; John Pawlowicz and Mark Fenton of the Alberta Geological Survey, who directed most of the field sampling; Chuck Fipke for valuable advice regarding indicator mineral tracing; staff of the Saskatchewan Research Council under the leadership of Alan Holsten and Bernard Gartner, who prepared the samples; Bruce Kjarsgaard of GSC for stimulating discussions on the alkaline igneous rocks of the Montana Alkaline Province; Irena Shetsen and Lawrence Andriashek of the Alberta Research Council, who provided very useful advice regarding lithological analyses; staff at Becquerel Labs, CANMET, CanTech Labs, CF Minerals, Consorminex, GSC, Overburden Drilling Management, XRAL and the University of Guelph for laboratory services; and Arlene Drake, Alexander FitzPatrick, Leanne Forman, Susan Lambert, and Dan Roberts, for assistance in the field and the office. We gratefully acknowledge the contribution that all these people, and others, made to the success of the project. However, we stress that the ideas presented here are those of the authors, for which we accept full responsibility.

REFERENCES

Alley, R.G., Blankenship, D.D., Bentley, C.R., and Rooney, S.T.
1986: Deformation of till beneath ice stream B, Antarctica. Nature, v. 322, p. 57-59.

1987a: Till beneath Ice Stream B. 3. Till deformation: evidence and implications. Journal of Geophysical Research, v. 92, p. 8921-8929.

Alley, R.G., Blankenship, D.D., Rooney, S.T., and Bentley, C.R.
1987b: Till beneath Ice Stream B. 4. A coupled ice-till flow model. Journal of Geophysical Research, v. 92, p. 8931-8940.

Ballantyne, B. and Harris, D. (*this volume*)
1997: Alluvial platinum-group minerals and gold in Alberta: Results from the "orientation studies project" and their significance to exploration. *In* Exploring for Minerals in Alberta: Geological Survey of Canada Geoscience Contributions, Canada-Alberta Agreement on Mineral Development (1992-1995), R.W. Macqueen (ed.). Geological Survey of Canada, Bulletin 500, p. 279-329.

Bayrock, L.A.
1962: Heavy minerals in till of central Alberta. Journal of the Alberta Society of Petroleum Geology, v. 10, p. 171-184.

Bayrock, L.A. and Pawluk, S.
1967: Trace elements in tills of Alberta. Canadian Journal of Earth Sciences, v. 4, p. 597-607.

Bobrowsky, P. and Rutter, N.W.
1992: The Quaternary geologic history of the Canadian Rocky Mountains. Géographie physique et Quaternaire, v. 46, p. 5-50.

Boulton, G.S.
1974: Processes and patterns of glacial erosion. *In* Glacial Geomorphology, D.R. Coates (ed.). State University of New York, Binghamton, p. 41-87.

1982: Subglacial processes and the development of glacial bedforms. *In* Research in glacial, glaciofluvial, and glaciolacustrine systems, R. Davidson-Arnott, W. Nickling and B.O. Fahey (eds.). Geo Books, Norwich, UK, p. 1-31.

1987: A theory of drumlin formation by subglacial sediment deformation. *In* Drumlin Symposium, J. Menzies and J. Rose (eds.). A.A. Balkema, Rotterdam, p. 25-80.

Boulton, G.S. and Hindmarsh, H.C.A.
1987: Sediment deformation beneath glaciers: rheology and geological consequences. Journal of Geophysical Research, v. 92, p. 9059-9082.

Boulton, G.S. and Jones, A.S.
1979: Stability of temperate ice sheets resting on beds of deformable sediment. Journal of Glaciology, v. 24, p. 29-43.

Brummer, J.J.
1978: Diamonds in Canada. CIM Bulletin, v. 71, p. 64-79.

Bustin, R.M.
1992: Organic maturation of the western Canadian sedimentary basin. International Journal of Coal Geology, v. 19, p. 319-358.

Christiansen, E.A.
1968: Pleistocene stratigraphy of the Saskatoon area, Saskatchewan, Canada. Canadian Journal of Earth Sciences, v. 5, p. 1167-1173.

1979: The Wisconsin deglaciation of southern Saskatchewan and adjacent areas. Canadian Journal of Earth Sciences, v. 16, p. 913-938.

1992: Pleistocene stratigraphy of the Saskatoon area, Saskatchewan, Canada: an update. Canadian Journal of Earth Sciences, v. 29, p. 1767-1778.

Clifton, H.E., Hunter, R.E., Swanson, F.J., and Phillips, R.L.
1969: Sample size and meaningful gold analysis. U.S. Geological Survey, Professional Paper 625-C, 17 p.

Craigie, E.
1993: Sampling techniques and the distribution of kimberlitic indicator minerals in glacial tills and sediments. *In* Diamonds: exploration, sampling, and evaluation, P. Sheahan and A. Chater (eds.). Prospectors and Developers Association of Canada, p. 237-248.

Darnley, A.G., Björklund, A., Bolviken, B., Gustavsson, N., Koval, P.V., Steenfelt, A., Tauchid, A., Xie Xuejing, Garrett, R.G., and Hall, G.E.M.
1995: A global geochemical database for environmental and resource management. UNESCO Earth Science Series 19, Paris, 122 p.

Davison, J.G.
1993: Diamond exploration samples: laboratory processing. *In* Diamonds: exploration, sampling, and evaluation, P. Sheahan and A. Chater (eds.). Prospectors and Developers Association of Canada, p. 313-342.

Dawson, F.M., Evans, C.G., Marsh, R., and Richardson, R.
1994: Uppermost Cretaceous and Tertiary strata of the western Canada sedimentary basin. *In* Geological Atlas of the Western Canada Sedimentary Basin, G.D. Mossop and I. Shetsen (compilers). Canadian Society of Petroleum Geologists and Alberta Research Council, p. 387-406.

Dawson, J.B. and Stephens, W.E.
1975: Statistical classification of garnets from kimberlites and associated xenoliths. Journal of Geology, v. 83, p. 589-607.

1976: Statistical classification of garnets from kimberlites and associated xenoliths - addendum. Journal of Geology, v. 84, p. 495-496.

Day, S.J. and Fletcher, W.K.
1987: The morphology, mineralogy, and behaviour of "fine-grained" gold from placer deposits of Alberta: sampling and implications for mineral exploration: Discussion. Canadian Journal of Earth Sciences, v. 24, p. 1502.

Deer, W.A., Howie, R.A., and Zussman, J.
1982: Rock-forming minerals, 2nd edition. Longman, New York.

DiLabio, R.N.W.
1989: Terrain geochemistry in Canada. Chapter 10. *In* Quaternary geology of Canada and Greenland, R.J. Fulton (ed.). Geological Survey of Canada, Geology of Canada, no. 1, p. 645-663 (also Geological Society of America, The Geology of North America, v. K-1).

Dreimanis, A.
1962: Quantitative gasometric determination of calcite and dolomite using Chittick apparatus. Journal of Sedimentary Petrology, v. 32, p. 520-529.

Dufresne, M.B., Olson, R.A., Schmitt, D.R., McKinstry, B., Eccles, D.R., Fenton, M.M., Pawlowicz, J.G., Edwards, W.A.D., and Richardson, R.J.H.
1994: The diamond potential of Alberta: a regional synthesis of the structural and stratigraphic setting, and other preliminary indications of diamond potential. Alberta Research Council, Open File Report 1994-10, 369 p.

Eden, P. and Bjorklund, A.
1995: Geochemistry of till in Fennoscandia from ultra-low density sampling. Journal of Geochemical Exploration, v. 52, p. 285-302.

Edwards, W.A.D.
1990: Placer gold occurrences in Alberta. Alberta Geological Survey, Open File Report 1990-9.

Evans, D.J.A. and Campbell, I.A.
1995: Quaternary stratigraphy of the buried valleys of the lower Red Deer River, Alberta, Canada. Journal of Quaternary Science, v. 10, p. 123-148.

Fenton, M.M.
1984: Quaternary stratigraphy of the Canadian Prairie. *In* Quaternary stratigraphy of Canada - A Canadian Contribution to IGCP Project 24, R.J. Fulton (ed.). Geological Survey of Canada, Paper 84-10, p. 57-68.

Fenton, M.M., Schreiner, B.T., Nielsen, E., and Pawlowicz, J.G.
1994: Quaternary geology of the western plains. *In* Geological Atlas of the Western Canada Sedimentary Basin, G.D. Mossop and I. Shetsen (compilers). Canadian Society of Petroleum Geologists and Alberta Research Council, p. 413-420.

Fipke, C.E. (ed.)
1989: The development of advanced technology to distinguish between diamondiferous and barren diatremes. Geological Survey of Canada, Open File 2124, 559 p. and 2 microfiche appendices.

Fipke, C.E., Gurney, J.J., and Moore, R.O.
1995: Diamond exploration techniques emphasising indicator mineral geochemistry and Canadian examples. Geological Survey of Canada, Bulletin 423, 86 p.

Fulton, R.J., Fenton, M.M., and Rutter, N.W.
1984: Summary of Quaternary stratigraphy and history, western Canada. *In* Quaternary stratigraphy of Canada - A Canadian Contribution to IGCP Project 24, R.J. Fulton (ed.). Geological Survey of Canada, Paper 84-10, p. 69-83.

Garrett, R.G.
1983: Sampling Methodology. Chapter 5. *In* Statistics and Data Analysis in Geochemical Prospecting, R.J. Howarth (ed.). Handbook of Exploration Geochemistry, v. 2, Elsevier, Amsterdam, p. 83-110.

1994: The distribution of cadmium in A horizon soils of the prairies in Canada and the adjoining United States. Geological Survey of Canada, Paper 94-1A, p. 73-82.

Garrett, R.G. and Thorleifson, L.H.
1993: Prairie Kimberlite Study - Soil and till geochemistry and mineralogy, low density orientation survey traverses,

Winnipeg-Calgary-Edmonton-Winnipeg, 1991. Geological Survey of Canada, Open File 2685, one diskette.

1994: The distribution of mercury in A and C horizon soils in the Prairies of Canada and adjoining United States. Conference on Mercury as a Global Pollutant, Whistler, B.C., July 10-14, 1994, Abstracts for Poster Session III.

1995: Kimberlite indicator mineral and soil geochemical reconnaissance of the Canadian prairie region. Geological Survey of Canada, Diamond Workshop Volume.

Giusti, L.
1986: The morphology, mineralogy, and behaviour of "fine-grained" gold from placer deposits of Alberta: sampling and implications for mineral exploration. Canadian Journal of Earth Sciences, v. 23, p. 1662-1672.

1987: The morphology, mineralogy, and behaviour of "fine-grained" gold from placer deposits of Alberta: sampling and implications for mineral exploration: Reply. Canadian Journal of Earth Sciences, v. 24, p. 1503.

Gravenor, C.P. and Bayrock, L.A.
1955: Use of indicators in the determination of ice-movement directions in Alberta. Geological Society of America Bulletin, v. 66, p. 1325-1328.

1956: Use of indicators in the determination of ice-movement directions in Alberta, Canada: a reply. Geological Society of America Bulletin, v. 67, p. 1105-1110.

1961: Glacial deposits of Alberta. *In* Soils in Canada, geological pedological, and engineering studies. Royal Society of Canada, Special Publication 3, p. 33-50.

Gravenor, C.P. and Kupsch, W.O.
1959: Ice-disintegration features in western Canada. Journal of Geology, v. 67, p. 48-64.

Gregory, G.P. and White, D.R.
1989: Collection and treatment of diamond exploration samples. *In* Kimberlites and related rocks 2: Their crust/mantle setting, diamonds and diamond exploration. Geological Society of Australia, Special Publication 14, p. 1123-1134.

Griffin, W.L., Cousens, D.R., Ryan, C.G., Sie, S.H., and Suter, G.F.
1989: Ni in chrome pyrope garnets: a new geothermometer. Contributions to Mineralogy and Petrology, v. 103, p. 199-202.

Griffin, W.L. and Ryan, C.G.
1993: Trace elements in garnets and chromites: evaluation of diamond exploration targets. *In* Diamonds: exploration, sampling, and evaluation, P. Sheahan and A. Chater (eds.). Prospectors and Developers Association of Canada, p. 185-212.

1995: Trace elements in indicator minerals: area selection and target evaluation in diamond exploration. Journal of Geochemical Exploration, v. 53, p. 311-337.

Griffin, W.L., Ryan, C.G., Gurney, J.J., Sobolev, N.V., and Win, T.T.
1994a: Chromite macrocrysts in kimberlites and lamproites: geochemistry and origin. *In* Proceedings of the Fifth International Kimberlite Conference, Volume 1, Kimberlites, related rocks and mantle xenoliths, H.O.A. Meyer and O.H. Leonardos (eds.). CPRM Special Publication 1/A, Brasilia, p. 366-377.

Griffin, W.L., Ryan, C.G., O'Reilly, S.Y., Nixon, P.H., and Win, T.T.
1994b: Trace elements in garnets from Tanzanian kimberlites: relation to diamond content and tectonic setting. *In* Proceedings of the Fifth International Kimberlite Conference, Volume 2, Diamonds: Characterization, Genesis, and Exploration, H.O.A. Meyer and O.H. Leonardos (eds.). CPRM Special Publication 1/B, Brasilia, p. 346-356.

Gurney, J.J.
1984: A correlation between garnets and diamonds in kimberlites. *In* Kimberlite Occurrence and Origin: a basis for conceptual models in exploration, J.E. Glover and P.G. Harris (eds.). University of Western Australia Publication 8, p. 143-166.

Gurney, J.J. and Moore, R.O.
1993: Geochemical correlations between kimberlitic indicator minerals and diamonds. *In* Diamonds: exploration, sampling, and evaluation, P. Sheahan and A. Chater (eds.). Prospectors and Developers Association of Canada, p. 147-172.

Gurney, J.J. and Zweistra, P.
1995: The interpretation of the major element compositions of mantle minerals in diamond exploration. Journal of Geochemical Exploration, v. 53, p. 293-309.

Gwyn, Q.H.J. and Dreimanis, A.
1979: Heavy mineral assemblages in tills and their use in distinguishing glacial lobes in the Great Lakes region. Canadian Journal of Earth Sciences, v. 16, p. 2219-2235.

Halferdahl, L.B.
1965: The occurrence of gold in Alberta rivers. Alberta Research Council, Economic Mineral Files, Open File Report 65-11.

Harris, D.C. and Ballantyne, S.B.
1994: Characterization of gold and PGE-bearing placer concentrates from the North Saskatchewan River, Edmonton, Alberta. *In* Current Research 1994-E, Geological Survey of Canada, p. 133-139.

Hirvas, H. and Nenonen, K.
1990: Field methods for glacial indicator tracing. *In* Glacial Indicator Tracing, R. Kujansuu and M. Saarnisto (eds.). A.A. Balkema, Rotterdam, p. 217-248.

Jackson, L.E., Jr.
1980: Glacial history and stratigraphy of the Alberta portion of the Kananaskis Lake map area. Canadian Journal of Earth Sciences, v. 17, p. 459-477.

Kjarsgaard, B.A.
1992: Is Ni in Cr-pyrope a valid exploration tool?. *In* Current Research, Part E. Geological Survey of Canada, Paper 92-1E, p. 315-322.

1995: Research on kimberlites and applications of diamond exploration techniques in Saskatchewan. *In* Investigations completed by the Saskatchewan Geological Survey and the Geological Survey of Canada under the Geoscience Program of the Canada-Saskatchewan Partnership Agreement on Mineral Development (1990-1995), D.G. Richardson (ed.). Geological Survey of Canada, Open File 3119, p. 213-226.

Karrow, P.F.
1976: The texture, mineralogy, and petrography of North American tills. *In* Glacial Till, R.F. Legget (ed.). Royal Society of Canada, Special Publication 12, p. 83-98.

Klassen, R.W.
1992: Nature, origin, and age relationships of landscape complexes in southwestern Saskatchewan. Géographie physique et Quaternaire, v. 46, p. 361-388.

1994: Late Wisconsinan and Holocene history of southwestern Saskatchewan. Canadian Journal of Earth Sciences, v. 31, p. 1822-1837.

Leckie, D.A. and Cheel, R.J.
1989: The Cypress Hills Formation (Upper Eocene to Miocene): a semi-arid braidplain deposit resulting from intrusive uplift. Canadian Journal of Earth Sciences, v. 26, p. 1918-1931.

Leckie, D.A. and Craw, D. (*this volume*)
1997: Anomalous gold occurrences in Cretaceous and Tertiary conglomerates and gravels of Alberta. *In* Exploring for Minerals in Alberta: Geological Survey of Canada Geoscience Contributions, Canada-Alberta Agreement on Mineral Development (1992-1995), R.W. Macqueen (ed.). Geological Survey of Canada, Bulletin 500, p. 331-344.

Lehnert-Thiel, K., Loewer, R., Orr, R.G., and Robertshaw, P.
1992: Diamond-bearing kimberlites in Saskatchewan, Canada: The Fort à la Corne case history. Exploration and Mining Geology, v. 1, p. 391-403.

Little, E.C.
1995: A single-maximum-advance model of continental glaciation restricted to the Late Wisconsin, southwestern Alberta. M.Sc. thesis, University of Western Ontario, 229 p.

Mathews, W.H.
1974: Surface profiles of the Laurentide ice sheet in its marginal areas. Journal of Glaciology, v. 13, p. 37-43.

McDonald, B.C. and Kelly, R.G.
1968: Procedures used in sedimentology laboratory. Geological Survey of Canada, Limited Circulation Report, 18 p.

Metz, D.G.
1968: Examination of the durability of Saskatchewan aggregates. M.Sc. thesis, University of Saskatchewan.

Morgan, A.V.
1969: Lithology of the Erratics Train in the Calgary area. *In* Geomorphology: Selected Readings, J.G. Nelson and M.J. Chambers (eds.). Methuen, Toronto, p. 165-182.

Mossop, G.D. and Shetsen, I. (compilers)
1994: Geological Atlas of the Western Canada Sedimentary Basin. Canadian Society of Petroleum Geologists and Alberta Research Council, Calgary, 510 p.

Mountjoy, E.W.
1958: Jasper area Alberta, a source of the Foothills Erratics Train. Alberta Society of Petroleum Geology Journal, v. 6, p. 218-226.

Nurkowski, J.R.
1984: Coal quality, coal rank variation and its relation to reconstructed overburden, Upper Cretaceous and Tertiary plains coals, Alberta, Canada. American Association of Petroleum Geologists Bulletin, v. 68, p. 285-295.

Paré, D.
1982: Application of heavy mineral analysis to problems of till provenance along a transect from Longlac, Ontario to Somerset Island. M.A. thesis, Carleton University, 76 p.

Parfenoff, A., Pomerol, C., and Tourenq, J.
1970: Les mineraux en grains, methodes d'etudes et determination. Masson et Cie., Paris, 578 p.

Pawluk, S. and Bayrock, L.A.
1969: Some characteristics and physical properties of Alberta tills. Research Council of Alberta, Bulletin 26, 72 p.

Peuraniemi, V.
1990: Heavy minerals in glacial material. *In* Glacial Indicator Tracing, R. Kujansuu and M. Saarnisto (eds.). A.A. Balkema, Rotterdam, p. 165-185.

Rahmani, R.A. and Lerbekmo, J.F.
1975: Heavy mineral analysis of Upper Cretaceous and Paleocene sandstones in Alberta and adjacent areas of Saskatchewan. *In* Cretaceous System in the Western Interior of North America, W.G.E. Caldwell (ed.). Geological Association of Canada, Special Paper 13, p. 607-632.

Roed, M.A., Mountjoy, E.W., and Rutter, N.W.
1967: The Athabasca Valley Erratics Train, Alberta and Pleistocene ice movements across the continental divide. Canadian Journal of Earth Sciences, v. 4, p. 625-632.

Romaniuk, O.
1981: Gold of the Saskatchewan sands and gravels. B.Sc. thesis, University of Alberta, Edmonton.

Rutter, N.W.
1972: Geomorphology and multiple glaciation in the area of Banff, Alberta. Geological Survey of Canada, Bulletin 206, 54 p.

1984: Pleistocene history of the western Canadian ice-free corridor. *In* Quaternary stratigraphy of Canada – A Canadian Contribution to IGCP Project 24, R.J. Fulton (ed.). Geological Survey of Canada, Paper 84-10, p. 49-56.

Saarnisto, M.
1990: An outline of glacial indicator tracing. *In* Glacial Indicator Tracing, R. Kujansuu and M. Saarnisto (eds.). A.A. Balkema, Rotterdam, p. 1-13.

Schreiner, B.T.
1990: Lithostratigraphic correlation of Saskatchewan tills: a mirror image of Cretaceous bedrock. Saskatchewan Research Council Publication R-1210-3-E-90, 114 p.

Scott-Smith, B.H.
1995: Geology of the Sturgeon Lake 02 kimberlite block, Saskatchewan. Exploration and Mining Geology, v. 4, p. 141-151.

Severson, R.C. and Tidball, R.R.
1979: Spatial variation in total element concentration in soil within the Northern Great Plains coal region. U.S. Geological Survey, Professional Paper 1134-A, p. A1-A18.

Severson, R.C. and Wilson, S.A.
1990: Assessment of geochemical variability and a listing of geochemical data for surface soils of Eastern North Dakota and parts of Northeastern South Dakota and Northwestern Minnesota. U.S. Geological Survey, Open File Report 90-310, 58 p.

Shaw, J.
1982: Melt-out till in the Edmonton area. Canadian Journal of Earth Sciences, v. 19, p. 1548-1569.

Shaw, J. and Kellerhals, R.
1982: The composition of recent alluvial gravels in Alberta river beds. Alberta Research Council, Bulletin 41, 151 p.

Shetsen, I.
1981: Sand and gravel resources of the Lethbridge area. Alberta Research Council, Earth Sciences Report 81-4, 41 p.

1984: Application of till pebble lithology to the differentiation of glacial lobes in southern Alberta. Canadian Journal of Earth Sciences, v. 21, p. 920-933.

1987a: Quaternary geology, southern Alberta. Alberta Research Council Map, scale 1:500 000.

1987b: Quaternary geology, central Alberta. Alberta Research Council Map, scale 1:500 000.

Shilts, W.W.
1982: Glacial dispersal - principles and practical applications. Geoscience Canada, v. 9, p. 42-47.

1984: Till geochemistry in Finland and Canada. Journal of Geochemical Exploration, v. 21, p. 95-117.

Shilts, W.W. and Kettles, I.M.
1990: Geochemical-mineralogical profiles through fresh and unweathered till. *In* Glacial Indicator Tracing, R. Kujansuu and M. Saarnisto (eds.). A.A. Balkema, Rotterdam, p. 187-216.

Stalker, A.MacS.
1956: The Erratics Train, foothills of Alberta. Geological Survey of Canada, Bulletin 37, 28 p.

1976: Quaternary stratigraphy of the southwestern Canadian prairie. *In* Quaternary stratigraphy of North America, W.C. Mahaney (ed.). Dowden, Hutchinson, and Ross, Stroudsburg, Pa., p. 381-407.

Stalker, A.MacS. and Craig, B.G.
1956: Use of indicators in the determination of ice-movement directions in Alberta: a discussion. Geological Society of America Bulletin, v. 67, p. 1101-1104.

Stalker, A.MacS. and Harrison, J.E.
1977: Quaternary glaciation of the Waterton-Castle River region of Alberta. Bulletin of Canadian Petroleum Geology, v. 25, p. 882-906.

Stalker, A.MacS. and Vincent, J-S.
1993: Quaternary. Subchapter 4K. *In* Sedimentary cover of the craton in Canada, D.F. Stott and J.D. Aitken (eds.). Geological Survey of Canada, Geology of Canada, no. 5, p. 466-482 (also Geological Society of America, The Geology of North America, v. D-1).

Stott, D.F., Dixon, J., Dietrich, J.R., McNeil, D.H., Russell, L.S., and Sweet, A.R.
1993: Tertiary. Subchapter 4J. *In* Sedimentary cover of the craton in Canada, D.F. Stott and J.D. Aitken (eds.). Geological Survey of Canada, Geology of Canada, no. 5, p. 439-465 (also Geological Society of America, The Geology of North America, v. D-1).

Tharin, J.C.
1969: The foothills erratics train of Alberta, Canada. Michigan Academician, v. 2, p. 113-124.

Thorleifson, L.H. and Garrett, R.G.
1993: Prairie kimberlite study - till matrix geochemistry and preliminary indicator mineral data. Geological Survey of Canada, Open File 2745, one diskette.

Thorleifson, L.H., Garrett, R.G., and Matile, G.
1994: Prairie kimberlite study indicator mineral geochemistry. Geological Survey of Canada, Open File 2875, one diskette.

Thorleifson, L.H. and Kristjansson, F.J.
1993: Quaternary Geology and Drift Prospecting, Beardmore-Geraldton area, Ontario. Geological Survey of Canada, Memoir 435, 146 p.

Vonhof, J.A.
1965: The Cypress Hills Formation and its reworked deposits in southwestern Saskatchewan. *In* 15th Annual Field Conference Guidebook. Alberta Society of Petroleum Geologists, p. 142-161.

1969: Tertiary gravels and sands in the Great Plains. Ph.D. thesis, University of Saskatchewan, Saskatoon, 279 p.

Whitaker, S.T.
1980: The Flaxville Formation in the Scobey-Opheim area, northeastern Montana. M.Sc. thesis, University of Colorado, Boulder, 164 p.

Whitaker, S.H. and Christiansen, E.A.
1972: The Empress Group in Saskatchewan. Canadian Journal of Earth Sciences, v. 9, p. 353-360.

Young, R.R., Burns, J.A., Smith, D.G., Arnold, L.D., and Rains, R.B.
1994: A single, late Wisconsin, Laurentide glaciation, Edmonton area and southwestern Alberta. Geology, v. 22, p. 683-686.

WAS EOCENE MAGMATISM WIDESPREAD IN THE SUBSURFACE OF SOUTHERN ALBERTA? EVIDENCE FROM NEW AEROMAGNETIC ANOMALY DATA[1]

G.M. Ross, J. Mariano[2], R. Dumont[2], B.A. Kjarsgaard[2], and D. Teskey[2]
Geological Survey of Canada, Calgary

Abstract

New, high-resolution aeromagnetic anomaly data acquired over the Phanerozoic Western Canada Sedimentary Basin and the underlying Archean Medicine Hat Block of southern Alberta reveal the presence of striking short wavelength anomalies that are clearly distinct from longer wavelength anomalies from sources within the basement. The most dramatic anomalies comprise a series of northwest-striking, linear features, up to 30 km long, between the towns of Milk River and Lethbridge. A second, less prominent, set of north-northeast–trending anomalies occurs south of the city of Medicine Hat. A ground magnetometer survey conducted over one of the anomalies south of Lethbridge indicated that the anomalies are real and cannot be attributed to cultural sources, or are artifacts of the acquisition program. Modeling of the anomalies suggests that their source lies within the sedimentary column at depths of about 250 m or less. The linear nature of the anomalies and their subparallel disposition in a swarm is similar to the aeromagnetic expression of mafic dyke swarms in the Canadian Shield. We believe that the southern Alberta anomalies represent dyke-like igneous bodies and further hypothesize that they are correlative with mafic potassic dykes of Eocene age exposed in the Sweet Grass Hills of southern Alberta and northern Montana. If correct, this hypothesis implies that dyke emplacement and associated extension occurred over a broad region of southern Alberta and may represent an eastward continuation of the association of Eocene alkaline magmatism and extension observed in the southern Canadian Cordillera. This may have important implications for understanding the formation of, and exploration for, hydrocarbon traps in the sedimentary section formed by post-Cretaceous fault movement and development of fracture porosity.

Résumé

Un nouveau levé aéromagnétique à haute résolution effectué dans la région du bloc de Medicine Hat (partie sud de l'Alberta) révèle la présence d'anomalies haute fréquence qui se distinguent nettement de celles à forte longueur d'onde localisées dans le substratum rocheux. Parmi les plus spectaculaires, on compte une série d'anomalies linéaires mesurant jusqu'à 30 km parallèlement à leur orientation nord-ouest, entre les villes de Milk River et de Lethbridge. Un deuxième ensemble d'anomalies subradiales d'orientation nord et nord-est a été identifié au sud de Medicine Hat (Alberta). Les anomalies observées près de Lethbridge ont été contrevérifiées sur le terrain au moyen d'un magnétomètre, et il ressort que les anomalies sont réelles et ne peuvent pas être attribuées à des sources artificielles produites lors du programme d'acquisition ou d'origine anthropique. La modélisation des anomalies incite à situer leur source dans l'empilement sédimentaire, à des profondeurs d'environ 250 m ou moins. La nature linéaire des anomalies et leur disposition subparallèle en un «essaim» s'apparente aux essaims de dykes du Bouclier canadien, notamment ceux de Mackenzie. Selon les auteurs, les anomalies linéaires observées dans le sud de l'Alberta pourraient représenter des massifs en forme de dykes, analogues aux dykes potassiques mafiques et aux roches ignées éocènes affleurant dans les collines Sweetgrass du sud de l'Alberta et du nord du Montana. Si cette hypothèse est confirmée, cela signifie qu'une vaste région du sud de l'Alberta a été marquée par l'intrusion de dykes et par des phénomènes d'extension associés, tout comme la partie sud de la Cordillère canadienne qui a connu un épisode éocène de magmatisme alcalin et d'extension. Cela pourrait influer de façon importante sur la compréhension des pièges d'hyrocarbures de l'empilement sédimentaire, pièges créés par le mouvement des failles après le Crétacé; l'exploration visant à identifier ces structures en serait aussi modifiée.

---

[1]Canada-Alberta Agreement on Mineral Development
[2]Geological Survey of Canada, 1 Observatory Crescent, Ottawa, Ontario K1A 0E8

INTRODUCTION

Over the last 10 years, public domain aeromagnetic anomaly data for Alberta have been acquired through surveys flown by the Geological Survey of Canada, data donations from industry, and recently, through a GSC-Industry consortium. Much of the data for southern Alberta held by the National Geophysical Data Centre in Ottawa was acquired through a donation by PanCanadian Petroleum Limited. The data were derived from surveys flown in the 1960s and originally compiled into contoured magnetic intensity maps. The GSC digitized the contour maps and integrated these data into the national database. With the recent increase in exploration activity in southern Alberta, principally by the diamond/mining industry, this region was targeted for a modern high-resolution survey under the Canada-Alberta Agreement on Mineral Development. The rationale for choosing this region, even though regional coverage already existed, was the knowledge that the basement of the region, the Medicine Hat Block, was composed of Archean crust and, therefore, perhaps an old mantle keel was preserved beneath the crust, thereby making the region prospective for diamond-bearing igneous rocks.

In the fall of 1992, the GSC contracted a high-resolution survey to be undertaken by Sander Geophysics Ltd. A total of 33 940 line-km of data were collected over the region of southern Alberta referred to as the Cypress Hills survey area (Fig. 1). Flight lines consisted of east-west lines spaced at 800 m and north-south control lines spaced at 5 km with a mean terrain clearance of 150 m. These acquisition parameters are typical of those used by the GSC for regional surveys flown over the exposed shield but represent a new level of detail for a government survey flown over a sedimentary basin. The new data confirm

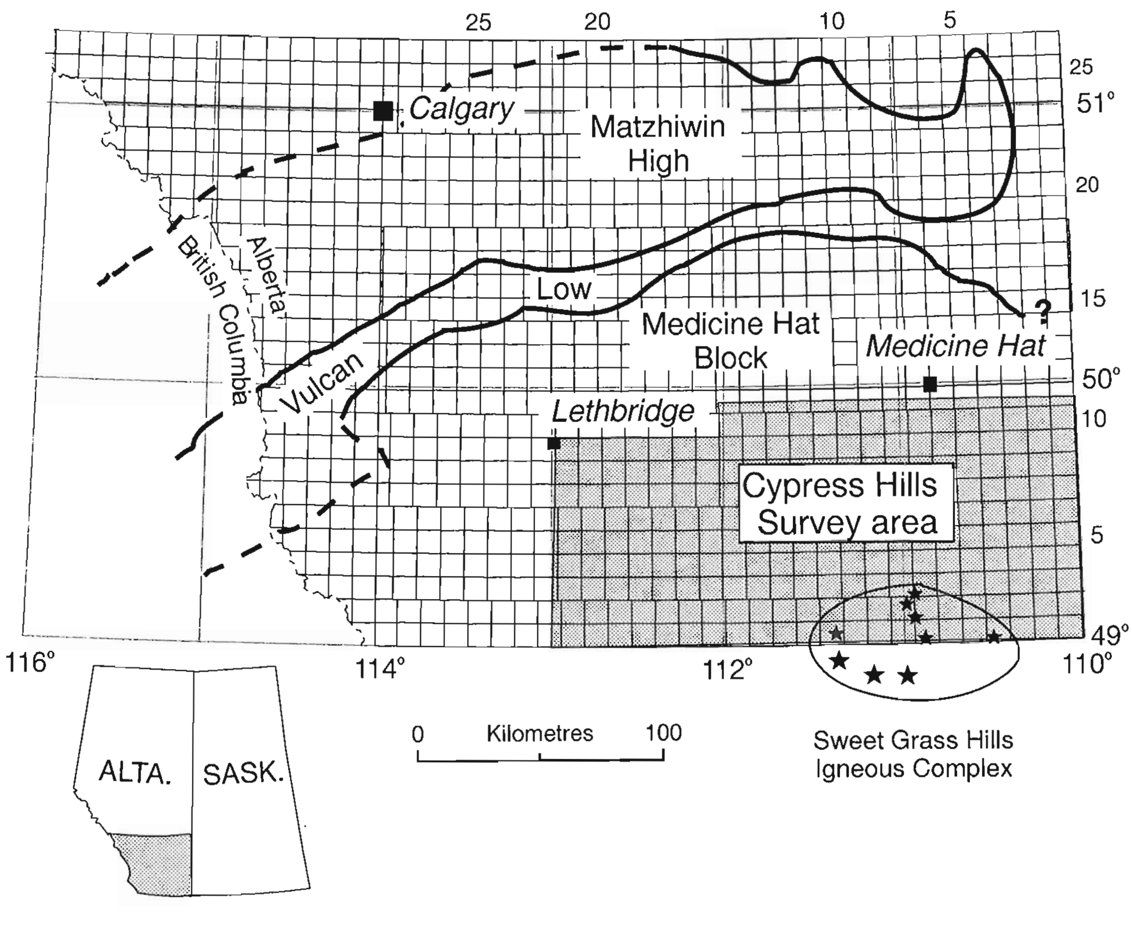

Figure 1. A location map with a township and range grid showing the location of the Cypress Hills survey area in southern Alberta (shaded). Major basement domains defined on the basis of aeromagnetic signature are shown (from Ross et al., 1991). The Sweet Grass Hills Igneous Complex is shown: small stars indicate occurrences of small plugs, dykes and vents in southern Alberta; large stars indicate the larger igneous centres in northern Montana (from Kjarsgaard, 1994).

the long wavelength, basement-sourced aeromagnetic anomalies observed in the PanCanadian data and also contain unusual high-wavenumber anomalies within the sedimentary section. The purpose of this paper is to describe these anomalies, document their shallow source within the sedimentary section, and speculate on the possible origin and significance of the anomalies. This further amplifies preliminary interpretations published by Ross et al. (1994a).

Magnetic data

Figure 2 is a map of the total intensity aeromagnetic field after removal of the International Geomagnetic Reference Field. The map is dominated by a broad wavelength aeromagnetic fabric consisting of northwest-trending linear anomalies, previously interpreted to be caused by sources in the the crystalline basement rocks that underlie the sedimentary section, at a depth ranging from 1.7 to 2.2 km (Ross et al., 1991). Examination of the drill core of basement rocks and dating using U-Pb zircon geochronology indicates that the basement in this region is Archean in age (2.6–3.2 Ga) and composed largely of granitic gneisses referred to as the Medicine Hat Block (Villeneuve et al., 1993; Davis et al., 1995). In general, aeromagnetic signals in Alberta are derived largely from susceptibility contrasts in the crystalline basement as there is little contribution from the weakly magnetized sedimentary section (Ross et al., 1994b). However, between the towns of Lethbridge and Milk River, several relatively narrow, high-wavenumber anomalies are apparent as northwest-trending lineaments (Fig. 2) in addition to north-trending anomalies southwest of Medicine Hat.

In order to enhance the high-wavenumber content of the observed data, the first vertical derivative of the total intensity data was calculated (Fig. 3). The resultant map was then illuminated from the northeast in order to enhance the northwest-trending fabric of the high-wavenumber anomalies. It should be noted that the derivative process tends to amplify the noise within the data set so that caution should be exercised in the interpretation of some of the anomalies. Two distinct suites of anomalies are present. In the western part of the survey area, between Lethbridge and Milk

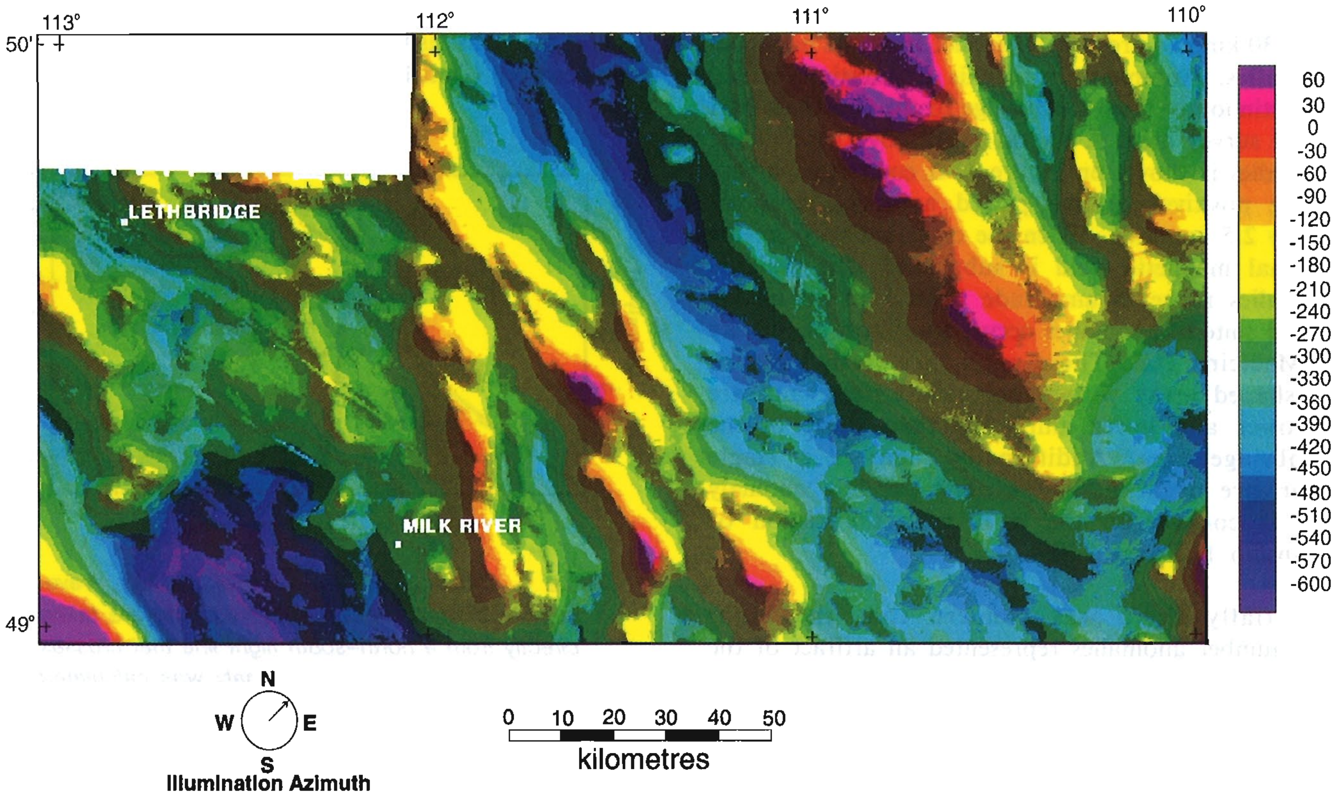

Figure 2. An aeromagnetic anomaly map for the Cypress Hills survey area. The International Geomagnetic Reference Field was removed for an altitude of 1.1 km. The resultant anomaly map was colour-shaded with a contour interval of 30 nT and illuminated from the northeast. Note the northwest-trending series of linear anomalies between the towns of Lethbridge and Milk River.

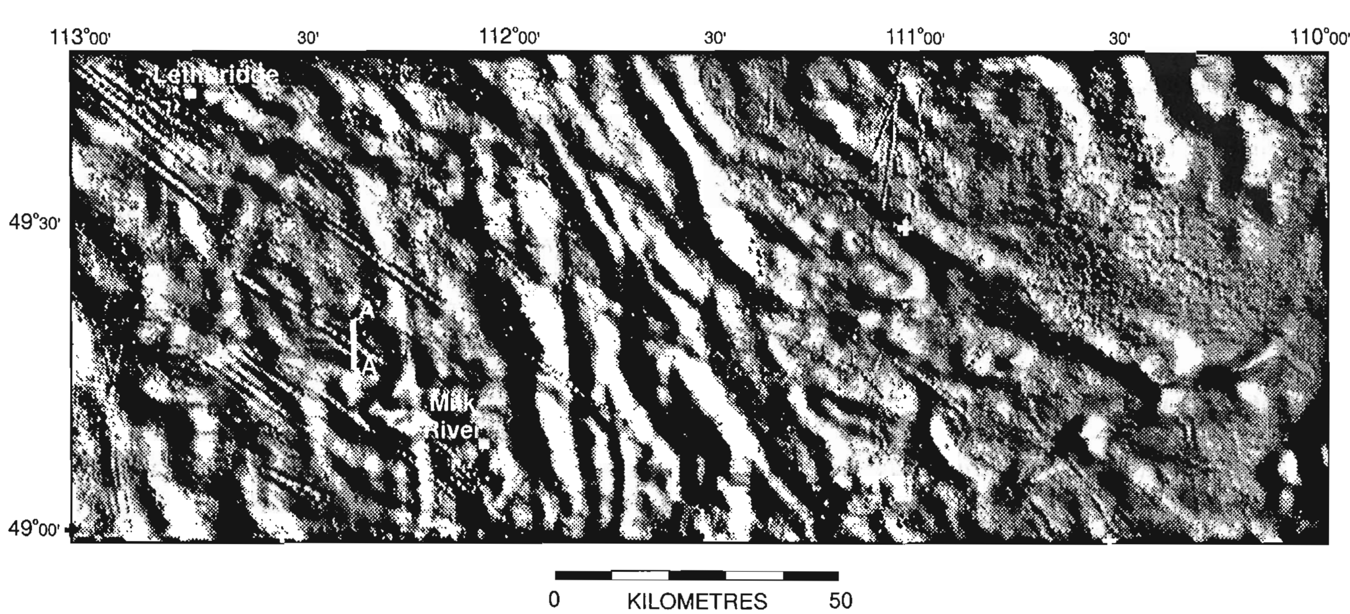

__Figure 3.__ Shaded first vertical derivative of the aeromagnetic anomaly data with illumination from the northeast. The derivative process used to compute this map amplifies noise in the data as exemplified by the small anomalies that give rise to a "rough" texture in the vicinity of Lethbridge and Milk River. Line A shows the location of the analog record and ground magnetometer survey shown in Figures 4 and 5, respectively.

River, several northwest-trending (120°-300°), high-wavenumber anomalies are continuous for distances of up to 30 km and are clearly distinct from the basement anomalies. Anomalies with this orientation extend discontinuously from Lethbridge to the southeast part of the survey area. A typical profile over one of the anomalies is shown on Figure 4. It consists of a very strong positive-negative paired anomaly, approximately 2.5 km wide. When the contribution from the regional magnetic field is subtracted, the residual anomalies range in amplitude from 5 to 40 nT. A second suite of anomalies occurs southwest of the city of Medicine Hat. These anomalies form a small, fan-shaped array with a northward trend and are narrower and lower amplitude than those in the Lethbridge area. Additionally there is a single occurrence of a curvilinear north-trending anomaly that is concave to the east, near the region of Township 1, Range 24W4.

Initially there was concern that the high-wavenumber anomalies represented an artifact of the survey data acquisition or processing. However, they are continuous between flight lines and surveys conducted on different days and thus are unlikely to represent an artifact of the acquisition. Furthermore, an independent survey has confirmed the anomalies south of Lethbridge (John Peirce, pers. comm., November 1995). They were then suspected to represent a cultural feature such as a pipeline. Consultation of pipeline maps showed that this was not the case. In addition, the region containing the anomalies southwest of Medicine Hat in Seven Persons Coulee area was visited and no obvious cultural source was observed (Don Lawton, pers. comm., June 1995).

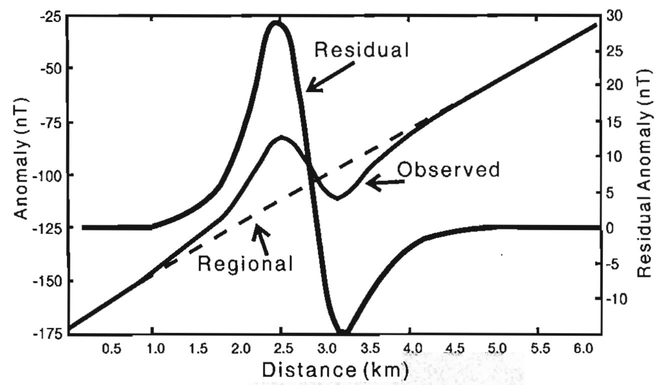

__Figure 4.__ Typical profile over one of the high wavenumber anomalies. The observed data are taken directly from a north–south flight line that crosses the anomaly. A regional anomaly was calculated by fitting a low-order polynomial to the data and was removed from the observed data to derive the residual anomaly. The asymmetry and wavelength of the residual anomaly is typical of the 20 profiles examined, although the amplitudes vary from 5 to 40 nT. Note that the scale on the right is for the residual anomaly and the scale on the left is for the regional and observed anomalies.

A ground survey was conducted over an anomaly south of Lethbridge with the hopes of replicating the observed airborne anomaly. The results are shown (Fig. 5) for a ground magnetometer survey conducted in a farmer's field that is underlain by one of the most prominent high-wavenumber anomalies. The survey was conducted using a proton precession magnetometer at an altitude of approximately 2.5 m. The results of the ground survey shown in Figure 5 have been continued upward to the elevation of the aeromagnetic flight line and show excellent agreement with respect to the asymmetry, wavelength and intensity of the airborne anomaly. This suggests that this particular anomaly, and by extrapolation many of the high-wavenumber anomalies, is real and is not an artifact of acquisition, nor is it caused by cultural effects such as a buried pipeline.

To further clarify the source of these anomalies, the observed residual anomaly was compared with model responses calculated using a cultural source and a "concentrated" (highly magnetized) basement source (Fig. 6). A point source with a 1 m radius was placed at a depth of 3 m to approximate a cultural source, such as a buried pipeline. The modeled magnetic response of this source produced a narrow, high-amplitude anomaly that has a distinctly shorter wavelength than the observed anomaly. Similarly, the basement source, which was placed at a depth of 2 km to approximate the depth to basement in this region, produced a substantially longer wavelength anomaly than that observed. Both of the modeled responses suggest that the source of the observed anomalies must be within the sedimentary section.

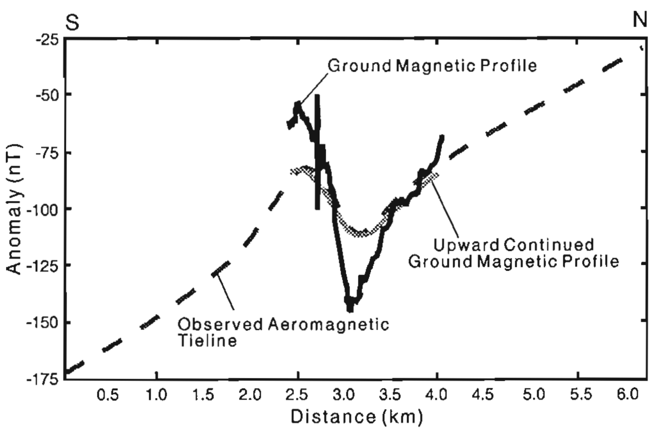

Figure 5. *Results of a ground magnetometer survey over one of the anomalies. The magnetometer survey was conducted at an altitude of 2.5 m and was continued upward to an altitude of 150 m to approximate the altitude of the aeromagnetic survey.*

Interpretation

Two potential interpretations of the anomalies are considered. The first is that they may represent igneous dykes related to the igneous rocks found within the Sweet Grass Hills of northern Montana and southernmost Alberta (Kjarsgaard, 1994, 1997). The second interpretation is that the linear anomalies could represent magnetization along fault zones induced as a consequence of alteration during structurally controlled hydrocarbon emplacement and seepage. We will consider this option first.

The migration of hydrocarbons can result in the generation of a reducing chemical environment and the concomitant alteration of minerals in contact with the fluids or precipitation of new minerals. This has been suggested to result in the precipitation of ferrimagnetic minerals such as magnetite and pyrrhotite. It is also possible that in situ minerals, such as hematite and/or pyrite, can undergo alteration and reduction to more ferrimagnetic species (Donovan et al., 1979; Elmore and Crawford, 1990; Machel and Burton, 1991). If seepage is controlled by structural features such as fault zones, then it is conceivable that seepage-related alteration could result in the formation of magnetic anomalies colinear with the fault zone. This geochemical-geophysical paradigm has formed the

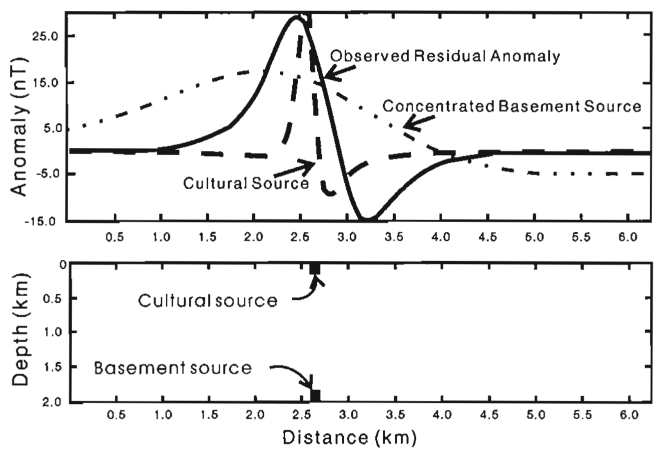

Figure 6. *Computed magnetic responses for different magnetic sources (shallow cultural source and concentrated basement source) in comparison with the observed anomaly profile. Note that a basement source produces a much longer wavelength anomaly than observed whereas the cultural source results in a much narrower response than observed. When compared to the models, the wavelength characteristics of the observed anomalies suggest a shallow source, likely in the upper part of the sedimentary section.*

basis for the contention that high-resolution aeromagnetic surveys can be used to explore for oilfields (Donovan et al., 1979). The classic locality is the Cement Field in western Oklahoma, an extreme case where hydrocarbon seepage has developed along the crest of a faulted anticline in late Paleozoic rocks and appears to be associated with a narrow (0.5 km), locally high-amplitude (60 nT), positive magnetic anomaly.

Subsequent petrologic and petrophysical work (Reynolds et al., 1990, 1991) concluded that the observed anomalies at the Cement Field were likely the result of contributions from cultural sources including buried well casings and spherules of drilling steel within the drill holes. Modeling by Reynolds et al. (1991) of the most ferrimagnetic intervals affected by seepage-related diagenesis, at Cement Field, resulted in a very weak positive anomaly of 7 nT (Fig. 7). Similarly, examples of magnetized fault planes in northeastern British Columbia (Ebner et al., 1995) and northern Alberta (John Peirce, pers. comm., November 1995) rarely exceed 1 nT in amplitude. We discount a hydrocarbon seepage origin for the Cypress Hills anomalies based on their nonassociation with hydrocarbon production trends discussed below and their locally very high amplitudes (up to 40 nT; Fig. 4), which are far greater than could be produced even under the most favourable circumstances of seepage alteration (Fig. 7)

The interpretation that the linear anomalies represent shallow dyke-like igneous bodies is attractive because of the presence of igneous rocks in southern

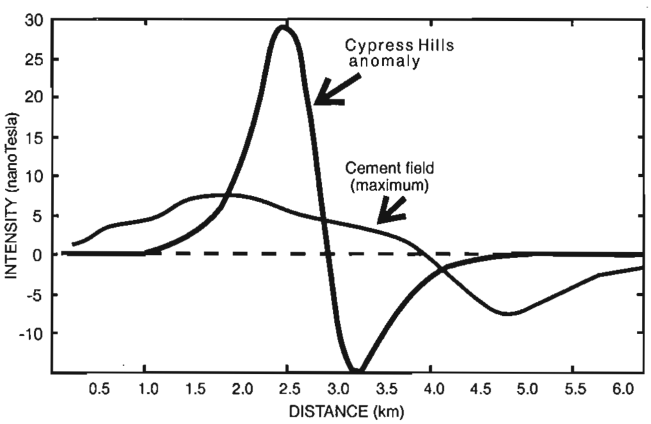

Figure 7. *Comparison of the observed magnetic anomaly with that produced by the magnetic response of a mineralized zone composed predominantly of pyrrhotite formed by hydrocarbon seepage alteration. The seepage-related response is taken from Reynolds et al. (1990) and was calculated assuming a susceptibility of 55.7 x 10^{-3}A/m.*

Alberta. The Sweet Grass Intrusives consist of shallow plutonic rocks that range in composition from calcalkaline diorite porphyry to mafic ultrapotassic rocks that are the northernmost surface occurrences of the Tertiary Montana Alkalic Province (Kjarsgaard, 1994). Seven areas in southern Alberta, south of Milk River, contain outcrops of igneous intrusive material that comprise dykes, sills and small extrusive vent complexes of mafic alkalic rocks known as minettes (Kjarsgaard, 1994). These rocks commonly consist of phenocrysts of olivine + phlogopite + diopside in a groundmass of mica (phlogopite–biotite solid solution) + salite + sanidine + magnetite + apatite with lesser amounts of calcite and apatite. Field and laboratory measurements of the magnetic susceptibilities of fresh minettes (Table 1) indicate that the mafic minettes have susceptibility of sufficient magnitude to produce the observed anomalies, in accord with the presence of modal magnetite. Comparison of magnetic anomaly data with known occurrences of minettes show that some are associated with a positive magnetic signature. We examined the magnetization in sedimentary strata adjacent to minette dykes and sills and found that there was virtually no change in the susceptibility as a consequence of thermal metamorphism associated with minette intrusion.

To further test the dyke interpretation of the magnetic anomalies, preliminary 2.5-D models were constructed (Fig. 8). While the dyke geometry produces a reasonable fit in comparison with the observed profile, a dyke that terminates in a shallow sill or a vent complex produced a more accurate fit to the observed anomalies. It is considered unlikely, however, that either of the latter geometries would have horizontal continuity comparable to the observed anomalies (i.e., up 30 km strike length). Our preliminary modelling thus appears to support a shallow dyke-like source for these anomalies. If this interpretation is correct, it implies that dykes like those observed in the Sweet Grass Hills are more widespread than previously recognized and may cover an area of over 10 000 km^2 (Fig. 9). A comparison between the Cypress Hills anomalies and the aeromagnetic signature of mafic dykes exposed in the Canadian Shield shows a close match in both spatial patterns and profile asymmetry (Schwarz et al., 1987; West and Ernst, 1991). We therefore conclude that the most likely interpretation of the linear magnetic anomalies is that they are dykes.

There is some regional evidence to support this conclusion. First, the linear pattern of the dykes presumably records an increment of extensional strain produced during crustal dilation and magma emplacement. Regional extension is known to have affected a broad region of the southern Canadian

Table 1

Magnetic susceptibilty of selected igneous rocks, Sweet Grass Hills, southern Alberta. All data are reported in x10^{-2} amps/metre (SI units)

A. Laboratory susceptibilities measured with a hand-held Scintrex susceptibility meter on sawn rock faces. Locality numbers and sample numbers are reported in Kjarsgaard (1994).

Locality	Sample no.	Lithology	Susceptibility
1	205	diorite porphyry	0.87
2	222B	olivine minette	2.26
3	200A	olivine minette	2.77
4	224E	olivine minette	3.77
5	221A	olivine minette	1.89
6	217B	minette	1.51
7	225	felsic minette	0.31

B. Field measurements of magnetic susceptibilities measured in a section through a minette sill that intrudes Cretaceous sedimentary rocks exposed at Middle Butte, Montana (48°51'N, 111°20'W). Measurements were made with a hand-held Scintrex susceptibility meter held on smooth rock faces. Average susceptibility for the minette is 1.8. Height is in metres above base.

Height	Lithology	Susceptibility
0.0	sandstone	0.0
0.5	sandstone	0.1
1.0	sandstone	0.1
1.5	shale	0.0
2.0	sandstone	0.0
2.5	minette	1.2
3.0	minette	1.8
3.5	minette	2.4
4.0	minette	2.0
4.5	minette	1.9
5.0	minette	1.9
5.5	minette	1.8
6.0	minette	1.9
6.5	minette	1.6
7.0	minette	1.5
7.5	minette	1.9
8.0	minette	1.8

C. Field measurements made within a dyke composed of light brown minette along the south side of Middle Butte. The dyke trends 005°N and has a steep dip of 65° or more to the east. The measurements were taken over a random area of about 10 m^2 and result in an average susceptibility of 2.47.

1: 2.4	2: 2.4	3: 2.5	4: 2.9
5: 2.8	6: 1.8	7: 2.8	8: 2.2
9: 2.5	10: 2.4		

D. Field measurements were made within a well-exposed sill of fresh gray minette at Middle Butte. Average susceptibility is 2.64.

1: 2.1	2: 2.9	3: 2.6	4: 2.6
5: 2.6	6: 2.7	7: 2.7	8: 2.5
9: 3.0	10: 2.3	11: 3.0	12: 2.7
13: 0.0		14: 0.5	
(sandstone at base of sill)		(sandstone at top of sill)	

E. Field measurements of a weathered minette sill at Middle Butte. Random susceptibility measurement were made over a 15 m^2 area. Average susceptibility is 2.23.

1: 2.5	2: 2.2	3: 2.4	4: 2.9
5: 2.0	6: 2.0	7: 2.0	8: 2.1
9: 1.6	10: 2.6		

F. A short segment of weathered, phlogopite-rich minette dyke exposed in Bear Creek (described in Kjarsgaard, 1994). The dyke trends 005° and is nearly vertical and about 4 m wide. The low average susceptibility of 1.70 may reflect the weathered nature of this occurrence.

1: 0.5	2: 1.4	3: 1.7	4: 1.5
5: 1.5	6: 1.4	7: 1.3	8: 1.6
9: 1.2	10: 1.4	11: 1.4	12: 1.8
13: 1.2	14: 1.2	15: 1.4	

G. Coulee 29 consists of a volcanic vent complex of minette breccia and tuff that is intruded by relatively late, irregular minette dykes and sills (Kjarsgaard, 1994). The breccias are generally of low susceptibility, especially in contrast to the intrusive, coherent minette dykes. Two sets of measurements were made on separate occurrences of fresh minette dyke about 1 km apart. The susceptibilities in the Cretaceous sedimentary rocks range from 0.0 to 0.1, and the susceptibilities in the minette breccias range from 0.0 to 0.4. The susceptibilities in the fresh minette are considerably higher, 2.04 and 1.85 for localities A and B, respectively.

Set A:

1: 3.0	2: 1.9	3: 2.1	4: 2.4
5: 1.8	6: 2.0	7: 1.8	8: 1.7
9: 1.7	10: 2.0		

Set B:

1: 2.0	2: 2.4	3: 2.0	4: 2.0
5: 1.5	6: 1.4	7: 1.4	8: 1.7
9: 2.0	10: 2.1		

H. Black Butte is a boss-like plug of feldspar-rich minette (Kjarsgaard, 1994). The minette is weathered in outcrop but somewhat fresher along small exposures adjacent to the road. Measurements were taken over an area of about 400 x 200 m, covering the known outcrop of the minette. The average susceptibility is 1.29.

1: 1.0	2: 1.4	3: 1.2	4: 1.4
5: 1.1	6: 1.4	7: 1.2	8: 2.2
9: 0.8	10: 1.2	11: 1.3	

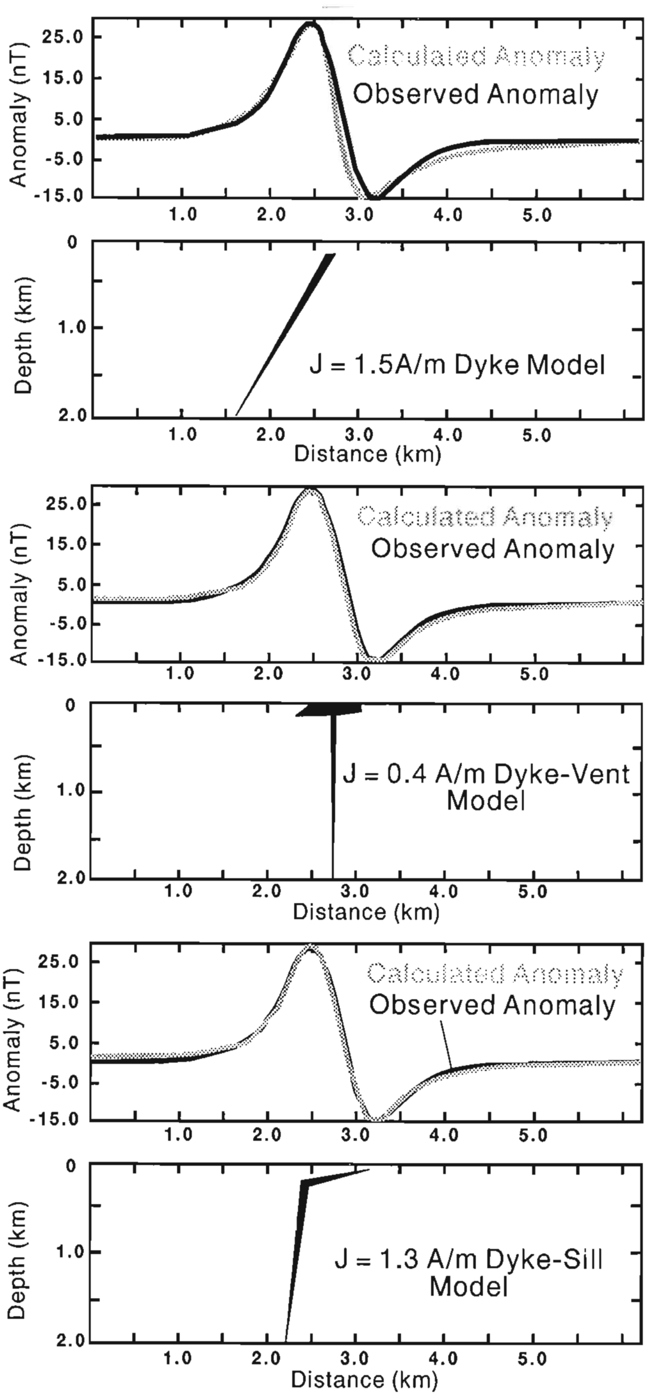

Figure 8. *Preliminary 2.5-D modelling of the aeromagnetic linears as dykes. The models indicate that the depth to the source is less than 200 m. The shallow position of the dykes within upper Cretaceous strata would be consistent with the Eocene age of minette dykes exposed in the Sweet Grass Hills and associated igneous rocks. A vertical or steeply-dipping dyke-like body produces a reasonable fit with the data although a better match is computed using a dyke that terminates in a sill or a vent. However, it is unlikely that either of these latter geometries would persist for strike distances of 30 km, the length of the longest anomaly. In addition, plug-like minettes in southern Alberta (e.g., Black Butte; Kjarsgaard, 1994) produce a definite subcircular anomaly. J is the magnetic contrast in amps/metre x 10^{-2}.*

Cordillera during the Eocene (ca. 55–52 Ma; Parrish et al., 1988) and was associated with the emplacement of alkaline igneous rocks of the Kamloops volcanics, Coryell syenite, and finally ca. 45 Ma lamprophyres. It should be pointed out that these rocks are a considerable distance west (over 350 km) of the westernmost dyke anomaly known in southern Alberta. Recent determination of the age of minette dykes in the Milk River area of southern Alberta, a northern extension of the Sweet Grass Hills magmatism, indicates an emplacment age of 50.3+/-0.5 Ma, overlapping with the ages of alkaline magmatism in the southern Canadian Cordillera (Davis and Kjarsgaard, 1994). Our interpretation of the magnetic data in southern Alberta suggests that the region affected by extension and emplacement of alkaline magmas extended much farther east and north than previously recognized. Recent analyses of the helium isotopic composition of gases in Alberta indicate the presence of anomolous ^3He in gas samples from a broad region of southern Alberta (Hiyagon and Kennedy, 1992), perhaps reflecting the effects of mantle degassing and

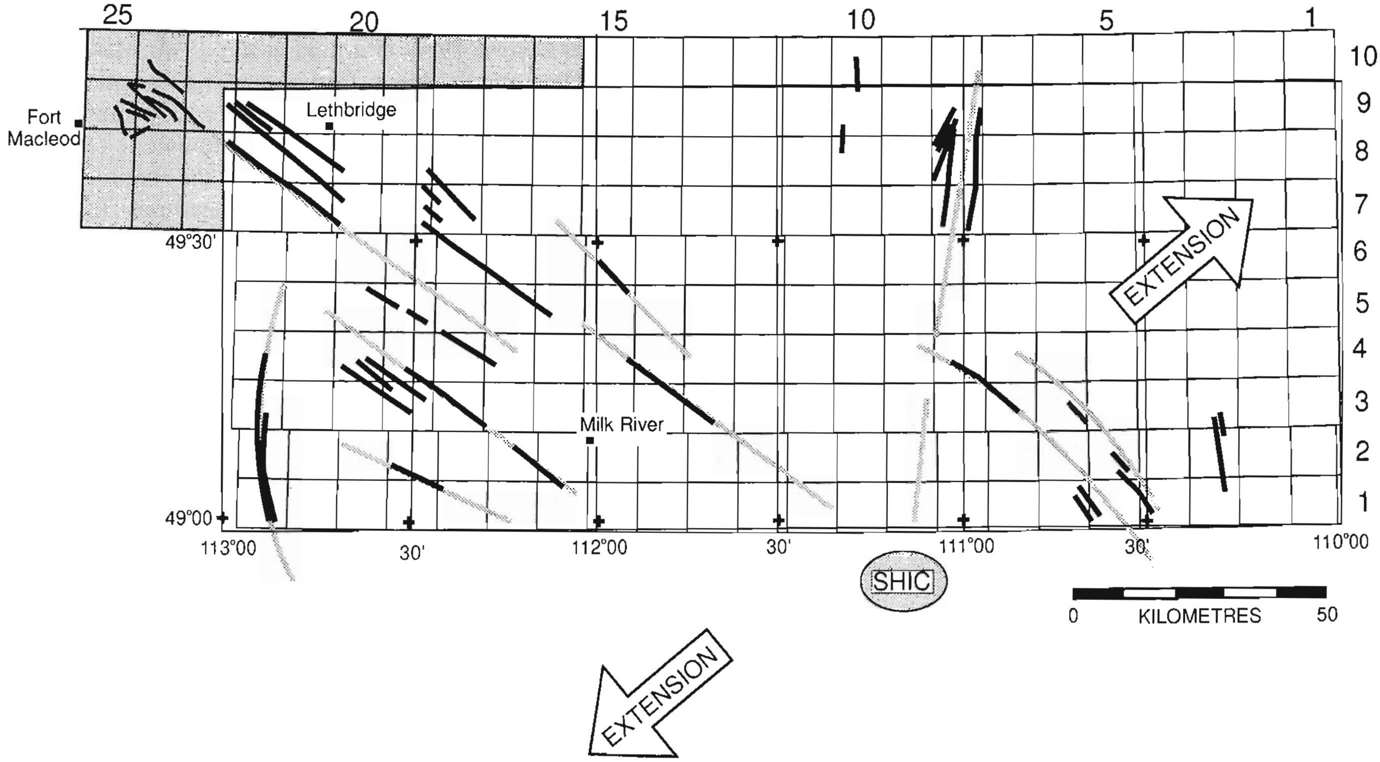

Figure 9. A plot of the trends of high wavenumber magnetic linears interpreted as dykes on a township and range grid. The shaded lines behind the magnetically-defined (black) linears emphasize the general pattern of the dykes which appear to converge in the region of the Sweet Grass Hills Igneous Complex (SHIC). This pattern of subradial and curvilinear dykes is similar to the patterns seen around hotspots and volcanic centres (e.g., Ernst et al., 1995). A postulated northeast–southwest extension direction is show by the arrows. The shaded area in the northwest is beyond the limit of the Cypress Hills survey. The northwest-trending linears east of Fort Macleod are normal faults identified on the basis of seismic reflection data (from Wright et al., 1993). Note the close alignment of the magnetically defined linears and the faults.

infiltration of mantle helium into the sedimentary section (cf. Oxburgh et al., 1986).

Tests

The interpretation that the magnetic anomalies are related to dykes is testable. Ground inspection of coulee walls in areas west of Milk River and along St. Mary River west of Lethbridge failed to reveal any outcrop correlation. We examined well records to determine if any of the petroleum wells in the region had intersected dyke material. We limited our search to well logs and searched the shallow parts of logs for a combined high-velocity (low travel time) sonic response and a positive gamma ray kick, the latter reflecting the high potassium content of the minettes (4–7%; Kjarsgaard, 1994). This search covered more than 30 wells, mostly south of Lethbridge, and failed to identify any potential minettes. Examination of seismic reflection data recorded over these anomalies may also aid in unraveling the origin of these anomalies. However, if the dyke inclinations are as steep as the modelling indicates, they may be difficult to recognize on vertical incidence reflection profiles. The ultimate test may be the direct drilling of one of the anomalies.

Implications for petroleum exploration

If the dyke interpretation of the linear anomalies is correct, it may have consequences for petroleum exploration in southern Alberta. The presence of dykes requires extension and formation of dilational fractures to host the dyke magmas. Those fractures that are filled with minette magma are the ones that have been detected in the aeromagnetic survey. Dilatant fractures that are not filled with dyke magma may still be present but invisible to aeromagnetic survey techniques at the present level of resolution (Fig. 10). Nonetheless, the presence of the dykes requires the presence of faulting, most likely along

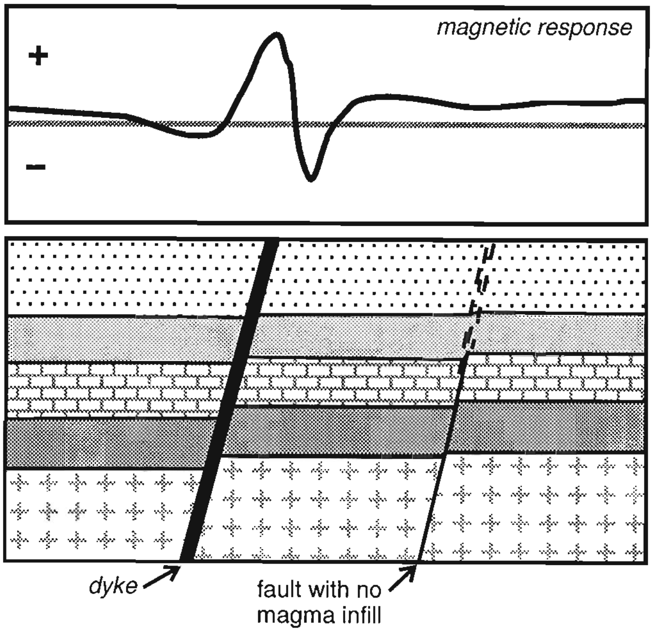

Figure 10. Diagram showing the postulated expression of extension in the form of dykes, which will result in a magnetic anomaly, and coeval faults that are magnetically transparent. Note the fracture zone developed in the upper part of the fault zone. This figure is based loosely on an interpretation of seismic data presented by Wright et al. (1993).

trends parallel to the dyke trends. A potential example is found in the region east of Fort Macleod that is characterized by small faults with a northwest–southeast trend (120°–130°) and a normal sense of displacement (Fig. 9; Wright et al., 1993). According to Wright et al. (1993), seismic data across the faults show that they are characterized by a steep dip and that they cause displacement of sub-Mississsippian (Devonian and Cambrian) strata.

Above the Devonian, the faults lose their displacement but the projection of the fault zones and adjacent rocks are characterized by oil staining and fracturing in the Mississippian Banff Formation and the mid-Cretaceous base of the Fish Scales zone. When the fault array is plotted with the trace of the magnetic linears to the southeast, they lie directly along strike with the magnetic linears in the Lethbridge area (Fig. 9). We suggest that these faults represent an example of post-Cretaceous fractures formed during Eocene extension but apparently unassociated with dyke emplacement. Similarly, there are two hydrocarbon fields in southern Alberta that are anomalously linear along a trend that parallels the dyke trends (Chin Coulee and Del Bonita; Fig. 11). The Del Bonita field is similar to the Reagan field which produces from Mississippian strata in faulted antiform that has a north-northwest-trending fault along its eastern flank (Putnam et al., 1995; McCourt, 1958). We were unable to find reservoir descriptions of the Chin Coulee region, but the alignment of producing wells in that area is quite anomalous relative to the unoriented fields typical of the region. We suggest that northwest-trending fractures formed during Eocene extension may have played a role in hydrocarbon entrapment and should be considered in the search for structural traps and fracture-related porosity.

CONCLUSIONS

High-resolution magnetic anomaly data recorded in southern Alberta have revealed the presence of short wavelength, linear, magnetic anomalies that are quite distinct from longer wavelength anomalies in the Archean basement of the region. Based on the magnetic response, linearity, swarm-like geometry of the anomalies, and comparison with exposed examples from the Canadian Shield, they are interpreted by analogy with the exposed Sweet Grass Hills igneous rocks, as dykes of mafic igneous rock that were emplaced during the Eocene (ca. 50 Ma). We discount a hydrocarbon seepage origin because the anomalies are more intense than could be produced by even the most altered examples from the Cement Field in Oklahoma, and they are not generally associated with known producing pools in southern Alberta. The anomalies cover a broad region of southern Alberta and represent an eastern and northern continuation of the association of alkaline magmatism and Eocene extension that characterizes the southeastern Canadian Cordillera and the Montana Alkalic province. The presence of the dykes records an increment of post-Cretaceous extension and thereby may provide a mechanism for the generation of hydrocarbon traps through structure and or fracturing.

Acknowledgments

John Mariano was supported by an NSERC post-doctoral fellowship with the Continental Geoscience Division (GSC Ottawa). Discussions with Ted Glenn (Chevron Canada), Lorne Kelsch (PanCanadian Petroleum), John Peirce (GEDCO), and John Broome (GSC Ottawa) have been very helpful in formulating and testing some of the ideas presented in this paper. Formal reviews were completed by Andrew Okulitch, John Broome and John Peirce. Mike Staniland and Bruce Palmer are thanked for help with retrieval of well data and examination of well logs for evidence of the elusive dykes.

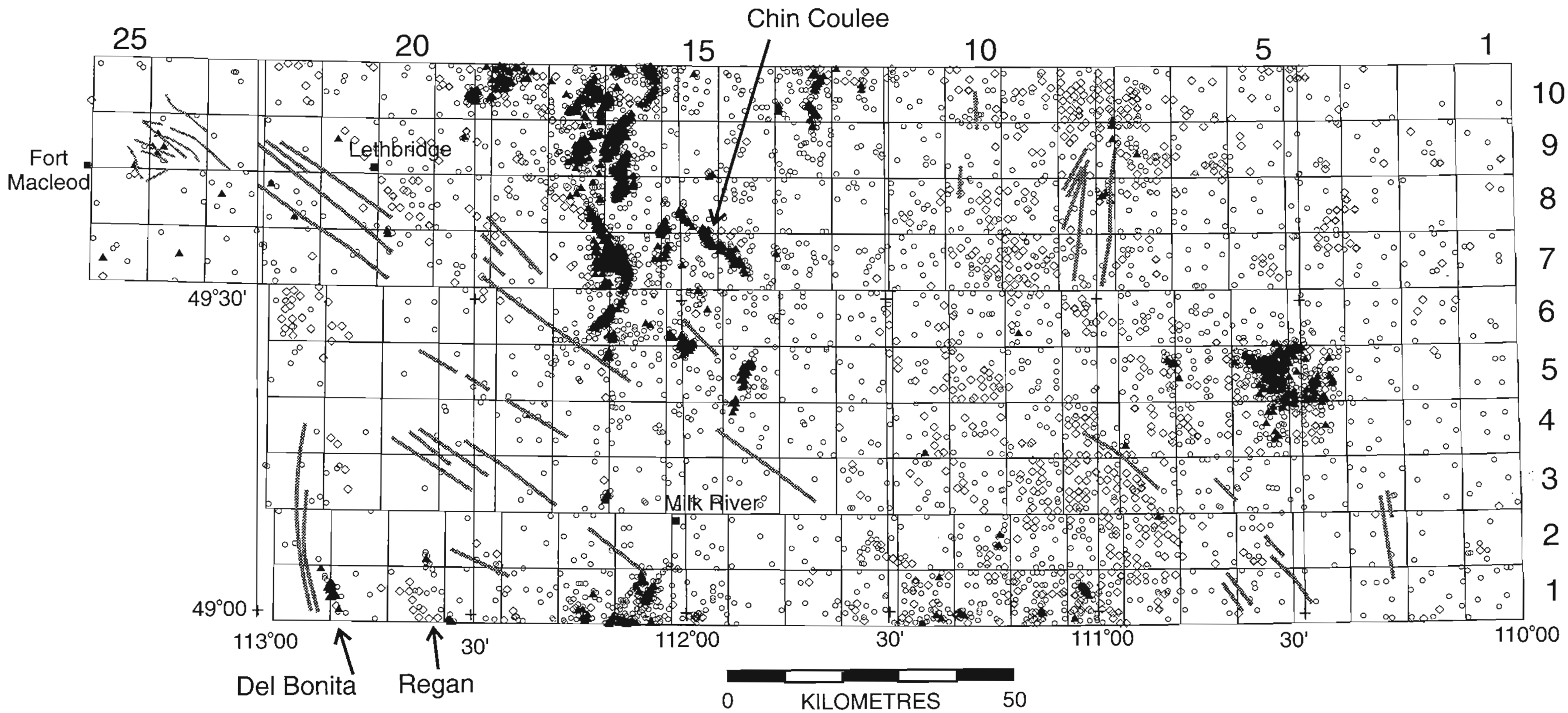

Figure 11. *Plots of well intersections in the survey area with the magnetic linears. Filled triangles, oil wells; open diamonds, gas wells; open circles, no production or dry tests. In order to limit well density and enhance legibility, the well search was conducted to exclude shallow wells above the Second White Specks (Cretaceous). Structurally-controlled fields at Del Bonita and Reagan are shown along with the anomalosly linear Chin Coulee field. The linears in the Fort Macleod area are from Wright et al. (1993) and are not interpreted as dykes.*

REFERENCES

Davis, W.J., Berman, R., and Kjarsgaard, B.
1995: U-Pb geochronology and isotopic studies of crustal xenoliths from the Archean Medicine Hat Block, northern Montana and southern Alberta: Paleoproterozoic reworking of Archean lower crust. *In* Lithoprobe Report No. 47, G.M. Ross (ed.), p. 329-334.

Davis, W.J., and Kjarsgaard, B.A.
1994: A Rb-Sr phlogopite-whole rock isochron age for olivine minette from the Milk River area, southern Alberta. *In* Radiogenic Age and Isotopic Studies: Report 8. Geological Survey of Canada, Current Research 1994-F, p. 11-14.

Donovan, T.J., Forgey, R.L., and Roberts, A.A.
1979: Aeromagnetic detection of diagenetic magnetite over oilfields. American Association of Petroleum Geologists Bulletin, v. 63, p. 245-248.

Ebner, E., Peirce, J., and Marchand, N.
1995: Part Four: Interpretation of aeromagnetic data. Canadian Society of Exploration Geophysicists Recorder, v. 20, p. 8-11.

Elmore, R.D. and Crawford, L.
1990: Remanence in authigenic magnetite: testing the hydrocarbon-magnetite hypothesis. Journal of Geophysical Research, v. 95, p. 4539-4549.

Ernst, R.E., Head, J.W., Parfitt, E., Grosfils, E., and Wilson, L.
1995: Giant radiating dyke swarms on Earth and Venus. Earth Science Reviews, v. 39, p. 1-58.

Hiyagon, H. and Kennedy, B.M.
1992: Noble gases in CH_4-rich gas fields, Alberta, Canada. Geochimica et Cosmochimica Acta, v. 56, p. 1569-1589.

Kjarsgaard, B.A.
1994: Potassic magmatism in the Milk River area, southern Alberta: petrology and economic potential. *In* Current Research 1994-B, Geological Survey of Canada, p. 59-68.

1997: (*this volume*) Diamonds in Alberta: studies of potential host rocks of deep-seated origin and applications of indicator mineral exploration techniques. *In* Exploring for Minerals in Alberta: Geological Survey of Canada Geoscience Contributions, Canada-Alberta Agreement on Mineral Development (1992-1995), R.W. Macqueen (ed.). Geological Survey of Canada, Bulletin 500, p. 185-207.

Machel, H.G. and Burton, E.A.
1991: Causes and spatial distribution of anomolous magnetization in hydrocarbon seepage environments. American Association of Petroleum Geologists Bulletin, v. 75, p. 1864-1876.

McCourt, J.H.
1958: Reagan Field. *In* Montana Oil and Gas Fields Symposium, Montana Geological Society, p. 203-204.

Oxburgh, E.R., O'Nions, R.K., and Hill, R.I.
1986: Helium isotopes in sedimentary basins. Nature, v. 324, p. 632-635.

Parrish, R.R., Carr, S.D., and Parkinson, D.L.
1988: Eocene extensional tectonics and geochronology of the southern Omineca Belt, British Columbia and Washington. Tectonics, v. 7, p. 188-212.

Putnam, P., Klovan, E., Hedinger, A.S., Hopkins, J.C., and Ward, G.
1995: The Mississippian succession in the plains of southwestern Alberta and northwestern Montana: Stratigraphic and structural architecture, trapping styles and future opportunities. Canadian Society of Petroleum Geologists Reservoir, v. 22, p. 3, 4.

Reynolds, R.J., Webring, M., Grauch, V.S.J., and Tuttle, M.
1990: Magnetic forward models of Cement oil field, Oklahoma, based on rock magnetic, geochemical, and petrologic constraints. Geophysics, v. 55, p. 344-353.

Reynolds, R.J., Fishman, N.S., and Hudson, M.R.
1991: Sources of aeromagnetic anomalies over Cement oil field (Oklahoma), Simpson oil field (Alaska) and the Wyoming-Idaho-Utah thrust belt. Geophysics, v. 56, p. 606-617.

Ross, G.M., Parrish, R.R., Villeneuve, M.E., and Bowring, S.A.
1991: Geophysics and geochronology of the crystalline basement of the Alberta Basin, western Canada. Canadian Journal of Earth Sciences, v. 28, p. 512-522.

Ross, G.M., Broome, J., and Miles, W.
1994b: Potential fields and basement structure, Western Canada Sedimentary Basin. *In* Geological Atlas of Western Canada Sedimentary Basin, G.D. Mossop and I. Shetsen (compilers). Canadian Society of Petroleum Geologists and Alberta Research Council, p. 37-41.

Ross, G.M., Mariano, J., and Dumont, R.
1994a: Was Eocene magmatism widspread in the subsurface of southern Alberta? Evidence from new aeromagnetic anomaly data. Lithoprobe Report No. 37, p. 240-249.

Schwarz, E.J., Hood, P.J., and Teskey, D.J.
1987: Magnetic expression of Canadian diabase dykes and downward modelling. *In* Mafic dyke swarms, H.C. Halls and W.F. Fahrig (eds.). Geological Association of Canada, Special Paper 34, p. 153-162.

Villeneuve, M.E., Ross, G.M., Theriault, R.J., Miles, W., Parrish, R.R., and Broome, J.
1993: Tectonic subdivision and U-Pb geochronology of the crystalline basement of the Alberta basin, western Canada. Geological Survey of Canada, Bulletin 447, 86 p.

West, G.F. and Ernst, R.E.
1991: Evidence from aeromagnetics on the configuration of Matachewan dykes and the tectonic evolution of the Kapuskasing Structural Zone, Ontario, Canada. Canadian Journal of Earth Sciences, v. 28, p. 1797-1811.

Wright, G.N., McMechan, M.E., and Potter, D.E.G.
1993: Structure and architecture of the Western Canada Sedimentary Basin. *In* Geological Atlas of Western Canada Sedimentary Basin, G.D. Mossop and I. Shetsen (compilers). Canadian Society of Petroleum Geologists and Alberta Research Council, p. 25-40.

GEOLOGICAL SETTING AND ORIGIN OF MICRODISSEMINATED AU-AG-CU MINERALS, FORT MACKAY REGION, NORTHEASTERN ALBERTA[1]

Hugh J. Abercrombie and Rui Feng[2]
Geological Survey of Canada, Calgary

Abstract

Newly discovered gold, silver, copper and related metallic minerals occur in rocks of the Western Canada Sedimentary Basin and underlying Precambrian basement near Fort MacKay, Alberta. The minerals include microdisseminated native, intergrown, and alloyed metals, and metal-chloride, -oxide, -carbonate, and -sulphide minerals deposited in pores and in microveinlets associated with fractures and diagenetically altered fabrics. Typical alteration minerals include hematite, microcrystalline quartz, Ce-carbonate, monazite, and native S.

A major structural feature at Fort MacKay is the dissolution edge of the Middle Devonian Prairie Formation, Upper Elk Point Group. Salt dissolution over a 20–30 km wide band paralleling the basin margin caused significant vertical displacement and collapse of overlying sediments. Three hydrochemical zones have been recognized: a lower, relatively oxidized, brine regime (>200 000 mg/l; Precambrian, Elk Point); an intermediate, relatively reduced, saline regime (10 000 to 70 000 mg/l; Beaverhill Lake, Woodbend); and an upper, fresh to brackish regime (1000 to 10 000 mg/l; Mannville and younger), locally bitumen-saturated.

Microdisseminated polymetallic mineralization is proposed to have occurred by mobilization and transport of gold and other metals in oxidizing, halide-rich brines derived from the Elk Point Group at a maximum paleotemperature of about 90°C. Metal deposition probably was related to changes in redox potential along the flow path; deposition may, in part, be related to the presence of hydrocarbons. The basin-wide distribution of halite in the Prairie Formation and its removal by dissolution over large areas of the WCSB may signify regional potential for similar occurrences across western Canada.

Résumé

Une minéralisation d'or, d'argent, de cuivre et de métaux associés de "type Prairie" vient d'être découverte dans des roches du bassin sédimentaire de l'Ouest canadien et dans le socle précambrien sous-jacent près de Fort MacKay (Alberta). La minéralisation se compose, d'une part, d'éléments métalliques microdisséminés à l'état natif, en intercroissance de même que sous la forme d'alliages et, d'autre part, de minéraux métalliques (chlorures, oxydes, carbonates et sulfures) déposés dans des pores et des microfilonnets associés à des fractures et à des fabriques altérées pendant la diagenèse. Les minéraux d'altération typiques sont notamment l'hématite, le quartz microcristallin, le carbonate de cérium, la monazite et le soufre natif.

Dans la région de Fort MacKay, l'une des principales caractéristiques structurales est le biseau de dissolution de la Formation de Prairie du Dévonien moyen (partie supérieure du Groupe d'Elk Point). La dissolution du sel, sur une bande de 20 à 30 km de largeur longeant la marge du bassin, est à l'origine du déplacement vertical significatif et de l'effondrement des roches sédimentaires sus-jacentes. On distingue trois zones hydrochimiques : un régime inférieur de saumures relativement oxydés (>200 000 mg/l; Précambrien, Elk Point); un régime intermédiaire d'eaux salines, relativement réduites (10 000 à 70 000 mg/l; Beaverhill Lake, Woodbend); un régime supérieur d'eaux fraîches à saumâtres (1 000 à 10 000 mg/l; Mannville et plus récent), localement saturé en bitume.

---

[1]Canada–Alberta Agreement on Mineral Development, Project C1.12
[2]Global Pacific Minerals, Suite 830, 789 West Pender Street, Vancouver, British Columbia V6C 1H2

La minéralisation de type Prairie serait, selon ce qui est proposé, causée par la mobilisation et le transport de l'or et d'autres métaux par l'intermédiaire de saumures oxydantes riches en halures provenant du Groupe d'Elk Point (paléotempérature maximale d'environ 90 °C). Le dépôt des métaux est probablement lié aux variations du potentiel d'oxydo-réduction le long de la trajectoire d'écoulement; le dépôt pourrait être, en partie, lié à la présence d'hydrocarbures. La répartition à l'échelle du bassin de la halite dans la Formation de Prairie et son élimination par dissolution sur de vastes zones du bassin sédimentaire de l'Ouest canadien pourraient signifier l'existence possible de minéralisation de type Prairie dans tout l'Ouest canadien.

INTRODUCTION

Transport of metals in sedimentary brines is recognized as an important process in the formation of sedimentary ore deposits. In the Western Canada Sedimentary Basin (WCSB), fluid flow is believed to have played an important role in the movement and accumulation of both hydrocarbons and metals (Garven and Freeze, 1984; Hitchon, 1984; Garven, 1989; Anderson and Macqueen, 1989; Masters, 1984; Nesbitt and Muehlenbachs, 1994). Flow of fluids within the WSCB has occurred as a consequence of repeated burial and uplift of the basin through a protracted period from late Precambrian to the present. Because the WCSB contains the largest single accumulation of hydrocarbons in the world in the Cold Lake, Athabasca-Wabasca, and Peace River heavy oil deposits (Masters, 1984), as well as significant conventional hydrocarbon resources, it is primarily regarded as an energy basin. However, world class deposits of Zn and Pb have been mined at Pine Point in southern Northwest Territories (Fig. 1a), and occurrences of similar mineralization have been identified elsewhere in the basin (Hitchon, 1993; Olson et al., 1994).

Gold, silver, copper and other metals are soluble in waters over a range of compositions and over a range of surface and subsurface conditions. In sedimentary basins, however, only a limited range of water compositions and pressure and thermal regimes can be called upon to mobilize, transport and deposit metals (Hanor, 1979; Sverjensky, 1984, 1987; Jaireth, 1994; Bloom et al., 1992). The capacity of sedimentary basin waters to leach and transport metals is dictated by their composition and redox state, metal availability, the existence of permeable pathways for fluid flow, and pressure-temperature (P-T) conditions imposed through basin evolution. Furthermore, precipitation of metallic minerals is a complex interplay between the properties of the fluid as controlled by changes in temperature and pressure along the flow path, and the geochemical environment which is dictated largely by the lithology and redox state of the flow system.

Based upon the discovery of novel microdisseminated mineral assemblages in the Fort MacKay region of northeastern Alberta (Abercrombie and Feng, 1994a), a new model for metal transport and deposition in sedimentary rocks has been proposed. Microdisseminated polymetallic minerals are inferred to have been deposited from oxyhalide brines of sedimentary evaporative-diagenetic origin (Abercrombie and Feng, 1994b; Feng and Abercrombie, 1994) and placer accumulations of these metals have also been documented (Giusti, 1986; Ballantyne and Harris, *this volume*). Brines of this character are known to exist in the Middle Devonian Prairie Formation and adjacent units throughout much of the WCSB (Hitchon et al., 1971; Aulstead and Spencer, 1985; Wittrup and Kyser, 1990; Connolly et al., 1991a). Models for the evolution of fluid flow in the WCSB show that the eastern, updip margin of the sedimentary sequence has been a region for discharge of deep formation waters throughout the history of the WCSB (Hitchon, 1984; Garven, 1989). Contemporary evidence of high salinity brines in the Fort MacKay region confirms the discharge of saline waters and brines at surface within the Athabasca River valley (Ells, 1926; Carrigy, 1959; Borneuf, 1982; J. Cody, pers. comm., 1995) and the existence of such brines in the shallow subsurface (Hackbarth and Nastasa, 1979).

Evidence for the occurrence of microdisseminated Au, Ag, Cu and related metals, metallic minerals, and alteration has been found in rocks ranging from Precambrian to Cretaceous age. Although the stratigraphic thickness of sedimentary rocks in the Fort MacKay region is only on the order of 300 to 350 m, virtually all important sedimentary lithologies are represented. Importantly for mineral exploration, the section also shows strong redox contrasts ranging from relatively oxidized Precambrian basement and Lower to Middle Devonian redbed evaporites, to relatively reduced argillaceous limestones of the Waterways Formation of the Beaverhill Lake Group, and to strongly reducing conditions in bitumen saturated sandstones of the Lower Cretaceous McMurray Formation. Similar strongly reducing conditions occur

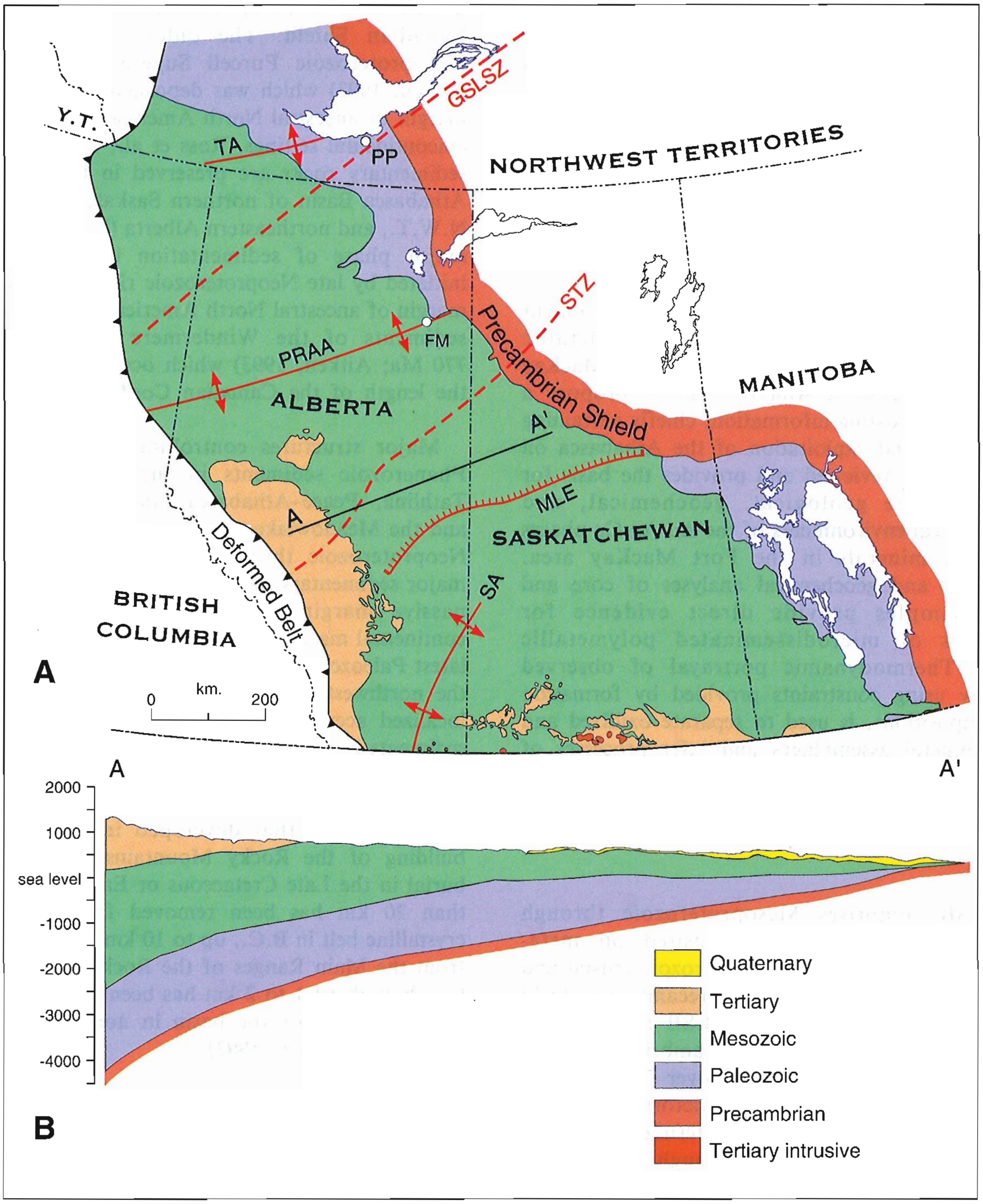

***Figure 1. A.** Geological map of the Western Canada Sedimentary Basin showing sedimentary and igneous rock distribution by age, major basement shear zones (dotted lines), and major structural features affecting deposition of Phanerozoic sediments (solid lines). **B.** Geological cross-section showing vertical distribution of sedimentary rocks by age along cross-section A–A'. GSLSZ, Great Slave Lake Shear Zone; STZ, Snowbird Tectonic Zone; TA, Tathlina Arch; PRAA, Peace River–Athabasca Arch; MLE, Meadowlake Escarpment; SA, Sweetgrass Arch; PP, Pine Point; FM, Fort MacKay.*

in the Waterways Formation where bitumens have penetrated beneath the sub-Cretaceous unconformity and in organic-rich laminites of the Middle Devonian Winnipegosis Formation. Gold is not, however, restricted to the sedimentary section. Allan (1920) reported gold values of $13.00 per ton (approx. 22 g/t) in samples of basement granitoids in the Athabasca Oils No. 1 drill hole completed on the east bank of the Athabasca River between Fort MacKay and Bitumount in 1912.

The objectives of this paper are to document occurrences of microdisseminated polymetallic minerals and associated alteration in the Fort MacKay region of northeastern Alberta, and to propose a genetic model. Existing information, chiefly pertaining to exploration and exploitation of the Athabasca oil sands deposit, is reviewed and provides the basis for establishing the geological, geochemical, and hydrogeological environments of the Au-Ag-Cu phases and related minerals in the Fort MacKay area. Petrographic and geochemical analyses of core and outcrop samples provide direct evidence for occurrences of microdisseminated polymetallic minerals. Thermodynamic portrayal of observed mineralogy using constraints provided by formation water compositions, is used to separate oxidized and reduced mineral assemblages and infer processes of metal transport and precipitation.

Geology

The WCSB comprises Mesoproterozoic through Tertiary sedimentary rocks deposited on metamorphosed Archean and Paleoproterozoic crustal and supracrustal assemblages of the Precambrian Shield (Figs. 1a, b). In the east, the WCSB thins depositionally and erosionally against Precambrian basement rocks; in the west it thickens to over 7 km and is delimited by the Rocky Mountain deformation front (Fig. 1b). To the north the WCSB terminates against the Tathlina Arch (Fig. 1a), although sedimentary rocks of comparable ages and lithologies are present in basins and mobile belts that formed peripherally to the Precambrian craton and extend northward into the Canadian Arctic Islands. To the south, age-equivalent sedimentary rocks are preserved across much of the west-central U.S.A. Additional information on regional scale lithostratigraphy and structure of the WCSB is available in Mossop and Shetsen (1994).

Tectonic evolution

Four main unmetamorphosed tectono-sedimentary assemblages occur within the WCSB and adjacent deformed belt or in intracratonic basins in the adjacent Canadian Shield. The oldest assemblage is the Mesoproterozoic Purcell Supergroup (1.2–1.7 Ga; Aitken, 1993) which was deposited along the western margin of ancestral North America in intracratonic to epicontinental settings (Ross et al., 1989). Correlative sedimentary rocks are preserved in the intracratonic Athabasca Basin of northern Saskatchewan, southern N.W.T., and northeastern Alberta (Fig. 2). The second major phase of sedimentation in the WCSB was initiated by late Neoproterozoic rifting of the western margin of ancestral North America and is preserved in sediments of the Windermere Supergroup (570–770 Ma; Aitken, 1993) which occur in outcrop along the length of the Canadian Cordillera.

Major structures controlling the distribution of Phanerozoic sediments in the WCSB include the Tathlina, Peace-Athabasca, and Sweetgrass arches, and the Meadowlake escarpment (Fig. 1a). From late Neoproterozoic through early Mesozoic, the third major sedimentary succession, a dominantly Paleozoic passive margin sequence, was deposited at the continental margin and in intracratonic basins. During latest Paleozoic and earliest Mesozoic, submergence of the northwestern part of the cratonic margin led to localized accumulation of Triassic to Early Jurassic sediments in incised and partly fault controlled basins. The fourth major sedimentary succession comprises Middle Jurassic to Paleocene rocks deposited in a foreland basin that developed in response to the building of the Rocky Mountains. Since maximum burial in the Late Cretaceous or Early Tertiary, more than 20 km has been removed from the Omineca crystalline belt in B.C., up to 10 km has been removed from the Main Ranges of the Rocky Mountains, and less than about 1 to 2 km has been removed from the eastern margin of the basin in northeastern Alberta (Willett and Issler, 1992).

Stratigraphy

Fort MacKay, Alberta, is located near the northeastern margin of the WCSB (Fig. 2). High grade metamorphic rocks of the Precambrian Shield outcrop about 100 km northeast of Fort MacKay and, farther northeast, Precambrian sedimentary rocks of the Athabasca Basin are exposed at surface. The Phanerozoic sedimentary column in the Athabasca River valley at Fort MacKay lies unconformably on basement and is only about 300 m thick. It is, however, highly diverse, comprising rocks of virtually all important sedimentary lithologies (Fig. 3). The Precambrian through Mesozoic section is exposed in an erosional window along the Clearwater and Athabasca rivers (Fig. 2).

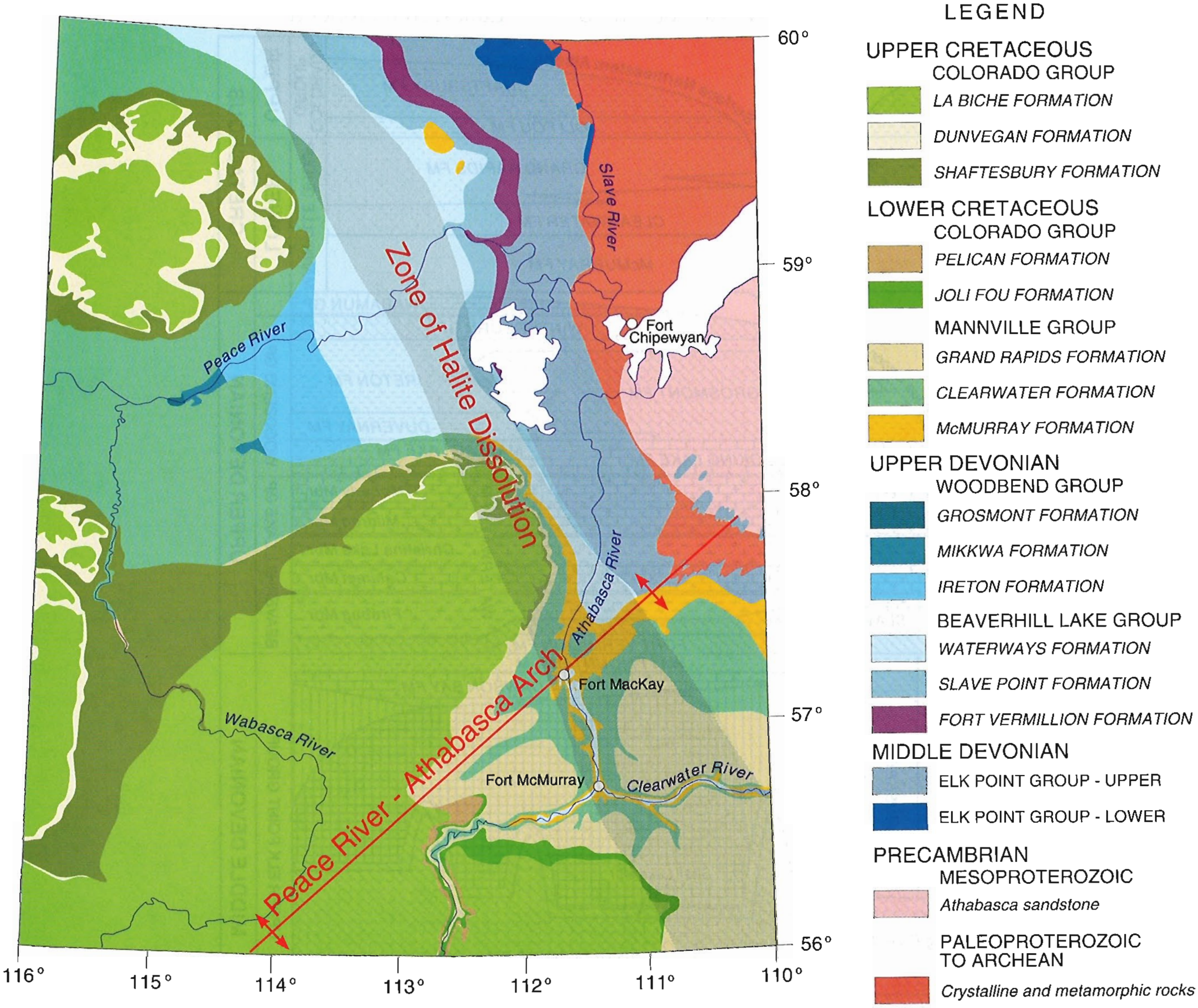

Figure 2. *Geological map of northeastern Alberta. The zone of halite dissolution in the Prairie Formation, Elk Point Group, is indicated by shading and the trace of the Peace River–Athabasca Arch (PRAA) is indicated by the solid line.*

Precambrian basement

Basement rocks in northeastern Alberta comprise a diverse suite of highly metamorphosed Archean to Paleoproterozoic ortho- and paragneisses cut by strike slip shear zones. These rocks show evidence for regional prograde metamorphism and deformation to granulite grade and superimposed retrograde metamorphism through amphibolite to greenschist grade. At Fort MacKay, basement rocks consist of highly strained ortho- and paragneisses of the Taltson Magmatic Zone (McDonough et al., 1993; McDonough, 1996, *this volume*). Alteration of basement gneisses is common and may include Paleoproterozoic retrograde greenschist facies alteration (chlorite-epidote) and later low temperature interaction of basement rocks by sedimentary basin derived waters (McDonough and Abercrombie, 1995).

Paleozoic platform margin

In northeastern Alberta, the Paleozoic platform margin succession is represented by shallowly westward dipping Devonian strata; stratigraphic relationships are illustrated schematically in Figure 3. Throughout this area, the Elk Point Group unconformably overlies the Precambrian Shield and is exposed in a northwestward trending belt paralleling the eastern margin of the WCSB. Upper Devonian rocks of the Beaverhill Lake

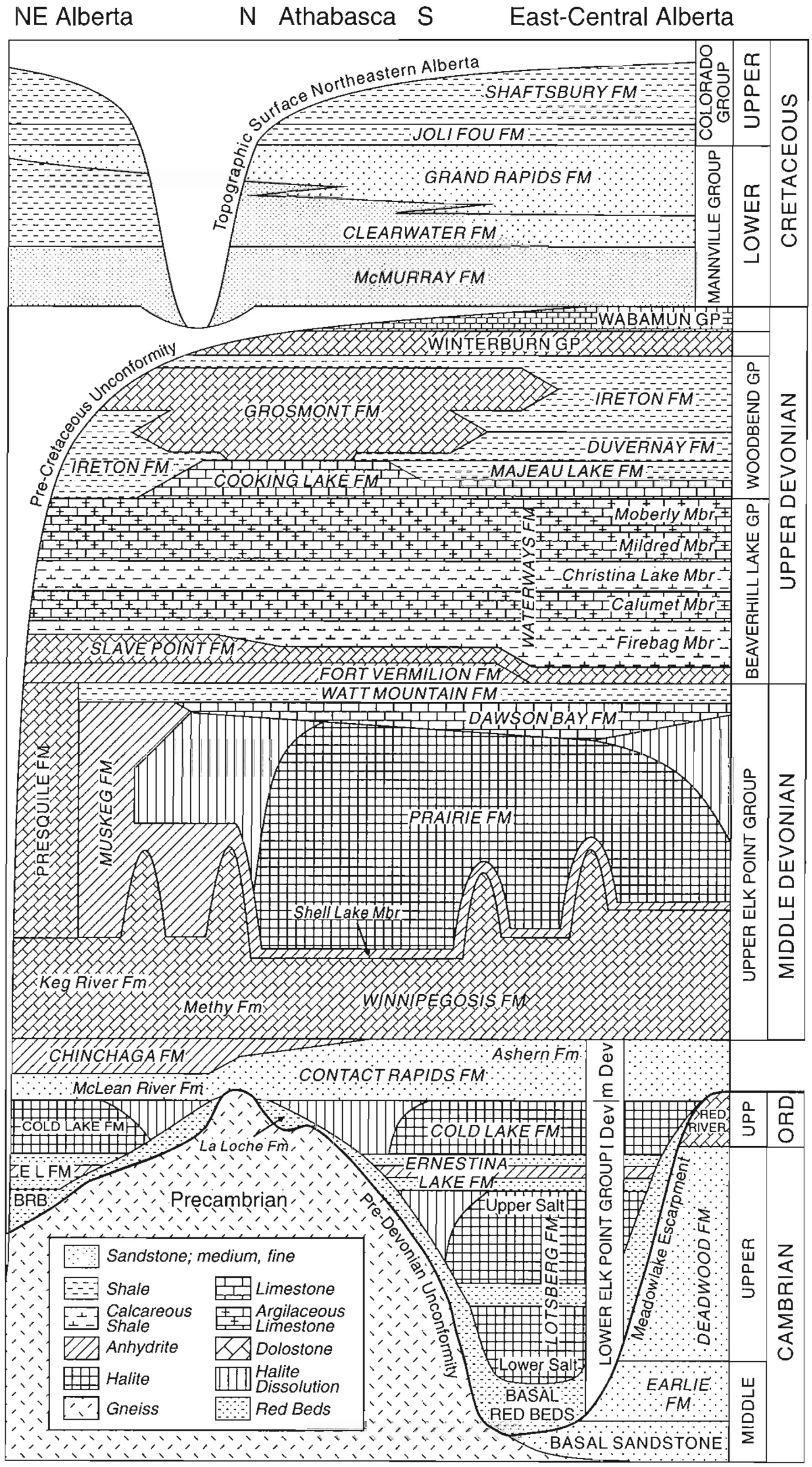

Figure 3. *Lithostratigraphic column for northeastern Alberta schematically illustrating stratigraphic relations along the eastern margin of the Western Canada Sedimentary Basin in Alberta. Modified after Turner and McPhee (1994).*

Group lie unconformably on the Elk Point Group and are overlain in succession by the Upper Devonian Woodbend, Winterburn, and Wabamun groups (Fig. 3).

Elk Point Group

The Lower to Middle Devonian Elk Point Group consist of a series of redbed evaporite sequences interbedded with dolostone, limestone, and shale that were deposited in a series of subbasins that formed in topographic lows on the pre-Devonian erosion surface (Meijer Drees, 1986). North of the Meadowlake Escarpment (Figs. 1, 3) and throughout much of northeastern Alberta it lies directly on Precambrian basement. Vertical successions through the Lower Elk Point Group vary along the eastern margin of the WCSB (Fig. 3), but generally consist of Basal Red Beds (or equivalent La Loche Formation) overlain by redbed salt deposits of limited extent. In outcrop, the Basal Red Beds infill depressions in the Precambrian surface (Fig. 4a) and locally reach thicknesses of up to 30 m (Norris, 1963). Two lithofacies are recognized. The oldest is a highly altered to sapropelic regolith which locally may be found in place or as debris flows infilling topographic lows on the pre-Devonian erosion surface. The second lithofacies is a more widely distributed hematitic sandstone to siltstone redbed.

The Lower Elk Point Group is thin in the immediate vicinity of Fort MacKay where both the Lotsberg and Cold Lake salts (Fig. 3) are absent due to nondeposition on a regional high on the Precambrian surface coincident with the trend of the Peace River–Athabasca Arch (Fig. 1; Benthin, 1973). The Lotsberg and southern Cold Lake salts underlie a large area of east-central Alberta and extend northward to within about 100 km of Fort McMurray (Hamilton, 1971; Meijer Drees, 1986). Low bromine contents of the Lotsberg and southern Cold Lake salts, and the absence of sulphate and carbonate minerals, suggest that these salts were deposited in a nonmarine setting (Wardlaw and Watson, 1966).

The Middle Devonian Upper Elk Point Group was deposited in a broad northwestward trending basin bounded to the east by the Precambrian Shield and to the west by the West Alberta Ridge. The basal unit of the Upper Elk Point Group is the Winnipegosis Formation (equivalent to the Keg River and Methy formations) which consists of fossiliferous dolostone with minor organic-rich laminites. The largest accumulations of salt in the WCSB occur in the Upper Elk Point and include thickly bedded primary and secondary halite of the Prairie Formation (Hamilton, 1971; Meijer Drees, 1986). With the exception of the lower Lotsberg salt, post-depositional salt dissolution has moved the eastern limit of all Elk Point salt units to the west by a variable amount since the Upper Devonian (Figs. 2, 3; Hamilton, 1971). The Watt Mountain Formation shale marks the top of the Elk Point Group and is associated with a regional unconformity separating Middle Devonian from Upper Devonian strata.

Beaverhill Lake Group

The Fort Vermillion (anhydrite evaporite) and Slave Point (limestone) formations, which make up the lower part of the Beaverhill Lake Group, are thinly developed or absent in the region of Fort MacKay. Here the uppermost Waterways Formation of the Beaverhill Lake Group consists of >200 m of calcareous shale, argillaceous limestone, and limestone, and has been subdivided regionally into five members. Limestones typically are silty, thinly bedded to nodular, and less commonly are massive to rubbly (Fig. 4b) with abundant bioclastic debris.

Pyrite of probable early diagenetic origin is common in the Waterways Formation, both as fine disseminations in argillaceous limestones and replacing bioclastic fragments. It also occurs in vertical pyrite-healed fractures up to about 5 mm thick (Fig. 4b). Bitumen locally fills intracrystalline pores, dissolution cavities, and vertical fractures in the Waterways Formation. Native sulphur is observed in drill core near the base of the Waterways Formation where it is associated with vuggy, recrystallized limestone, locally pyrite bearing, and was reported in outcrop by Norris (1963). Where they are exposed immediately beneath the pre-Cretaceous unconformity, Waterways limestones may show red-orange staining due to alteration of disseminated pyrite. This is particularly well developed in exposures of Moberly Member (Fig. 3) on the west bank of the Athabasca River at Fort MacKay. Here, 1 to 2 m of intensely red-ochre coloured, unlithified clay-rich silt that may represent a preserved soil developed at the pre-Cretaceous unconformity, overlies mottled orange and tan weathering limestone.

Woodbend Group

The Woodbend Group is the youngest Upper Devonian unit represented in the Fort MacKay region; its subcrop edge parallels the eastern margin of the WCSB west of the Athabasca River. The Woodbend Group consists of the Cooking Lake and overlying Grosmont

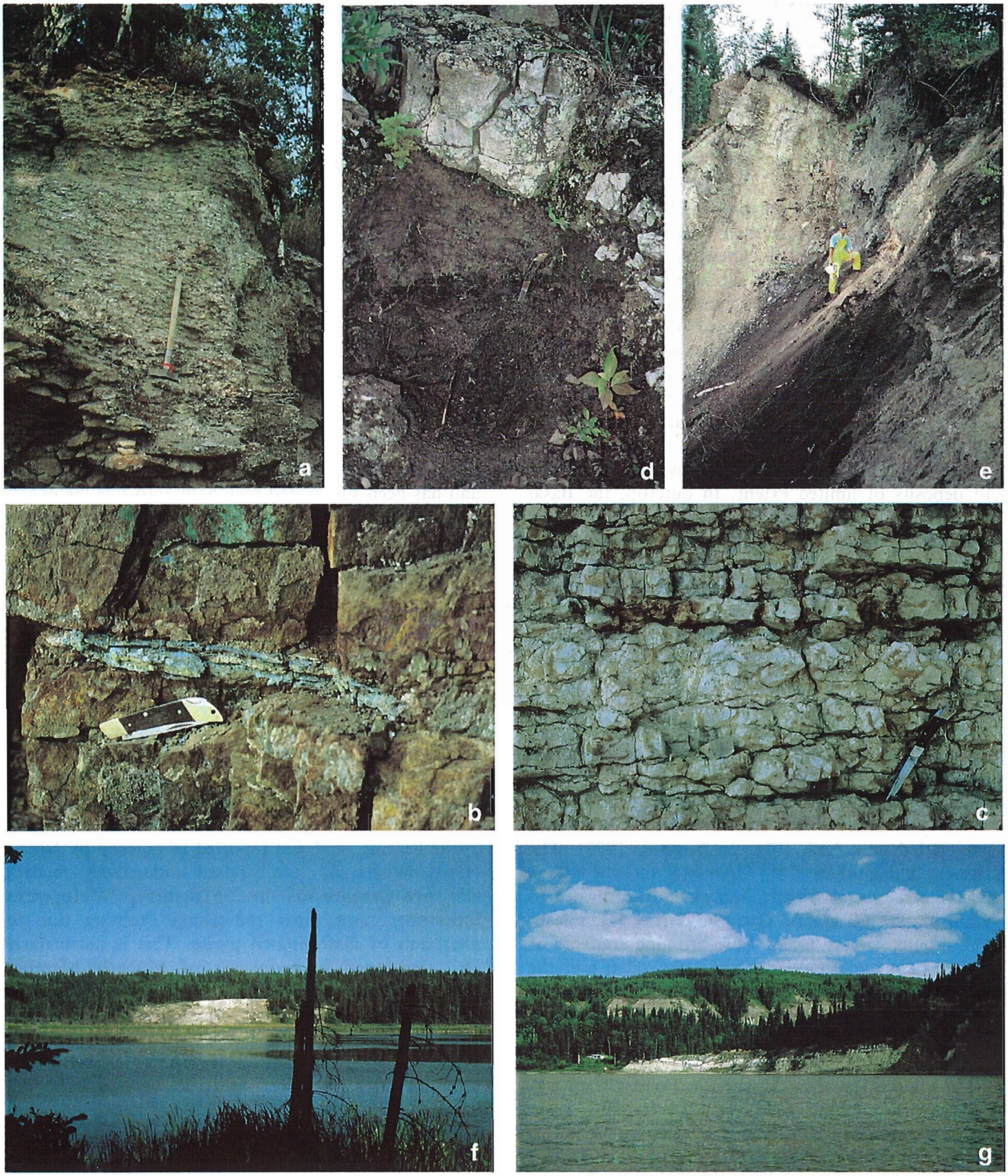

carbonate platformal sequences and associated basinal shales of the Majeau Lake, Duvernay, and Ireton formations. The Upper Ireton Formation, a thick regional shale unit, mantles the Grosmont platform and is overlain, far to the southwest, by reef to platformal dolostones and limestones of the Winterburn and Wabamun groups.

Mesozoic-Tertiary Foreland Basin

Leckie and Smith (1992) recognized five major cycles of foreland basin sedimentation in the WCSB, each bounded by major unconformities or lithological discontinuities. The first cycle ranges from Late Jurassic to earliest Cretaceous and is not preserved in northeastern Alberta. Mesozoic sediments of northeastern Alberta represent cycles 2 and 3 of Leckie and Smith (1992) and consist of the Lower Cretaceous Mannville and Mid- to Upper Cretaceous Colorado groups, respectively.

Mannville Group

Lower Mannville Group siliciclastics infilled broad northwestward trending valleys flanked by upland regions of uneroded pre-Cretaceous strata that were not fully buried until Upper Mannville time. In northeastern Alberta, the Lower Mannville Group is represented by the McMurray Formation, a quartz-rich sandstone deposited in fluvial to estuarine environments under fresh to brackish water conditions. It is thickest in depressions developed on the pre-Cretaceous erosion surface and appears to thicken into the Athabasca River valley. In the Fort MacKay-Fort McMurray region, poorly lithified, bitumen-saturated sands of the McMurray Formation host the Athabasca oil sands deposit, the biodegraded remnant of a supergiant oilfield (Creaney and Allan, 1992; Masters, 1984).

On the banks of the Athabasca River upstream from Fort MacKay, near where the Beaver and Muskeg rivers enter the Athabasca River, an unusually hard, quartz cemented sandstone, informally named the "Beaver River sandstone", occurs within the lower unit of the McMurray Formation (Fenton and Ives, 1982; Ives and Fenton, 1985). Mapping in the Muskeg-Beaver rivers area has identified outcrops and subcrops of the Beaver River sandstone (BRS) over an elongate 25 km^2 region south and east of Fort Mackay (Abercrombie, unpublished data). Due to the extremely hard, quartz cemented nature of this unit, Ells (1926) suggested that these outcrops were Precambrian quartzites. Examination of rock exposures shows that quartz cemented Beaver River sandstone is underlain and overlain by a heavy oil-bearing, fine to medium grained sandstone that is indistinguishable from the lower unit of the McMurray Formation (Fig. 4c). The Beaver River sandstone locally is porous and contains small quantities of bitumen. The McMurray Formation is overlain by lithofeldspathic sandstones and shales of the Clearwater and Grand Rapids formations of the Upper Mannville Group.

Colorado Group

The Colorado Group is the youngest stratigraphic unit exposed in northeastern Alberta. It is a thick assemblage of predominantly marine and locally organic-rich shale deposited in the Cretaceous western interior seaway. Periodic lowering of relative base level within the seaway resulted in progradation of nearshore sediments into the basin. These are preserved in a series of shale-encased tabular sandstone to conglomerate bodies of local to regional extent. Shales of the Lower Colorado Group have been examined by Bloch et al. (in press) who have refined the subsurface stratigraphic nomenclature across the WCSB. The revised stratigraphy has not been utilized in field mapping and is not reflected in Figures 2 or 3.

***Figure 4.** Field photographs. **a.** Regolithic debris flow of the Lower to Middle Devonian Basal Red Beds (La Loche Formation) unconformably overlies and infills depressions on altered Precambrian granitoid rocks at Stony Islands, Slave River. **b.** Nodular limestone of the Upper Devonian Moberly Member, Waterways Formation, exposed in outcrop along the Athabasca River south of Fort MacKay. The limestone is cut by pyrite-bitumen filled fractures, now oxidized and outlined by rusty iron staining. **c.** Quartz-cemented quartz sandstone of the Beaver River sandstone (BRS) exposed in a borrow pit west of the Athabasca River near the mouth of the Beaver River. At this location the Beaver River sandstone is underlain and overlain by bitumen-impregnated sandstone of the lower member of the McMurray Formation. This indicates that the Beaver River sandstone is of probable diagenetic facies of the McMurray Formation and is Cretaceous in age. **d.** Down-faulted block of bitumen-impregnated sandstone of the lower member of the McMurray Formation lies within a narrow graben cut into bedded limestones of the Moberly Member of the Waterways Formation exposed along the Muskeg River east of Fort MacKay. **e.** Calcite-malachite-azurite vein cutting altered Precambrian granitoid rocks, Stony Islands, Slave River. **f.** Sulphate-carbonate tufa mound developed at the site of brine discharge at Saline Lake in the Athabasca River valley south of Fort MacKay. The tufa mound rises approximately 12 m above the lake surface. **g.** Clay-altered argillaceous limestones of the Moberly Member, Waterways Formation, unconformably overlain by altered sandstones of the McMurray Formation on the east bank of the Athabasca River at the mouth of McLean Creek north of Fort McMurray. The alteration is interpreted to mark the site of a brine discharge zone.*

Structure

Regional maps of Precambrian structure across the WCSB portray a simple westward tilted surface with little evidence of differential relief. This is primarily a function of the regional map scale and lack of Precambrian drill intersections. More detailed investigations show that locally the basement surface is irregular and is cut by faults that were active during deposition of Cambrian and possibly younger strata.

Carrigy (1959), Hackbarth and Nastasa (1979), and Cotterill and Hamilton (1995), among others, have used a variety of surface and subsurface methods to infer structures in the vicinity of Fort MacKay and all show faults cutting the Precambrian surface and Phanerozoic formations. The best documented fault is the Sewetakun Fault, which is inferred to follow the trace of the Athabasca River between Fort McMurray and Fort Mackay (Hackbarth and Nastasa, 1979). West-side-down movement of 83 m at the top of the Precambrian and 75 m at the top of the Winnipegosis Formation indicates that the Sewetakun Fault has been active over a prolonged period of time from Precambrian through at least Middle Devonian. The work of Hackbarth and Nastasa (1979) and others shows that the Sewetakun Fault is one of numerous north-northwestward-trending, west-side-down faults that cut Devonian strata in the region. Cotterill and Hamilton (1995) have mapped a number of northeastward trending faults parallel to the axis of the Peace River–Athabasca Arch. These faults propagate into Phanerozoic cover and may be seen at surface (Fig. 4d).

Dissolution of salt from the Middle Devonian Prairie Formation (Figs. 2, 3) has had a profound effect on local to regional scale structures throughout northeastern Alberta. Salt removal has affected all overlying units structurally, and has been active since at least late Devonian time. Structural surfaces of post-Elk Point strata show dip reversals across the zone of salt dissolution, and isopachs of these same formations show thickening in the region of dip reversals. This indicates that removal of salt occurred prior to or during sedimentation, providing accommodation space for accumulation of anomalous thicknesses of overlying sediments. An example of this is the Bitumount subbasin north of Fort MacKay, where thickening of the McMurray Formation by up to 60 m can be attributed to dissolution of underlying Prairie Formation salts.

Structures related to salt removal include sink-holes and elongate fault-bounded depressions ranging in size from a few tens of metres to linked depressions several kilometres in width and tens of kilometres in length (Dufresne et al., 1994). Logging of cores from the Fort MacKay area reveals many high angle faults and fractures in Waterways Formation limestones that may be related to vertical movement along the Sewetakun fault due to salt removal or karsting of the pre-Cretaceous unconformity surface. Larger, subbasin scale salt removal is recorded by thickened accumulations of post-Elk Point strata where they overlie and infill salt solution structures. Collapse and solution breccias related to dissolution of Prairie Formation salts are widely distributed in overlying evaporite and carbonate rocks of the Upper Elk Point and Beaverhill Lake groups. Along the Athabasca and Clearwater rivers and their tributaries, where limestones of the Waterways Formation of the Beaverhill Lake Group are exposed at surface and overlie zones of salt removal, bedding within the Waterways and the lower part of the McMurray Formation is gently folded into domes and depressions with a wavelength of 1 to 3 km and amplitude of at least 30 to 40 m. These depressions have been linked to salt removal at depth. Surface outcrops of the Waterways Formation exposed along the Athabasca River valley west of the western regional limit of salt solution (Fig. 2) dip shallowly to the west but are otherwise undeformed. Other structural manifestations of salt removal include numerous sink holes in the present-day land surface, and sand-filled depressions in the pre-Cretaceous erosion surface.

Jointing and fractures are common in Waterways Formation exposures along the Athabasca River valley and its tributaries. Most are unmineralized, but many contain bitumen and are stained red-orange to brown due to alteration of pyrite to ferric oxyhydroxide minerals (Fig. 4b). Locally, Waterways Formation limestones are brecciated and in places cemented by networks of finely crystalline ferric oxyhydroxide (after pyrite) and silica (Feng and Abercrombie, 1994).

Mineralogy

Normal optical methods for mineral identification cannot be used for identifying microdisseminated mineralogy due to its extremely small particle size; typical Au and related metallic phases range from <0.5 to 10 μm and are therefore best described as microdisseminated. Instead, high resolution scanning electron microscope (SEM) imaging is required for mineral identification or determining element associations in finely intermixed compounds. This method has advantages and disadvantages. The principal advantage is that it permits imaging of metallic particles as small as a few hundred nanometres. Secondly, by using an energy dispersive X-ray spectrometer (EDS), qualitative chemical composition data can be obtained to assist in mineral identification. The disadvantage of this technique is that with such small particle sizes it is difficult to ascertain with certainty whether an element association observed by EDS analysis of a single spot is indicative of a distinct phase or reflects spectral contributions from two or more intimately intermixed, but distinct phases.

The mineralogy of microdisseminated phases was determined using SEM imaging of 35 samples including rock chips, polished thin sections, and rock slabs. These included samples of: i) Precambrian basement granitoids (core only), ii) Basal Red Bed sandstone (core only), iii) Waterways Formation limestone (core and outcrop), and iv) Beaver River sandstone (outcrop only). All samples were carbon coated prior to analysis and examination was conducted using backscattered electron (BSE) imaging. EDS was used qualitatively to assist in identification of mineral phases observed by BSE imaging.

Sample preparation initially involved the production of doubly polished uncovered thin sections and singly polished chip mounts. During the polishing process it was observed that microdisseminated minerals were being plucked and removed from the surface being polished. For this reason, preparation procedures were modified such that only fractured, unpolished surfaces were examined. Under this revised procedure, rock and chip samples are fractured, mounted on SEM stubs, and carbon coated prior to analysis. This modified procedure has proven to be successful in preventing the loss of microdisseminated particles of gold and other minerals in the preparation stage. Caution must be taken, however, to ensure that the samples are not exposed to sources of metallic contamination prior to examination. Periodic blank checks involving carbon coating and SEM–EDS examination of frosted glass slides can be used to detect contamination. Use of frosted glass slides is preferred over polished glass because the rougher surface better simulates the fractured rock surface.

SEM imaging was done at GSC Calgary using a Cambridge Stereoscan 150 Mk II equipped with a Robinson RBC-150 FML backscattered electron detector and a Kevex 7000 EDS system. Supplementary analyses were carried out at GSC Ottawa using a Leica 440 SEM and a Link light element EDS system. Results of SEM examinations are presented below and are summarized in Table 1.

The morphologies of micron sized particles imaged by SEM normally are difficult to distinguish, therefore the word "particle" is used generically to describe discrete minerals present in the sample. Where SEM examination shows that a particle is flat, it is described as a "flake". The use of SEM–EDS on unpolished surfaces permits qualitative determination of particle composition. Where possible, particle morphology and qualitative chemistry were used to identify minerals or apparently homogeneous phases. In the text and in Table 1, mineral names and stoichiometric mineral compositions are used to identify minerals or mineral classes which could be identified with reasonable certainty (i.e., quartz - SiO_2; monazite - $(Ce, La)PO_4$). However, due to the complexity of the rare earth element (REE) carbonate phases, identification of individual mineral species is impossible from qualitative SEM–EDS data and therefore $CeCO_3$ refers to a family of light rare earth carbonate minerals. Because the EDS system used was not equipped to analyze O, minerals identified as oxides are tentative identifications and are referred to in italics (e.g., *$PbSb_2O_4$, Sb_2O_3, SnO_2*). In many cases SEM–EDS examination revealed the presence of metallic alloys, for example Cu-Zn (brass). Where SEM-BSE examination showed metallic alloys to be homogeneous, the specific phases are indicated by hyphenating the constituent elements with the qualitatively most abundant element first (e.g., Cu-Zn, brass; Au-Ag, electrum). Gold has also been observed by SEM-EDS in close spatial association with Al, Si, and Ca as *Au-Al*, *Au-Si*, or *Au-Ca* elemental associations. These unusual elemental associations are referred to in italics to indicate that their identification as distinct phases has not been confirmed.

Precambrian basement

Ten basement granitoid samples from core samples taken from holes drilled near Fort MacKay were examined (Figs. 5a–d). The samples display steeply dipping mylontic fabrics, interpreted as a result of ductile–brittle shear deformation, and foliation expressed by chlorite and epidote with associated K-feldspar. In altered basement rocks, hematite is the predominant metallic alteration mineral, occurring as nodules, veinlets, and thin films on fracture surfaces. Quartz and pyrite are less abundant and also occur in veins and nodules. Minor native S locally is associated with pyrite. Monazite and $CeCO_3$ micro-veinlets are widespread and locally are associated with calcite veinlets.

SEM–EDS examination of basement rocks revealed widespread occurrences of microdisseminated Pb-bearing minerals such as $PbCl_2$, $PbCO_3$, and *$PbSb_2O_4$* (Fig. 5a). Chlorargyrite (AgCl) and native Ag are also widely distributed and associated with Pb

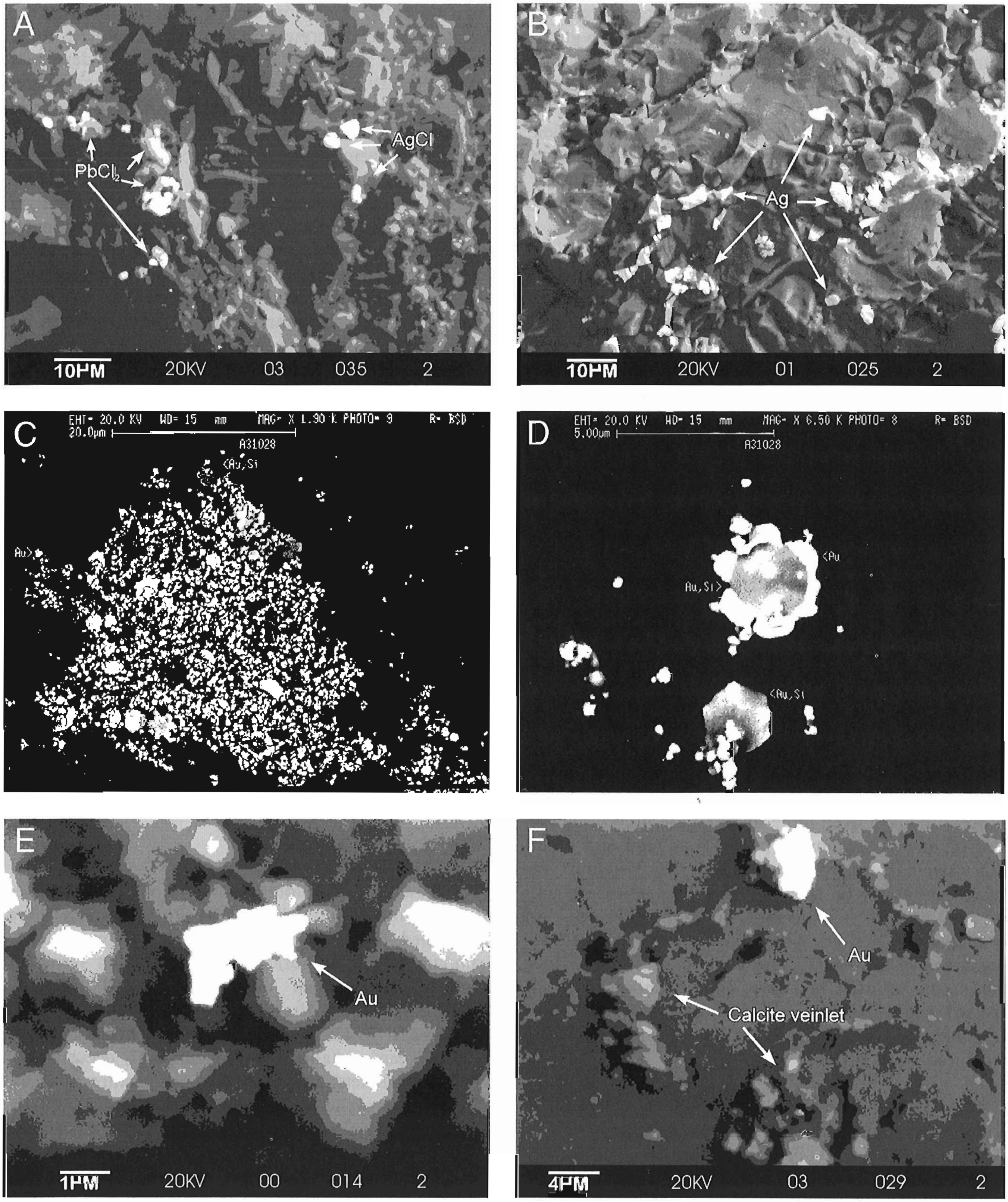

minerals, monazite, and calcite (Figs. 5a, b). Less abundant metallic phases include native Cu, Cu-Zn, Sb_2O_3, SnO_2, $CuSb_2O_6$, scheelite, and $BiCl_3$. Native Au was also observed in two samples as aggregates or as small disseminated particles of <1 to ~ 5 μm in diameter (Fig. 5c, d). Gold appears to be associated with native Cu, and less commonly with Ag-bearing minerals. Generally, Au, Ag, and Pb minerals are more abundant in samples near the pre-Devonian erosion surface. SEM-EDS examination of small 5 to 10 μm particles of *Au-Si* (Fig. 5d) using an SEM-EDS equipped with a light element EDS detector indicates that this element association apparently occurs in the absence of oxygen, sulphur, and carbon because none of these peaks were detected by light element EDS examination of *Au-Si* particles.

Basal Red Beds

The Basal Red Beds consist of medium to coarse grained quartz, K-feldspar, biotite, and muscovite, with halite, gypsum, and hematite cements and fracture coatings. There is a gradual upward change from massive, coarse grained and poorly sorted sandstone to shaly redbeds cut by many thin (0.2 to 0.8 cm), subhorizontal gypsum veins with vertical growth fabrics. Alteration minerals observed by SEM-EDS include $CeCO_3$, monazite, calcite, NaCl, KCl, and hematite; native S also was observed.

Metallic phases found on freshly broken surfaces of the sandstones and shales include relatively abundant Cu and Cu-Zn, and lesser amounts of AgCl, native Ag, $PbCl_2$, $PbCO_3$, $(Cu,Zn)Cl_2$, $FeCl_2$, Cu-Fe sulphide, and trace SnO_2, Sb_2O_3, $PbSb_2O_4$, and loosely bound native Au and Au+salt associations (Fig. 5e). Some $PbCO_3$, Ag, Sb_2O_3, and SnO_2 particles were observed in horizontal gypsum veins. Gold and related mineralization is dominantly microdisseminated, although alteration minerals may be up to several hundred microns in size.

Beaverhill Lake Group

Waterways Formation Beaverhill Lake Group argillaceous limestone samples examined by SEM-EDS contain calcite and 1 to 5 per cent detrital quartz, illite, chlorite, K-feldspar, and trace amounts of zircon and apatite (Figs. 5f, 6a-f). Bitumen staining is widespread in samples collected at surface and in core samples near the pre-Cretaceous unconformity where it occurs in pores and along fractures. Bitumen content may reach about 5 per cent by volume in these samples. Apart from the extensive ferric oxyhydroxide-quartz vein networks observed at surface, other relatively common minerals observed by SEM-EDS include quartz, apatite, monazite, $CeCO_3$, rutile, Fe-Ni-Cr oxides, and pyrite. Silicification is observed in some samples, and occurs as quartz micro-veinlets and disseminated microcrystalline quartz. In surface samples, hematite or ferric oxyhydroxide veinlets associated with quartz, calcite, and illite occur commonly along micro-fracture zones; core samples with vertical pyrite-bitumen filled fractures may be unaltered equivalents of these samples. Secondary calcite forms micro-veinlets or nodules in association with pyrite, illite, chlorite, apatite, monazite, rutile, and less commonly, hematite. Disseminated pyrite, which occurs in ovoid, framboidal, and irregular shapes within the limestone matrix, probably is of early biogenic origin. Elsewhere, secondary pyrite is associated with calcite micro-veining.

Gold is most abundant in the Waterways Formation samples relative to other rock units examined. On freshly broken limestone surfaces, microdisseminated Au (Fig. 5f), and *Au-Ca* and *Au-Al* elemental associations were observed as very small particles, ranging in size from <0.1 μm to ~ 5 μm. Qualitative light element EDS analysis indicated that these particles contain little or no oxygen, seemingly ruling out the possibility that these mixtures are oxides or carbonates, although it has been suggested that oxygen X-ray emission lines may have been absorbed by other nearby elements (G. LeCheminant, pers. comm., 1994). Au-Si compounds have been synthesized in the laboratory as amorphous alloys (Hasegawa, 1991), and recovery of Au-bearing Al particles in stream sediments from northeastern Alberta has been reported (S.B Ballantyne, pers. comm., 1995). Native Al has

__Figure 5.__ Backscattered electron (BSE) SEM photomicrographs. The brightness of BSE-SEM images is directly proportional to the mean atomic weight of the substrate, meaning that dense, high molecular weight substances (e.g., gold) appear bright while less dense substances (e.g., calcite, quartz) are darker. __A.__ Associated 1 to 5 μm $PbCl_2$ and AgCl particles occur on a fractured surface of Precambrian granitoid rock. 1110 ft.; drillhole Athabasca No. 1. __B.__ Native Ag occurs on the surface of a fractured epidote in altered Precambrian granitoid rocks. 910 ft.; drillhole Ells Gold No. 1. __C.__ An aggregate of <0.5 to 3 μm Au and Au-Si particles on a cut and polished surface of altered Precambrian granitoid. 1028 ft.; drillhole Athabasca No. 3. __D.__ Enlargement of photomicrograph C showing bright 1 μm particles of Au rimming hexagonal Au-Si particles. Oxygen was not detected by light element EDS analysis of the hexagonal Au-Si particles. __E.__ A single 2 μm particle of native Au occurs on a fractured surface of a redbed siltstone. 925 ft.; drillhole Athabasca No. 1. __F.__ A single 5 μm gold particle occurs within the pore space in a micritic limestone. This grain is associated with microcrystalline calcite, which occurs in a veinlet that follows the boundary between two calcite grains. Surface sample F-02.

recently been reported in oceanic sediments proximal to a hydrothermal vent system (Devkov et al., 1995).

The largest gold particle observed was 400 μm in diameter, but most commonly Au occurs as 1–5 μm particles surrounded by a cloud of sub-micron particles (Fig. 6a–c). Gold shows a close relationship with other metallic minerals, which may occur as alloys (Fig. 6c) or native metals (Fig. 6d). Gold also displays relationships to alteration, with more silicified limestones containing more Au particles. Au-salt relationships are also observed in the limestone samples (Fig. 6e). In hand specimen, Au-bearing rocks show few apparent signs of alteration, but microscopic monazite is observed as an alteration product in many samples (Fig. 6f).

Silver minerals, including native Ag and AgCl, are relatively less common in Waterways Formation limestones, and are not as widely distributed as Au. Although Ag locally is associated with Au or is present as electrum, Ag- and Au-bearing minerals apparently do not co-exist at the micron to millimetre scale. Native Cu and Cu-Zn (brass) are the most common metallic minerals in the limestones, and occur as disseminated particles, flakes, and aggregates of flakes, or in association with Au particles (Fig. 6d, e), with calcite and clay, or with salts (Fig. 6e). $PbCO_3$ and $PbCl_2$ also are widely distributed but are less abundant than Cu and Cu-Zn. Trace metallic minerals include native Zn, Ni-Co-Cr oxide, SnO_2, Sb_2O_3, native Bi, $BiCl_3$, and scheelite.

Beaver River sandstone

Beaver River sandstones are oil-stained and variably porous. Secondary calcite, NaCl, KCl, monazite, and $CeCO_3$ occur locally with hematite and pyrite. In some parts of the sandstone sequence ferric oxyhydroxides may be as high as 10 per cent, imparting a brown colour to the rocks. Au-bearing particles were identified by SEM-EDS of the Beaver River sandstone, both in polished thin sections and on freshly broken surfaces. Au phases, including native Au (1–5 μm), Au-Ag, and Au-Cd, are less abundant than in the Beaverhill Lake limestones. Other metallic minerals and elemental associations observed include Ag, Cd-Pb, Cu, Cu-Zn, Sb_2O_3, and SnO_2.

Summary of metallic minerals and alteration

In the samples examined, the most abundant Au and other microdisseminated polymetallic minerals occur in the Waterways Formation of the Upper Devonian Beaverhill Lake Group. Here Au occurs in association with Ag, Cu, Zn, Pb, Cd, Fe, Cr, Ni, Sb, Bi, Cl, Ca, Al, and Si. Gold is next most abundant in basement rocks where it is associated with Ag, Cu, Pb, Sb, Sn, W, Si, and Cl. Gold and related minerals are least abundant in samples of the Basal Red Beds and BRS, although the sample set ($n=35$) is by no means comprehensive and these results should be viewed as preliminary only. Results are unavailable for much of the evaporite and carbonate sections of the Lower and Upper Elk Point groups.

Mineralogical data, summarized in Table 1, were collected and synthesized prior to establishing the relations between redox state and alteration and it is therefore impossible to integrate the observations summarized in Table 1 directly into a discussion of redox state. Examination of the alteration and metallic minerals (Table 1) shows that microdisseminated polymetallic minerals are associated with reduced (e.g., pyrite), oxidized (e.g., hematite), and intermediate oxidation (e.g., native S) levels, indicating that studies relating redox indicator assemblages to alteration and microdisseminated minerals should be carried out.

A unique feature of the alteration mineralogy is the widespread occurrence of Ce-bearing phosphate and carbonate minerals in all units examined. Ce occurs in two valence states; under reducing conditions as Ce^{3+} and under oxidizing conditions as Ce^{4+}. In oxic near-surface oceanic waters, microbially mediated oxidation of Ce^{3+} results in production of less soluble Ce^{4+} which preferentially is removed from the water column resulting in a "negative Ce anomaly" (values

__Figure 6.__ BSE-SEM photomicrographs. __A.__ A single 1 μm gold particle observed within the pore space in a micritic limestone. Upper Devonian Waterways Formation; surface sample F-02. __B.__ Microdisseminated gold particles ranging in size from <0.2 to 1.3 μm in size occur on a fractured surface of Waterways Formation limestone. Upper Devonian Waterways Formation; surface sample F-20. __C.__ A group of native gold grains ranging in size from <1 to 7 μm occur with a single Cu-Zn particle on a fractured surface of micritic limestone. Upper Devonian Waterways Formation; surface sample F-20. __D.__ A150 μm sheaf of native copper flakes occurs within an enlarged pore in argillaceous limestone. Upper Devonian Waterways Formation; surface sample 93-AI. __E.__ A single 3 μm AuAg alloy (electrum) particle occurs in association with gypsum and halite in a pore in micritic limestone. Upper Devonian Waterways Formation; surface sample WK-14. __F.__ Authigenic monazite replacing microcrystalline dolomite. Middle Devonian Elk Point Group; 161.5 m; drillhole T3.

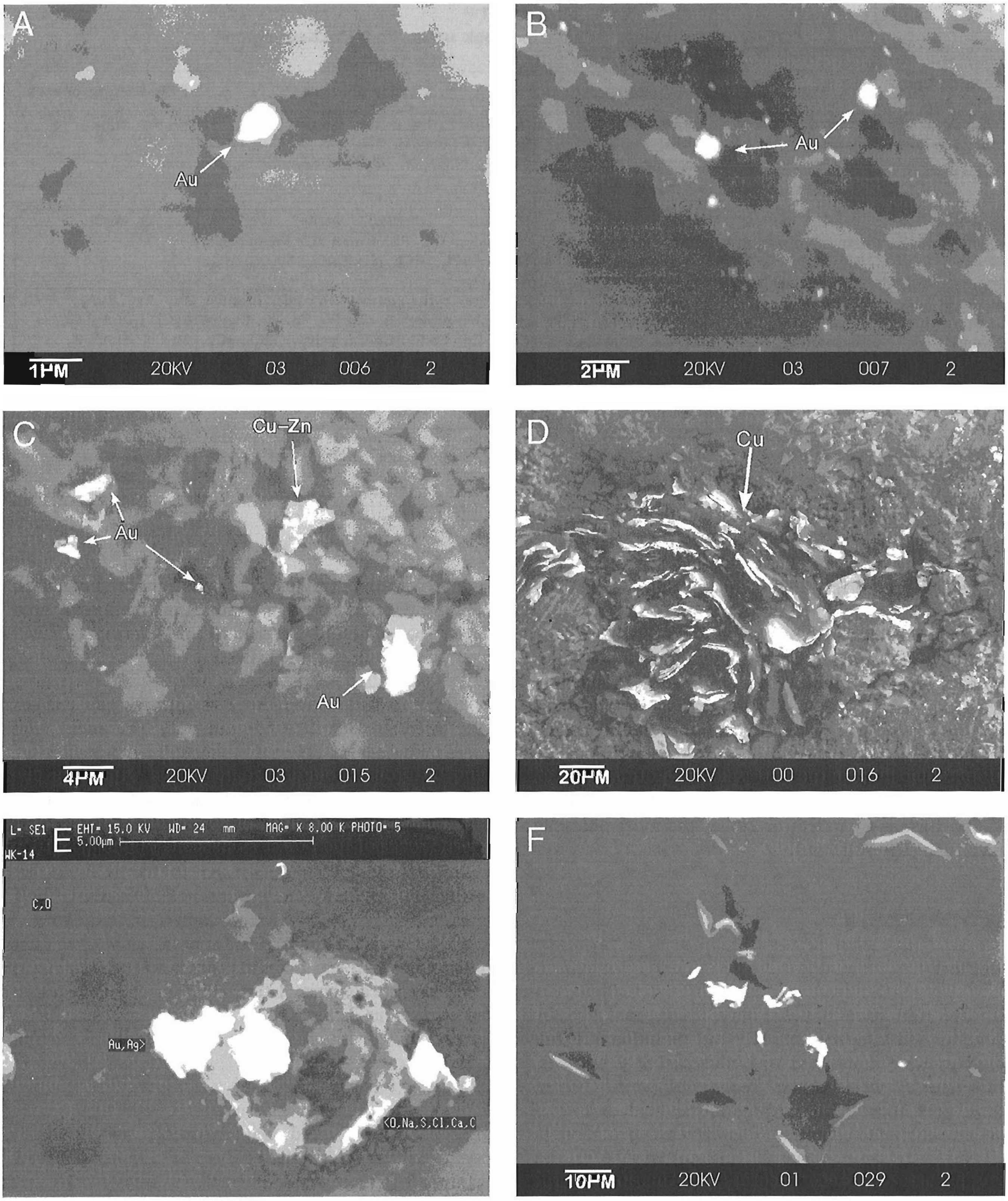

less than 1) characteristic of ocean waters (Sholkovitz and Schneider, 1991). In suboxic to anoxic ocean waters and pore fluids from anoxic marine sediments the Ce anomaly commonly is "positive" (greater than 1) reflecting the enhanced solubility of cerium as Ce^{3+} under reducing conditions. Although little information is available on the concentrations of rare earth elements (REE) in sedimentary brines, the apparent

Table 1
Summary mineralogy of selected rock units, Fort MacKay region

Rock Unit/ Age	Lithology[1]	Alteration	Metallic Minerals	PGM-bearing phases
TaltsonMagmatic Zone; 1.8–2.0 Ga	Altered granitoid gneisses	Epidote, chlorite, calcite, quartz, monazite, barite, $CeCO_3$, native S, and NaCl, KCl	Hematite, pyrite, galena, scheelite (Fe,Ti, Cr)-oxides, Cu, Pb, $PbCl_2$, $FeCl_2$, $PbCO_3$, *$PbSb_2O4$, Sb_2O_3, SnO_2*	Au, Ag, AgCl, *Au-Si*
Basal Red Beds; Middle Devonian	Regolith and red sandstone,reddish green siltstone; thin gypsum veins	Gypsum, monazite, quartz, native S, $CeCO_3$, (Na, K)Cl	Hematite, scheelite, barite (Fe,Ti,Cr, Ni)-oxides, Cu, Pb, Cu-Zn (Cu,Fe)-sulphide, $FeCl_2$, $PbCl_2$, $NiCl_2$, $(Cu,Zn)Cl_2$, *Sb_2O_3, SnO_2, $PbSb_2O_4$*	Au, Ag, AgCl
Beaverhill Lake Group; Upper Devonian	Limestone, argillaceous limestone, fossiliferous limestone	Calcite, quartz, hematite, illite, chlorite, monazite, barite, native S, $CeCO_3$, (Na,K)Cl, KCl	Hematite, pyrite, quartz, Ni-oxide, ilmenite, (Fe,Cr,Ni)-oxide, Cu, Cd, Pb, Zn, Sn, Cu-Zn, Cu-Fe-Zn, Cu-Sb, Cd-Zn, galena, Sb_2S_3 (Cu, Sn)-sulphide (Ni,Co)-sulphide, $PbCl_2$, $FeCl_2$, $BiCl_3$, $PbCO_3$, *Sb_2O_3, SnO_2*	Au, Ag, AuAg, AuCl, AgCl, (Au,Ag)-Cl, Au-Cu, Au-Cu-Z, Au-Ag-Cu, Au-Cd, Cd-Zn-Au, Au-Zn, Au-Pd, Ti-Au, Cu-Ag, *Au-Ca, Au-Al, Au-Si*
Beaver River sandstone; Cretaceous	Fine grained, quartz and goethite cemented quartz sandstone	Calcite, quartz, monazite, illite, $CeCO_3$, NaCl, KCl, chlorite	Hematite, geothite, ilmenite (Fe,Ni,Ti)-oxide, Cu, Zn, Pb, Cu-Zn, Cd-Pb, Sb_2S_3, *Sb_2O_3, SnO_2*	Au, Ag, AuAg, Au-Cd, AgCl, *Au-Si*

[1]Lithological descriptions reflect the type of samples examined

enrichment in Ce in rocks in northeastern Alberta is consistent with i) the presence of oxidized brines and ii) microbial mediation of redox reactions. However, the close spatial association of reduced, elemental, and oxidized sulphur species and abundant Ce minerals tends to indicate that a complex array of redox processes proceed simultaneously. The presence of Ag-, Pb-, Bi-, Cu-, and Fe-chloride minerals, and the Au+salt association, indicate that Cl is a major component of mineralizing solutions, making oxidized, Cl-rich formation waters or brines the most plausible metal carrying solutions.

GEOCHEMISTRY

Methods

Surface and core samples have been analyzed by solution- and laser ablation-ICP-MS. Solution ICP-MS analyses were conducted on pulverized 2 g samples. The samples were reacted sequentially with 7.5 ml nitric acid then 7.5 ml hydrofluoric acid and were subsequently decomposed by microwave digestion in sealed teflon bombs for 20 minutes at 180°C and 100 psi. The samples were cooled, decanted, heated to dryness and redissolved in 15 ml 50:50 HCl–HBr. The samples were then diluted 55–110 times with a 1000 ppm KI solution and analyzed for Au by solution ICP-MS using a VG PQ II Turbo+ ICP-MS. For most samples, a white, insoluble residue remained after digestion. Gold was detected by laser ablation ICP-MS analysis of some residues, indicating that the digestion method did not result in complete extraction of gold from the samples. The results of solution ICP-MS analyses are shown in Table 2.

Small rock chips were broken from samples selected for laser ablation ICP-MS analysis. The rock chips were mounted in a teflon sample holder and placed in a sealed quartz glass cell which was flooded by ICP-MS grade Ar. The incident laser beam was focused above the sample surface and was rastered on 100 μm centres over a 400 x 400 μm area. Vaporized ablated material was carried in a stream of Ar to the ICP-MS for analysis. The ICP-MS was calibrated against NIST standard glass 612 which contains approximately 5 ppm Au. Internal calibration for each sample was done using Ca which was obtained for these rocks by X-ray fluorescence analysis. Laser ablation ICP-MS results are shown in Table 3.

Results

The maximum gold concentration measured by solution mode ICP-MS analysis is 130 ppb from a sample of Waterways Formation limestone. Laser ablation ICP-MS results for gold on a similar suite of samples yielded maximum average concentrations of gold of 1.08 ppm in a sample of Beaver River sandstone (average of 4 raster patterns) and 1.60 ppm in limestone of the Waterways Formation. Laser ablation ICP-MS results typically are higher by an

Table 2
Solution ICP-Ms analyses for surface and core samples

	Unit	Lithology	Au (ppm; g/t)
Surface Samples			
RR45	Beaver River sandstone	Oil-stained quartz sandstone	0.020
RR21	Beaver River sandstone	Oil-stained quartz sandstone	0.020
WK31	Beaver River sandstone	Oil-stained quartz sandstone	0.001
WK06	Lower McMurray Fm	Iron-stained quartz sandstone	0.014
WK15	Waterways Fm	Limestone	0.001
RR41	Waterways Fm	Limestone	0
RR09	Waterways Fm	Limestone	0.030
F18	Waterways Fm	Limestone	0.005
F19	Waterways Fm	Limestone	0.010
F02	Waterways Fm	Limestone	0.005
F22	Waterways Fm	Limestone	0.006
F01	Waterways Fm	Limestone	0.008
Core Samples			
T3 124.98 m	Waterways Fm	Limestone	0.020
T3 147.6 m	Waterways Fm	Limestone	0.130
T4 313.08 m	Basal Red Beds	Redbed	0.040
T4 315.6 m	Basal Red Beds	Redbed	0.014
86-2R 919 ft.	Winnipegosis Fm	Limestone	0.014

order of magnitude than corresponding solution ICP-MS analyses. The presence of detectable Au in residues, as noted above, implies that solution ICP-MS results may be low by an unknown amount. Although the results provided in Tables 2 and 3 are not fully quantitative, they suggest that maximum concentrations of gold determined by both solution and laser ablation ICP-MS may be anomalous given that the mean gold concentration in lithified limestone is 7 ppb (Boyle, 1979).

Inconsistencies between assay methods also have been reported by industry and may be related to the widespread distribution of dispersed organic material or bitumen in these rocks. Gatellier and Disnar (1989) encountered problems in obtaining reliable gold analyses of organic-rich rocks, and showed that gold was not solubilized by hot $HCl/HF/HNO_3$ digestion of intimately mixed gold and organic material. Furthermore, their study showed that roasting of samples at 900°C for 12 hours resulted in significant increases in Au contents due to liberation of Au by breakdown of organic material. An intimate association of Au with hydrocarbons, or with dispersed organic material, may prevent total recovery of gold by conventional extraction techniques. This may be further complicated by the micron sized gold particles which, upon liberation by destruction of organic material, may escape recovery due to their extremely small particle size.

BASIN EVOLUTION AND WATER-ROCK INTERACTION

Paleothermometry

On the basis of apatite fission track analysis and inversion modeling, Willett and Issler (1992) and Issler (pers. comm., 1995) infer maximum paleotemperatures of about 90°C at 60 Ma at the Precambrian surface during deepest Laramide burial in the region of Fort MacKay. Their data also show that Lower Cretaceous Mannville Group samples collected from cores taken to the west of Fort MacKay attained an estimated maximum temperature of about 75°C at this time.

Although there are few constraints on the pre-Cretaceous thermal history of Paleozoic rocks in northeastern Alberta, work at Pine Point (Fowler et al., 1993; Macqueen and Powell, 1983; Powell and Macqueen, 1984) and in central Alberta (Meijer Drees et al., 1995) shows no evidence for a regional Paleozoic thermal event that could give rise to temperatures significantly in excess of 90°C in northeastern Alberta. Powell and Macqueen (1984) and Fowler et al. (1993) inferred localized introduction of heated fluids in the Pine Point area. At Pine Point it is probable that small-scale thermal anomalies reflect hydrothermal activity associated with aggressive replacement textures and hydrothermal dolomitization documented at Pine Point by, among many others, Beales and Jackson (1966), Anderson and Macqueen (1989), and Qing and Mountjoy (1994). Morrow and Aulstead (1995) provided evidence consistent with a Late Devonian to Carboniferous age for coarsely crystalline dolomite of the diagenetic Manetoe and Presquile lithofacies of the southern N.W.T. Fluid inclusion homogenization temperatures for Presquile dolomite at Pine Point range between 92 and 106°C (Qing and Mountjoy, 1994). No evidence for similar coarsely crystalline replacement dolomite has been reported in the Fort MacKay region of northeastern Alberta.

Table 3
Laser ablation ICP-MS analyses for surface samples

Sample	Unit	Lithology	Raster Area	CaO (%)	Rh (ppm)	Pd (ppm)	Pt (ppm)	Au (ppm)
RR45	Beaver River sandstone	Oil-stained quartz sandstone	1	0.06	0	0	0	3.48
			2	0.06	0	0	0	0.05
			3	0.06	0	0.01	0	0.78
			4	0.06	0	0	0	0.02
			Avg.	**0**	**0**	**0**	**0**	**1.08**
WK06	Beaver River sandstone, Lower McMurray Fm	Fe-stained quartz sandstone	1	0.11	0	0.01	0	0.08
			2	0.11	0	0.02	0	0.07
			3	0.11	0	0.02	0	0.05
			4	0.11	0	0.02	0	0.06
			5	0.11	0	0.04	0	0.14
			6	0.11	0	0.03	0	0.07
			7	0.11	0	0.05	0	0.09
			8	0.11	0	0.02	0	0.04
			9	0.11	0	0.02	0	0.14
			Avg.	**0.11**	**0**	**0.02**	**0**	**0.08**
RR09	Waterways Fm	Limestone	1	54.4	0.01	0.01	0	0.13
			2	54.4	0.01	0.02	0	0.05
			3	54.4	0.02	0.01	0	0.11
			4	54.4	0.01	0.01	0	2.17
			5	54.4	0.02	0.02	0	0.09
			6	54.4	0.01	0.01	0	0.16
			Avg.	**54.4**	**0.01**	**0.01**	**0**	**0.45**
WK15	Waterways Fm	Limestone	1	53.4	0.01	0.4	0	3.71
			2	53.4	0.01	0.01	0	0.51
			3	53.4	0	0.05	0	2.29
			4	53.4	0.01	0.02	0	0.87
			Vein	53.4	0.01	0.06	0	0.63
			Avg.	**53.4**	**0.01**	**0.03**	**0**	**1.60**
WK30B	Waterways Fm	Limestone	1	52.4	0.01	0.01	0.01	0.35
			2	52.4	0.02	0.01	0.01	0.53
			3	52.4	0.02	0.01	0.01	0.19
			4	52.4	0.02	0.01	0.01	0.18
			5	52.4	0.02	0.01	0.01	0.12
			Avg.	**52.4**	**0.02**	**0.01**	**0.01**	**0.27**
RR43A	Waterways Fm	Limestone	1	50.3	0.02	0.01	0.01	0.16
			2	50.3	0.02	0.01	0.01	0.15
			3	50.3	0.02	0.02	0	1.05
			4	50.3	0	0	0	0.02
			5	50.3	0	0.01	0	0.11
			6	50.3	0	0	0.01	0.25
			7	50.3	0	0	0	0.16
			8	50.3	0	0	0.01	0.31
			9	50.3	0	0	0	0.12
			10	50.3	0	0	0	0.04
			11	50.3	0	0	0	0.07
			12	50.3	0	0	0	0.66
			13	50.3	0	0	0.01	0.18
			14	50.3	0	0	0	0.08
			15	50.3	0	0	0	0.16
			Avg.	**50.3**	**0**	**0**	**0.01**	**0.23**

Alteration of Precambrian basement

Evidence for alteration of basement rocks by fluids of probable sedimentary origin is most abundant near the upper contact with overlying Phanerozoic sedimentary rocks. Although it is not pervasively developed, alteration of the upper 1 to 5 m or more of basement gneisses is common and ranges from minor hematitization along the margins of quartz and calcite veinlets, to near complete low temperature recrystallization of original metamorphic and igneous fabric, producing a fine grained, variegated orange-red to maroon mixture of quartz, clays, carbonate, and hematite. Norris (1963) described sapropelic alteration of rocks at the Precambrian surface, which is consistent with the arid continental conditions that persisted at the time of deposition of the Basal Red Beds.

McDonough and Abercrombie (1995) investigated reported occurrences of copper minerals (Godfrey, 1986) at Stony Islands, Slave River, northeastern Alberta. At Stony Islands, a regolithic debris flow unit of the La Loche Formation (Basal Red Beds) directly overlies pristine to altered Precambrian granitoid gneisses (Fig. 4a). Altered Precambrian gneisses locally are gossanous or calcitized and are cut by 2 to 5 cm wide calcite-azurite-malachite veins (Fig. 4e) that pass upwards into coarse conglomeratic units of the La Loche Formation. The latter is cemented by azurite- and malachite-bearing calcite identical in appearance and continuously traceable to vein-calcite cutting basement rocks.

Although the origin of the calcite veins is not known with certainty, it is unlikely that the vein calcite and calcite cement were sourced from the high metamorphic grade metaigneous basement rocks at Stony Islands. Penetration of carbonate-rich fluids originating within the sedimentary sequence into basement rocks is a much more plausible scenario and strongly implies that fluids derived from the sedimentary basin have interacted with basement rocks. Regionally, it is likely that flow of sedimentary brines in basement rocks is controlled by the distribution of fractures. Fracturing may be expected along major crustal shear zones, such as the Great Slave Lake Shear Zone and the Snowbird Tectonic Zone (Fig. 1), as well as along later, brittle faults cutting Proterozoic rocks (McDonough, 1997, *this volume*) and pre-Laramide faults cutting sedimentary rocks of the WCSB.

Borehole televiewer logging of a wildcat well (7-32-89-10 W4; C.W. Hunt, pers. comm.) drilled to a depth of 1450 m in the vicinity of Fort McMurray, Alberta, shows that basement granitoid gneisses of the Taltson Magmatic Zone (McDonough, 1997, *this volume*) are fractured to a depth of 450 m beneath the Precambrian surface. Analyses of waters recovered from drill stem tests in this interval show that the waters are brines of probable sedimentary origin (Abercrombie, unpublished data), in agreement with Bottomley et al. (1994) who concluded, on the basis of B isotopic signatures, that a significant component of waters found in mines in the Precambrian Shield originated as sedimentary brines. Therefore, interaction between sedimentary basin brines and basement rocks may be an integral part of brine evolution in near-basement parts of the basin.

Salt solution and karsting

Water-rock interaction has had a significant effect on the physical properties and structure of Phanerozoic rocks in northeastern Alberta. Dissolution of Elk Point Group halite units by inflowing waters at the eastern margin of the basin has resulted in removal of halite over a minimum distance of 20 to 30 km from the present solution edges of all but the lower Lotsberg salt (Hamilton, 1971; Meijer Drees, 1986). This has led to the development of collapse breccias in overlying rocks and these may have provided conduits for subsequent fluid flow and karst development. Locally, collapse breccias may be infilled with coarsely crystalline calcite and/or bitumen.

Development of solution cavities and karsting occurred at unconformities such as the post-Elk Point Group exposure surface (Fig. 3), developed at the level of the Watt Mountain Formation shale, and the pre-Cretaceous erosion surface. For instance, the Grosmont carbonate platform is extensively karsted where it subcrops beneath the pre-Cretaceous unconformity. Collapse features have been identified on the pre-Cretaceous unconformity (Fig. 4d) and the presence of numerous sinkholes in the contemporary land surface attests to the continuation of karsting to the present (Tsui and Crudden, 1984)

Redox zonation

Sulphur has been documented in three valence states in Paleozoic formations in northeastern Alberta. Oxidized S (S^{+6}) chiefly occurs as gypsum and anhydrite in evaporite rocks, whereas reduced S (S^{-2}) dominantly occurs as pyrite in reduced marine limestones and shales. Occurrences of native S (S^{o}) demarcate the transition between relatively more oxidized and more reduced redox zones. Iron also shows variations in redox state, occurring in oxidized form as hematite and in reduced form as pyrite.

Redox zonation can be represented by constructing a phase diagram showing the relative stability of mineral and aqueous species observed in rocks from northeastern Alberta. Stability relations for selected mineral and aqueous species in the system Ca-Fe-H-C-O-S are shown in Figure 7, in terms of pH and the logarithm of oxygen fugacity (fO_2;

corresponding approximately to the partial pressure of oxygen). This diagram has been constructed for water compositions typical of Middle Devonian brines from northeastern Alberta (Hitchon, 1993) at a temperature of 25°C and using thermodynamic parameters from the SUPCRT92 database (Johnson et al., 1993) and Robie et al. (1979). Increasing oxygen fugacity (less negative $\log(fO_2)$ represents increasingly oxidized conditions; a surface water in equilibrium with the atmosphere would have a $\log(fO_2)$ value of approximately -3.6.

The phase diagram shown in Figure 7 can be used to place constraints on the redox conditions in the subsurface in northeastern Alberta. Based on the presence of calcite and/or dolomite throughout most of the Paleozoic succession, and on the presence of white mica or illite in clastic units of the Elk Point Group, pH is constrained to range between about 5 and 6 in Paleozoic rocks from northeastern Alberta. This is consistent with the results of Hitchon (1993), who showed that pH calculated under reservoir conditions for Paleozoic formation waters from northeastern Alberta most commonly ranged from 5.0 to 5.9. Based on the occurrence of calcite-anhydrite-hematite throughout much of the Lower Elk Point Group, oxygen fugacity in these rocks must lie above the hematite-pyrite boundary and therefore must be greater than a minimum $\log(fO_2)$ value of -64.5. Although not shown in Figure 7, the occurrence of native Cu in hematite-bearing clastic and carbonate units (Table 1) provides some information on maximum oxygen fugacity levels within the Elk Point Group. The presence of native Cu and the apparent absence of oxygen-bearing Cu minerals such as cuprite and tenorite, mean that the maximum oxygen fugacity at this location probably was no higher than about -51 at 25°C.

The co-existence of calcite, pyrite, and bitumen, and the absence of anhydrite and native S, is consistent with oxygen fugacities below the anhydrite stability curve. Such conditions probably occur in reduced marine limestones and dolostones of the Waterways and Winnipegosis formations where the presence of calcite buffers oxygen fugacities to values above the lower redox limit of calcite stability. Below $\log(fO_2)$ levels of -71.6 in the presence of water, $CO_{2(g)}$ is reduced to methane and oxygen. The reverse reaction, whereby oxygen combines with methane to yield carbon dioxide and water, may serve as an analogue for hydrocarbon biodegradation. Under these conditions, calcite is unstable and the assemblage pyrite-bitumen would therefore record lowest oxygen fugacities, hence the most reducing conditions. This could occur in the McMurray Formation, where both

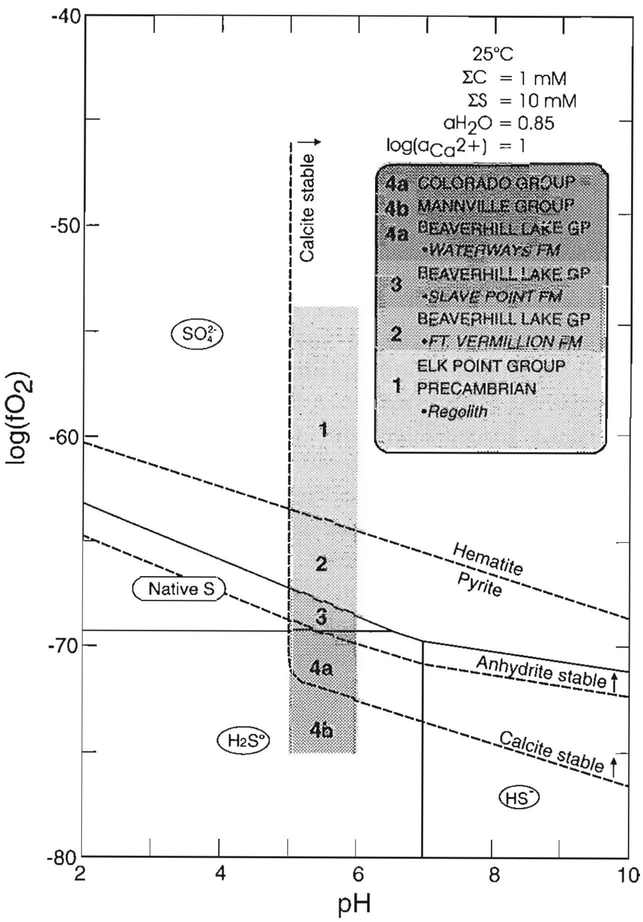

Figure 7. *pH versus log (fO_2) diagram showing mineral-fluid phase relations in the Fe-C-O-H-S system at 25°C calculated for conditions in the D1 aquifer system in northeastern Alberta. Thin solid lines show the boundaries between predominance fields for sulphur species including native S. Dashed lines show the stability limits for minerals. The shaded region illustrates conditions prevailing through the stratigraphic column and shows that strong redox contrasts are evident within the stratigraphic column.*

pyrite and biodegraded bitumens occur in bitumen-saturated quartz sandstones, or in open fracture systems in carbonate rocks where fluids are isolated chemically from the bulk rock. The wide distribution of biodegraded oils in the McMurray Formation and in the Beaverhill Lake Group below and near the sub-Cretaceous unconformity, suggests that hydrocarbon biodegradation can be called upon to reduce the relatively more oxidized waters originating in the Elk Point Group. Work is underway to carefully document mineral associations and parageneses to more accurately constrain redox conditions throughout the stratigraphic column in the Fort MacKay area.

Origin of native sulphur

Native S occurs regionally in the stratigraphic interval between the base of the Waterways Formation and the top of the Elk Point Group, and locally along fractures cutting organic-rich laminites of the Winnipegosis Formation and marine limestones of the Waterways Formation. Formation of native S can occur by a number of biochemical and thermochemical pathways through oxidation of sulphide or reduction of sulphate. At temperatures below 80 to 100°C native S can be produced by bacterial sulphate reduction (BSR) with accompanying oxidation of organic material. The organic source can either be immature organic detritus or liquid hydrocarbons in the case of native sulphur associated with salt in the Gulf Coast, U.S.A., and elsewhere (Ruckmick et al., 1979). At temperatures above 100 to 120°C, bacterial reactions are unimportant and thermochemical sulphate reduction (TSR) becomes possible for kinetic reasons. The dissolution of gypsum or anhydrite and the production of oxidized carbonate species, dominantly bicarbonate and gaseous CO_2, results in precipitation of calcite as a product of both BSR and TSR (Hutcheon et al., 1995; Machel et al., 1995).

In the absence of localized introduction of heated fluids during pre-Cretaceous burial, sulphate reduction is constrained to have occurred below a maximum temperature of 90°C and therefore likely occurred through BSR in a manner similar to evaporite-hosted native S deposits of the Trans-Pecos region of west Texas (Hentz et al., 1989). Discharge of saline, H_2S-bearing brines in springs at Saline Lake and elsewhere in the Athabasca River valley (Ells, 1926; Carrigy, 1959; Borneuf, 1982; J. Cody, pers. comm., 1995) suggests that BSR may be active in the subsurface of northeastern Alberta to the present day. Further chemical, isotopic, and petrological investigations of the occurrence of native sulphur and its relation to redox processes are underway.

Silica cementation of the Beaver River sandstone

The quartz cemented Beaver River sandstone is unique in relation to other Mesozoic sandstones in the eastern part of the WCSB. It is extremely unusual for sandstones that have never been buried below about 1-2 km to be intensely quartz cemented (Bjørlykke and Egeberg, 1993; Abercrombie et al., 1994). Silica solubility rises rapidly with temperature and is favoured under relatively more alkaline conditions. Abundant quartz cement therefore implies the cooling of warm, alkaline waters with elevated silica content. This, however, is inconsistent with the burial history and quartz-rich bulk composition of the McMurray Formation.

Because the McMurray Formation has not been buried to depths sufficient to dissolve significant quantities of silica, and because of its quartz-rich composition which is consistent with relatively more acidic rather than alkaline conditions (Hutcheon et al., 1989), it is unlikely that the waters which transported silica to the Beaver River sandstone originated within the McMurray Formation. It is suggested that the Beaver River sandstone represents a geochemical or diagenetic facies of the lower unit of the McMurray Formation which formed in a paleo-discharge zone where warm, somewhat alkaline waters rising along fractures cutting Waterways Formation limestones were discharged into the basal McMurray Formation. Elevated silica concentrations in these waters were unsustainable once the fluid passed into the cooler, quartzose sands of the basal McMurray Formation, and the precipitation of quartz, or more probably metastable silica polymorphs, occurred as a result. This interpretation is supported by the presence of silica microveinlets in underlying Devonian strata where precipitation of silica minerals would also have been initiated by cooling of upward flowing silica-charged waters (Feng and Abercrombie, 1994) in a thermal spring.

The presence of a silicifed sandstone in the basal McMurray Formation may be of importance to localization of microdisseminated polymetallic mineralization. If, as suggested here, the Beaver River sandstone records discharge of warm waters, these waters may have carried metals from depth to the base of the Cretaceous sandstones. Silicification is common in Carlin-type deposits where it may be associated with gold mineralization (Berger and Bagby, 1993). The Beaver River sandstone may therefore be a key element in documenting flow of heated waters in the region, particularly if it can be demonstrated by drilling that a silica replacement "stockwork" or fracture system underlies outcrops of the Beaver River sandstone.

HYDROGEOLOGY

Paleohydrogeology

Two dimensional models for hydrogeological evolution of the WCSB consistently show the northeastern onlap/erosional edge of the basin to be a site of regional discharge for either compactionally or gravitationally driven west-to-east flow (e.g., Hitchon, 1984;

Garven and Freeze, 1984; Garven, 1989). This may be true at some times. However, it can be shown, for instance, that during the Middle Devonian, when nonmarine salts of the Lotsberg Formation accumulated in a nonmarine basin south of the Peace River–Athabasca Arch (Fig. 1), a basin-scale hydrological divide between eastward and westward flow must have occurred some distance into the basin. The position of this divide would have moved through space and time such that rocks in the eastern part of the basin would at some times have experienced westward flow of descending, low-salinity waters of meteoric origin and at other times have experienced eastward flow of warm, ascending, higher salinity, basin-derived fluids.

Accurate reconstruction of basin paleohydrogeology may be possible, but is beyond the scope of this paper. Significant information exists regarding the present-day hydrogeology of northeastern Alberta and can be used to portray contemporary flow systems in the region, however. The usefulness of this approach can be assessed once accurate information on the spatial distribution of alteration and micro-disseminated polymetallic minerals is available to be compared with present-day flow. Mismatches between the distributions of observed mineralogy/alteration and present-day water types would imply that paleoflow differed from present flow and may provide constraints useful in mineral exploration. Studies of the mineralogy and compositions of unaltered, altered, and metallic mineral-bearing rock units are underway to assess this possibility.

Present-day hydrogeology

Hackbarth and Nastasa (1979) identified three hydrostratigraphic units in the Fort MacKay–Fort McMurray region. These are summarized in Table 4 and illustrated in Figure 8. Pre-Prairie Formation rocks including the Basal Red Beds, Contact Rapids, and Winnipegosis formations make up D1, which is equivalent to the combined Basal aquifer and Contact Rapids–Winnipegosis aquifer system of Bachu and Underschultz (1993). On the basis of results presented above, it is suggested that fractured and altered rocks of Precambrian age underlying the Basal Red Bed sequence should also be included in D1. West of the Athabasca River, D1 is characterized by up-dip flow to the northeast, with salinities exceeding 300 000 mg/l total dissolved solids (TDS), decreasing to <50 000 mg/l TDS east of the Athabasca River (Hackbarth and Nastasa, 1979; Bachu and Underschultz, 1993).

Table 4
Hydrostratigraphy in the Fort MacKay region, northeastern Alberta (modified from Hackbarth and Nastasa, 1979)

Hydrostratigraphic Unit	D1	D2	KQ
Stratigraphic Units	Precambrian Elk Point Gp	Beaverhill Lake Gp Woodbend Gp	Mannville Gp Quaternary
Salinity (as TDS; mg/L)	>200 000	10 000–70 000	>5000
Aqueous sulphide (bisulphide, HS^-)	not detected	present	present

The D2 hydrostratigraphic unit of Hackbarth and Nastasa (1979) is equivalent to the Beaverhill Lake–Cooking Lake aquifer system of Bachu and Underschultz (1993) and comprises the Slave Point, Beaverhill Lake and Cooking Lake formations. To the west of the zone of salt solution of the Prairie Formation, D1 and D2 are separated by the Prairie–Watt Mountain aquiclude system. To the east, where impermeable halite units of the Prairie Formation have been dissolved and the Watt Mountain and Fort Vermillion formations are thin, D1 and D2 merge. Regionally, formation water salinities within D2 are <70 000 mg/l, although a number of tests from D2 near Bitumount, north of Fort MacKay, reported salinities in excess of 200 000 mg/l TDS (Hackbarth and Nastasa, 1979).

The uppermost flow unit, the KQ hydrostratigraphic unit of Hackbarth and Nastasa (1979), comprises clastic rocks of the Lower Cretaceous Mannville Group and Quaternary alluvium. In upland areas of the Birch and Pelican mountains west of the Athabasca River, and on Stony Mountain south of the Athabasca and Clearwater rivers, Colorado Group shale outcrops mark the base of the Colorado aquitard system, which splits KQ into separate Cretaceous and Quaternary aquifer systems. Across much of the WCSB, the Colorado aquitard has acted as a regional seal for flow of waters (Connolly et al., 1991a, b) and oils (Creaney and Allan, 1992).

Based on calculated head distributions, flow within D2 west of the Athabasca River is inferred to be to the northeast (Hackbarth and Nastasa, 1979). Measured salinities of waters sampled from observation wells near Bitumount show that highly saline waters derived from solution of the Prairie Evaporite Formation presently flow upwards into the Beaverhill Lake and overlying McMurray formations at this location.

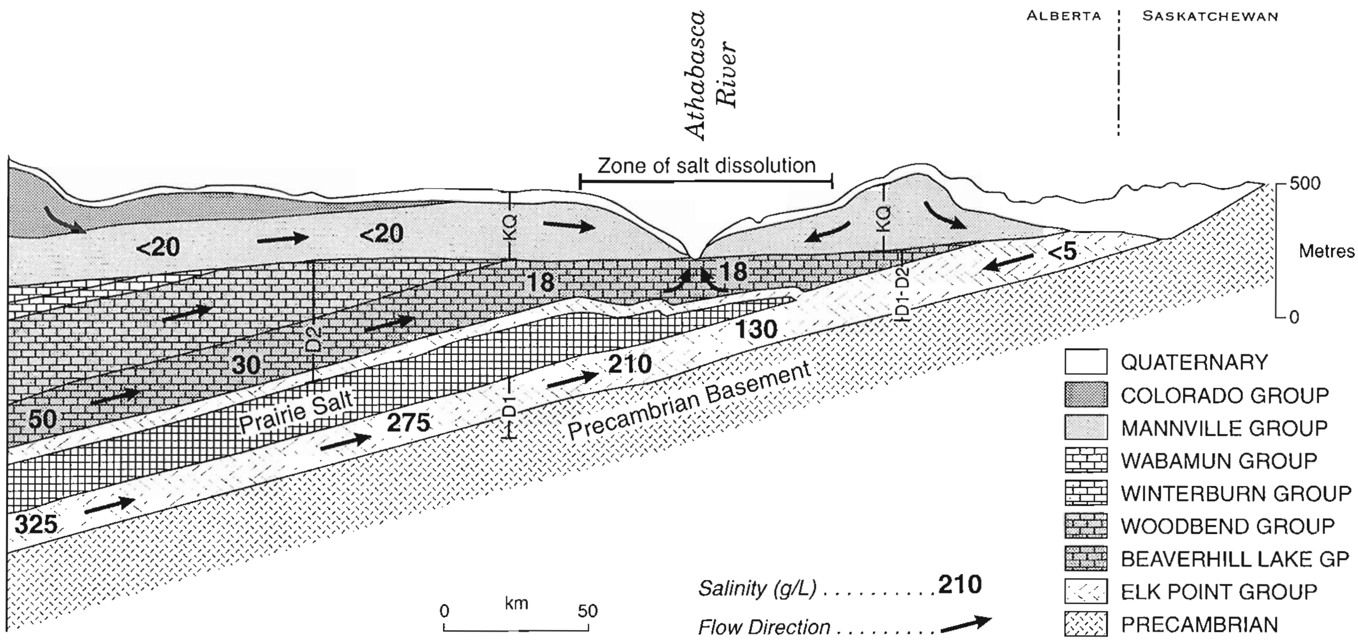

Figure 8. *Schematic representation of the hydrogeology of the Athabasca River valley in the region of Fort MacKay. Arrows indicate flow direction and are derived from potentiometric surfaces constructed from measured pressures. Numerals indicate formation water salinity in grams/litre. West of the Athabasca River the D1 and D2 aquifer systems are separated by impermeable strata of the Prairie Formation salt and Watt Mountain shale. East of the Athabasca River the D1 and D2 aquifer systems merge due to dissolution of halite in the Prairie Formation. The Athabasca River valley is the major discharge point for all aquifer systems. Modified after Bachu and Underschultz (1993).*

Examination of salinity maps for the Beaverhill Lake Formation show that salinities >100 000 mg/l are observed in D2 in a narrow zone underlying and following the course of Athabasca River from north of Bitumount to the Beaver River–Muskeg River area south of Fort MacKay (Hackbarth and Nastasa, 1979). It is of interest to note that this is approximately the same area underlain by silica cemented sandstones of the Beaver River sandstone of the Lower McMurray Formation, and is near an active discharge zone at Saline Lake (Fig. 4f). Other evidence for fluid discharge and alteration is apparent in the Athabasca River valley south of Saline Lake (Fig. 4g).

GENETIC MODEL

The salient features of the genetic model for microdisseminated polymetallic minerals are illustrated in Figure 9, as they relate to Au-Ag-Cu phases and related alteration discovered in the Fort MacKay region of northeastern Alberta. Although the importance of oxidized brines in mobilizing and transporting metals was recognized by Feng and Abercrombie (1994), the recognition of the role of redox processes in localizing alteration and deposition of microdisseminated metallic minerals is an important new element of the genetic model. The following explanation is an attempt to reconcile the unusual mineralogy and geochemistry of Au-bearing rocks in the Fort MacKay area with constraints imposed by geochemical principles and the geology and hydrogeology of the region.

The source of metals cannot be documented with certainty, but it is suggested that metals probably originated in the basement. There is good evidence that sedimentary brines have interacted with basement rocks in the past in northeastern Alberta and are associated with copper mineralization (McDonough and Abercrombie, 1995). Basement-penetrating faults are known in the Fort MacKay area (Carrigy, 1959, 1973; Hackbarth and Nastasa, 1979) and fractured and altered granites have been documented to a depth of hundreds of metres beneath the buried Precambrian surface near Fort MacKay. Metals also may have originated in the sedimentary section. Work carried out by Thiede (1975) and Thiede and Cameron (1978) in determining the Cu, Pb, and Zn contents of Elk Point Group rocks in Saskatchewan showed that it is anomalously enriched in these metals compared to other evaporite basins worldwide. Therefore, the source of metals may not be restricted to basement rocks.

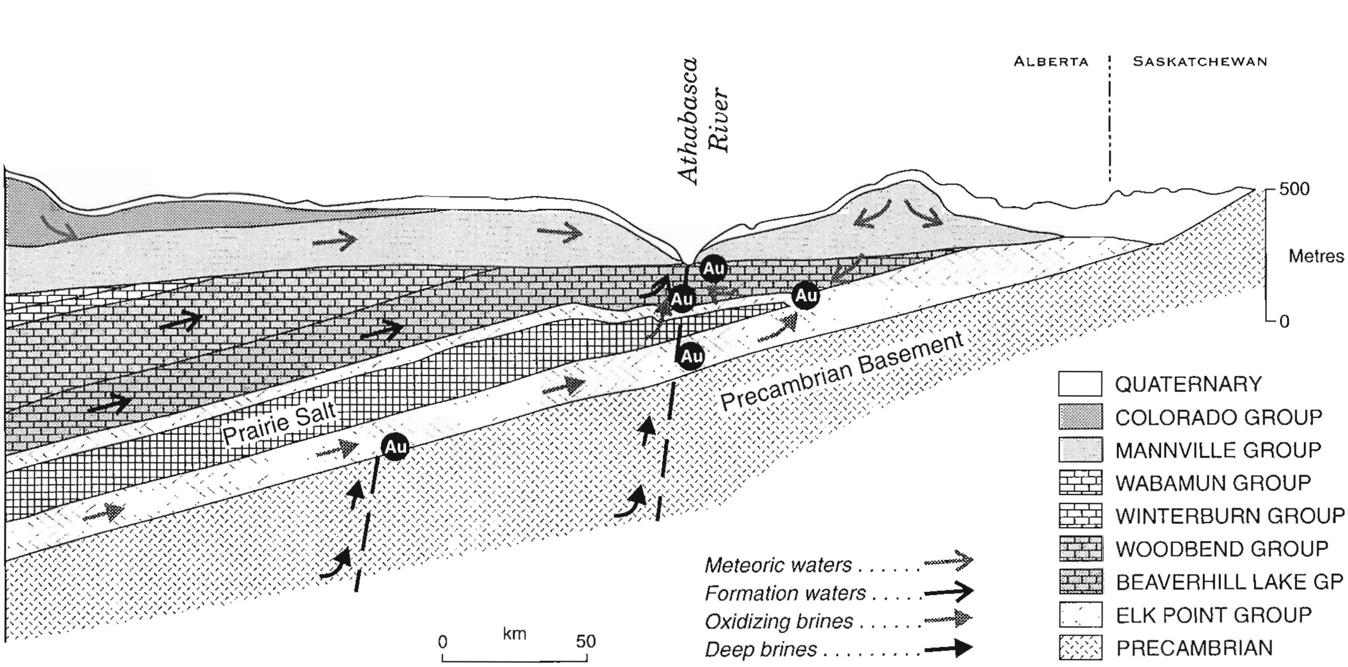

***Figure 9.** Genetic model for microdisseminated polymetallic minerals, northeastern Alberta. Brines originating in the Prairie Formation descend by density drive where they are oxidized by reaction with hematite and anhydrite, at which point they are capable of scavenging and transporting metals. Present and past fluid flow has dominantly been updip to the east and has resulted in focused discharge of metal-bearing brines along collapse structures associated with salt dissolution and karsting at the sub-Cretaceous unconformity. The Au symbols indicate possible sites of gold precipitation at regional or structurally controlled, microbially mediated redox boundaries.*

The solubility of gold, silver, copper and other metals in saline brines is chiefly a function of redox state, pH, and brine composition (e.g., Jaireth, 1992, 1994; Thornber, 1992). Geochemical calculations show that Au, Ag, and Cu chloride, bromide, and iodide complexes are the most stable species in highly saline, oxidized, neutral to acidic brines at low temperature. Sverjensky (1987) and Bloom et al. (1992) have calculated the geochemical evolution of a saline brine during migration in a sedimentary basin. If formation waters first react with sulfate-rich evaporates (anhydrite) and then react with a typical redbed assemblage (hematite), oxygen fugacities well into the hematite field can be attained. Under these conditions, Au, Ag, Cu and other metals, including platinum group elements, are soluble as chloride complexes.

Mobilization and transport of metals occurred upon interaction of highly oxidizing brines originating in halite evaporite units of the Prairie Formation with basement rocks or metal-enriched sedimentary rocks. These brines may have been original residual evaporite brines, or conceivably they may have originated as low-salinity waters of meteoric origin which dissolved halite of the Prairie Formation such that their salinities rose to levels approaching halite saturation. Under both scenarios, reaction with anhydrite and hematite in red bed-evaporite sequences of the Elk Point Group would have produced an oxidized brine capable of leaching and transporting Au and other metals. Gold solubilities in the latter scenario, however, would have been greatly enhanced if the brines approached halite saturation while retaining atmospheric oxidization levels (Jaireth, 1992). The existence of oxidized brines is supported by the observation that formation waters from the "Granite Wash" have higher Fe and Mn contents than those from other aquifers (Hitchon, 1993) and by the presence of native Cu (Table 1), both of which are indicative of relatively oxidizing conditions.

Precipitation of microdissmeninated polymetallic minerals occurred as oxidized brines crossed major redox boundaries. On the basis of the distribution of native S in rocks in northeastern Alberta, it is apparent that redox boundaries developed both locally in structurally controlled settings and regionally at major stratigraphic boundaries (Fig. 9). At least three significant stratigraphically controlled, microbially mediated redox boundaries exist at Fort MacKay. The lowermost is the contact between unaltered, reduced basement granitoid rocks and oxidized basement rocks at or below the Precambrian surface. This boundary is in part stratigraphically controlled by the Precambrian-Lower Devonian erosion surface, but may extend some distance below this surface. The second redox boundary is the contact between organic-rich laminites and marine limestones of the Winnipegosis Formation and the underlying redbed-evaporite sequence of the Lower Elk Point Group. The uppermost redox boundary occurs at the Slave Point–Watt Mountain interval which marks the contact between the underlying, oxidized Elk Point Group and overlying, reduced, argillaceous marine limestones of the Beaverhill Lake Group.

Macroscopic native S also has been observed in fractures cutting the organic-rich Winnipegosis Formation laminites and bitumen-bearing Waterways Formation marine limestones. This occurrence of native S is interpreted to record microbial reduction of oxidized, SO_4-rich waters where they flowed through reduced, organic-rich units — either immature dispersed organic material in the Winnipegosis laminites or liquid hydrocarbons in the Waterways Formation. Although the importance of fracture flow in relation to microdisseminated polymetallic minerals has not yet been determined, focused flow of metal-bearing brines along fracture systems and localized redox reactions potentially may be important in forming greater concentrations of these minerals in parts of the Western Canada Sedimentary Basin.

Within reduced Waterways Formation limestones and bitumen-saturated Cretaceous sandstones, migration of metals as halide complexes is not likely. However, remobilization of metals by bisulphide or polysulphide complexes is possible, and could lead to remobilization and secondary enrichment of original microdisseminated polymetallic minerals. This mechanism might also help explain microdisseminated gold observed in Cretaceous sandstones (Feng and Abercrombie, 1994) and coals (Dufresne et al., 1994) of the Mannville Group, and gold observed within the lower part of the Colorado Group (S.B. Ballantyne, pers. comm., 1995). It is also possible that oxidized metal-bearing brines originating in the Elk Point Group could have migrated to the base of the Colorado Group prior to migration of hydrocarbons into Mannville Group reservoirs during the Laramide Orogeny.

The general geochemical environments and the proposed genetic model described above are similar to those of redbed Cu deposits and the unconformity-related Au-PGE-U mineralization in the South Alligator mineral field, Australia (e.g., Sverjensky, 1987; Eugster, 1989; Bloom et al., 1992). The microdisseminated polymetallic minerals documented here are, however, distinguished by the diversity of metallic elements present, the abundance of metal alloys, oxides, chlorides, and carbonates, and their variable redox states. The potential for broader distribution of microdisseminated polymetallic minerals across the WCSB is worthy of further investigation given that the geology, geochemistry, and hydrogeology of the Fort MacKay region is similar to that of much of the eastern margin of the WCSB. The distribution of halite within the Prairie Formation is shown in Figure 10. If, as proposed, oxidizing, halide-rich waters are required to mobilize and transport metals, the wide distribution of halite and halite dissolution indicates that there is potential for regional development of such fluids across the WCSB. The presence of halide-rich brines and metal-enriched redbed-evaporite sequences of the Elk Point Group across much of the WCSB suggests good potential for discovery of additional occurrences of microdisseminated polymetallic minerals.

CONCLUSIONS

A novel assemblage of microdisseminated Au-Ag-Cu and other metallic minerals has been discovered in Phanerozoic sedimentary rocks and Precambrian basement at Fort MacKay, northeastern Alberta. This assemblage consists predominantly of <0.1 to 10 μm sized particles of native elements, including Au, Ag, Cu, Zn, Pb, Fe, Bi, and S, intergrown or alloyed metals including Au-Ag, Au-Cd, Cu-Zn, Cu-Zn-Au, Fe-Cu-Zn, Cd-Zn, and possible *Au-Al, Au-Si,* and *Au-Ca*, and is associated with a wide variety of metal-chloride, -oxide, -carbonate, -phosphate, and -sulphide minerals. Microdisseminated polymetallic minerals occur in pores and veinlets and do not appear to be replacive. They may be localized in proximity to vertical fracture systems related to collapse structures associated with dissolution of halite in the Prairie Formation and normal faults perpendicular to the axis of the Peace River–Athabasca Arch. Microdisseminated native Cu and Cu-Zn are the most common and widespread microdisseminated metallic phases. Laser ablation ICP-MS and solution ICP-MS analyses of rocks from the Fort MacKay region of northeastern Alberta support the presence of Au and related polymetallic phases originally detected by SEM–EDS. Based on the initial examinations reported above, gold and related polymetallic minerals are most abundant in the Waterways Formation of the Beaverhill Lake Group.

The proposed genetic model for microdisseminated polymetallic minerals in the WCSB involves metal scavenging and transport by residual evaporite brines originating in the Prairie Formation and other halite-bearing evaporite units of the Elk Point Group. The maximum temperature of deposition is estimated

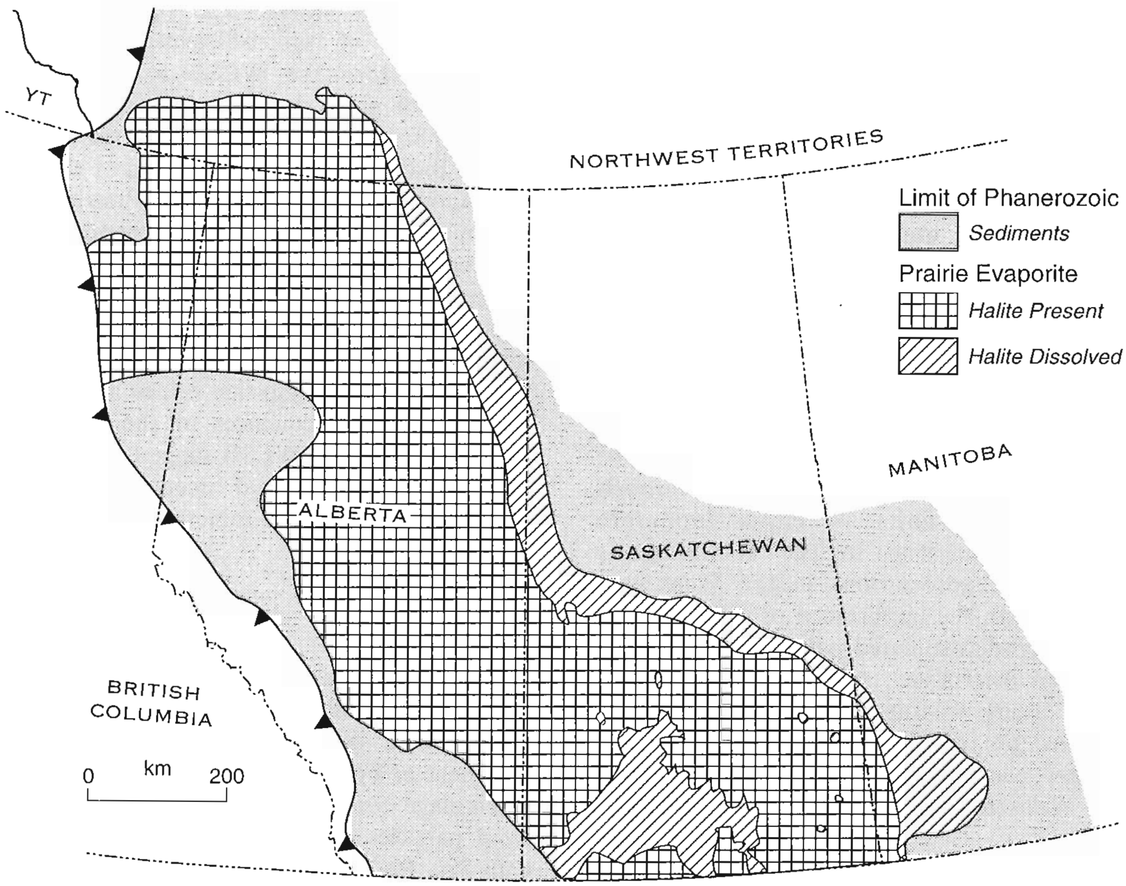

***Figure 10.** Regional distribution of halite facies of Prairie Formation showing areas of salt dissolution. Widespread dissolution of salt near the eastern updip margin of the basin and the consequent formation of saline brines implies that large areas of western Canada may be prospective for additional occurrences of Prairie-type mineralization.*

from burial reconstruction and apatite fission track analysis to be <90°C in northeastern Alberta. Assuming that the oxidation potential of the brines can be set by reaction with hematite and anhydrite present in redbed and evaporite units of the Elk Point Group, transport of Au and related metals by oxyhalide complexes is possible. Metals likely were mobilized as brines flowed through basement, but may also have been derived from sedimentary rocks of the Elk Point Group. Deposition occurs as metal-bearing brines flow through stratigraphically and structurally controlled, microbially mediated redox boundaries where bacterial reactions caused reduction of oxyhalide complexes, releasing metals for precipitation.

Of importance to genetic models for the origin of microdisseminated polymetallic minerals is the recognition of microbially mediated redox reactions in controlling oxidation potential in rocks in northeastern Alberta. Regionally, redox zonation is controlled by stratigraphy, but locally it is controlled by structure. Major regional redox boundary surfaces include: i) the contact between oxidized (altered) and reduced (unaltered) Precambrian basement, ii) the contact between reduced marine carbonates of the Winnipegosis Formation and underlying, more oxidized evaporites of the Lower Elk Point Group, and iii) the Slave Point–Watt Mountain interval, which separates reduced marine limestones of the Beaverhill Lake Group from more oxidized evaporites of the Upper Elk Point Group. Redox boundaries are marked by the occurrence of native S of probable microbial origin. The occurrence of native S on vertical to sub-vertical fractures cutting organic-rich laminites of the Winnipegosis Formation and reduced marine limestones of the Waterways Formation indicates that locally, oxidized brines have penetrated vertically into reduced rocks, suggesting a structural control on at least some proportion of the microdisseminated minerals.

The discovery of microdisseminated Au-Ag-Cu minerals at Fort MacKay provides a new opportunity for mineral exploration research in a largely unexplored region of western Canada. Based on the model presented above, major factors for localization of microdisseminated polymetallic minerals include i) a source of saline brines, ii) generation of an oxidizing brine by reaction with hematite and anhydrite, iii) focusing of flow along vertical structures or upward cross-formational flow through regional redox boundaries, and iv) active microbial reduction of SO_4 and other species, which requires v) the presence of organic material, either as dispersed immature organic matter or as hydrocarbons. Because the geology and geochemical environments of the Fort MacKay region are similar across much of the eastern part of the WCSB, it is suggested that the potential for discovery of additional occurrences of microdisseminated Au-Ag-Cu and other polymetallic minerals is high.

Acknowledgments

This work is funded by Alberta-Canada Mineral Development Agreement, and received funding and in-kind support from Alberta Geological Survey, Birch Mountain Resources Ltd., Focal Resources Ltd., NSR Resources Inc., and Tintina Mines Ltd. The samples used in this study were provided by Focal Resources Ltd., H.M.S. Properties Ltd., NSR Resources Inc., and Tintina Mines Ltd. The authors have benefitted from discussion with geologists from the above companies, especially S.F. Sabag of Tintina Mines Ltd., V. Pratico of Birch Mountain Resources Ltd., and E. Allen and L. Smith of Focal Resources Ltd., K. Richardson of H.M.S. Properties Ltd., and W. Hamilton and R. Richardson of Alberta Geological Survey. We thank J. Wong and D. Walker for their assistance with SEM examinations.

REFERENCES

Abercrombie, H.J., Bloch, J.D., Hutcheon, I.E., and de Caritat, P.
1994: Silica activity and the smectite-illite reaction. Geology, v. 22, p. 539–542.

Abercrombie, H.J. and Feng, R.
1994a: Gold and PGE anomalies in Phanerozoic sedimentary rocks, northeastern Alberta - potential for new deposits? Program and Abstracts, Calgary Mining Forum, Calgary Mineral Exploration Group Society, p. 51.

1994b: Prairie-type disseminated gold-silver-copper mineralization in the Western Canada Sedimentary Basin: brine-associated native and alloyed metals, chlorides, oxides, and carbonates. Abstracts with Programs, Geological Society of America, v. 26, p. 83.

Aitken, J.D.
1993: Proterozoic sedimentary rocks; Subchapter 4A. *In* Sedimentary Cover of the Craton in Canada, D.F. Stott and J.D. Aitken (eds.). Geological Survey of Canada, Geology of Canada, no. 5, p. 81–95.

Allan, J.A.
1920: Second Annual Report on the Mineral Resources of Alberta. Government of Alberta, Edmonton.

Anderson, G.M. and Macqueen, R.W.
1989: Mississippi Valley-type lead-zinc deposits. Ore Deposit Models, R.G. Roberts and P.A. Sheahan (eds.). Geoscience Canada Reprint Series 3, p. 79–90.

Aulstead, K.L. and Spencer, R.J.
1985: Diagenesis of the Keg River Formation: fluid inclusion evidence. Bulletin of Canadian Petroleum Geology, v. 33, p. 167–183.

Bachu, S. and Underschultz, J.R.
1993: Hydrogeology of formation waters, northeastern Alberta basin. American Association of Petroleum Geologists, Bulletin, v. 77, p. 1745–1768.

Ballantyne, S.B., Harris, D.C., and Sabag, S.F.
1995: Mineralogical results from insoluble residues obtained from cold HF digestion of precious metal-bearing strata, Fort MacKay, Alberta. Abstracts, Geological Survey of Canada, Forum 1995.

Ballantyne, S.B. and Harris, D.C. (*this volume*)
1997: Alluvial platinum-group minerals and gold in Alberta: results from the "orientation studies project" and their significance to exploration. *In* Exploring for Minerals in Alberta: Geological Survey of Canada Geoscience Contributions, Canada-Alberta Partnership on Minerals (1992–1995), R.W. Macqueen (ed.). Geological Survey of Canada, Bulletin 500, p. 279–329.

Beales, F.W. and Jackson, S.A.
1966: Precipitation of lead-zinc ores in carbonate rocks as illustrated by Pine Point ore field. Canadian Institute of Mining and Metallurgy, Transactions, v. 75, p. B278–B285.

Benthin, H.L.
1973: Conventional oil possibilities in the Fort McMurray area. *In* Guide to the Athabasca Oil Sands Area, M.A. Carrigy and J.W. Kramers (eds.). Alberta Research Council, Information Series 65, p. 163–172.

Berger, B.R. and Bagby, W.C.
1993: The geology and origin of Carlin-type gold deposits. *In* Gold Metallogeny and Exploration, R.P. Foster (ed.). Blackie, Glasgow and London, p. 210–248.

Bjørlykke, K. and Egeberg, P.K.
1993: Quartz cementation in sedimentary basins. American Association of Petroleum Geologists, Bulletin, v. 77, p. 1538–1548.

Bloch, J.D., Schroder-Adams, C.J., Leckie, D.A., Craig, J., and McIntyre, D.J.
in press: Shale of the Cretaceous Lower Colorado Group in western Canada: geochemistry, micropaleontology, sedimentology and hydrocarbon potential. Geological Survey of Canada, Bulletin.

Bloom, M.S., Gilbert, D.J., Gammons, C.H., and Wilde, A.R.
1992: Reaction path modeling for hydrothermal Au-PGE mineralization at Coronation Hill and similar deposits of the South Alligator Mineral Field, Australia. *In* Water-Rock Interaction, Y.K. Kharaka and A.S. Maest (eds.). Balkema, Rotterdam, p. 1569–1573.

Borneuf, D.
1982: Springs of Alberta. Alberta Research Council, Earth Sciences Report 82-3, 95 p.

Bottomley, D.J., Grégoire, D.C., and Raven, K.G.
1994: Saline groundwaters and brines in the Canadian shield; geochemical and isotopic evidence for a residual evaporite brine component. Geochimica et Cosmochimica Acta, v. 58, p. 1483–1498.

Boyle, R.W.
1979: The Geochemistry of Gold and its Deposits. Geological Survey of Canada, Bulletin 280, 584 p.

Carrigy, M.A.
1959: Geology of the McMurray Formation, Part III, General geology of the McMurray area. Research Council of Alberta, Memoir 1, 130 p.

1973: Mesozoic geology of the Fort McMurray area. *In* Guide to the Athabasca Oil Sands Area, M.A. Carrigy and J.W. Kramers (eds.). Alberta Research Council, Information Series 65, p. 77–101.

Connolly, C.A., Walter, L.M., Baadsgaard, H., and Longstaffe, F.J.
1991a: Origin and evolution of formation waters, Alberta Basin, Western Canada Sedimentary Basin. I. Chemistry. Applied Geochemistry, v. 5, p. 375–396.

1991b: Origin and evolution of formation waters, Alberta Basin, Western Canada Sedimentary Basin. II. Isotopic systematics and water mixing. Applied Geochemistry, v. 5, p. 397–414.

Cotterill, D.K. and Hamilton, W.N.
1995: Geology of Devonian limestones in northeast Alberta. Alberta Geological Survey, Open File Report 1995-7.

Creaney, S. and Allan, J.
1992: Petroleum systems in the foreland basin of Western Canada. *In* Foreland Basins and Fold Belts, R.W. Macqueen and D.A. Leckie (eds.). American Association of Petroleum Geologists, Memoir 55, p. 279–308.

Devkov, V.M., Mandova, E.D., Dimitrov, K.B., and Rekkalov, K.N.
1995: Native aluminum in metalliferous sediments from the East Pacific Rise axial zone (21°S). Marine Geology, v. 123, p. 87–103.

Dufresne, M.B., Henderson, B.A., Fenton, M.M., Pawlowicz, J.G., and Richardson, R.J.H.
1994: The mineral deposits potential of the Marguerite River and Fort MacKay areas, northeast Alberta (NTS 74E). Alberta Research Council, Alberta Geological Survey, Open File Report 1994-9.

Ells, S.C.
1926: Bituminous sands of northern Alberta; occurrence and economic possibilities; report on investigations to the end of 1924; topographical maps. Department of Mines, Canada, Mines Branch Report 632, 239 p.

Eugster, H.P.
1989: Geochemical environment of sediment-hosted Cu-Pb-Zn deposits. Geological Association of Canada, Special Paper 36, p. 111–126.

Feng, R. and Abercrombie, H.J.
1994: Disseminated Au-Ag-Cu mineralization in the Western Canada Sedimentary Basin, Fort MacKay, Northeast Alberta: A new gold deposit type. *In* Current Research 1994-E. Geological Survey of Canada, p. 121–132.

Fenton, M.M. and Ives, J.W.
1982: Preliminary observations on the geological origins of Beaver River sandstone. *In* Archaeology in Alberta 1981, Occasional Paper No. 19. Archaeological Survey of Alberta, p. 166–169.

Fowler, M.G., Kirste, D.M., Goodarzi, F., and Macqueen, R.W.
1993: Optical and geochemical classification of Pine Point bitumens and evidence for their origins from two separate source rocks. Energy Sources, v. 15, p. 315–337.

Garven, G.
1989: A hydrogeologic model for the formation of the giant oil sand deposits of the Western Canada Sedimentary Basin. American Journal of Science, v. 284, p. 105–166.

Garven, G. and Freeze, A.
1984: Theoretical analysis of the role of groundwater flow in the genesis of stratabound ore deposits. 2. Quantitative results. American Journal of Science, v. 284, p. 1085–1174.

Gatellier, J.-P. and Disnar, J.-R.
1989: Organic matter and gold-ore association in a hydrothermal deposit, France. Applied Geochemistry, v. 4, p. 143–150.

Giusti, L.
1986: The morphology, mineralogy, and behaviour of "fine-grained" gold from placer deposits of Alberta: sampling and implications for mineral exploration. Canadian Journal of Earth Sciences, v. 23, p. 1662–1672.

Godfrey, J.D.
1986: Geology of the Precambrian Shield of northeastern Alberta. Alberta Research Council, Map 1986-1, scale 1:250,000.

Hackbarth, D.A. and Nastasa, N.
1979: The hydrogeology of the Athabasca oil sands area, Alberta. Alberta Research Council, Bulletin 38, 39 p.

Hamilton, W.N.
1971: Salt in east-central Alberta. Research Council of Alberta, Bulletin 29, 53 p.

Hanor, J.S.
1979: The sedimentary genesis of hydrothermal fluids. *In* Geochemistry of Hydrothermal Ore Deposits, Second Edition, H.L. Barnes (ed.). New York, John Wiley, p. 157-172.

Hasegawa, R.
1991: Amorphous magnetic minerals - a history. Journal of Magnetism and Magnetic Materials, v. 100, p. 1-12.

Hentz, T.F., Price, J.G., and Gutierrez, G.N.
1989: Geologic occurrence and regional assessment of evaporite-hosted native sulfur, Trans-Pecos, Texas. Bureau of Economic Geology, Report of Investigations No. 184, 70 p.

Hitchon, B.
1984: Geothermal gradients, hydrodynamics, and hydrocarbon occurrences, Alberta, Canada. American Association of Petroleum Geologists, Bulletin, v. 68, p. 713-743.

1993: Geochemistry of formation waters, Northern Alberta, Canada: Their relation to the Pine Point ore deposit. Alberta Geological Survey, Open File Report 1993-14.

Hitchon, B., Billings, G.K., and Klovan, J.E.
1971: Geochemistry and origin of formation waters in the Western Canada Sedimentary Basin, Part III. Factors controlling chemical compositions. Geochimica et Cosmochimica Acta, v. 35, p. 567-598.

Hutcheon, I., Abercrombie, H.J., Shevalier, M., and Nahnybida, C.
1989: A comparison of formation reactivity in quartz-rich and quartz-poor reservoirs during steam assisted thermal recovery. *In* The Fourth UNITAR/UNDP International Conference on Heavy Crude and Tar Sands Proceedings, Volume 2, Geology, Chemistry, R.F. Meyer and E.J. Wiggins (eds.). Paper No. 235, p. 747-757.

Hutcheon, I., Krouse, H.R., and Abercrombie, H.J.
1995: Controls on the origin and distribution of elemental sulfur, H_2S and CO_2 in Paleozoic hydrocarbon reservoirs in western Canada. *In* Geochemical Transformations of Sedimentary Sulfur, M.A. Vairavamurthy and M.A. Schoonen (eds.). American Chemical Society Symposium Series, p. 426-438.

Ives, J.W. and Fenton, M.M.
1985: Progress Report for the Beaver River Sandstone Geological Source Study, Permit No. 83-54 Final Report. Report on file, Archaeological Survey of Alberta, Edmonton, 70 p.

Jaireth, S.
1992: The calculated solubility of platinum and gold in oxygen-saturated fluids and the genesis of platinum-palladium and gold mineralization in the unconformity-related uranium deposits. Mineralium Deposita, v. 27, p. 42-54.

1994: Transport of gold and silver in oxygen-saturated fluids and the formation of high-fineness gold in saprolitic and supergene environments. Australian Journal of Earth Sciences, v. 41, p. 181-189.

Johnson, J.W., Oelkers, E.H., and Helgeson, H.C.
1993: SUPCRT92: A software package for calculating the standard molal thermodynamic properties of minerals, gases, aqueous species, and reactions from 1 to 5000 bars and 0 to 1000°C. Computers and Geosciences, v. 8, p. 899-947.

Leckie, D.A. and Smith, D.G.
1992: Regional setting, evolution and depositional cycles of the Western Canadian foreland basin. *In* Foreland Basins and Fold Belts, R.W. Macqueen and D.A. Leckie (eds.). American Association of Petroleum Geologists, Memoir 55, p. 9-46.

Machel, H.G., Krouse, H.R., and Sassen, R.
1995: Products and distinguishing criteria of bacterial and thermochemical sulfate reduction. Applied Geochemistry, v. 10, p. 373-390.

Macqueen, R.W. and Powell, T.G.
1983: Organic geochemistry of the Pine Point lead-zinc ore field and region, Northwest Territories, Canada. Economic Geology, v. 78, p. 1-26.

Masters, J.A.
1984: Lower Cretaceous oil and gas in western Canada. *In* Elmworth - Case Study of a Deep Basin Gas Field. American Association of Petroleum Geologists Memoir, 38, p. 1-34.

McDonough, M.R. *(this volume)*
1997: Structural controls and age constraints on sulphide mineralization, southern Taltson magmatic zone, northeastern Alberta. *In* Exploring for minerals in Alberta: Geological Survey of Canada Geoscience Contributions, Canada-Alberta Partnership on Minerals (1992-1995), R.W. Macqueen (ed.). Geological Survey of Canada, Bulletin 500, p. 13-29.

McDonough, M.R. and Abercrombie, H.J.
1995: Mineral occurrences in Middle Devonian carbonates, Salt River and Stony Islands (Slave River) areas, northeastern Alberta. *In* Current Research 1995-B. Geological Survey of Canada, p. 125-130.

McDonough, M.R., Grover, T.W., McNicholl, V.J., and Lindsay, D.D.
1993: Preliminary report of the geology of the southern Taltson magmatic zone, northeastern Alberta. *In* Current Research, Part C. Geological Survey of Canada, Paper 93-1C, p. 221-232.

Meijer Drees, N.C.
1986: Evaporitic Deposits of Western Canada. Geological Survey of Canada, Paper 85-20, 118 p.

Meijer Drees, N.C., Palmer, B.C., Fowler, M.G., Stasiuk, L.D., Nowlan, G.S., and McGregor, D.C.
1995: Petroleum geology of the Middle Devonian Winnipegosis and Prairie formations in east-central Alberta. *In* Proceedings of the Oil and Gas Forum 95, J.S. Bell, T.D. Bird, T.L. Hillier, and P.L. Greener (eds.). Geological Survey of Canada, Open File 3058, p. 103-111.

Morrow, D.W. and Aulstead, K.L.
1995: The Manetoe dolomite - a Cretaceous-Tertiary or a Paleozoic event? Fluid inclusion and isotopic evidence. Bulletin of Canadian Petroleum Geology, v. 43, p. 267-280.

Mossop, G.D. and Shetsen, I. (compilers)
1994: Geological Atlas of the Western Canada Sedimentary Basin. Canadian Society of Petroleum Geologists and Alberta Research Council, Calgary, 510 p.

Nesbitt, B.E. and Muehlenbachs, K.
1994: Paleohydrology of the Canadian Rockies and origins of brines, Pb-Zn deposits and dolomitization in the Western Canada Sedimentary Basin. Geology, v. 22, p. 243-246.

Norris, A.W.
1963: Devonian stratigraphy of northeastern Alberta and northwestern Saskatchewan. Geological Survey of Canada, Memoir 313.

Olson, R.A., Richardson, R.J.H., and Eccles, D.R.
1994: Regional metallogenic evolution of Alberta. Alberta Research Council, Open File Report 1994-8, 50 p.

Powell, T.G. and Macqueen, R.W.
1984: Precipitation of sulphide ores and organic matter-sulphate reactions at Pine Point, Canada. Science, v. 224, p. 63-66.

Qing, H. and Mountjoy, E.W.
1994: Formation of coarsely crystalline, hydrothermal dolomite reservoirs in the Presquile barrier, Western Canada Sedimentary Basin. American Association of Petroleum Geologists Bulletin, v. 78, p. 55-77.

Robie, R.A., Hemingway, B.S., and Fisher, J.R.
1979: Thermodynamic properties of minerals and related substances at 298.15 K and 1 bar (105 Pascals) pressure and at higher temperatures. United States Geological Survey, Bulletin 1452, 456 p.

Ross, G., McMechan, M.E., and Hein, F.J.
1989: Proterozoic History: The Birth of the Miogeocline. *In* Western Canada Sedimentary Basin - A Case History, B.D. Ricketts (ed.). Canadian Society of Petroleum Geologists, p. 79-104.

Ruckmick, J.C., Wimberly, B.H., and Edwards, A.F.
1979: Classification and genesis of biogenic sulfur deposits. Economic Geology, v. 74, p. 469-474.

Sholkovitz, E.R. and Schneider, D.L.
1991: Cerium redox cycles and rare earth elements in the Sargasso Sea. Geochimica et Cosmochimica Acta, v. 55, p. 2737-2744.

Sverjensky, D.A.
1984: Oil field brines as ore-forming solutions. Economic Geology, v. 79, p. 23-37.

1987: The role of migrating oil field brines in the formation of sediment-hosted Cu-rich deposits. Economic Geology, v. 82, p. 1130-1141.

Thiede, D.S.
1975: Geological implications of variation in heavy metal content in the Elk Point evaporite sequence, Saskatchewan, Canada. M.Sc. thesis dissertation, University of Wisconsin, Madison, unpublished, 192 p.

Thiede, D.S. and Cameron, E.N.
1978: Concentration of heavy metals in the Elk Point evaporite sequence, Saskatchewan. Economic Geology, v. 73, p. 405-415.

Thornber, M.R.
1992: The chemical mobility and transport of elements in the weathering environment. *In* Regolith Exploration Geochemistry in Tropical Terrains, C.R.M. Butt and H. Zeegers (eds.). Commonwealth Scientific and Industrial Research Organization, p. 79-96.

Tsui, P.C. and Crudden, D.M.
1984: Deformation associated with gypsum karst in the Salt River Escarpment, northeastern Alberta. Canadian Journal of Earth Sciences, v. 21, p. 949-959.

Turner, A. and McPhee, D.
1994: Analysis of Paleozoic core data for the evaluation of potential Pb-Zn mineralization in northeastern Alberta. Alberta Research Council, Open File Report 1994-18.

Wardlaw, N.C. and Watson, D.W.
1966: Middle Devonian salt formations and their bromide content, Elk Point area, Alberta. Canadian Journal of Earth Sciences, v. 3, p. 263-274.

Willett, S.D. and Issler, D.R.
1992: Apatite fission track thermochronometry applied to the Western Canada Sedimentary Basin - A case history from the Peace River Arch region. *In* Low Temperature Thermochronology, Mineralogical Association of Canada, Short Course Handbook, v. 20, p. 157-188.

Wittrup, M.B. and Kyser, T.K.
1990: The petrogenesis of brines in Devonian potash deposits of western Canada. Chemical Geology, v. 82, p. 103-128.

Appendix 1
Locations

Surface Samples

Sample	Formation	Lithology	NTS	UTM E	UTM N
F-01	Waterways	Limestone	74E/4	464130	6334440
F-02	Waterways	Limestone	74E/4	464130	6334490
F-18	Waterways	Limestone	74E/4	464820	6332180
F-19	Waterways	Limestone	74E/4	464950	6332510
F-20	Waterways	Limestone	74E/4	464980	6332340
F-22	Waterways	Limestone	74E/4	465020	6332340
RR-9	Waterways	Limestone	74E/4	462990	6337930
RR-21	McMurray (BRS)	Sandstone	74E/4	464540	6336900
RR-41	Waterways	Limestone	74E/4	465130	6336540
RR-43A	Waterways	Limestone	74E/4	465780	6337900
RR-45	McMurray (BRS)	Sandstone	74E/4	464640	6338610
WK-6	McMurray	Sandstone	74E/4	463560	6337580
WK-14	Waterways	Limestone	74E/4	463950	6338310
WK-15	Waterways	Limestone	74E/4	464420	6335370
WK-30B	Waterways	Limestone	74E/4	464810	6338090
WK-31	McMurray (BRS)	Sandstone	74E/4	464680	6338110
93-A1	Waterways	Limestone	74E/4	464060	6332450

Diamond Drill Holes

Name	Company	Year	NTS	UTM E	UTM N
T3	Tintina	1993	74E/4	463725	6338090
T4	Tintina	1993	74E/4	463390	6335700
86-2R	HMS Properties Ltd.	1986	74E/4	465010	6330220
Athabasca No. 1	Scurry Rainbow	1962	74E/5	461410	6345880
Athabasca No. 3	Scurry Rainbow	1962	74E/5	461300	6346050
Ells Gold No. 1	374624 Alberta Ltd.	1988	74E/5	459455	6351252

ALLUVIAL PLATINUM-GROUP MINERALS AND GOLD IN ALBERTA: RESULTS FROM THE "ORIENTATION STUDIES PROJECT" AND THEIR SIGNIFICANCE TO EXPLORATION[1]

S.B. Ballantyne and D.C. Harris
Mineral Resources Division, Ottawa

Abstract

This project characterizes heavy mineral concentrates (HMC), gold and platinum-group minerals (PGM) in modern river placer deposits and unconsolidated paleoplacer fluvial systems. Gold and PGM grains of 25 μm and larger were recovered consistently in the field using washed/sieved material which was panned using a conical pan (metal batelle). Gold and PGM grains also were donated by individuals and mineral exploration companies. Gold morphology varies throughout the grain sizes examined (tens of micrometres to millimetres). Chemical composition ranges from electrum to gold (550–950 fineness). Rivers draining the mid-Cretaceous Shaftesbury Formation in northeastern Alberta contain pristine-shaped gold grains encrusted with Cu-Fe and Fe-sulphides. Edmonton district preglacial to interglacial Saskatchewan sands and gravels yielded alluvial gold grains and pristine bacterial gold growths on paleoplacer gold substrates. Some homogeneous gold grains contain up to 14.1 wt.% Pt, 8.0 wt.% Pd, and 4.0 wt.% Ag. The most abundant PGM discrete phases are Pt-Fe and Os-Ir-Ru-Pt alloys, occurring as platelets, discs, rods, spheres and crystals. Compositions of the Os-Ir-Ru-Pt alloys plot in the fields of osmium, iridium, ruthenium and rutheniridosmine; these alloys also commonly contain inclusions of chalcopyrite, bornite, osmium, PGM sulphides, tellurides or arsenides. Alluvial chrome spinels also recovered from HMC from central Alberta have major and trace element compositions strongly supporting derivation from deep mantle sources. The occurrence of placer gold-PGM in gravels is uncommon worldwide; comparison to ore deposit settings globally may offer explanations.

Résumé

Le présent projet vise à caractériser les concentrés de minéraux lourds, l'or et les éléments du groupe du platine dans des dépôts placériens modernes et des réseaux fluviaux à paléoplacers non consolidés. Des grains d'or et les éléments du groupe du platine de 25 μm et plus ont été récupérés de façon continue sur le terrain en utilisant des sédiments lavés et tamisés à l'aide d'une batée conique (batalle métallique). De plus, certaines personnes et des sociétés d'exploration minière ont donné des grains d'or et les éléments du groupe du platine. La morphologie de l'or varie selon la granulométrie, laquelle va de quelques dizaines de micromètres à quelques millimètres. La composition chimique, quant à elle, passe de l'électrum à l'or (finesse 550-950). Dans les rivières drainant la Formation de Shaftesbury du Crétacé moyen dans le nord-est de l'Alberta, il y a des grains d'or de forme primitive incrustés de sulfures de Cu-Fe et de Fe. Les sables préglaciaires à interglaciaires du district d'Edmonton, en Saskatchewan, contiennent des grains d'or alluvial et des croissances bactériennes d'or encore intactes sur des substrats d'or paléoplacérien. Certains grains d'or homogènes ont des proportions allant jusqu'à 14,1 % en poids de Pt, 8,0 % en poids de Pd et 4,0 % en poids d'Ag. Les phases distinctes les éléments du groupe du platine les plus abondantes sont les alliages de Pt-Fe et d'Os-Ir-Ru-Pt, existant sous la forme de plaquettes, de disques, de tiges, de sphères et de cristaux. La composition des alliages d'Os-Ir-Ru-Pt se situe dans les champs de l'osmium, de l'iridium, du ruthénium et de la ruthéniridasmine; ces alliages contiennent également des inclusions en forme de «goutelettes» de chalcopyrite, de bornite, d'osmium, de sulfures des éléments du groupe du platine, de tellurures ou d'arséniures. Des spinelles chromifères de ruisseau extraits de concentrés de minéraux lourds provenant du centre de l'Alberta ont une composition en éléments majeurs et traces qui appuie fortement une origine mantellique profonde. La présence d'or et les éléments du groupe du platine placériens dans des graviers est inhabituelle partout dans le monde et une comparaison avec d'autres minéralisations de ce type à l'échelle mondiale pourrait fournir des explications.

[1]Canada-Alberta Agreement on Mineral Development, Project C1.51

INTRODUCTION

In 1992, the authors initiated an orientation study project in central Alberta (Figs. 1-3) as part of the contribution to the Canada-Alberta Agreement on Mineral Development (1992-1995). This paper describes an investigation into Alberta placer gold and platinum group minerals (PGMs) hosted by Tertiary and Quaternary clastic unconsolidated sediments. Their possible sources and the genetic settings for their accumulation in the Western Canada Sedimentary Basin (WCSB) are also considered.

Gold, silver and platinum-group elements constitute the noble or precious metals. In nature, they commonly occur together as native metals, alloys and minerals. Although gold placers are common throughout the world, the occurrence of gold and PGMs together in the placer environment is much more restricted. Generally, the primary sources for placer PGMs are considered to be mafic to ultramafic rocks, in particular, large-scale layered igneous intrusions and ophiolitic complexes.

The occurrence of placer gold and PGMs in Alberta has long been noted (e.g., Hoffman, 1891; Allan, 1920, 1924), but the fact that Alberta placers are hosted within drainages of WCSB sedimentary strata without known mafic to ultramafic rocks remains an enigma.

Reconnaissance sample collection of panned heavy mineral concentrate (HMC) material was initiated in central Alberta in the autumn of 1992. During the following two field seasons further orientation-scale sampling and the examination of donated HMC material was completed. Sample collection sites were chosen for those drainages that had been previously reported in the literature to contain both alluvial gold and "platinum" grains. Generally the "platinum" grains were not properly characterized in earlier work.

The project was designed to verify the presence of placer-paleoplacer gold and PGMs at specific sites and to characterize the PGMs in relation to their specific drainages. Gold grains and other heavy minerals contained in the "black sand" HMC were also examined and identified in an attempt to further define the provenance and genetic origin of the gold and PGMs. The new baseline data collected during these orientation surveys is expected to encourage informed speculation as to the possible origin(s) of the gold and PGMs in the WCSB. Alberta has no present or past production of platinum-group elements alone, and gold production is presently restricted to hobby placer miners and by-product production of several sand and gravel aggregate operations.

Alluvial gold and platinum in Alberta

Alluvial gold mining in Alberta started in 1858 (Tyrrell, 1915). Prospectors from Minnesota tested Alberta streams and rivers on their way to the Fraser River, where gold had been discovered in 1857. The Geological Survey of Canada's (GSC) involvement in documenting Alberta alluvial gold resources began in 1859 when Dr. James Hector explored the North Saskatchewan River. Hector reported that specimens of placer gold had been collected in the vicinity of Edmonton *(in* Tyrrell, 1915).

American prospectors discovered gold on the North Saskatchewan River at Rocky Mountain House in 1860-1861. By 1862, Fraser River miners had left British Columbia and arrived at Fort Edmonton, where they sluiced and panned the North Saskatchewan River. In fact, in 1862, miners such as Thomas Clover convinced 62 of 175 prospectors from eastern Canada, the Overlanders, to mine placer gold at Fort Edmonton rather than continue west. In 1866, disillusioned but experienced miners from the Kootennay River, British Columbia, took part in a short-lived stampede to Edmonton (Tyrrell, 1915). James Gibbons, the inventor of the "grizzly dump box" and sluice mining method, claimed to be able to produce 0.8 ounces of gold per day between spring break-up and fall freeze-up on the North Saskatchewan River.

In 1887, the first dredge was built on the North Saskatchewan River (Tyrrell, 1915). In 1898, there were twelve dredges working the river, but the Klondike Gold Rush soon overshadowed Alberta production, so that by 1907 only one dredge remained in operation. During visits in 1895 and 1898, G.M. Dawson of the GSC estimated that about 300 miners were working "paying" bars 100 km upstream and downstream from Fort Edmonton.

From 1887 to 1912 gold returns from the North Saskatchewan River, as given by the Department of Mines of Canada, totalled 14 684 fine ounces (Tyrrell, 1915). Tyrrell suggested that at least that amount was also recovered during the 26 "boom" years from 1861 to 1886. No records of production were kept for this initial river-bar-mining discovery period, however.

G. Christian Hoffmann, reporting on work completed by the Chemistry and Mineralogy division of the GSC, was the first to describe "native platinum found, in association with gold, on the bars of the North Saskatchewan River, in the neighbourhood of Edmonton, district of Alberta, Northwest Territories" (Hoffmann, 1891, 1892). He noted that until then, native platinum had been found only in British Columbia and Quebec. A member of his staff, Mr. R.A.A. Johnston, examined a platinum-bearing sample and noted about "one-fourth of the platinum to be magnetic".

Sampling locations and methodology

Modern drainages

In central Alberta, HMC accumulation sites in modern drainages were located during the months of September and October at low water levels in streams and rivers. The sampling sites included "heads and tails" of point and mid-channel gravel bars, and sediment "classification" sites on meanders or on bends of the water course (Plate 1, Table 1). Some of the sampling sites had been located previously by other surveys (Giusti, 1983) where gold and platinum grain recovery had been reported. Many of these localities on the North Saskatchewan River were probably worked during Alberta's historical placer mining period $\simeq$1862-$\simeq$1907). These localities are today often utilized by hobby placer miners in the Edmonton area.

Paleoplacers

A network of rivers flowed across the western plains before the last glaciation. HMC, including gold and platinum, accumulated in river beds now represented by the Saskatchewan gravels (paleoplacers) in part exposed at Villeneuve, Entwistle and Heatherdown. A number of present-day aggregate-sand-and-gravel producers have exploited these paleoplacers, utilizing various gold and platinum recovery processes as part of their sand-gravel washing operations. This "by-product" placer gold and platinum recovery accounts for most of Alberta's modern production. Permission was obtained to enter a number of Edmonton area gravel-pit operations, and reconnaissance orientation paleoplacer HMC samples were panned from accessible sedimentary strata exposed on pit walls and floors (Plate 2).

As well as the orientation field collection of samples, important research material was provided to the authors from other sources. Mr. Frank Scheibein, an Edmonton area hobby placer miner, provided gold and PGM concentrates collected from the North Saskatchewan River near the Capilano Bridge within the City of Edmonton (Plates 4, 5). Mr. Tom Bryant, author and long-time Alberta placer prospector, provided a selection of large gold grains recovered from Alberta aggregate sand and gravel washing gold recovery systems (Plates 12-16). The gold concentrate (#12106) and PGM concentrate (#5611) curated in the National Mineral Collection Systematic Reference Series at the GSC, Ottawa, and donated by Mr. William Pearce in 1891, were also examined in this study (Plate 3). These two concentrates are the same material examined by Mr. R.A.A. Johnston of the "Laboratory of the Survey" and reported as the third example of native platinum found in Canada (Hoffman, 1892)[1].

Panning methods

Conical gold pans are used throughout the third world to recover alluvial and lateritic gold grains. The so-called "flat" or "California" gold pan is widely used in North America by hobbyists and placer miners to recover or test for placer gold.

For our orientation survey, we used a modified version of a "field kit" for gold exploration developed by the well-known placer gold consultant Mr. Mike W. Milner. The kit consists of a set of metal sieves and screens that nest in conical metal gold pans or batelles, reproducing the shape of a traditional third-world conical pan (Plate 1). In modern placer mining, the simultaneous classification and washing of potential "pay" material before sluicing and concentration of the HMC is considered necessary to enhance gold grain recovery. The same principles are used with the Milner field kit. Unconsolidated clastic material or till can be progressively washed and sieved into smaller grain sizes, because the nested screens allow the finest material to be captured in the conical metal bottom pan.

An improvement to the Milner field kit was developed by Mr. Robin Day of Edmonton. He modified the metal batelle shape by steepening the sides of the cone. Mr. Day's improvements allow for more complete removal of clay-rich sample material, providing the necessary reduction of "lights" to "heavies" required for our mineralogical examinations. Subsequent examination of the HMCs concentrated and recovered from the central cone of the batelle revealed that gold and platinum grains less than 63 μm (the silt-size fraction) are obtained consistently through the use of this methodology (Plates 4-7, 9, 10, 16).

[1]It is of note that until our present MDA study, no further mineralogical data from the Pearce concentrates were available (see Harris and Ballantyne, 1994). In fact, Alberta placer localities were reported to contain platinum but confirmation and mineralogical description of the PGMs were lacking until this study. Not surprisingly, little speculation is apparent in the scientific literature as to primary source(s) for the alluvial PGM grains dispersed in specific drainages within Alberta.

Table 1
Central Alberta GSC–MDA Orientation HMC Survey

Sample Site	Sample site no.	Section	Township	Range	Longitude	Latitude	W	Estimate of heavies	Gold grains recovered	PGMs recovered	Sulphide estimate	Barite	Ilmenite grains	Chromite recovered
Villineuve Onoway Channel	1	29	54	26	113.82	53.59	4							
Eden Lake Onoway Two Tert. Sask. Gravel	2	1	54	2	114.17	53.53	5							
Upland Sand and gravel Evensburg	3	30	53	6	114.85	53.50	5		31		no		2	1
Pembina River Evensburg Park	4	29	53	7	114.97	53.50	5	good	13		no		3	
McLeod River	5	5	52	18	116.54	53.38	5	good	300+	6	limonite py pseudomorphs		2	1
Embarras River	6	5	52	18	116.53	53.37	5	poor	21	1	no		1	1
McLeod River	7	3	50	23	117.18	53.22	5	poor	4	2	4%		1	
Gregg River	8	6	49	24	117.40	53.14	5	poor	no		4%			2
Upper McLeod River	9	14	48	22	117.04	53.03	5	poor	1		10%			4
Upper Embarras River	10	28	48	21	116.92	53.09	5	good	8		no			2
Lovett River	11	23	47	20	116.75	52.99	5	moderate	6		no			3
Pembina River	12	5	46	18	116.51	52.85	5	moderate	49	1	1%		2	17
Brazeau River	13	16	45	18	116.50	52.00	5	poor	no		20%			
Cardinal River	14	7	14	18	116.54	52.78	5	very poor	no		3%			
Blackstone River	15	18	43	16	116.27	52.63	5	poor	no		20%			2
North Ram River	16	24	38	15	115.99	52.11	5	poor	1		4%			1
Bighorn River Crescent Falls	17	26	39	17	116.32	52.30	5	poor	no		5%	60%		
Cripple Creek	18	29	37	14	115.95	52.12	5	moderate poor blacks	no	11	4%	5%		
Ram River (South) Rimbey	19	7	36	13	115.83	52.00	5	very poor	no		4%	60%		
Prairie Creek	20	7	38	9	115.26	52.17	5	moderate	3		no			3
Main Ram River	21	19	39	10	115.41	52.28	5	poor	no		15%			3
North Sask. River	22	19	39	10	115.41	52.29	5	poor	1		4%	15%		1
Baptiste Creek	23	30	41	11	115.52	52.47	5	moderate	2		no		5	1
Red Deer River	24	18	29	20			4	extreme	27		no			
North Sask. River	26	14	54	3	110.51	53.63	4	very good	300+	1	no		3	
North Sask. River Heinsburg Bridge	27	28	55	4	110.71	53.74	4	extreme	400+	1	no		2	
Outwash Gravel Pit	28	24	56	7	111.07	53.81	4	moderate	8		no			
North Sask River	29	24	56	7	111.07	53.81	4	extreme	168	4	no			
North Sask. River	30	14	55	9	111.37	53.70	4	extreme	156	1	no		5	1
North Sask. River	31	34	55	12	111.83	53.72	4	moderate	600+	3	no			
North Sask. River	32	5	58	15	112.29	53.91	4	moderate	55	1	no			
North Sask. River	33	6	58	17	112.60	53.90	4	moderate	17	1	no			
North Sask. River	34	32	58	19	112.87	53.97	4	good	79	2	no			
North Sask. Riverf Vinca Bridge	35	36	56	21	113.05	53.79	4	very good	200+	2	no			
North Sask. River Fort Sask.	36	31	54	22	113.27	53.62	4	moderate	121		no		1	2

Sample preparation and examination

Overburden Drilling Management Limited, Nepean, Ontario was contracted to separate visible gold and PGM grains from the previously panned HMC obtained at the field sample sites.

After gold and PGM separation was complete, the recovered HMC material was sent to Orex Laboratories Ltd. in Burnaby, British Columbia. Their laboratory facilities were contracted to extract so-called "diamond indicator" kimberlitic/lamproitic heavy minerals such as garnet, chromite, ilmenite and chrome diopside. This sample preparation involved classification into magnetic, paramagnetic and non-magnetic fractions. These fractions were sent to J.J. Gurney's analytical laboratories in Capetown, South Africa for identification and selection of potential diamond indicator heavy minerals. The selected grains were mounted and polished, and detailed electron probe microanalysis was performed on each grain. Subsequently, the data and grain mounts were returned to the GSC mineralogical laboratory facilities in Ottawa. Further major element and trace element electron probe microanalysis was performed at the Ottawa GSC laboratories as a check, and to provide new elemental data (Ni, Zn). These data are reported in Table 2.

Gold and PGM grains were examined by:

1. binocular microscope to determine various phases based on size, shape and colour;
2. SEM backscattered imagery and energy dispersive (EDS) analyses of phases and/or gangue;
3. examination under the reflecting microscope;
4. quantitative chemical analysis of all phases possible using an electron microprobe (core, rim, inclusions, and intergrowths; and
5. qualitative documentation of complex intergrowths and tiny inclusions using SEM-EDS characterization and backscattered imagery.

The GSC mineralogical laboratory in Ottawa provided the SEM system and CAMECA SX-50 electron microprobe fitted with four wavelength-dispersive spectrometers (WDS) and one EDS spectrometer. Two quantitative analysis analytical routines with operating conditions of 20 kv and 20 na were used. A 12-element routine was applied for the gold grains and related phases and a 15-element routine was used for the platinum-group element grains (for details see Harris and Ballantyne, 1994).

X-ray powder pattern diffraction identification and analysis was conducted at GSC Ottawa on selected ferroan platinum alloys.

Sample examination: discussion

In all geochemical HMC orientation programs for gold and PGMs it is important to examine and identify the accompanying heavy minerals. These grains commonly contain minerals or suites of minerals associated with specific types of gold and platinum group element deposits. This is also the underlying premise in gathering data from the diamond indicator heavy minerals. Their overall abundance and specific elemental compositions may assist in identifying potential diamond-bearing source rocks or target areas. Chromite is an excellent example of a heavy mineral found in placers that may be derived from diamond-bearing or non-diamond bearing kimberlitic or lamproitic rocks, mafic-ultramafic platinum group-element-enriched rocks (layered-Alaskan-type intrusions or ophiolite complex type) and Motherlode district-style mesothermal gold-bearing quartz veins hosted in ultramafics or liswainites.

Another gold and PGM grain recovery and separation laboratory technique involving new technology was tested as part of this orientation study. The "Carbad" process, developed in Australia, has been tested on hard rock and alluvial ores. It employs a surface wetting recovery technique that exploits the natural oleophilicity/hydrophobicity of gold and PGM particles when in contact with a carbon-hydrocarbon media. The technology causes selective agglomeration of small gold particles, some as small as sub-micron size. Examples of material recovered by this method by Envi-Tech. Inc. of Edmonton, Alberta, are shown in Plates 9 and 10.

Results and discussion

Thirty-six sites were visited in the course of this study (Table 1; Fig. 1). Fourteen samples were found to contain 1 to 11 grains of PGMs; 25 samples contained 1 to over 600 gold grains. Sulphides (pyrite) or limonite pseudomorphs after pyrite were recognized at 14 sites and abundant barite was noted at four sites.

Within the heavy mineral suite picked for diamond indicator minerals, 16 samples contained chromite (chrome spinel), 11 samples contained ilmenite grains and seven samples hosted both chromite and ilmenite grains. No indicator garnets or chrome diopside were found in the size fraction of plus 100 μm used in the selection of the diamond indicator minerals.

During our last field season, both wet-sieved unprocessed bulk river sediment samples and heavy mineral panned concentrate material obtained with batelles were provided to Envi-Tech. Inc. of

Table 2
Alberta Chromites (Chrome Spinels) - GSC-MDA HMC Survey

Sample Site	River	Grain	% AL_2O_3	CR_2O	FE_2O_3	V_2O_3	TiO_2	FEO	MGO	MNO	ZNO	Zn ppm	NIO	Ni ppm
3	Evensburg	3	7.90	54.93	6.16	0.21	0.19	21.21	7.17	0.44	0.26	2088	0.07	550
5	McLeod River	9	17.11	45.26	7.37	0.17	1.47	13.24	14.45	0.21	0.08	642	0.25	1964
6	Embarras River	10	17.34	47.29	5.85	0.19	0.85	13.28	14.03	0.22	0.07	562	0.25	1964
7	McLeod River	12	12.52	50.88	6.66	0.16	0.29	18.89	9.52	0.36	0.16	1285	0.12	943
8	Gregg River	13	9.27	46.31	14.10	0.12	0.59	20.00	8.48	0.49	0.17	1365	0.15	1178
8	Gregg River	14	16.82	46.55	6.73	0.14	1.21	13.01	14.37	0.20	0.08	642	0.26	2043
9	Upper McLeod River	15	18.06	41.44	8.93	0.19	1.79	15.18	13.43	0.20	0.08	642	0.25	1964
9	Upper McLeod River	17	18.29	41.50	7.90	0.18	1.30	19.65	10.24	0.27	0.13	1044	0.24	1886
9	Upper McLeod River	18	10.86	53.01	3.89	0.25	0.11	19.28	8.36	0.34	0.21	1687	0.07	550
10	Upper Embarras River	19	6.71	51.14	14.84	0.04	0.34	12.78	12.84	0.31	0.08	642	0.17	1335
10	Upper Embarras River	20	12.35	52.78	4.37	0.28	0.15	20.02	8.61	0.36	0.22	1767	0.07	550
11	Lovett River	21	16.89	50.84	0.40	0.18	0.15	22.39	7.43	0.28	0.58	4659	0.02	157
11	Lovett River	23	33.50	29.59	5.71	0.18	0.17	17.12	12.79	0.24	0.24	1928	0.18	1414
12	Pembina River	24	8.39	49.47	11.16	0.07	0.47	21.71	6.94	0.62	0.37	2972	0.11	864
12	Pembina River	25	27.45	38.99	4.80	0.15	0.44	10.15	16.92	0.20	0.06	482	0.23	1807
12	Pembina River	26	8.67	55.07	5.93	0.12	0.21	20.77	7.76	0.38	0.10	803	0.13	1021
12	Pembina River	27	14.77	51.34	5.27	0.16	0.32	14.96	12.48	0.28	0.07	562	0.18	1414
12	Pembina River	28	22.25	44.61	3.14	0.26	0.05	17.06	11.62	0.29	0.23	1847	0.09	707
12	Pembina River	29	10.52	37.71	23.90	0.05	0.92	12.89	13.59	0.25	0.05	401	0.26	2043
12	Pembina River	30	18.80	43.75	7.58	0.17	1.30	13.93	14.23	0.21	0.06	482	0.26	2043
12	Pembina River	31	17.77	47.15	6.06	0.13	1.08	12.89	14.68	0.19	0.07	562	0.25	1964
12	Pembina River	32	35.18	31.57	3.77	0.12	0.36	11.81	16.75	0.17	0.08	642	0.20	1571
12	Pembina River	33	22.96	45.49	1.61	0.24	0.11	16.50	12.18	0.25	0.21	1687	0.09	707
12	Pembina River	34	21.11	44.43	4.09	0.26	0.07	19.26	10.02	0.34	0.51	4097	0.08	628
12	Pembina River	35	16.33	49.91	5.43	0.13	0.75	10.95	15.48	0.20	0.05	401	0.16	1257
12	Pembina River	37	19.83	47.31	2.86	0.31	0.06	17.77	10.96	0.31	0.24	1928	0.08	628
12	Pembina River	38	19.85	42.19	7.16	0.19	1.29	15.27	13.35	0.21	0.08	642	0.24	1886
12	Pembina River	40	16.74	46.09	7.45	0.16	1.42	12.96	14.64	0.18	0.07	562	0.24	1886
12	Pembina River	41	17.46	44.69	7.08	0.15	1.29	14.49	13.46	0.24	0.08	642	0.25	1964
12	Pembina River	42	17.24	45.20	7.31	0.21	1.36	14.56	13.58	0.25	0.08	642	0.24	1886
15	Blackstone River	43	9.35	52.04	12.33	0.04	0.43	9.79	15.30	0.22	0.06	482	0.19	1493
15	Blackstone River	44	34.64	31.17	3.10	0.16	0.40	15.25	14.32	0.22	0.21	1687	0.18	1414
16	North Ram River	45	17.70	47.73	4.05	0.23	0.10	20.13	9.19	0.35	0.26	2088	0.05	392
21	North Ram River	46	9.18	47.27	13.08	0.13	0.54	20.73	8.07	0.40	0.17	1365	0.10	785
21	Main Ram River	48	21.28	41.62	6.56	0.23	0.32	18.75	10.63	0.30	0.22	1767	0.13	1021
22	North Sask. River	50	16.87	50.65	4.48	0.12	0.73	10.76	15.69	0.22	0.05	401	0.20	1571
23	Baptise Creek	52	15.86	50.63	4.87	0.16	0.90	12.65	14.54	0.22	0.07	562	0.15	1178

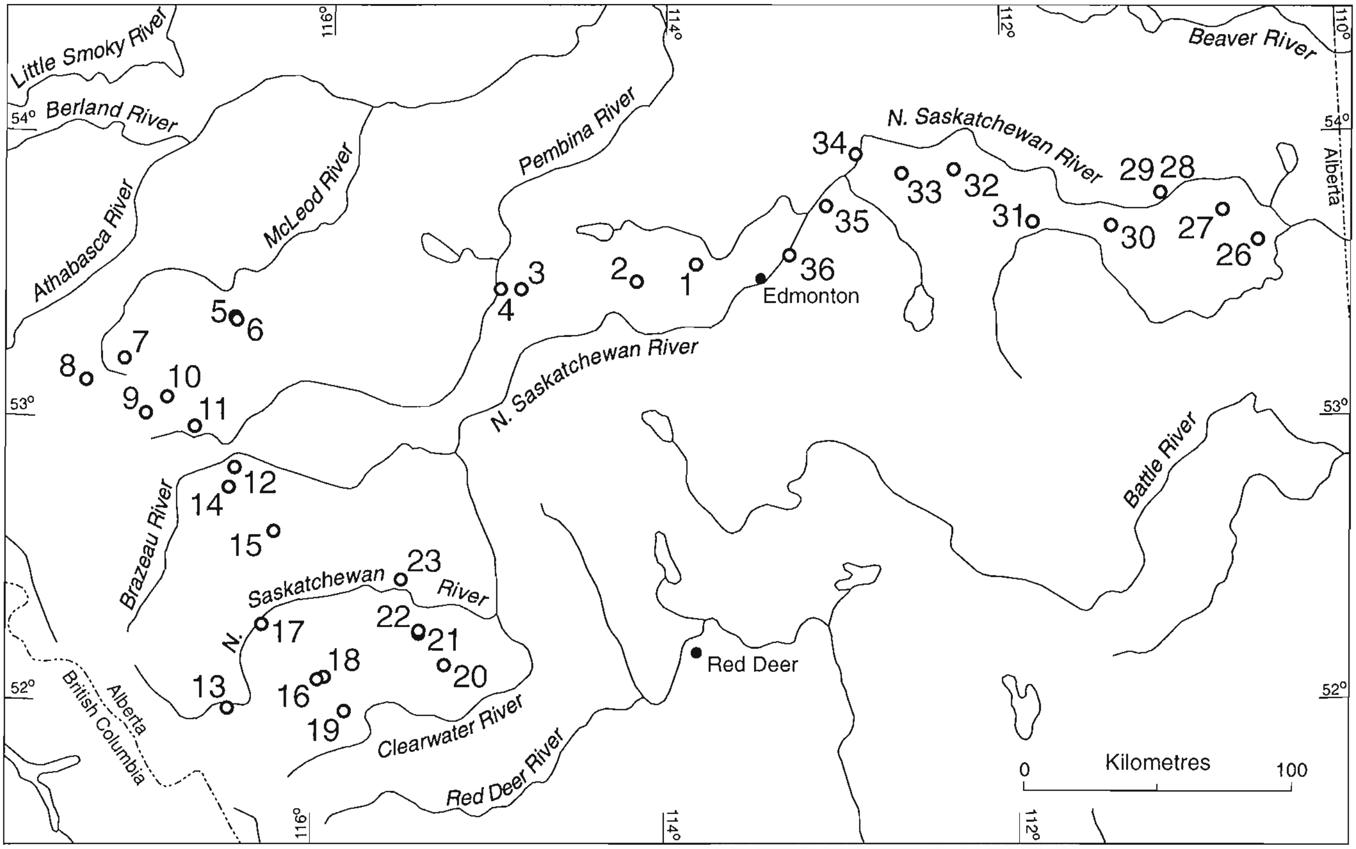

Figure 1. *Central Alberta study area sample location map, sites 1–23, 26–36. For precise locations and additional data, see Table 1.*

Edmonton, Alberta, for further processing using their carbon-hydrocarbon adsorbent. Samples collected by the senior author from selected sites on the Athabasca River and in Fort MacMurray drainage systems were found to contain fine to plus 100 μm particles of gold or electrum (Plates 9, 10). Gold particles containing up to 80 per cent gangue (in our tests, limonitic material), hydrophobic sulphides and gold grains below the lower limit of gravity processes (i.e., less than 50 μm) were recovered by Envi-Tech. Inc. Our sample sites did not yield any PGM grains in this test suite so the ability of the Carbad process to recover the variety of PGM found in central Alberta drainages (Harris and Ballantyne, 1994), could not be confirmed.

Platinum-group minerals

As reported by Harris and Ballantyne (1994), the principal PGMs from the North Saskatchewan River are Pt-Fe alloys (ferroan platinum), Os-Ir-Ru alloys, rare native platinum, hongshiite and sperrylite (Plates 3–5). The ferroan platinum alloys occur mainly as platelets up to 400 μm in diameter, as rods up to 600 μm in length and as spheres of less than 100 μm. Their (Fe,Cu,Ni) contents range from 10 to 32 wt.% with minor to trace amounts of Os, Ir, Rh, Pd and Ru; inclusions consist of chalcopyrite, bornite and PGMs such as native osmium, cooperite, irarsite, hollingworthite and unidentified phases of Rh-S and Rh-Ir-As-S. Harris and Ballantyne (1994) illustrated a number of the typical shapes and forms of grains observed in these samples. These alloys and their inclusions are considered to represent a primary high-temperature paragenesis.

The second most abundant PGM grains are the Os-Ir-Ru alloys. The Os-Ir-Ru grains are similar in appearance to the Pt-Fe alloy platelets, but are more silvery in colour. Analyses of these alloys show that they plot in the compositional fields of osmium, ruthenium, iridium and rutheniridosmine. The data for some of the Os-Ir-Ru alloys indicate a slightly narrower miscibility gap than that previously defined by compositions of material from other worldwide occurrences. This could be indicative of derivation from higher temperature rocks than ultramafic-mafic intrusions.

Gold-bearing alloys and gold grains

The gold-bearing alloys are the most abundant grains of economic interest in the HMC from placer and paleoplacer environments (Plates 6–8). SEM and electron microprobe analyses indicate a wide range in compositions, with grains commonly displaying zoning between core and rim. The compositions of the more pristine and homogeneous gold grains range in fineness (parts per thousand pure gold) from 550 to over 950. The majority of these pristine grains have a fineness greater than 800 and can be classified as "native gold"; those with a fineness of less than 800 are classified as "electrum". Some gold grains were found to be alloyed with mercury, which varied from a thin surface rim, to irregular replacement, to almost complete replacement. These grains can be mistaken for PGMs because of their silvery colour. Gold grains with mercury contents of up to 40.7 wt.% were analyzed. The source of the mercury is believed to be anthropogenic. Other gold grains were found to contain platinum and palladium in concentrations reaching 14.1 wt.% Pt, 8.0 wt.% Pd and 4.0 wt.% Ag. A common origin with the PGMs is indicated. Gold and gold alloy grains of similar sizes, textures and compositions have also been reported from bedrock in the Fort MacKay region of north-central Alberta by Feng and Abercrombie (1994), and Abercrombie and Feng (1996; *this volume*).

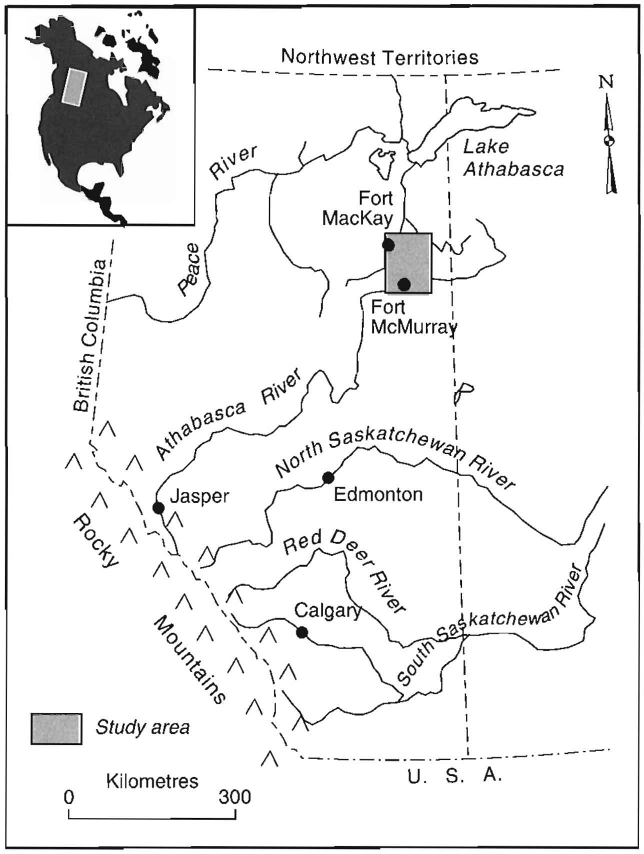

***Figure 2.** Northeastern Alberta study area, Fort McKay – Fort McMurray area. See Figure 3 for detail.*

Gold grains: alteration and modification in paleoplacer environments

Probable bacteriological modification

Examination of the surface textures of gold grains from paleoplacer settings of central and northern Alberta indicates that they have been significantly modified (Plates 9–16). Irregular surfaces, including "mamillary" forms, are clearly evident. At a fine scale, "mounds" made up of an open-textured network of intricate branching and multi-levelled "filaments" of pure gold (i.e., lacking silver or any other metals), reach above the substrate more than 200 μm (Plates 9–11). In some cases, similar forms have been modified by subsequent transportation of grains (Plate 10). These textures appear to result from bacterial colonization and precipitation of pure gold on the surfaces of gold grains. The relationship of these apparently bacteriologically-generated forms to the general surface textures of gold grains is shown in Plates 9 to 16. In particular Plates 12 and 13 illustrate the multi-layered nature and lace-like texture of the features interpreted as of bacteriological origin.

The Alberta material examined in this study is very similar to identical (in some respects) to the genus *Pedomicrobium*-like budding bacteria from Australia and Alaska described by Bischoff (1994) and Watterson (1992), respectively.

Bischoff et al., (1992) also provided detailed evidence for the microbial accumulation of gold in the alluvial environments of Venezuela. Undulating filamentous appendages of gold aggregates from Venezuela are described as *Chrysoagyrtus venezuelaensis*.

Inorganic modification

The mammillary, mound and branching textures visible in Plates 10 to 13 indicate bacteriological activity. It seems equally clear, however, that some gold has been dissolved and re-precipitated authigenically in these paleoplacer deposits, without the influence of bacteria. The strongest evidence of such authigenic activity lies in the persistent occurrence of gold grains exhibiting highly irregular shapes (Plates 6–8). The following discussion provides an interpretation of how such authigenic modification of gold grains may have occurred in the Alberta paleoplacers, and compares the Alberta examples with similar textures seen in alluvial gold deposits in Central Otago, New Zealand.

In the recycled gravels, the depositional environment of the first stage of authigenic, irregular-shaped gold grain development is interpreted as being acidic, reducing and dominated by sulphur derived from the oxidation of pyrite. This silver-bearing, irregular gold contains rare, delicate, octahedral gold crystals or portions of crystals that reflect in situ formation. The thiosulphate ion may be responsible for both Au and Ag transport in chloride-poor surficial environments under neutral to alkaline conditions (Webster and Mann, 1984; Webster, 1986).

The second stage of gold accumulation is marked by pure gold overgrowths that occur on silver-bearing, coarse gold grains and other authigenic minerals such as marcasite. Changing groundwater conditions during uplift and Holocene erosion are believed responsible for the accumulation of authigenic gold, silica, kaolinite and marcasite (colloform banding, framboid, and crystal structures) as well as cavity-filling and replacement textures (see Watterson, 1992). Second-stage gold overgrowth apparently occurred when gold was dissolved under neutral-alkaline, oxidizing or reducing conditions and transported by HS^- or possibly by humic acid complexes. This pure gold precipitated under acidic conditions as chemically accreted "mustard" (regular, diffuse rims) and/or thin to concentric layers of gold-marcasite ± silica and kaolinite. With further uplift marcasite would have broken down owing to its rapid oxidation in the surficial environment, and produced iron oxide remnants on these authigenic gold surfaces.

Youngson and Craw (1993) and Craw and Youngson (1993) described authigenic gold chemical accretion and residual concentration recycling processes in the world class alluvial deposits of Central Otago, New Zealand. These authors described chemical processes that led to substantial gold grain coarsening and higher fineness composition during Pleistocene-Recent uplift and alluvial sedimentation. These processes may be continuing today within local gold concentrations in channel lag deposits in alluvial fan environments. Authigenic gold deposition has occurred during uplift and reworking of each younger gravel sequence, although the precise nature of the chemical processes active in Central Otago groundwaters is not understood (Clough and Craw, 1989; Youngson and Craw, 1993). Otago authigenic

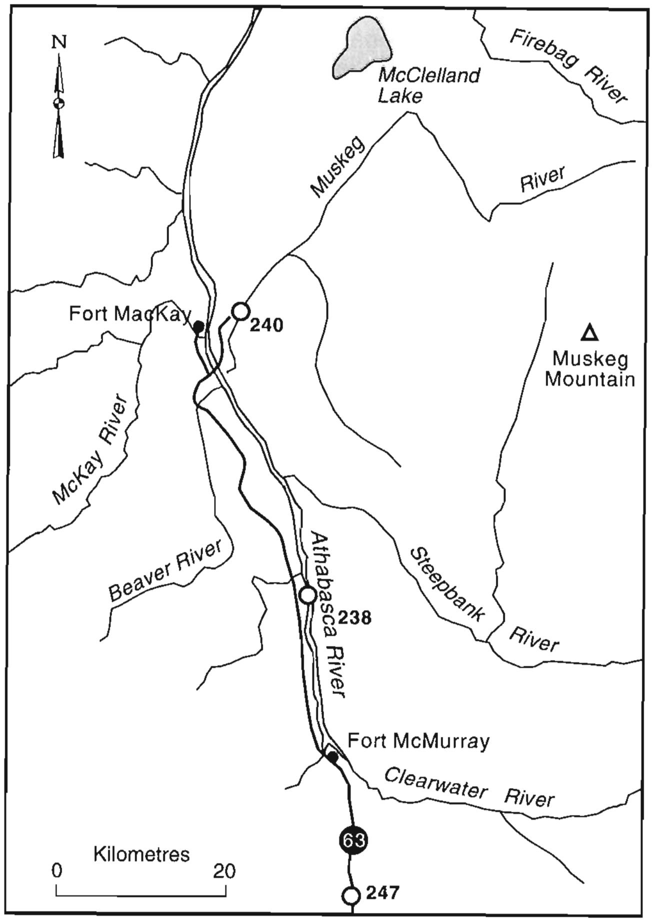

Figure 3. Northeastern Alberta study area showing locations of samples 238 (Plate 10), 240 (Plate 9), and 247 (Plate 16). These HMC sample sites were panned by the senior author as part of GSC–MDA methodology transfer to private industry exploration programs.

gold occurs as: amorphous coatings and protrusions, cement between detrital gold grains, overgrowths of lattice intergrowths, and embayment growths around inclusions of authigenic clays or detrital minerals (Youngston and Craw, 1993). Rare, worm-like masses of gold occurring in cavities in nugget-sized grains may be due to bacterial processes (ibid., 1993). Craw (1992) also examined gold reprecipitation in normal fluvial sediments in Southland, New Zealand (Waimumu Stream). There the major discrepancy between very fine grained (1-20 μm) primary vein gold and coarse (1-6 μm) gold particles found in fluvial sediments can be ascribed to diagenetic welding and recrystallization during or after recycling induced by transport deformation (Craw, 1992).

In Canada, gold grains showing similar textures have been described. Giusti (1986) noted spongy rims on Alberta alluvial gold grains, and Eyles (1990) described postdepositional nugget accretion (composite grains) from British Columbia's Cariboo gold placers.

Experimental aspects of gold grain modification

Chemical and biochemical transport-accumulation of gold in the surficial environment is an area of ongoing research and discussion. Aspects of the topic may have important implications for understanding gold and PGM distribution in source rocks and streams in the WCSB.

Bacteria-produced amino acids were found to solubilize native gold at neutral and alkaline pH, and further resulted in amino acid transport of colloidal gold (Lyalikava and Mokeicheva, 1969; Mineyev, 1976). Southam and Beveridge (1994) conducted experiments in the laboratory at 60°C (low-temperature diagenesis) and at atmospheric pressure, whereby a soil bacterium (*Bacillus subtillis*) solubilized native gold under acidic conditions. Within a few months bacterially derived organic compounds transformed colloidal gold into *in vitro* hexagonal-octahedral gold crystals 20 μm in size, which later aggregated to form 50 μm-sized gold grains. Their low-temperature sediment diagenesis-simulated laboratory model (Southam and Beveridge, 1994) adequately demonstrates bacterial capacity to bind metals, namely gold, and reinforces the perhaps unappreciated role of bacteria in authigenic/diagenetic mineral deposit formation.

Discussion

Placer gold and secondary gold, pyrite-marcasite and base metal sulphides in Alberta are known to have been modified and/or precipitated in the subsurface in major channels at reduction fronts significantly distal (up to 400 km) from the source for the now preserved noble-metal and polymetallic deposits. Systematic sampling of stratigraphy within gravel pits was not within the scope of our orientation study. However, Alberta sand and gravel washing operations produce "alluvial?" gold as a by-product, and account for all of Alberta's present-day gold production. It is entirely possible that fine gold is being liberated from "fossil-redox" secondary sulphide deposits now in contact with the new, post-glacial, oxidizing groundwater hydrology regime. The portions of gravel pits that host heavy black manganese and rusty-red iron oxide coatings on sands and gravels are not presently being processed or washed for HMC recovery. The past down-channel transport of gold and base metals in solution in acidic, oxidizing Tertiary groundwaters, to be redeposited in unconsolidated sediments at reduction front environments (such as clay, carbonaceous material, iron sulphide zones) should be more extensively evaluated in Alberta and elsewhere in Canada. The fact that "specialized" gold-adsorbing bacterial colonies may have been active in past or present environments or that they may be presently active in the groundwater flow regime should also be considered.

Sources of alluvial platinum group minerals, gold and gold alloy grains

As noted above, the textures and compositions of PGM grains, particularly the alloys and inclusions, support a primary, high-temperature origin. Sources for PGMs and alloys normally might include kimberlite/lamproite, ophiolitic complexes or Alaskan-type basic intrusives - none of which, with the exception of small kimberlite lamproite bodies in the Grande Prairie area, are known in Alberta. Basic/ultrabasic rocks of this sort may occur in the Canadian Shield or the Cordillera, and it is possible that extra-basinal rocks of this type are most likely sources. Clearly, further work is required. Whatever the source(s) of the PGM grains, their widespread distribution and distinctive compositions seem to indicate more than one local source.

The gold grains and gold alloys may also have an origin outside the WCSB, but we do know that there are at least two possible intrabasinal sources. These include the Cretaceous Shaftesbury Formation (Plate 8), and Devonian carbonates in the Fort McKay region. Plates 17 and 18 illustrate precious and base metal occurrences on freshly broken rock surfaces from diamond drill core in Devonian carbonates, and also insoluble residues from these carbonates. Noteworthy are minute occurrences of gold, gold-silver, copper, copper-zinc, molybdenum and native platinum group grains/crystals. Similar metal/alloy occurrences in these carbonates and associated units of the Fort McKay region are discussed in detail by Feng and Abercrombie (1994) and Abercrombie and Feng (1997; *this volume*). The sizes, shapes, textures and compositions of metallic occurrences from the Shaftesbury Formation and the Devonian carbonates indicate these units may have served as intrabasinal sources for at least some of the gold occurrences and possibly some of the PGM grains.

Diamond indicator minerals in heavy mineral concentrates

Alberta is now experiencing unprecedented exploration for diamond-bearing source rocks. HMC drainage sampling programs can detect potential source areas because several minerals associated with diamond-bearing host rocks are resistant. Key diamond indicator minerals widely used in assessing diamond potential are Cr-pyrope garnet, chromite (chrome spinel), pyrope-almandine garnet and ilmenite (Fipke et al., 1995). These minerals are known to survive exposure to weathering and erosional processes and subsequent glacial dispersion and transport into the surficial environment. Some of these diamond "indicator" minerals are known to have unique chemical and visual characteristics. Because they are also "heavy" minerals, they will accumulate at alluvial Au and PGM concentration sites within drainage systems.

As part of this project, we attempted to recover diamond indicator minerals from the HMCs. Although no pyrope garnet grains or chrome diopside were recovered, we did obtain a number of ilmenite and chromite grains. A total of 27 ilmenite grains were recovered from 11 sample localities (Table 1), as well as 37 chromite grains from 14 sample localities (Table 2), including 17 chromite grains from one locality (Pembina River). Table 2 provides compositional data on the chromite grains recovered.

Figure 4 compares TiO_2, Al_2O_3 and Ni (ppm) compositional data for chromites from this study with chromite compositional data provided by Griffin and Ryan (1993) and Griffin et al. (1994) for kimberlites and lamproites. It can be seen that many of the chromite grains recovered in this study plot outside the suggested compositional ranges for kimberlite and lamproite in Griffin and Ryan (1993), although Griffin and Ryan's (1993) chromite compositional data as indicators of diamond potential have been questioned (e.g., Kjarsgaard, 1997; *this volume*). Table 2 provides additional compositional data that may be of value when comparing chromites recovered from this study with those of other studies. Readers are also referred to the discussion in Kjarsgaard (1997; *this volume*).

In this study, compositions of recovered chromites yield a maximum concentration of Cr_2O_3 of 55.07 wt.% (Table 2). Many Alberta TiO_2 chromite concentrations fall within the 1.00–1.64 wt.% range, closely following those of kimberlitic pipes of high or increased diamond potential (1.26–1.61 wt.%) reported for the Zimni-Coast of the former Soviet Union situated within the southeastern White Sea region. Cr_2O_3 versus Al_2O_3 and TiO_2 plots for chromite compositions from Alberta also have trends comparable to Zimni Coast kimberlite pipes. The presence of ilmenite, which reflects reducing environments, favours the preservation of diamonds because most ilmenite has crystallized within the kimberlite magma. High Cr_2O_3 and MgO contents reflect low Fe^{3+}/Fe^{2+} ratios, indicating a highly reducing environment (low oxygen fugacity = low Fe^{3+} picroilmenites). MgO versus Cr_2O_3 plots (not shown here) and inferred Fe^{3+}, Fe^{2+} values based on stoichiometric calculations indicate that some ilmenites recovered in this study may be derived from kimberlite source rocks which could have preserved diamonds. Maximum Cr_2O_3 content of ilmenites is 4.88 wt.% with an accompanying 10.97 wt.% MgO concentration.

It is generally accepted that PGM placers may originate from mafic-ultramafic intrusions (Alaskan-type) or from basic to ultrabasic rocks (Alpine, ophiolite complex-type). However, it is also recognized that potentially diamond-bearing volcanic vents (lamproite) and diatremes (kimberlites) are complex hosts for mantle-derived ultramafic xenoliths in megacryst/macrocryst/matrix potassic ultrabasic rocks. Primary PGM enrichment is commonly clearly associated with chromite (chrome spinel) segregations in Alaskan-type and also Alpine-type or ophiolitic (podiform) rocks. Chrome spinels are also ubiquitous in kimberlites and olivine lamproites. As our knowledge of mineral chemistry continues to improve it is becoming clear that spinel composition trends for specific elements may overlap, or that significant differences in spinel compositions may exist within and between diatremes within the same diatreme field. We must bear these factors in mind when examining diamond indicator ilmenite and chromite geochemical composition trends. For example, in dogmatically assigning "indicator" chromites to specific source rocks (ophiolite, lamproite, kimberlite or Alaskan ultramafics) we perhaps run the risk of not considering that Alberta PGM and Au-Ag-Pt-Pd alloys might be derived from diamond-bearing, mantle-sourced rocks.

CONCLUSIONS

1. Gold and PGM grains of 25 μm and larger were recovered consistently in the field from washed and sieved material at more than 35 modern river drainage sites and 5 unconsolidated paleoplacer sites as exposed in gravel pits.

2. Alluvial gold and PGM grains range from common elliptical to ovoid disc and plate-shaped, to a variety of less common elongate and irregular

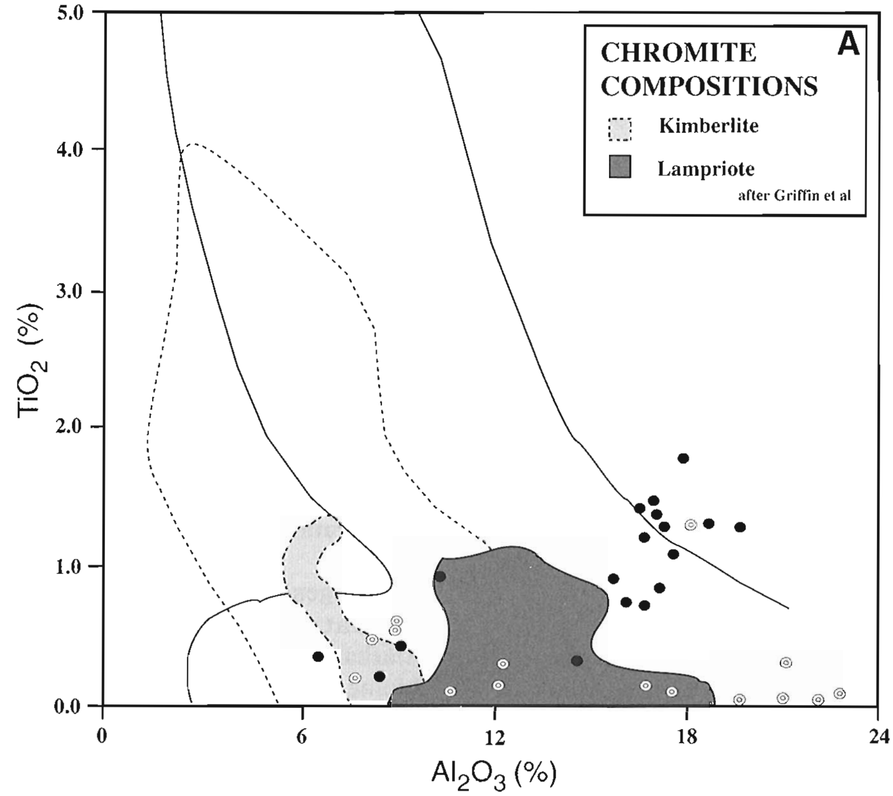

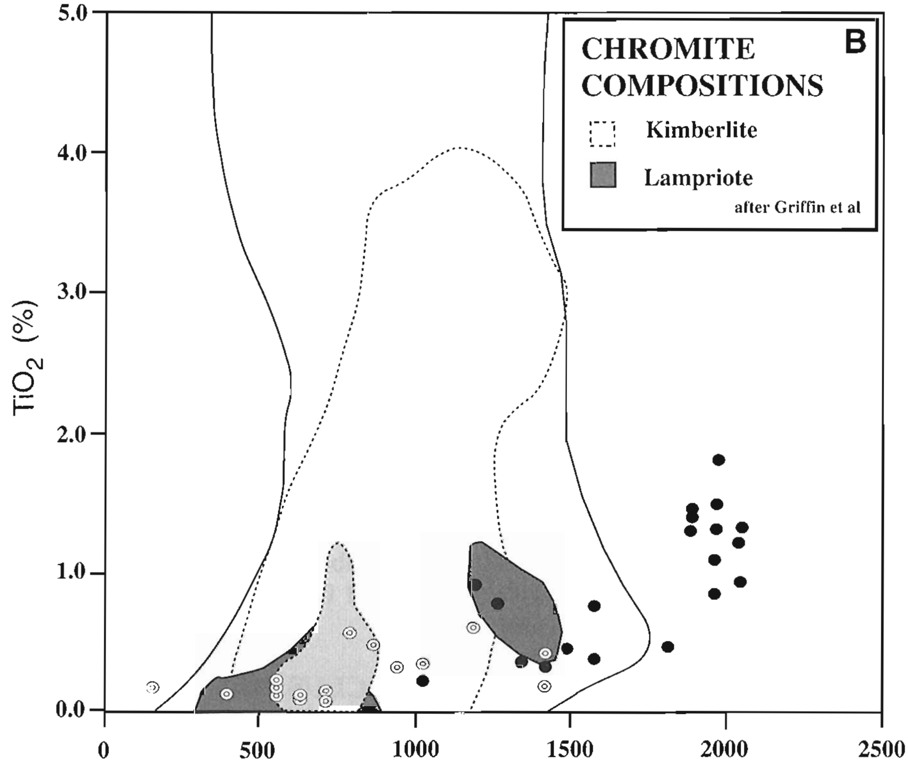

Figure 4. *Chromite (chrome spinel) compositions of grains recovered from Alberta HMCs in this study. Light and dark shaded areas are identified as diamond-associated kimberlite and lamproite fields by Griffin and Ryan (1993) and Griffin et al. (1994). See Table 2 and text for discussion.*

grains, in some cases modified by in situ diagenetic processes.

3. There appear to be two main types of alluvial precious metal grains: native gold and gold-bearing alloy grains; and PGM grains.

4. The native gold grains and gold-bearing alloy grains are the most abundant and appear to be of the greatest economic interest. They display a wide range of compositions, and many grains display zoning between the core and rims. Compositions of more pristine and homogeneous grains range in fineness from 550 to over 950.

5. PGM grains include Pt-Fe alloys (ferroan platinum) and Os-Ir-Ru alloys with inclusions of other platinum-group metals, and/or chalcopyrite or bornite. The textures and compositions of the majority of PGM grains examined in this study indicate a primary, high-temperature origin.

6. The surfaces of many alluvial grains, in both modern drainages and particularly in paleoplacer deposits, show evidence of modification, probably by bacterial processes. SEM studies show a variety of delicate, worm-like appendages, protrusions and irregular blobs on many grains. On some grains, "filaments" are clearly evident, pseudomorphed by gold. SEM-EDS spot analysis of these surface features demonstrates that they commonly are composed of high-purity gold, without silver, PGM or other elements, further supporting a bacterial origin. Some modern drainage gold grains also show bacterial(?) surface textures, but these features commonly appear to be flattened as compared with the delicate features shown by gold grains in paleoplacer deposits, suggesting that the modern drainage grains have been transported after modification of grain surfaces.

7. There is evidence of agglomeration of gold grains by bacterial precipitation of gold, as certain clusters of grains in paleoplacer deposits show bacterially-produced(?) "bridges" linking smaller grains into larger agglomerates.

8. Some agglomeration of grains may also have taken place by inorganic precipitation of gold, as has been demonstrated from similar settings in New Zealand. The strongest evidence of inorganic precipitation of gold lies in the persistent occurrence of gold grains of highly irregular shapes, which lack evidence of the action of organisms.

9. The compositional complexity, diversity, and abundance of gold and PGM grains in Alberta are unusual when these occurrences are compared with similar modern to Tertiary-aged occurrences elsewhere in the world.

10. Possible local, intrabasinal sources (as opposed to Cordilleran Orogen or Canadian Shield sources) for the widespread alluvial gold and PGM grains discovered in this study include lamproite, kimberlite or similar diatreme rocks that have intruded the sedimentary section, with known Alberta occurrences to date only verified for the Grande Prairie region. Other possible intrabasinal sources, for gold grains at least, include the Cretaceous Shaftesbury Formation of north-central Alberta, and the Devonian carbonates of the Fort McKay region of northern Alberta.

11. Some production of alluvial gold grains occurs at present from operating gravel pits in Alberta, and there is potential for further production. Evaluation of specific sites, including documenting the stratigraphic location of actual or potential gold occurrences at individual gravel pit operations, is a viable means of encouraging increased production.

12. As a part of this study, a limited number of chromite (chrome spinel) and ilmenite grains were recovered. These minerals are used widely as diamond indicator minerals in heavy mineral diamond exploration programs. The compositions of some of the chromites recovered are consistent with derivations from kimberlite or lamproite pipes that could bear diamonds. The occurrence of chromite grains in this alluvial material is regarded as a favourable sign in the search for diamond-bearing igneous rocks in Alberta.

Acknowledgments

Understanding of the possible origins of Alberta gold and PGMs has increased considerably during the course of this study, and assessment of the economic potential of the occurrences will undoubtedly follow. We gratefully acknowledge the efforts and cooperation of our colleagues at the Geological Survey of Canada (GSC), Alberta Geological Survey and the Alberta Research Council. As well, members of the mineral exploration community provided essential support for our investigations. We thank Takla Star Resources, Tintina Mines Limited, Marum Resources, Focal Resources, Birch Mountain Resources and the former Lac Minerals. Their contributions of samples and support broadened the scope of our sampling capabilities and research. This study was supported financially by the Canada-Alberta Agreement on Mineral Development, 1992-1995.

REFERENCES

Abercrombie, H.J. and Feng, R. (*this volume*)
1997: Geological setting and origin of microdisseminated Au-Ag-Cu minerals, Fort MacKay region, northeastern Alberta. *In* Exploring for Minerals in Alberta: Geological Survey of Canada Geoscience Contributions, Canada-Alberta Agreement on Mineral Development (1992-1995), R.W. Macqueen (ed.). Geological Survey of Canada, Bulletin 500, p. 247-277.

Allan, J.A.
1920: First Annual Report on the Mineral Resources of Alberta Report 1, (Gold, p. 50-53). Edmonton, Alberta Research Council, 104 p.

1924: Placer gold on Athabasca River. *In* Geological Investigations during 1914; Report 12, (Gold, p. 43). Edmonton, Alberta Research Council, p. 24-45.

Bischoff, G.C.O.
1994: Gold-adsorbing bacteria as colourisers on alluvial placer gold. Neues Jahrbuch für Geologie und Paläontologie Abhandlungen, band 194, 2/3, p. 187-209.

Bischoff, G.C.O., Coenraads, R.R., and Lusk, J.
1992: Microbial accumulation of gold: an example from Venezuela. *In* Neues Jahrbuch für Geologie und Paläontologie, Abhandlungen, v. 185, p. 131-159.

Clough, D.M. and Craw, D.
1989: Authigenic gold-marcasite association: evidence for nugget growth by chemical accretion in fluvial gravels, Southland, New Zealand. Economic Geology, Scientific Communication, v. 84, p. 953-958.

Craw, D.
1992: Growth of alluvial gold particles by chemical accretion and reprecipitation, Waimumu, New Zealand. New Zealand Journal of Geology and Geophysics, v. 35, p. 157-164.

Craw, D. and Youngson, J.H.
1993: Aluvial gold placer formation on actively rising mountain ranges, Central Otago, New Zealand. Sedimentary Geology, v. 85, p. 623-635.

Eyles, N.
1990: Post-depositional nugget accretion in Cenozoic placer deposits, Cariboo mining district, British Columbia. *In* Exploration in British Columbia, 1989. Victoria, British Columbia Ministry of Energy, Mines and Petroleum Resources, p. 147-169.

Feng, R., and Abercrombie, H.J.
1994: Dissseminated Au-Ag-Cu mineralization in the Western Canadian Sedimentary Basin, Fort MacKay, northeastern Alberta: a new gold deposit type. *In* Current Research, 1994-E. Geological Survey of Canada, p. 121-132.

Fipke, C.E., Gurney, J.J., and Moore, R.O.
1995: Diamond exploration techniques emphasizing indicator mineral geochemistry and Canadian examples. Geological Survey of Canada, Bulletin 423, 86 p.

Giusti, L.
1983: The distribution, grades and mineralogical composition of gold-bearing placers in Alberta. M.Sc. thesis, University of Alberta, Edmonton, 397 p.

1986: The morphology, mineralogy and behaviour of 'fine grained' gold from placer deposits of Alberta: sampling and implications for mineral exploration. Canadian Journal of Earth Sciences, v. 23, p. 1662-1672.

Giusti, L. and Smith, D.G.W.
1984: An electron microprobe study of some Alberta placer gold. Tschermaks Mineralogische und Petrographische Mitteilungen, v. 33, p. 187-202.

Griffin, W.L. and Ryan, C.J.
1993: Trace elements in garnets and chromites: evaluation of diamond exploration targets. *In* Diamonds: Exploration, Sampling and Evaluation, P.A. Sheahan and A. Chater (eds.). Short Course Proceedings, Prospectors and Developers Association of Canada, Toronto, p. 187-211.

Griffin, W.L., Ryan, C.J., Gurney, J.J, Sobolev, N.V., and Win, T.T.
1994: Chromite macrocrysts in kimberlites and lamproites: geochemistry and origin. *In* Proceedings of the Fifth International Kimberlite Conference, Brazil, v. 1, Kimberlites, related rocks and mantle xenoliths, H.O.A. Meyer and O.H. Leonardos (eds.). Comphania de Pequisa de Recursos Minerais, Special Publication 1A, p. 366-377.

Harris, D.C. and Ballantyne, S.B.
1994: Characterization of gold and PGE-bearing placer concentrates from the North Saskatchewan River, Edmonton, Alberta. *In* Current Research 1994-E. Geological Survey of Canada, p. 133-139.

Hoffman, C.
1891: Chemical contributions. Geological Survey of Canada Annual Report, v. V, p. 66A, 65R.

1892: Mineralogical Notes. *In* Chemical Contributions to the Geology of Canada from the Laboratory of the Survey. Geological Survey of Canada, printed by S.E. Dawson, Ottawa, p. 65R.

Kjarsgaard, B.A. (*this volume*)
1997: Diamonds in Alberta: studies of potential host rocks of deep-seated origin and applications of indicator mineral exploration techniques. *In* Exploring for Minerals in Alberta: Geological Survey of Canada Geoscience Contributions, Canada-Alberta Agreement on Mineral Development (1992-1995), R.W. Macqueen (ed.). Geological Survey of Canada, Bulletin 500, p. 185-207.

Lyalikova, N.N. and Mokeicheva, L.Y.
1969: The role of bacteria in gold migration in deposits. Geokhimiya, v. 38, p. 805–810.

Mann, S.
1992: Bacteria and the Midas touch. Nature, News and Views, Plant Biology, v. 357, p. 358–360.

Mineyev, G.G.
1976: Organisms in the gold migration - accumulation cycle. Geokhimiya, v. 13, p. 577–582.

Shaw, J. and Kellerhals, R.
1982: The composition of recent alluvial gravels in Alberta River beds. Alberta Research Council, Bulletin 41, p. 151.

Southam, G. and Beveridge, J.T.
1994: The in vitro formation of placer gold by bacteria. Geochimica et Cosmochimica Acta, v. 58, no. 20, p. 4527–4530.

Tyrrell, J.B.
1915: Gold on the North Saskatchewan River. Canadian Mining Institute Transactions, v. 18, p. 160–173.

Watterson, J.R.
1992: Preliminary evidence for the involvement of budding bacteria in the origin of Alaskan placer gold. Geology, v. 20, p. 315–318.

Webster, J.G.
1986: The solubility of gold and silver in the system Au-Ag-S-O_2-H_2O and 25°C and atmosphere 29. Geochimica et Cosmochimica Acta, v. 50, p. 1827–1845.

Webster, J.G. and Mann, A.W.
1984: The influence of climate, geomorphology and primary geology on the supergene migration of gold and silver. Journal of Exploration Geochemistry, v. 22, p. 21–42.

Youngson, J.H. and Craw, D.
1993: Gold nugget growth during tectonically induced sedimentary recycling, Otago, New Zealand. Sedimentary Geology, v. 84, p. 71–88.

Plate 1

Sampling Methods

The samples for this study were primarily obtained using the in situ field classification and panning methodology depicted in photographs A–D.

Coarse gravel sites were selected as far from the bank as possible at low water levels. The top one third of a metre or so of gravel was shovelled into the nestled sieves and conical-pan system (**A** and **B**). The material was well hand-washed and mixed successively into the four fractions as depicted in **D** by using a plastic flour scoop (see **A**). The less-than-one-millimetre-sized material was saved in the bottom batelle. This material was well mixed; clean water was added to remove all clay or rusty water from the pan before actual reduction of the "lights" from the pan was begun (see **D**). The degree of slope of the modified steepened sides of the cone shaped pan is illustrated in **C**. The swirling of clean water and washed material in the conical pan allowed the "light" material to spill over the lip of the pan while the "heavies" were captured in the central vortex. After reduction of the lights the "heavy" minerals were swirled. They too could be easily reduced or separated by careful dipping and spilling over the lip of the pan. The gold and platinum grains were left in the very bottom of the central vortex. A small water squirt bottle (**C**) and the plastic flour scoop were used to remove the "black sand" and gold-PGMs into a numbered plastic bag. Excess water was decanted from the plastic bag before closing it with plastic ties. By shaking the bag, the gold and PGMs could be concentrated into the bottom corner of the bag. These grains could often be examined with a hand lens or they could be viewed in the dimple in the very bottom of the pan before flushing into the plastic bag.

Well-rounded quartzite pebbles dominate the river-bed material at this sample site (**A**, **B** and **D**). The Rocky Mountains- and Foothills- derived Proterozoic and Paleozoic rocks (quartzites and limestones) are generally more resistant to wear during transport than the less-resistant Cenozoic and late Mesozoic mudstones, shales and sandstones exposed at the surface. However, even in Alberta's large rivers, important, locally-derived Tertiary and Cretaceous rocks such as ironstones, coal, bentonite, sandstones, and preglacial gravels can dominate the river-bed material. In our study, the western extent of the continental Laurentide glaciation's influence on river-bed material (exotic granite and gneiss pebbles) could be easily approximated by the presence of excessive quantities of "erratic" metamorphic garnets recovered during panning of the HMC. Although modern central Alberta river systems obtain bed material from successions of continental and Cordilleran glacial deposits, downcutting and incision processes are predominant in the plains reaches. (Shaw and Kellerhals, 1982). It can be assumed active degrading and differential fluvial transport of locally derived river-bed materials can be obtained from some sections of the rivers and their tributaries. Close inspection of the complex history of river valleys is a prerequisite for the interpretation of the HMC data obtained. Regional and detailed follow-up HMC surveys using the batelle modified field kit has shown clearly that the Precambrian shield and the interior of British Columbia can no longer be presented as the sole sources of the gold-PGM and chromite grains at the expense of local sources hosted by Alberta strata.

PLATE 1

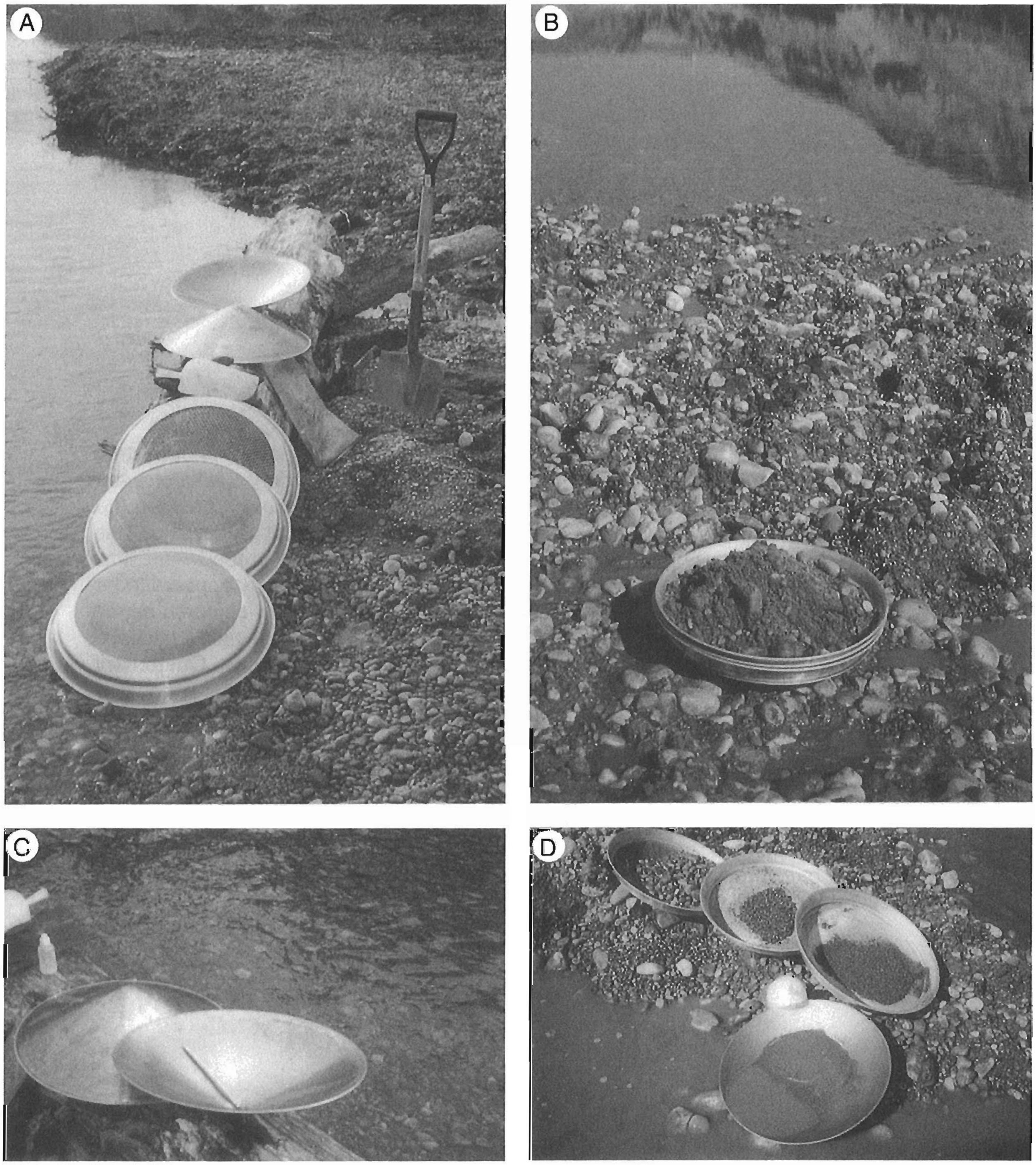

Plate 2

Paleoplacer Gravels

Preglacial alluvial fan and river channel deposits now exposed in industrial aggregate-pit operations west of Edmonton (**A–F**). These Tertiary Saskatchewan sands and gravels reveal complex multiple transport phases. Considerable grain-size sorting has taken place during fluvial sedimentological processing. This has produced porosity differences that now result in selective groundwater flow regimes within the strata. In some cases, the present-day hydrology appears to be different from Tertiary flow (as evidenced from dry, perched, rusty coloured sands and gravels). The magnitude of the effects of the postglacial valley isostatic vertical rebound, preglacial valley infill by glacial fluvial deposits, Quaternary denudation, and slope downcutting associated with orogenesis are suggested processes responsible for these hydrological changes.

In Alberta, the economic potential for the formation of auriferous paleoplacers in settings similar to those of New Zealand (Craw and Youngson, 1993) is yet to be adequately assessed. However, past climatic, hydrological and geomorphological features evident in present aggregate-pit operations and the heavy mineral material recovered from these and other preglacial deposits in Alberta suggest that further detailed study is warranted.

PLATE 2

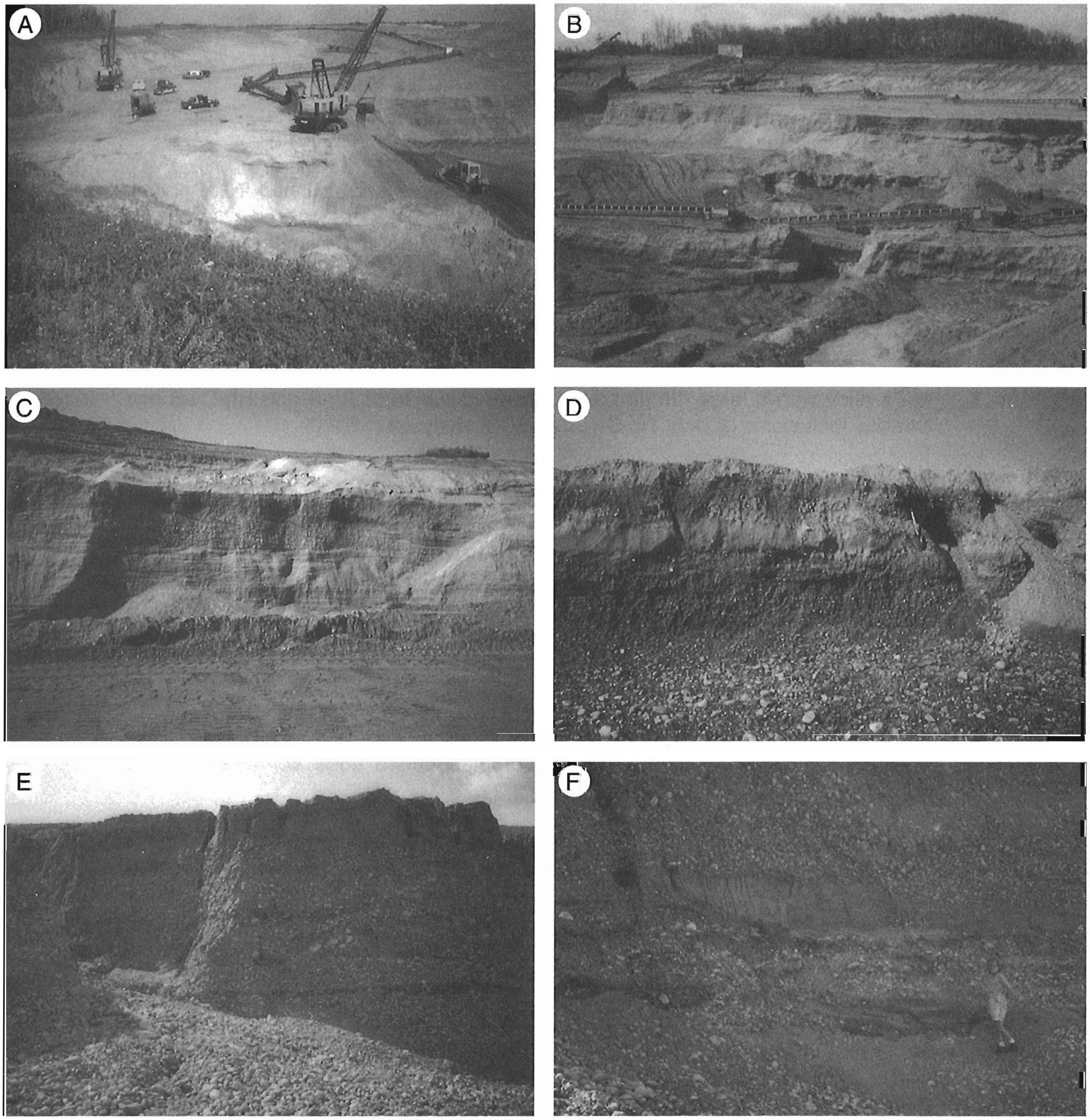

Plate 3

Platinum-Group Mineral Grains, 1891 Sample (#5611)

A–F. SEM backscattered electron images of resin-mounted and polished PGM grains. Scale is given at top of each photograph. This sample was collected by Mr. M. Pearce and donated in 1891 to the National Mineral Collection Systematic Reference Series at the Geological Survey of Canada, Ottawa. It is identified as coming from the North Saskatchewan River near Fort Edmonton. This material is similar to that recovered during this study. Other SEM image examples can be found in Harris and Ballantyne (1994).

A. Pt-Fe alloy with a large (20 μm), intergrowth inclusion of Rh-S and Rh-Cu-S and satellite inclusions of only Rh-S (SEM–EDS analysis).

B. Ir-Os alloy with crystalline Cu-S inclusions and spheroid SiO_2 and crystalline Mg-silicate inclusions (SEM–EDS analysis).

C. Pt-Fe alloy grain with numerous randomly distributed small inclusions of intergrown Rh-Cu-S and Rh-S phases (SEM–EDS analysis).

D. Pt-Fe alloy grain with three, spherical, K-Al-silicate, droplet-like inclusions (SEM–EDS analysis).

E. Pt-Fe alloy grain with a single Rh-S inclusion containing diffuse filigreed growths of Pt-Fe alloy within it and along its circular edge. This is a rare texture. Most sulphide inclusions have crystalline or droplet-defined edge contacts with the enclosing Pt-Fe or Os-Ir-Ru alloy host.

F. Pt-Fe alloy grain containing three, tiny Pd-As inclusions and a larger spheroid inclusion. Within the K-Al-silicate sphere, five minute crystals of Pt-As are visible.

In general, Alberta Pt-Fe alloys (ferroan platinum) and alloys of Os-Ir-Ru were found to contain a diverse variety of droplets and inclusions. They are composed of silicates, base metal sulphides, platinum group-element-bearing sulphides and platinum-group- element-bearing arsenides, tellurides and antimonides. In some cases, Os-Ir-Ru alloys and Pt-Fe alloys were found to be intergrown in complex forms (see Harris and Ballantyne, 1994). Native platinum grains and hongshiite (Pt-Cu alloy) were also analyzed (ibid.). The complexity and diversity of the alluvial PGM material from Alberta as compared to other worldwide placers was not known prior to this orientation study.

PLATE 3

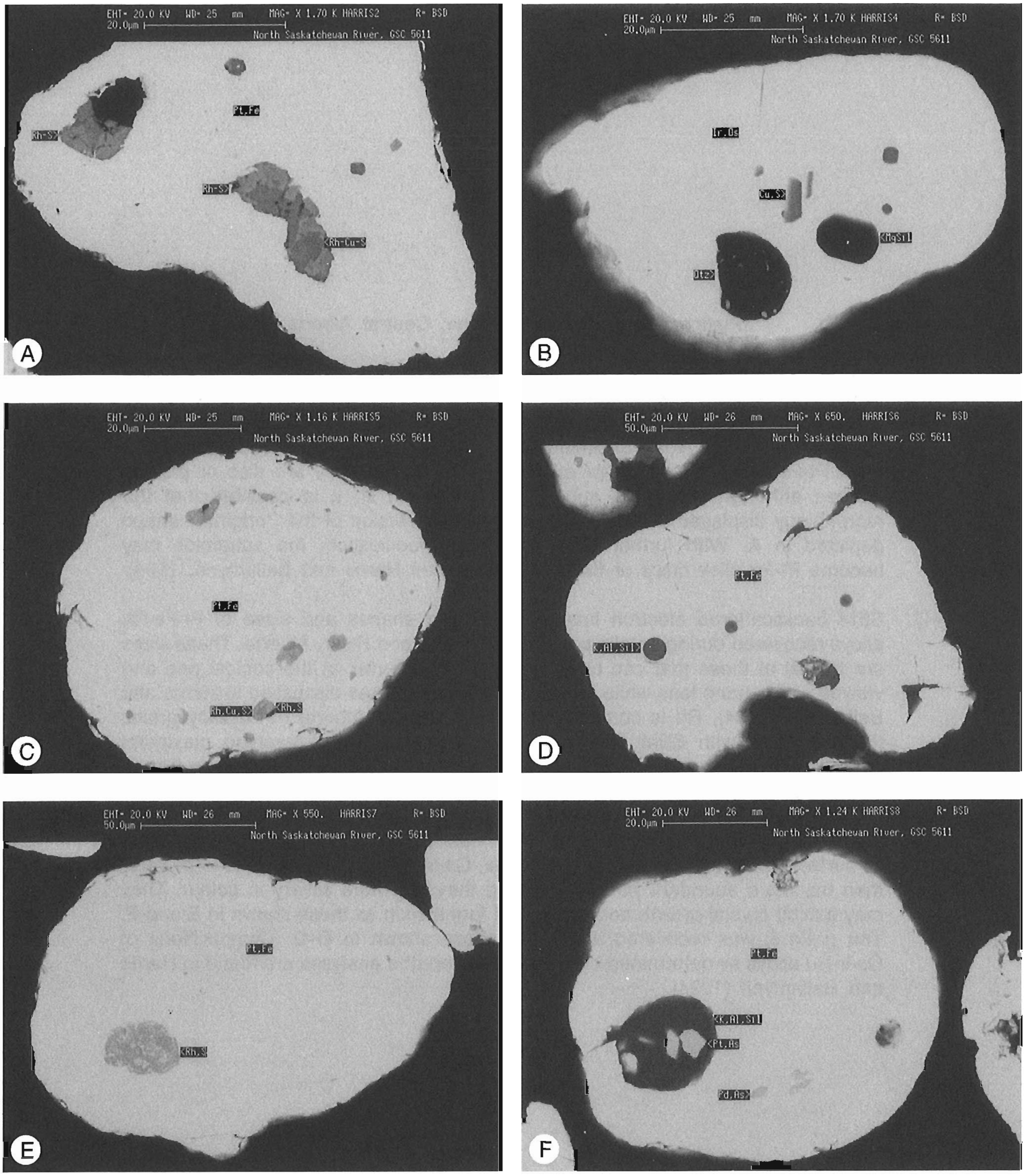
EHT= 20.0 KV WD= 25 mm MAG= X 1.70 K HARRIS2 R= BSD
20.0μm
North Saskatchewan River, GSC 5611
Pt,Fe
Rh-S>
Rh-S>
<Rh-Cu-S
A
EHT= 20.0 KV WD= 25 mm MAG= X 1.70 K HARRIS4 R= BSD
20.0μm
North Saskatchewan River, GSC 5611
Ir,Os
Cu,S>
<MgSil
Qtz>
B
EHT= 20.0 KV WD= 25 mm MAG= X 1.16 K HARRIS5 R= BSD
20.0μm
North Saskatchewan River, GSC 5611
Pt,Fe
Rh,Cu,S>
<Rh,S
C
EHT= 20.0 KV WD= 26 mm MAG= X 650. HARRIS6 R= BSD
50.0μm
North Saskatchewan River, GSC 5611
Pt,Fe
K,Al,Sil>
D
EHT= 20.0 KV WD= 26 mm MAG= X 550. HARRIS7 R= BSD
50.0μm
North Saskatchewan River, GSC 5611
Pt,Fe
<Rh,S
E
EHT= 20.0 KV WD= 26 mm MAG= X 1.24 K HARRIS8 R= BSD
20.0μm
North Saskatchewan River, GSC 5611
Pt,Fe
<K,Al,Sil
<Pt,As
Pd,As>
F

Plate 4

Platinum-Group Mineral Grains, Central Alberta

A. SEM backscattered electron photomicrograph images of an approximately 40 μm Pt-Fe alloy crystal. Note the smooth face and modified "spheroid" faces on the rest of the crystal. This material was donated by Mr. Frank Scheibein, who collected it from the North Saskatchewan River within the city limits of Edmonton. Most Pt-Fe alloys recovered or examined during this study are disc or platelet shaped although some are spheres as shown in **B**. It is possible that the morphology displayed in **B** is a slightly modified version of the "original" shape depicted in **A**. With further fluvial transport modification, the spheroids may become Pt-Fe alloy discs or flattened plates (see Harris and Ballantyne, 1994).

B–D. SEM backscattered electron images of various shapes and sizes of Pt-Fe-Rh alloys recovered during batelle panning of the McLeod River, Alberta. These sizes are typical of those that can be recovered in the vortex of the conical pan and viewed with a hand lens while at the field sample site. As discussed in Harris and Ballantyne (1994), Rh is commonly detected in most Alberta Pt-Fe alloy grains (EDS analysis with SEM). Minor to trace amounts of Rh reaching maximum quantitative analyses of 7.3 wt.% were determined by electron microprobe (Harris and Ballantyne, 1994).

E–F. Backscattered electron image of an Os-Ir-bearing alloy grain (**E**) and a close-up of its surface texture (**F**). In Alberta drainages, Os-Ir-Ru alloys were found to be rarer than the more abundant Pt-Fe alloys and they are more silvery in colour. They may exhibit crystal growth and hexagonal forms such as those shown in **E** and **F**. The grain **E** was recovered along with those shown in **B–D**. Compositions of Os-Ir-Ru alloys as determined by electron microprobe analyses are found in Harris and Ballantyne (1994).

PLATE 4

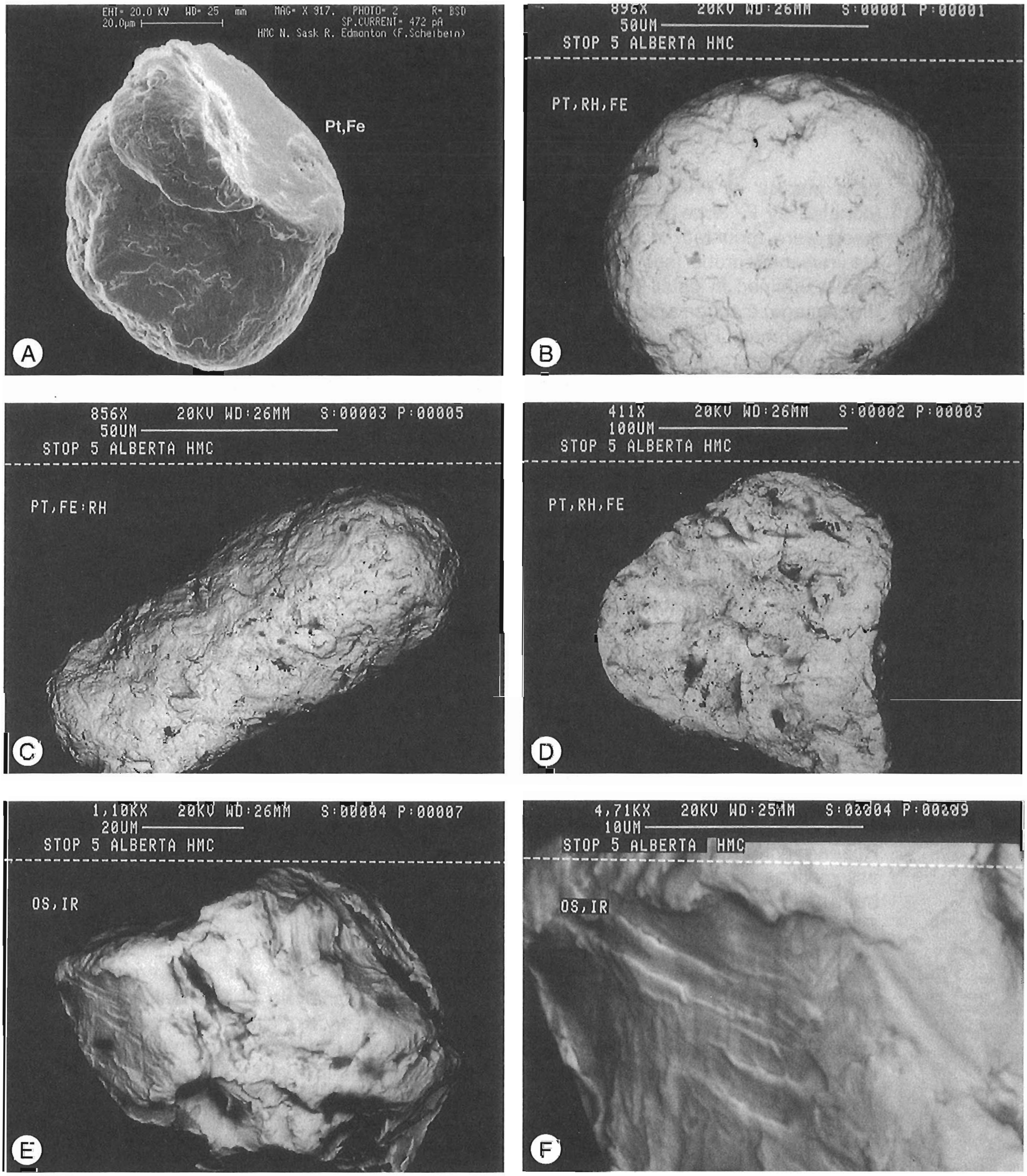
EHT= 20.0 KV WD= 25 mm MAG= X 917. PHOTO= 2 R= BSD
20.0µm
SP.CURRENT= 472 pA
HMC N. Sask R. Edmonton (F.Scheibein)
Pt,Fe
A
896X 20KV WD:26MM S:00001 P:00001
50UM
STOP 5 ALBERTA HMC
PT,RH,FE
B
856X 20KV WD:26MM S:00003 P:00005
50UM
STOP 5 ALBERTA HMC
PT,FE:RH
C
411X 20KV WD:26MM S:00002 P:00003
100UM
STOP 5 ALBERTA HMC
PT,RH,FE
D
1,10KX 20KV WD:26MM S:00004 P:00007
20UM
STOP 5 ALBERTA HMC
OS,IR
E
4,71KX 20KV WD:25MM
10UM
STOP 5 ALBERTA HMC
OS,IR
F

Plate 5

Platinum and Gold Grains

A–C. SEM images of Pt-Fe alloys from the North Saskatchewan River, Edmonton (donated by F. Scheibein). Larger sized disc and plate shaped grains such as these were mounted in araldite resin, polished and analyzed quantitatively by electron microprobe (see Plate 3). Before mounting, the surfaces of the grains were examined in detail (**A** and **B**) in secondary (left image) and backscattered (right image) electron modes to determine the presence of mineral gangue (Si,O in **A**) and primary PGM growth or cleavage features (**B**). No mineral gangue or chromite intergrowths commonly associated with PGM enrichment in Alaskan or ophiolite-complex type deposits were identified with the PGMs examined in this Alberta study. Photo **C** shows other Pt-Fe grain shapes typically found in central Alberta drainages.

D. A backscattered electron SEM image of a Au-Pt alloy flake recovered during sampling on the McLeod River. The black line across the centre of the image is dust contamination on the SEM stub. Unfortunately, this grain was lost during the attempt to mount it in resin. However, as reported in Harris and Ballantyne (1994), other gold-PGM-bearing homogeneous grains were found by quantitative electron microprobe analyses to contain as much as 14.1 wt.% Pt, 8.0 wt.% Pd, and 4.0 wt.% Ag. Other gold grain analyses revealed minor concentrations of Pt or Cu, and Sn or Ni. The grain in **D** contains no silver. It contains homogeneous and almost equal proportions of Au and Pt as determined by detailed SEM–EDS analysis at various points across the grain's surface.

These rare alluvial gold grains (such as **D**), with significant to minor weight percentages of Pt, Pd, Cu, Ni, Sn and Hg, are found in many Alberta drainages (see Harris and Ballantyne, 1994; also Giusti and Smith, 1984). They range in composition from complex, very inhomogeneous metals to homogeneous alloys. Research literature on the origin of these grains and their complex metal associations is not revealing. Similar textures are apparent in material derived from bedrock, northern Alberta (Feng and Abercrombie, 1994; Abercrombie and Feng, 1996).

E–F. A backscattered electron image of a typical silt sized pure gold grain recovered during panning of Alberta drainages. The SEM–EDS analysis of the delicate surface textures revealed in **F** does not indicate the presence of silver or mercury. Many gold grains examined in this study show surface amalgamation of mercury resulting in the thin surface rim of the gold grain having a texture similar to **E** and **F**.

PLATE 5

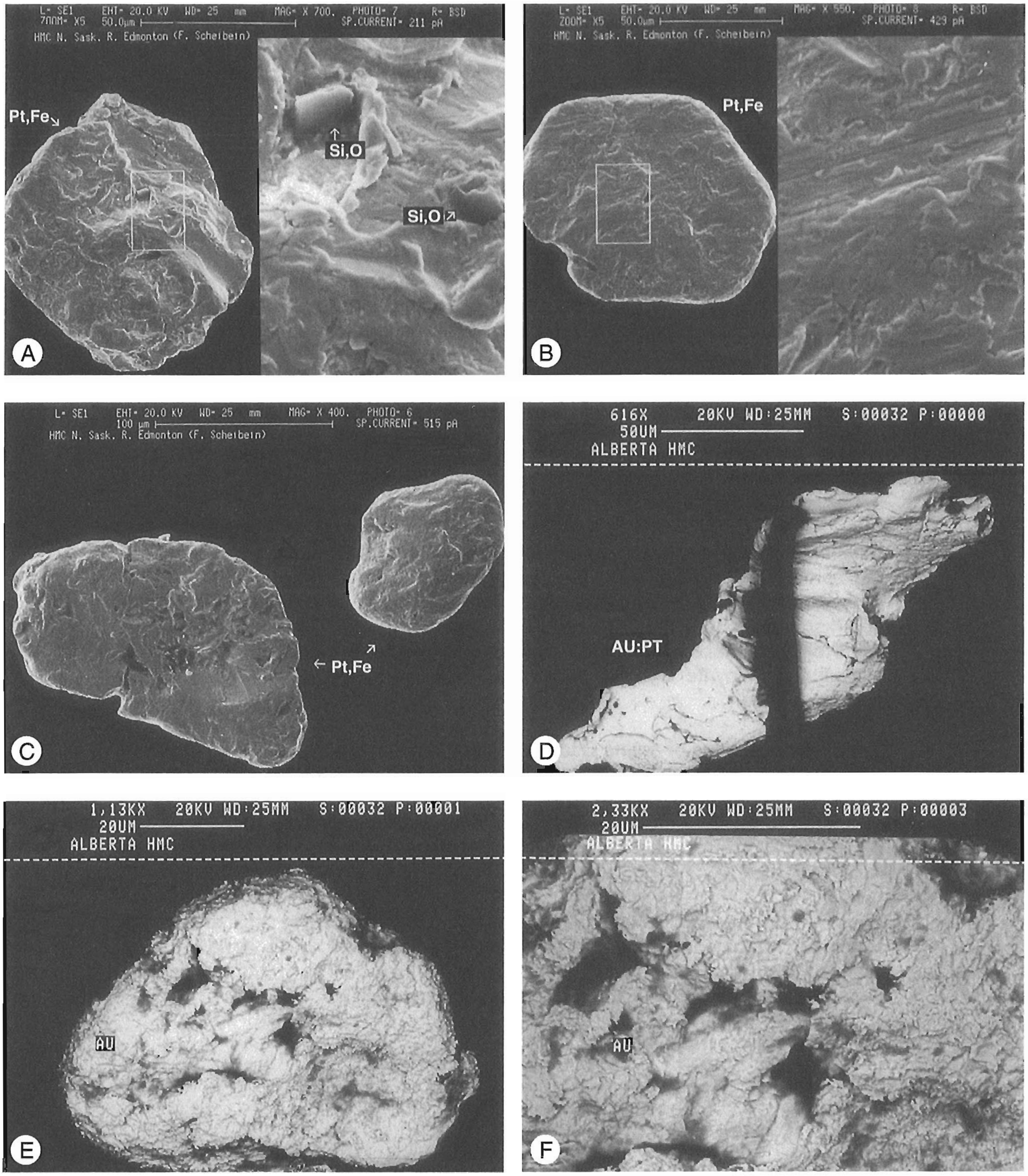
L= SE1 EHT= 20.0 KV WD= 25 mm MAG= X 700. PHOTO= 7 R= BSD
ZOOM= X5 50.0µm SP.CURRENT= 211 pA
HMC N. Sask. R. Edmonton (F. Scheibein)
Pt,Fe
Si,O
Si,O
A
L= SE1 EHT= 20.0 KV WD= 25 mm MAG= X 550. PHOTO= 8 R= BSD
ZOOM= X5 50.0µm SP.CURRENT= 429 pA
HMC N. Sask. R. Edmonton (F. Scheibein)
Pt,Fe
B
L= SE1 EHT= 20.0 KV WD= 25 mm MAG= X 400. PHOTO= 6
100 µm SP.CURRENT= 515 pA
HMC N. Sask. R. Edmonton (F. Scheibein)
Pt,Fe
C
616X 20KV WD:25MM S:00032 P:00000
50UM
ALBERTA HMC
AU:PT
D
1,13KX 20KV WD:25MM S:00032 P:00001
20UM
ALBERTA HMC
AU
E
2,33KX 20KV WD:25MM S:00032 P:00003
20UM
ALBERTA HMC
AU
F

Plate 6

Gold Grains

A. A grain showing a delicate intergrowth of silver sulphide and native silver with attached complex gangue. This 20 μm pristine alluvial grain is the only HMC-recovered silver-only grain found in GSC or industry panning surveys.

B. A pristine grain from outcrop in the McIvor River area showing presumably crystalline forms of chalcopyrite (EDS peaks) embedded by gold and silver.

C. A gold and silver grain recovered from a heavy mineral concentrate from drainages of the Shaftesbury Formation rock units. This grain is a unique polycrystalline aggregate of modified octahedra.

D–F. Examples of relatively large, pristine, gold and silver alluvial grains recovered from the same HMC sample site. The grains exhibit imbedded gangue ranging in composition from quartz to potassium-aluminum-silicate and calcium-iron-magnesium carbonate. Grain **D** also has numerous individual blotches of iron oxide on its surface. These may represent the remanent oxidation products of individual iron pyrite crystals or framboids that were previously affixed to the grain's surface.

The surface textures of grains **C** to **F** are smooth and show no indication of pitting due to silver dissolution or possible bacterial surface growths. Their pristine surfaces and delicate appendages or crystal shape features can be directly compared to those of grain **B**, which was recovered from outcrop. Little transport in the alluvial environment is suggested by the delicate forms exhibited by grains **A** to **F**.

These grains were collected by Tintina Mines Ltd. staff during their exploration surveys of north-central Alberta. The grains were recovered by Consoridex Ltd. of Hull, Quebec using tabling and super panning techniques. The grains were picked and examined by SEM at the GSC mineralogical facility.

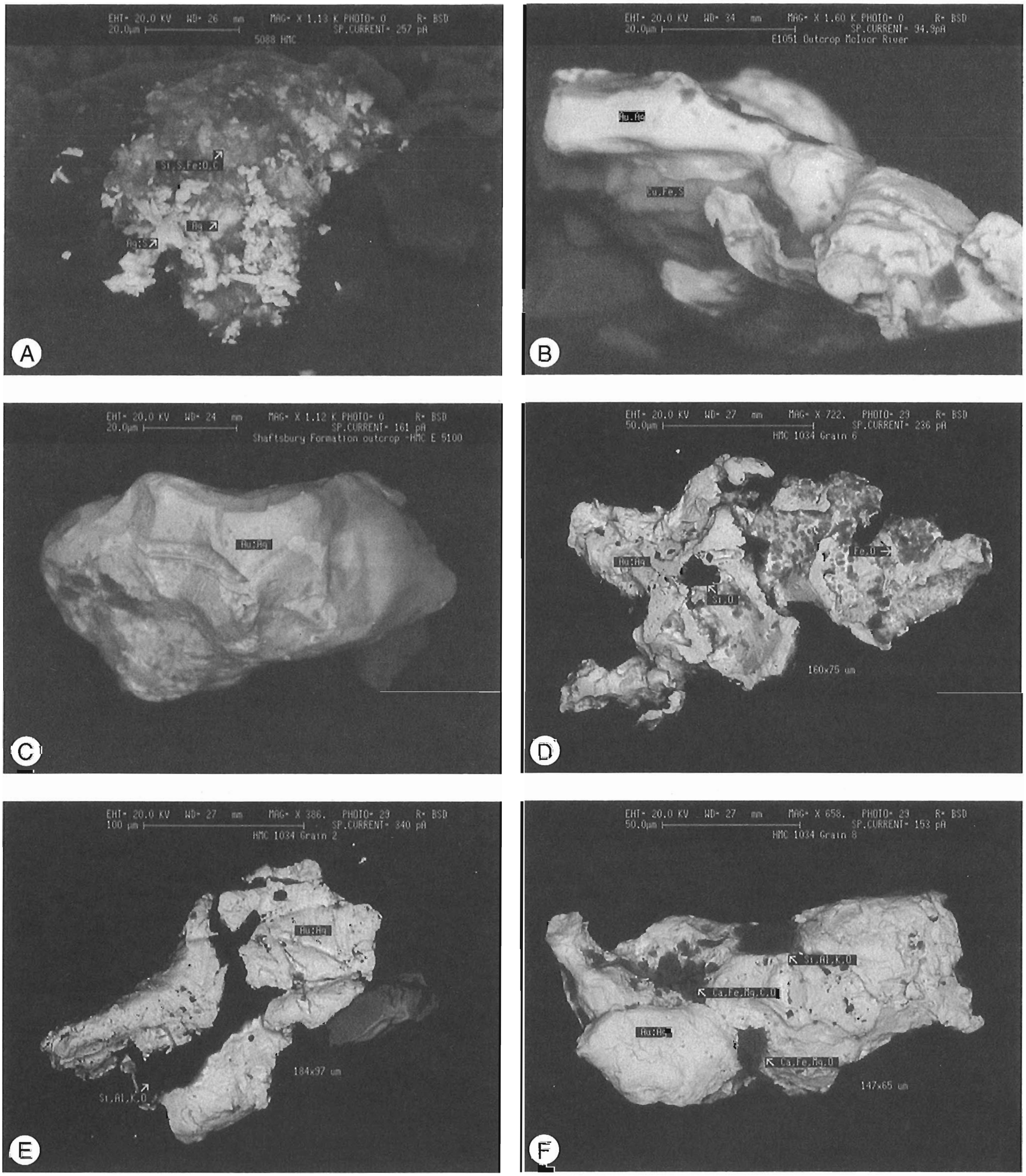
A
B
C
D
E
F
Au:Ag
160x75 um
184x97 um
147x65 um

Plate 7

Gold Grains

A–B. A polycrystalline aggregate of gold and silver octahedra exceeding 100 μm in size. The grain was recovered during HMC alluvial sampling, and exhibits mirror-smooth, even surfaces and crystallographic growth forms such as microlaminae and plane faces (**B**). This pristine grain shows little evidence of dissolution or physical deformation, suggesting recent introduction into the alluvial environment.

C–D. Elongate, polycrystalline forms of gold and silver octahedra approximately 40 μm in width. Relict plane faces are evident and preserved lamination features probably reflect zonal growth. The mirror-smooth surfaces and sharp edges of some regular microlaminae and faces suggest that twinning may have occurred. These pristine forms also suggest recent introduction into alluvial drainages.

E–F. Large gold and silver polycrystalline aggregates.

Grain **F** exhibits a more modified form of the pristine features of grain **E**. It probably reflects different growth conditions rather than physical deformation. The mirror smooth, plane-faced forms are evident in each grain as amalgamated octahedra. Our interpretation of these forms is that they have been little modified in the alluvial environment. They depict the physical forms present in the weathered profile or host rock lithology from which they were derived.

Plates A–F are examples of grains recovered from the reconnaissance alluvial HMC sampling conducted by Tintina Mines Ltd. (see Plate 6 caption).

PLATE 7

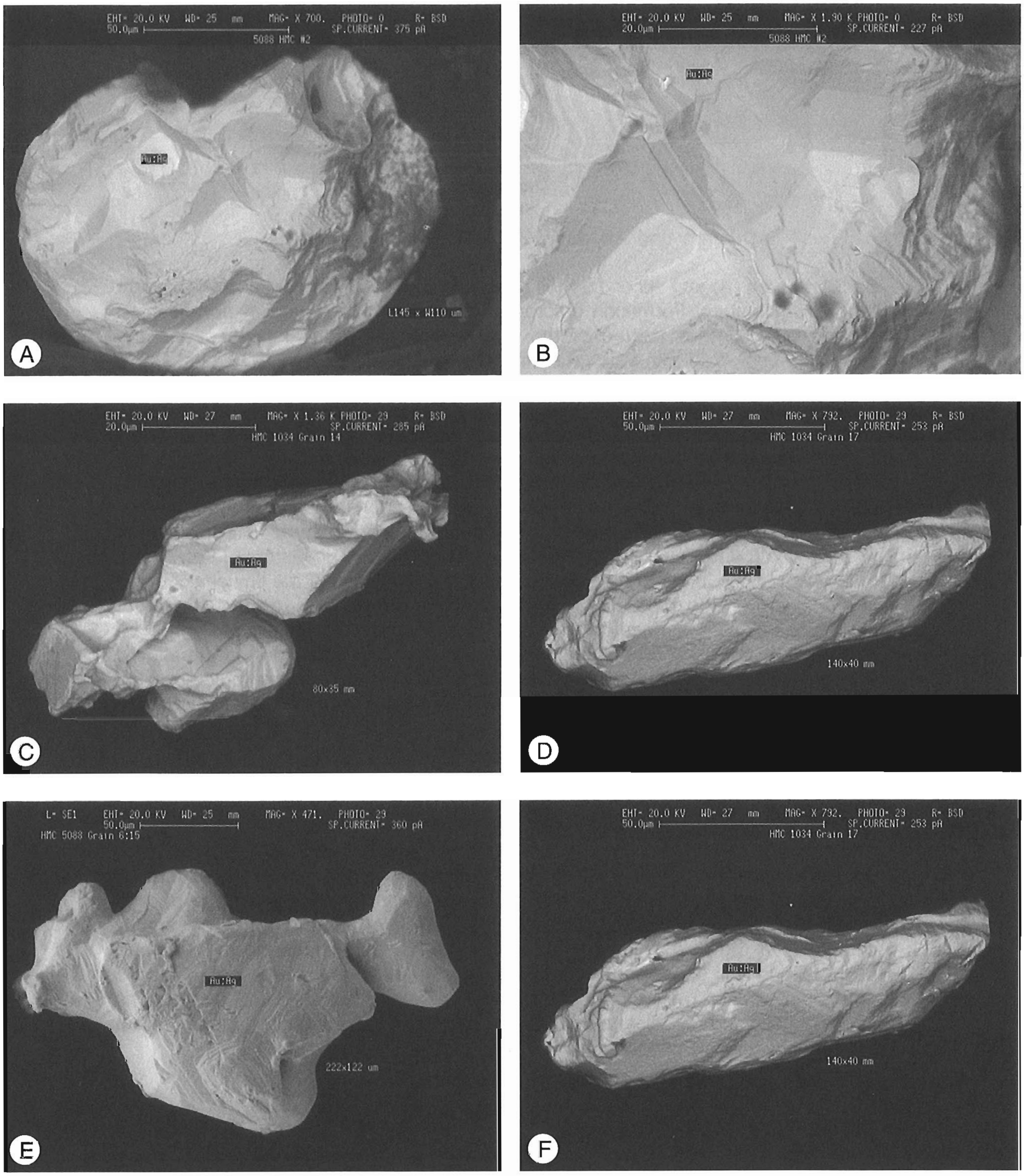

EHT= 20.0 KV WD= 25 mm MAG= X 700. PHOTO= 0 R= BSD
50.0µm SP.CURRENT= 375 pA
5088 HMC #2
Au:Ag
L145 x W110 um
A
EHT= 20.0 KV WD= 25 mm MAG= X 1.90 K PHOTO= 0 R= BSD
20.0µm SP.CURRENT= 227 pA
5088 HMC #2
Au:Ag
B
EHT= 20.0 KV WD= 27 mm MAG= X 1.36 K PHOTO= 29 R= BSD
20.0µm SP.CURRENT= 285 pA
HMC 1034 Grain 14
Au:Ag
80x35 mm
C
EHT= 20.0 KV WD= 27 mm MAG= X 792. PHOTO= 29 R= BSD
50.0µm SP.CURRENT= 253 pA
HMC 1034 Grain 17
Au:Ag
140x40 mm
D
L= SE1 EHT= 20.0 KV WD= 25 mm MAG= X 471. PHOTO= 23
50.0µm SP.CURRENT= 360 pA
HMC 5088 Grain 6:15
Au:Ag
222x122 um
E
EHT= 20.0 KV WD= 27 mm MAG= X 792. PHOTO= 23 R= BSD
50.0µm SP.CURRENT= 253 pA
HMC 1034 Grain 17
Au:Ag
140x40 mm
F

Plate 8

Outcrop and Alluvial Gold Grains with Chalcopyrite

A–B. Backscattered (**A**) and secondary (**B**) images of a plus 50 μm gold and silver grain from a Shaftesbury Formation outcrop in the McIvor River area of north-central Alberta. The surface texture of the gold and silver grain is pristine and the copper-iron-sulphide minerals (presumed to be chalcopyrite by EDS peaks) are intergrown with the precious metals.

C–D. Backscattered images of a pristine gold and silver grain recovered during heavy mineral panning reconnaissance sampling by Tintina Mines Ltd. This grain and others recovered from streams draining Shaftesbury Formation rock units is remarkable for its pristine shape and copper-iron-sulphide mineral intergrowths. Gangue of quartz and aluminum silicates is also present. The presumed chalcopyrite (by EDS peaks) is crystalline and appears to be distributed on quartz or in depressions in the grain's surface. The sharp outlines of the tiny chalcopyrite crystals show little oxidation. The smooth surface of the grain with intact protrusions (**C**) and surface casts of lost host minerals (see centre of **D**) may be explained by a very short residence time and distance of transport in the alluvial environment. It is suspected that this and other similar copper-sulphide-bearing gold and silver grains have recently entered their respective drainages as a result of active slope failure.

Compare the grain in (**C**) to those in (**A**) and (**E**), which are in situ outcrop recovered grains.

E–F. Backscattered (**E**) and secondary (**F**) images of a plus 100 μm gold and silver grain recovered from the same Shaftesbury Formation outcrop as **A**. Intergrowths of presumably chalcopyrite and quartz are completely interbedded in the pristine gold and silver grain. The composition and gangue of this grain may be directly compared to the river-drainage-derived grain in **C**. Consoridex of Hull, Quebec, using tabling and super panning techniques, recovered the grains in **A**, **C** and **E** and other similar grains from HMC material and unconsolidated rock debris (shale?) collected by Tintina Mines Ltd. during reconnaissance and follow-up exploration surveys conducted in north-central Alberta in 1994.

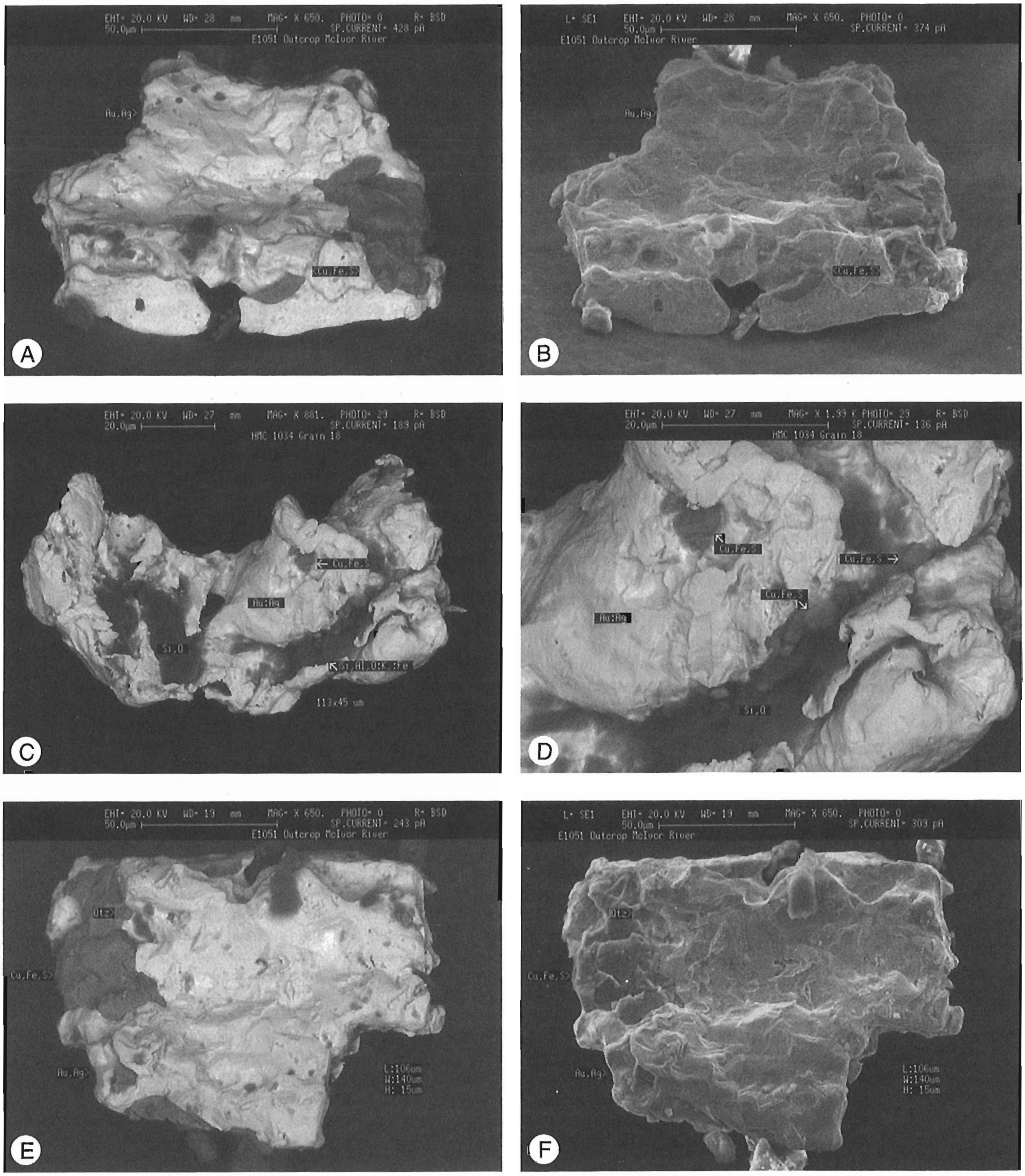
EHT= 20.0 KV WD= 28 mm MAG= X 650. PHOTO= 0 R= BSD
50.0µm
SP.CURRENT= 428 pA
E1051 Outcrop McIvor River
Au,Ag>
<Cu,Fe,S>
A
L= SE1 EHT= 20.0 KV WD= 28 mm MAG= X 650. PHOTO= 0
50.0µm
SP.CURRENT= 374 pA
E1051 Outcrop McIvor River
Au,Ag>
<Cu,Fe,S>
B
EHT= 20.0 KV WD= 27 mm MAG= X 881. PHOTO= 23 R= BSD
20.0µm
SP.CURRENT= 189 pA
HMC 1034 Grain 18
Cu,Fe,S
Au:Ag
Si,O
Si,Al,O,K,Fe
113x45 um
C
EHT= 20.0 KV WD= 27 mm MAG= X 1.33 K PHOTO= 23 R= BSD
20.0µm
SP.CURRENT= 136 pA
HMC 1034 Grain 18
Cu,Fe,S
Cu,Fe,S
Au:Ag
Cu,Fe,S
Si,O
D
EHT= 20.0 KV WD= 19 mm MAG= X 650. PHOTO= 0 R= BSD
50.0µm
SP.CURRENT= 243 pA
E1051 Outcrop McIvor River
Cu,Fe,S>
Au,Ag>
L:106um
W:140um
H: 15um
E
L= SE1 EHT= 20.0 KV WD= 19 mm MAG= X 650. PHOTO= 0
50.0µm
SP.CURRENT= 309 pA
E1051 Outcrop McIvor River
Cu,Fe,S>
Au,Ag>
L:106um
W:140um
H: 15um
F

Plate 9

Gold Grains Showing Bacterial(?) Textures

A–B. A plus 100 μm alluvial gold grain recovered by panning on the Athabasca River near Hinton, Alberta. The complete surface of the grain in **A** is covered in modified to slightly flattened gold "filament" and crystal structures (**B**).

Microbial involvement in the formation of placer gold has been described by Watterson (1992). Laboratory experiments proving the in vitro formation of placer gold by *Bacillus subtilis* have been simulated by Southam and Beveridge (1994). In the latter, low-temperature diagenesis experiment, bacterial autolysis resulted in the formation of hexagonal-octahedral gold crystals that were observed to aggregate into ≃50 μm sized forms (see **B** and **D**). Craw (1992) described the coarsening and accretion of detrital gold flakes by low-silver-content, spongy textured, reprecipitated, "new-rim" gold. Craw (1992) did not attribute the Waimumu, New Zealand, diagenetically welded detrital and secondary gold sample material to bacterial deposition; however, Alberta material documented in this study suggests the possibility of microbial processes in gold particle growth (Plates 9–16).

Authigenic gold deposition, and growth either chemical or microbial, is generally described as an almost "pure" gold rimming process as compared to the higher silver content cores of the grains. SEM-EDS spot analysis of the surface of the grains in **A** and **C** can be compared. Moderate silver content was determined for the surface of the grains in **A** and **B** but not for those in **C** and **D**. The new "pure" gold forming the delicate structures as shown in **D** is the most common feature of Alberta samples. It is not known if the moderate concentrations of silver observed on the surface of the grain in **A** and **B** is due to very thin "rimming". The detrital grains' core silver content may have actually been measured. Authigenic Ag gold-zoned rims have been identified as "inner" rims during overgrowth addition cycles onto pre-existing grains in Central Otago, New Zealand (Youngson and Craw, 1993). These authors attributed the distinctly different Ag contents of "outer" versus "inner" rims as being a reflection of different groundwater solution chemistry during gold recycling processes. Perhaps the SEM-EDS spot surface analysis of the grain in **A** and **B** reflects the higher silver contents of such an "inner rim".

C–D. Secondary electron images of a gold grain recovered from panning site #240 on the Muskeg River, in northeastern Alberta. Morphological characteristics exhibited in these images are typical of Alberta alluvial gold samples. Elliptical to oblate discoid shapes predominate. However, detailed examination of the gold grain surfaces by SEM usually reveals delicate appendages, protrusions, irregular blobs, worm-like blebs of gold on multilayered exteriors, shallow depressions and meandering crevasses or embayments, irregular pits in a modified smooth surface (see **A–F**), and, in some cases, impurities such as clay minerals and quartz. The high purity, delicate-textured appendages shown in **D** do not reveal pitting, but the comparatively smooth-surfaced (hammered appendages) exterior of the multilayered grain contains numerous irregular pits and crevasses.

E–F. Secondary electron images of a gold grain recovered by panning on the Athabasca River. **F** is a close-up of the area outlined by the white rectangle shown in the center of **E**. This mottled-textured and multilayered grain reveals meandering crevasses and embayments, some of which appear to be engulfing the mineral quartz (see upper right in **E** and detail in **F**). The exterior surface of pure Au (**E**) appears to be an agglomeration of modified or hammered delicate appendages or protrusions such as the better-preserved examples shown in **B** and **D**. The grain in **E** was also found to contain tiny Cu-Zn (alloy?) growths on an embedded quartz grain host (**F**). The processes that have led to Cu-Zn deposition are not known; however, bacterial metal-binding capacity in the genesis of certain ore deposits has been recognized. The fact that bacteria accumulate gold and cause it to exist as the native metal in highly variable morphologies (Southam and Beveridge, 1994; Bischoff, 1994) allows speculation that other microbes could have the ability to specifically accumulate other metals or combinations of metals. During this study many Alberta HMC samples were found to contain spheres to flakes of native base metals or alloys of base metals. Perhaps exotic groundwater solution and precipitation of metals and alloys enhanced secondary gold growth cycles such as shown in **E** and **F**.

Sample locations: **A–B**, #239, Athabasca River near Hinton; **C–D**, #240, Muskeg River, northeastern Alberta (Fig. 3); **E–F**, #280, northeastern Alberta, Athabasca River.

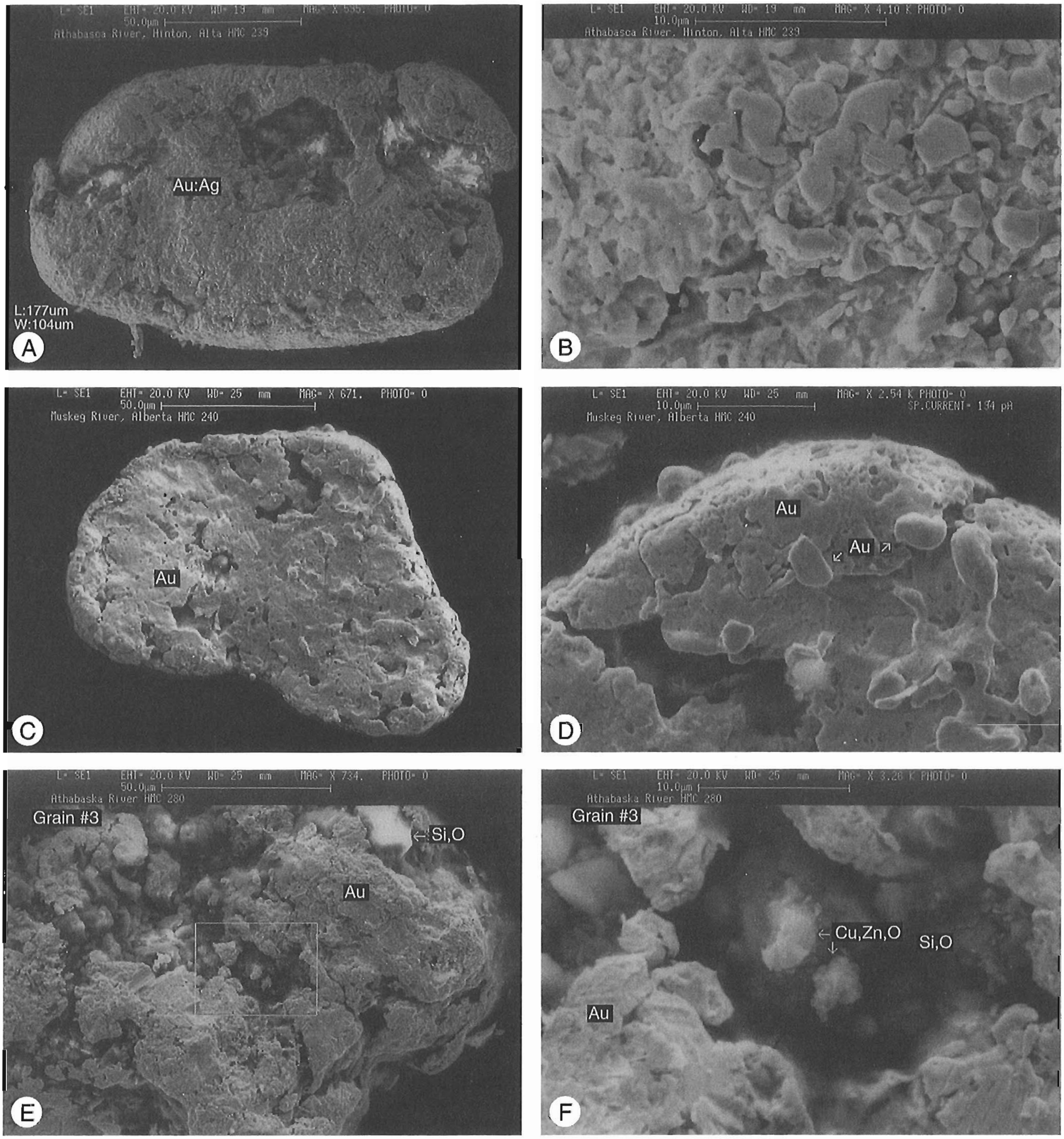
Athabasca River, Hinton, Alta HMC 239
Au:Ag
L:177um
W:104um
A
Athabasca River, Hinton, Alta HMC 239
B
Muskeg River, Alberta HMC 240
Au
C
Muskeg River, Alberta HMC 240
Au
Au
D
Athabaska River HMC 280
Grain #3
Si,O
Au
E
Athabaska River HMC 280
Grain #3
Cu,Zn,O
Si,O
Au
F

Plate 10

Gold Grains Showing Bacterial(?) Textures

A. Disc-shaped alluvial gold- and silver-bearing grain recovered by panning on the Athabasca River near Hinton, Alberta. The grain surface appears to be covered in probable bacterial growths that have been slightly flattened or modified during river transport.

B. Close-up of the geometry of the mound-like appendage adhering to the rim surface of the grain in **A**. Probable bacterial growth structures are clearly evident. Many of the protrusions have tiny black holes in their centres.

C. A gold-only grain recovered from the same site as **A**. It shows no silver peak by EDS. See below.

D. A gold-only grain similar to that in **C** in that its surface has been greatly modified by transport so the probable bacterial growth textures or holes in the sponge-texture are preserved and appear as black holes in the surface. Compare to **A** and **B** images.

E. A copper-zinc metal flake adhering to the pristine surface of an Si, Al, Mg, Fe, O mineral grain. Both Cu and Zn are major EDS peaks. Note that this metal protrudes sharply over the top or upper edge of the host mineral grain. The metal flake appears to "nestle" into and along a chipped indent and terrace structure exposed on the surface of the host grain.

F. A large gold- and silver-bearing grain recovered by panning from the same site as the grain shown in **E**. The surface of this grain is covered in probable bacterial growths similar to those of **A**.

All the grains in **A–F** were recovered from HMCs obtained by GSC panning. These black sands were treated by Envi-Tech. Inc. **E** demonstrates that native metals other than gold and silver may be recovered by exploiting natural hydrophobicity when in contact with a carbon-hydrocarbon media.

Sample locations: **A–E**, #238, Athabasca River, northeastern Alberta (Fig. 3).

PLATE 10

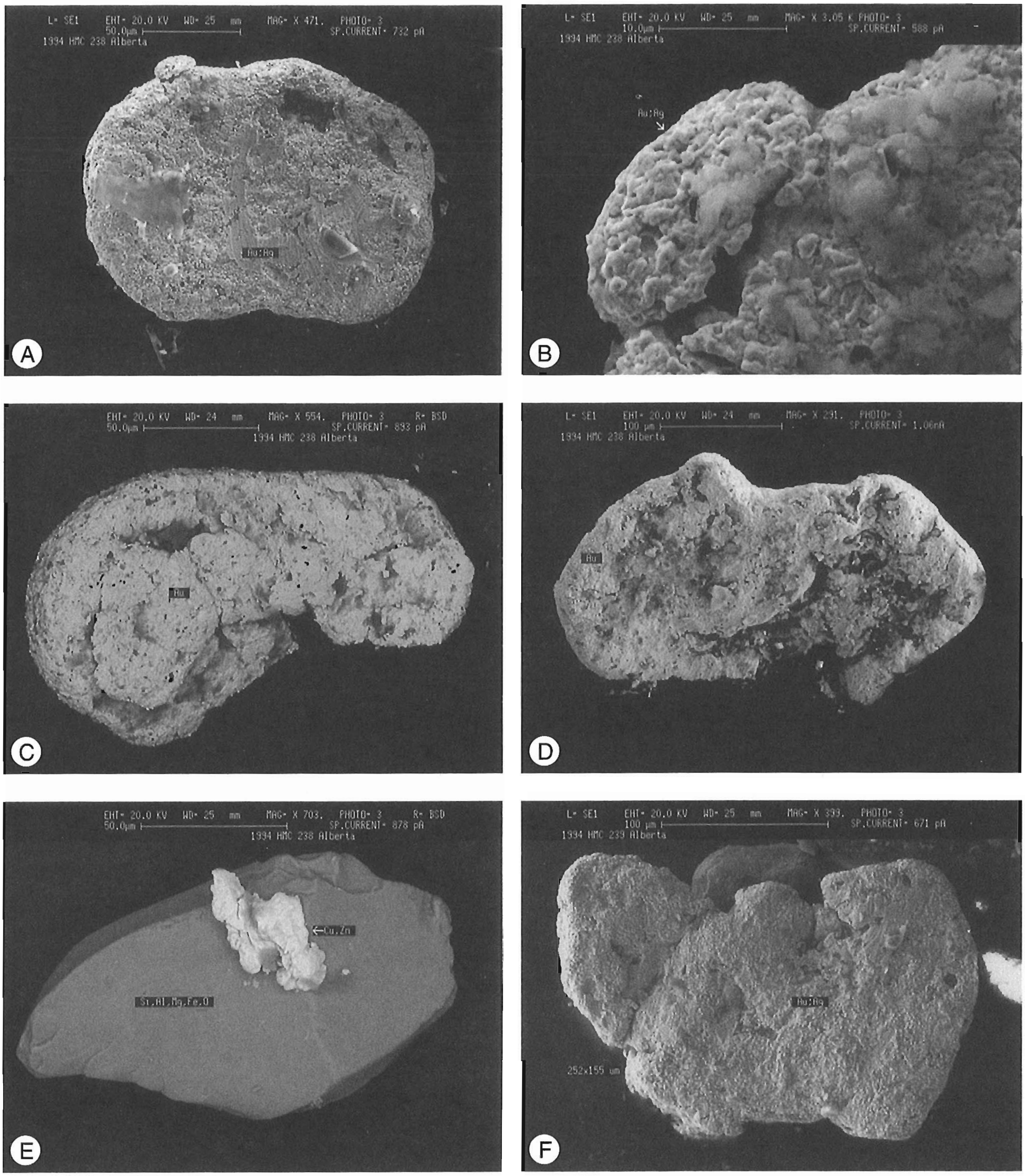

Plate 11

Gold Grain showing Bacterial(?) Textures and Transport Features

A–E. Secondary electron photomicrographs and backscattered electron images (**B**, **D**, **F**) (i.e., respective pairs) of an alluvial gold specimen donated by Tom Bryant who collected it from Alberta gravel pit gold recovery operations. This flattened, disc-shaped specimen is approximately 1.2 mm in diameter and exhibits alluvial transport features such as a distorted bent shape (**E** and **F**) and overfolded edges (**A** and **B**). The disc's surface or substrate appears to have been completely colonized by gold-adsorbing bacteria so that its irregular growth form can be morphologically described as "mamilliary" or "mustard" gold. The probable colonization of the specimen by gold-adsorbing bacteria is convincing in that a ovoid gold "mound" (500 μm) has formed an open-textured network of intricate branching and multi-levelled filaments of gold that reaches more than 200 μm above the substrate. EDS analyses of many points on the gold "mound" colony and from all over the surface of the disc showed the complete absence of silver or any other metals. It appears that bioaccumulation of pure gold has occurred in situ on previously fluvially transported gold particles found in the Tertiary paleochannels of Alberta.

PLATE 11

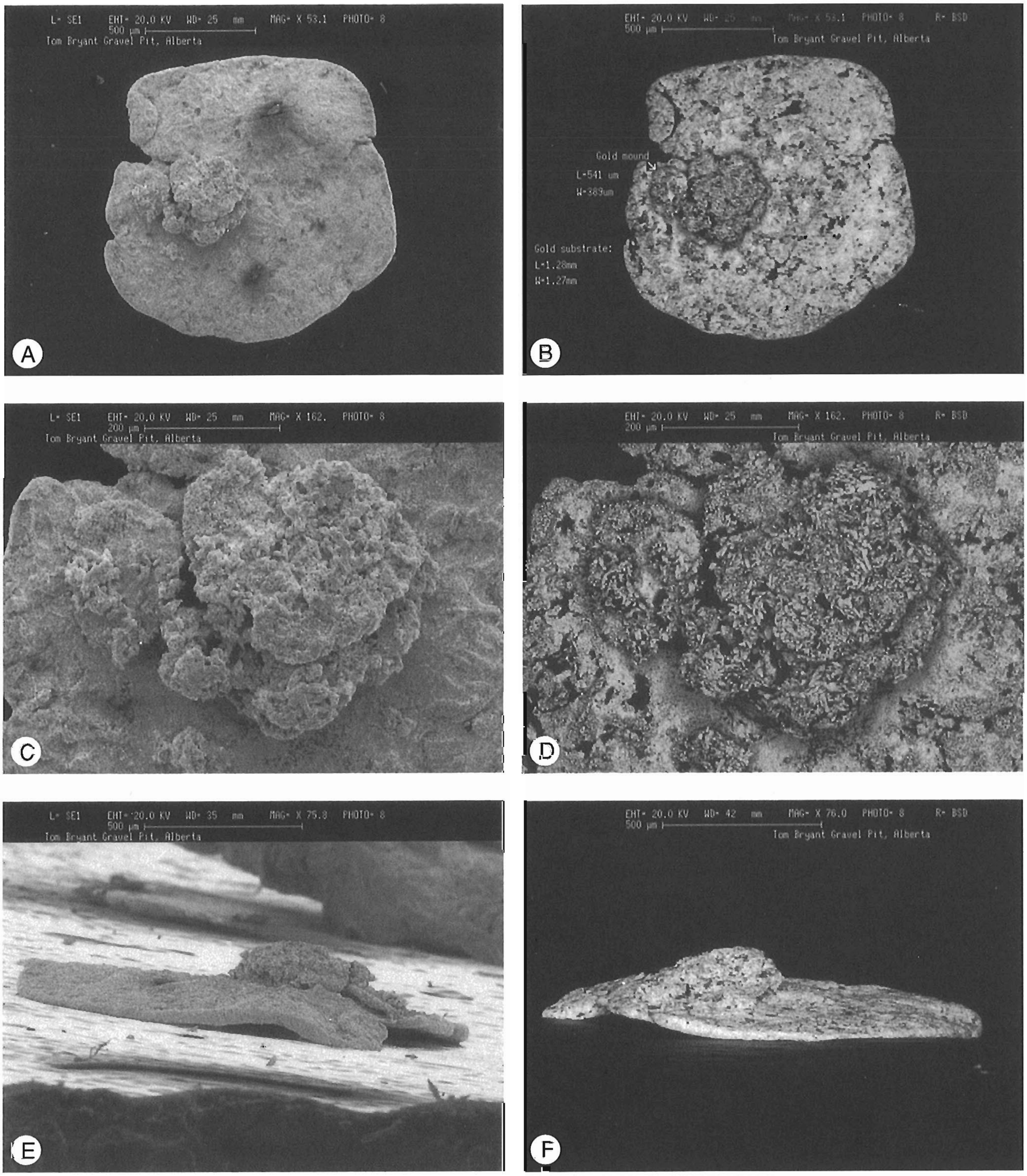
L- SE1 EHT- 20.0 KV WD- 25 mm MAG- X 53.1 PHOTO- 8
500 µm
Tom Bryant Gravel Pit, Alberta
A
EHT- 20.0 KV PHOTO- 8 R- BSD
500 µm
Tom Bryant Gravel Pit, Alberta
Gold mound
L=541 um
W=389um
Gold substrate:
L=1.28mm
W=1.27mm
B
L- SE1 EHT- 20.0 KV WD- 25 mm MAG- X 162. PHOTO- 8
200 µm
Tom Bryant Gravel Pit, Alberta
C
EHT- 20.0 KV WD- 25 mm MAG- X 162. PHOTO- 8 R- BSD
200 µm
Tom Bryant Gravel Pit, Alberta
D
L- SE1 EHT- 20.0 KV WD- 35 mm MAG- X 75.8 PHOTO- 8
500 µm
Tom Bryant Gravel Pit, Alberta
E
EHT- 20.0 KV WD- 42 mm MAG- X 76.0 PHOTO- 8 R- BSD
500 µm
Tom Bryant Gravel Pit, Alberta
F

Plate 12

Bacterial(?) Textures on Gold Grain Seen in Plate 11

A–B. Secondary photomicrographs of a vertically multi-layered pure gold "mound". The images are from different sides of the disc-shaped substrate. The lace-like texture and the delicate shapes and porous gaps of these surface bacterial(?) features indicate there was no transport after the development of these features.

C–D. Secondary and backscattered SEM images, respectively, of an edge and upper surface portion of the disc-substrate. The irregular outlines of the distinctive shapes are more closely packed than in the gold mound. A distinct ridge pattern or lattice of "filaments" or "buds"(?) can be seen protruding above the disc's surface in the centre-right portion of the image.

E–F. Secondary electron close-up images of the major gaps shown as holes in the gold "mound" in views (**A** and **B**).

Agglomerates of undulating and branching "filaments" are evident in the above images. These features are highly variable in diameter and length. (Note the 20 μm scale bar at the top of each image in the black bar area).

Sample collected by Tom Bryant from gravel pit operations.

PLATE 12

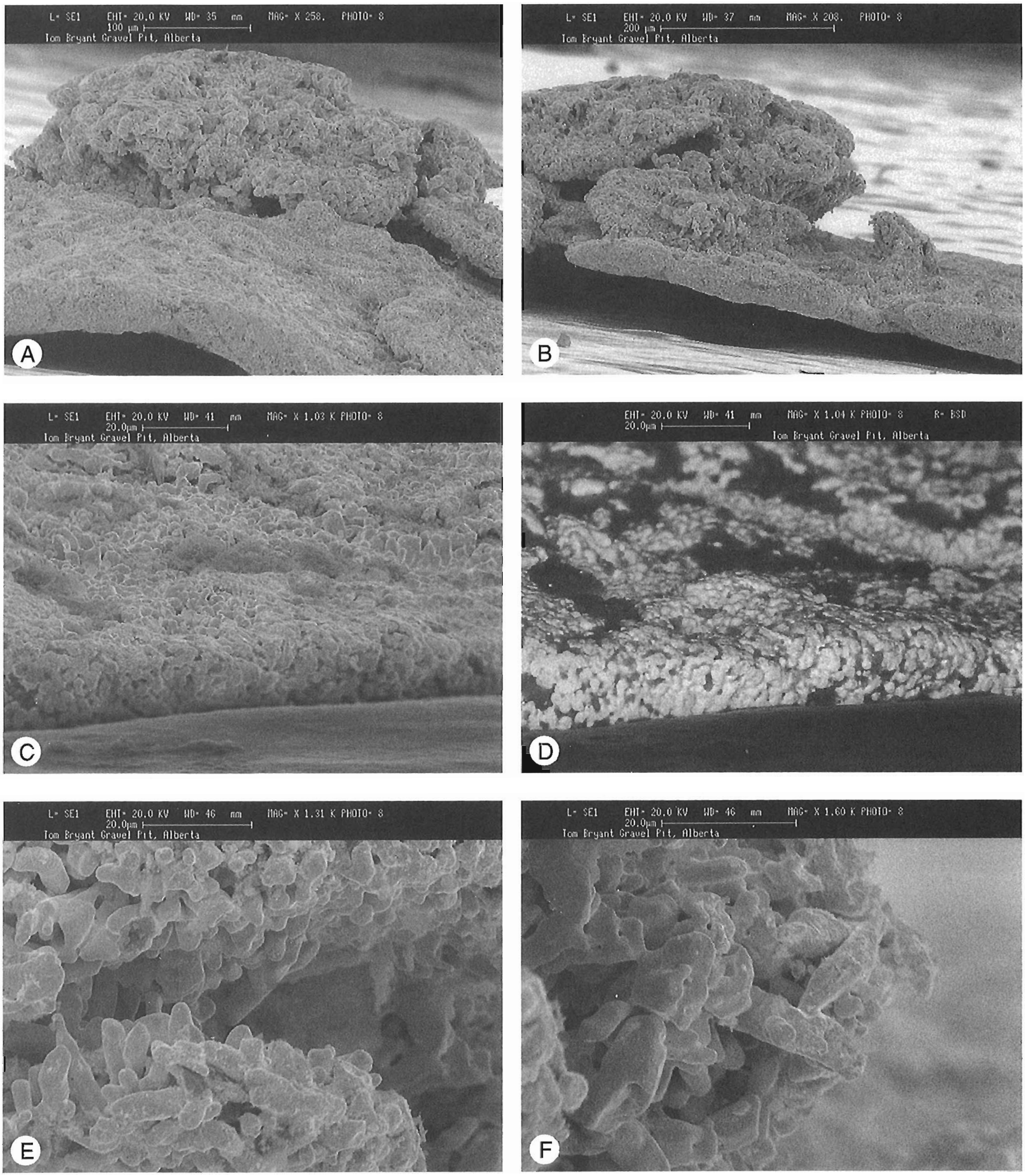
L= SE1 EHT= 20.0 KV WD= 35 mm MAG= X 258. PHOTO= 8
100 µm
Tom Bryant Gravel Pit, Alberta
A
L= SE1 EHT= 20.0 KV WD= 37 mm MAG= X 208. PHOTO= 8
200 µm
Tom Bryant Gravel Pit, Alberta
B
L= SE1 EHT= 20.0 KV WD= 41 mm MAG= X 1.03 K PHOTO= 8
20.0µm
Tom Bryant Gravel Pit, Alberta
C
EHT= 20.0 KV WD= 41 mm MAG= X 1.04 K PHOTO= 8 R= BSD
20.0µm
Tom Bryant Gravel Pit, Alberta
D
L= SE1 EHT= 20.0 KV WD= 46 mm MAG= X 1.31 K PHOTO= 8
20.0µm
Tom Bryant Gravel Pit, Alberta
E
L= SE1 EHT= 20.0 KV WD= 46 mm MAG= X 1.60 K PHOTO= 8
20.0µm
Tom Bryant Gravel Pit, Alberta
F

Plate 13

Pure Gold Bacterial(?) Textures on Alluvial Gold Grain

A–E. Secondary electron photomicrograph images demonstrate the nature and size of "filaments" on alluvial gold grains. Image **B** is an enlargement of the left-central part of image **A**; images **C** and **D** are close-ups of typical "bacterial" filaments; **E** and **F** are close-ups of features interpreted as budding hyphae.

E is a top view down the cylinder shape of a single "filament" showing an indentation at its tip. It appears that pure gold did not completely fill the original living cell so now a partly infilled cavity is preserved.

F is a close-up image of the external ribbed surface of a "filament". Close examination of images (**B** and **D**) shows numerous examples of these striae. A possible explanation is that during gold accumulation the inferred organic bacterial cell collapsed after the initial coat of pure gold was deposited on the surfaces. The black holes in the surfaces of the "buds" (**F**) and (**D**), are closely associated with the ultra-fine ribbed layers. They may indicate incomplete pure gold coating after collapse.

The sample was collected by Tom Bryant from Alberta gravel pit operations. Note that it is the same sample as illustrated in Plates 11, 12.

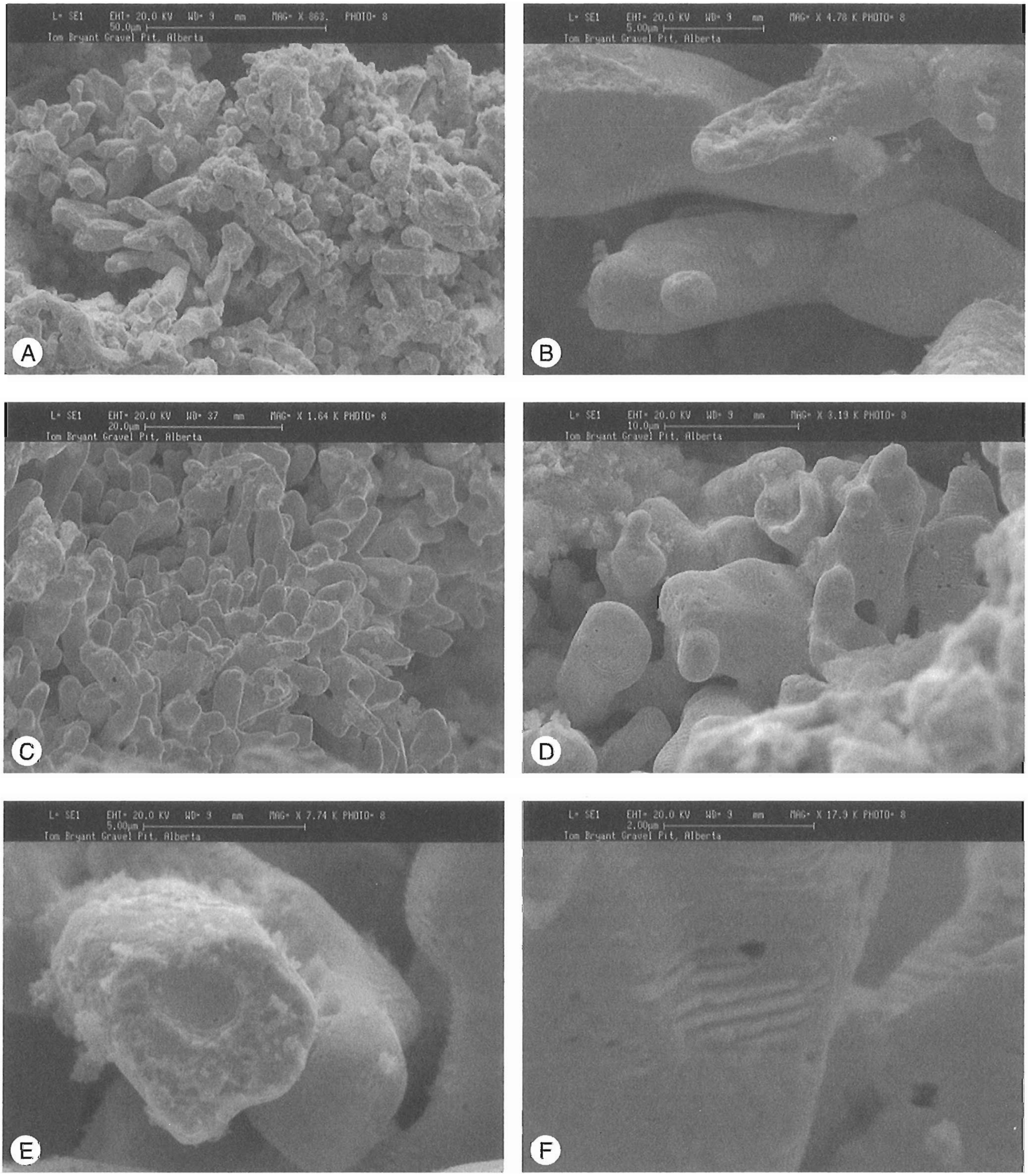
L= SE1 EHT= 20.0 KV WD= 9 mm MAG= X 863. PHOTO= 8
50.0μm
Tom Bryant Gravel Pit, Alberta
A
L= SE1 EHT= 20.0 KV WD= 3 mm MAG= X 4.78 K PHOTO= 8
5.00μm
Tom Bryant Gravel Pit, Alberta
B
L= SE1 EHT= 20.0 KV WD= 37 mm MAG= X 1.64 K PHOTO= 8
20.0μm
Tom Bryant Gravel Pit, Alberta
C
L= SE1 EHT= 20.0 KV WD= 9 mm MAG= X 3.19 K PHOTO= 8
10.0μm
Tom Bryant Gravel Pit, Alberta
D
L= SE1 EHT= 20.0 KV WD= 9 mm MAG= X 7.74 K PHOTO= 8
5.00μm
Tom Bryant Gravel Pit, Alberta
E
L= SE1 EHT= 20.0 KV WD= 3 mm MAG= X 17.9 K PHOTO= 8
2.00μm
Tom Bryant Gravel Pit, Alberta
F

Plate 14

Bacterial(?) Textures on Gold Grains

A. A more "massive" example of numerous placer gold particles and other heavy mineral particles (ilmenite?) now fused together by lattice and lace-like structures. This backscattered electron image clearly shows that crystalline, non-gold, alluvial minerals can be engulfed by microbial(?) "new" gold growths onto and between substrate detrital gold grain hosts.

B. A close-up secondary electron image of a portion of **A.** Gold layers and bridges across open spaces (black portion) between gold grains are evident. Single spheroids and ultrafine structures cover the host substrate gold particles.

C. A secondary electron image of a single 40 μm sized gold-adsorbing bacteria colony that has grown vertically above the pre-colonized probable gold-covered surface of the host detrital gold particle. Distinct single hyphae(?) and morphologically curled collapsed(?) structures are evident.

D. A backscattered electron image of an inferred colony of gold-adsorbing bacteria that has used a heavy mineral grain as a substrate (dark part of image) or engulfed it as a result of colony geometry during growth.

E. A secondary electron image of short "budding hyphae"(?) (note the 5 μm scale bar at the top of the image) showing the ultrafine, preserved colony morphology. A process of growth whereby gold in colloidal and/or ionic solution is accumulated on older cells as the colony enlarges by continuous budding can be envisioned by careful examination of this image.

F. This secondary electron image of a 5 μm spheroid shape of "new" gold is an unusual morphology compared to those found on the surface of the grains in **A**. It could have been a framboidal pyrite grain deposited with the other heavy minerals found in **A** that has now been replaced by gold. It could also be a different gold-adsorbing bacterioform as compared to the "filamentous" appendages more commonly observed (**C** and **E**).

This sample was collected by Tom Bryant from Alberta sand and gravel pit washing operations.

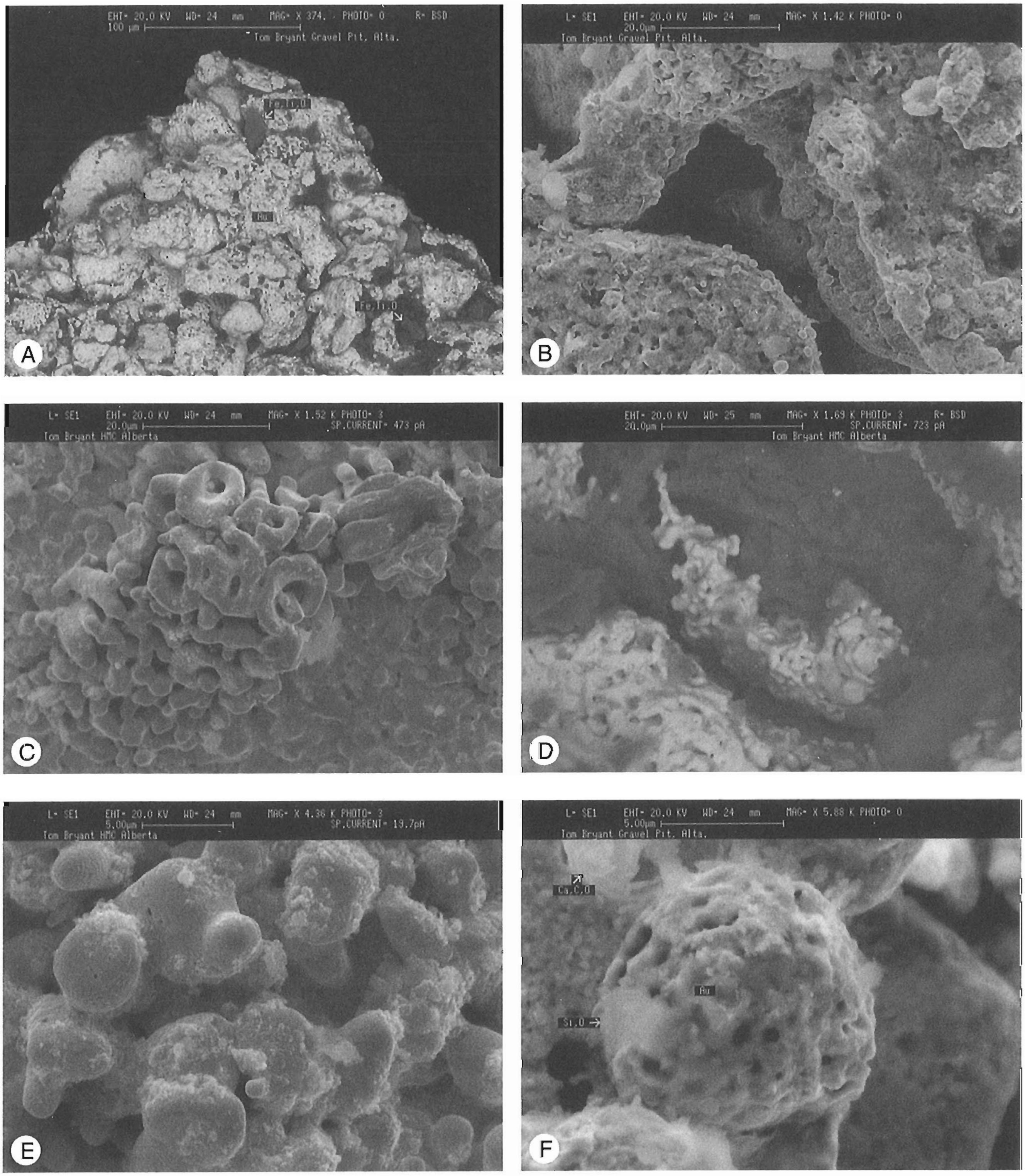
EHT= 20.0 KV WD= 24 mm MAG= X 374. PHOTO= 0 R= BSD
100 µm
Tom Bryant Gravel Pit, Alta.
Au
A
L= SE1 EHT= 20.0 KV WD= 24 mm MAG= X 1.42 K PHOTO= 0
20.0µm
Tom Bryant Gravel Pit, Alta.
B
L= SE1 EHT= 20.0 KV WD= 24 mm MAG= X 1.52 K PHOTO= 3
20.0µm
SP.CURRENT= 473 pA
Tom Bryant HMC Alberta
C
EHT= 20.0 KV WD= 25 mm MAG= X 1.69 K PHOTO= 3 R= BSD
20.0µm
SP.CURRENT= 723 pA
Tom Bryant HMC Alberta
D
L= SE1 EHT= 20.0 KV WD= 24 mm MAG= X 4.36 K PHOTO= 3
5.00µm
SP.CURRENT= 19.7pA
Tom Bryant HMC Alberta
E
L= SE1 EHT= 20.0 KV WD= 24 mm MAG= X 5.88 K PHOTO= 0
5.00µm
Tom Bryant Gravel Pit, Alta.
Au
F

Plate 15

Bacterial(?) Agglomeration of Gold Grains

A. Secondary electron image of an agglomeration of detrital gold grains now "fused" together by "new" gold of probable bacterial origin. The 100 μm scale bar at the top of the image shows that the cup-shaped detrital grain is now attached to a series of less than 50 μm grains of variable shapes normally attributed to placer gold (i.e., distinct signs of transport).

B. Close-up secondary electron image of the delicate textures bridging the formerly separate placer grains. Most of the alluvial grains show some degree of bacterial(?) colonization on or between their surfaces as depicted in this image. In this sample, all SEM–EDS analyses peaks either from bacterial(?) gold structures or from host detrital grain surfaces show pure gold (no silver was detected). According to Mann (1992) this gold purity implies bacterial cell wall binding properties selective for gold.

C–D. Secondary and backscattered electron images of a portion of the bridge shown in **B** at the location marked "new gold" in image **A**. Gold-adsorbing bacteria(?) shapes are clearly evident as are voids and space between the alluvial grains (black areas). Less than 5 μm quartz grains (Si,O) have been engulfed by the growing structure. It is not known if this silica was deposited from the same solutions carrying the gold, if it is colloidal silica, or if it is detrital in origin.

E–F. Secondary and backscattered electron images of a portion (approximately 40 μm across) of an alluvial grain surface now hosting numerous bacterioform(?) gold structures. The spherical single cell shapes may represent swarmer cells not unlike those shown in Bischoff (1994) and Watterson (1992) from Australia and Alaska, respectively.

This specimen was donated by Tom Bryant from his collection of large gold particles recovered from Alberta sand and gravel pit operations. It provides compelling evidence that gold precipitation of probable bacterial origin can occur after gold particle deposition and lodgement in the sediment. Microbially induced gold deposition and accumulation therefore may give rise to "nugget" formation in some cases. Any subsequent re-cycling of this specimen into the drainage system would lead to a larger "single nugget" as compared to the numerous original single grains originally present in these alluvial clastic sediments.

PLATE 15

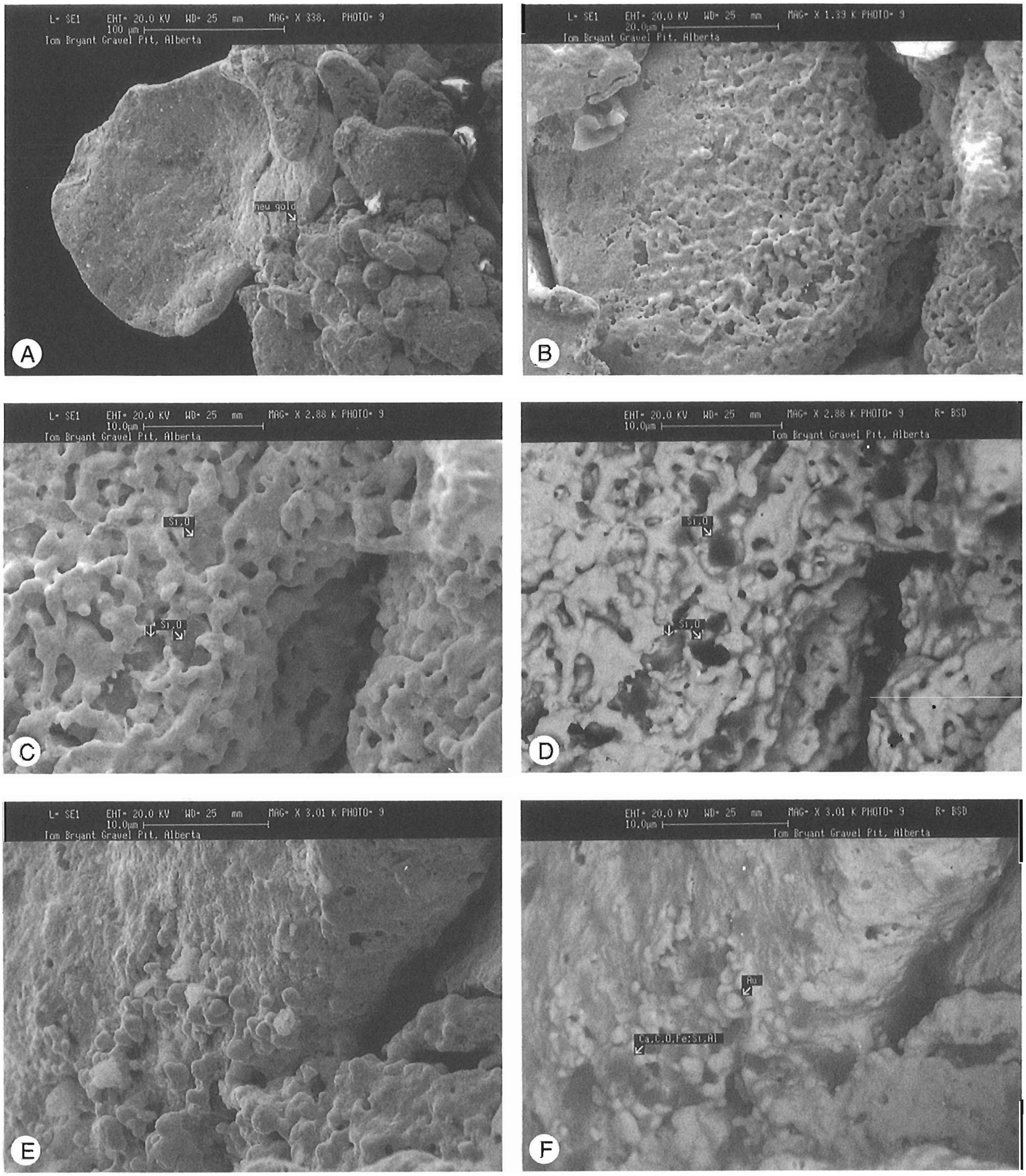

L= SE1 EHT= 20.0 KV WD= 25 mm MAG= X 338. PHOTO= 9
100 μm
Tom Bryant Gravel Pit, Alberta
new gold
A
L= SE1 EHT= 20.0 KV WD= 25 mm MAG= X 1.33 K PHOTO= 9
20.0μm
Tom Bryant Gravel Pit, Alberta
B
L= SE1 EHT= 20.0 KV WD= 25 mm MAG= X 2.88 K PHOTO= 9
10.0μm
Tom Bryant Gravel Pit, Alberta
Si,O
Si,O
C
EHT= 20.0 KV WD= 25 mm MAG= X 2.88 K PHOTO= 9 R= BSD
10.0μm
Tom Bryant Gravel Pit, Alberta
Si,O
Si,O
D
L= SE1 EHT= 20.0 KV WD= 25 mm MAG= X 3.01 K PHOTO= 9
10.0μm
Tom Bryant Gravel Pit, Alberta
E
EHT= 20.0 KV WD= 25 mm MAG= X 3.01 K PHOTO= 9 R= BSD
10.0μm
Tom Bryant Gravel Pit, Alberta
Au
Ca,C,O,Fe;Si,Al
F

Plate 16

Bacterial(?) Textures on Gold Grains

A. Disc shaped alluvial gold- and silver-bearing grain. The grain exhibits a sponge-like surface texture with mineral surface intergrowths. Much of the surface area of this grain could be considered modified bacterial growths (slightly flattened during transport but many black holes still preserved).

B. This gold- and silver-bearing grain reveals important surface characteristics as shown in detail in **C**, **D** and **E**. Generally its surface indicates modified bacterial(?) growths that have been slightly flattened (**C**). At the "5 o'clock" position a groove-like gash in the delicate surface matte is evident. Normally such a structure is ascribed to transport contact (**D**).

C. A close-up view of the modified bacterial(?) growths on the grain surface and an internal quartz-rich 20-μm-long exposure, the grey area. Note that quartz lies in a depression relative to the surrounding bright "sponge-like" and silver surface and that bright, thread-like metals lie on top of the quartz (**E**).

D. A close-up view of the "gash" noted in **B**. Gold and silver were detected by EDS as major compositions and at similar concentrations both deep within the groove and at the sponge-like surface. Copper and zinc-metal "shard-like" flakes less than 5 μm in size are found affixed across the groove-like structure in the deepest portion of the "gash". Small grey holes are found in the outer surface gold and silver patina and along and within the groove lines. It is possible that the grooves are not mechanical scratches made during transport. They may represent casts of clay minerals now no longer embedded into the bacterial(?) surface of the grain.

E. A close-up of the "bright" threads on the surface of the embedded quartz (dark grey) shown in **C**. It is obvious that both a copper and zinc metal area (medium grey) were affixed to the quartz prior to the "bright" gold and silver being attached to the surface of the copper and zinc. Owing to their small size (1–2 μm) knowledge about the interrelationship of copper, zinc, gold and silver has been restricted to their EDS determinations on exposures on the surface of the grains.

Both **A** and **B** grains were recovered by initial panning followed by heavy mineral concentrate carbon-hydrocarbon adsorbent treatment by Envi-Tech. Inc.

Sample location: #247, northeastern Alberta (Fig. 3).

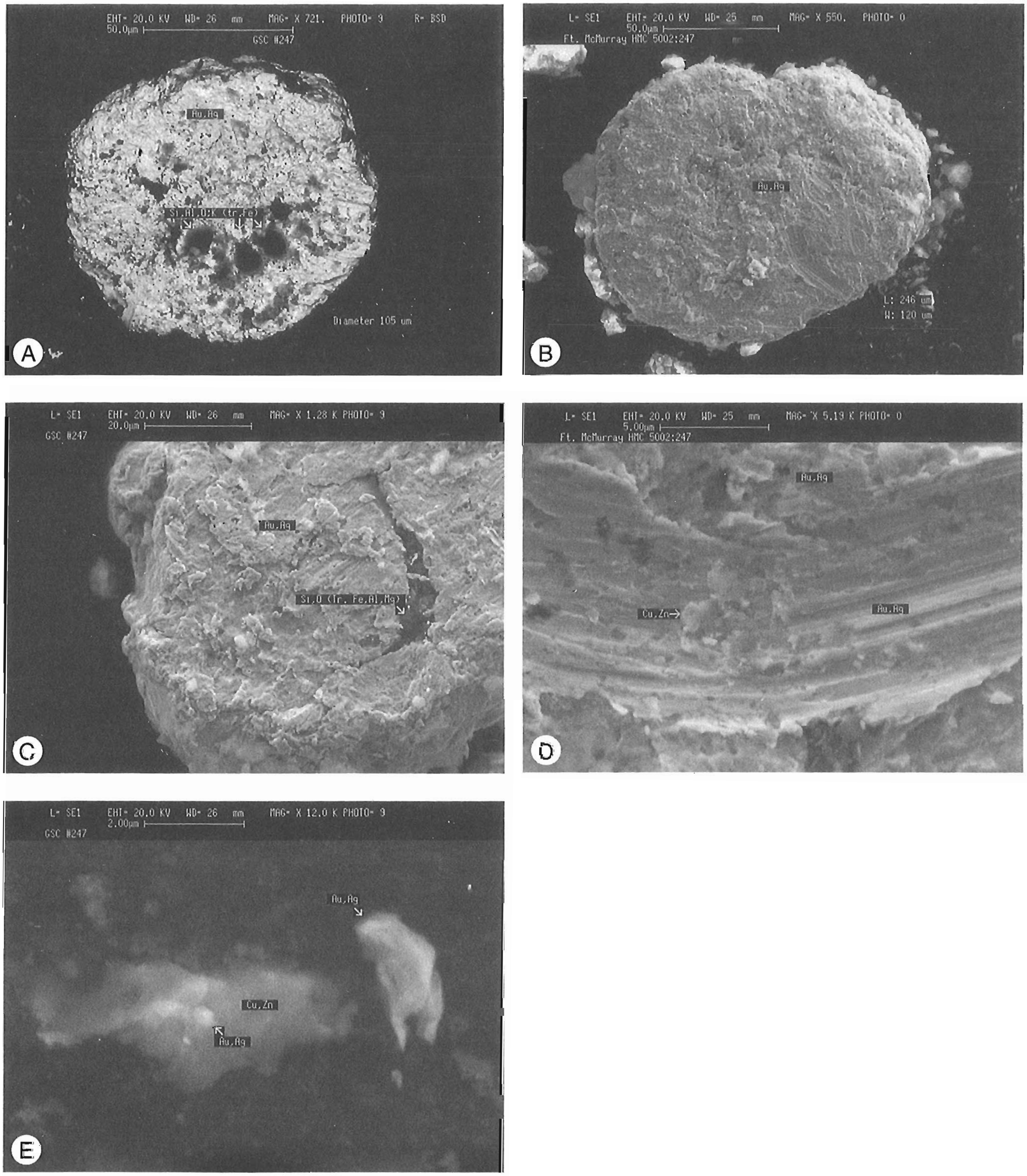
EHT= 20.0 KV WD= 26 mm MAG= X 721. PHOTO= 9 R= BSD
50.0µm
GSC #247
Au,Ag
Si,Al,O,K (tr.Fe)
Diameter 105 um
A
L= SE1 EHT= 20.0 KV WD= 25 mm MAG= X 550. PHOTO= 0
50.0µm
Ft. McMurray HMC 5002:247
Au,Ag
L: 246 um
W: 120 um
B
L= SE1 EHT= 20.0 KV WD= 26 mm MAG= X 1.28 K PHOTO= 9
20.0µm
GSC #247
Au,Ag
Si,O (Tr. Fe,Al,Mg)
C
L= SE1 EHT= 20.0 KV WD= 25 mm MAG= X 5.19 K PHOTO= 0
5.00µm
Ft. McMurray HMC 5002:247
Au,Ag
Cu,Zn
Au,Ag
D
L= SE1 EHT= 20.0 KV WD= 26 mm MAG= X 12.0 K PHOTO= 9
2.00µm
GSC #247
Au,Ag
Cu,Zn
Au,Ag
E

Plate 17

Metals in Rock Chips, Devonian Carbonates, Fort McKay Area

A–F. A series of SEM backscattered electron photomicrographs of diamond drill core rock chips from three different drill holes (supplied by Tintina Mines Limited; see T2, T3, T4 in title at top of each image) and from three different vertical depths (26.2, 188.6 and 147.96 m) of Devonian stratigraphy, Fort MacKay, Alberta. A scale bar in micrometres is depicted in the top black title area of each image.

In this study freshly broken rock chips were mounted on carbon tape on an SEM stub. The sample was examined by rotating and tilting the SEM stage to expose all of the fresh rock chip "faces". For the present exploratory study of the Devonian carbonate section rocks, a simple rock chip surface was examined. Exposures of Devonian carbonate strata are known to outcrop in the downcut incised drainages where HMC sampling was tested in the Fort McMurray study area (Fig. 3). Assuming a local source for some of the recovered HMC material, it is prudent to examine potential source rocks in order to interpret the complexities of the HMC mineralogy.

A. A photomicrograph of a portion of a rock chip approximately 2 μm farther down the drill hole from the sample area of Plate 18. This ridged portion of the chip shows a series of native copper and gold flakes and leaves hosted in calcium carbonate rock matrix. EDS analysis shows that the copper and gold particles are variable in size, pure, and discrete in composition. The fresh surface break along the ridge edge shows that these native metals are distributed at various depths throughout this portion of the chip. These metallics could be easily liberated from the rock to be concentrated in HMC accumulation sites within a local drainage system.

B. A different face of the same rock chip shown in **A**. This fresh exposed ridge shows thousands of molybdenite mineral particles (bright colour) attached to a calcium carbonate host rock matrix. Jedwab (1993) considered molybdenite to be demonstratably syngenetic/diagenetic with copper sulphides in the Shaba, Zaire setting. In this carbonate sample from Fort MacKay, the native gold and copper are mutually exclusive of the molybdenite (sulphide) concentrations found in the same chip. The mineralogical form (**A**) of the native copper and gold found in this chip rules out any possibility that they are of detrital derivation.

C. A photomicrograph of a portion of a rock chip from the Devonian carbonate section at 188.6 m vertical depth. The fresh surface break exposed 50 μm Au and Cu flakes and Sr sulphate minerals encrusted in a Ca-Mg carbonate rock matrix.

D. A close-up photomicrograph of another portion of the same rock chip as **C** showing a series of leaves and flakes composed of native copper, Cu-Zn "brass" intermetallics and a Cu-Au minor Zn mixture. Sulphide species were found to be absent in the chip examined.

E. A photomicrograph of a portion of a freshly broken rock chip face showing a series of 50 μm and smaller Cu-Zn (brass) leaves, shards and flakes exposed at variable depths within the calcium carbonate matrix.

F. A typical tiny Au-Ag spheroid delicately attached to the surface of the carbonate matrix host rock.

This SEM–EDS search over exposed rock chip surfaces added insights as to the size, shapes, distribution and relative abundance and integration of the complex species of native metals (base and precious), intermetallics, alloys and sulphides-sulphates.

It is now reasonable to hypothesize that WCSB rocks have been sources in the past and can continue to contribute some of the unusual HMC species observed in this study of alluvial Au and PGMs in both paleo- and modern Albertan drainage systems.

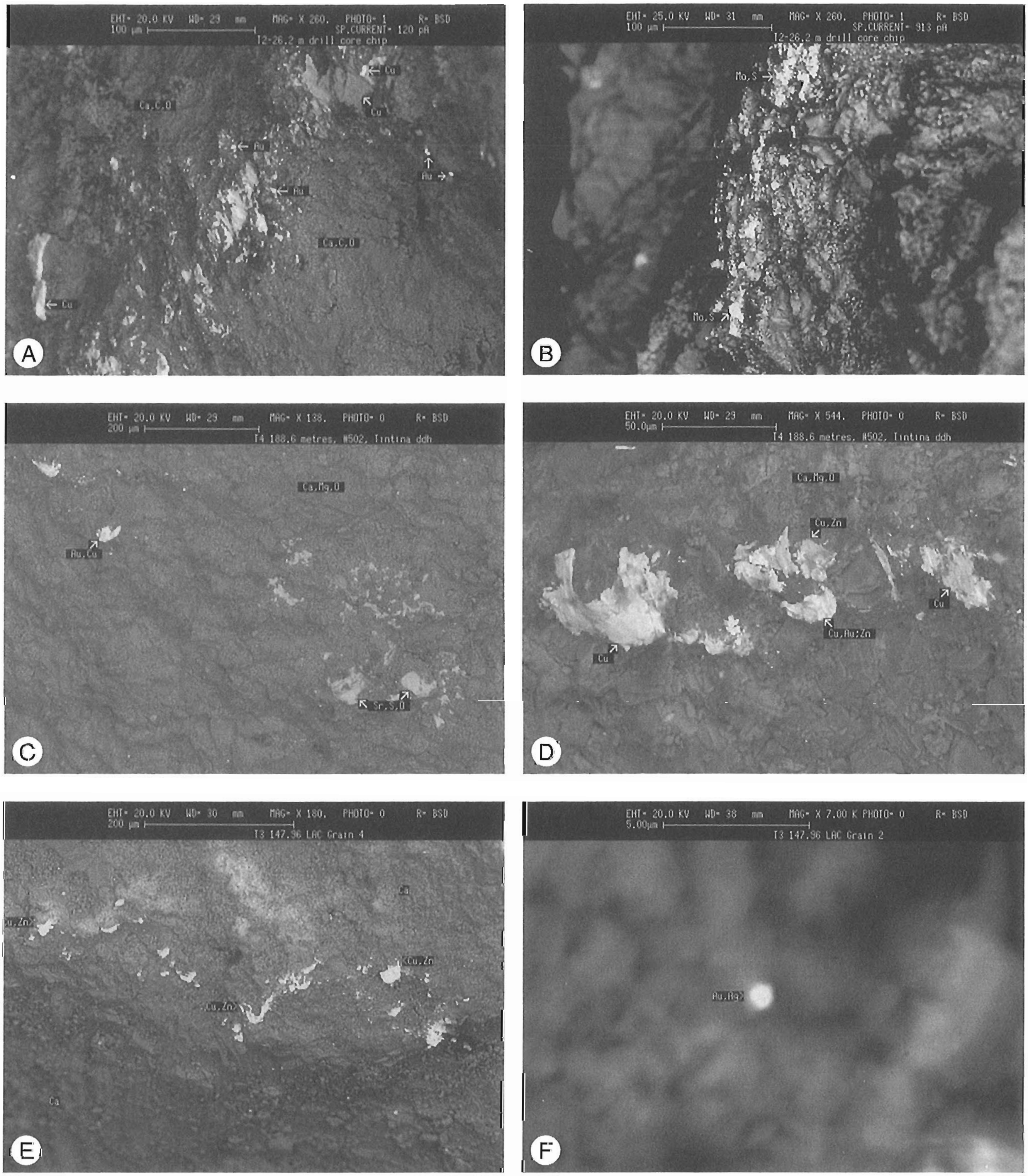
A
B
C
D
E
F

Plate 18

Metals in Insoluble Residues, Devonian Carbonates, Fort McKay Area

A–F. A series of backscattered electron (**A**, **B**, **D**, **F**) and secondary electron (**C**, **E**) SEM images of residual, insoluble material recovered from drill core after cold HF-acid dissolution. The insoluble species were collected on filter paper and then mounted (pressed) onto carbon-coated tape and then onto SEM stubs for examination. The hydrofluoric acid leaching concentration method did not demand crushing or grinding of the rocks so very small, individual, insoluble mineral species could be examined by SEM–EDS. However, the selective properties of the leach can dissolve important alteration-ore minerals (i.e., they may be lost) while others persist through the treatment. During sample preparation very small or friable individual mineral species may also be lost.

A–D. Diamond drillcore was provided by Tintina Mines Limited from a 0.76 m interval starting from 21.64 m and drilled into the Devonian carbonate section of the Fort MacKay horst located some 50 km north of Fort McMurray Alberta (Fig. 3). The section was logged as muddy limestone containing bitumen coatings on fracture surfaces. GSC laboratory whole rock geochemistry determined that the sample contained 0.22 wt.% S, 15.3 wt.% SiO_2, 36.3 wt.% CaO, 32.7 wt.% CO_2 and 3.17 wt.% MgO. Tintina Mines Limited reported enriched precious metal values for this 0.76 m interval.

A. This 50 μm intergrowth of native silver and AgS appears to be associated with organic material (CO). The sample stubs were not carbon coated as carbon tape was used for mounting. The grey CaF on the mount is an insoluble result of the HF-carbonate dissolution process.

B. A 1 μm Au-Ag particle now encrusted by CaF.

C. A 200 μm ZnS particle showing pristine crystal faces.

D. A typical 2 μm particle which by EDS analysis revealed major Au + Ag and minor Cu + Zn in its composition.

E–F. This sample material came from the same source and hole as the **A–D** sample, but was collected from a 1.83 m interval starting from 24.38 m down the vertical hole, The section was logged as limestone containing shell fragments and minor, wispy, bituminous threads. Whole rock geochemistry revealed that this section is different in composition from the **A–D** section. The sample contained 0.13 wt.% S, 1.36 wt.% SiO_2 (less), 50.8 wt.% CaO (more), 43.3 wt. CO_2 (more) and 0.77 wt.% MgO (less). This section reportedly contained lower precious metal enrichment compared to the **A–D** section.

E. A 2 μm native platinum shard recovered from the insoluble residue after cold HF dissolution.

F. A 50 μm long Ni-Cu-Zn alloy showing delicate leaf-like appendages and ridges along its overall wire-shape.

Native metals and complex alloys were commonly encountered in HMC from Alberta paleo- and modern drainage systems. Gold, silver and platinum native metals, alloys and intermetallics are present in Alberta sedimentary strata. In this particular case base metal sulphides, silver sulphides and iron sulphides accompanied the complex noble metals hosted in the Devonian carbonate rocks near Fort MacKay, Alberta.

PLATE 18

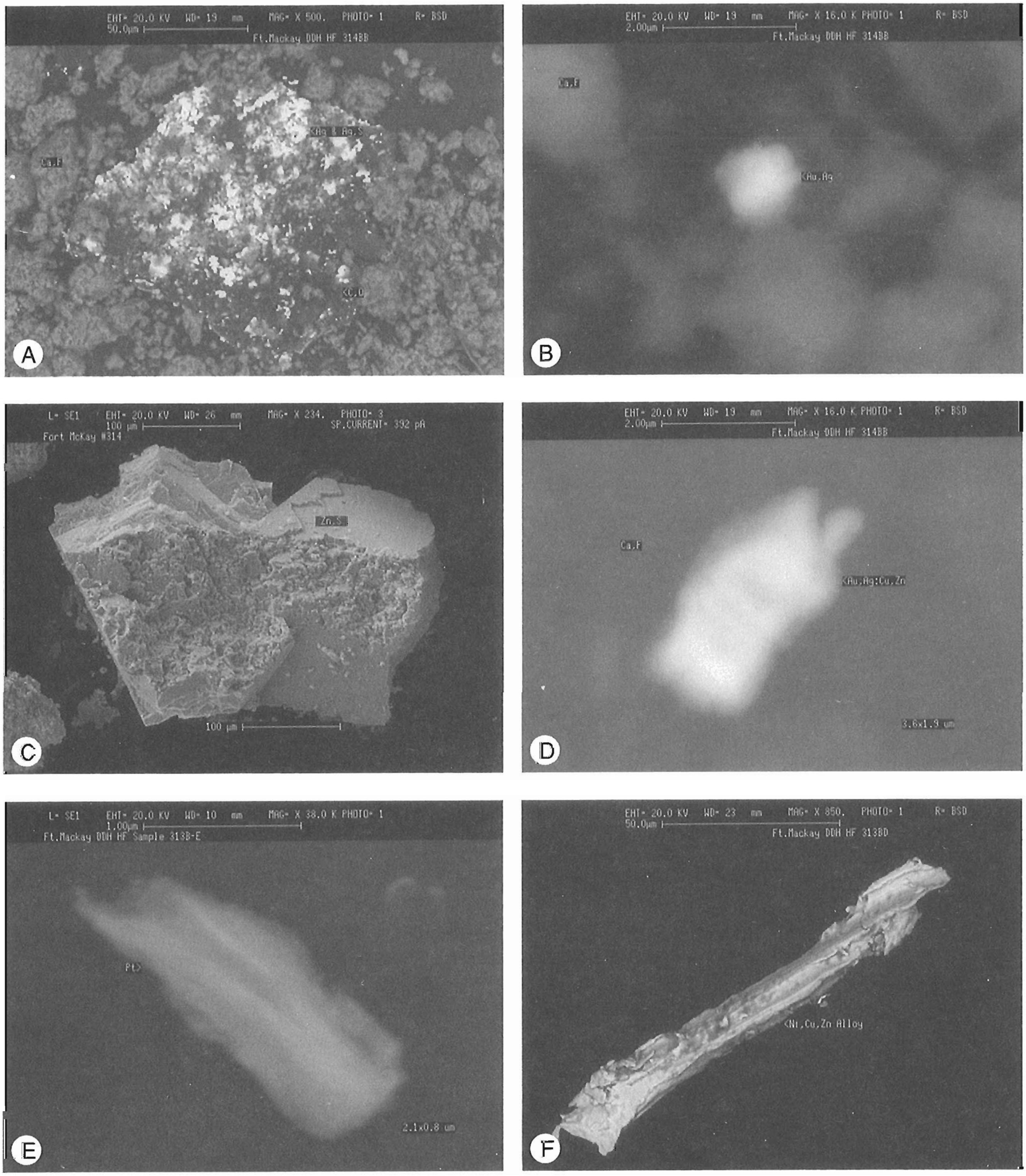
EHT= 20.0 KV WD= 19 mm MAG= X 500. PHOTO= 1 R= BSD
50.0μm
Ft.Mackay DDH HF 314BB
Ca,F
A
EHT= 20.0 KV WD= 19 mm MAG= X 16.0 K PHOTO= 1 R= BSD
2.00μm
Ft.Mackay DDH HF 314BB
Ca,F
<Au,Ag
B
L= SE1 EHT= 20.0 KV WD= 26 mm MAG= X 234. PHOTO= 3
100 μm
SP.CURRENT= 392 pA
Fort McKay #314
Zn,S
100 μm
C
EHT= 20.0 KV WD= 19 mm MAG= X 16.0 K PHOTO= 1 R= BSD
2.00μm
Ft.Mackay DDH HF 314BB
Ca,F
<Au,Ag:Cu,Zn
3.6x1.9 um
D
L= SE1 EHT= 20.0 KV WD= 10 mm MAG= X 38.0 K PHOTO= 1
1.00μm
Ft.Mackay DDH HF Sample 313B-E
Pt>
2.1x0.8 um
E
EHT= 20.0 KV WD= 23 mm MAG= X 850. PHOTO= 1 R= BSD
50.0μm
Ft.Mackay DDH HF 313BD
<Ni,Cu,Zn Alloy
F

ANOMALOUS GOLD OCCURRENCES IN CRETACEOUS AND TERTIARY CONGLOMERATES AND GRAVELS OF ALBERTA[1]

D.A. Leckie and D. Craw[1]
Geological Survey of Canada, Calgary

Abstract

Reconnaissance surveys of lithified Cretaceous conglomerate and generally nonlithified Tertiary gravel in outcrop in southern to central Alberta indicate anomalous values of detrital gold at several levels. Background gold levels are considered to be 2 to 5 ppb, based on about 200 analyses. The highest gold values of up to 910 ppb were obtained from an igneous-clast conglomerate in the Albian Blairmore Group, southern Rocky Mountain Foothills. Tertiary gravels of Swan Hills and Cypress Hills have values between <2 and 21 and <2 and 44 ppb, respectively. The basal Cretaceous Cadomin Formation of the Alberta Foothills has values of 2 to 5 ppb with one value of 17 ppb. Gold occurrences in the foreland basin deposits appear to have been influenced by the position of the drainage divide associated with the accretionary prism to the west. "Windows" of gold deposition exist in the succession owing initially to exposure of Omineca Belt primary gold deposits due to uplift, followed by cutoff of source by lateral eastward-stepping of the drainage divide. The Western Canada foreland basin contains three such gold deposition "windows", the last of which is still open. Although the gold values obtained for this study may not yet be of direct economic interest, some occurrences are anomalous and should be investigated further.

Résumé

Sur un territoire allant de la partie sud à la partie centrale de l'Alberta, un échantillonnage de reconnaissance de conglomérats et de graviers lithifiés et non lithifiés du Crétacé et du Tertiaire a mis en évidence des valeurs anomales d'or détritique à plusieurs niveaux. Les teneurs de fond en or ont été situées à une valeur entre 2 et 5 ppb, sur la base d'environ 200 analyses. Les concentrations d'or les plus élevées allant jusqu'à 910 ppb ont été obtenues d'un conglomérat à clastes ignés du Groupe de Blairmore (Albien), dans la partie sud des contreforts des Rocheuses. Les graviers tertiaires des collines Swan et des collines Cypress contiennent respectivement des teneurs en or variant entre <2 et 21 ppb et entre <2 et 44 ppb. Les concentrations d'or de la partie basale de la Formation de Cadomin (Crétacé), dans les contreforts de l'Alberta, s'échelonnent de 2 à 5 ppb, avec une seule valeur atteignant 17 ppb. Dans le bassin d'avant-pays, les indices aurifères semblent varier selon la position de la ligne de partage des eaux de drainage qui dépend du prisme d'accrétion à l'ouest. Il existe dans la succession des «fenêtres» de minéralisation aurifère attribuables initialement à la mise en surface de gisements d'or primaire du Domaine d'Omineca par soulèvement et, par la suite, isolement de la source en raison d'un déplacement latéral vers l'est de la ligne de partage des eaux de drainage. Le bassin d'avant-pays de l'Ouest du Canada contient trois fenêtres de minéralisation aurifère de ce genre, la dernière affleurant encore. Même si les concentrations d'or obtenues pour cette étude peuvent ne pas être d'un intérêt économique direct pour le moment, certains indices sont des anomalies et devraient donc être étudiés plus en profondeur.

[1]Department of Geology, University of Otago, Dunedin, New Zealand

INTRODUCTION

Sediments of the Western Canada foreland basin and overlying post-Eocene succession were derived predominantly from the rising Canadian Cordillera to the west from Jurassic time to the present. Detrital gold, with a few exceptions, is relatively rare in these rocks (Olson et al., 1994), largely because most of the terrestrial sediments originated in source terranes which did not contain bedrock gold concentrations. In contrast, detrital gold is relatively common in modern rivers such as the Bow, Peace and North Saskatchewan (located on Fig. 1; Edwards, 1990; Guisti, 1986), but the sources for gold in these rivers have not been thoroughly established. Until recently (Craw and Leckie, 1996; Leckie and Craw, 1995), there has been no evidence presented for the existence of paleo-placer gold in the Rocky Mountains and foothills of southwestern Alberta (e.g., Edwards, 1990; Horachek, 1994), although the presence of gold has long been rumored (Riley, 1946; Riley et al., 1968; Lone Pine Publishing, 1991). In general, common misconceptions of the regional geology of the area have made a search for commercial volumes of gold in southern Alberta appear futile.

This study demonstrates that anomalous concentrations of detrital gold occur at several levels of the Mesozoic succession. Although this gold may not yet be of direct economic interest, some of the occurrences appear to warrant further investigation. These gold occurrences also provide information on the relationships between regional tectonic processes and gold accumulation in a foreland basin setting (Leckie and Craw, 1995; Craw and Leckie, 1996).

Here, we summarize the results of a reconnaissance investigation of some potential gold-bearing conglomerate/gravel paleoplacer units in Alberta. These units (Fig. 2) include: 1) the lowermost Cretaceous Cadomin Formation in southwestern Alberta; 2) an Albian-aged igneous-clast conglomerate within the Blairmore Group of southwestern Alberta; 3) Oligocene conglomerate of the Cypress Hills

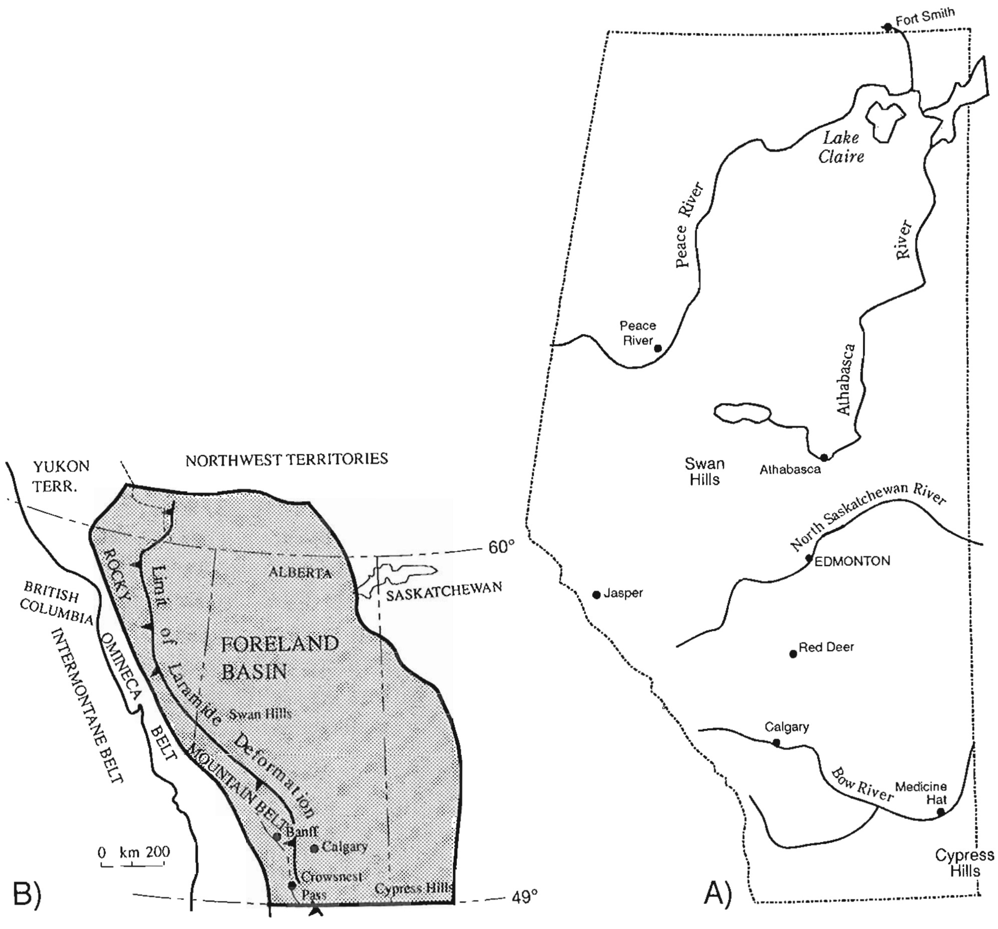

*Figure 1. **A)** General location map. Locations of detailed studies referred to in this paper are shown. **B)** Location map of the Canadian Cordillera and adjacent foreland basin, showing the main tectonic subdivisions.*

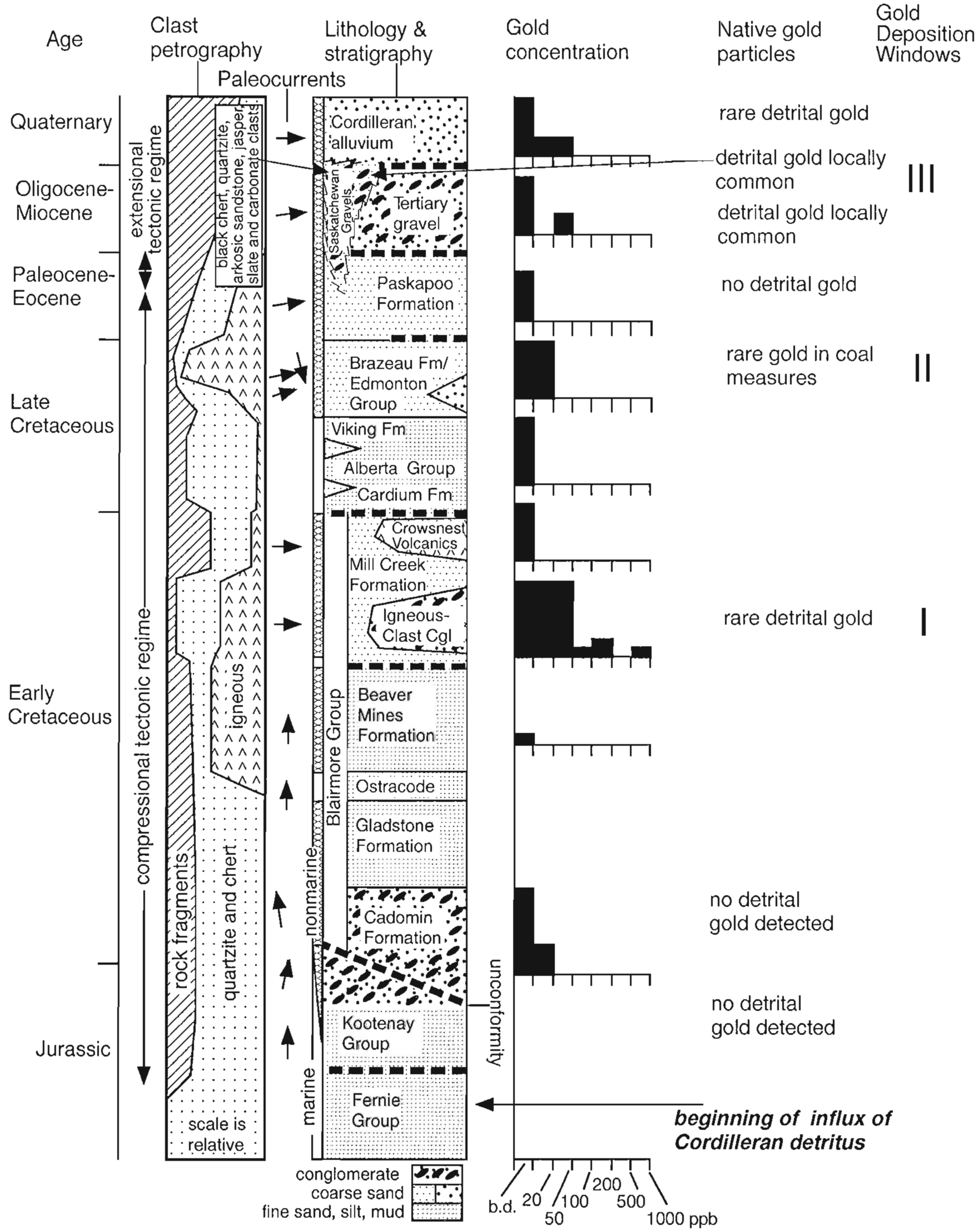

Figure 2. *Generalized stratigraphic column for the Western Canada Foreland Basin (center), summarizing principal lithologies, identifying the main conglomerate levels, and indicating the marine or nonmarine character of the various parts of the section. Paleocurrent data are from Leckie (unpublished), Mack and Jerzykiewicz (1989), Eberth and Hamblin (1993), and Hamblin and Walker (1979). Stratigraphic variations in sandstone and conglomerate composition (left) are summarized and generalized from Urbatt (1988), and Mack and Jerzykiewicz (1989). Histograms of gold analyses (Leckie and Craw, 1995; Horachek, 1994; this study) from the various units (right) indicate anomalous gold concentrations. Histograms are indicative only; there is insufficient space to display more than about six "detection" analyses.*

Formation in the Cypress Hills of southeastern Alberta; and 4) Tertiary conglomerate in the Swan Hills of central Alberta. Interpretive aspects and descriptive detail may be found in Craw and Leckie (1996) and Leckie and Craw (1995).

METHODS

Samples of unconsolidated sand matrix from the Tertiary Cypress Hills Formation in the Cypress Hills, Tertiary Swan Hills gravel, and modern sediment were obtained by removing clasts larger than 1 cm diameter with a sieve. For the lithified conglomerates of the Cadomin Formation, igneous-clast conglomerates in the Blairmore Group, and lithified outcrops of the Cypress Hills Formation, samples of sandstone matrix were collected after the removal of pebbles and cobbles. For each sample, approximately 500 g of sand or sandstone matrix were collected from which 30 g were analyzed for gold using fire assay and atomic absorption spectrometry (Cantech Laboratories Inc., Calgary, and Loring Laboratories Ltd., Calgary). Detection limits are 2 ppb (Cantech) and 5 ppb (Loring Laboratories Ltd.).

BACKGROUND GOLD LEVELS

Typical background gold content for most rocks in the Cretaceous Blairmore Group is about 2 ppb (Leckie and Craw, 1995). Two Crowsnest volcanic samples, and one sample from the Mill Creek Formation have detectable Au, quoted at 10 ppb with a 5 ppb detection limit, indicating that background may be as high as 10 ppb in some rock types. Fire assay/atomic absorption spectrometry analyses of sediments elsewhere in the Cretaceous succession show that gold concentrations are below detection (5 ppb; D. Leckie, unpublished data), and confirm the generally low Au background. A single sample of Cadomin Formation conglomerate from the Crowsnest Pass area has 17 ppb Au, probably an anomalous value. Our results are consistent with those of Horachek (1994), who obtained maximum assay results of 16 ppb from Cadomin and other Cretaceous sediments. Only 13 of Horachek's (1994) 134 samples had values between 5 and 16 ppb. However, Horachek (1994) did not sample the igneous-clast conglomerate within the Blairmore Group which we find contains anomalous gold values.

The conglomerate analyses show that there are significant but low levels of anomalous gold concentrations in many samples. These elevated concentrations are undoubtedly due to the selective manner in which samples were taken to maximize the likelihood of obtaining heavy mineral concentrations. The lowest values, which approach the expected background of about 2 to 5 ppb, show that this biased sampling method was not always successful, but the low values provide a local background level against which to compare the rest of the data. One high value (80 ppb) was obtained from a sandstone of the associated Mill Creek Formation directly overlying the conglomerates, as well as from within the conglomerate matrix itself.

GEOLOGICAL HISTORY

The Mesozoic western North American foreland basin (Fig. 1b) was an elongate trough which developed between a continental margin magmatic arc and the North American craton. Two collisional events, the Early Jurassic to Cretaceous Columbian Orogeny and the Late Cretaceous to Paleocene Laramide Orogeny, resulted in the formation of five tectono-stratigraphic zones in western Alberta and British Columbia. These include the Rocky Mountain, Intermontane (Fig. 1b), and Insular belts, consisting primarily of non- to weakly metamorphosed to low-grade volcanic and sedimentary strata. These three belts are separated by two sutural complexes, the Omineca Belt (Fig. 1b) and Coast Plutonic Belt, comprising high-grade metamorphic and plutonic rocks. The clastic sediments of the foreland basin form a westward-thickening wedge of unmetamorphosed detritus. Details of the clastic wedges and their relationships to tectonic events can be found in Maqueen and Leckie (1992).

During latest Paleocene or middle Eocene time, Cordilleran tectonics changed from transpressional deformation to large-scale extension (Coney and Harms, 1984). Uplift associated with the extension resulted in the development of a basin-wide Eocene unconformity and deposition of extensive boulder-gravel sheets across the western part of the basin. Modern drainage patterns likely became established during this time. Uplift and erosion continued during the Neogene and early Pleistocene, recycling the Paleocene- to Oligocene-aged gravels into preglacial valleys now containing the Saskatchewan Sands and Gravels. During the Pleistocene, Cordilleran-derived glacial outwash gravels were transported eastward from valley glaciers and piedmont lobes in the Rocky Mountains (Stalker, 1968; Jackson et al., 1982). This post-Paleocene period is unnamed in geological literature on western Canada, but for discussion purposes, we refer to it as part of the foreland basin.

GOLD IN THE WESTERN CANADA FORELAND BASIN AND YOUNGER SUCCESSION

Apart from work on the modern river gravels (Halferdal, 1965; Giusti, 1986), few serious attempts have been made to ascertain the presence of gold in the foreland basin and younger succession of Alberta (Edwards, 1990; Horachek, 1994; Leckie and Craw, 1995). However, Craw and Leckie (1996) show that gold occurs in southern Alberta at four stratigraphic levels (Fig. 2) and that the rest of the section is relatively barren. Figure 2 illustrates a simplified Mesozoic stratigraphy for southern Alberta plotted against representative gold values and dominant rock types. Gold occurrences in these four stratigraphic levels are outlined below. Elsewhere, gold values ranging from 0.02 to 1 oz/ton have also been reported from the ironstone oolites of the Coniacian Badheart Formation in northwestern Alberta (Marum Resources Ltd., unpublished promotional data).

Craw and Leckie (1996) defined the concept of gold depositional "windows" (Fig. 3) from Mesozoic to modern sediments. Windows of gold deposition exist in a foreland basin succession between the exposure of primary gold deposits due to uplift and the cutoff of source by lateral stepping of the drainage divide. The western Canada foreland basin contains three such gold deposition windows (Fig. 2), the last of which is still open. Figure 2 specifically shows how the gold depositional windows are applied to Lower and Middle Cretaceous sediments.

MODERN RIVERS

Gold occurs in modern river gravels of southern Alberta (Rutherford, 1937; Halferdal, 1965; Guisti, 1986; Edwards, 1990; Harris and Ballantyne, 1994), most significantly in regions that were glaciated by Pleistocene continental ice sheets. Till derived from the Canadian Shield (Laurentide drift) to the north and northeast has been reworked into modern streams, as

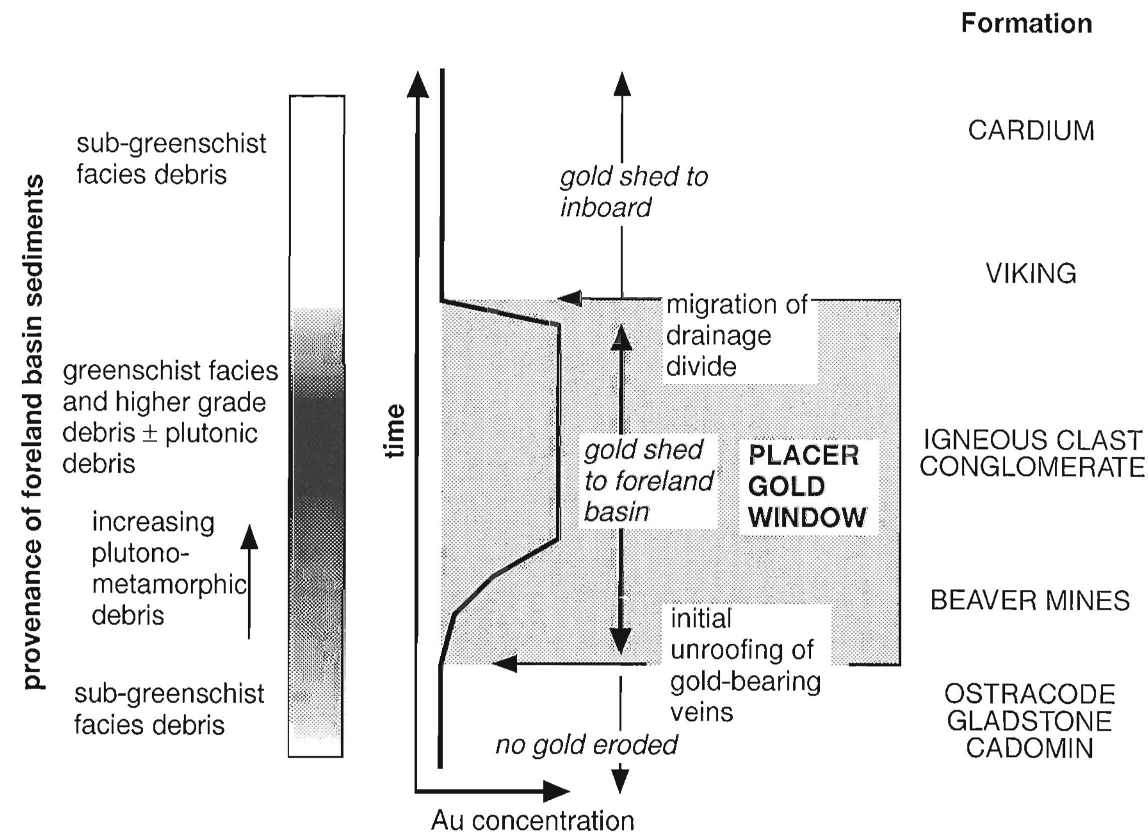

Figure 3. *Conceptual sketch of an ideal detrital gold window in a foreland basin sequence, based on data in Figure 2. Cadomin to Cardium stratigraphy (see Fig. 2) is shown as an example. Modified from Craw and Leckie (in press).*

shown by the presence of igneous and high-grade metamorphic clasts. Presumably some gold, which is common in the Canadian Shield (Boyle, 1979), became concentrated in this way into modern Alberta rivers.

In addition to the Laurentide ice sheet, Cordilleran glaciers flowed eastward to just beyond the Rocky Mountain Foothills, depositing outwash gravels which partly filled the major valleys (Stalker, 1961). These gravels generally do not contain shield-derived material (Jackson et al., 1982), but they do contain clasts of rock types exposed in the Main and Front Ranges, and Foothills. Gold generally is rare in these valley-fill outwash gravels (Leckie and Craw, unpublished data; Edwards, 1990), but it does occur as a heavy mineral in modern gravels or young terraces near the headwaters of the main rivers.

The Red Deer, North Saskatchewan and Bow rivers occupy preglacial, gravel-filled valleys for parts of their reaches (Stalker, 1961). At least 1 t of gold has been mined from the North Saskatchewan River in the last 100 years (Tyrrell, 1915; Horachek, 1994). The source of the gold is enigmatic, but the most productive reaches along the river correspond to locations where the modern rivers have incised into and reworked the preglacial valley fills (Rutherford, 1937).

PREGLACIAL AND TERTIARY GRAVELS

Tertiary gravels, ranging in age from late Eocene to Pliocene (Figs. 2, 4), are preserved in isolated uplands throughout Alberta and southern Saskatchewan, including Del Bonita, Wood Mountain, Grimshaw, Cypress Hills, Hand Hills, Nose Hill and Swan Hills (Rutherford, 1937; Russell, 1948, 1971; Vonhof, 1969; Leckie and Cheel, 1989). The gravels, which overlie a major unconformity throughout most of the basin, are typically quartzose and arkosic sandstone, chert and jasper, with clasts up to 50 cm in diameter. At the time of deposition, overthrusting in the Cordillera had virtually ceased, and the orogen and foreland basin were being isostatically uplifted and eroded (Price and Mountjoy, 1970; Price et al., 1985).

Saskatchewan sands and gravels

The Saskatchewan Sands and Gravels (Figs. 2, 4; McConnell, 1885) in southern and central Alberta are westward-derived, "preglacial", late Tertiary to Early Pleistocene deposits composed of quartzose sandstone, black chert, arkosic sandstone and jasper (Rutherford, 1937; Stalker, 1968; Westgate et al., 1976). These gravels are characterized by an absence of igneous and metamorphic material derived from the Canadian

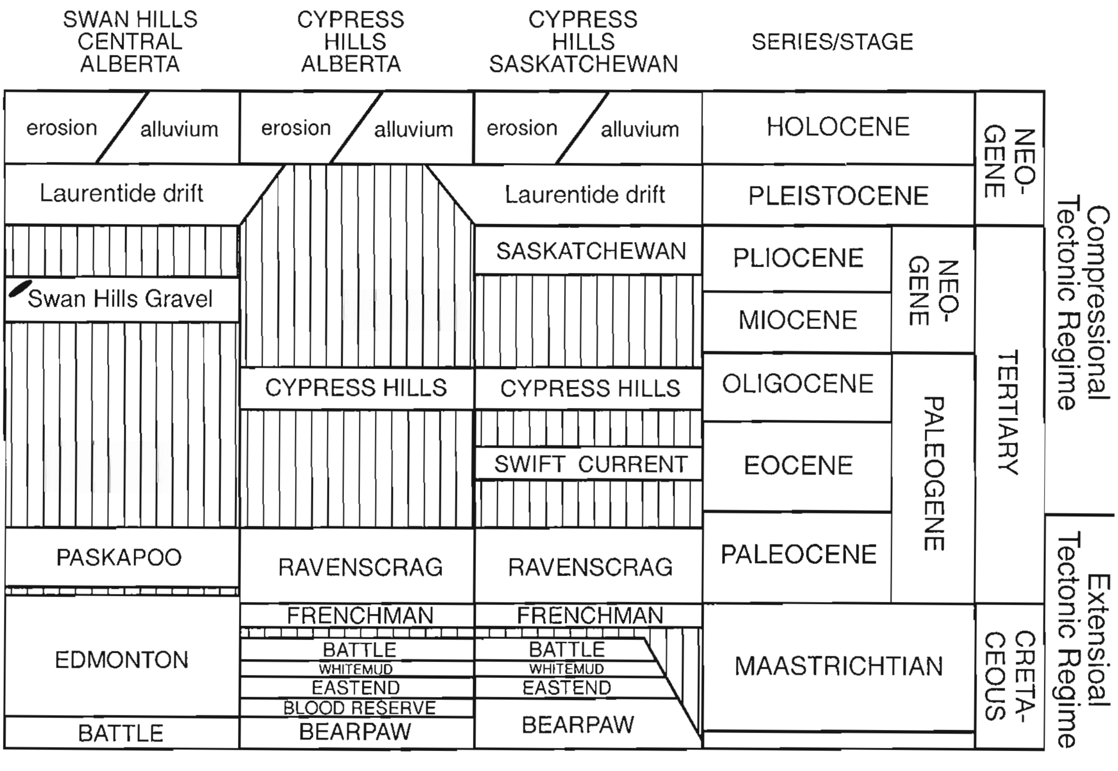

Figure 4. *Stratigraphy of Tertiary gravels in Swan Hills of central Alberta and Cypress Hills of southern Alberta and Saskatchewan.*

Shield and occur within preglacial valleys, commonly up to 122 m deep and 8 to 24 km wide (Stalker, 1968). The major preglacial valleys are dendritic, northeast-trending and generally correspond to the present drainage systems of the North Saskatchewan, Red Deer, Bow, Oldman, South Saskatchewan, Waterton, Belly, and St. Mary rivers, and Willow Creek (Stalker, 1961, 1968; Westgate et al., 1976). The Saskatchewan Gravels have been interpreted as erosional remnants of the older, Tertiary gravel described in the following section (McConnell, 1885; Stalker, 1968; Westgate et al., 1976).

Swan Hills

The uplands of the Swan Hills and Whitecourt area are capped by unconsolidated, Tertiary cobble to boulder gravel (Fig. 4). The dominant lithology is quartzite with lesser amounts of sandstone, chert and other rock types (Vonhof, 1969). Paleocurrent data (Vonhof, 1969; this study) indicates a northeastward-flowing fluvial system. The distribution of these Tertiary gravels was mapped by St. Onge (1974). The gravels are gold-bearing as indicated by assay analyses and panning (Fig. 5). Gold values from 12 localities, as indicated by assay analyses, range from 4 to 16 ppb with no general pattern. Some of these values, though low, can be considered as anomalous. Native gold was recovered by panning from Whitecourt Mountain and there was only minute recovery of native gold from gravels on the Swan Hills, 70 km to the north-northeast. Edwards (1990) obtained values of 0 to 0.002 oz/ton from Whitecourt Mountain and 25 ppb from Swan Hills.

The higher native gold content on Whitecourt Mountain may have resulted from northeastward transport of gold by a Tertiary predecessor of the Athabasca River in the Jasper area (Vonhof, 1969; Craw and Leckie, 1996). The source of the gold may be from post-metamorphic quartz veins occurring in the greenschist facies Neoproterozoic rocks west of Yellowhead Pass (Fig. 4) (Craw and Leckie, 1996).

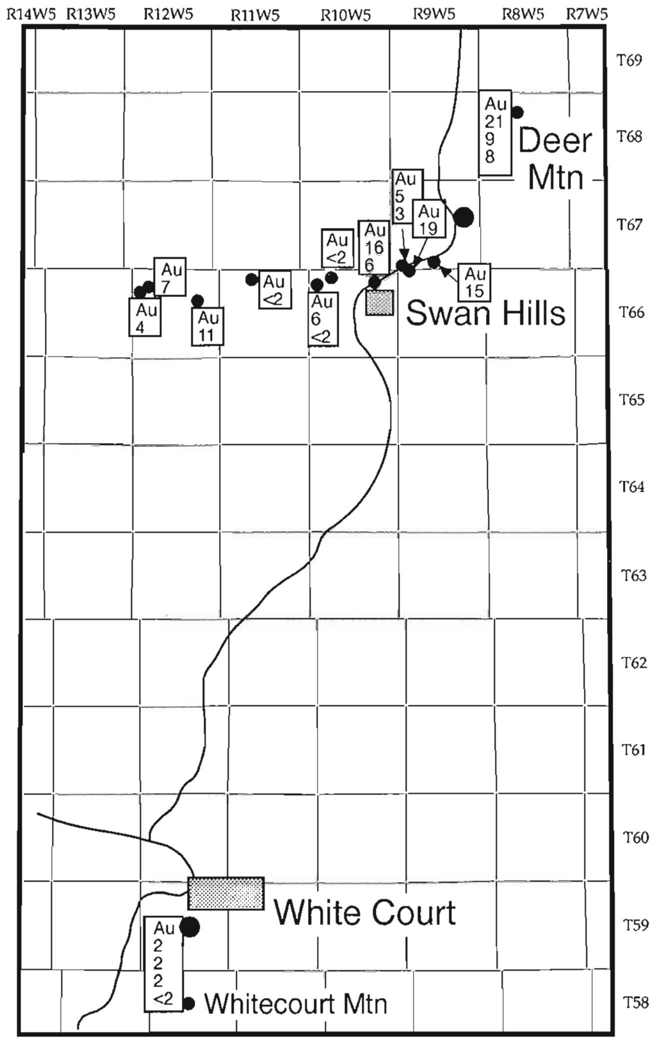

Figure 5. Location map for samples taken in this study from Tertiary gravels at Swan Hills, with gold analyses shown for each locality. Localities at which free gold was obtained are indicated with black circles. Multiple samples were collected at most sites.

Cypress Hills Formation

The Late Eocene to Early Oligocene (Storer, 1975) Cypress Hills Formation (Fig. 4) outcrops on the plateau crest of the Cypress Hills in southeastern Alberta and southwestern Saskatchewan (Fig. 1a). The lithological makeup and sedimentology of these outcrops has been described in detail by Furnival (1946), Vonhof (1969) and Leckie and Cheel (1989). The degree of lithification of the Cypress Hills conglomerate is variable, locally forming calcite-cemented, vertical ridges (Kupsch and Vonhof, 1967). Generally, the gravel is unlithified and the sand matrix can be panned for native gold. The Cypress Hills Formation is made up primarily of gravel with minor sand and silt lenses. The gravel consists of well-rounded clasts, up to 40 cm, of quartzite, chert, arkose, limestone, and dolomite. Minor but important igneous clasts include porphyritic basalt and andesite, trachyte, phonolite, flow-banded rhyolite and obsidian, and porphyritic and equigranular granitoids. Rare metamorphic clasts include argillite, granite gneiss and metaquartzite.

The Cypress Hills Formation was laid down as a braidplain deposit with paleocurrents indicating transport toward the northeast (Leckie and Cheel, 1989). Local recycling is indicated by debris-flow deposits interlayered with the braided-river sediments. An angular unconformity separates the base of the Cypress Hills Formation from that of the underlying Ravenscrag Formation. The basal contact is irregular and marked by incision with fluvially-scoured potholes and channels.

On the Cypress Hills, 47 samples from 14 localities (Fig. 6) were assessed by fire assay. The Cypress Hills data show that many of the analyses are marginally anomalous, and some distinctly anomalous values occur. Only one value (44 ppb) is high enough to represent a small free native gold grain (Leckie and Craw, 1995). Other anomalous gold analyses probably indicate local chemical mobility of secondary gold derived from the dissolution of detrital flakes (Leckie and Craw, 1995). Edwards (1990) recovered 0 to 10 ppb gold values from five samples of the Cypress Hills gravel in Alberta.

Detrital gold is rare and difficult to separate from Cypress Hills gravels by gold pan because of its fine grain size (up to 100 μm). Under the scanning electron microscope, gold grains are seen to be discoid with irregular margins. Surface textures are highly irregular and pitted, with some delicate apophyses. The overall appearance is typical of detrital gold in Alberta (Guisti, 1986; Leckie and Craw, 1995; Harris and Ballantyne, 1994), but some post-depositional chemical modification has occurred (cf. Youngson and Craw, 1993; Leckie and Craw, 1995). Semiquantitative energy dispersive analysis of spots on gold surfaces show that there is no detectable silver present.

UPPER CRETACEOUS TO PALEOCENE SEDIMENTS

Upper Cretaceous to Paleocene units in western Alberta consist primarily of lithic sandstones, with thin coals and conglomerates (Irish, 1970; Mack and Jerzykiewicz, 1989; Eberth and Hamblin, 1993). We did not sample these Upper Cretaceous to Paleocene sediments and only refer to them briefly in reference to Figure 2. A significant proportion of the lithic material is volcanic detritus (up to 90% locally; Fig. 3) with subordinate low-grade metamorphic, carbonate and chert fragments (Mack and Jerzykiewicz, 1989; Potocki and Hutcheon, 1992). The rare plutonic material of igneous and metamorphic origin is presumed to have been derived from the Omineca Belt (Tyrrell, 1915; Mack and Jerzykiewicz, 1989).

Boyle (1979) suggested, with limited data, that Upper Cretaceous to Paleocene sediment may contain gold paleoplacers in the Rocky Mountain Front Ranges, although evidence for gold enrichment is sparse. Some conglomerate samples from the Brazeau Formation in the catchment of the North Saskatchewan River (Fig. 2) contain low, but

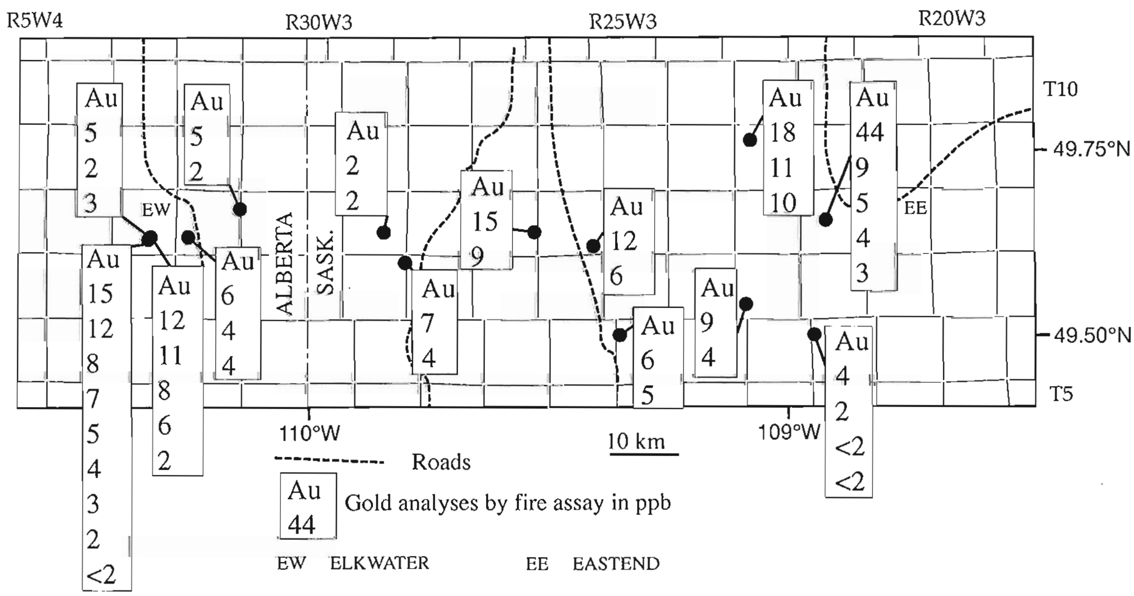

Figure 6. Location map for samples taken in this study from the Oligocene Cypress Hills Formation in the Cypress Hills, with gold analyses shown for each locality. Localities at which free gold was obtained are indicated with black circles. Multiple samples were collected at most sites.

anomalous, gold concentrations (up to 13 ppb); however, no detrital gold has been detected (Horachek, 1994). Tyrrell (1915) reported native gold in concentrates from coal in the Edmonton Group.

ALBIAN IGNEOUS-CLAST CONGLOMERATE IN THE BLAIRMORE GROUP

An Albian-aged (Early Cretaceous), igneous-pebble to cobble conglomerate infills nine known paleovalleys up to 22 km wide and 60 m deep, incised into the Beaver Mines and Mill Creek strata (Blairmore Group) of southwestern Alberta (Figs. 7, 8; Leckie and Craw, 1995; Leckie and Krystinik, 1995). The east-northeast trend of the valleys is well constrained and the conglomerate can be traced eastward for up to 66 km in several adjacent thrust slices in the Rocky Mountain Foothills and Main Ranges (Fig. 8); this trend is confirmed by paleocurrent data (Leckie and Krystinik, 1995). The conglomerate is distinctive because it contains abundant igneous clasts derived from the western Omineca Belt 250 km to the west (Fig. 1b; Norris et al., 1965; Urbatt, 1988; Leckie and Krystinik, 1995), prior to the rise of the modern Rocky Mountains. Clast petrography includes granitoids, mafic volcanics, low-grade metamorphic rocks and shallow level post-metamorphic quartz veins formed from meteoric fluids.

This igneous-clast conglomerate is well lithified, and separation of detrital gold is difficult. Some detrital gold flakes have been collected, but most indications of anomalous gold content (up to 910 ppb) are derived from geochemical analysis (Fig. 9; Leckie and Craw, 1995). The conglomerate contains detrital gold grains up to 150 μm in diameter and chemical analyses indicate widespread anomalous gold concentrations (up to 910 ppb Au) in conglomerate matrix. Gold contents in these igneous-clast conglomerates exceed those reported from the richest modern placers in Alberta (c.f. Guisti, 1986; Edwards, 1990; Horachek, 1994). The levels of enrichment detected in this study are locally comparable to modern economic placers which contain at least 200 to 300 ppb Au, and preferably around 1 ppm Au, in unconsolidated gravels (Boyle 1979). The gold is very fine grained, due to its distance from the presumed source (about 250 km, not palinspastically restored), and probable post-depositional mobility.

The conglomerate is too strongly lithified to allow normal panning of the sediment to extract gold. Hence, we collected gold liberated during the

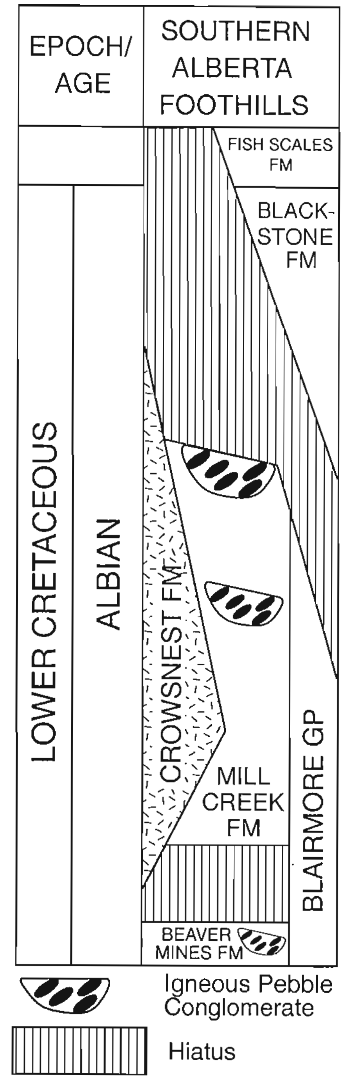

Figure 7. *Stratigraphic occurrence of igneous pebble conglomerate in Albian Beaver Mines and Mill Creek Formations (from Leckie and Krystinik, 1995).*

weathering process in samples of weathered debris below scarp outcrops, principally under overhangs, and on degraded outcrop surfaces. This technique met with limited success, and three samples (Fig. 9) yielded free grains of native gold. Free gold grains less than about 50 μm across are extremely difficult to save in a gold pan, and some may have been lost. Also, gold grains still attached to appreciable nonmetallic minerals possibly will have been lost in the panning process.

The gold grains are small (maximum dimension 150 μm) and irregular in shape, with broadly rounded exterior surfaces and irregular cavitation. In detail, the grain surfaces are highly convoluted locally, with

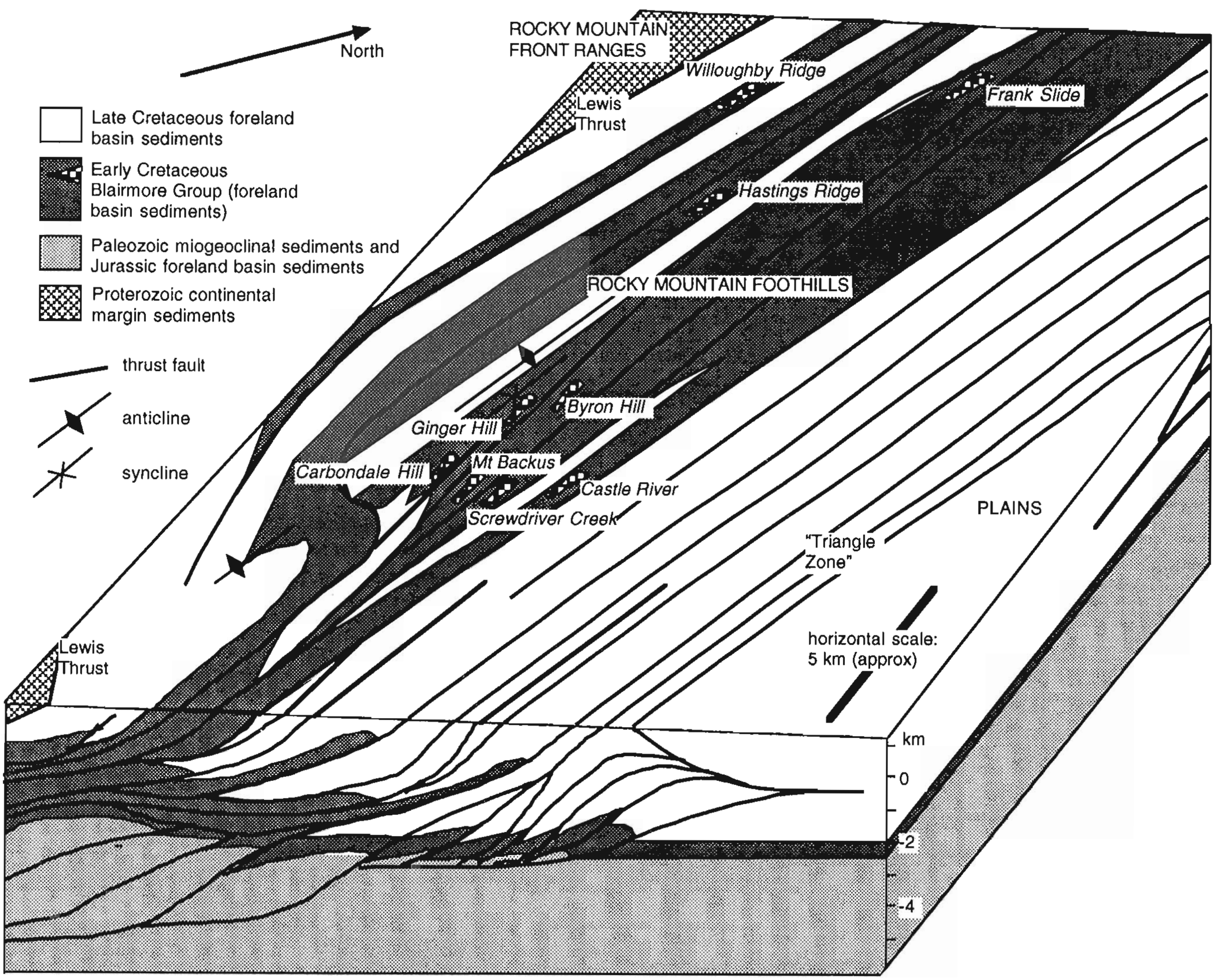

Figure 8. Occurrences of igneous-clast conglomerate within the Blairmore Group in the Rocky Mountain Foothills of southwestern Alberta, south of Crowsnest Pass (Highway 3). For reference, Frank Slide refers to the Frank Slide interpretive centre in the municipality of Crowsnest Pass.

delicate gold protuberances and scaly gold coatings on a 1 to 10 μm scale. Smooth-walled holes or cavities extend into gold grains for up to 10 μm. These textures are characteristic of detrital gold grains which have experienced both solution and overgrowths in conglomerate matrix after deposition (Guisti 1986; Youngson and Craw, 1993). Discontinuous coatings of limonite, silica and dolomite occur and likely were derived from the conglomerate cement.

CADOMIN FORMATION

The Cadomin Formation (Fig. 2) is a pebble to cobble conglomerate occurring along the length of the Rocky Mountain Foothills. The conglomerate is extremely highly indurated by silica cement. The age of the Cadomin Formation is poorly constrained but it is considered to be directly underlain by the basal Cretaceous unconformity and is therefore Aptian to Neocomian in age. The conglomerate is up to 200 m thick and was deposited in a north- to northwest-flowing braided river deposit (D.A. Leckie and R.J. Cheel, unpublished data). The Cadomin conglomerates appear to represent an interval of tectonic quiescence in the Cordillera when much of the proto-Rocky Mountains and eastern foreland basin were being isostatically uplifted and sediments older than Hauterivian were being bevelled regionally (Leckie and Smith, 1992; McMechan and Thompson, 1993). Dominant sediment sources were Paleozoic carbonates and clastics and Precambrian quartzites which flanked the North American craton and are now present in the Rocky Mountain Belt (Rapson, 1965; Potocki and Hutcheon, 1992).

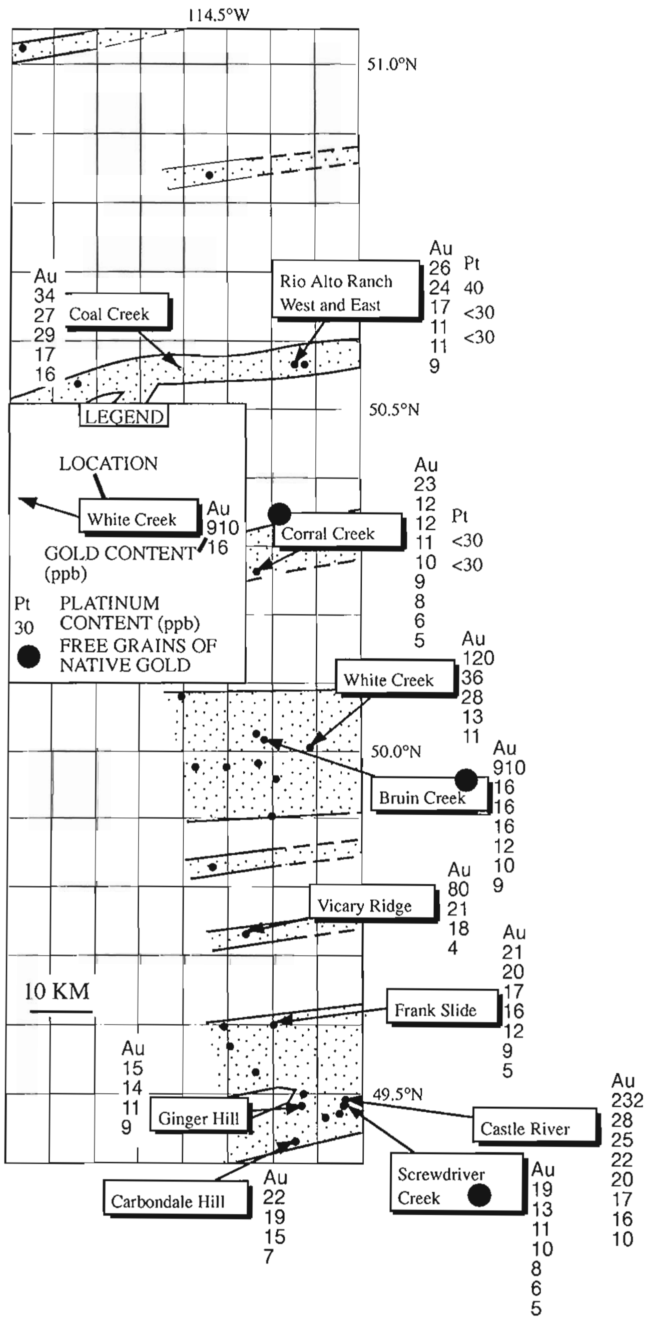

Figure 9. Location map for samples taken in this study from the igneous-clast conglomerate in the Blairmore Group (details in Leckie and Craw, 1995), with gold analyses shown for each locality. Localities at which free gold was obtained are indicated with black circles. Multiple samples were collected at most sites.

Twenty samples of matrix from outcrops of the Cadomin Formation in the Crowsnest Pass of southern Alberta were processed by fire assay. All but one of the values were in the 2 to 5 ppb range (Fig. 10). One sample from the Oldman River had a value of 17 ppb.

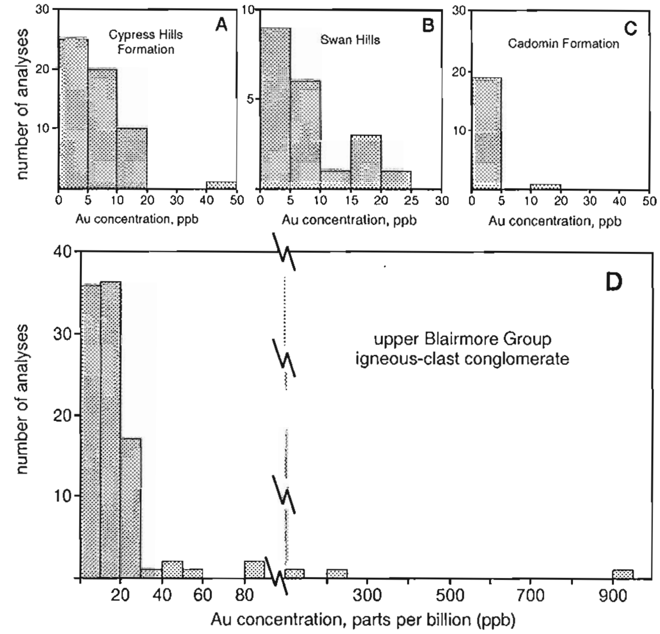

Figure 10. Histogram of results of fire assay analyses of samples of matrix from: A) the Cypress Hills Formation, B) Swan Hills, C) Cadomin Formation in the Crowsnest Pass area, and D) upper Blairmore Group igneous-clast conglomerate in the southern Alberta Foothills.

In general, we consider the Cadomin Formation to be devoid of anomalous gold values.

INTERPRETATION OF GOLD DISPERSAL IN THE FORELAND BASIN

In the early stages of uplift of the Rocky Mountain Cordillera, no gold-bearing rocks were exposed in what was to become the Omineca Belt (Fig. 1b), and thus no placer gold deposits could form from Omineca Belt sources in sediments of the Jurassic to Early Cretaceous Fernie through Beaver Mines formations (Fig. 2). Once the Omineca Belt had been eroded deeply enough to expose gold sources, a pulse of detrital gold passed into the foreland basin within the igneous-pebble conglomerate in the Blairmore Group (Figs. 2, 7, 10; Leckie and Craw, 1995). However, as compression in the Cordilleran orogen continued, the drainage divide shifted eastward, and the Omineca detrital gold was rerouted westward. Effectively, this eastward shift of the drainage divide blocked fluvial systems from flowing eastward from the gold-bearing Omineca Belt into the foreland basin. This process was repeated during Late Cretaceous–early Tertiary Laramide compression, but fewer deep-seated crystalline rocks of the Omineca Crystalline Belt were being eroded then, and gold was apparently less common. Hence, the placer gold passed into the foreland basin in a window of time between source unroofing by collision-driven uplift and erosion, and the collision-driven stream capture that cut off the supply of gold outboard to the east in the foreland belt. This placer gold window shown in Figure 3 was derived from the two Cretaceous pulses (Fig. 2).

Apparently another partly complete placer gold window followed the period of foreland basin deposition in the Early Tertiary (Fig. 2) when the watershed shifted westward to the Rocky Mountains and up-thrusted, sparingly gold-bearing, Neoproterozoic–Cambrian strata east of the new divide were eroded. Because no major compression has occurred since then, the drainage divide has not shifted significantly and this window remains open. Gold was shed into late Tertiary piedmont gravels (Swan Hills, Cypress Hills), and continues to be shed into the modern rivers. However, no richer sources of gold, which presumably occur in deeper parts of the section, have been exposed and so the amount of placer gold is small. The current window could close in the future because of drainage capture in several places (Craw and Leckie, 1996).

Paleoplacers in the Cretaceous and Tertiary strata described above have been uplifted and eroded during Tertiary regional extension and uplift. Hence, gold from these paleoplacers should reappear in modern streams near the source. Gold, redeposited from the Edmonton Group, could have been eroded and redeposited, together with newly eroded Rocky Mountain gold, in the Tertiary gravels capping remnant highlands such as the Swan Hills and Hand Hills. Continued uplift and erosion of the uplands resulted in the concentration of gold in the multiple networks which deposited the Saskatchewan Gravels. As noted above, further concentration of gold in modern alluvium has taken place where current rivers (especially North Saskatchewan and Red Deer rivers) have eroded the older Saskatchewan sands and gravels (Rutherford, 1937).

CONCLUSIONS

Analyses of gold contents of Mesozoic to modern conglomerates (or gravels) in southern to central Alberta show that there are significant, but low, levels of anomalous gold concentrations in many samples. Gold occurs in four intervals of the foreland basin succession: gravels of modern rivers draining the Rocky Mountain Belt; middle to late Tertiary gravels derived from the Rocky Mountains; Late Cretaceous to Early Tertiary sands and gravels; and a distinctive Early Cretaceous igneous-clast conglomerate in the Blairmore Group. The last interval is the most distinctly enriched in gold, in strong contrast with background gold concentrations in the underlying conglomeratic Cadomin Formation. The gold concentrations in the igneous-clast conglomerate demonstrate that paleoplacers derived from the Canadian Cordillera have accumulated in the Western Canada foreland basin, a sedimentary succession previously dismissed as a host for detrital gold. The Tertiary conglomerates at Swan Hills and Cypress Hills have low but anomalous values and also should be further investigated.

Acknowledgments

This manuscript was critically read by A.P. Hamblin and R.W. Macqueen.

REFERENCES

Boyle, R.W.
1979: The geochemistry of gold and its deposits. Geological Survey of Canada, Bulletin 280, 584 p.

Coney, P.J. and Harms, T.A.
1984: Cordilleran metamorphic core complexes: Cenozoic extensional relics of Mesozoic compression. Geology, v. 12, p. 550–554.

Craw, D. and Leckie, D.A.
1996: Tectonic controls on detrital gold dispersal into a foreland basin: an example from the Western Canada Foreland Basin. Journal of Sedimentary Research, v. 66, p. 559–566.

Eberth, D.A. and Hamblin, A.P.
1993: Tectonic, stratigraphic and sedimentological significance of a regional discontinuity in the upper Judith River Group (Belly River wedge) of southern Alberta, Saskatchewan, and northern Montana. Canadian Journal of Earth Sciences, v. 30, p. 174–200.

Edwards, W.A.D.
1990: Placer gold occurrences in Alberta. Alberta Research Council, Alberta Geological Survey, Open File Report 1990-9, unpaginated.

Furnival, G.M.
1946: Cypress Lake map-area, Saskatchewan. Geological Survey of Canada, Memoir 242, 161 p.

Guisti, L.
1986: The morphology, mineralogy, and behavior of "fine-grained" gold from placer deposits of Alberta: sampling and implications for mineral exploration. Canadian Journal of Earth Sciences, v. 23, p. 1662–1672.

Halferdal, L.B.
1965: The occurrence of gold in Alberta Rivers. Alberta Research Council, Economic Mineral Files, Open File Report 65-11, unpaginated.

Hamblin, A.P. and Walker, R.G.
1979: Storm-dominated shallow marine deposits: the Fernie Kootenay (Jurassic) transition, southern Rocky Mountains. Canadian Journal of Earth Sciences, v. 23, p. 1673–1690.

Harris, D.C. and Ballantyne, S.B.
1994: Characterization of gold and PGE-bearing placer concentrates from the North Saskatchewan River, Edmonton, Alberta. *In* Current Research 1994-E, Geological Survey of Canada, p. 133–139.

Horachek, Y.
1994: Investigation of potential paleoplacers in the Cretaceous strata of the North Saskatchewan River watershed. Alberta Research Council, Open File Report 1994-19, 28 p.

Irish, E.J.W.
1970: The Edmonton Group of south-central Alberta. Bulletin of Canadian Petroleum Geology, v. 18, p. 125–155.

Jackson, L.E., Jr., MacDonald, G.M., and Wilson, M.C.
1982: Paraglacial origin for terraced river sediments in Bow Valley, Alberta. Canadian Journal of Earth Sciences, v. 19, p. 2219–2231.

Kupsch, W.O. and Vonhof, J.A.
1967.: Selective cementation in Tertiary sands and gravels, Saskatchewan. Canadian Journal of Earth Sciences, v. 4, p. 769–775.

Leckie, D.A. and Cheel, R.J.
1989: The Cypress Hills Formation (Upper Eocene to Miocene): a semi-arid braidplain deposit resulting from intrusive uplift. Canadian Journal of Earth Sciences, v. 26, p. 1918–1931.

Leckie, D.A. and Craw, D.
1995: Westerly derived Early Cretaceous gold paleoplacers in the Western Canada foreland basin, southwestern Alberta: tectonic and economic implications. Canadian Journal of Earth Sciences, v. 32, p. 1079–1092.

Leckie, D.A. and Krystinik, L.F.
1995: The Cretaceous Igneous-Clast Conglomerate in the Blairmore Group, Rocky Mountain Foothills and adjacent subsurface (Bow Island Formation), Alberta, Canada. Bulletin of Canadian Petroleum Geology, v. 43, p. 320-342.

Leckie, D.A. and Smith, D.G.
1992: Regional setting, evolution, and depositional cycles of the Western Canada Foreland Basin. *In* Foreland Basins, R.W. Macqueen and D.A. Leckie (eds.). American Association of Petroleum Geologists, Memoir 55, p. 9–46.

Lone Pine Publishing
1991: The Lost Lemon Mine. Lone Pine Publishing, Edmonton, 63 p.

Mack, G.H. and Jerzykiewicz, T.
1989: Provenance of post-Wapiabi sandstones and its implications for Paleocene tectonic history of the southern Canadian Cordillera. Canadian Journal of Earth Sciences, v. 26, p. 665–676.

Macqueen, R.W. and Leckie, D.A. (eds.)
1992: Foreland Basins and Foldbelts. American Association of Petroleum Geologists, Memoir 55, 460 p.

McConnell, R.G.
1885: Report on the Cypress Hills, Wood Mountain and adjacent country. Geological Survey of Canada, Annual Report 1, pt. C, p. 1C–169C.

McMechan, M.E. and Thompson, R.I.
1993: The Canadian Cordilleran Fold and Thrust Belt south of 66°N and its influence on the Western Interior Basin. *In* Evolution of the Western Interior Basin, W.G.E. Caldwell and E.G. Kauffman (eds.). Geological Association of Canada, Special Paper 39, p. 73–90.

Norris, D.K., Stevens, R.D., and Wanless, R.K.
1965: K-Ar age of igneous pebbles in the McDougall-Segur Conglomerate, southeastern Canadian Cordillera. Geological Survey of Canada, Paper 65-26, 11 p.

Olson, R.A., Dufresne, M.B., Freeman, M.E., Richardson, R.J.H., and Eccles, D.R.
1994: Regional metallogenic evaluation of Alberta. Alberta Research Council, Open File Report 1994-10, 191 p.

Potocki, D.J. and Hutcheon, I.
1992: Lithology and diagenesis of sandstones in the Western Canada Foreland Basin. *In* Foreland Basins, R.W. Macqueen and D.A. Leckie (eds.). American Association of Petroleum Geologists, Memoir 55, p. 229–258.

Price, R.A., Monger, J.W.H., and Roddick, J.A.
1985: Cordilleran cross-section: Calgary to Vancouver, trip 3. *In* Field Guides to geology and mineral deposits in the southern Canadian Cordillera, D. Tempelman-Kluit (ed.). Geological Society of America Cordilleran Section Meeting, Vancouver, British Columbia, p. 3.1–3.85.

Price, R.A. and Mountjoy, E.W.
1970: Geologic structure of the Canadian Rocky Mountains between Bow and Athabasca Rivers — A progress report. *In* Structure of the Southern Canadian Cordillera, J.O. Wheeler (ed.). Geological Association of Canada, Special Paper 6, p. 7–25.

Rapson, J.E.
1965: Petrography and derivation of Jurassic–Cretaceous clastic rocks, southern Rocky Mountain, Canada. American Association of Petroleum Geologists Bulletin, v. 49, p. 1426–1452.

Riley, D., Primrose, T., and Dempsey, H.
1968: The Lost Lemon Mine. Frontier Publishing, Calgary, 40 p.

Riley, D.E.
1946: The Lost Lemon Mine. Alberta Folklore Quarterly, v. 2, p. 15–18.

Russell, L.S.
1948: The geology of the southern part of the Cypress Hills, southwestern Saskatchewan. Saskatchewan Department of Mineral Resources, Report 8.

1971: Paleontology of the Swan Hills area, north-central Alberta. Royal Ontario Museum, Life Sciences Contribution 71, p. 1-31.

Rutherford, R.L.
1937: Saskatchewan gravels and sands in central Alberta. Transactions of the Royal Society of Canada, Section 4, v. 31, p. 81-95.

St. Onge, D.A.
1974: The geomorphology of the Swan Hills area, Alberta. Geological Survey of Canada, Paper 74-26, 6 p.

Stalker, A.MacS.
1961: Buried valleys in central and southern Alberta. Geological Survey of Canada, Paper 60-32, 13 p.

1968: Identification of Saskatchewan gravels and sands. Canadian Journal of Earth Sciences, v. 5, p. 155-163.

Storer, J.E.
1975: Middle Miocene mammals from Cypress Hills, Canada. Canadian Journal of Earth Sciences, v. 12, p. 520-522.

Tyrrell, J.B.
1915: Gold on the North Saskatchewan River. Transactions of the Canadian Mining Institute, v. 18, p. 160-173.

Urbatt, R.R.
1988: Provenance of the Lower Cretaceous (Albian) McDougall-Segur Conglomerate, southwestern Alberta. B.Sc. Thesis, University of Calgary, 85 p.

Vonhof, J.A.
1969: Tertiary sands and gravels in the Canadian Great Plains. Ph.D. Thesis, University of Saskatchewan, 279 p.

Westgate, J.A., Kalas, L., and Evens, M.E.
1976: Geology of the Edmonton area, Alberta. Field Trip C8 Guidebook, Geological Association of Canada and Mineralogical Association of Canada, Joint Meeting, May, 1976, Edmonton, 49 p.

Youngson, J.H. and Craw, D.
1993: Gold nugget growth during tectonically-induced sedimentary recycling. Sedimentary Geology, v. 84, p. 71-88.

SUMMARY AND CONCLUSIONS[1]

R.W. Macqueen
Geological Survey of Canada, Calgary

Abstract

What have we learned from the federally supported geoscience studies of the Canada–Alberta Partnership on Minerals (MDA)? For the exposed Precambrian Shield, the major area of federal MDA geoscience funding, geological studies outline: a new tectonic/radiometric framework with 3 types of sulphide occurrences; a high potential for uranium-polymetallic mineralization; and the distribution/origin of glacial materials. A regional geophysical survey demonstrates significant differences in igneous rocks, and reveals some sulphide mineralization. A regional lake sediment/water geochemical survey indicates locally anomalous values of Au and U. A digitally based integration of Shield studies permits sophisticated mineral potential assessments and rapid access to geoscience data. Diamond-related studies of Alberta minettes/kimberlites, and appraisal of diamond potential within the new Precambrian crustal blocks, provide a new diamond exploration framework for Alberta. A low-density indicator mineral/geochemical survey of southern Alberta demonstrates that one in two till samples contains indicator minerals, and identifies several areas favourable for kimberlite occurrence. An aeromagnetic survey of southeastern Alberta suggests the presence of an igneous dyke swarm of probable Eocene age, possibly with diamond potential. Exciting MDA-funded geoscience studies in the Fort McKay region verify disseminated gold, silver and copper mineralization in Paleozoic rocks. Studies of Tertiary/Recent gravels in central Alberta clarify the nature and distribution of anomalous amounts of gold and platinum group elements with economic potential. Studies of the Crowsnest Volcanics of southwestern Alberta reveal their origin, and offer a better assessment of their potential for economic mineralization.

Résumé

Qu'avons-nous retiré des études géoscientifiques menées dans le cadre de l'Entente Canada-Alberta sur l'exploitation minérale (EEM) et financées par le gouvernement fédéral? En ce qui concerne la partie affleurante du Bouclier canadien, principale région où les fonds fédéraux ont été versés pour la réalisation de travaux géoscientifiques dans le cadre de cette EEM, les études géologiques ont permis d'établir un nouveau cadre tectonique et de nouvelles limites radiométriques considérant trois types d'indices de sulfures; de faire ressortir un potentiel élevé en minéralisation polymétallique riche en uranium; et de décrire tant la répartition que l'origine de matériaux glaciaires. Un levé géophysique régional a révélé des différences significatives au sein des roches ignées et la présence de quelques minéralisations en sulfures. Un levé géochimique régional des sédiments et des eaux lacustres a indiqué des anomalies locales d'or et d'uranium. Une intégration numérique des études portant sur le Bouclier a permis des évaluations sophistiquées du potentiel minéral et un accès rapide à l'information géoscientifique. Les études sur la teneur en diamant des minettes et des kimberlites de l'Alberta, mais aussi l'évaluation du potentiel diamantifère dans les blocs crustaux précambriens récemment identifiés, ont abouti à la définition d'un nouveau cadre pour l'exploration du diamant en Alberta. Dans le sud de l'Alberta, un échantillonnage des minéraux indicateurs et un levé géochimique à faible densité ont mis en évidence le fait qu'un échantillon de till sur deux contient des minéraux indicateurs; il a donc été possible de délimiter plusieurs zones où il pourrait y avoir des indices de kimberlites. Dans le sud-est de l'Alberta, un levé aéromagnétique a fait ressortir la présence d'un essaim de dykes ignés d'âge éocène probable, peut-être diamantifère. La présence d'une minéralisation disséminée d'or, d'argent et de cuivre dans des roches paléozoïques de la région de Fort MacKay a été confirmée par des travaux géoscientifiques financés par l'EEM, lesquels tavaux ont été des plus stimulants. Des études sur des graviers tertiaires et holocènes dans le centre de l'Alberta ont permis de définir la nature et la répartition des anomalies d'or et des éléments du groupe du platine offrant un potentiel économique. Dans le sud-ouest de l'Alberta, les études sur les volcanites de Crowsnest ont révélé leur origine et permis de mieux évaluer leur potentiel économique.

[1]Canada-Alberta Agreement on Mineral Development, Project C1.61

Precambrian Shield of Northeastern Alberta

Bedrock geological mapping

M.R. McDonough's 1:50 000 scale geological mapping has shown that the bulk of the rocks of northeastern Alberta belong to the Taltson magmatic zone, and are mostly Paleoproterozoic in age (2.5-1.6 Ga), rather than Archean. Although the rocks are typically complex, strongly deformed and not well exposed, the southern part of the Taltson magmatic zone is dissected by three, regional, north-trending shear zones that may host mineralization. Within the framework outlined by McDonough (1997), three types of sulphide occurrences are recognized, all of them governed by or associated with penetrative greenschist grade deformation. This deformation is constrained by radiometric dating to the period 1860 - 1800 Ma (McDonough, 1997). One type of occurrence is hosted by shear zones; all three types of occurrences (McDonough, 1997) appear worthy of further investigation. The search for other kinds of deposits, e.g., gold or molybdenum located in granitic rocks, gold in metasedimentary rocks, etc. (Charbonneau et al., 1997) should be facilitated by the existence of the new suite of 1:50 000 scale geological maps.

Surficial studies

J.M. Bednarski's work on the surficial deposits of the shield area of northeastern Alberta confirms that much of the area is only sparsely covered by glacial deposits despite extensive scour during the last glaciation. The nature of the surficial deposits, their distribution and their origin, including extensive deltaic and lacustrine deposits, is clear from this regional-scale work. Bednarski also provides geochemical data obtained from 336 samples in the region, analyzed for ten elements including Au, As, Pb, U and Zn (Bednarski, 1997). These geochemical data add to the regional lake sediment and water geochemical data discussed by McCurdy (1997). Study of all of these geochemical data permits recognition of anomalous values that should prove interesting for mineral exploration. Knowledge of the nature and distribution of the surficial materials is also of value in interpreting the origin and significance of diamond indicator minerals. As noted by Kjarsgaard (1997) for the southern and central part of Alberta, interpretation of indicator mineral data is not a trivial matter, especially over most of Alberta, where multiple glacial and erosional events have taken place.

Regional geophysical and geochemical surveys

The regional geophysical survey by B.W. Charbonneau and colleagues, and the regional lake sediment and water geochemical survey by McCurdy and colleagues offer basic data available digitally. Broad outlines of the geology of the region are revealed by the geophysical data, including major lithological units, major fault or shear zones, and abrupt contacts. The presentation of the geophysical data (Charbonneau et al., 1994) in the form of digitally derived maps complete with graphic presentation of multi-element data offers the potential for near pinpointing of anomalies, and for comparison, by computer or by visual inspection, of individual survey lines or individual elements one with another. Some 146 stacked multiparameter profiles are provided in the open file data (Charbonneau et al., 1994). In other areas of Canada, Nova Scotia for example (see Shives et al., 1995), geophysical signatures have been linked clearly to mineralization. The Alberta data do not yet permit linkages to mineralization, partly because the area is relatively unexplored. Exceptions to this statement are provided by some VLF anomalies, which appear to coincide with sulphide-rich metasedimentary bands, and uranium anomalies that outline some uranium occurrences. The digital nature of this survey permits easy integration with other data sets, including geochemical data.

Regional lake sediment and water geochemical data including analysis of 35 elements from 1160 sampling sites (Friske et al., 1994; McCurdy, 1997) were completed in northeastern Alberta to National Geochemical Reconnaissance standards. Accordingly these data permit comparison of analytical values of a given element both within the area surveyed, and with other areas outside of northern Alberta. The contoured plots from these data (uranium, molybdenum, gold, zinc, nickel and copper; and the pathfinder elements arsenic and antimony) presented by McCurdy (1997) reveal interesting anomalies. These anomalies, considered in their context of bedrock geology (including geological structure) and surficial geology, suggest that a number of areas warrant further detailed studies or mineral exploration. The geochemical data also indicate, as might be suspected, that in areas of thick overburden, glacial processes played a major role in accounting for the distribution of the elements examined. North of Lake Athabasca, where glacial cover is thin to non-existent, geochemical analyses appear to reflect bedrock geology closely, and thus offer the most promise for detecting potential economic mineralization in bedrock. McCurdy (1997) recommends several specific bedrock areas for uranium and gold exploration, and a number of areas south of Lake Athabasca where placer gold may occur in economically interesting concentrations.

Mineral potential mapping

The objectives of the data integration project of C-J. Chung and colleagues (Chung et al., 1997) were to develop digitally based methods of integrating diverse data sets from the Shield of northeastern Alberta, and to produce maps of mineral potential for various economic elements from the integrated data. The methods developed are preliminary, partly because of the absence of known economic deposits on the Shield of northern Alberta and thus a less-than-ideal database for comparison of all the data sets with known economic mineralization. Nevertheless, it is significant that the statistical relationships derived for the various data sets from the area were capable of detecting at least 75% of the 36 known anomalous occurrences of gold in a "training area" chosen from the northeastern Alberta Shield. The ability to use all of the data available - satellite data to airborne geophysical data, to digitally prepared geological map data, to regional geochemical data - offers much promise in narrowing down areas for exploration in this large and minimally explored region. Further publications are expected on this topic and for this area (C-J. Chung, pers. comm., 1996).

Unconformity-related uranium deposits

In 1994-95, Canada was the world's leading producer of uranium (Whillans, 1996), most of it from the rich uranium-polymetallic deposits of the Athabasca Basin of northern Saskatchewan (Ruzicka, 1995). V. Ruzicka's assessment of the potential for the occurrence of similar, rich uranium-polymetallic deposits in the Alberta portion of the Athabasca Basin is favourable. Indeed Ruzicka (1997) offers eight specific recommendations to those conducting exploration in the area, based on the characteristics of the Saskatchewan deposits and his extensive knowledge of global uranium deposits. Even though they rarely outcrop, the richly productive unconformity-related deposits of Saskatchewan have specific signatures, and thus must be found by "blind" exploration drilling, carefully guided by all the relevant clues that can be assembled. Significant exploration features for the Athabasca Basin include proximity to Archean basement granitoid rocks, the presence of faults and fractures, geochemical anomalies, and zones of argillic or chloritic alteration - all features that are prominently associated with most unconformity-related deposits (Ruzicka, 1995; 1997). Of note to uranium explorationists is the recent discovery that high resolution seismic reflection data of the type acquired in the LITHOPROBE project provide sharp and detailed images of the contact between the overlying Athabasca Basin sediments and the underlying crystalline basement at depths of 0.5 to 2 km, and at the same time identify the all-important faults and shear zones within the basement and Athabasca Basin cover rocks, where such zones are present (Clowes, 1996, p. 122). For further research on uranium metallogeny in Athabasca Basin settings, Ruzicka (1997) offers a number of suggestions aimed at refining the exploration model for these deposits, not least of which is determining the geochronology of mineralization events.

Crowsnest Formation: Origin and mineral potential

The Southwestern Minerals subprogram of the Canada-Alberta MDA supported only the Crowsnest Formation (CNF) project, although other related work on gold paleoplacer deposits in Cretaceous and Tertiary rocks of southwestern Alberta was supported by other funding and is reported on herein (Leckie and Craw, 1997). An important goal of the CNF project was to gain a better understanding of the nature and origin of this unusual and distinctive volcanic unit, which has been suggested to have potential for gold, diamonds, base metals, garnets (as abrasives) and building stone. The composition, origin and distribution of the unit all have a bearing on these potential commodities and uses. Accordingly the approach followed by T.D. Peterson and colleagues was mapping and sampling of the Crowsnest Formation, followed by detailed petrographic and geochemical study. Their work shows that the unit is made up of large volumes of vocaniclastic sandstones with relatively minor, mildly potassic trachytes and phonolites containing phenocrysts of sanidine, titanite, analcite and other minerals. Peterson et al. (1997) suggest that the CNF magmas probably originated by partial melting of metasomatized lithosphere near the crust-mantle boundary (~25-30 km depth). As would be expected for such a setting, primary gold and base metal concentrations are very low, and low-grade metamorphism did not produce anomalous vein or stratiform concentrations (Bégin et al., 1995; Peterson et al., 1997). The best potential for the CNF may be for industrial minerals, specifically analcite, although the presence of iron-bearing minerals as contaminants and alteration products detracts from possible commercial use of analcite from CNF. There is also some potential for gem quality analcite, which in the best examples has an attractive dark green colour and striking appearance. As an abrasive, melanite garnet, which may comprise 10% by volume of some of the CNF volcaniclastic sandstones, may have some potential (Peterson et al., 1997).

Diamond subprogram

Study of potential host rocks from deep-seated settings

The major increase in staking in Alberta from 1990-1995 (Kjarsgaard, 1997) was most strongly related to diamond exploration (Dufresne et al., 1996). Does Alberta have diamond potential? This is one of the central questions underlying the work of B.A. Kjarsgaard and colleagues on kimberlites and related rocks from Alberta settings. No definitive answer may yet be provided to this question, but a clearer understanding of the nature, distribution and origin of rocks of deep-seated origin has been achieved (Kjarsgaard, 1997; and references therein). Important supporting data relevant to the possible occurrence of diamond deposits in Alberta is provided by the work of Ross and colleagues (1991; also Villeneuve et al., 1993), with their identification of tectonic domains in the Precambrian basement of Alberta, including the distribution of Archean-aged crustal blocks. Such blocks are considered as favourable or even essential for the occurrence of diamond-bearing rocks (e.g. Fipke et al., 1995). In his study of Alberta occurrences of deep-seated rocks, Kjarsgaard (1997) also notes the difficulty of applying diamond indicator mineral analysis effectively in exploration in the western Canadian plains because of the complex sedimentological history that these minerals have had in such settings.

Three areas of occurrence of rocks of deep-seated origin are known in Alberta: the Sweet Grass minettes in the south, considered to be part of the Montana Alkaline Province (Kjarsgaard, 1997); the Mountain Lake area to the northeast of Grande Prairie (Leckie et al., 1997; Kjarsgaard, 1996; 1997); and the Buffalo Hills kimberlites of northern Alberta (Northern Miner, 1997). Newspaper reports that appeared in the spring of 1997 indicate that one of the three kimberlite bodies sampled by Ashton Mining on their Buffalo Hills property contains both micro and macro diamonds (the boundary between microdiamonds and marcro-diamonds is 1/2 mm). Although minettes in general are considered to have low potential for diamonds, the Sweet Grass minettes have compositional aspects which justify further examination (Kjarsgaard, 1997). In addition, a minette dyke in the Churchill Province, N.W.T., is richly diamondiferous (McCrae et al., 1996). The two other occurrences either are undergoing or have undergone active exploration for diamonds. The Mountain Lake diatreme appears to have very limited potential for diamond occurrence based on the chemistry of its contained heavy minerals; the diatreme body is made up of ultrabasic volcanic or vocanogenic rocks, neither kimberlite nor lamproite in compositon (Leckie, Kjarsgaard et al., 1997). It is worth noting that the Fort à la Corne area of north-central Saskatchewan, with more than 70 known pipes or geophysical anomalies interpreted as pipes (Kjarsgaard, 1996), was unknown until 1988, but was discovered initially using Geological Survey of Canada regional aeromagnetic survey maps (Kjarsgaard, 1996). Will Alberta prove host to large numbers of pipes? As discussed by Dufresne et al. (1996) and Kjarsgaard (1997), diamond indicator minerals and some diamonds have been discovered widely in Alberta from Quaternary deposits and modern drainage; the problem in locating the sources is the complexity of the sedimentary history of these materials, in particular multi-stage recycling of materials.

In all occurrences of rocks of deep-seated origin, the information to be obtained by field outcrop, drill core and geophysical studies includes the distribution, shape or form, and extent of a particular occurrence [pipe(s) of some sort at the Grande Prairie (Mountain Lake) and Buffalo Hills occurrences, and dykes, plugs and vent complexes at the Sweet Grass Hills occurrences (Kjarsgaard, 1997)]. Petrological and trace element studies indicate the nature and depth of origin of these bodies, and offer some indication of the likelihood of economic diamond occurrence. Locating pipes offers promise, but really is only the beginning in terms of assessing diamond potential. Dufresne et al. (1996) and Kjarsgard (1997) indicate the steps to be followed in study and assessment of the diamond potential of rocks of deep-seated origin.

Indicator mineral and geochemical reconnaissance

Thorleifson and Garrett's (1997) kimberlite indicator mineral and geochemical survey of Alberta, conducted as one part of a series of Canadian prairie-wide surveys, shows an average of one indicator mineral per two samples. The kimberlite indicator minerals Cr-pyrope, Cr-diopside and Mg-ilmenite, as well as gold in several forms, are present in the surface till of Alberta in a non-random distribution (Thorleifson and Garrett, 1997). Indicator mineral studies, combined with geochemical analysis of samples, provide information on the bedrock source of the till samples. Although the problem of multi-stage recycling greatly complicates interpretations, clear distinctions commonly can be made between Canadian Shield-derived materials and Cordilleran-sourced materials (Thorleifson and Garrett, 1997). The systematic data obtained by the Canada-Alberta MDA survey provide a regional background for detailed collection and interpretation of indicator mineral data on a more local scale. Indeed there now is a wealth of indicator mineral and geochemical data that one hopes will be compared with surficial deposit data, integrated and evaluated, so that future understanding and interpreting of multi-stage recycling of indicator minerals will be less daunting than at present. The soil indicator mineral data seem to be less promising for mineral exploration, but the soil geochemical data are of immediate and continuing value in environmental and agricultural investigations (e.g., Garrett, 1994).

Cypress Hills aeromagnetic survey

These new high-resolution aeromagnetic anomaly data (Stone, 1993a,b) led to the recognition of striking short wave length anomalies by Ross and colleagues (Ross et al., 1997). The reasonable interpretation of these features put forward by Ross et al. (1977) is that they are real features (not artifacts), they are located within the sedimentary section, near the surface (~250 m or less), and are similar in distribution and size to known dyke swarms in the Canadian Shield. As such, these "dykes" (for they have yet to be verified as dykes) may represent a continuation into eastern Alberta of the Montana Alkaline Province Eocene-aged volcanics, exposed in southernmost Alberta in the Sweet Grass Hills (Kjarsgaard, 1997). This is an exciting prospect, and one that needs to be confirmed by detailed ground magnetic or gravity surveys, accompanied by drilling of the most suitable anomalies.

Meanwhile an important aspect of these linear features of the Cypress Hills may be their role in the generation of shallow structural traps for hydrocarbons in Cretaceous sediments of southeastern Alberta (Ross et al., 1997).

Precious metals: Gold and platinum group elements

Modern and Tertiary placer and paleoplacer occurrences

Before Canada-Alberta MDA studies began in 1992, the only known Alberta gold occurrences that have produced small amounts of gold intermittently since the 1880s, and still produce measurable amounts of gold for hobby placer "miners", are certain gravel bar locations on the North Saskatchewan River in the Edmonton region, and a number of Tertiary-aged gravel deposits also in the Edmonton region. Accordingly it was decided to investigate these occurrences systematically (Harris and Ballantyne, 1994; Ballantyne and Harris, 1997; and references therein). S.B. Ballantyne and colleagues in their Canada-Alberta MDA-funded studies were consistently able to recover gold and PGE grains from a large number of localities. Microscopic, scanning electron microscope, and electron microprobe studies of collected grains were carried out. Gold grains seem to be the most abundant. They occur in a variety of shapes and sizes, and range in composition from electrum to gold (550-950 fineness). The grains studied include some donated by individuals and mining companies.

In paleoplacer settngs from the Tertiary-aged Saskatchewan sands and gravels, gold grain surfaces commonly contain distinctive bacterial? growths. PGM grains are also abundant in both modern and Tertiary-aged material, occurring as platelets, rods, discs, spheres and crystals, and with compositions including Pt-Fe, Os-Ir-Ru-Pt alloys (Ballantyne and Harris, 1997). A possible in-basin source for gold and PGE grains is the mid-Cretaceous Shaftesbury Formation of northeastern Alberta, where pristine gold grains occur encrusted with Cu-Fe and Fe-sulphides.

The presence of complex and diverse precious metal grains in Alberta modern and Tertiary gravels is unusual when these Alberta occurrences are compared with similar modern to Tertiary-aged settings elsewhere in the world: what might this mean? Future studies should address several questions. What is the source of these alluvial grains? Are there geographic differences in the nature, composition, morphology and abundance of these grains? Is it possible that the grains are derived from ultrabasic intrusives or pipes intruding the Alberta Basin? Or are the grains most likely derived from outside the basin, e.g., from the

Cordillera? How important is bacterial or other postdepositional modification of grains? Answers to these questions should also provide a better assessment of the economic potential of these materials. Meanwhile there is continuing potential for small-scale recovery of gold and PGE grains from commercial gravel operations in central Alberta (S.B. Ballantyne, pers. comm., 1996).

Microdisseminated Au-Ag-Cu minerals, Fort McKay region

Following closely behind the interest in diamond occurrences in Alberta in terms of ground staked between 1990 and 1996 is a new type of precious metal occurrence, termed "microdisseminated Au-Ag-Cu minerals" by Abercrombie and Feng (1997). These minerals and probable alloys occur in rocks of the Western Canada Sedimentary Basin and underlying Precambrian basement near Fort McKay, Alberta. Abercrombie and Feng (1997) describe these occurrences, note their location near the dissolution edge of the Middle Devonian Prairie Formation, and present a hypothesis to explain the origin and distribution of these exciting occurrences. Three hydrochemical zones characterize the region: a lower, relatively oxidized brine regime; an intermediate, relatively reduced saline regime; and an upper, fresh to brackish regime, locally bitumen-saturated (Abercrombie and Feng, 1997). The hypothesis proposed to explain these occurrences involves mobilization and transport of gold and other metals in oxidizing, halide-rich brines derived from the Elk Point Group at a maximum paleotemperature of about 90°C, with deposition occurring in reducing zones, probably produced by microbial reduction of sulphate, and probably related to the presence of organic matter or hydrocarbons.

A striking aspect of the setting in which these occurrences are located is that it is not unique to the Fort McKay region: there appears to be potential for similar occurrences in many other places along the dissolution edge of evaporites in this and other similar basins elsewhere. Many questions arise regarding these occurrences. What controls the initial release of metals? What focussing mechanisms operate? How and when does deposition occur? And (perhaps most important of all) if these occurrences are to move from the realm of geological curiosities to deposits with economic potential, have mechanisms operated to concentrate metals, and if so, how and where? These and related questions are paramount in the exploration programs that have been underway in the region since 1993.

Anomalous gold occurrences in Cretaceous and Tertiary conglomerates and gravels, Southwestern Alberta

In a report of a research project conducted independently of the Canada-Alberta MDA work, D.A. Leckie and D. Craw have identified gold values that range up to 910 parts per billion (ppb) in lithified conglomerates and gravels of southwestern Alberta. Although the gold values reported are not of economic interest, the fact that they are well above background values of about 2 to 5 ppb indicates that further investigation is warranted. A distinctive, igneous-pebble-bearing conglomerate in the Blairmore Group (Early Cretaceous) contains the highest gold values detected. The suggested source for the gold found in these rocks is primary gold deposits of the Omineca Crystalline Belt of the Cordillera to the west. Leckie and Craw postulate the existence of "windows" of gold derivation and deposition from the Omineca Belt based on specific times of uplift of the Belt followed later by source cutoff by eastward-stepping of the drainage divide. Because gold is known in modern gravels of the area that drains the Rocky Mountain Belt, it appears that the latest gold window to the Omineca Belt is still open.

Sweet Grass Hills and environs

Eocene-aged volcanics that crop out in the Sweet Grass Hills of southern Alberta (Kjarsgaard, 1997) may have some potential for gold and/or silver, although anomalous values of gold have not been found to date. In Montana, rocks of the Montana Alkaline Province locally contain gold and silver (Gavin, 1991). The Cypress Hills linear features, if they are intrusive dykes (Ross et al., 1997) as discussed above, may have potential for gold occurences similar to those of the Montana Alkaline Province.

Closing comments

As noted above, geoscience was one part of the Canada-Alberta MDA program, with the federal components as discussed herein. The provincial program, as well as federal and provincial activities in technology development and economic development, are reviewed briefly in the document Canada-Alberta Partnership on Minerals (1996). The exisiting geological database in Alberta is large and growing, but until the 1980s much of it was most strongly related to oil, gas, and coal exploration. The intention of the geoscience segment of the Canada-Alberta MDA was to create or improve the geological framework that enhances mineral exploration, leads to increased exploration, and ultimately to economically viable, producing mineral deposits. Time will tell how successful the Canada-Alberta MDA projects have been in meeting these goals. Meanwhile, the level of interest in mineral deposits in Alberta is high, especially in the potential for diamond or gold deposits. Mineral exploration activity has increased significantly in Alberta, and it is our hope that the geoscience reported herein will contribute to the successful search for non-fuel mineral resources.

ACKNOWLEDGMENTS

This volume, planned to summarize or interpret GSC-supported Canada-Alberta MDA research, owes its origin mainly to those scientists, contractors, technicians and other helpers who completed or contributed to the work. Selection of the projects and initial levels of financial support was made by a number of individuals including Walter Nassichuk and Grant Mossop of GSC Calgary, Murray Duke and others in the Mineral Resources Division of GSC Ottawa, and Sandy Colvine, formerly of Continental Geosciences Division of GSC Ottawa. Early discussions about the scope and nature of the Canada-Alberta MDA also involved Jan Boon and Wylie Hamilton of the Alberta Geological Survey, and Michael Day of Alberta Energy, all of Edmonton. Gerry Ross of GSC Calgary offered initial guidance and enthusiasm, and later contributed to the program. Thanks are due also to the critical readers of the papers included in this volume, acknowledged in individual papers.

Once underway in 1992, federally and provincially supported Geoscience projects were monitored by the Geoscience Technical Committee consisting of Jan Boon of the Alberta Geological Survey; Don Currie of the Alberta Chamber of Resources, Edmonton; and Roger Macqueen of GSC Calgary. Rick Richardson of the Alberta Geological Survey provided guidance to the Geoscience Technical Committee. Reg Olson of Apex Geoscience Ltd., Edmonton, provided advice and guidance to the Geoscience Technical Committee on request. The financial and technical recommendations of the Geoscience Technical Committee were discussed and accepted, modified or (on occasion) rejected by the Management Committee at semi-annual meetings, co-chaired by Al Clark of the Mining Sector of Natural Resources Canada, Ottawa, and Paul Precht of Alberta Energy, Edmonton. The other members of the Management Committee were Grant Mossop of GSC Calgary, and Dave Luff of Alberta Energy. Jurgen Kleta and Katherine Wood of Alberta Energy skillfully handled the tabulation of progress reports and accounting data for the Management Committee and its meetings. Dan Richardson of Federal-Provincial-Territorial Liaison Office, GSC Ottawa, is especially thanked for keeping track of the funding over the life of the program, 1992-1997.

Claudia Thompson and Billie Chiang of GSC Calgary handled secretarial duties competently and cheerfully. Peter Neelands and Mike Staniland of GSC Calgary helped with figure preparation for some of the papers. Brian Ortman and Doug Lemay at GSC Calgary looked after the many diagrams in myriad computer programs and formats. Daniel Lebel of GSC Calgary helped with some necessary changes in French translation. This volume was edited initially by Tim Hillier, formerly of GSC Calgary, and the final stages completed by Jo Monro of GSC Calgary. Pat Greener and Hilde King skillfully and patiently completed the final text preparation for publication.

REFERENCES

Abercrombie, H.J. and Feng, R.
1997: Geological setting and origin of microdisseminated Au-Ag-Cu minerals, Fort McKay region, northeastern Alberta. *In* Exploring for Minerals in Alberta: Geological Survey of Canada Geoscience Contributions, Canada-Alberta Agreement on Mineral Development (1992-1995), R.W. Macqueen (ed.). Geological Survey of Canada, Bulletin 500, p. 247–277.

Ballantyne, S.B. and Harris, D.C.
1997: Alluvial platinum-group minerals and gold in Alberta: results from the "orientation studies project" and their significance to exploration. *In* Exploring for Minerals in Alberta: Geological Survey of Canada Geoscience Contributions, Canada-Alberta Mineral Development Agreement (1992-1995), R.W. Macqueen (ed.). Geological Survey of Canada, Bulletin 500, p. 279-329.

Bednarski, J.M.
1997: Quaternary geololgy along the shield margin, northeastern Alberta. *In* Exploring for Minerals in Alberta: Geological Survey of Canada Geoscience Contributions, Canada-Alberta Agreement on Mineral Development (1992-1995), R.W. Macqueen (ed.). Geological Survey of Canada, Bulletin 500, p. 81–105.

Bégin, N.J., Ghent, E.D., and Beiesdorfer, R.E.
1995: Mineralogical and geochemical analyses and economic potential of the Crowsnest volcanics. *In* Current Research, 1995-E, Geological Survey of Canada, p. 11-25.

Canada-Alberta Partnership on Minerals
1996: Program Summary. Alberta Geological Survey, Geological Survey of Canada, 104 p.

Charbonneau, B.W., Holman, P.B., and Hetu, R.J.
1994: Airborne geophyscal survey of northeastern Alberta NTS 74L/14,15, 74M/11-3, 6-11, 14,16. Geological Survey of Canada, Open File 2807.

1997: Airborne gamma ray spectrometric-magnetic-VLF survey of northeastern Alberta. *In* Exploring for Minerals in Alberta: Geological Survey of Canada Geoscience Contributions, Canada-Alberta Agreement on Mineral Development (1992-1995), R.W. Macqueen (ed.). Geological Survey of Canada, Bulletin 500, p. 107-131.

Chung, C-J., Rencz, A.N., and Zhang, A.
1997: Data integration study for mineral potential mapping in northeastern Alberta. *In* Exploring for Minerals in Alberta: Geological Survey of Canada Geoscience Contributions, Canada-Alberta Agreement on Mineral Development 1992-1995), R.W. Macqueen (ed.). Geological Survey of Canada, Bulletin 500, p. 155-161.

Clowes, R.
1996: LITHOPROBE Phase IV: Multidisciplinary Studies of the Evolution of a Continent - A Progress Report. Geoscience Canada, v. 23, p. 109-123.

Dufresne, M.B., Eccles, D.D., McKinstry, B., Schmitt, D.R., Fenton, M.M., Pawlowicz, J.G., and Edwards, W.A.D.
1996: The diamond potential of Alberta. Bulletin 63, Alberta Geological Survey, Edmonton, 158 p.

Fipke, C.E., Gurney, J.J., and Moore, R.O.
1995: Diamond exploration techniques emphasizing indicator mineral geochemistry and Canadian examples. Geological Survey of Canada, Bulletin 423, 86 p.

Friske, P.W.B., McCurdy, M.W., Day, S.J., Gross, H., Balma, R.G., Lynch, J.J., and Durham, C.C.
1994: National Geochemical Reconnaissance lake sediment and water data, northeastern Alberta (Parts of NTS 74E, 74L, and 74M). Geological Survey of Canada, Open File 2856.

Garrett, R.G.
1994: The distribution of cadmium in A soil horizons of the prairies in Canada and the adjoining United States. Geological Survey of Canada, Paper 94-1A, p. 73-82.

Gavin, B.
1991: Precious-metal mineralization in the Bearpaw Mountains and Sweet Grass Hills, north-central Montana. *In* Guidebook of the Central Montana Alkalic Province, D.W. Baker and R.B. Berg (eds.). Montana Bureau of Mines Special Publication 100, p. 55-62.

Harris, D.C. and Ballantyne, S.B.
1994: Characterization of gold and PGE-bearing placer concentrates from the North Saskatchewan River, Edmonton, Alberta. *In* Current Research, 1994-E. Geological Survey of Canada, p. 133-139.

Kjarsgaard, B.A.
1996: Prairie kimberlites. *In* Searching for Diamonds in Canada, A.N. LeCheminant, D.G. Richardson, R.N.W. DiLabio and K.A. Richardson (eds.). Geological Survey of Canada, Open File 3228, p. 67-72.

1997: Diamonds in Alberta: studies of potential host rocks of deep-seated origin and applications of indicator mineral exploration techniques. *In* Exploring for Minerals in Alberta: Geological Survey of Canada Geoscience Contributions, Canada-Alberta Agreement on Mineral Development (1992-1995), R.W. Macqueen (ed.). Geological Survey of Canada, Bulletin 500, p. 185-207.

Leckie, D.A. and Craw, D.
1997: Anomalous gold occurrences in Cretaceous and Tertiary conglomerates and gravels of Alberta. *In* Exploring for Minerals in Alberta: Geological Survey of Canada Geoscience Contributions, Canada-Alberta Agreement on Mineral Development (1992-1995), R.W. Macqueen (ed.). Geological Survey of Canada, Bulletin 500, p. 331-344.

Leckie, D.A., Kjarsgaard. B.A. et al.
1997: Geology of a Late Cretaceous possible kimberlite at Mountain Lake, Alberta - chemistry, petrology, indicator minerals, aeromagnetic signature, age, stratigraphic position and setting. Geological Survey of Canada, Open File 3441, 200 p.

McCurdy, M.W.
1997: Interprertation of geochemical data from lake sediments and waters over Precambrian rocks in northeastern Alberta (NTS 74E, 74L, 74M). *In* Exploring for Minerals in Alberta: Geological Survey of Canada Geoscience Contributions, Canada-Alberta Agreement on Mineral Development (1992-1995), R.W. Macqueen (ed.). Geological Survey of Canada, Bulletin 500, p. 133-154.

McCrae, N.D., Armitage, A.E., Miller, A.R., Roddick, J.C., Jones, A.L., and Mudry, M.P.
1996: The diamondiferous Akluilak lamprophyre dyke, Gibson Lake area, N.W.T. *In* Searching for diamonds in Canada, A.N. LeCheminant, D.G. Richardson, R.N.W. DiLabio, and K.A. Richardson (eds.). Geological Survey of Canada, Open File 3228, p. 101-107.

McDonough, M.R.
1997: Structural controls and age constraints on sulphide mineralization, southern Taltson Magmatic Zone, northeastern Alberta. *In* Exploring for Minerals in Alberta: Geological Survey of Canada Geoscience Contributions, Canada-Alberta Agreement on Mineral Development (1992-1995), R.W. Macqueen (ed.). Geological Survey of Canada, Bulletin 500, p. 13-29.

Northern Miner
1997: "Winter drilling program uncovers kimberlites at Buffalo Hills in Alberta". March 10, 1997, p. 21.

Peterson, T.D., Currie, K.L., Ghent, E.D., Bégin, N.J., and Beiersdorfer, R.E.
1997: Petrology and economic geology of the Crowsnest Volcanics, Alberta. *In* Exploring for Minerals in Alberta: Geological Survey of Canada Geoscience Contributions, Canada-Alberta Agreement on Mineral Development 1992-1995), R.W. Macqueen (ed.). Geological Survey of Canada, Bulletin 500, p. 163–184.

Ross, G.M., Mariano, J. Dumont, R., Kjarsgaard, B.A., and Teskey, D.
1997: Was Eocene magmatism widespread in the subsurface of southern Alberta? Evidence from new aeromagnetic anomaly data. *In* Exploring for Minerals in Alberta: Geological Survey of Canada Geoscience Contributions, Canada-Alberta Agreement on Mineral Development (1992-1995), R.W. Macqueen (ed.). Geological Survey of Canada, Bulletin 500, p. 235–246.

Ross, G.M., Parrrish, R.R., Villeneuve, M.E., and Bowring, S.A.
1991: Geophysics and geochronology of the crystalline basement of the Alberta Basin, western Canada. Canadian Journal of Earth Sciences, v. 28, p. 512–522.

Ruzicka, V.
1995: Unconformity-type uranium deposits. *In* Mineral Deposit Modeling, Geological Association of Canada Special Paper 40, R.V. Kirkham, W.D. Sinclair, R.I. Thorpe and J.M. Duke (eds.). p.125–149. (dated 1993).

1997: Metallogenic features of the Uranium-polymetallic mineralization of the Athabsasca Basin, Alberta, and a comparison with others parts of the basin. *In* Exploring for Minerals in Alberta: Geological Survey of Canada Geoscience Contributions, Canada-Alberta Agreement on MineralDevelopment (1992-1995), R.W. Macqueen (ed.). Geological Survey of Canada, Bulletin 500, p. 31–79.

Shives, R.B.K., Ford, K.L., and Charbonneau, B.W.
1995: Applications of Gamma ray spectrometric/magnetic/ VLF-EM surveys. Geological Survey of Canada, Open File 3061, 82 p.

Stone, P.E.
1993a: High resolution aeromagnetic total field survey of the Cypress Hills area, Alberta. 6 sheets (black and white). Scale 1:100 000. Geological Survey of Canada, Open File Report 2588, Map 1 - 82H/NE (south half); Map 2 -72E/NW; Map 3 - 72E/NE; Map 4 - 82H/SE; Map 5 - 72E/SW; Map 6 - 72E/SE.

1993b: Coloured maps: aeromagnetic residual and total field colour Interval maps with line contours, Cypress Hills area, southern Alberta. Scale 1:100 000. Map C9865G - 82H/NE (south half); Map C9866G - 72E/NW; Map C9867G - 72E/NE; Map C9868G - 82H/SE; Map C9869G - 72E/SW; Map C9870G - 72E/SE.

Thoreifson, L.H. and Garrett, R.G.
1997: Kimberlite indicator mineral and geochemical reconnaissance of southern Alberta. *In* Exploring for Minerals in Alberta: Geological Survey of Canada Geoscience Contributions, Canada-Alberta Agreement on Mineral Development (1992-1995), R.W. Macqueen (ed.). Geological Survey of Canada, Bulletin 500, p. 209–233.

Villeneuve, M.E., Ross, G.M., Theriault, R.J., Miles, W., Parrish, R.R., and Broome, J.
1993: Tectonic subdivision and U-Pb geochronology of the crystalline basement of the Alberta Basin, western Canada. Geological Survey of Canada, Bulletin 447, 86 p.

Whillans, R.T.
1996: Uranium. *In* 1995 Canadian Minerals Yearbook. Minerals and Metals Sector, Natural Resources Canada, E. Godin (ed.). Ottawa, p. 64.1–64.17.

APPENDIX
ALBERTA MINERAL DEVELOPMENT AGREEMENT PROJECTS

FEDERALLY FUNDED CANADA–ALBERTA MDA GEOSCIENCE PROJECTS

Five scientifc subprograms plus a coordination subprogram make up the Geological Survey of Canada portion of Canada–Alberta MDA studies. These subprograms, the 15 projects included within them, and the project leaders when the work was underway, are listed below. Authors' addresses are given in the papers included in this volume, except for those authors whose affilitations have changed since the work reported on herein was completed (for current addresses, see the list at the end of this Appendix). Information on publications from these projects can also be obtained from:

GSC Bookstore Geological Survey of Canada 601 Booth Street Ottawa, Ontario K1A OE8	GSC Calgary Bookstore Geological Survey of Canada (Calgary) 3303-33 Street N.W. Calgary, Alberta T2L 2A7

Northeastern Minerals Subprogram

- Tectonic evolution of the Precambrian Shield of northeastern Alberta; M.R. McDonough, GSC Calgary.
- Metallogenic studies of U-polymetallic mineralization of the Athabasca Basin and adjacent area; V. Ruzicka, Mineral Resources Division, Ottawa.
- Quaternary geology and till geochemistry; J. Bednarski, Terrain Sciences Division, Calgary.
- Airborne gamma-ray spectrometer-magnetics-VLF plus interpretation and follow-up; B.W. Charbonneau, Mineral Resources Division, Ottawa.
- Geochemical surveys; P.W.B. Friske, Mineral Resources Division, Ottawa.
- Data Integration, northeastern minerals program; C-J. Chung, Mineral Resources Division, Ottawa.

Southwestern Minerals Subprogram

- Mineral potential, metamorphism and petrogenesis of the Crowsnest Volcanics; T.D. Peterson, Continental Geoscience Division, Ottawa.

Diamond Subprogram

- Kimberlite mineralogy, petrology and geochemistry; B.A. Kjarsgaard, Continental Geoscience Division, Ottawa.
- Geochemical and mineralogical reconnaissance; L.H. Thorleifson, Terrain Sciences Division, Ottawa.
- Aeromagnetic survey, Cypress Hills; P.E. Stone, Continental Geoscience Division, Ottawa.
- Preliminary stratigraphic test to support mineral exploration, northern Alberta; B.A. Kjarsgaard, Continental Geoscience Division, Ottawa; also Alberta Geolgical Survey, Edmonton.
- Geochemical and stratigraphic setting of the Shaftesbury Formation in northern Alberta, and its potential to host ore deposits; R.W. Macqueen, GSC Calgary.

Industrial Minerals Subprogram

- Brine resources of Alberta; H.J. Abercrombie, GSC Calgary.

General Subprogram

- Orientation studies; S.B. Ballantyne, Mineral Resources Division, Ottawa.

Coordination

- Coordination and publication; R.W. Macqueen, GSC Calgary.

PROVINCIALLY FUNDED ALBERTA MDA GEOSCIENCE PROJECTS

Information on the following provincially supported Alberta MDA projects and resulting publications can be obtained from:

Alberta Geological Survey
7th Floor, North Petroleum Plaza
9945 - 108 Street
Edmonton, Alberta, T5K 2G6

The following geoscience projects were included in the provincially funded geoscience program. Projects that were completed by industry have the name of the company conducting the study; all other projects were completed by members of the Alberta Geological Survey. Further information and publications may be obtained from the Alberta Geological Survey. The first ten projects are closely related to GSC-supported projects listed above.

Precambrian Shield

- Evaluation of mineralization potential of selected areas of northeast Alberta; C.W. Langenberg, Alberta Geological Survey, Edmonton.
- Mineral deposits potential of the Marguerite River area; Alberta Geological Survey and Apex Geoscience Ltd., Edmonton.
- Analysis and cataloguing of Precambrian Shield rock samples; W.A.D. Edwards, Alberta Geological Survey, Edmonton.

Quaternary Surveys

- Reconnaissance mineral and geochemical survey with emphasis on northern Alberta; M.M. Fenton, Alberta Geological Survey, Edmonton.
- Surficial geology mapping and Quaternary stratigraphy of the Peace River and High Level-Fort Vermillion areas of northern Alberta; M.M. Fenton, Alberta Geological Survey; and Geology Department, University of Alberta, Edmonton.

Commodities: Gold, Diamonds, Lead-Zinc

- Investigation of potential paleoplacers in the Cretaceous strata of the North Saskatchewan River watershed; GEO-ING Resource Consulting Ltd., Edmonton.
- Regional synthesis of the structural and stratigraphic setting of Alberta to assist industry in the search for diamondiferous diatremes; Apex Geoscience Ltd., and Alberta Geological Survey, Edmonton.
- Analysis of Paleozoic core data for the evaluation of potential Pb-Zn deposits in northeastern Alberta; D. McPhee and A. Turner, consultants, Calgary.

Hydrogeochemistry, Brines

- Study of the hydrogeochemistry of northern Alberta with specific reference to the possible occurrence of Zn-Pb deposits; Hitchon Geochemical Services Ltd., Sherwood Park, Alberta.
- Evaluation of potential for the recovery of industrial minerals from Alberta brines; S. Bachu, Alberta Geological Survey, Edmonton.

Southern Alberta Rift

- Geological mapping, prospecting and sampling of the southern Alberta Rift; R.A. Olson Consulting Ltd. (Apex Geoscience Ltd.), Edmonton.
- Reconnaissance structural-stratigraphic study of the southern Alberta rift in southwest Alberta; R.A. Olson Consulting Ltd. (Apex Geoscience Ltd.), Edmonton.

Structural and Building Materials

- Mapping and resource exploration of the Tertiary and preglacial formations of Alberta; W.A.D. Edwards, Alberta Geological Survey, Edmonton.

- Mineral aggregate commodity analysis; W.A.D. Edwards, Alberta Geological Survey, Edmonton.

- Mineral aggregate database and deposit map series; W.A.D. Edwards, Alberta Geological Survey, Edmonton.

- Regional synthesis and characterization of industrial limestones in Alberta; W.N. Hamilton, Alberta Geological Survey, Edmonton.

- Mineral resource mapping of main mountain corridors; W.N. Hamilton, Alberta Geological Survey, Edmonton.

- Commodity profiling of principal industrial and metallic minerals in Alberta; W.N. Hamilton, Alberta Geological Survey, Edmonton.

Oil Sands

- Assessment of the potential of co-product minerals and metals in Alberta oil sands deposits; D.W. Devenny, Gulf Canada Resources, Calgary.

General Projects

- Mineral information system; D.A. Wynne, Alberta Geological Survey, Edmonton.

- Geoscience coordination, public open houses and final publication of provincially funded projects; Alberta Geological Survey and Apex Geoscience Ltd., Edmonton.

Other projects were conducted as part of the Canada–Alberta Mineral Development Agreement (1992-1995) as follows. All are reported on elsewhere (e.g. Canada-Alberta Partnership on Minerals, 1996). Further information about these projects and reports resulting from them may be obtaned from the sources given, or from the Alberta Geological Survey, Edmonton.

FEDERALLY SUPPORTED PROJECTS

Mining and Minerals Technology

- Heavy minerals recovery from Syncrude and Suncor centrifuge plant tailings; D. Currie, Alberta Chamber of Resources, Edmonton.

- Microwave smelting of low rank coals and oxide minerals; Alberta Research Council, Edmonton.

- Clay carbo-chlorination study; H.A. Simons Ltd., Calgary.

- Engineering design and preliminary feasibility of Envi-Tech adsorption technology for fine gold recovery process; TMCL Engineering, Ottawa.

- Novel technology for gold recovery from Alberta placer deposits; J. Janiak, Envi-Tech Inc., Edmonton.

Development Studies

- Fort Chipewyan granite as an aggregate source; D. Scafe, Alberta Geological Survey, Edmonton.

- Evaluation of leonardite resources of Alberta; Retread Resources Ltd., Sherwood Park, Alberta.

- Economic analysis of extracting calcium and magnesium chloride from Alberta brines; D.B. Cross and Associates Ltd., Calgary.

- Review of Alberta limestone production, marketing, distribution and future development possibilities; Holter Geological Services, Ferndale, Washington.

- Alberta MDA worldwide web server; Alberta Geological Survey, Edmonton.

PROVINCIALLY SUPPORTED PROJECTS

Technology Development

- Development of an expanded light-weight plaster structural-type building product for agricultural or light-weight industrial use; Polar Powders and Technologies Inc., Calgary.

- Establishing diamond exploration sample processing methodology and facilities for Alberta; TerraMin Research Labs Ltd., Calgary.

- Development of enhanced methodology for the analysis of indicator minerals in potential diamond-bearing ores in Alberta; Loring Laboratories Ltd., Calgary.

- Diamond recovery by selective adsorption; J. Janiak, Envi-Tech Inc., Edmonton.

- Preliminary study of the environmental impact of Envi-Tech fine gold recovery process; TMCL Engineering, Ottawa.

Economic Development

- Whitehorse Mining Initiative; Whitehorse Mining Initiative Secretariat, Ottawa.

- Diamond market study; R. Vandenberg, Maple Leaf Resources, Edmonton.

- IGWG native representatives (Inter-Governmental Working Group on Aboriginal Participation in the Mining Industry of Canada).